Interrogating the relationship between the tumour microenvironment and its infiltrating immune cells in Ovarian Cancer

by

Rachel Louise Pounds

A thesis submitted to the University of Birmingham for the degree of

DOCTOR OF PHILOSOPHY



Institute of Cancer and Genomic Sciences
College of Medical and Dental Sciences
University of Birmingham

May 2023

UNIVERSITY OF
BIRMINGHAM

University of Birmingham Research Archive

e-theses repository

This unpublished thesis/dissertation is copyright of the author and/or third parties. The intellectual property rights of the author or third parties in respect of this work are as defined by The Copyright Designs and Patents Act 1988 or as modified by any successor legislation.

Any use made of information contained in this thesis/dissertation must be in accordance with that legislation and must be properly acknowledged. Further distribution or reproduction in any format is prohibited without the permission of the copyright holder.

ABSTRACT

Ovarian cancer (OC) is the sixth most common cancer amongst women, with approximately 7,500 new cases diagnosed each year in the United Kingdom. The complex ovarian tumour microenvironment is poorly understood, while the nature and role of tumour-infiltrating NK cells in OC progression remains unclear. To analyse the cell type contexture of OC tissue, two single cell sequencing techniques were performed on omental tumour biopsies from patients with advanced OC. The scRNAseq analysis focused on portraying an immunogenic tumour microenvironment and determined the characteristics of a dysfunctional NK cell population, implying NK reactivation upon chemotherapy exposure. In contrast, scATACseq data identified significant epithelial tumour cell heterogeneity and demonstrated an increase in chromatin accessibility for oncogenes and transcription factors related to cancer stem cells following chemotherapy treatment. Utilising a large prospective cohort of OC patient samples, the phenotype and function of NK cells in peripheral blood, primary ovarian tumour and metastatic omental tumour was explored. Flow cytometric analysis has revealed that peripheral blood NK cells are activated in OC, while NK cell inhibition occurs following tumour infiltration. Results have shown the adaptations to NK cell receptors in advancing disease and the specific inhibitory NK features associated with poor patient outcomes. The OC NK cells demonstrated a reduced ability to proliferate and expand upon exposure to cells lacking HLA and secreted fewer cytokines than the non-cancerous control samples. Instead, the OC NK cells were highly cytotoxic towards K-562 cells and primary ovarian tumours. Interestingly, the NK cell cytotoxicity to primary ovarian tumours was dependent on the activation receptor, DNAM-1. The significance of DNAM-1 in the tumour-immune response was demonstrated, identifying it as a possible biomarker that can be used as a target for NK-mediated immunotherapy.

ACKNOWLEDGEMENTS

First of all, I would like to thank my supervisor Professor Paul Moss, for his inspiration, reassurance and direction during this thesis. Both his constructive feedback and genuine support have been invaluable over the past years.

Mr Jason Yap has provided precious support and mentorship across both the laboratory and clinical environments over the last 10 years. I thank him for his patience, kindness and endless encouragement that has motivated me to continue challenging myself during this project.

I would like to express my gratitude to Dr Jianmin Zuo, who has been full of insights and offered practical guidance within the laboratory to tackle this PhD.

I must also mention Professor Sean Kehoe who has been a valued supervisor throughout my academic career and first provided me the opportunity to undertake scientific research.

Miss Kavita Singh, Mr Janos Balega and Professor Sudha Sundar have been invaluable in the clinical setting, and without their assistance I would not have been able to collect the required samples for my study. I also thank the patients at City Hospital, Birmingham, for their consent in using their samples for my laboratory research.

To all those in Professor Paul Moss' extended team, I thank you for your support. Dr Hayden Pearce and Dr Wayne Croft have been instrumental in helping me navigate through the intricacies of this research and analyse the accompanying data. Rachel Bruton deserves a special mention for her continued support and advice.

Thanks to the MRC for funding this research and awarding me the clinical research training fellowship position.

Finally, I would like to thank my family, particularly my husband, Matt, my children, Oscar and Freya, and my parents, Nick and Sue. I will be forever grateful for their endless strength, understanding and love.

TABLE OF CONTENTS

ABSTRACT ……..... I

ACKNOWLDEGEMENTS …… II

TABLE OF CONTENTS ……... III

LIST OF FIGURES ……..……..XII

LIST OF TABLES ……..... XXIII

ABREVIATIONS ……..…… XXV

Chapter 1: Introduction ……...……... 1

1.1 Ovarian Cancer ……..…...……..…… 2

1.1.1 Epidemiology of Ovarian Cancer ……... 2

1.1.2 Aetiology and Pathophysiology of Epithelial Ovarian Cancer …….. 3

1.1.3 Symptoms and Diagnosis of Ovarian Cancer …… 5

1.1.4 Disease staging ……...… 6

1.1.5 Ovarian Cancer Management ……. 8

1.1.6 Ovarian Cancer Prognosis and Patient Outcomes ……... 10

1.2 Clinical Challenges in Ovarian Cancer ……..……... 12

1.2.1 The Development of Resistance to Chemotherapy Treatment in Ovarian Cancer ……...…… 12

1.2.2 Tumour Heterogeneity in Ovarian Cancer ……...….. 13

1.3 The Tumour Microenvironment and the Immune Response ... 15

1.3.1 Ovarian Cancer and the Tumour Microenvironment ……... 15

1.3.2 Immunosurveillance and Tumour Progression ……..... 18

1.3.3 Immune Escape Mechanisms in the Ovarian Tumour Microenvironment ..… 19

1.3.4 The Clinical Importance of the Immune Response in Ovarian Cancer ……... 19

1.3.5 The Tumour-specific Immune Response following Chemotherapy Treatment ……..…. 20

1.4 Natural Killer cells in Ovarian Cancer ……..... 21

1.4.1 Natural Killer cell Development and Maturation ……. 21

1.4.2 Identification of Target cells and Natural Killer Cell Activation ……..……. 21
1.4.3 Natural Killer Inhibition and Recognition of "self" ……..... 22
1.4.4 The Functional Response of Activated Natural Killer cells …… 24
1.4.5 The Role of Natural Killer cells in Advanced Ovarian Cancer ……... 25
1.5 Immunotherapy and Targeted Cancer Drugs ……...…...…...… 27
1.5.1 Currently Approved Agents in Ovarian Cancer ……... 27
1.5.2 Immunotherapy Clinical Trials in Ovarian Cancer ……..… 29
1.5.3 Natural Killer cell Therapy in Ovarian Cancer ……..... 31
1.6 PhD Aims and Objectives ……..……..... 33

Chapter 2: Materials and Methods ……...……. 35

2.1 Part 1: Analysis of the study cohort …..……..……...……. 36
2.1.1 The cohort population ……..……. 36
2.1.1.1 Identification and recruitment to the cohort population ……. 36
2.1.1.2 Ethical approval …….. 37
2.1.2 Clinicopathological characteristics of the cohort population ……. 37
2.1.2.1 Definition of the clinicopathological characteristics …….. 37
2.1.3 Management of the cohort population ……...…. 38
2.1.3.1 Description of the treatment and management outcomes …….. 38
2.1.4 Study cohort clinical outcomes …….. 39
2.1.4.1 Disease recurrence and progression free survival …….. 40
2.1.4.2 Patient death and overall survival ……..…. 40
2.1.5 Statistical analysis…… 40
2.1.6 Study cohort sample collection ……..... 41
2.1.6.1 Peripheral blood collection ……..……...……..... 41
2.1.6.2 Tissue biopsy collection ……./……..... 41
2.2 Part 2: Laboratory Techniques ……... 42
2.2.1 Tissue culture ……. 42
2.2.1.1 Basic culture medium ……. 42
2.2.1.2 The K-562 cell line ……. 42
2.2.2 Preparation of patient samples ……... 43

2.2.2.1 Processing of patient blood samples ……..… 43
2.2.2.2 Processing of patient tissue samples ……...… 44
2.2.2.3 Cryopreservation of patient samples ……... 44
2.2.2.4 Thawing of patient samples ……...…….. 45
2.2.2.5 Flash freezing patient tissue samples …….. 45
2.2.3 NK cell phenotype analysis ……. 45
2.2.3.1 Flow cytometry of patient samples ……. 45
2.2.4 Cytotoxicity analysis ……... 49
2.2.4.1 NK cell isolation ……...… 49
2.2.4.2 Labelling of K-562 cells ……..…… 50
2.2.4.3 Co-culture of NK cells and K-562 cells …….. 50
2.2.4.4 Flow cytometric analysis of NK cell cytotoxicity ……... 50
2.2.5 Cytokine production …… 51
2.2.5.1 NK cell stimulation ……. 51
2.2.5.2 Intracellular and surface cytokine staining …….. 52
2.2.5.3 Flow cytometric analysis of NK cell cytokine production …….. 52
2.2.6 Real-time quantitative PCR (qPCR) of NK cell ligands ……..… 53
2.2.6.1 RNA extraction from ovarian tissue …… 53
2.2.6.2 RNA conversion to cDNA …….. 54
2.2.6.3 Amplification and measurement of target genes ……. 55
2.2.7 Expression of NK ligands on normal and malignant epithelial cells within ovarian biopsies ……... 57
2.2.8 NK cell cytotoxicity following co-culture with ovarian tissue …….. 58
2.2.8.1 Co-culture of ovarian tissue and NK cells ……... 58
2.2.8.2 Cytotoxicity of NK cells following co-culture with ovarian tissue ……. 58
2.2.8.3 NK activation receptor blocking and cytotoxicity ……..... 59
2.3 Part 3: Single Cell Sequencing ……..…….. 61
2.3.1 Single cell RNA sequencing …….. 61
2.3.1.1 Sample preparation for single cell RNA sequencing ……. 61
2.3.1.2 Cell sorting of tumour samples for single cell RNA sequencing ……... 62
2.3.1.3 Library preparation for 10X sequencing ……..... 64
2.3.1.4 Analysis of the single cell RNA sequencing data …… 65
2.3.1.5 Unsupervised clustering and major cell lineage annotation ……. 66

2.3.1.6 NK cell cluster identification and annotation …….. 65
2.3.1.7 Cluster proportion comparisons …….. 67
2.3.1.8 Signature scoring ……..… 67
2.3.1.9 Differential expression …… 68
2.3.1.10 Gene Set Enrichment Analysis (GSEA) …….. 68
2.3.1.11 Correlation analysis. ……..…. 68
2.3.2 Single cell ATAC sequencing …… 68
2.3.2.1 Sample preparation and nuclei extraction for single cell ATAC sequencing … 68
2.3.2.2 Library preparation for 10X single cell ATAC sequencing ……... 70
2.3.2.3 Analysis of the single cell ATAC sequencing data ……..…. 71
2.3.2.4 Differential peak analysis ……... 72
2.3.2.5 Unsupervised clustering and major cell lineage annotation ……..…. 72
2.3.2.6 Differential transcription factor motif enrichment …….…… 73

Chapter 3: Heterogeneity and Transcriptional Profiles of tumour and immune cells in Ovarian Cancer 74

3.1 Introduction …….. 75

3.2 Single cell RNA Sequencing of Ovarian Cancer ……..... 76

3.2.1 The sample cohort ……...…. 76
3.2.2 Composition of omental samples evaluated by single cell RNA sequencing ….. 79
3.2.3 Analysis of single cell RNA sequencing data …….. 80
3.2.3.1 Clustering and identification of major cell types ……. 80
3.2.3.2 Cell clustering according to tissue type and OC treatment …….. 85
3.2.3.3 Annotation of major cell types with chemotherapy exposure ……..… 87
3.2.3.4 Interrogation of NK cell ligands within omental tissue ……... 92
3.2.3.5 Clustering and identification of NK cell subpopulations ……. 94
3.2.3.6 Interrogation of NK cell clusters according to tissue type and OC treatment … 96
3.2.3.7 Annotation of NK cells with chemotherapy exposure ……..… 101
3.2.4 Summary of the single cell RNA sequencing analysis in ovarian cancer …….. 104

3.3 Single cell ATAC sequencing of ovarian cancer samples ……. 105

3.3.1 The sample population ……..…. 105

3.3.2 Preparation of specimens ……..…….. 107
3.3.3 Analysis of single cell ATAC sequencing data …….…… 107
3.3.3.1 Clustering and identification of major cell types …….. 107
3.3.3.2 Differences in chromatin landscape following chemotherapy exposure …….. 113
3.3.4 Summary of the single cell ATAC sequencing analysis in ovarian cancer ….. 118
3.4 Discussion …… 119

Chapter 4: Analysis of NK cell Phenotype in Ovarian Cancer … 131

4.1 Introduction …… 132
4.2 Study cohort …… 133
4.3 Analysis of NK cells within the study cohort ……... 133
4.3.1 Patient samples evaluated …… 133
4.3.2 Identification of NK cells …… 136
4.3.3 Evaluation of NK cell sub-populations and phenotype …… 139
4.4 Analysis of peripheral NK cell phenotype …….. 142
4.4.1 The proportion of NK cells within the circulating blood …….. 142
4.4.2 The type of NK cells within the circulating blood ……..…. 144
4.4.3 The expression of receptors on NK cells within the circulating blood ……. 151
4.4.3.1 Activation receptors on the peripheral NK cells ……... 151
4.4.3.2 Inhibitory receptors on the peripheral NK cells …… 154
4.4.4 Summary of the peripheral NK cell phenotype …… 157
4.5 Assessment of NK phenotype following ovarian infiltration …. 157
4.5.1 The proportion of NK cells within ovarian tissue …… 157
4.5.2 The type of NK cells within the ovarian tissue ……..... 159
4.5.3 The expression of receptors on ovarian tissue infiltrating NK cells ……. 165
4.5.3.1 Activation receptors on the ovarian NK cells ……..... 165
4.5.3.2 Inhibitory receptors on the ovarian NK cells …… 168
4.5.4 Summary of the ovarian infiltrating NK cell phenotype ……... 170
4.6 Assessment of NK cell phenotype following omental tissue Infiltration …..... 170
4.6.1 The proportion of NK cells within omental tissue ……..... 170

4.6.2 The type of NK cells within the omental tissue …… 172
4.6.3 The expression of receptors on omental tissue infiltrating NK cells ……..... 178
4.6.3.1 Activation receptors on the omental NK cells ……... 178
4.6.3.2 Inhibitory receptors on the omental NK cells ……... 181
4.6.4 Summary of the omental infiltrating NK cell phenotype ……..… 183
4.7 The correlation between peripheral, ovarian tissue and omental tissue NK cells …..... 183
4.7.1 The association between paired PBMC NK cells and ovarian NK cells …… 183
4.7.1.1 The proportion and type of NK cells …….. 183
4.7.1.2 Analysis of NK activation receptors …….. 190
4.7.1.3 Analysis of NK inhibition receptors ……... 192
4.7.2 The association between matched PBMC NK cells and omental NK cells …… 193
4.7.2.1 The proportion and type of NK cells ……...… 193
4.7.2.2 Analysis of NK activation receptors ……... 201
4.7.2.3 Analysis of NK inhibition receptors ……..... 203
4.7.3 The association between paired ovarian and omental tumour NK cells ……..204
4.7.3.1 The proportion and type of NK cells ……... 204
4.7.3.2 Analysis of NK activation receptors ……... 209
4.7.3.3 Analysis of NK inhibition receptors …… 210
4.7.4 Summary of the correlation between the peripheral blood, ovarian and omental NK cells …….. 211
4.8 Discussion ……..……..…… 212

Chapter 5: The correlation of NK cell Phenotype with Clinical Outcomes in Ovarian Cancer ……... 217
5.1 Introduction ……... 218
5.2 Study cohort …….. 218
5.3 Explanatory variables of the study cohort…….. 219
5.3.1 Patient characteristics and histopathological variables ……... 219
5.3.1.1 Patient age at the time of surgical intervention ……... 219
5.3.1.2 Patient ethnicity ……... 219
5.3.1.3 Disease stage ……... 220

5.3.1.4 Peritoneal Cancer Index …….. 220
5.3.1.5 Histopathological findings …….. 220
5.3.1.6 Metastatic Omental disease ……. 221
5.3.1.7 Serum CA-125 level at the time of surgical intervention …… 222
5.3.1.8 Absolute lymphocyte count at the time of surgical intervention ……..… 223
5.3.2 Patient management and treatment variables ……..…… 225
5.3.2.1 Type of surgical intervention …… 225
5.3.2.2 Cytoreduction ……..… 226
5.3.2.3 Chemotherapy treatment and response ……..... 227
5.4 Patient outcomes ……..….. 229
5.4.1 Disease recurrence and analysis of progression free survival …….. 229
5.4.2 Analysis of disease specific death ……..... 232
5.5 The association between NK phenotype and clinical outcomes … 236
5.5.1 The correlation between NK cells, patient survival and disease recurrence …..... 236
5.5.1.1 Recurrence of disease and the proportion of NK cells ……. 236
5.5.1.2 Patient survival and the proportion of NK cells ……... 239
5.5.1.3 Disease recurrence based on the NK cell subpopulation ……. 241
5.5.1.4 Patient survival based on the NK cell subpopulation ……...… 244
5.5.1.5 Disease recurrence based on NK cell receptors ……... 247
5.5.1.6 Patient survival based on NK cell receptors ……. 256
5.5.2 Disease severity and NK cell phenotype …….. 265
5.5.2.1 NK cells and disease stage ……... 265
5.5.2.2 NK cells and tumour burden …… 266
5.5.3 NK cells and chemotherapy response …….. 270
5.5.4 DNAM-1 expression and patient outcomes ……. 274
5.5.4.1 DNAM-1 expression and disease stage ……..…….. 274
5.5.4.2 DNAM-1 expression and CA-125 level ……...……..... 276
5.5.4.3 DNAM-1 expression and omental metastatic disease …….. 278
5.5.5 Summary of the association between NK phenotype and clinical outcomes ….. 280
5.6 Discussion ……..….. 281

Chapter 6: Functionality study of NK cells and interaction with primary Ovarian Cancer cells 286

6.1 Introduction 287

6.2 Function of the peripheral NK cells 288

6.2.1 NK cell cytotoxicity 288

6.2.1.1 Defining NK cell killing 288

6.2.1.2 The NK cell cytotoxicity study cohort 291

6.2.1.3 Peripheral NK cell cytotoxicity analysis 294

6.2.1.4 Correlations between NK cell cytotoxicity and clinical findings 298

6.2.1.5 Correlations between NK cell cytotoxicity and NK phenotype 302

6.2.2 NK cell cytokine production 306

6.2.2.1 Detecting NK cell cytokines 306

6.2.2.2 The NK cytokine study cohort 309

6.2.2.3 Analysis of NK cell cytokine production 310

6.2.2.4 Correlations between NK cytokine production and clinical outcomes 320

6.2.2.5 Correlations between NK cell cytokine production and NK phenotype 327

6.2.3 Summary of peripheral NK cell function 331

6.3 Interaction between ovarian tumour tissue and NK cells 333

6.3.1 Identification of NK cell ligands on tumour tissue 333

6.3.2 The study cohort for NK ligand analysis 334

6.3.3 Transcription analysis of NK cell ligands on ovarian tumour tissue 335

6.3.4 Correlations between tumour ligands and patient outcomes 338

6.3.5 Correlation between NK ligands and NK phenotype data 344

6.3.6 Summary of NK cell ligand expression upon ovarian tumours 348

6.4 The expression of NK ligands on epithelial cells within ovarian biopsies 349

6.4.1 Detecting NK ligands expressed by epithelial cells within ovarian biopsies..... 349

6.4.2 Comparison of NK ligands between normal and malignant epithelial cells 352

6.4.3 Summary of NK ligand expression in normal and malignant epithelial cells 353

6.5 The recognition of primary ovarian tumour cells by NK cells 354

6.5.1 NK cell cytotoxicity following co-culture with ovarian tumour cells 354

6.5.1.1 Detecting NK cell killing of tumour cells ……...… 354
6.5.1.2 The co-culture study population ……..…… 357
6.5.1.3 Ovarian - NK cell co-culture analysis ……. 359
6.5.1.4 Correlation between NK cell killing and clinical outcomes …… 364
6.5.2 The contribution of NK activating receptors to NK cell cytotoxicity ……. 368
6.5.2.1 Receptor inhibition and NK cell killing …….. 368
6.5.2.2 The co-culture population for receptor inhibition ……... 369
6.5.2.3 Analysis of NK activation receptor inhibition ……..... 369
6.5.3 Summary of the NK cell response to ovarian tumour tissue ……... 372
6.6 Discussion ……..….. 373

Chapter 7: General Discussion and Future Work ……...……...…. 379

7.1 Tumour Heterogeneity and Transcriptional Profiling of Ovarian Cancer …..……..……...……. 380
7.2 NK cell Phenotype, Functionality and Clinical Relevance in Ovarian Cancer …….. 383
7.2.1 NK cell Phenotype …… 385
7.2.2 NK cell Phenotype and Clinical Relevance …… 386
7.2.3 NK cell Functionality ……..…. 387
7.2.4 DNAM-1 in Ovarian Cancer ……... 390
7.3 Limitations and Future Directions …… 391
7.4 Conclusion …….. 392

Chapter 8: References ……...……..…. 394

LIST OF FIGURES

Figure 1.1: Anatomical illustration of an ovarian tumour …… 3
Figure 1.2: Advanced OC is managed with either upfront primary surgery or upfront primary chemotherapy followed by interval debulking surgery ……...……9
Figure 1.3: Cancer stem cells give rise to new chemo-resistant tumour ……13
Figure 1.4: Types of tumour cell heterogeneity in cancer ……..… 14
Figure 1.5: The structure and components of the tumour microenvironment in OC ……. 16
Figure 1.6: NK response following the detection of MHC class I molecules on normal healthy cells and tumour cells ……. 23
Figure 1.7: NK cell-initiated antibody-dependent cell-mediated cytotoxicity (ADCC) …… 25
Figure 1.8: Mechanism of action of anti-angiogenic agents …….. 28
Figure 1.9: Mechanism of action of PARP inhibitors …… 28
Figure 2.1: Analysis of NK phenotype in patient blood and tissue samples …….. 48
Figure 2.2: The amplification plot for cDNA undergoing PCR ……. 56
Figure 2.3: The NK cell and ovarian co-culture with addition of antibodies to inhibit NK cell Receptors …….. 60
Figure 2.4: The gating strategy to identify and sort cell populations within digested omental tumour tissue ……..... 63
Figure 2.5: The generation of GEM's during library preparation for single cell RNA Sequencing …….. 65
Figure 2.6: Creation of GEM's and barcoding during library preparation for single cell ATAC Sequencing ……... 71
Figure 3.1: Clustering of the high-level cell types in omental deposits from HGSOvCa Patients …… 81
Figure 3.2: Markers utilised to identify major cell types ……... 83
Figure 3.3: Identification of major cell types within omental samples …….. 84
Figure 3.4: Clustering of cells based on treatment and tissue type ……..... 85
Figure 3.5: Profile of major cell type proportions by sample, treatment and tissue type …... 86
Figure 3.6: The proportion of major cell types in the CD45+ve and CD45-ve populations based on tissue type ……. 87
Figure 3.7: The proportion of major cell types in the CD45-ve and CD45+ve populations based on NACT treatment ……... 88

Figure 3.8: Modulation of gene expression within major cell types following chemotherapy exposure ……... 89
Figure 3.9: The proportion of cell types in the CD45-ve and CD45+ve populations based on chemotherapy response score …….. 90
Figure 3.10: The proportion of cell types in the CD45-ve and CD45+ve populations based on disease recurrence following chemotherapy treatment ……. 91
Figure 3.11: The expression of NK ligands on major cell types within omental tumour ….. 93
Figure 3.12: Profile of differential expression of NK ligands following chemotherapy Exposure ……..……94
Figure 3.13: Clustering of the major lymphocyte cell populations in all omental samples ... 95
Figure 3.14: Identification of NK subtypes within omental tissue …….…… 95
Figure 3.15: Expression of makers genes within the different NK cell clusters ……..... 95
Figure 3.16: Gene expression of NK cell marker genes depicting NK cell function ……. 96
Figure 3.17: Expression profile of receptors for NK activation and inhibition ……. 97
Figure 3.18: Expression profile of genes for NK cytokines ……... 99
Figure 3.19: The proportion of NK cell clusters based on tissue type ……. 100
Figure 3.20: The proportion of NK cell clusters based on chemotherapy exposure …… 100
Figure 3.21: The proportion of NK cell clusters by chemotherapy response score ……. 101
Figure 3.22: The proportion of NK cell clusters by disease recurrence following chemotherapy treatment ……...……...… 102
Figure 3.23: Gene expression and functional divergence following chemotherapy treatment and upon disease recurrence ……. 103
Figure 3.24: Clustering of high-level cell types cells within metastatic omental tumour Deposits ……..... 108
Figure 3.25: Identification of the major high-level cell types within metastatic omental tumour deposits ……... 109
Figure 3.26: Gene activity of major cell type marker genes …… 110
Figure 3.27: Identification of the major high-level cell types marker genes ……... 110
Figure 3.28: Cluster proportions based on patient sample ……. . 112
Figure 3.29: Major high-level cell types within patient samples ……. 113
Figure 3.30: Cells within high-level cell clusters ……..… 113
Figure 3.31: UMAP of cells within metastatic omental tumour based on treatment …….. 114
Figure 3.32: Cluster proportions stratified by chemotherapy treatment …….. 114
Figure 3.33: Major cell type chromatin accessibility marker peak profile …….. 115

Figure 3.34: Transcription factor motif enrichment profile of marker motifs enriched within major cell type marker peaks ……... 116
Figure 3.35: Chromatin accessibility in the major cell types following chemotherapy ….. 117 treatment.
Figure 3.36: Motif enrichment analysis of gene transcription in major cells depending on chemotherapy exposure and patient samples ……...… 118
Figure 4.1: Blood and tissue samples collected within the study cohort ……. 135
Figure 4.2: The gating strategy implemented to identify the NK cell population within each blood (PBMC) sample following flow cytometry ……. 137
Figure 4.3: The gating strategy implemented to identify the NK cell population within each tissue biopsy (TILS) sample following flow cytometry ……..... 138
Figure 4.4: The gating strategy used to identify the different NK cell sub-populations …. 139
Figure 4.5: Histograms demonstrating the expression of NK cell surface receptors ……... 141
Figure 4.6: The proportion of CD56 positive NK cells within the peripheral blood of patients with OC and with normal ovaries ……..…… 142
Figure 4.7: The proportion of CD56 positive NK cells within the peripheral blood of all patients in the study cohort ……..... 144
Figure 4.8: The proportion of NK subsets within each PBMC sample in the study cohort ..147
Figure 4.9: Comparison of the proportion of NK subsets between patients with normal ovaries and patients with OC ……..... 149
Figure 4.10: The proportion of the NK cell subsets across the different patient groups …. 150
Figure 4.11: PBMC NK cells with high expression of activation receptors in patients with OC and normal ovaries ……... 152
Figure 4.12: PBMC NK cells with high expression of activation receptors in the four patient groups ……... 153
Figure 4.13: PBMC NK cells with high expression of inhibitory receptors in OC patients compared to normal ovary patients …….. 155
Figure 4.14: PBMC NK cells with high expression of inhibitory receptors in the four patient groups ……... 156
Figure 4.15: The proportion of CD56 positive NK cells infiltrating into ovarian tissue …. 158
Figure 4.16: The proportion of CD56 positive NK cells infiltrating into ovarian tissue …. 159
Figure 4.17: The proportion of NK subsets within each ovarian tissue biopsy sample ….. 161
Figure 4.18: The incidence of the ovarian infiltrating NK cell subsets in OC and normal ovarian tissue ……..…….. 163

Figure 4.19: The incidence of the ovarian infiltrating NK cell subsets across the different patient groups …….. 164
Figure 4.20: Activation receptors in normal ovarian and OC tissue ……..... 166
Figure 4.21: Ovarian NK cell activation receptor across four patient groups …….. 167
Figure 4.22: Inhibitory receptors on tissue infiltrating NK within OC and normal ovary ... 168
Figure 4.23: Ovarian NK cell inhibitory receptors across four patient groups …… 169
Figure 4.24: Proportion of infiltrating NK cells within omental tissue …… 171
Figure 4.25: Proportion of infiltrating NK cells within normal omentum, chemotherapy naïve omental tumours and chemotherapy exposed omental tumours …….. 172
Figure 4.26: The proportion of NK subsets within each omental tissue biopsy sample ….. 174
Figure 4.27: The type of infiltrating NK cell subsets in omental tumour and normal omental tissue ……..... 176
Figure 4.28: The proportion of the omental infiltrating NK cell subsets across the different patient groups …….. 177
Figure 4.29: NK activation receptors in normal omentum and omental tumour ……. 179
Figure 4.30: Omental NK cell activation receptors across the patient groups ……. 180
Figure 4.31: NK cell inhibitory receptors in normal omentum and omental tumour …...… 181
Figure 4.32: Omental NK cell inhibitory receptors across three patient groups …….. 182
Figure 4.33: Correlation between the proportion of NK cells within the PBMC to matched ovarian tumour ……. 184
Figure 4.34: Correlation between CD56 and CD16 expression in PBMC NK cells and paired ovarian tumour NK cells …….. 185
Figure 4.35: Correlation between the proportion of NK cells within the PBMC to matched ovarian tumour in both primary surgery and neoadjuvant chemotherapy OC patients …… 186
Figure 4.36: Correlation between PBMC and ovarian NK cell CD56 and CD16 expression in both primary surgery and neoadjuvant chemotherapy patients …… 187
Figure 4.37: Correlation between the proportion of NK cells within PBMC to matched ovarian tissue in patients with normal ovaries and benign ovaries ……. 188
Figure 4.38: Correlation between paired PBMC and ovarian NK cell CD56 and CD16 expression in patients with normal and benign ovaries ……... 189
Figure 4.39: Expression of activation receptors on ovarian tumour infiltrating NK cells and matched PBMC NK cells in all OC patients ……... 191
Figure 4.40: Expression of inhibitory receptors on tumour infiltrating NK cells and matched

PBMC NK cells in all OC patients …….. 192
Figure 4.41: Correlation between the proportion of NK cells within the PBMC to matched omental tumour tissue ……..… 194
Figure 4.42: Correlation between CD56 and CD16 expression in PBMC NK cells and matched omental tumour NK cells …….. 195
Figure 4.43: Correlation between the proportion of NK cells within PBMC to matched omental tumour in primary surgery and neoadjuvant chemotherapy groups .. 197
Figure 4.44: Correlation between PBMC and omental NK cell CD56 and CD16 expression in both primary surgery and neoadjuvant chemotherapy OC patients …… 198
Figure 4.45: Correlation between the proportion of NK cells within the PBMC to matched normal omental tissue in patients with normal or benign ovaries …… 199
Figure 4.46: Correlation between PBMC and normal omental NK cell CD56 and CD16 expression in patients with normal and benign ovaries ……... 200
Figure 4.47: Expression of activation receptors on omental tumour infiltrating NK cells and matched PBMC NK cells in all OC patients ……...… 202
Figure 4.48: Expression of inhibitory receptors on omental tumour infiltrating NK cells and matched PBMC NK cells in all OC patients …… 203
Figure 4.49: Correlation between the proportion of NK cells within ovarian tumour and matched omental tumour samples ……... 205
Figure 4.50: Correlation between CD56 and CD16 expression in ovarian tumour NK cells and paired omental tumour NK cells ……... 206
Figure 4.51: Correlation between the proportion of NK cells within ovarian tumour and matched omental tumour in both primary surgery and neoadjuvant chemotherapy OC patients …….. 207
Figure 4.52: Correlation between ovarian tumour and omental tumour NK cell CD56 and CD16 expression in both primary surgery and neoadjuvant chemotherapy OC Patients …… 208
Figure 4.53: Expression of activation receptors on ovarian tumour infiltrating NK cells and matched omental tumour NK cells in all OC patients ……..… 209
Figure 4.54: Expression of inhibitory receptors on ovarian tumour infiltrating NK cells and matched omental tumour NK cells in all OC patients …….. 210
Figure 5.1: Kaplan-Meier plot demonstrating progression free survival in all OC patients in the primary surgery and neoadjuvant chemotherapy treatment groups ……. 231
Figure 5.2: Kaplan-Meier plot demonstrating progression free survival in advanced OC

(AOC) patients in the primary surgery and neoadjuvant chemotherapy treatment Groups ……... 232
Figure 5.3: Kaplan-Meier plot demonstrating overall survival in all OC patients in the primary surgery and neoadjuvant chemotherapy treatment groups …….. 235
Figure 5.4: Kaplan-Meier plot demonstrating overall survival in advanced OC (AOC) managed with primary surgery and neoadjuvant chemotherapy ……...… 235
Figure 5.5: The progression free survival of OC patients based on the proportion of NK cells within their peripheral blood ……...….. 237
Figure 5.6: The progression free survival of OC patients based on the proportion of NK cells within the ovarian tumour tissue samples ……. 238
Figure 5.7: The progression free survival of OC patients based on the proportion of NK cells within the omental tumour tissue samples ……... 238
Figure 5.8: The overall survival of OC patients based on the proportion of NK cells within the peripheral blood …….…….. 240
Figure 5.9: The overall survival of OC patients based on the proportion of NK cells within ovarian tumour tissue ……...……. 240
Figure 5.10: The overall survival of OC patients based on the proportion of NK cells within omental tumour tissue ……..… 241
Figure 5.11: The progression free survival of OC patients based on the proportion of NK cell subpopulations within peripheral blood samples …… 243
Figure 5.12: The overall survival of OC patients based on the proportion of NK cell subpopulations within peripheral blood samples ……... 246
Figure 5.13: The progression free survival of OC patients based on peripheral NK cell expression of activation receptor NKp46 …… 249
Figure 5.14: The progression free survival of OC patients based on peripheral NK cell expression of activation receptor CD57 ……..… 250
Figure 5.15: The progression free survival of OC patients based on peripheral NK cell expression of activation receptor DNAM-1 ……... 250
Figure 5.16: The progression free survival of OC patients based on peripheral NK cell expression of inhibiting receptor PD-1 …… 251
Figure 5.17: The progression free survival of OC patients based on ovarian NK cell expression of activation receptor NKp46 ……... 252
Figure 5.18: The progression free survival of OC patients based on ovarian NK cell expression of activation receptor DNAM-1 …… 252

Figure 5.19: The progression free survival of OC patients based on ovarian NK cell expression of activation receptor CD57 ……..… 253
Figure 5.20: The progression free survival of OC patients based on ovarian NK cell expression of inhibiting receptor PD-1 ……...… 253
Figure 5.21: The progression free survival of OC patients based on omental NK cell expression of activation receptor NKp46 …… 254
Figure 5.22: The progression free survival of OC patients based on omental NK cell expression of activation receptor DNAM-1 …… 254
Figure 5.23: The progression free survival of OC patients based on omental NK cell expression of activation receptor CD57 …….. 255
Figure 5.24: The progression free survival of OC patients based on omental NK cell expression of inhibiting receptor PD-1 ……... 255
Figure 5.25: The overall survival of OC patients based on peripheral NK cell expression of activation receptor DNAM-1 ……...… 258
Figure 5.26: The overall survival of OC patients based on peripheral NK cell expression of activation receptor NKp46 …….. 259
Figure 5.27: The overall survival of OC patients based on peripheral NK cell expression of activation receptor CD57 ……. 259
Figure 5.28: The overall survival of OC patients based on peripheral NK cell expression of inhibiting receptor PD-1 …….. 260
Figure 5.29: The overall survival of OC patients based on ovarian NK cell expression of activation receptor DNAM-1 ……... 261
Figure 5.30: The overall survival of OC patients based on ovarian NK cell expression of activation receptor NKp46 ……..…… 261
Figure 5.31: The overall survival of OC patients based on ovarian NK cell expression of activation receptor CD57 ……. 262
Figure 5.32: The overall survival of OC patients based on ovarian NK cell expression of inhibiting receptor PD-1 …….. 262
Figure 5.33: The overall survival of OC patients based on omental NK cell expression of activation receptor DNAM-1 ……... 263
Figure 5.34: The overall survival of OC patients based on omental NK cell expression of activation receptor NKp46 …….. 263
Figure 5.35: The overall survival of OC patients based on omental NK cell expression of activation receptor CD57 ……. 264

Figure 5.36: The overall survival of OC patients based on omental NK cell expression of inhibiting receptor PD-1 …….. 264
Figure 5.37: The mean proportion of NK cells in peripheral blood, ovarian tumour and omental tumour depending on disease stage ……... 265
Figure 5.38: The proportion of each NK cell subtype within the peripheral blood depending on disease stage ……...… 266
Figure 5.39: The proportion of NK cells within the peripheral blood, ovarian tumour and omental tumour depending on PCI value …… 267
Figure 5.40: The proportion of NK cells with high expression of activation receptors based on PCI ……... 268
Figure 5.41: The proportion of NK cells with high expression of inhibitory receptors based on PCI value ……..……...… 269
Figure 5.42: The proportion of NK cells in blood and tumour tissue based on CRS ……... 270
Figure 5.43: The proportion of NK cells with high expression of activation receptors based on CRS ……. 272
Figure 5.44: The proportion of NK cells with high expression of inhibitory receptors based on CRS ……..... 273
Figure 5.45: NK cells with high expression of DNAM-1 based on disease stage ……... 275
Figure 5.46: NK cells with high expression of DNAM-1 based on CA-125 level …….. 277
Figure 5.47: NK cells with high expression of DNAM-1 based on the presence of omental tumours in OC patients …… 279
Figure 6.1: The gating strategy implemented to identify live K-562 cells ……... 289
Figure 6.2: Identification of live K-562 cells following NK cell co-culture …… 290
Figure 6.3: Kaplan-Meier plot demonstrating progression free survival in the primary surgery and neoadjuvant chemotherapy patients utilised in the cytotoxicity assay ….. 293
Figure 6.4: Kaplan-Meier plot demonstrating overall survival in the primary surgery and neoadjuvant chemotherapy patients utilised in the cytotoxicity assay ……... 293
Figure 6.5: Killing of K-562 cells by NK cells from healthy donor and OC samples ….. ...294
Figure 6.6: Cytotoxicity of peripheral NK cells obtained from healthy donors and patients with OC ……. 296
Figure 6.7: Cytotoxicity of peripheral NK cells obtained from healthy donors, primary surgery OC patients and neoadjuvant chemotherapy OC patients …… 297
Figure 6.8: Cytotoxicity of peripheral NK cells in OC patients based on the presence of metastatic omental disease ……..... 298

Figure 6.9: Cytotoxicity of peripheral NK cells in OC patients who recurred compared to those who remained disease free ……... 299
Figure 6.10: Cytotoxicity of peripheral NK cells in OC patients who died compared to those who were alive ……..... 300
Figure 6.11: Kaplan-Meier plot demonstrating progression free survival in OC patients with NK cytotoxicity below and above the median value …… 301
Figure 6.12: Kaplan-Meier plot demonstrating overall survival in OC patients with NK cytotoxicity below and above the median value ……. 301
Figure 6.13: Proportion of peripheral NK cells in OC patients based on degree of NK Cytotoxicity ……. 302
Figure 6.14: Type of peripheral NK cells in OC patients based on NK cytotoxicity …….. 303
Figure 6.15: Expression of activation receptors on NK cells with low and high levels of Cytotoxicity ……..… 304
Figure 6.16: Expression of inhibitory receptors on NK cells with low and high levels of Cytotoxicity ……. 305
Figure 6.17: The gating strategy implemented to identify the NK cell population within peripheral blood samples following flow cytometry ……..… 307
Figure 6.18: The NK cell population from an unstimulated PBMC sample and a stimulated PBMC sample co-cultured with K-562 cells ……. 308
Figure 6.19: Histograms demonstrating NK cell cytokine production ……..... 309
Figure 6.20: Proportion of NK cells in unstimulated and stimulated PBMC samples ……. 311
Figure 6.21: Cytokine production from unstimulated peripheral NK cells …….. 314
Figure 6.22: Cytokine production from stimulated peripheral NK cells …….. 315
Figure 6.23: The difference in cytokine production between unstimulated and stimulated NK cells in healthy donor, primary surgery and chemotherapy samples …….. 318
Figure 6.24: The difference in cytokine production between unstimulated and stimulated NK cells in healthy donor and combined OC samples ……..… 319
Figure 6.25: Proportion of peripheral NK cells in OC patients based on presence of omental Disease ……. 321
Figure 6.26: The proportion of NK cells with stimulation in OC patients who suffered a recurrence of disease compared to those who remained disease free ……. 322
Figure 6.27: Cytokine production in stimulated NK cells based on disease recurrence ..… 323
Figure 6.28: Kaplan-Meier plots demonstrating progression free survival in OC patients based on the level of cytokines produced by NK cells ……. 325

Figure 6.29: Kaplan-Meier plots demonstrating overall survival in OC patients based on amount of cytokine production …… 326
Figure 6.30: Comparison of the proportion of NK cell subpopulations between patients with high and low cytokine production ……... 328
Figure 6.31: The correlation between the expression of NK activation receptors and degree of cytokine production ……. 330
Figure 6.32: The correlation between the expression of NK inhibitory receptors and degree of cytokine production ……. 331
Figure 6.33: Quantitative PCR data demonstrating the transcription level of 18S within HGSOvCa and benign ovarian tissue biopsies ……..... 336
Figure 6.34: Quantitative PCR data demonstrating the relative transcription of NK cell activating ligands on HGSOvCa tissue and benign ovarian tissue ……. 337
Figure 6.35: Quantitative PCR data demonstrating the relative transcription of NK cell inhibition ligands on HGSOvCa tissue and benign ovarian tissue …….…. 338
Figure 6.36: Transcription of NK ligands on HGSOvCa tissue based on chemotherapy Exposure …….. 339
Figure 6.37: Disease recurrence and transcription of NK ligands on HGSOvCa tissue ….. 341
Figure 6.38: Survival and the transcription of NK ligands on HGSOvCa tissue ……..… 342
Figure 6.39: Kaplan-Meier plot showing progression free survival based on transcription levels for NK ligands on tumour tissue ……... 343
Figure 6.40: Kaplan-Meier plot showing overall survival based on transcription levels for NK ligands on tumour tissue ……...… 344
Figure 6.41: Comparison of the type of tumour infiltrating NK cells between tumours with high and low transcription levels for the NK ligands ……..… 346
Figure 6.42: Expression of activating receptors on NK cells within tumour tissue based on the levels of corresponding NK ligands ……. 347
Figure 6.43: Expression of inhibiting receptors on NK cells within tumour tissue based on the levels of corresponding NK ligands …… 348
Figure 6.44: The gating strategy to detect Epcam positive epithelial cells within tumour Biopsies …….. 350
Figure 6.45: Identification of epithelial cell population and expression of NK ligands …. 351
Figure 6.46: The expression of NK ligands upon normal epithelial cells and malignant cells within ovarian tumour biopsies ……... 353

Figure 6.47: The gating strategy implemented to identify the live ovarian tumour cells following co-culture with NK cells ……. 356
Figure 6.43: Expression of inhibiting receptors on NK cells within tumour tissue based on the levels of corresponding NK ligands ……..... 358
Figure 6.49: Healthy donor NK cell killing after co-culture with ovarian tissue …… 361
Figure 6.50: Autologous NK cell killing after co-culture with ovarian tissue ……. 362
Figure 6.51: NK cell killing after co-culture with ovarian tissue ……. 363
Figure 6.52: NK cell killing after co-culture with ovarian tumour treated with and without Chemotherapy …….. 365
Figure 6.53: NK cell killing of ovarian tumour in those who recurred and those who remained free of disease ……...… 366
Figure 6.54: NK cell killing of ovarian tumour in those who died and those alive …… 366
Figure 6.55: Kaplan-Meier plot showing progression free survival in those with low and high levels of NK cytotoxicity following culture with ovarian tumour tissue …… 367
Figure 6.56: Kaplan-Meier plot showing overall survival in those with low and high levels of NK cell cytotoxicity following culture with ovarian tumour tissue …… 368
Figure 6.57: NK cell killing of ovarian tumour cells with the inhibition of NK activating Receptors ……..… 370
Figure 6.58: Flow cytometric analysis of NK killing following NK receptor inhibition …. 371
Figure 7.1: Comparison of tumour-infiltrating NK cells and peripheral NK cells …….…. 384
Figure 7.2: The mechanisms utilised by ovarian cancer cells to inactivate NK cells and reduce NK cell-mediated cytotoxicity ……...…… 388

LIST OF TABLES

Table 1.1: The FIGO Staging for Ovarian Cancer (2014) ……...… 7
Table 1.2: Significant findings from single cell RNA sequencing studies of the TME in ovarian cancer …..……. 18
Table 1.3: Clinical application and outcomes of the NICE approved targeted cancer drugs in OC ……...……. 29
Table 1.4: NK cell therapies and outcomes from clinical use …….32
Table 2.1: NK cell activating receptor antibody panel ……..……. 46
Table 2.2: NK cell inhibiting receptor antibody panel ……..……. 47
Table 2.3: Surface stain antibodies utilised in the cytokine assay ……..… 53
Table 2.4: Intracellular antibodies utilised in the cytokine assay ……... 53
Table 2.5: Primer probes used in qPCR to detect NK cell ligands …… 55
Table 2.6: Conditions for DNA amplification with PCR ……... 56
Table 2.7: Antibodies to detect epithelial cells within ovarian tissue and their expressed NK ligands ……... 57
Table 2.8: Antibodies used to detect NK cell killing of ovarian tissue …….. 59
Table 2.9: Antibodies added to co-culture to block NK cell receptors …….. 59
Table 2.10 Antibodies added to the single cell solution for cell sorting …… 62
Table 3.1: Characteristics and baseline variables of the patients in the scRNAseq cohort … 78
Table 3.2: The cells sequenced for every patient in the scRNAseq cohort ……... 79
Table 3.3: Characteristics and baseline variables of patients who provided samples for scATACseq analysis ……... 106
Table 3.4: The nuclei sequenced in each sample in the scATAC cohort ……. 107
Table 4.1: The mean proportion of PBMC NK subsets in the different patient groups ...… 146
Table 4.2: The mean proportion of NK subsets within ovarian tissue ……. 160
Table 4.3: The mean proportion of NK subsets within omental tissue ……...…. 173
Table 5.1: Patient characteristics and histopathological variables ……... 224
Table 5.2: Patient management and treatment …… 228
Table 5.3: Disease recurrence based on treatment modality ……... 230
Table 5.4: OC related death based on treatment modality ……... 234
Table 5.5: OC recurrences based on the proportion of NK cells …… 236
Table 5.6: Disease-specific death and the proportion of NK cells ……... 239

Table 5.7: OC recurrences based on the proportion of PBMC NK cell subpopulations ….. 242
Table 5.8: OC related death based on the proportion of PBMC NK cell subpopulations … 244
Table 5.9: Proportion of women with disease recurrence based on low and high expression of NK receptors ……..… 248
Table 5.10: Mortality from OC with low and high expression of NK receptors ……..….. 257
Table 6.1: Cytotoxicity assay patient characteristics and outcomes……. 292
Table 6.2: Mean cytotoxicity of peripheral NK cells in healthy donors and OC patients ... 295
Table 6.3: Cytokine assay patient characteristics and outcomes …….. 310
Table 6.4: Mean percentage of cytokines produced by stimulated and unstimulated NK cells within PBMC samples ……. 313
Table 6.5: Characteristics and outcomes of patients included in the NK ligand analysis … 335
Table 6.6: Characteristics and outcomes of patients included in the Ovarian-NK cell co-culture analysis ……...… 359
Table 6.7: Cytotoxicity of healthy donor (HD) NK cells and autologous NK cells when cultured with ovarian tumour, benign ovary and normal ovary ……. 362

ABREVIATIONS

ADDC: Antibody-dependent cell-mediated cytotoxicity

APOD: Apolipoprotein D

ATAC: Assay for Transposase-Accessible Chromatin

B2M: Beta-2-microglobulin

BGCS: British Gynaecological Cancer Society

BRCA: Breast cancer gene

BSA: Bovine serum albumin

CA-125: Cancer antigen 125

CAR: Chimeric antigen receptor

CAF: Cancer associated fibroblast

CEA: Carcinoembryonic antigen

CIK: Cytokine induced killer cells

CFSE: Carboxyfluorescein succinimidyl ester

COL1A1: Collagen type 1 alpha 1

CRS: Chemotherapy response score

CSC: Cancer stem cell

CT: Computerised tomography

CTLA-4: Cytotoxic T-lymphocyte associated protein 4

DAMP: Damage-associated molecular pattern

DCN: Decorin

DEG: Differentially expressed gene

DMSO: Dimethyl sulfoxide

DNA: Deoxyribonucleic acid

DNAM-1: DNAX accessory molecule 1

EDTA: Ethylenediaminetetra acetic acid

EMT: Epithelial-to-mesenchymal transition

EOC: Epithelial ovarian cancer

EPCAM: Epithelial cell adhesion molecule

FACS: Fluorescence-activated cell sorting

FBS: Fetal Bovine Serum

FIGO: International Federation of Obstetrics and Gynaecology

FOXP3: Forkhead box P3

G-CSF: Granulocyte colony-stimulating factor

GEM: Gel beads in emulsion

GM-CSF: Granulocyte-macrophage colony-stimulating factor

HD: Healthy donor

HER2: Human epidermal growth factor receptor 2

HGSOvCa: High-grade serous ovarian cancer

HLA: Human Leukocyte Antigen

HNPCC: Hereditary non-polyposis colorectal cancer

HRA: Health research authority

IDO: Indoleamine 2,3-dioxygenase

IDS: Interval debulking surgery

IFN: Interferon

IL: Interleukin

KRAS: Kirsten rat sarcoma viral oncogene homologue

KRT: Keratin

LSI: Latent semantic indexing

LYZ: Lysozyme

MACS: Magnetic-activated cell sorting

MDSC: Myeloid-derived suppressor cell

MDT: Multi-disciplinary team

MFAP5: Microfibril associated protein 5

MgCl2: Magnesium chloride

MHC: Major histocompatibility class

MICA/B: Major histocompatibility complex (MHC) class I chain-related protein A/B

MRI: Magnetic resonance imagine

NaCl: Sodium chloride

NACT: Neoadjuvant chemotherapy

NICE: National Institute for Health and Care Excellence

NK: Natural killer cells

NKG2A/D/C: Natural Killer group 2A/D/C

NKp30/44/46: Natural Killer protein 30/44/46

OC: Ovarian cancer

OS: Overall survival

PARP: Poly adenosine diphosphate-ribose polymerase

PBMC: Peripheral blood mononuclear cell

PBS: Phosphate buffered saline

PCA: Principle component analysis

PCI: Peritoneal cancer index

PD-1: Programmed cell death protein 1

PDL-1: Programmed cell death protein ligand 1

PDPN: Podoplanin

PDS: Primary debulking surgery

PECAM1: Platelet and endothelial cell adhesion molecule 1

PI: Propidium iodide

PFS: Progression free survival

PTPRC: Protein tyrosine phosphatase receptor type C

PVR: Polio virus receptor

PVRL2: Polio virus receptor-related 2

qPCR: Quantitative polymerase chain reaction

RMI: Risk of malignancy index

RNA: Ribonucleic acid

Rpm: Revolutions per minute

RPMI: Roswell Park Memorial Institute medium

scATACseq: Single cell ATAC sequencing

scRNAseq: Single cell RNA sequencing

SPRI: Solid phase reversible immobilisation

STIC: Serous tubal intraepithelial carcinoma

TAH + BSO: Total abdominal hysterectomy and bilateral salpingo-oopherectomy

TF-IDF: Term frequency-inverse document frequency

TGF: Transforming growth factor

TILs: Tumour infiltrating lymphocytes

TME: Tumour microenvironment

TNF: Tumour necrosis factor

TRAIL: Targeting TNF-related apoptosis- inducing ligand

Treg: Regulatory T cell

TREM1: Triggering receptor expressed on myeloid cells 1

TRIS-HCl: Tris(hydroxymethyl)aminomethane hydrochloride

ULBP: UL16 binding protein

UMAP: Uniform manifold projection

UMI: Unique molecular index

VEGF: Vascular endothelial growth factor

WFDC1/2: Whey acidic protein four disulphide core domain protein 1/2

Chapter 1:

Introduction

1.1 Ovarian Cancer

1.1.1 Epidemiology of Ovarian Cancer

Ovarian cancer (OC) is the sixth most common cancer amongst women, with approximately 7,500 new cases diagnosed each year in the United Kingdom. This accounts for 4% of all new cancer diagnoses in females. Typically occurring in post-menopausal women, the highest incidence rates are in the 75 to 79-year age group, with over a quarter of all new cases occurring in those over the age of 75 years. There are roughly 4,100 deaths from OC each year within the United Kingdom; almost half are in the cohort women over the age of 75 years [1]. Although the age-standardised incidence rates of OC in the United Kingdom actually reduced by 5% between the years 2006 and 2018, it is expected that the rate will have increased by almost 15% by the year 2035, to 32 new cases per 100,000 women per year [1, 2]. While there are no differences in OC incidence based on deprivation, rates are higher in women of White ethnicity compared to women from Asian, Black and mixed ethnic groups [1, 3].

Around 90% of OC cases are of epithelial cell (EOC) origin, with the most common and also most aggressive subtype being high-grade serous ovarian cancer (HGSOvCa) [1, 4-6]. Other less common types of epithelial tumours include low-grade serous OC, endometrioid OC, clear cell OC and mucinous tumours. Rarer, non-epithelial tumours can originate within ovarian germ cells (such as ovarian teratomas), ovarian sex cords or stroma (sex cord stromal tumours, commonly granulosa cell tumours) and surrounding soft tissues (sarcomas) [1]. This thesis concentrates on epithelial cell tumours, particularly the high-grade serous subtype because this is not only the most prevalent form of OC - it is also the deadliest and currently available treatments remain unsatisfactory.

1.1.2 Aetiology and Pathophysiology of Epithelial Ovarian Cancer

The aetiology of EOC remains poorly understood [7]. Evidence suggests that early tumorigenesis actually occurs within the fallopian tubes. Through the examination of salpingo-oopherectomy specimens, prophylactically removed in women who have a hereditary OC risk associated with mutated BRCA genes, dysplasia has frequently been discovered in the distal fimbria of the tube, the likely site of origin [7-11]. Furthermore, the high-grade serous subtype, HGSOvCa, seems to develop from a precursor lesion within the tube, serous tubal intraepithelial carcinoma (STIC), before then spreading towards the ovary [1, 4, 8, 9, 12]. Figure 1.1 illustrates the anatomy of the ovaries and their relationship with the fallopian tubes.

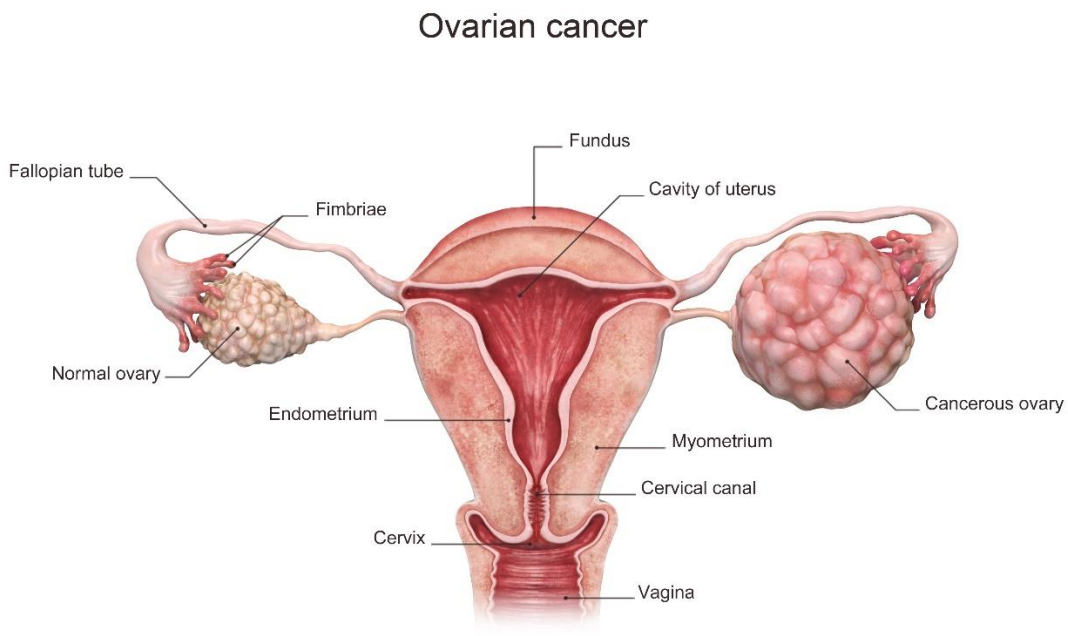


Figure 1.1: Anatomical illustration of an ovarian tumour
The comparison of a normal ovary to a malignant ovarian tumour, in relation to the fallopian tubes, uterus, cervix and vagina.

Figure adapted from St. John's Cancer Institute, 2023 [13]

Following neoplastic transformation, the tumour cells initially metastasise away from the ovary and fallopian tube via direct spread and by lymphatic drainage. Here malignant deposits have the ability to readily implant on the surface of the peritoneum, omentum and bowel mesentery. In addition, tumour cells flow through fluid within the peritoneal cavity, following a natural current along the right paracolic gutter up to the liver and diaphragm [11, 14, 15].

Carcinogenesis is thought to occur following the complex interaction between multiple factors; a hereditary or genetic predisposition is likely modified by numerous environmental aspects [7]. One pathophysiological theory involves the constant and repetitive trauma and repair that occurs to the ovarian epithelium during ovulation. The incurred genetic disruptions within the epithelial cells then lead to neoplastic transformation. Moreover, the number of ovulatory cycles is related to mutations in the tumour suppressor gene p53, resulting in defective DNA repair and increasing the risk of ovarian pathogenesis [7, 14-18]. This "incessant ovulation hypothesis" supports the notion that reduced ovulation, for example due to pregnancy and oral contraceptive use, is protective against OC development [7, 19]. In comparison, increased ovulation (through nulliparity, never using oral contraceptives, early menarche or late menopause) is shown to increase the risk of OC [20].

Another hypothesis for ovarian tumour development includes sustained inflammatory insults to the ovarian epithelium or fallopian tube, for example with chronic salpingitis, pelvic inflammatory disease and endometriosis [7, 21, 22]. Other concepts describe reproductive hormones, such as oestrogens and androgens, as well as excess gonadotrophins directly stimulating and disrupting the normal ovarian epithelium [23, 24]. Additional risk factors for OC include: smoking, obesity, infertility and exposure to environmental toxins (such as Talcum powder) [25-28].

While the development of ovarian tumours is associated with several somatic and germline mutations, whole exome sequencing has shown they have a low to intermediate mutational burden (with between 20 and 40 mutations per tumour) when compared to other malignancies [5, 11, 29-32]. Abnormalities within the p53 gene are the most frequent mutations found in OC, present in 50% to 80% of serous ovarian tumours, and in almost all (95%) cases of advanced high-grade serous tumours [5, 33-36]. Up to 20% of HGSOvCa cases can also have altered expression of the proto-oncogenes, *HER2/neu* and *AKT2*, as well as silencing of the tumour suppressor gene, *p16* [37-39]. In contrast, mucinous, endometrioid and low-grade epithelial tumours are significantly more likely to have mutations in the oncogenes *BRAF* and *KRAS*, along with dysfunctional *PTEN*, a tumour suppressor gene [40-42].

A number of inherited genetic mutations are also associated with OC [11, 43]. In all ovarian tumours, between 10% and 15% harbour an inherited germline mutation in the *BRCA1* or *BRCA2* proteins [44], increasing to 20% with acquired somatic *BRCA* mutations also included [35, 45]. These genes are critical in repairing damaged DNA via the homologous recombination repair pathway [45-47], with a lifetime OC risk of 30%-44% and 27% caused by *BRCA1* and *BRCA2* mutations respectively [48, 49]. Mutations in DNA mismatch repair genes (specifically, *MSH2*, *MSH6* and *MLH1*) and deletions within the gene *EPCAM* are seen in the condition Lynch Syndrome, previously known as Hereditary non-polyposis colorectal cancer (HNPCC). While subjecting women to a lifetime OC risk of around 12%, OC caused by Lynch syndrome accounts for 2% to 3% of all ovarian malignancies [43, 50-53].

1.1.3 Symptoms and Diagnosis of Ovarian Cancer

The signs and symptoms of OC are typically vague and tend to initially be insignificant to most patients. Specifically, the common symptoms reported include: abdominal bloating and pain,

reduced appetite, early satiety, frequent or urgent urination, weight loss, altered bowel habits and generalised fatigue [1].

Upon presentation, the diagnostic tools utilised include the serum tumour marker, CA-125 and ultrasound scan of the abdomen and pelvis [54]. A risk of malignancy index (RMI) score is then calculated using the CA-125 level, ultrasound findings and menopausal status. This predicts the likelihood a patient has OC, with all those women with a score of 250 or greater referred to a specialist gynaecological cancer centre [47, 54]. Here, following discussion by the multi-disciplinary team, patients may undergo additional investigations if deemed necessary. These may include further serum tumour markers (for example, CEA), additional imaging (CT scan, MRI), cytological analysis of ascitic fluid aspirated from the abdominal cavity or fluid obtained from pleural effusions, and histological diagnosis through image guided biopsies or laparoscopic biopsies [47]. The results can assist in confirming a diagnosis, explore the histological type of OC, evaluate the disease stage and also allow treatment strategies to be planned for each patient.

1.1.4 Disease staging

The majority of patients (over 70%) present when tumours have already spread beyond the pelvis and are unfortunately found to have advanced stage disease at the time of diagnosis [1]. The International Federation of Gynaecological Oncologists (FIGO) 2014 staging system for cancers of the ovary, fallopian tube and peritoneum, which was last updated in 2018, classifies each case depending on the size and location of the ovarian tumour and any metastatic spread [55-57]. Table 1.1. demonstrates the 2014 FIGO staging system for ovarian, fallopian tube and peritoneal cancers. The stage of disease determines the treatment options available and influences the rates of recurrence and survival.

Table 1.1: The FIGO Staging for Ovarian Cancer (2014) [55-57]

The FIGO staging system for ovarian, fallopian tube and peritoneal cancers (2014)	
Stage I	**Tumour confined to ovaries / fallopian tubes**
Stage IA	*Tumour within one ovary / tube*
Stage IB	*Tumour within both ovaries / tubes*
Stage IC	*Tumour within one or both ovaries / tubes plus:* - *IC1: tumour capsule ruptures during surgery* - *IC2: Capsule ruptures prior to surgery or tumour present on ovary / tube surface* - *IC3: Neoplastic cells within peritoneal washings or ascites*
Stage II	**Tumour involving one or both ovaries / tubes, with extension into pelvis or peritoneal cancer**
Stage IIA	*Extension to uterus / fallopian tubes / ovaries*
Stage IIB	*Extension to other pelvic intraperitoneal structures*
Stage III	**Tumour involving one or both ovaries / tubes, or peritoneal cancer, plus tumour in the peritoneum beyond the pelvis and / or tumour within the retroperitoneal lymph nodes**
Stage IIIA1	*Tumour within the retroperitoneal lymph nodes only:* - *IIIA1(i): greatest dimension up to 10mm* - *IIIA1(ii): greatest dimension over 10mm*
Stage IIIA2	*Microscopic tumour within the peritoneum beyond the pelvis +/- retroperitoneal lymph nodes*
Stage IIIB	*Macroscopic tumour within the peritoneum beyond the pelvis and up to 2cm greatest dimension +/- retroperitoneal lymph nodes*
Stage IIIC	*Macroscopic tumour within the peritoneum beyond the pelvis and over 2cm greatest dimension (including to the capsule of liver and spleen without parenchymal disease) +/- retroperitoneal lymph nodes*
Stage IV	***Additional distant metastasis***
Stage IVA	*Neoplastic cells within pleural effusion*
Stage IVB	*Parenchyma metastasis / metastasis to extra-abdominal organs, inguinal lymph nodes or lymph nodes beyond the abdominal cavity*

1.1.5 Ovarian Cancer Management

The National Institute for Health and Care Excellence (NICE) and the British Gynaecological Cancer Society (BGCS) have published guidelines for the management of OC [47, 58, 59]. The surgical resection for all stages of suspected OC should be performed at a specialist gynaecological cancer centre, with evidence that this improves survival [47, 60].

The treatment of early OC (stages I and II) includes surgical resection of the tumour plus sampling of ascitic fluid or peritoneal washings from within the abdominal cavity, biopsies taken from the peritoneum, omentectomy and the assessment of lymph nodes if appropriate. Following this, platinum-based chemotherapy treatment is offered to all women with early OC, except those with low grade stage I disease [47].

Current standard treatment for advanced OC (stages III and IV) consists of cytoreductive surgery and chemotherapy [47]. Here, surgical intervention aims to remove all macroscopically visible disease (termed complete cytoreduction), which is associated with significantly prolonged overall survival (OS) and progression-free survival (PFS) [47, 61-63]. Chemotherapy is given with six courses of platinum-based drugs (namely, Carboplatin), either as a single agent or in combination with the drug Paclitaxel, determined by patient's fitness [59]. Primary debulking surgery (upfront surgery followed by six adjuvant chemotherapy cycles) is the gold standard treatment in patients with a good performance status and where complete or optimal cytoreduction (where residual disease is less than 1cm in size) is deemed possible [47]. Interval debulking surgery (three or four neoadjuvant chemotherapy cycles before surgical resection, followed by three subsequent adjuvant chemotherapy cycles) is non-inferior and has been shown to reduce morbidity in those patients who have a significant disease burden or where achieving complete or optimal cytoreduction remains uncertain [63,

64]. Figure 1.2 demonstrates the different treatment pathways; upfront primary debulking surgery and upfront neoadjuvant chemotherapy with interval debulking surgery.

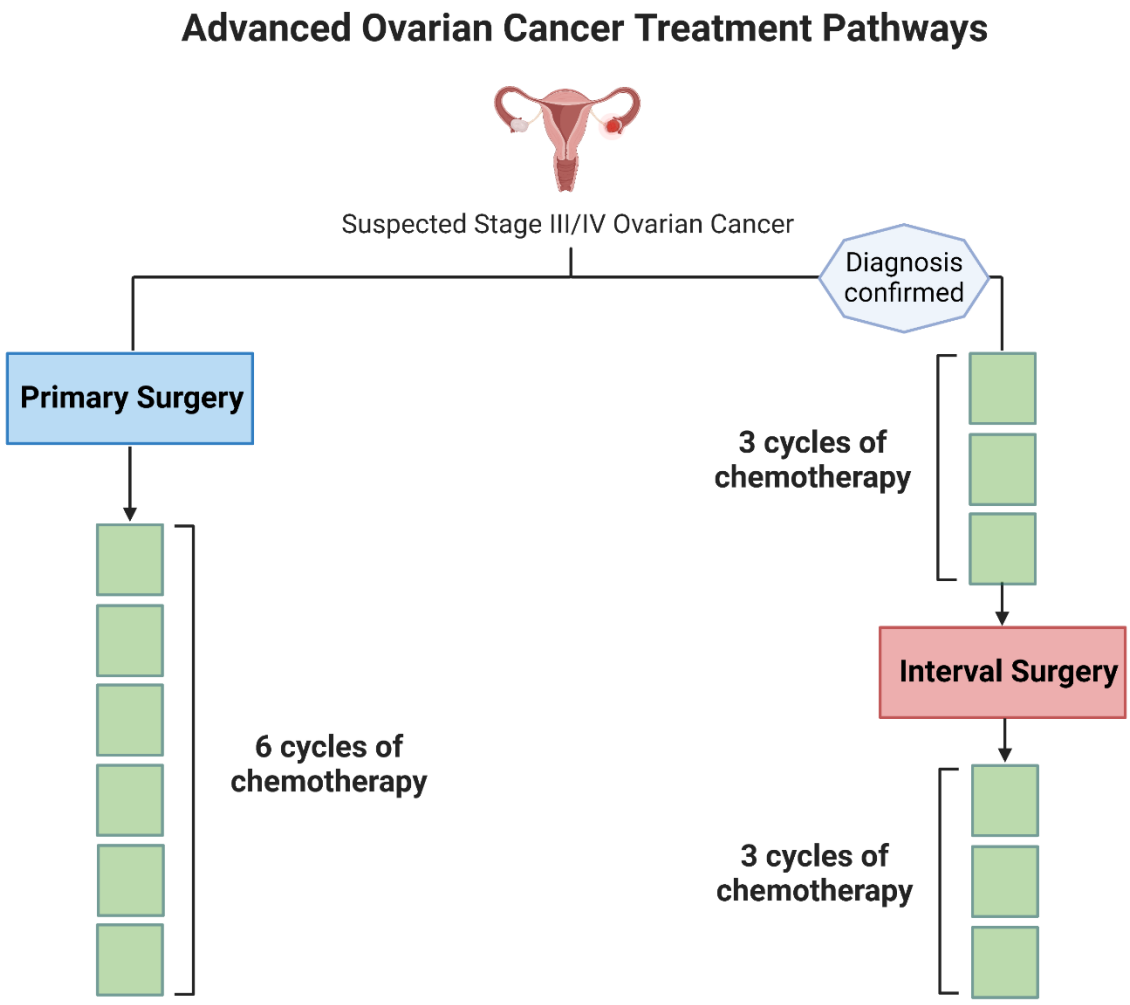


Figure 1.2: Advanced OC is managed with either upfront primary surgery or upfront primary chemotherapy followed by interval debulking surgery

Following suspected FIGO stage III/IV disease, and discussion at the multi-disciplinary team meeting, patients may undergo primary debulking surgery followed by six cycles of carboplatin-based chemotherapy. Alternatively, three cycles of neoadjuvant carboplatin-based chemotherapy are given following a histological diagnosis or cytological confirmation of disease. Interval debulking surgery is then performed before three further cycles of carboplatin-based chemotherapy.

OC has a predilection to metastasise in the first instance to the omentum, a large fatty fold of visceral peritoneum that covers the abdominal organs [65, 66]. The omentum is believed to create an optimal environment to actively support the rapid growth of tumour deposits [66-70]. Metastatic omental disease has an important role in OC progression; it is associated with a poor prognosis, including reduced chemotherapy response and worsened survival rates [66, 69, 71]. With the majority of stage III/IV disease found to have omental disease, an omentectomy is therefore undertaken in all cases of both early and advanced OC [47, 67, 72].

The chemotherapy response score (CRS) is assigned through pathological examination of the omental tissue removed during surgery following chemotherapy treatment. CRS measures the degree of cell death following chemotherapy, is used as a surrogate marker to determine the response to chemotherapy treatment and predicts PFS [71]. CRS is scored in 3 levels: CRS 3 indicates a complete response to chemotherapy; CRS 2 indicates a moderate response; and CRS 1 indicates a poor response.

1.1.6 Ovarian Cancer Prognosis and Patient Outcomes

Although 80% of patients respond initially to chemotherapy, just over half are alive and disease free after 12 months of completing treatment. The majority develop resistance to chemotherapy and suffer disease recurrence within two years [64, 73]. Indeed, only one third are alive and disease free by 18 months [64]. Risk factors for disease recurrence include advanced stage, residual disease following surgery, metastatic spread to lymph nodes and *TP53* gene mutations [74, 75].

Recurrent disease is managed either by further chemotherapy or additional surgery, termed secondary debulking surgery, in very few selected cases; however, survival rates remain poor

[47]. Patients who responded to their initial first-line chemotherapy regimens of Carboplatin (with or without Paclitaxel) have a greater chance of responding to additional courses of chemotherapy. Disease recurrence can only be treated with a regimen of combined Carboplatin and Paclitaxel if both agents have not already been used. Paclitaxel can however, be given as a monotherapy in cases where advanced disease has not responded to Carboplatin. When these first-line therapies cannot be used further, or when they fail to control the disease, second-line chemotherapy agents can be offered instead [59, 76].

The 10-year net survival for all disease stages is just 35%. The 5-year survival for stage I is high at 95% and is 70% for stage II disease, while rates in advanced OC are just 25% and 15% for stages III and IV, respectively [1]. The amount of residual disease following surgical resection is also indicative of prognosis, particularly sub-optimal cytoreduction (where disease at least 1cm in size remains) leading to inferior survival [64]. The Peritoneal Cancer Index (PCI) evaluates the extent of metastatic peritoneal disease in advanced OC and is also a significant factor for patient survival [77]. Additional predictors for poor survival outcomes include: tumours with high-grade serous histology, poor WHO (World Health Organisation) grade of tumour differentiation, the presence of ascites within the abdominal cavity, positive lymph nodes, *BRCA1* mutations, a reduced number of somatic mutations, patients age over 70 years at diagnosis, black ethnicity, smoking, obesity, fewer tumour-infiltrating lymphocytes and abnormal laboratory markers: higher CA-125 levels, raised platelet-lymphocyte ratio, and abnormal fasting glucose [74, 78-88].

1.2 Clinical Challenges in Ovarian Cancer

1.2.1 The Development of Resistance to Chemotherapy Treatment in Ovarian Cancer

Along with the majority of OC cases presenting with advanced disease, one of the main clinical challenges in managing these patients is the frequent and rapid development of resistance to chemotherapy drugs. Despite tumours initially responding to the standard cytotoxic agents, carboplatin and paclitaxel, the sensitivity to treatment reduces over time and two thirds of women relapse in just eighteen months from diagnosis [39, 89, 90]. The precise mechanisms by which cancer cells become tolerant to chemotherapy drugs remain unclear [91]. It is likely that both the tumour cells and the surrounding structures adapt during treatment, working together to overcome the effects of chemotherapy and create an environment that supports tumour growth and progression. The tumour cells that survive chemotherapy, in other words those that have developed treatment resistance, have avoided or survived the DNA damage caused by the chemotherapy [91]. The methods by which tumour cells establish this ability is likely to involve genomic alterations. In addition to the ubiquitous p53 mutation found in ovarian cancer, chemotherapy has been shown to induce whole genome mutations, ineffective repair following DNA damage, as well as epigenetic alterations and the subsequent deviations in cancer cell phenotype [91-95].

In addition, a collection of cells within solid malignancies are recognised as being tumorigenic and are termed “cancer stem cells” or “tumour initiating cells”. These cells are known to be enhanced within OC and are inherently resistant to chemotherapy drugs [91, 96]. While chemotherapy goes on to destroy the other chemo-sensitive tumour cells, these resistant cancer stem cells survive, proliferate and form a new, genetically beneficial, chemo-resistant tumour. This is described in Figure 1.3 [97]. Furthermore, the process called epithelial-to-mesenchymal transition (EMT), whereby cancer cells become capable of invading surrounding structures and

metastasising, plays a crucial role in the development of OC chemo-resistance [98, 99]. It is most likely that a combination of these mechanisms, mutations and tumour stem cells all contribute to the development of treatment failure and tumour progression.

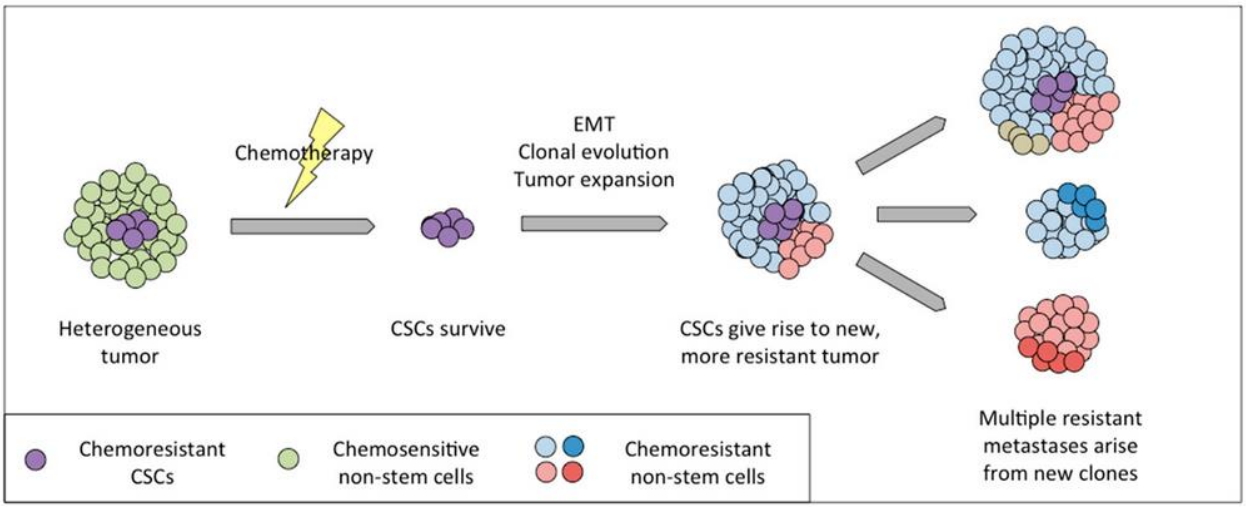


Figure 1.3: Cancer stem cells give rise to new chemo-resistant tumour
The chemo-resistant cancer stem cells (CSC) survive chemotherapy treatment, allowing tumour cells to expand and evolve into new, chemo-resistant clones, allowing OC to progress and metastasise despite ongoing treatment.

Figure adapted from Roberts et al., 2019 [97]

1.2.2 Tumour Heterogeneity in Ovarian Cancer

Another major obstacle in OC is the wide diversity of tumour cell types. Indeed, OC cells can differ in their mutational burden, gene expression profiles, phenotypes, motility, potential for angiogenesis, ability to proliferate, immunogenicity and capabilities to metastasise [100-102]. Distinct variations in cancer cells can occur between different patients with the same type of tumour, called inter-patient heterogeneity. It can also arise between different tumours within the same patient, for example between the primary tumour site and metastatic tumour deposits, known as inter-tumour heterogeneity. Finally, intra-tumour heterogeneity is seen when

differing cell types occur within the same tumour [103-105]. In fact, the complexity of intra-tumour heterogeneity is demonstrated when altered cells are evident within a single biopsy sample as well as between numerous biopsies obtained from different locations within the same tumour mass [106]. Figure 1.4 portrays the different types of heterogeneity that occurs within OC patients [105]. As tumours progress, the extent of intra-tumour heterogeneity also advances, with clusters of cells forming different subpopulations based on their genetic signatures and transcription profiles [106, 107].

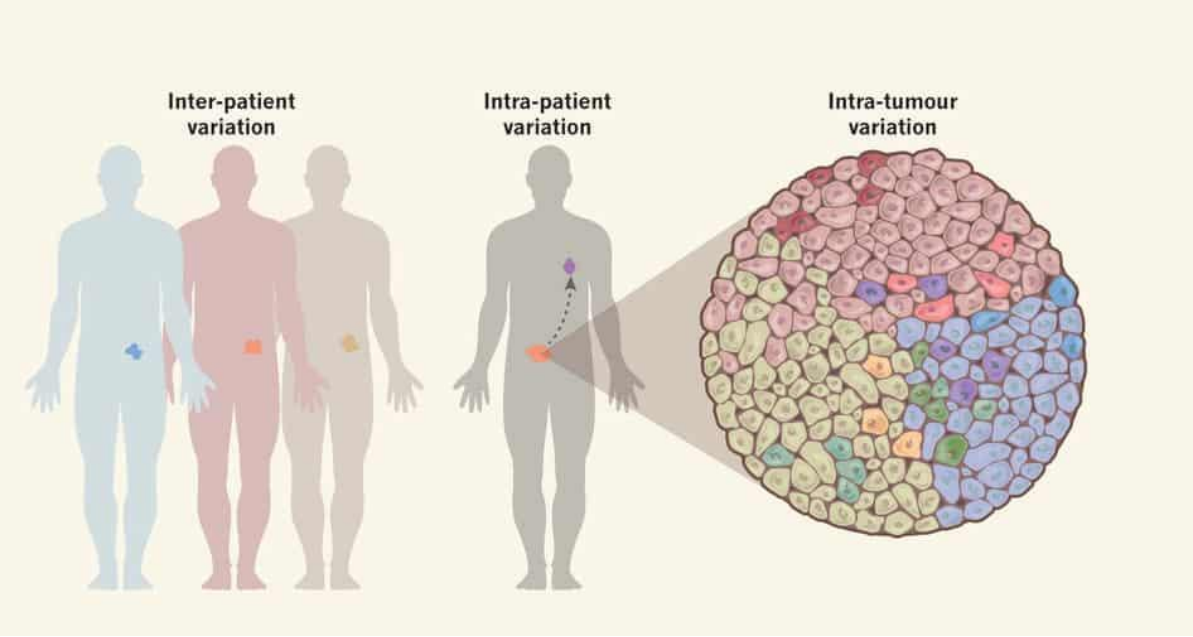


Figure 1.4: Types of tumour cell heterogeneity in cancer
Tumour cell heterogeneity is evident between patients (inter-patient heterogeneity), between different tumour sites in the same patient (intra-patient or inter-tumour heterogeneity) and within the same tumour mass (intra-tumour heterogeneity).

Figure adapted from Fox et al., 2014 [105]

The clinical implications of tumour heterogeneity are seen when these differing subpopulations vary in their response to treatments. Due to alterations in their molecular signatures, it is common for some tumour subpopulations to have an inferior or minimal response to treatment. This creates an opportunity where small populations of drug insensitive cells continue to expand and treatments then fail. Indeed, those patients with extensive intra-tumour heterogeneity typically have greater treatment resistance and worsened outcomes [107]. In addition, certain tumour biomarkers or specific tumour cell populations that can influence prognosis, or even determine the therapies offered to patients, may go undetected when heterogeneity occurs between tumour locations or biopsy sites within the same tumour mass [106].

1.3 The Tumour Microenvironment and the Immune Response

1.3.1 *Ovarian Cancer and the Tumour Microenvironment*

The tumour microenvironment (TME) describes the complex arrangement of cells and structures surrounding a tumour, particularly stromal cells (including fibroblasts and adipocytes), immune cells, blood vessels and the extracellular matrix, [108-110] as illustrated in Figure 1.5 [111]. Components of the TME communicate though the extracellular matrix, via cell-to-cell contact and following cytokine or chemokine secretion [112]. Cancer cells attempt to manipulate the TME to create a setting that supports tumour survival and growth, angiogenesis and metastatic spread. The TME and the immune cells therein can function to both encourage tumour progression as well as acting to suppress and prevent tumour invasion [108-110]. Indeed, the net function and the overall effects of the TME influences tumour advancement, control and regression [113].

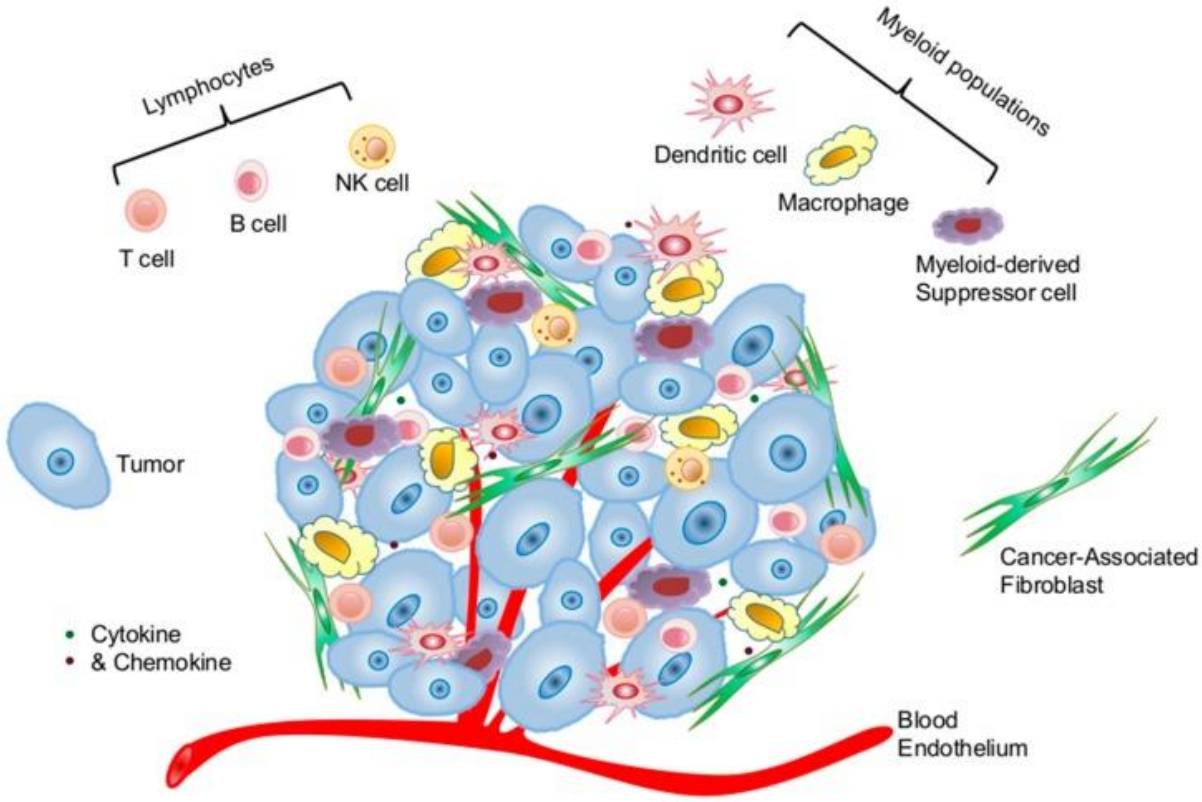


Figure 1.5: The structure and components of the tumour microenvironment in OC
The ovarian TME consists of tumour cells, endothelial cells, various different immune cells, fibroblasts, adipocytes, extracellular matrix and red blood cells within blood vessels.

Figure adapted from Cui et al., 2016 [111]

Detailed knowledge of the cellular composition within the TME can be acquired through RNA sequencing analysis at the single cell level [114]. By interrogating the transcriptional profiles and gene expression of individual cells, a detailed characterisation of tumour, immune and stromal cells within the TME can be established [114, 115]. The identification of different subpopulations of cells with unique genetic signatures allows cell heterogeneity to be examined within samples, across biopsy sites and also between patients. Table 1.2 highlights the key findings from the single-cell analysis studies performed in OC.

Table 1.2: Significant findings from single cell RNA sequencing studies of the TME in ovarian cancer

Study	Sample details	Clinical details	Key findings
Winterhoff et al. [116]	1 x tumour biopsy, depleted of infiltrating immune cells, 92 cells sequenced	Stage III HGSOvCa, pre-chemotherapy	Two cell populations identified: epithelial and stromal cells. Cancer stem cell and EMT genes expressed in stromal cells.
Xu et al. [117]	7 x tumour + 5 x non-malignant samples, 59,324 cells (33,000 tumour cells)	Stage I/II/III OC, pre-chemotherapy	Tumour samples: large epithelial population with 8 tumour subpopulations and EMT expressed, cancer associated fibroblasts, immune populations with large CD8 T cells and macrophage clusters. Normal sample: mainly fibroblasts.
Deng et al. [118]	10 x tumour samples + 1 normal ovary sample from 6 OC patients, 55802 cells	Stage I/II/III, 5 x Primary + 3 x metastatic HGSOvCa, 1 x normal ovary, 2 endometrioid OC. Pre-chemotherapy	10 populations of cells, large epithelial subset, immune cells and fibroblasts EMT features in malignant samples. ERBB2 and HOXB-AS3 genes in metastatic samples.
Olalekan et al. [119]	6 omental samples, 9885 cells	Stage III/IV, 5 serous, 1 mixed Mullerian tumour Pre-chemotherapy	9 major cell types: large epithelial population, immune cells and fibroblasts, cancer stem cells identified.
Shih et al. [120]	8 OC patients, 14 biopsies: 4 x omental + 9 x ovarian tumour + 1 benign ovary, 2900 cells	Stage I/III/IV, low- and high-grade serous OC + peritoneal tumour, 1 post-chemotherapy	16 cell populations including 4 epithelial, stromal, immune and fibroblasts clusters. Majority of cells epithelial in primary tumours, mainly immune in metastasis.
Hornburg et al. [121]	15 OC samples: 5 samples each of 3 phenotypes: Epcam+CD45- (tumour; 40539 cells), Epcam-CD45- (stromal); 35296 cells), Epcam-CD45+ (immune; 15049 cells)	OC, stage/histology not clear	Detailed T cell analysis within the 3 cell sorted groups. Large T cell, myeloid and fibroblasts populations. Differing T cell populations and fibroblasts between phenotype groups.
Izar et al. [122]	1.Ascitic fluid, 11 patients, 22 samples, 11,000 cells 2. 3 ascites, 2 primary tumours, xenograft models, 35,957 cells	HGSOvCa, 4 pre-chemotherapy, others exposed to chemotherapy.	7 major cell types including 18 subpopulations: immune cells were most common cell type (various subpopulations), 5 subpopulations of tumour cells, fibroblasts.
Zhang et al. [123]	11 patients 93,650 cells	Stage III/IV, HGSOvCa, paired Pre- and post-chemotherapy omentum/peritoneum	Stress associated state during chemotherapy. Two thirds of cells were immune cells (10 clusters), smaller tumour populations (12 clusters), 5 stromal clusters including cancer associated fibroblasts.

1.3.2 Immunosurveillance and Tumour Progression

The immune system can be separated into two different categories: the innate and adaptive immune systems [124]. The non-specific innate immune system generates an initial and rapid response to pathogens and tissue damage upon recognition of a limited number of targets [124, 125]. The innate immune response involves a number of different cells, including: macrophages, neutrophils, mast cells, dendritic cells and natural killer (NK) cells [125]. Meanwhile, the adaptive immune system is antigen-dependent, where a large number of specific antigens can be detected, generating immunological memory for an increased and more efficient response following subsequent exposure. Cells involved in the adaptive response include T cells and B cells [124, 125].

The recognition of tumour antigens and the interactions between immune and cancer cells in the TME have great importance in controlling tumour cell survival and progression [126, 127]. Following cancer cell detection, the ensuing anti-tumour immune response involves both the innate and adaptive immune systems, which act to eliminate the cancer by destroying malignant cells through a variety of different mechanisms. These include cytokine secretion to prevent tumour proliferation and angiogenesis, as well as inducing tumour cell apoptosis [127-129]. Any residual tumour cells are held in equilibrium, controlled by the immune system in a dormant state [130]. During this period, genetic and epigenetic changes can allow tumour cells to develop mechanisms to overcome this control exerted by the immune cells, enabling them to evade the anti-tumour immune response [127-129].

1.3.3 Immune Escape Mechanisms in the Ovarian Tumour Microenvironment

Ovarian tumours evolve a range of mechanisms to reduce immune recognition, including recruitment of regulatory T cells (Tregs) which produce inhibitory cytokines, such as interleukin (IL)-10 and transforming growth factor (TGF)-beta), and suppress T cell function [131-138]. Cytokines also disrupt dendritic cell function whilst tumours secrete indoleamine 2,3-dioxygenase (IDO), preventing T cell proliferation, and prostaglandin E2, which is involved in tumour growth and progression [110, 131, 135, 139-142]. Myeloid-derived suppressive cells (MDSC) and cancer-associated fibroblasts (CAF) also have immune suppressive properties and [113, 141, 143], as such, the combined actions of multiple immunosuppressive factors lead to disease progression, treatment failure and unfavourable prognostic implications [113, 131, 141, 143, 144].

1.3.4 The Clinical Importance of the Immune Response in Ovarian Cancer

The nature of the immune cell infiltrate within the ovarian TME has an important impact on prognosis [110, 145]. Increased numbers of tumour infiltrating lymphocytes (TILs) correlate positively with patient survival and CD4+ and/or CD8+ TILs are associated with favourable outcome [86, 87, 146-153]. However, OC is often defined as a 'cold' tumour which describes a suppressed immune environment where T cells are excluded, unreactive and unable to directly contact tumour cells, limiting T cell-mediated cytotoxicity, a profile that progresses as tumours advance and metastasise [110, 154-159].

The mutational burden in OC also impacts upon the immune composition within the TME. Tumours with a *BRCA* or *TP53* mutation have higher numbers of TILs, compared to those without mutations [160-162]. In addition, the TILs within these mutated tumours have greater expression of certain immune checkpoint receptors, such as the programme cell death protein,

PD-1. Therefore, OC cases with specific mutations have increased immunogenicity, which correlates with treatment response, patient outcomes and survival [160].

1.3.5 The Tumour-specific Immune Response following Chemotherapy Treatment

Exposure to chemotherapy has been shown to directly alter the composition of the TME [163]. Cytotoxic treatment advantageously modulates and enhances the immune response, seen with the expansion and activation of CD4+ T cells, CD8+ T cells, NK cells and B cells [104, 163-166]. The immunosuppressive nature of the TME is reversed; there is a reduction of inflammatory tumour-promoting cytokines, decreased number of Tregs and MHC class I molecules are upregulated, causing antigen presentation and triggering an adaptive immune attack [104, 165-168]. In addition, the cellular stress response and tumour cell apoptosis following chemotherapy leads to immunogenic cell death. The subsequent production of damage-associated molecular patterns, known as DAMPs, recruit antigen presenting cells and sensitise tumour cells to a targeted immune response [163, 169-171].

Transcriptomic evaluation with single cell sequencing has detected the chemotherapeutic alterations within the TME, including malignant and stromal populations [115, 123, 168, 172, 168]. Examination of tumour cells has identified an increased stress associated state following chemotherapy, with pro-inflammatory cytokines, paracrine signalling and the expression of cellular stress gene signatures [123]. In addition, an increase in the proportion of cancer stem cells has been observed [168]. By comparing the transformed tumour cell populations in treatment resistant samples to those susceptible to chemotherapy, there is differing cell adhesion molecules and cell surface signalling [168, 172]. There is also a reduction in the tumour-promoting cancer-associated fibroblasts and decreased stromal cell proliferation [163, 167, 168].

1.4 Natural Killer cells in Ovarian Cancer

1.4.1 Natural Killer cell Development and Maturation

Natural Killer (NK) cells are lymphocytes and comprise ~10-15% of circulating blood lymphocyte cells [173]. They develop within the bone marrow and are also present within extramedullary locations such as secondary lymphoid tissues [173-176]. NK cells are a critical part of the innate immune system with the ability to destroy both virally infected cells and tumour cells without prior sensitisation and in an antigen-independent manner [154, 173, 176-180].

NK cells are identified by the presence of CD56 and the absence of CD3 cell surface markers [179]. Furthermore, there are two differing sub-populations of NK cells based on the expression of CD16 and CD56. Firstly, a mature cytotoxic population that makes up around 90% of all NK cells and is characterised by low expression of CD56 and high expression of CD16 (termed $CD56^{dim}CD16^{bright}$). A smaller cytokine-producing subset has high levels of CD56 and low or negative CD16 expression (either $CD56^{bright}CD16^{dim}$ or $CD56^{bright}$ $CD16^{neg}$) [173, 180-182].

1.4.2 Identification of Target cells and Natural Killer Cell Activation

NK cells possess activating receptors, such as the killer activation receptors (known as KAR), one of which is the natural-killer group 2, member D receptor (NKG2D). Other key NK activating receptors include: NKG2C, DNAM-1 (DNAX accessory molecule-1) and natural cytotoxicity receptors such as NKp30 (NK cell p30-related protein) and NKp46 (NK cell p46-related protein) [175, 183]. When cells within the body suffer DNA damage or a cellular stress response occurs, certain ligands are expressed on the surface of the distressed cell. NK activation receptors can bind to these stress ligands, triggering NK cell stimulation and activation [182, 184-186]. In addition, major histocompatibility complex (MHC) class I-related

chain A (MICA) and B (MICB), produced by stressed tumour cells, can also directly activate NK cells when they are detected by the activating receptor NKG2D [187-188].

1.4.3 Natural Killer Inhibition and Recognition of "self"

NK cells also have inhibitory receptors, such as killer-cell immunoglobulin-like receptors (KIR), NKG2A, Ly49A (C-type lectin-like receptor subfamily A) and TIGIT (T-cell immunoglobulin and immunoreceptor tyrosine-based inhibitory motif), which act to prevent an NK response when stimulated [182, 183, 186]. These receptors, specifically KIRs, recognise classical MHC class I molecules, such as the class I human leucocyte antigens (HLA-A, HLA-B and HLA-C). These are present on normal healthy cells, thereby allowing NK cells to identify "self" from damaged, altered neoplastic and virally infected cells that lose their MHC class I molecules [173, 177, 182, 186]. Importantly, this "self" recognition of normal cells can override NK activation receptor-ligand interactions [175]. Tumours often down regulate HLA class I expression, thereby triggering NK cell activation and enhancing NK-mediated killing of tumour cells [154, 189-192], as well as expressing activatory stress ligands [141]. Figure 1.6 demonstrates the different NK cell reactions upon recognition of "self", "missing self" and "altered self" MHC class I molecules.

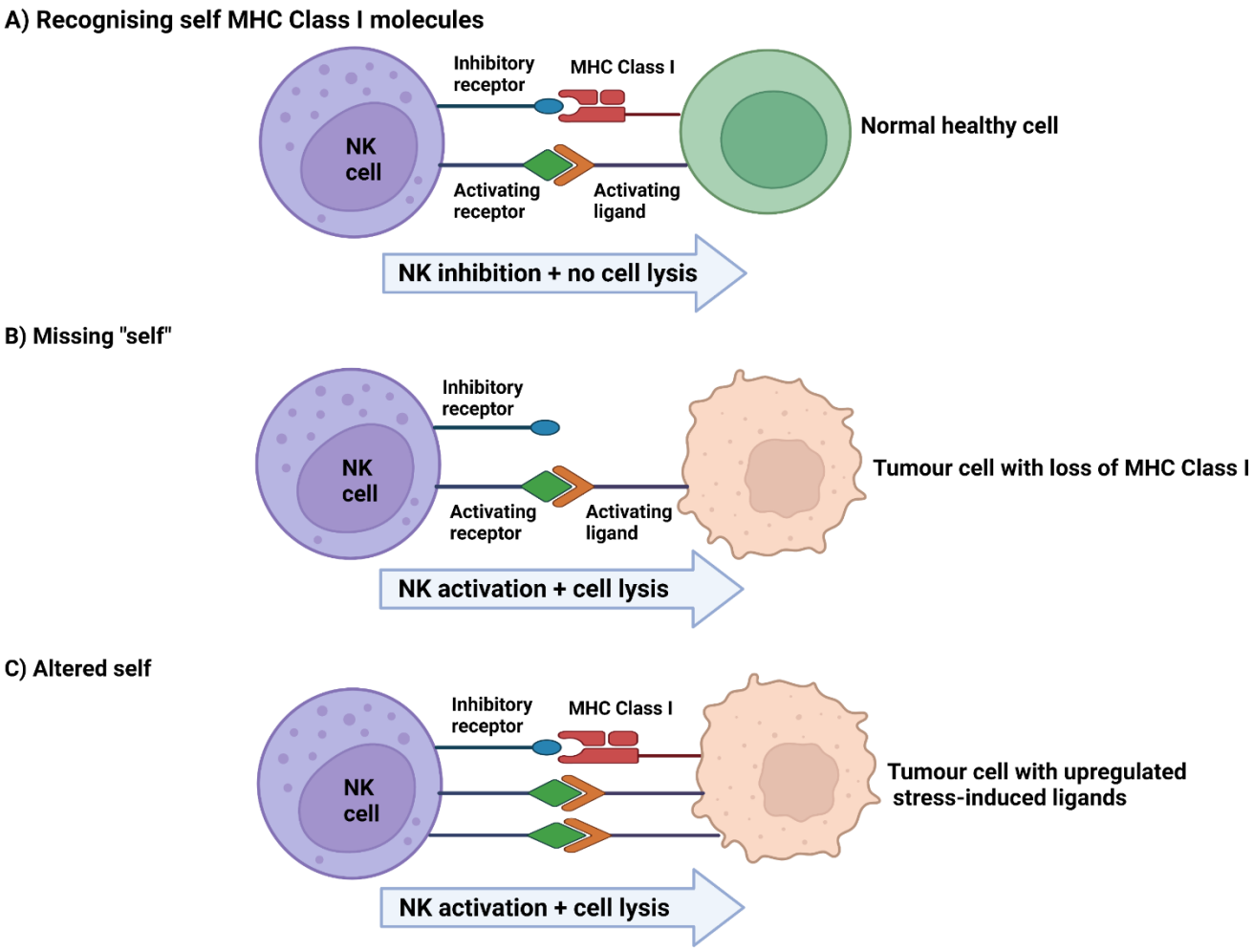


Figure 1.6: NK response following the detection of MHC class I molecules on normal healthy cells and tumour cells

NK cells have varying responses depending on the MHC class I molecules detected: A) "Self" MHC class I on normal healthy cells strongly inhibit NK cells, overruling any coinciding NK activation signalling, resulting in no NK cell-mediated attack; B) NK cells identify "missing self" when tumour cells downregulate MHC class I molecules, leading to a loss of NK inhibition and allowing NK cells to initiate tumour cell lysis; C) NK cells are activated and attack tumour cells when they upregulate stress-induced or "altered self" ligands, superseding any inhibitory signalling.

In contrast to the downregulation of classical HLA class I molecules, tumours sometimes upregulate the expression of HLA-E. Here, the HLA-E ligands bind to the NK inhibitory receptor, NKG2A, thus inactivating the NK cells and preventing NK cytolysis. This 'escape mechanism' is a further attempt by tumours to avoid an NK-mediated immune response. [193-196]. The variable expression and stimulation of the NK receptors leads to differing functional properties of NK cells, with the overall action determined by the balance of the activating and inhibiting receptors [182, 197, 198].

1.4.4 The Functional Response of Activated Natural Killer cells

NK cells are activated when signalling from activatory receptors overcomes stimulation from inhibitory receptors [173, 177, 186, 199, 200]. The less mature $CD56^{bright}$ NK cell population is less cytotoxic but has an immunoregulatory role with production of cytokines and chemokines such as interferon (IFN)-gamma, granulocyte-macrophage colony stimulating factor (GM-CSF), tumour necrosis factor (TNF)-alpha and IL-10. These recruit additional immune cells and enhance immune responses [154, 173, 175, 177-180]. NK cells release cytolytic granules containing perforin and granzymes or upregulate the "death receptor" ligands FasL (Fas ligand) and TRAIL [175, 201-206]. They are also involved in antibody-dependent cell-mediated cytotoxicity (ADCC) via recognition of antibody through surface Fc receptors (Figure 1.7) [175, 207-209].

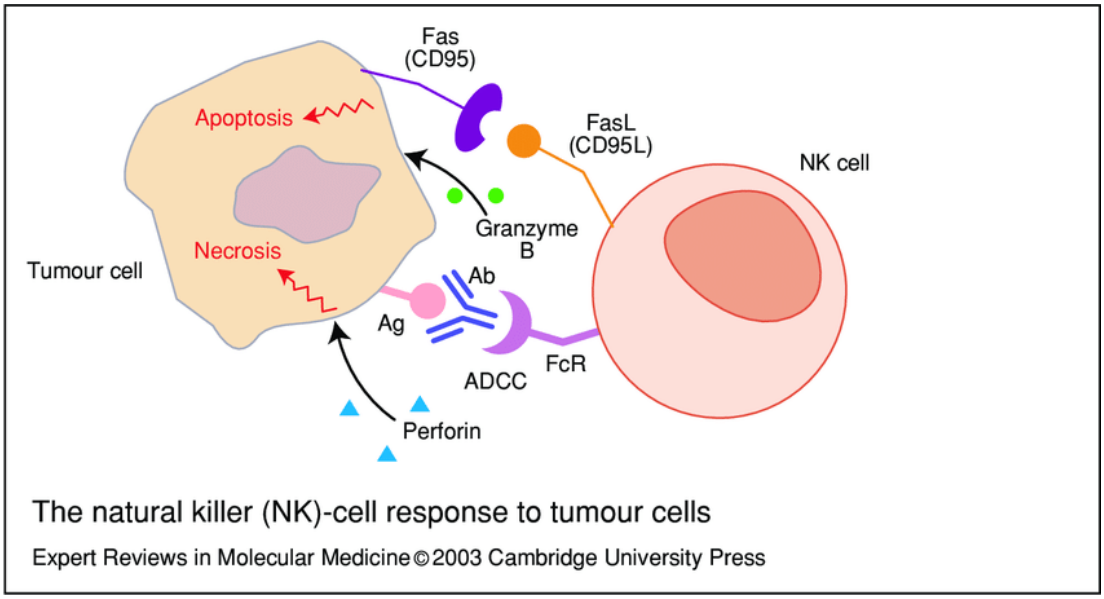


Figure 1.7: NK cell-initiated antibody-dependent cell-mediated cytotoxicity (ADCC)
NK cells use antibody-dependent cell-mediated cytotoxicity to kill tumour cells. The Fc receptor (FcR) on the NK cell binds to an antigen (Ag) on the tumour cell surface through the Fc portion of a tumour specific antibody (Ab). The Fas ligand (FasL or CD95L) on the NK cell also interacts with the tumour cell through Fas (CD95). These initiate the release of perforin and granzyme B to cause tumour cell death through apoptosis and necrosis.

Figure adapted from Mitra et al., 2003 [207]

1.4.5 The Role of Natural Killer cells in Advanced Ovarian Cancer

Studies have shown that tumour infiltrating NK cells have lower levels of proliferation, cytokine production and cytotoxicity than those circulating in peripheral blood [156, 210, 211]. Growth factors and cytokines, such as TGF-beta, produced by the tumour cells may contribute to this profile [131, 132, 150, 151, 154, 180, 199, 212-216]. An example of this is seen with frequent downregulation of NK activation receptors in this setting [150, 211, 212, 217].

Chronic expression of tumour ligands can lead to downregulation of NK activating receptors, as seen with tumour ligand CD155 and NK receptor DNAM-1 [150, 192, 200]. Tumour escape

can also occur through release of soluble forms of tumour ligands which saturate NK receptors. [177, 213]. Ovarian tumours can secrete soluble NKG2D ligands such as MICA, MICB and the ULBP ligands, leading to the downregulation of activating receptor NKG2D and subsequently reducing NK cytokine production and cytotoxicity [192, 187, 213, 218]. In contrast to activating membrane-bound NKG2D ligands, the soluble ligands prevent an immune response and have unfavourable prognostic outcomes [213, 218-220].

Another method utilised by ovarian tumours to create an immunosuppressive environment includes expression of migration inhibitory factor (MIF). This downregulates NKG2D and increases production of the checkpoint protein B7-H6, which reduces the NK activating receptor NKp30 [151, 221-229]. Ovarian tumours reduce NK cytokine secretion, while producing Mucin-16 (also known as the OC serum biomarker, CA-125) which protects tumours from an NK-mediated attack and encourages neoplastic proliferation [151, 223-229]. They can also cause the upregulation of the inhibitory NK immune checkpoint receptors such as CTLA-4, PD-1 and Tactile (CD96), which prevent NK activation towards tumour cells [150, 200, 225, 226].

NK cells have been shown to have prognostic implications for OC patients. Improved clinical outcomes and increased survival are associated with a greater total number of NK cells, increased amounts of peripheral blood NK cells, higher expression of NK activation receptors and increased NK penetration into ovarian tumour tissues [230-232]. Indeed, high levels of tumour-infiltrating NK cells are associated with increased OS, while reduced peripheral blood NK cell counts and decreased peripheral blood NK cell activity, measured with cytokine production, are related with poor OS [232]. In comparison, the presence of NK cells in

malignant peritoneal and pleural effusions have been shown to correlate with reduced OS [230].

1.5 Immunotherapy and Targeted Cancer Drugs

1.5.1 Currently Approved Agents in Ovarian Cancer

While immunotherapy drugs have been successful in advancing the management of other malignancies, results in OC have been disappointing [147]. This may be partly related to recruitment of patients with advanced disease into clinical trials [147, 157, 158, 233, 234] but tumour heterogeneity, reduced tumour HLA expression, a lack of targetable antigens, an immunosuppressive tumour environment and immune evasion mechanisms are all likely to contribute [109, 154]. HGSOvCa has a low to intermediate tumour mutation burden which limits a patient's ability to mount an immune response [180, 235-237]. Chemotherapy has been shown to improve response rates to immunotherapy treatment, making immunotherapy drugs an attractive therapeutic option alongside and following chemotherapy regimens [166, 238, 239].

Two classes of targeted drugs are approved by NICE in the UK and recommended for the treatment of advanced OC [47, 240-246]. Anti-angiogenic drugs, such as Bevacizumab, are monoclonal antibodies that target vascular endothelial growth factor (VEGF), shown in Figure 1.8, whilst PARP (poly ADP ribose polymerase) inhibitors, such as Olaparib and Niraparib are also approved [240, 241, 243-246]. In the presence of BRCA mutations, resulting in the loss of DNA repair via the homologous recombination repair pathway, tumour cells become reliant on PARP for DNA repair. By inhibiting PARP and therefore preventing DNA repair, an increase in DNA damage can lead to tumour cell death and improved response to chemotherapy (Figure 1.9) [45, 247, 248].

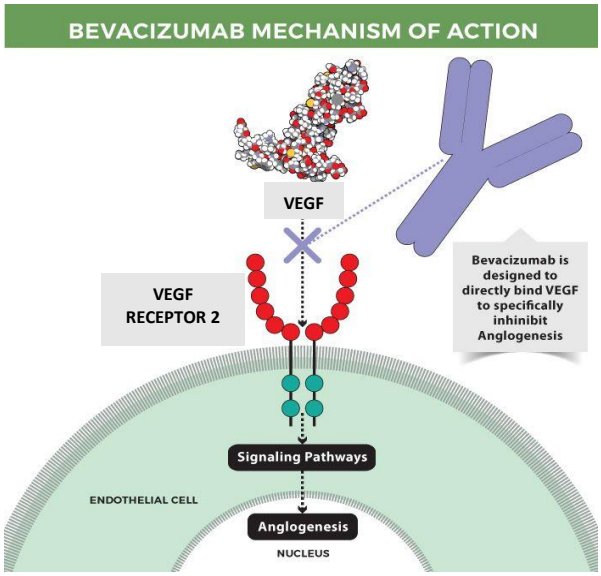


Figure 1.8: Mechanism of action of anti-angiogenic agents

The anti-angiogenic agent, Bevacizumab, binds to VEGF and inhibits the signalling required for angiogenesis, preventing tumour growth.

Figure adapted from HealioLearn ImmunoOncology [249]

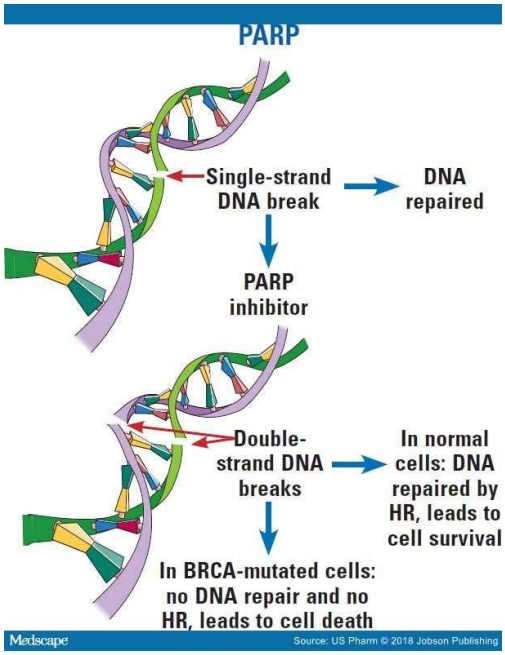


Figure 1.9: Mechanism of action of PARP inhibitors

The homologous recombination (HR) repair pathway and PARP can repair DNA damage. When PARP is inhibited, cells rely on HR for DNA repair. In BRCA mutations, HR is prevented and DNA cannot be repaired if PARP is also inhibited, leading to cell death.

Figure adapted from Iqbal et al., 2018 [250]

Table 1.3 shows the clinal application of these two approved targeted agents and patient outcomes following use.

Table 1.3: Clinical application and outcomes of the NICE approved targeted cancer drugs in OC

Type of Immunotherapy	Agent	Clinical application	Outcomes
Anti-angiogenic / anti-VEGF	Bevacizumab [47, 240-242, 251-254]	- Alongside first-line chemotherapy in stage IV - With NACT in stage III - In stage III if suboptimal cytoreduction at surgery - Maintenance therapy for up to 15 months after chemotherapy completed	- Increased PFS - OS not improved
PARP inhibitor	Olaparib, [243, 245]	With BRCA1/2 mutation: - Maintenance therapy in stage III/IV -Following good response to first-line platinum chemotherapy (incl. in relapse of platinum-sensitive disease)	- Prolonged PFS in relapsed platinum-sensitive OC - Delayed time to chemo-resistance when given as maintenance
PARP inhibitor	Niraparib [244, 246, 247, 255]	With BRCA1/2 mutation: - Maintenance in stage III/IV following good chemotherapy response Without BRCA1/2 mutation: - Recurrence of platinum-sensitive disease	- Prolonged PFS (improvements in PFS are less in those without BRCA mutation)
Combined Anti-angiogenic + PARP inhibitor	Bevacizumab + Olaparib, [242]	-Combined maintenance therapy in stage III/IV if previously responded to combined chemotherapy and Bevacizumab, and if tumours have defective homologous recombination repair systems/BRCA mutation	-Delayed disease progression

1.5.2 Immunotherapy Clinical Trials in Ovarian Cancer

Early clinical studies exploring the efficacy of immunotherapeutic agents in OC have been discouraging. Tumours upregulate inhibitory receptors, such as CTLA-4 and PDL-1, that limit immune activation [150, 200, 255, 256]. Blockade of these checkpoints can elicit anti-tumour immunity and trials of checkpoint inhibiting drugs targeting PD-1 and CTLA-4 have shown anti-tumour activity, disease stability and delayed progression in some cases [256-258].

However, response rates have typically been low at just 10-15%, with disease controlled in less than half of participants [257, 258]. Similarly, trials of checkpoint inhibitors in combination with anti-angiogenic treatments or PARP inhibitors have shown poor response rates and even disease progression during treatment [259-262].

Other immunotherapies given alongside chemotherapy have yielded varying results, but unfortunately no improvements in PFS or OS in advanced platinum resistant disease [263]. Anti-CA-125 monoclonal antibody trials have found conflicting outcomes; some with no survival benefits when given as a maintenance therapy, while some positive outcomes are evident when given alongside adjuvant chemotherapy [264, 265]. Although early vaccination studies initially showed promising findings, recent phase III vaccine studies have unfortunately failed to do so [266, 267]. Adoptive cell therapy, specifically using cytokine-induced killer cells, has delayed progression in advanced disease but is yet to show increases in OS [268]. Regrettably, trials of other adoptive cell therapies have not demonstrated measurable or improved responses [269]. Early clinical studies and in vivo studies of engineered T cells (T cell receptor and chimeric antigen receptor (CAR)-T cells), targeting mesothelin, folate receptor, Her2 and CA-125, have given promising results by eradicating or reducing tumour burden, albeit with small numbers of participants [231, 266, 270-272].

Current ongoing clinical trials are exploring additional immunotherapy treatments, typically in platinum resistant and recurrent OC. These trials include phase III and IV studies of: immune checkpoint inhibitor drugs targeting the PD-1/PD-L1 pathway [273-279], PARP inhibitor drugs [276, 280-282], antiangiogenic drugs [283], monoclonal antibodies and cancer vaccines targeting P53, CA-125, folate receptor, TGF-beta and cancer testis antigen [266, 267, 284].

1.5.3 Natural Killer cell Therapy in Ovarian Cancer

Natural Killer cells have the ability to use a number of different methods to target ovarian tumour cells and overcome tumour escape mechanisms [109]. As such, there is great potential for successful NK immunotherapies in OC. Unfortunately, the efficacy of such treatments to date have mainly been impeded due to high levels of toxicity and adverse effects occurring in early phase clinical trials [154, 200]. A number of different NK therapies have so far been explored in OC, shown in Table 1.4.

Table 1.4: NK cell therapies and outcomes from clinical use

NK cell therapy	Clinical findings
NK cell activation with IL-2 [285, 286]	Phase II trial: limited persistence of NK cells and no NK expansion. Further trials ongoing.
NK cell activation with IL-2 + 13-cis-retinoic [287]	Increased NK cell numbers, decreased VEGF, improved PFS and OS in platinum sensitive advanced disease.
NK cell activation with IL-15 [190, 288]	Pre-clinical: increases NK cytotoxicity, activates NK cells, increased cytokine activity.
Adoptive transfer of cytokine-induced killer (CIK) cells [289]	A phase II trial : improved PFS survival.
Intraperitoneal NK infusion [290-292]	Pre-clinical studies in mouse xenograft models: increased circulating NK levels, kills intraperitoneal tumours. Early clinical safety trials in recurrent OC are ongoing.
Anti-PD-1 treatment [158, 265, 266, 293]	Pre-clinical: improved NK cytokine release and retained cytotoxicity. Phase I trial: stable disease in 44%, all patients have partial response, only 4% tumours shrink by over 30%. Phase II with Bevacizumab: improved response rate in platinum sensitivity:
Anti-TIGIT treatment [294]	Pre-clinical: prevents NK exhaustion.
Anti- NKG2A treatment [295]	Pre-clinical: prevents NK cell inhibition increases NK cytotoxicity.
Bispecific monoclonal antibody targeting both EPCAM and CD3 [296]	Phase I trial: T and NK cell activation in ascitic fluid of patients.
Anti-folate receptor antibody [297]	Phase II: improved overall response rate and prolonged PFS. Phase III trial ongoing.
Engineered CAR-NK cells directed towards NKG2D [298, 299]	Pre-clinical xenograft modes: prevents tumour growth and prolongs survival, less cytotoxic than CAR-T cells. Phase I trial using the NKG2D ligand with a CAR-NK is ongoing.
Engineered CAR-NK towards mesothelin [271, 300]	Phase I trial: no adverse effects, clearance of pleural effusion. Further trials are ongoing.
Engineered CAR-NK towards CD24 [301]	Pre-clinical: cytotoxicity towards OC cells in vitro.

It is likely that a combination of NK therapies will be required to improve patient outcomes. Approaches that can block multiple NK inhibition pathways or simultaneously prevent NK dysfunction while also augmenting NK activation may be required [154, 200]. As such, while NK cells remain a critical component of the OC immune response and have great potential to

help improve disease outcomes, further understanding of tumour-immune heterogeneity, NK function and tumour evasion is needed to better target therapies.

1.6 PhD Aims and Objectives

Ovarian cancer is the sixth-leading cause of death from cancer amongst women, and with the majority relapsing and developing treatment failure within two years, there is an urgent need to identify novel therapeutic approaches for these women [1, 64, 73]. There is a lack of detailed understanding surrounding ovarian tumour cell heterogeneity and the specific mechanisms associated with resistance to chemotherapy treatment. The complex ovarian TME is also poorly understood, with limited knowledge of how these tumours influence and evade the immune response. The nature and role of the tumour infiltrating lymphocytes, specifically the NK cells, in OC development and progression also remains unclear and warrants further investigation.

The research described in this thesis was compelled by the vital necessity for greater understanding of this disease, specifically the need to identify new biomarkers that can be used as targets for novel immunotherapy protocols. Throughout this thesis, I have aimed to establish the following:

1. A detailed characterisation and transcriptional analysis of both tumour and immune cell heterogeneity in ovarian tumours, prior to and after chemotherapy, exploring molecular mechanisms associated with treatment resistance and immune recognition within the tumour microenvironment.

2. An interrogation of the OC immune landscape using an established cohort of OC patient samples, focusing on the phenotype of both peripheral and tumour infiltrating NK cell populations and their relationship to disease outcomes.
3. A comprehensive exploration of the typical behaviour and function of NK cells, concentrating on the alterations with chemotherapy and methods of immune evasion that can guide the introduction of stratified immunotherapy protocols in women with OC.

Chapter 2:

Materials and Methods

2.1 Part 1: Analysis of the study cohort

2.1.1 The cohort population

The cohort population consisted of 80 patients with OC who were managed in the Pan Birmingham Gynaecological Cancer Centre between 2017 and 2022. Of these, 40 patients underwent primary surgery followed by 6 cycles of platinum-based adjuvant chemotherapy. The primary surgery was either cytoreductive primary debulking surgery (PDS) for advanced OC (stage III/IV; n=28, 70.0%) or standard surgery for early OC (stage I/II; n=12, 30.0%). The other 40 OC patients in the cohort received platinum-based neoadjuvant chemotherapy, followed by interval debulking surgery (IDS) and additional adjuvant chemotherapy for advanced OC.

A further 20 patients who did not have OC (or any other malignancy) were recruited as controls. This included 10 patients who had surgery for a benign ovarian mass, with final histology showing either an ovarian fibroma or cystadenoma. The remaining 10 patients had histologically normal ovaries and fallopian tubes, with surgery performed for benign gynaecological conditions (n=8, 80.0%) or risk reduction surgery (n=2, 20.0%) due to an increased risk of developing OC.

2.1.1.1 Identification and recruitment to the cohort population

The patients within the study cohort were identified during the Gynaecological Oncology multi-disciplinary team (MDT) meetings held weekly at the Pan Birmingham Gynaecological Cancer Centre (PBGCC). Patients were recruited prior to surgical intervention during their routine pre-operative management.

2.1.1.2 Ethical approval

All participants were recruited and consented as part of the ethically approved Health Research Authority (HRA) trial, titled "Investigation into new biomarkers for diagnosing and treating ovarian cancer", with IRAS project identification 225991 and protocol number RD 17-225. Local ethical approval was acquired from the Sandwell and West Birmingham NHS Trust, with Research & Development identification 18CAN26.

2.1.1 Clinicopathological characteristics of the cohort population

The baseline clinicopathological characteristics of the cohort population that were assessed in the analysis include: age, ethnicity, disease stage, peritoneal cancer index (PCI), histopathological diagnosis, presence of metastatic omental disease, serum CA-125 level and the serum absolute lymphocyte count. This data was obtained from clinical records and the PBGCC's electronic database.

2.1.2.1 Definition of the clinicopathological characteristics

- *Age:* the age in years recorded on the day of surgical intervention.
- *Ethnicity:* the patient's identity defined by cultural characteristics.
- *Disease stage:* patients with OC were staged based on surgical findings and following histopathological inspection of resected specimens according to the 2014 FIGO staging criteria for ovarian cancer.
- *Peritoneal Cancer Index (PCI):* the staging score assigned to OC patients at the time of surgery based on the presence and size of peritoneal tumours within the abdominal cavity [302].
- *Histopathological diagnosis:* the histological type of tumour or benign lesion, as determined by the Histopathology consultant.

- *BRCA status:* the presence of germline or somatic mutations in the BRCA1 or BRCA2 proteins.
- *Metastatic omental disease*: the presence of metastatic tumour within the omental tissue following histopathological inspection of surgical specimens.
- *Serum CA-125 level:* the CA-125 value (units per millilitre or U/ml) from peripheral blood samples obtained at the time of surgical intervention.
- *Serum absolute lymphocyte count*: the value **(**1x10*9/L) from peripheral blood samples obtained at the time of surgical intervention.

2.1.2 Management of the cohort population

Details of the treatments received by the study population and the management outcomes that were collated in the analysis include: the type of surgery undertaken, the surgical procedures performed, the surgical cytoreduction score, the use of neoadjuvant chemotherapy and chemotherapy response score. The operation records, clinical notes and histopathology reports were used to acquire this information.

2.1.2.1 Description of the treatment and management outcomes

- *Type of OC surgical intervention*: surgery was defined as primary surgery if no previous chemotherapy treatments had been given. This included standard primary surgery in early OC (stage I/II disease) or cytoreductive primary debulking surgery (PDS) in advanced OC (stage III/IV). Surgery was classed as interval debulking surgery (IDS) if patients had received neoadjuvant chemotherapy for advanced OC prior to their surgical resection.
- *Surgical procedure:* the operation records were utilised to determine the surgical procedures undertaken. These included: tissue biopsies only, total abdominal

hysterectomy plus bilateral salpingo-oopherectomy (TAH + BSO), omentectomy and any additional surgical procedures (including bowel resection and resection of upper abdominal organs). Standard primary surgery (for early OC) included TAH + BSO and omental biopsy. Cytoreductive surgery for advanced OC (PDS and IDS) consisted of TAH + BSO, omentectomy and any of the additional surgical procedures.

- *Cytoreduction score:* following thorough inspection of the abdominal cavity by the operating surgeons, complete cytoreduction (R0) was assigned when all macroscopic disease had been removed surgically. Optimal cytoreduction (R1) was classed as remaining visible disease up to 10mm in size, while suboptimal (R2) described remaining visible disease greater than 10mm in size.
- *Chemotherapy treatment:* for the OC patients who received neoadjuvant chemotherapy, details of the type of chemotherapy and number of cycles received were obtained from the hospital records.
- Chemotherapy response score (CRS): following neoadjuvant chemotherapy, the cytotoxic effects on tumour cells were graded pathologically and scored according to the response to chemotherapy: complete response (CRS 3), moderate response (CRS 2) or poor response (CRS 1). The CRS grade was obtained upon review of histopathology records.

2.1.3 Study cohort clinical outcomes

Details on patient outcomes were acquired from the PBGCC's electronic records and included: the development of disease recurrence, the time for disease recurrence to occur, survival status, and time to disease-specific death, if applicable. All patients were followed up until the study end date of 10.1.2023.

2.1.3.1 Disease recurrence and progression free survival

The time to disease recurrence was calculated from the treatment completion date (the date of completing adjuvant chemotherapy) to the date that a recurrence was confirmed, either pathologically or radiologically. This time period was used to give the progression free survival (PFS). In cases where there was no evidence of disease recurrence, the PFS was determined using the date they were last seen and remained free of disease.

2.1.3.2 Patient death and overall survival

The survival status for all patients in the study cohort were reviewed on the study end date of 10.1.2023. The time to disease-specific death and overall survival were calculated from the date of diagnosis to the recorded date of death. When patients remained alive, their overall survival time was established from diagnosis date to the end date of the study follow-up period.

2.1.4 Statistical analysis

Statistical analysis was performed using Graphpad Prism software, version 9.2.0. The Mann-Whitney U and Kruskal Wallis tests were used to analyse continuous and unpaired variables, while the Chi-squared test examined categorical variables. Analysis of Variance (ANOVA) was used to compare the means between the different patient groups. Survival rates (progression free survival and overall survival) were estimated using the Kaplan Meier method, with the Mantel-cox test used to compare survival distributions. Statistical significance was regarded with p values of less than 0.05.

2.1.5 Study cohort sample collection

All participants in the study cohort provided a peripheral blood sample and where possible, tissue biopsy samples were also obtained.

2.1.6.1 Peripheral blood collection

Peripheral blood samples were taken from all patients immediately prior to anaesthetic induction for their surgical debulking procedure. The blood samples were collected in BD Vacutainer heparin tubes, with approximately 10ml of blood obtained from each patient. Samples were anonymised, stored at room temperature and transferred to the University of Birmingham laboratories for processing.

2.1.6.2 Tissue biopsy collection

Biopsy samples were obtained from ovarian and omental tissues immediately following their surgical removal while in the operating theatre. The specific location and size of all biopsies were approved by both the operating consultant Gynaecological Oncology surgeon as well as a Histopathology consultant. This guaranteed that optimal tumour tissue was collected for research use while ensuring that clinical staging was not affected. Tissue samples were placed immediately in basic culture media, anonymised, stored at 4℃ and transferred to the University of Birmingham.

2.2 Part 2: Laboratory techniques

2.2.1 Tissue culture

2.2.1.1 Basic culture medium

The basic medium used for tissue culture in the experiments described was sterile RPMI 1640 media (Fisher Scientific Ltd; catalogue number 15450564), with additional 2mM L-glutamine at pH 7.0 (Gibco, ThermoFisher Scientific; catalogue number 25030081). The media was supplemented with 10% sterile heat-inactivated foetal bovine serum (FBS; ThermoFisher Scientific; catalogue number 11550356) and 1% sterile antibiotics (penicillin 10,000 units/ml and streptomycin 10mg/ml; Sigma Aldrich; catalogue number P4333). The basic media was stored at 4℃ and warmed to 37℃ prior to use.

2.2.1.2 The K-562 cell line

The K-562 cell line was sourced from ATCC [303]. It is an immortalised cell line, which originated from a patient with chronic myelogenous leukaemia and is known to lack HLA expression [304]. It therefore directly stimulates NK cells and generates a cytotoxic NK cell response.

The K-562 cells are non-adherent and were cultured in T25 Corning tissue culture flasks, using basic tissue culture medium, and were incubated at 37℃ with 5% CO2. The medium was renewed every three days: the cell solution was transferred to a sterile 50ml universal tube and was centrifuged at 1200rpm for 5 minutes at room temperature. The supernatant was discarded and the cell pellet resuspended in 10ml of fresh basic medium before being transferred back to a T25 culture flask. The cells were passaged every five to seven days, when at a density of 0.7 - 0.8x10^6 cells per ml. They were re-plated at a concentration of 0.4x10^6 cells in every ml of basic media. The cells were cryopreserved by centrifuging the

cell solution at 1200rpm for 5 minutes at room temperature, the supernatant removed and the pellet resuspended in K-562 freezing medium. This consisted of 90% FBS (ThermoFisher Scientific; catalogue number 11550356) and 10% DMSO (Dimethyl Sulfoxide, ThermoFisher Scientific; catalogue number J66650-AK), with 1ml added to $5x10^6$ K-562 cells, which was then transferred to a cryovial. These were cooled slowly within Nalgene Mr Frosty freezing containers and placed in -80 freezers.

2.2.2 Preparation of patient samples

2.2.2.1 Processing of patient blood samples

Peripheral blood samples (approximately 10ml per sample) were collected in BD Vacutainer heparin tubes (ThermoFisher Scientific; catalogue number 19267676) and stored at room temperature for up to three hours. The whole blood from each sample was added to 10ml of basic media and layered on top of 20ml of sterile Lympholyte-H (Tebu-Bio; catalogue number CL5015) solution in a sterile 50ml universal tube. The tube was centrifuged at room temperature for 25 minutes at 1800rpm, set to maximum acceleration and minimal deceleration. This separated the whole blood sample based on density gradient, creating a layer of lymphocyte and monocyte cells, known as peripheral blood mononuclear cells (PBMC). The PBMC layer was removed and added to basic media, giving a total volume of 40ml. The remaining cells from the whole blood (platelets, erythrocytes, neutrophils and any non-viable cells) were discarded. The collected PBMC's were centrifuged for 10minutes at room temperature at 1600rpm before the supernatant was removed and 10ml of basic media added. Samples were either incubated at 37°C and used within six hours or were cryopreserved for future analysis.

2.2.2.2 Processing of patient tissue samples

Tissue biopsies were preserved in basic media at 4℃ following collection at the time of surgical resection. Following transfer to the laboratories, each tissue sample was sectioned into pieces of 2mm diameter and transferred into a sterile 6-well culture plate. The samples were covered with 2ml of basic media and incubated overnight at 37℃ with 5% CO2. The following day, the diced tissue and media from the 6-well plate were sieved through a 40 µM cell strainer. This filtered solution was then diluted with 20ml of basic media and centrifuged at room temperature for 5 minutes at 1500rpm. The supernatant was removed and the pellet resuspended in 2ml of sterile red blood cell lysis buffer (Cambridge, Bioscience; catalogue number RBCL-1). After a 10-minute incubation period at room temperature, 8ml of basic media was added and the sample centrifuged at 1500rpm for 5 minutes. Following removal of the supernatant, red blood cell lysis buffer was added for a second time if the tissue pellet seemed heavily bloodstained on visual inspection. Once free from red blood cells, the resulting cell pellet was resuspended in 10ml of basic media. If further analysis was not performed immediately, samples were cryopreserved for future use.

2.2.2.3 Cryopreservation of patient samples

Patient samples, including the extracted PBMC, filtered non-enzymatic tissue samples and the enzymatic tissue samples, were cryopreserved if not used immediately after processing. Samples were centrifuged to give a pellet before being resuspended in 1ml of freezing medium, giving a final density of $1x10^6$ per ml. The freezing medium consisted of 50% basic media, 40% FBS (ThermoFisher Scientific; catalogue number 11550356) and 10% DMSO (ThermoFisher Scientific; catalogue number J66650-AK). The samples were then transferred to cryovials and stored within Nalgene Mr Frosty freezing containers in vapor phase nitrogen

freezers. All samples were stored at the University of Birmingham, in line with our ethical agreement and in compliance with the 2004 Human Tissue Act.

2.2.2.4 Thawing of patient samples

The cryopreserved patient samples were retrieved from storage in liquid nitrogen immediately prior to further use in the laboratory. The cryovials were quickly heated in a water bath until samples had completely thawed. The samples were then transferred to sterile universal tubes and warmed basic media slowly added.

2.2.2.5 Flash freezing patient tissue samples

The cancerous biopsies were visually inspected to identify segments containing solid tumour deposits. These samples, along with the normal and benign biopsies, were detached from excess vascular or fatty tissues and were sectioned into 5mm size pieces. These were placed individually into cryovials, which were immersed immediately into liquid nitrogen for at least 10 minutes for rapid cooling. After this snap freezing, the cryovials were transferred into vapor phase nitrogen freezers for storage.

2.2.3 NK cell phenotype analysis

2.2.3.1 Flow cytometry of patient samples

Flow cytometric analysis was used to assess the NK cell phenotype in the patient PBMC samples and the filtered tissue samples. Following peripheral blood processing and non-enzymatic tissue processing (Methods sections 2.2.2.1 and 2.2.2.2, respectively), two 5ml FACS tubes were prepared for every blood samples to be analysed, and the same prepared for each tissue sample. The single cell solutions from both the PBMC and filtered tissue samples were counted using a haemocytometer and each FACS tube had $1x10^6$ of the required cells

added. The FACS tubes were centrifuged at 1500rpm for 10 minutes, the supernatant removed and the remaining pellet resuspended in 75µl of sterile PBS (ThermoFisher Scientific; catalogue number J61196-AP). Antibodies were prepared as described in Tables 2.1 and 2.2 for two separate NK cell antibody panels and were distributed as shown in Figure 2.1. The samples were incubated on ice for 30 minutes in the dark before 500µl of sterile PBS was added. The tubes were centrifuged at 1500rpm for 5 minutes, the supernatant discarded and the pellet resuspended in 150µl of PBS. Propidium iodide (PI; Miltenyi Biotec; catalogue number 130-093-233) was added to each sample (1µl) and samples processed on the Gallios flow cytometer (Beckman Coulter Life Sciences). Kaluza, Flow Cytometry Analysis Software (Beckman Coulter, analysis version 2.1), detected the proportion of NK cells within samples, the types of NK cells and expression of activating and inhibiting NK cell receptors.

Table 2.1: NK cell activating receptor antibody panel

Antibody	Conjugate	Antibody details (manufacturer; catalogue number)	Antibody volume per sample (µl)
CD3	FITC	Biolegend; 344804	2.5
CD16	PE	Biolegend; 302008	5
CD14	ECD	Beckman Coulter; B92391	3
CD19	ECD	Beckman Coulter; 6604551	3
PI	ECD	Miltenyi Biotec; 130093233	1
NKp46	PerCP-Cy5.5	Biolegend; 137610	5
CD56	PE/Cy7	Biolegend; 318318	5
NKG2C	APC	Biolegend; 250704	2
CD45	AF700	Biolegend; 304024	5
DNAM-1	APC-Fire750	Biolegend; 338320	5
CD57	PB	Biolegend; 359608	2.5
NKG2D	BV510	Biolegend; 320816	5

Table 2.2: NK cell inhibiting receptor antibody panel

Antibody	Conjugate	Antibody details (manufacturer, catalogue number)	Antibody volume per sample (µl)
CD3	FITC	Biolegend; 344804	2
PD-1	PE	Biolegend; 329905	3
CD14	ECD	Beckman Coulter B92391	3
CD19	ECD	Beckman Coulter 6604551	3
PI	ECD	Miltenyi Biotec; 130093233	1
CTLA-4	PerCP-Cy5.5	Biolegend; 349928	3
CD56	PE/Cy7	Biolegend; 318318	5
TIGIT	APC	Biolegend; 372706	5
CD45	AF700	Biolegend; 304024	5
CD94	APC-Fire750	Biolegend; 305518	5
CD16	PB	Biolegend; 302008	5
CD69	BV510	Biolegend; 310936	5

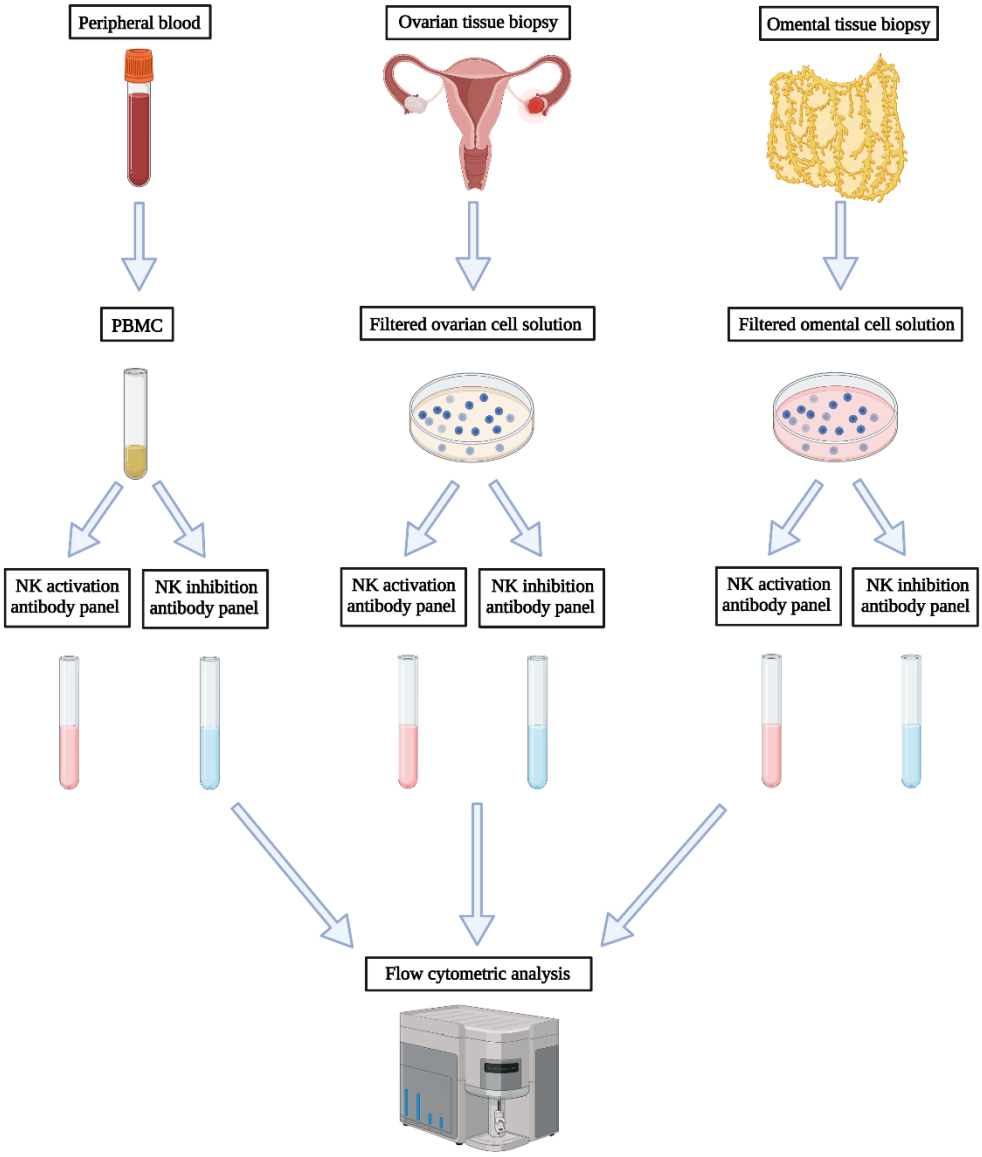


Figure 2.1: Analysis of NK phenotype in patient blood and tissue samples
Patient blood and tissue biopsies were processed and stained with two antibody panels before flow cytometric analysis interrogated NK cell phenotype.

2.2.4 Cytotoxicity analysis

2.2.4.1 NK cell isolation

NK cell enrichment was performed using The EasySep™ Human NK cell Isolation kit (STEMCELL Technologies, catalogue number 17955). Patient PBMC samples were centrifuged at 1500rpm for 5 minutes at room temperature. The cell pellet was resuspended in 4.5ml of sterile MACS buffer, consisting of PBS (ThermoFisher Scientific; catalogue number J61196-AP), 2 mmol Ethylenediaminetetra-acetic acid (EDTA; Corning; catalogue number 46-0340Cl) and 2% newborn calf bovine serum (ThermoFisher Scientific; catalogue number 16010159). Samples were counted using a haemocytometer, transferred to sterile 5ml polystyrene round-bottom tubes and centrifuged at 4℃ for 5 minutes at 1500rpm. The pellet was suspended in the MACS buffer, giving a concentration of $1x10^7$ cells in 200µl of MACS buffer. Isolation Cocktail (12.5µl; from the EasySep™ kit) was added to each sample, which was then incubated at room temperature for 5 minutes. The RapidSpheres vial (from the EasySep™ kit) was vortexed for 1 minute and 12.5µl added to each sample. MACS buffer was added, giving a total of 2.5ml, and pipetted gently to mix. The tubes were placed in the EasySep™ magnet and incubated for 5 minutes. The magnet was then inverted (with the tubes still in place), pouring the cell suspension (isolated NK cells) out of the tubes in the magnet into new 15ml universal tubes. The amount of NK cells in the collected cell suspension were calculated using a haemocytometer and topped up to 10ml with basic culture medium. The tubes were centrifuged at 1500rpm for 5 minutes at room temperature, the supernatant removed and cells resuspended in basic medium at a concentration of $1x10^6$ cells per ml. These isolated NK cells were incubated at 37℃ until used in the co-culture assay, for a maximum of 12 hours.

2.2.4.2 Labelling of K-562 cells

K-562 cells were cultured as described in section 2.2.1.2. The number of K-562 cells in each ml of medium was calculated using a haemocytometer and $10x10^5$ cells harvested for each patient sample to be used in the co-culture. These were transferred into a sterile 15ml universal tube and centrifuged at 1500rpm for 5 minutes at room temperature. In a separate tube, a 1µM solution of Carboxyfluorescein succinimidyl ester (CFSE; eBioscience; catalogue number 65-0850-84) was formulated: 1µl of a 5mM CFSE stock concentration (prepared by diluting 100µg CFSE with 36µl DMSO) was added to 5ml of sterile PBS warmed to 37℃. The centrifuged K-562 cells were resuspended in 1ml of the 1µM CFSE-PBS solution. These were incubated for 15 minutes at room temperature, before 10ml of basic medium was added and cells incubated again for an additional 10 minutes.

2.2.4.3 Co-culture of NK cells and K-562 cells

The K-562 cells, labelled with CFSE, were centrifuged at room temperature for 5 minutes at 1500rpm. The supernatant was discarded and the K-562 cells were suspended in basic medium at a concentration of $2x10^5$ per ml of media. Using a sterile, round bottom, 96-well plate, 100µl of labelled K-562 cells ($2x10^4$ cells) were transferred to six wells. To three of these wells, 100µl of the prepared isolated NK cells ($1x10^5$) were added, with 100µl of basic media added to the remaining three control wells. The 96-well plate was incubated at 37℃ for 16 hours.

2.2.4.4 Flow cytometric analysis of NK cell cytotoxicity

The 96-well plate was centrifuged at 1500rpm for 5 minutes. The supernatant (150µl) was pipetted from each well and 150µl of fresh basic medium added to each well. The solution in each well was transferred to sperate 5ml FACS tubes. CountBright™ beads (ThermoFisher

Scientific; catalogue number C36995) were vortexed and 10µl added to each FACS tube, along with 2µl of PI (Miltenyi Biotec catalogue number 130-093-233). The samples were processed on the Gallios flow cytometer (Beckman Coulter Life Sciences) and analysed using Kaluza, Flow Cytometry Analysis Software (Beckman Coulter, analysis version 2.1). By gating on the CFSE+PI cells, the live K-562 cells in each sample were calculated. To determine the concentration of K-562 cells per µl, the following equation was used: (the number of live K-562 cells divided by the number of CountBright™ beads in each sample) x (the bead count per 10µl divided by the total volume of the sample). The concentration of viable K-562 cells from the NK cell co-culture wells were then compared to the control wells without NK cells. This allowed the percentage of K-562 cells killed by the NK cells to be calculated.

2.2.5 Cytokine production

2.2.5.1 NK cell stimulation

Three sterile 5ml FACS tubes were prepared for each patient sample to be analysed: one as an unstimulated control tube for PBMC only, the second for PBMC and K-562 added to stimulate NK cells, and the third as a positive control with PBMC and eBioscience™ cell stimulation cocktail (500X; ThermoFisher Scientific; catalogue number 00-4970-93). The processed PBMC solution was counted using a haemocytometer and a total of $1x10^6$ PBMC cells transferred to each tube. The K-562 cells were counted and $1x10^6$ cells inserted into the second FACS tube for the stimulated sample. The eBioscience™ cell stimulation cocktail (1µl) was added to the third FACS tube for the positive control. The tubes were centrifuged at 1500rpm for 5 minutes at room temperature. The supernatant was discarded and the cell pellet was resuspended in 0.5ml of basic medium. To each tube, 1µl of eBioscience™ protein

transport inhibitor cocktail (500X; ThermoFisher Scientific; catalogue number 00-4980-03) was added and the samples incubated at 37℃ overnight.

2.2.5.2 Intracellular and surface cytokine staining

Following incubation, the tubes were centrifuged at 1500rpm for 5 minutes at room temperature with maximum deceleration. The supernatant was removed and the pellet gently mixed with 100µl of sterile PBS. Viability dye (LIVE/DEAD™ fixable red dead cell stain for 488nm excitation; ThermoFisher Scientific; catalogue number L23102) was prepared by diluting 1µl of the dye in 10µl of sterile PBS. The viability dye and surface stain antibodies were added as detailed in Table 2.3. Following incubation in the dark and on ice for 30 minutes, 2ml of sterile PBS was used to wash the samples and they were centrifuged at 1500rpm for 5 minutes with maximum deceleration. The resulting pellet was suspended in 100µl of eBioscience™ intracellular fixation buffer (ThermoFisher Scientific; catalogue number 00-8222-49). The tubes were vortexed for 10 seconds and incubated at 4℃ for 30 minutes. A 0.2% concentration of Triton-X 100 solution (Sigma-Aldrich; catalogue number 9036-19-5) was prepared with PBS and 100µl was transferred to each sample. The tubes were incubated on ice for 30 minutes before being washed with 2ml of sterile PBS and centrifuged at 2000rpm for 5 minutes at 4℃. The cell pellet was resuspended in 200µl of PBS, intracellular antibodies were added (Table 2.4) and samples incubated on ice and in the dark for 45 minutes. The cells were washed with 2ml of PBS, centrifuged at 2000rpm for 5 minutes at 4℃, and the pellet resuspended in 200µl of PBS.

2.2.5.3 Flow cytometric analysis of NK cell cytokine production

The samples were processed within 24 hours by the Gallios flow cytometer (Beckman Coulter Life Sciences). Kaluza, Flow Cytometry Analysis Software (Beckman Coulter,

analysis version 2.1), was utilised to measure the cytokines produced by the stimulated NK cells (PBMC cultured with K-562 cells), compared to the unstimulated NK cells (PBMC only) and the positive control NK cells (PBMC with eBioscience™ cell stimulation cocktail).

Table 2.3: Surface stain antibodies utilised in the cytokine assay

Antibody	Conjugate	Antibody details (manufacturer; catalogue number)	Antibody volume per sample (µl)
CD14	ECD	Beckman Coulter B92391	1.5
CD19	ECD	Beckman Coulter 6604551	1.5
Viability dye	ECD	ThermoFisher Scientific; 15530795	1
CD3	PerCP/Cy5.5	Biolegend; 300327	1.5
TGF-beta	APC	Biolegend; 141405	5
CD56	APC-Cy7	Biolegend; 318331	2.5
CD16	BV421	Biolegend; 302037	5

Table 2.4: Intracellular antibodies utilised in the cytokine assay

Antibody	Conjugate	Antibody details (manufacturer; catalogue number)	Antibody volume per sample (µl)
TNF-alpha	FITC	Biolegend; 502906	5
GM-CSF	PE	Biolegend; 502305	5
IL-10	PE-Cy7	Biolegend; 501419	5
IFN-gamma	AF700	Biolegend; 506515	5
IL-2	BV510	Biolegend; 503833	2.5

2.2.6 Real-time quantitative PCR (qPCR) of NK cell ligands

2.2.6.1 RNA extraction from ovarian tissue

Snap frozen tissue was utilised to quantify NK cell ligand expression on benign and malignant ovarian tissue. RNA extraction from the tissue biopsies was undertaken using the RNeasy Mini Kit (Qiagen; catalogue number 74104) and according to the manufacturer's protocol. Snap frozen tissue samples were removed from vapor phase nitrogen storage and immediately sectioned on a sterile petri dish with 600µl of buffer RLT (RNeasy lysis buffer

from the RNeasy Mini Kit) covering the tissue. The diced tissue and buffer were placed in sterile 1.5ml DNA-free tubes, which were centrifuged for 3 minutes at 13000rpm. The supernatant was removed and placed into a fresh 1.5ml sterile tube, along with 600µl of 70% ethanol. This solution was transferred into a RNeasy mini spin column, which was inserted into a sterile 2ml collection tube and centrifuged for 1 minute at 13000rpm. The flow-through waste was removed from the collection tube and 700µl of buffer RW1 (RNeasy washing buffer from the RNeasy Mini Kit) added to the spin column. This was centrifuged for 15 seconds at 13000rpm, before samples were centrifuged twice at 13000rpm with 500µl of buffer RPE (RNeasy washing buffer), initially for 15 seconds and again for 2 minutes. The spin column was inserted into a new 2ml collection tube, which was centrifuged at 13000rpm for 1 minute, before the spin column was placed into a new 1.5ml collection tube. RNase-free water (20µl; Qiagen; catalogue number 129112) was added to the spin column membrane and centrifuged again at 13000rpm for 1 minute. This resulted in RNA collecting at the base of the 1.5ml tube, which was kept on ice and the RNA concentration (ng/µl) determined using the Nanodrop Spectrophotometer version 1.8 (ThermoFisher Scientific).

2.2.6.2 RNA conversion to cDNA

The iScript cDNA Synthesis Kit (BioRAD; catalogue number 1708890) was used to convert RNA into complementary DNA (cDNA). RNase-free water was added to 1µg of RNA, 1µl of iScript Reverse Transcriptase and 4µl of 5x iScript reaction mix (from the iScript cDNA Synthesis Kit) in a 0.5ml RNA-free tube, giving a total volume of 20µl. The solution was processed in the Eppendorf 5333 Mastercyler Thermal Cycler, with priming occurring for 5 minutes at 25°C, reverse transcription for 20 minutes at 46°C and reverse transcriptase inactivation for 1 minute at 95°C. Finally, the sample was held at 4°C before the produced cDNA was diluted with RNase-free water to give a concentration of 5µg/µl.

2.2.6.3 Amplification and measurement of target genes

Within each well of a 96-well qPCR plate, the diluted cDNA (5µl) was combined with 1.25µl of the relevant primer probes (Table 2.5; Applied Biosystems), 12.5µl of TaqMan Universal Mastermix II (ThermoFisher Scientific; catalogue number 4440042) and 6.25µl of RNA-free water. For control wells, 5µl of either DNA-free water or a standardised plasmid was used (instead of the 5µl of cDNA). Standard plasmids containing certain copy numbers of relevant target gene sequences were used to generate standard curves. The plate was analysed on the 7500 real time PCR system (Applied Biosystems) for a total of 50 cycles, with the PCR conditions shown in Table 2.6. Figure 2.2 gives an example of cDNA amplification during PCR, including the standard curve. The copy numbers for each target gene were normalised by comparing to the transcription levels of the reference genes 18S and β2-microglobulin (B2M) within each sample. The data was evaluated using SDS software version 1.5 (Applied Biosystems).

Table 2.5: Primer probes used in qPCR to detect NK cell ligands

Primer	Assay Identification
MICA	Hs00792195_m1
MICB	Hs04187752_Mh
ULBP1	Hs00360941_m1
ULBP2	Hs00607609_mH
ULBP3	Hs00225909_m1
ULBP4	Hs01026642_m1
PVR	Hs00197846_m1
PVRL2	Hs00607609_m1
PDL-1	Hs00204257_m1
HLA-E	Hs03045171_m1
HLA-A	Hs01058806_g1
HLA-C	Hs00740298_g1
HLA-DR	Hs00219575_m1
18S	Hs03003631_g1
B2M	Hs00187842_m1

Table 2.6: Conditions for DNA amplification with PCR

PCR Stage	Temperature	Time
Holding stage	50℃	2 minutes
	95℃	10 minutes
Cycling stage (50 cycles)	95℃	15 seconds
	60℃	1 minute

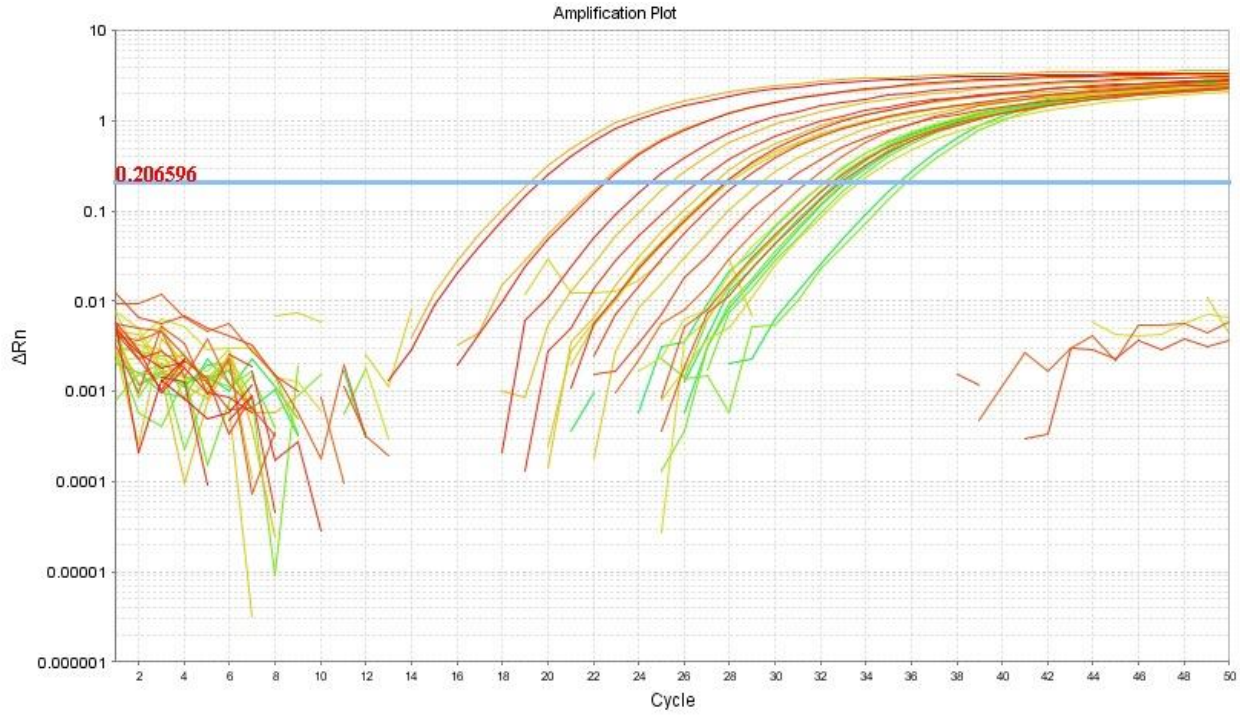


Figure 2.2: The amplification plot for cDNA undergoing PCR
Patient samples undergoing PCR to amplify cDNA using a primer for the MICA gene.

2.2.7 Expression of NK ligands on normal and malignant epithelial cells within ovarian biopsies

The expression of NK ligands by the epithelial cells within ovarian tissue biopsies were determined using flow cytometric analysis. The filtered tissue samples (processed according to section 2.2.2.2) were centrifuged at 1500rpm for 5 minutes at room temperature and the pellets resuspended 100µl of sterile PBS. These solutions were transferred to 5ml polystyrene, round bottom FACS tubes and stained with antibodies for the epithelial cell marker (Epcam) and NK ligands, documented in Table 2.7. They were incubated in darkness at 4°C for 40 minutes before 500µl of PBS was added. The samples were then centrifuged at 1500rpm for 5 minutes, the supernatants discarded and the pellets resuspended in 200µl of sterile PBS. PI (1µl; Miltenyi Biotec; catalogue number 130-093-233) was added and the samples processed on the Gallios Flow Cytometer (Beckman Coulter, USA). Kaluza analysis software detected the Epcam positive epithelial cell populations: tumour cells with high Epcam and low HLA class I expression, and normal healthy epithelial cells with lower Epcam and higher HLA class I. The expression of the NK ligands by the cells within the epithelial populations could then be evaluated.

Table 2.7: Antibodies to detect epithelial cells within ovarian tissue and their expressed NK ligands

Antibody	Conjugate	Antibody details (manufacturer; catalogue number)	Antibody volume per sample (µl)
Epcam	BV421	Biolegend; 324220	5
HLA-A/B/C	PE/Cy7	Biolegend; 311430	5
MHC Class II	APC/Cy7	Biolegend; 307618	5
PDL-1	BV510	Biolegend; 329734	5
MICA/B	AF700	R & D Systems; FAB13001N	5
ULBP1	PerCP	R & D Systems; FAB1380C	5
ULBP2/5/6	APC	R & D Systems; FAB1298A	5
ULBP3	AF488	R & D Systems; FAB1517G	5
ULBP4	PE	R & D Systems; FAB6285P	5

2.2.8 NK cell cytotoxicity following co-culture with ovarian tissue

2.2.8.1 Co-culture of ovarian tissue and NK cells

Filtered ovarian tissue samples (non-enzymatic processing described in section 2.2.2.2) were cultured with NK cells from processed PBMC samples (section 2.2.2.1). These NK cells were either obtained from the same patient (autologous NK cells) or from controls (healthy donor NK cells). The single cell solution of filtered ovarian tissue was counted using a haemocytometer and the sample divided equally between four or six 5ml FACS tubes: two tubes for tissue only, two tubes for tissue plus the addition of healthy donor NK cells and, if available, two tubes also for tissue along with autologous NK cells. As described in section 2.2.4.1, NK cells were isolated from PBMC samples and counted using a haemocytometer. The NK cells were added to the relevant FACS tubes in a 1:1 ratio to the amount of tissue cells. All tubes were topped up to 4ml with basic media and incubated overnight at 37°C.

2.2.8.2 Cytotoxicity of NK cells following co-culture with ovarian tissue

Following incubation, the FACS tubes were centrifuged at 1500rpm for 5 minutes at room temperature. The supernatant was discarded and the cell pellet resuspended in 100µl of sterile PBS. Antibodies were added to each FACS tube as described in Table 2.8, which were then incubated on ice, in the dark for 45 minutes. Samples were washed with 500µl of sterile PBS and were centrifuged for 5 minutes at 1500rpm. The supernatant was removed and the samples resuspended in 150µl of PBS with 1µl of PI (Miltenyi Biotec; catalogue number 130-093-233). The whole volume of the samples was processed on the Gallios flow cytometer (Beckman Coulter Life Sciences) and analysed using Kaluza Flow Cytometry Analysis Software (Beckman Coulter, analysis version 2.1) to count the live cells with high Epcam expression and low MHC class I expression, giving the total number of viable ovarian tissue/tumour cells in each sample. The number of live ovarian tissue/tumour cells from the

samples without NK cells was compared to the number of ovarian cells in the samples that had been co-cultured with additional NK cells. This allowed the degree of killing by NK cells to be calculated.

Table 2.8: Antibodies used to detect NK cell killing of ovarian tissue

Antibody	Conjugate	Antibody details (manufacturer; catalogue number)	Antibody volume per sample (µl)
Epcam	BV421	Biolegend; 324220	5
HLA-1	PE/Cy7	Biolegend; 311430	5
CD56	AF700	Biolegend; 318316	5

2.2.8.3 NK activation receptor blocking and cytotoxicity

Filtered tissue samples and isolated healthy donor NK cells were combined in a 1:1 ratio as described in section 2.2.8.1. Antibodies to block specific NK activating receptors were also added, documented in Table 2.9 and shown in Figure 2.3. Co-cultures were again incubated overnight and then processed as defined in section 2.2.8.2. Flow cytometric analysis and evaluation with Kaluza software to count the total number of Epcam positive ovarian tissue/tumour cells from: a) the isolated tissue cultures, b) the NK cell and tissue co-cultures, and c) the co-cultures plus NK receptor inhibiting antibodies. This determined the impact each of the NK cell receptors had on the ability for NK cells to kill ovarian tissue/tumour.

Table 2.9: Antibodies added to co-culture to block NK cell receptors

NK cell receptor target	Antibody details (manufacturer; catalogue number)	Concentration of antibody within co-culture
DNAM-1	Biolegend; 338302	0.5mg/ml
NKG2D	Biolegend; 320813	1mg/ml
NKp46	Biolegend; 331947	2mg/ml
NKp30	Biolegend; 325223	2mg/ml

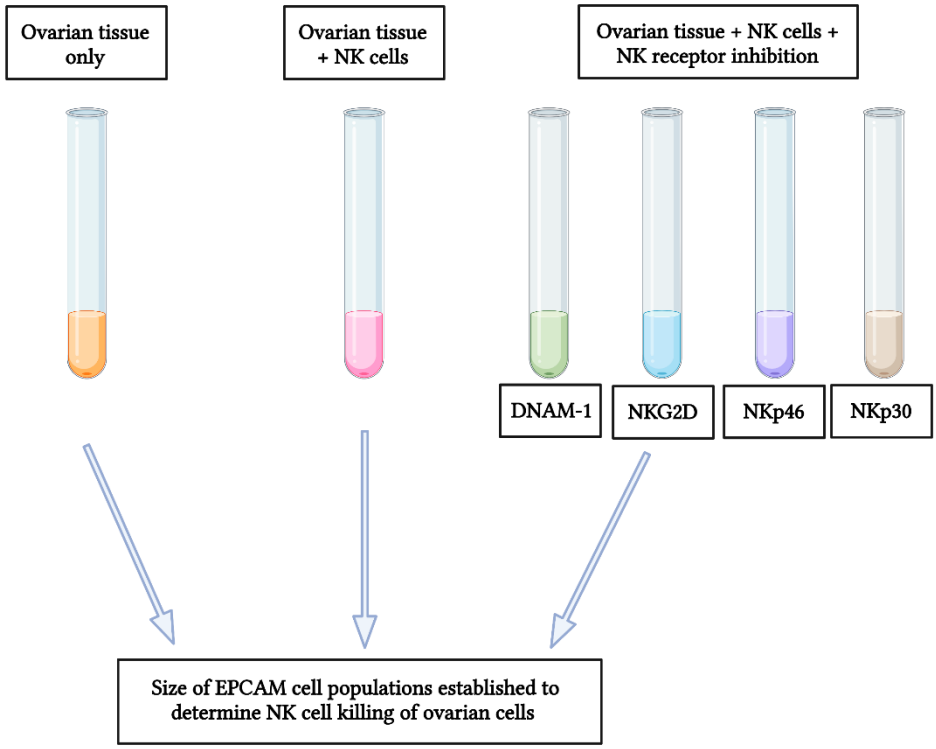


Figure 2.3: The NK cell and ovarian co-culture with addition of antibodies to inhibit NK cell receptors.

NK cell-mediated killing of ovarian tissue was established based on the size of Epcam positive cell populations.

2.3 Part 3: Single Cell Sequencing

2.3.1 Single cell RNA sequencing

2.3.1.1 Sample preparation for single cell RNA sequencing

Omental tumour samples were collected in the operating theatre and were immediately placed into MACS storage solution (Miltenyi Biotec; catalogue number 130-100-008) on ice. Within 30 minutes the tissues were sectioned into 2mm size pieces and placed into a 15ml sterile universal tube for digestion. Basic culture medium (3ml) was added along with 500µl of a collagenase (1500 units) and hyaluronidase (500 units) solution (StemCell Technologies; catalogue number 07912), 500µl of liberase TL (Sigma-Aldrich; catalogue number 05401020001) and 2µl (500 units) of benzonase nuclease (Merck; catalogue number E1014). The tube was rotated at 37°C for 90 minutes.

The digested sample was then filtered through a 100-micron cell strainer into a sterile 50ml universal tube. Basic media was used to wash the digestion tube to collect any residual cells, which was also filtered through the strainer, with the digested tissue collected in the 50ml tube. The sample was then filtered again through a 40-micron cell strainer, ensuring a single cell solution of digested tissue.

This was centrifuged at room temperature for 10 minutes at 1500rpm. The supernatant was removed and 2ml of red blood cell lysis buffer (Cambridge, Bioscience; catalogue number RBCL-1) was added to the cell pellet. This was incubated at room temperature for 10 minutes, before 8ml of basic medium was added and the sample centrifuged again at 1500rpm for 10 minutes. The supernatant was discarded, the pellet was mixed with 4ml of sterile MACS buffer (PBS, 2mM of EDTA (Corning) and 2% of newborn calf bovine serum

(ThermoFisher Scientific)) and the sample transferred to a 5ml sterile round bottom FACS tube.

Following a further centrifuge for 5 minutes at 1500rpm, the cell pellet was stained with 15µl of Fc receptor blocking solution (Biolegend; catalogue number 422302) and the sample incubated at 4°C for 5 minutes. Additional antibodies, described in Table 2.10, were then added and the sample incubated at 4°C for 25 minutes. After the addition of 4ml of MACS buffer, the sample was centrifuged at 1500rpm for 5 minutes at 4°C. The cell pellet was resuspended in 500µl of MACS buffer and 1.5µl of PI added. Keeping the sample on ice, it was transferred for cell sorting.

Table 2.10 Antibodies added to the single cell solution for cell sorting

Antibody	Conjugate	Antibody details (manufacturer; catalogue number	Antibody volume per sample (µl)
CD45	BV785	Biolegend; 304047	3
Epcam	APC	Biolegend; 324207	3
Podoplanin	FITC	Biolegend; 337025	3

2.3.1.2 Cell sorting of tumour samples for single cell RNA sequencing

The tumour biopsies, digested and processed to give a single cell solution, were sorted to identify three different cell types: immune cells with high CD45 expression, epithelial cells with high Epcam and low podoplanin expression, and fibroblasts with low Epcam and high podoplanin expression. Figure 2.4 shows the gating strategy used to identify and sort the different cell types. Dead and non-viable cells were identified with PI staining and removed by gating on the live single cell population. This removed and minimised the effect of cellular debris, with only live immune cells, epithelial cells and fibroblasts retained. The cells with

CD45 expression were collected into one FACS tube and the combined Epcam/podoplanin positive cells in another, along with basic medium. These two populations were combined, with CD45 positive cells making up 75% and the Epcam/podoplanin cells 25% of the final sample. The sorted cell populations were diluted in basic media to give a concentration of 1 x 10^6 cells per ml and centrifuged at 1700rpm for 10 minutes at 4°C. After supernatant was discarded the cell pellet was resuspended in basic media, maintaining a density of 1000 cells in every µl. The sample was then transferred on ice to the 10X Genomics Laboratory, where strict viability checks ensured live, high quality cells were included for sequencing.

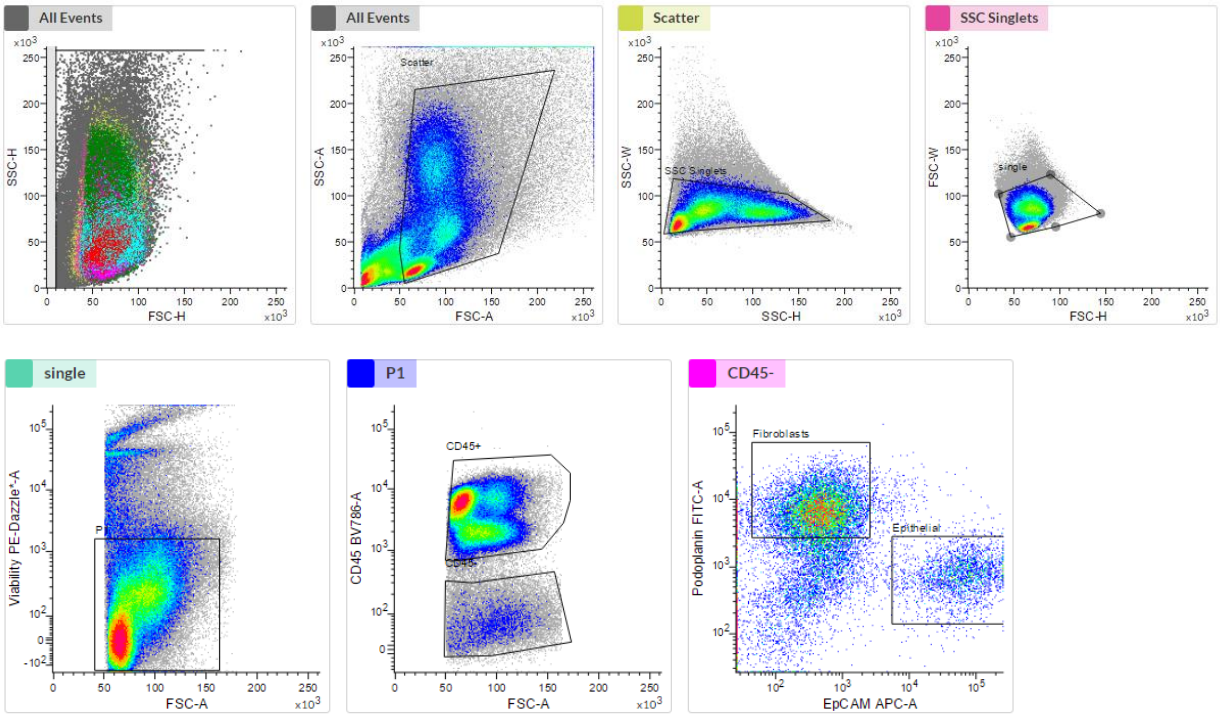


Figure 2.4: The gating strategy to identify and sort cell populations within digested omental tumour tissue.

Cell sorting identified: singlets, live cells (using PI, PE-Dazzle), CD45 positive immune cells, fibroblasts (high podoplanin and low Epcam expression) and epithelial cells (high Epcam and low podoplanin expression).

2.3.1.3 Library preparation for 10X sequencing

The samples were processed by the scientists within the 10X Genomics Sequencing laboratory at the University of Birmingham. Here, the Chromium Controller (10X Genomics) and the Single Cell 3' GEM, Library and Gel Bead kit (version 3.1; 10X Genomics; catalogue number PN-1000121) aimed to profile up to 10,000 individual live cells from each sample, using 10X barcodes to identify the transcriptome of each single cell [305]. Specifically, GEMs (Gel beads-in-emulsion) were produced, which combined gel beads with barcoded oligonucleotides, a single cell and partitioning oil, as shown in Figure 2.5. Within each GEM, the cell was lysed, the mRNA tagged with a 10X barcode and unique molecular identifier (UMI), and reverse transcription performed to produce cDNA. All the cDNA from each cell had the same oligonucleotide barcode, enabling transcripts to be mapped backed to their original cell source. The GEMs were then broken and the cDNA amplified using PCR. The cDNA was processed to generate a library for sequencing: the amplified cDNA was fragmented using enzymes and primer sequences added via end repair, A-tailing and adaptor ligation. The cDNA was then size selected with Solid Phase Reversible Immobilization (SPRI)-select reagents, cleaned using magnetic beads and the library amplified with PCR. The library quality was ensured by using a TapeStation High Sensitivity system. The final library to be sequenced included: primers, the 10X barcode (matched for each cell analysed), the UMI and the optimised cDNA. Illumina NEXTSeq was then used to sequence the sample, identifying 20,000-40,000 transcription reads per cell.

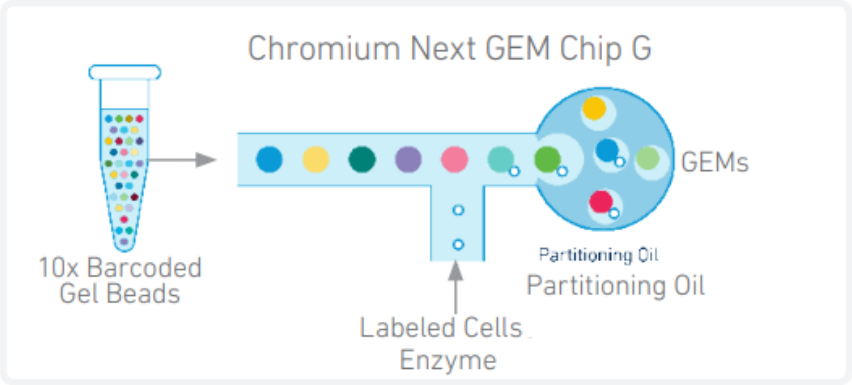


Figure 2.5: The generation of GEM's during library preparation for single cell RNA sequencing
Figure from the 10X Single Cell 3' GEM, Library and Gel Bead kit user guide [305].

2.3.1.4 Analysis of the single cell RNA sequencing data

The single cell RNA sequencing data was analysed by the Bioinformaticians within the Institute of Immunology and Immunotherapy and the Centre for Computational Biology at the University of Birmingham. The single cell data produced by Illumina NEXTSeq was interrogated using the Cell Ranger (version 5.0.1) analysis pipelines [306, 307]. Here, the BCL files containing raw sequencing data were converted into FASTQ files (cellranger mkfastq) and the reads were aligned to the Human Reference Genome (version GRCh38) with cellranger count. This generated the raw feature (gene) count matrix which corresponds to the counts of unique molecular identifiers (UMI) for features in every single cell. The raw UMI matrices were imported and further analysed using "R" (version 3.6.2).

Any doublets within the dataset (identified with DoubletFinder version 3.0) were removed. In addition, cells were eliminated if they had fewer than 500 genes detected, more than 3500 genes detected or if a high proportion (above 10%) of their genes mapped to mitochondrial RNA. When a particular gene was expressed in three cells or less, the genes were also discarded from

the analysis. Downstream analysis was conducted with Seurat (version 3.2.0). Cell cycle scores were calculated using Seurat CellCycleScoring function and the difference between G2M and S phase score quantified. Seurat SCTransform pipeline was followed for normalisation, regressing out % mitochondrial mapping and G2M-S phase score difference. SCTransform-normalised data for each sample was integrated following the SCTransform integration workflow on the top 8000 most variable features. The most variable features were then used for dimensionality reduction by principal component analysis and subsequent uniform manifold projection with PCs 1:20 that explained most of the variance observed.

2.3.1.5 Unsupervised clustering and major cell lineage annotation

To identify major lineage cell types, unsupervised clustering was applied using Seurat FindNeighbours and FindClusters which first connected cells together according to the "shared nearest neighbour" theory, generating a shared nearest neighbour graph and then optimised the modularity using the Louvain algorithm to identify cell clusters. The resolution parameter controlling cluster granularity was set to 0.8. Marker genes that were differentially overexpressed in each cluster compared to all other clusters were identified using Seurat FindAllMarkers with default parameters. Clusters were annotated with major lineage cell type using a combination of marker gene expression profiles and interrogating the expression of known canonical cell type marker genes.

2.3.1.6 NK cell cluster identification and annotation

For finer-grained analysis specifically of NK cell type, data was first subset on the NK cells before NK-population variable features were calculated with Seurat FindVariableFeatures (n = 3000 genes). This was followed by dimensionality reduction with PCA and UMAP (using PCs 1:20). Clustering was applied with FindClusters and canonical major cell type marker gene

expression profiles were assessed to remove non-NK cell clusters. Further filtering removed any remaining non-NK cells which had raw counts of > 0.5 for the T cell specific CD3D gene. Final NK cell-cluster marker genes were identified with FindAllMarkers and NK differentiation marker gene expression was assessed to annotate NK cell subsets. Genes of interest panels included NK ligands, NK receptors and cytokines. Average expression of these within the NK cell clusters, within the tissue types and also within treatment groups were calculated using Seurat AverageExpression function.

2.3.1.7 Cluster proportion comparisons

The proportions of different cell types were compared across the samples analysed, using the Wilcoxon rank sum test. This included stratifying cluster proportion between the type of tissue analysed (ovarian tumour metastatic deposits in the omentum and a non-malignant normal omental sample), and between chemotherapy exposed and chemotherapy naïve tissues.

2.3.1.8 Signature scoring

Gene set signatures of interest relating to NK cells were explored within the NK cell clusters using the AddModuleScore function in Seurat. Here the average gene expression levels within the individual cells of a cluster were calculated, removing any background expression from randomly selected control features. A positive signature score indicated that the signature is expressed more highly than expected given average population expression. The NK cell relevant gene-sets included Cytotoxicity, Exhaustion, NK Activating Receptors and NK Inhibitory Receptors. Scores were compared across tissue type using Wilcoxon rank sum test.

2.3.1.9 Differential expression

The differential expression of genes between treatment exposed and treatment naïve tissues, as well as between recurrence and no recurrence in the treatment exposed tissues, was assessed using Seurat FindMarkers with MAST (test.use="MAST").

2.3.1.10 Gene Set Enrichment Analysis (GSEA)

Gene set enrichment analysis was applied to differential expression results using the R package fgsea. Genes were ranked by log2FC and fgsea applied using HALLMARK gene set from the Molecular Signatures Database (MsigDb). Selected significantly enriched (Adjusted p-value <0.01) gene sets were visualised.

2.3.1.11 Correlation analysis

Spearman correlation was assessed between cell type proportions and the following clinical covariates: age; ca125 at surgery; PCI; progression free survival; overall survival using ggcorr. Scatter plots of selected correlations were plotted with ggscatter.

2.3.2 Single cell ATAC sequencing

2.3.2.1 Sample preparation and nuclei extraction for single cell ATAC sequencing

Tumour biopsies were obtained immediately following the surgical resection of omental tissue. The biopsy samples were placed in MACS storage solution (Miltenyi Biotec; catalogue number 130-100-008) on ice, were snap frozen in liquid nitrogen within 30 minutes and were then stored in vapor phase nitrogen freezers. The sample preparation for single cell ATAC sequencing involved the extraction of nuclei from the snap frozen tissues.

Prior to removing the biopsies from nitrogen storage freezers, four different buffers were prepared. For every sample to be processed, a 4ml wash buffer was formulated by combining: 3.5ml of nuclease-free water (ThermoFisher Scientific; catalogue number AM9932), 40µl of Tris-HCl (pH 7.4; Sigma-Aldrich; catalogue number 77-86-1), 8µl of NaCl (Sigma-Aldrich; catalogue number S8776), 12µl of $MgCl_2$ (Sigma-Aldrich; catalogue number 63069), 400µl of BSA (Miltenyi Biotec; catalogue number 130-091-376) and 40µl of Tween-20 (Sigma-Aldrich; catalogue number P1379). A 500µl 1X lysis buffer consisted of: 433µl of the nuclease-free water, 5µl Tris-HCl (pH 7.4), 1µl NaCl, 1.5µl $MgCl_2$, 5µl of Tween-20, 5µl Nonidet P40 substitute (Sigma-Aldrich; catalogue number 74385), 1µl of Digitonin (ThermoFisher Scientific; catalogue number 407560050) and 50µl of BSA. Lysis dilution buffer (4.5ml per sample) contained 3.98ml nuclease-free water, 45µl of Tris-HCl (pH 7.4), 9µl of NaCl, 13.5µl of $MgCl_2$ and 450µl of BSA. Following optimisation, a 0.1X lysis buffer for omental tumour processing was prepared with 500µl of the 1X lysis buffer and 4.5ml of the lysis dilution buffer. The buffers were kept on ice, along with a 7ml Dounce tissue homogeniser.

For the nuclei extraction, the tissue biopsies were removed from nitrogen storage freezers one at a time and kept on ice throughout. The tissue was immediately sectioned, while still frozen, into 1-2mm pieces and transferred into the cold homogeniser with 1ml of the 0.1X lysis buffer. The tissue was pushed to the base of the homogeniser and pestle A was turned 50 times with pressure. Another 50 turns were applied to the tissue using pestle B. The solution was transferred into a sterile 15ml tube and the homogeniser was rinsed with 1ml of the 0.1X lysis buffer, which was then also transferred into the new 15ml tube. The sample was incubated for of 20 minutes on ice before it was centrifuged at 500xG for 5 minutes at 4°C. The supernatant was discarded and the pellet resuspended in 2ml of new 0.1X lysis buffer.

Following another 20-minute incubation on ice, the sample was filtered through a 40-micron cell strainer and the solution was centrifuged again at 500xG for 5 minutes at 4°C. The supernatant was removed and 1ml of the wash buffer added to the cell pellet. The solution was filtered through a fresh 40-micron cell strainer and transferred into sterile 1.5ml Eppendorf tubes. The individual nuclei within the solution were counted and viability assessed using the Countess II FL automated cell counter (ThermoFisher Scientific). Diluted nuclei buffer (from the 10X Genomics Single Cell ATAC Library and Gel Bead Kit; catalogue number 1000175) was added to the sample to achieve a concentration of between 2000 to 3000 nuclei per µl for a targeted nuclei recovery of 4000 nuclei.

2.3.2.2 Library preparation for 10X single cell ATAC sequencing

Following nuclei extraction, the single-nuclei solutions were processed by the 10X Genomics Sequencing laboratory at the University of Birmingham. The Chromium Single Cell ATAC Solution and the Chromium Next GEM Single Cell ATAC Library and Gel Bead Kit were utilised according to the manufacturer's instructions [308]. Briefly, the diluted nuclei were added to a transposition solution, where transposase entered nuclei and fragmented the DNA in open chromatin regions, while adapter sequences were merged onto the DNA fragments. Individual transposed nuclei were joined with a barcoded gel bead and partitioning oil to create a GEM, shown in Figure 2.6. By dissolving gel beads, primers and 10x barcodes were added to single-stranded DNA, and the GEM's fragmented to collect the DNA. All of the transposed DNA fractions from the same nucleus were tagged with the same individual barcodes to identify the nucleus of origin after DNA pooling.

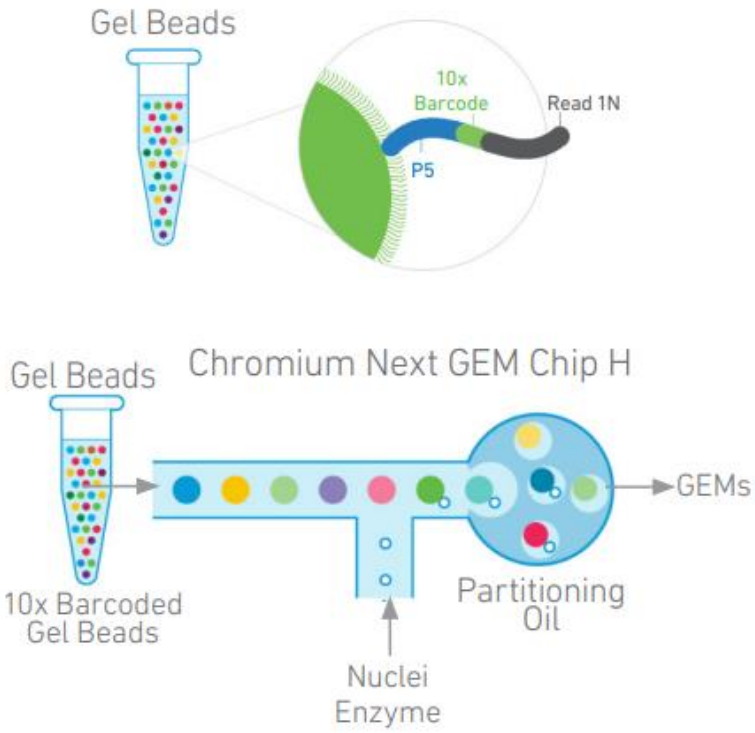


Figure 2.6: Creation of GEM's and barcoding during library preparation for single cell ATAC sequencing
Figure from Chromium Next GEM Single Cell ATAC Reagent user guide [308].

The samples were cleaned using Solid Phase Reversible Immobilization (SPRI) and silane magnetic beads. The DNA was then amplified using PCR and the quality assessed with Agilent TapeStation High Sensitivity D1000 ScreenTape. Sequencing was performed with Illumina NextSeq 500, aiming to analyse 4000 individual nuclei at a depth of 25,000 read pairs for every nucleus. The sequenced DNA reads could be correlated to each separate nucleus using the unique barcodes.

2.3.2.3 Analysis of the single cell ATAC sequencing data

For scATAC-seq analysis, sequencing reads were processed into FASTQ format and peak-barcode counts using Cell Ranger ATAC v2.0.0, aligning to the prebuilt Cell Ranger

GRCh38 human reference genome. The output of this was used as input to the Signac v1.6.0 R package. For integration of samplewise data a common peakset was created from overlapping peaks across all samples and filtered to remove those with peak width < 20 or > 10000. For each sample, per-cell fragments aligned to this common peak set was calculated using the FeatureMatrix function and stored in a new chromatin assay with CreateChromatinAssay function. Normalisation and dimensionality reduction were performed using Signac with latent semantic indexing (LSI) which consisted of running functions RunTFIDF; FindTopFeatures; RunSVD and finally RunUMAP. This normalised using term frequency-inverse document frequency (TF-IDF) and singular value decomposition followed by UMAP on the top 50% of peaks in terms of their sample variation. LSI components 2:30 were used in UMAP dimensionality reduction. Sample integration was performed using harmony RunHarmony function taking the merged sample data using reduction = "lsi" and the combined peaks assay as input parameters.

2.3.2.4 Differential peak analysis

Peak-level differential analysis identified peak sites with differential chromatin accessibility between major cell lineages and between treatment exposed and treatment naïve tissue using FindMarkers on the combined peaks assay. Peaks were considered differentially accessible if absolute log2FC > 0.25 and Benjamini Hochberg adjusted p-value < 0.01.

2.3.2.5 Unsupervised clustering and major cell lineage annotation

Harmony-adjusted cell embeddings were used for unsupervised clustering using Seurat functions FindNeighbours to generate the shared neighbour graph and FindClusters to identify clusters using resolution of 0.2 for coarse grained clustering. To estimate per cell gene activity from peaks data the Signac function GeneActivity was used and cluster markers

peaks and genes were identified using FindAllMarkers on the combined peaks and gene activity assays respectively. Clusters were annotated with major cell type lineage Lymphocyte, Myeloid, Fibroblast and Epithelial based on canonical cell type marker gene activity profile and chromatin accessibility profile at known major cell type defining gene loci.

2.3.2.6 Differential transcription factor motif enrichment

Transcription factor motif position frequency matrices were obtained using the R package JASPAR2020 and motif information added to the Signac object using the AddMotifs function. Per cell motif activity scores were calculated with RunChromVar on BSgenome.Hsapiens.hg38 and the combined peaks assay. Differential activity of motifs was assessed between major lineage cell types and between chemotherapy exposed and chemotherapy naïve tissues using FindMarkers on the motif activities.

Chapter 3:

Heterogeneity and transcriptional profiles of tumour and immune cells in Ovarian Cancer

3.1 Introduction

Although 80% of ovarian cancer (OC) patients initially respond to chemotherapy, the majority develop resistance and just over half are alive and disease free after 12 months of completing treatment [64, 73]. While the precise mechanisms remain unclear, chemoresistance is believed to result from the selection of treatment-resistant sub-populations of cells within a heterogeneous tumour [91, 116]. It is suggested that the malignant cells, the immune infiltrate and the tumour microenvironment (TME) adapt during chemotherapy treatment to support the growth and progression of surviving cancerous cells [91]. This would likely involve genomic changes, ineffective DNA damage repair and epigenetic alterations [91-95, 309].

As tumours progress, the extent of intra-tumour heterogeneity also advances, with clusters of cells forming different subpopulations based on their genetic signatures and transcription profiles [106, 107]. These differing malignant subpopulations vary in their response to treatments due to discrepancies in their molecular signatures [107]. The challenges in managing OC patients, overcoming treatment resistance and introducing novel tumour-specific therapeutic strategies are hampered by a lack of understanding of ovarian tumour heterogeneity. In addition, details of the precise immune cell infiltrate and the tumour-immune response remain unclear in OC, yet play an important role in treatment efficacy and the success of new immunotherapies [114, 115].

Sequencing analysis at the single cell level provides extensive knowledge of the cellular composition within the tumour microenvironment (TME) [114]. Any alterations to the tumour and immune landscape following exposure to chemotherapy treatment can consequently be detected by comprehensive transcriptomics evaluation [115]. Thus, the interrogation of individual malignant cells and immunogenomic analysis has identified variable gene

expression and transformed cell populations due to chemotherapeutic modulations within the TME [123, 168, 172]. This chapter aims to interrogate the heterogeneity of advanced metastatic ovarian tumours at the single cell level. This transcriptomic analysis aimed to focus on both the tumour and immune cell populations, their interactions within the TME, and mechanisms of immune recognition and tumour evasion. The detailed cell characterisation will also examine alterations following chemotherapy exposure and the molecular adaptations associated with treatment resistance. Two different sequencing techniques were used to evaluate OC tissue samples, undertaking a comprehensive analysis of the cell type contexture within the ovarian TME.

3.2 Single cell RNA Sequencing of Ovarian Cancer

3.2.1 The sample cohort

Single cell RNA sequencing (scRNAseq) was performed on OC tissue biopsies from 9 women with advanced OC. Tissue samples were obtained at the time of debulking surgery, with specimens obtained from the omentum due to OC having a predilection to metastasise here in the first instance [65, 66]. Indeed, omental tumour deposits are frequently found in advanced (FIGO stage III/IV) metastatic OC, which are significantly associated with poor clinical outcomes [66, 69, 71, 71]. In addition, from previous experience and earlier laboratory experiments, omental tissue samples are relatively straightforward to process and manipulate compared to necrotic and fragile ovarian tumour tissue.

All 9 patients in the cohort had high-grade serous OC (HGSOvCa). Cytoreductive primary debulking surgery (PDS) was performed in 5 patients, while 4 were recruited at the time of interval debulking surgery (IDS) following neoadjuvant chemotherapy (NACT). Metastatic tumour deposits within the omentum were histologically confirmed in 8 patients, while there

was no evidence of metastatic omental disease in one of the patients who underwent PDS. This normal omental sample was included in the analysis for comparison to the patients with omental tumours in the PDS and NACT groups.

Table 3.1 shows the characteristics and variables for the patients based on diagnosis and treatment group. These were matched for age, ethnicity, disease stage and *BRCA* status [35, 44, 45]. Patients also had similar peritoneal cancer index (PCI) and surgical cytoreduction scores (described in the Methods sections 2.1.21 and 2.1.3.1). A third of the patients in the cohort had recurred and died from their disease by the follow-up end date (10.01.2023), including 1 in the primary surgery group and 2 in the NACT group. There were no differences in progression free survival ($p = 0.8393$) and overall survival ($p = 0.2133$) between the patient groups in the cohort.

Table 3.1: Characteristics and baseline variables of the patients in the scRNAseq cohort

Variable	Primary surgery (n=4)	Neoadjuvant chemotherapy (n=4)	Normal omentum (n=1)
Age (years)			
Mean ± SD	60.0 ± 12.1	66.3 ± 8.2	72
Ethnicity	**n (%)**	**n (%)**	**n (%)**
White	3 (75.0)	2 (50.0)	1 (100.0)
Asian	0 (0.0)	1 (25.0)	0 (0.0)
Black	1 (25.0)	1 (25.0)	0 (0.0)
Disease stage	**n (%)**	**n (%)**	**n (%)**
3	3 (75.0)	1 (25.0)	0 (0.0)
4	1 (25.0)	3 (75.0)	1 (100.0)
PCI			
Median (range)	21 (14-25)	16 (12-18)	6
BRCA status	**n (%)**	**n (%)**	**n (%)**
normal	3 (75.0)	4 (100.0)	1 (100.0)
mutated	1 (25.0)	0 (0.0)	0 (0.0)
CA-125 (U/ml)			
Mean ± SD	898 ± 1398	2010 ± 1968	2013
Cytoreduction	**n (%)**	**n (%)**	**n (%)**
R0	1 (25.0)	3 (75.0)	1 (100.0)
R1	1 (25.0)	0 (0.0)	0 (0.0)
R2	2 (50.0)	1 (25.5)	0 (0.0)
Chemotherapy cycles	n/a	**n (%)**	n/a
3		1 (25.0)	
4		2 (50.0)	
6		1 (25.0)	
Chemotherapy Response score	n/a	**n (%)**	n/a
2		3 (75.0)	
3		1 (25.0)	
Disease recurrence	**n (%)**	**n (%)**	**n (%)**
Recurred	1 (25.0)	2 (50.0)	0 (0.0)
Disease-free	3 (75.0)	2 (50.0)	1 (100.0)
Survival	**n (%)**	**n (%)**	**n (%)**
Died	1 (25.0)	2 (50.0)	0 (0.0)
Alive	3 (75.0)	2 (50.0)	1 (100.0)

3.2.2 Composition of the omental samples evaluated by single cell RNA sequencing

Following tissue processing (described in the Methods section 2.3.1.1), which included digestion and the generation of a single cell solution, cell sorting (Methods section 2.3.1.2) ensured that each sample consisted of immune cells (with high CD45 expression), fibroblasts (with raised podoplanin expression) and epithelial cells (with elevated Epcam expression). To guarantee adequate immune cell number, the samples were enriched with sorted CD45 positive immune cells. As such, the reconstructed samples were comprised of 75% CD45 positive cells and 25% Epcam/podoplanin positive cells. Bioinformatic analysis then explored gene transcription patterns within the cell populations. The number of cells sequenced and analysed (shown in Table 3.2) from the OC samples ranged from 2271 to 6355 cells per sample, while the normal omental sample had a greater number of cells (20494).

Table 3.2: The cells sequenced for every patient in the scRNAseq cohort

Patient	Treatment group	Chemotherapy exposure	Cells sequenced
1	PDS OC	Nil	2271
2	PDS OC	Nil	4352
3	PDS OC	Nil	4062
4	PDS GIT / non-OC	n/a	Excluded
5	PDS normal omentum	Nil	20494
6	PDS OC	Nil	6355
7	NACT OC	6 cycles	6284
8	NACT OC	3 cycles	5764
9	NACT OC	4 cycles	3174
5	NACT OC	4 cycles	5244

3.2.3 Analysis of single cell RNA sequencing data

3.2.3.1 Clustering and identification of major cell types

The raw sequencing data from all the omental samples were processed and integrated as described in Methods section 2.3.1.4. Unsupervised clustering was applied to group together cells of a similar transcriptional profile. Highly expressed marker genes for each cluster were then interrogated to determine the subpopulation cell type. In total, 19 different major lineage cell types were identified: endothelial cells, epithelial cells, fibroblasts, and several immune cells, including macrophages, mast cells, monocytes, neutrophils, B cells, T cells and NK cells (Figure 3.1). From the CD45 positive immune cell clusters, the predominant cell type was CD8+ T cells, while there were also large subpopulations of CD4+ T cells, B cells and NK cells, shown in Figure 3.1 (A). Epithelial and fibroblast cell populations contributed the greatest proportion of non-immune cells.

Figure 3.1 (B) illustrates the cell clustering according to each patient sample. The different cell subpopulations are relatively consistent across the 9 samples. However, three of the patients who had received NACT had greater proportions of certain immune subpopulations: the sample from patient 5 (Pt5) had a high proportion of macrophages, the sample from patient 6 (Pt6) consisted mainly of B cells and the sample from patient 8 (Pt8) had large numbers of neutrophils.

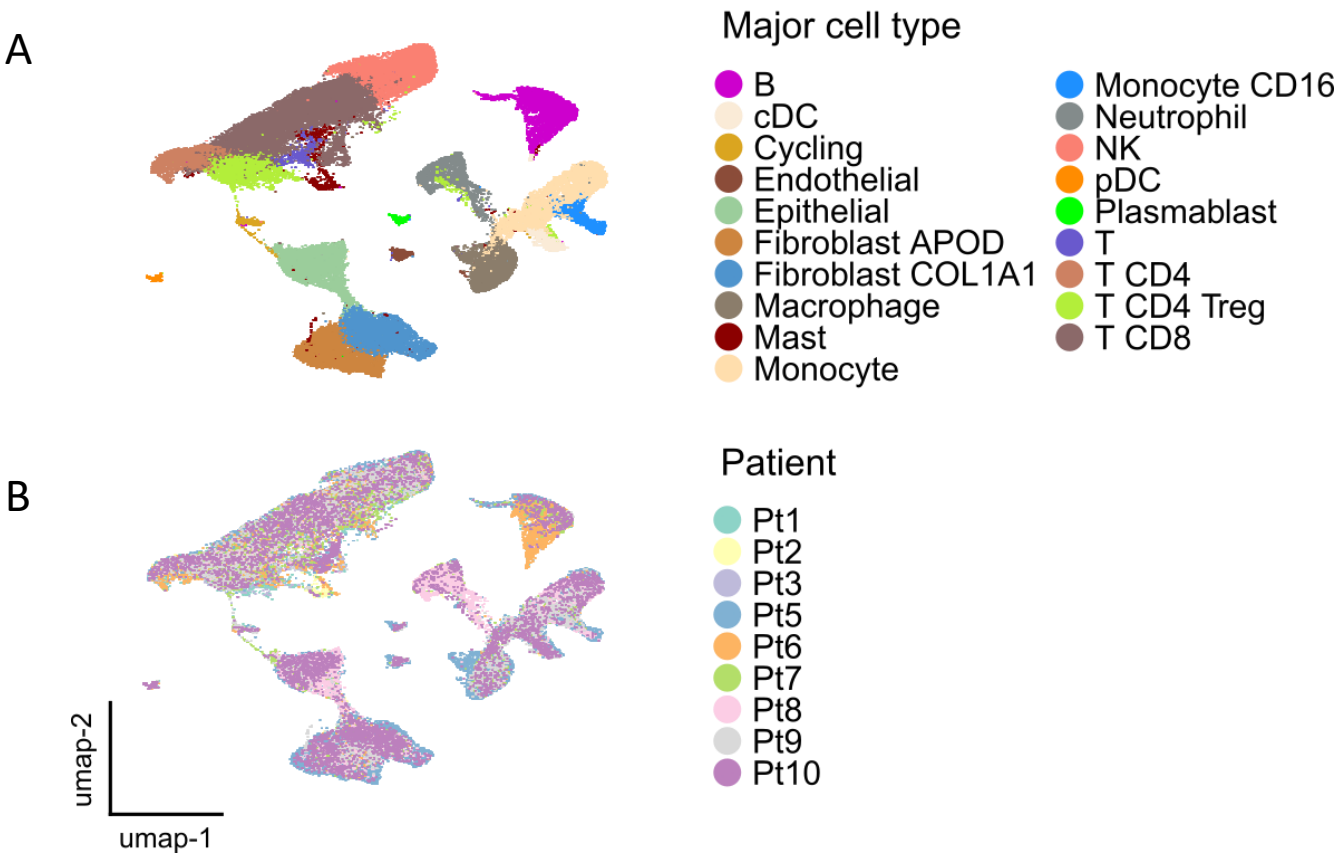


Figure 3.1 Clustering of high-level cell types in omental deposits from HGSOvCa patients. UMAP embedding of integrated scRNAseq data overlaid with high level cell type clusters (A) and patient source (B). The patient with normal omentum is labelled Pt5, while Pt4 was the non-OC sample and has been excluded from the analysis.

Canonical high-level cell marker genes were used to identify the different cell types. The raised expression of the specific marker genes by individual cells allowed cells to be clustered into the 19 subpopulations. (Figures 3.2 and 3.3). Within the CD45+ immune cells, the NK subpopulation was identified through high expression of *NKG7* (natural killer cell protein granule 7), which regulates NK cytotoxicity and influences tumour growth, and *PTPRC* (protein tyrosine phosphatase, receptor type C) which encodes the CD45 antigen [310, 311]. The CD4+ and CD8+ T cells were identified through elevated expression of *CD3G* (T-cell glycoprotein CD3 gamma chain), which is part of the T cell receptor, whilst the CD8+ T cell cluster expressed *CD8A* (CD8 antigen) and CD4+ Treg cells expressed high levels of *FOXP3*

(forkhead box P3) [312-314]. The neutrophil subpopulation had increased expression of *S100P*, the intracellular protein involved in neutrophil activation [315]. The monocyte differentiation marker *CD14* and gene *LYZ* (lysozyme) identified these cell clusters [316, 317]. Macrophages also expressed *CD163*, the scavenger receptor that is a macrophage transmembrane protein [318]. B cells were recognised with high *MS4A1* (membrane spanning 4-domains A1) expression, which is involved in B cell differentiation [319].

Of the non-immune cell populations, epithelial cells were identified with the gene *KRT18* (keratin 18), which encodes the filament chains found in epithelial tissues [320]. Within the high-level epithelial cell subpopulation, there was a subset of tumour cells with enhanced expression of OC biomarkers *MUC16* and *WFDC2*. *PECAM1* (platelet and endothelial cell adhesion molecule 1), a signalling receptor in blood and vascular cells, was used to identify the endothelial cell population [321]. The fibroblast cluster was detected with highly expressed *DCN* (the proteoglycan decorin which is produced by fibroblasts in the stroma), *COL1A1* (the gene collagen type I alpha 1, that is expressed by fibroblasts and produces collagen) and *MFAP5* (the glycoprotein microfibril associated protein 5 within the extracellular matrix) [322-325]. The cycling, or proliferating, cells were represented by raised *MK167*, which encodes the proliferation marker Ki-67 [326].

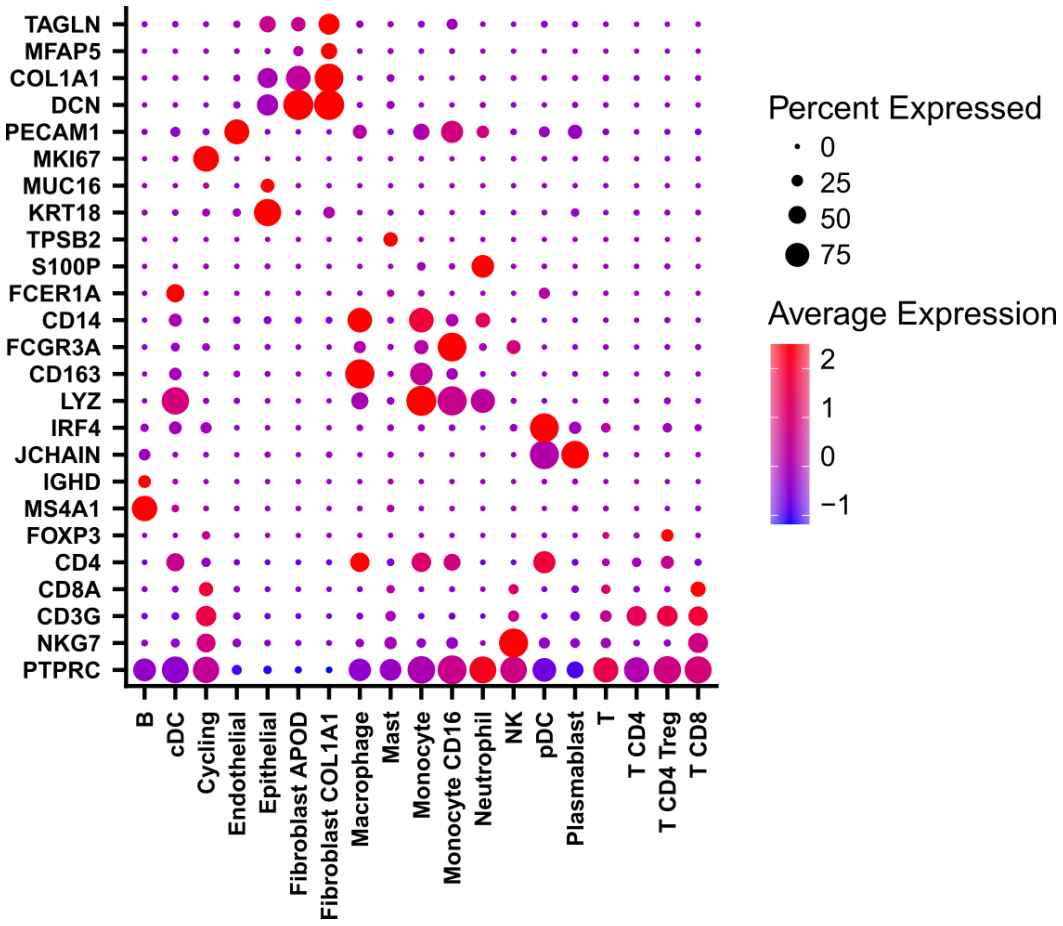


Figure 3.2 Markers utilised to identify major cell types

Dotplot showing average cluster-wise expression profile of a panel of canonical high-level cell type marker genes. The size of the dots indicates the proportion of cells within the cluster that are expressing a given gene.

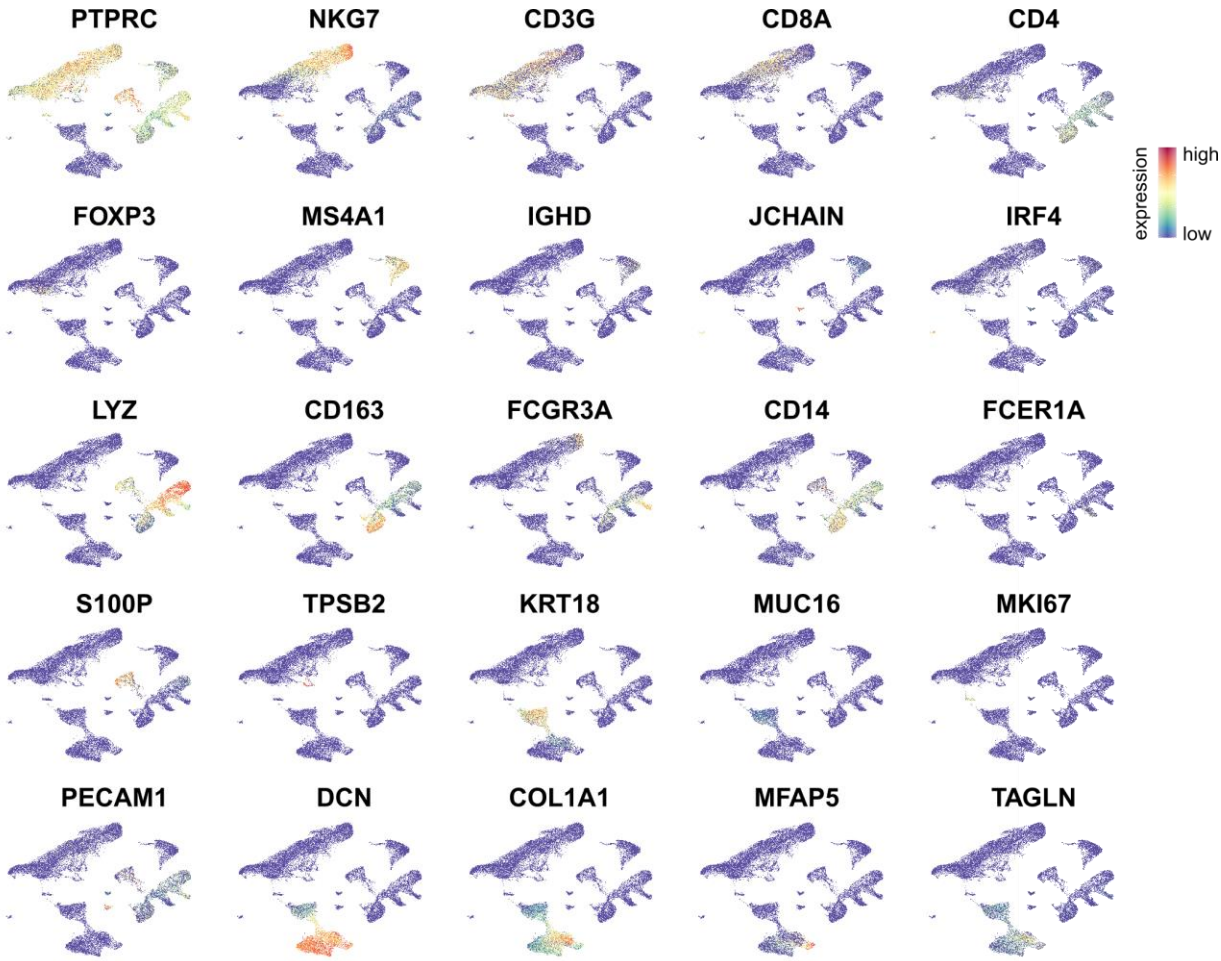


Figure 3.3 Identification of major cell types within omental samples.
UMAP embeddings overlaid with the expression of key marker genes for the major high-level cell types within omental tumour samples.

3.2.3.2 Cell clustering according to tissue type and OC treatment

The integrated data for the 8 omental tumour samples was then divided according to the treatment received: PDS (chemotherapy-naive) or NACT (chemotherapy-exposed), and compared to the single normal omentum sample (Figure 3.4).

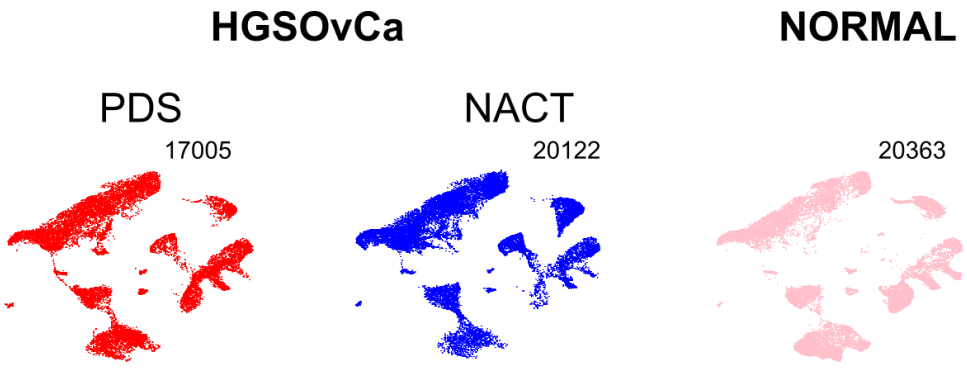


Figure 3.4 Clustering of cells based on treatment and tissue type.
UMAP embedding of integrated OC tissue scRNAseq data split by treatment condition (PDS/NACT) compared to the UMAP embedding of a single normal omentum sample. The total cell number is dictated above each plot.

The data suggest that chemotherapy exposure alters the proportion of cell types present in the tumour microenvironment (Figure 3.5). The combined NACT samples have increased CD8+ and CD4+ T cells, neutrophils and B cells, alongside reduced proportions of monocytes, macrophages and fibroblasts, when compared to the PDS samples. Omental tumour samples have a greater proportion of CD8+ and CD4+ T cells, neutrophils, mast cells and B cells compared to normal omentum whilst the normal omentum has increased macrophages and fibroblasts.

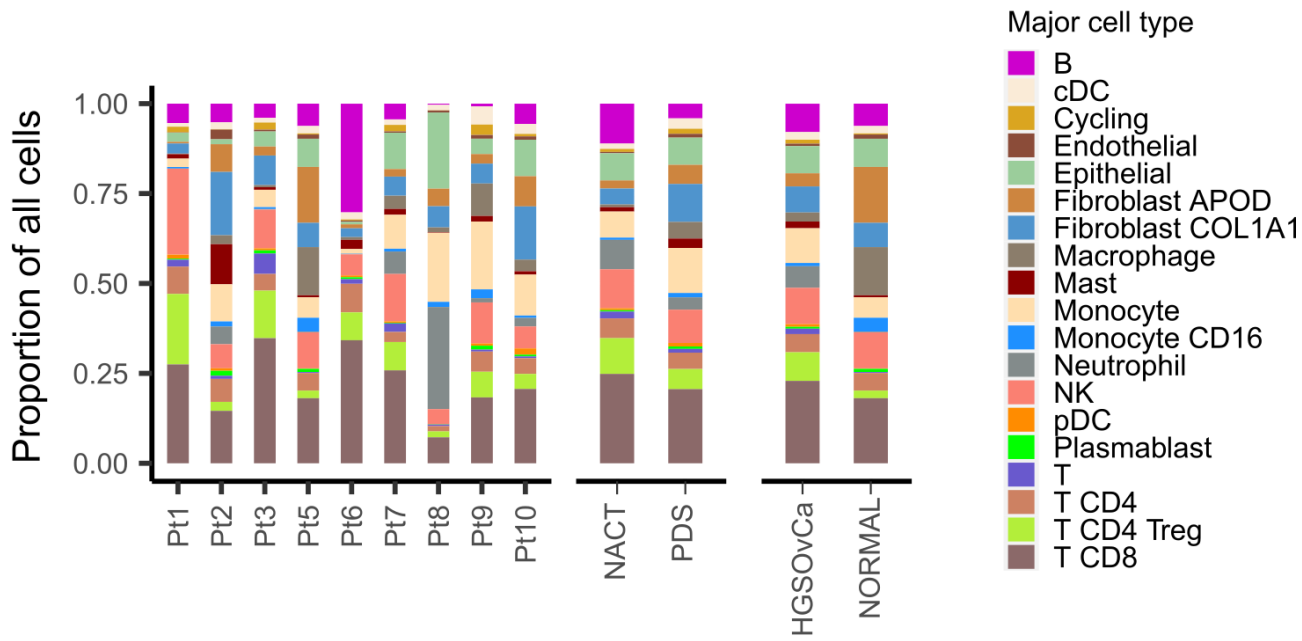


Figure 3.5 Profile of major cell type proportions by sample, treatment and tissue type.
Compositions of major lineage cell types within each omental sample, treatment category (NACT vs PDS) and tissue type (omentum with HGSOvCa/tumour deposits vs normal omentum).

Comparison of CD45+ and CD45- cells showed similar amounts of endothelial cells between the omental tumour samples and the normal omentum sample (Figure 3.6). Omental tumour had greater proportions of epithelial cells and COL1A1 fibroblasts, the cancer-associated fibroblasts, while APOD fibroblasts (normal adipose-derived stromal cells) were increased in the normal omentum [327]. Macrophages and NK cells were raised in normal omental tissue, with omental tumour consisting of more mast cells, monocytes, neutrophils and Treg cells. The other cell types (B cells, dendritic cells, cycling cells, plasmablasts, CD4+ and CD8+ T cells) were similar between the normal and malignant omental tumour.

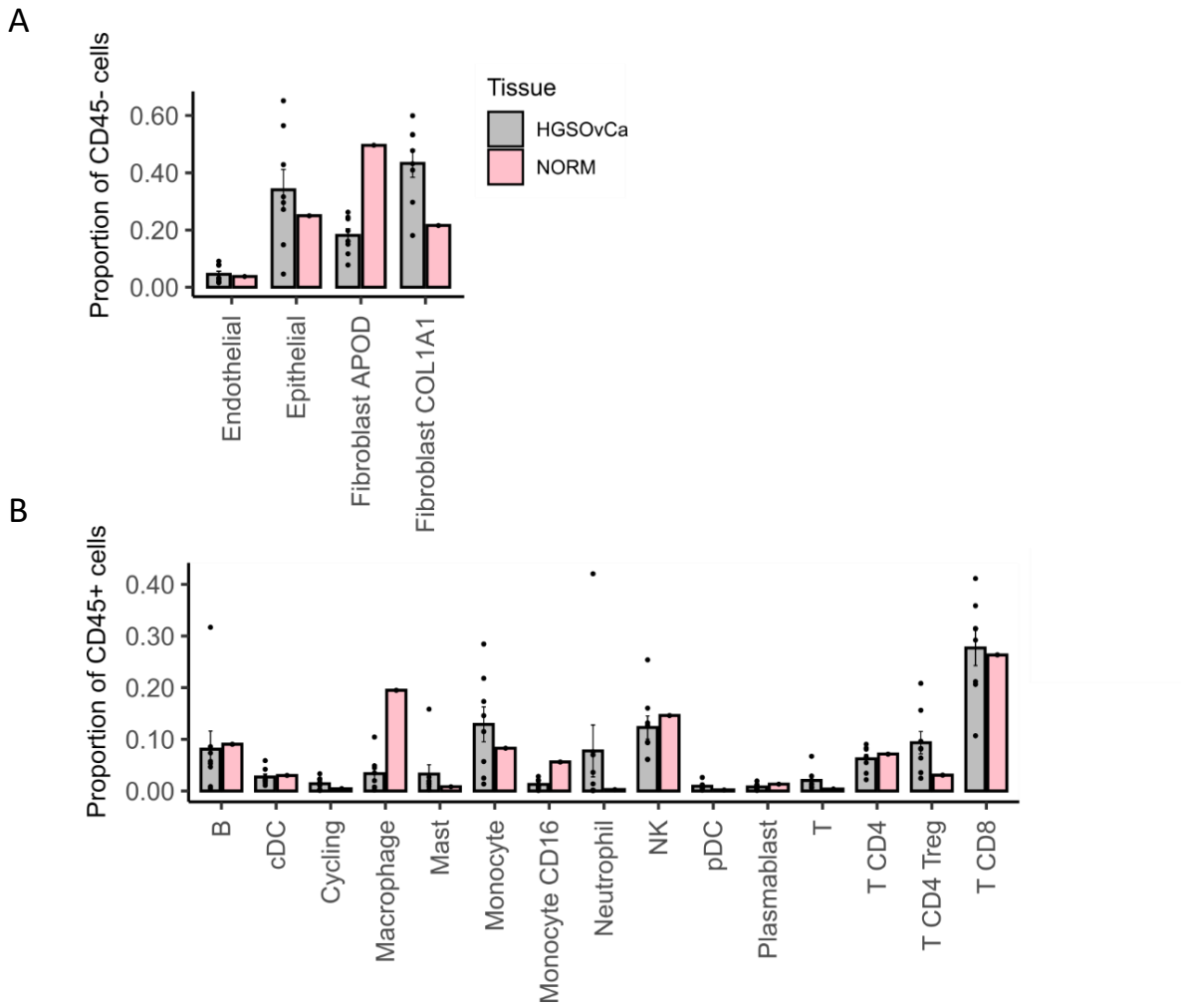


Figure 3.6 The proportion of major cell types in the CD45+ve and CD45-ve populations based on tissue type.

The proportion of major lineage cell types within the non-immune (A) and immune cell (B) compartments, stratified by HGSOvCa and normal omental tissue.

3.2.3.3 Annotation of major cell types with chemotherapy exposure

CD45+ and CD45- populations were then stratified by exposure to chemotherapy treatment (Figure 3.7). The only significant alteration was a reduction in the proportion of macrophages following chemotherapy (NACT group) ($p < 0.03$). Although there were trends with NACT, particularly reduced endothelial, monocytes, mast and dendritic cells, along with increased epithelial, B, Treg and CD8+ T cells, these differences were not significant.

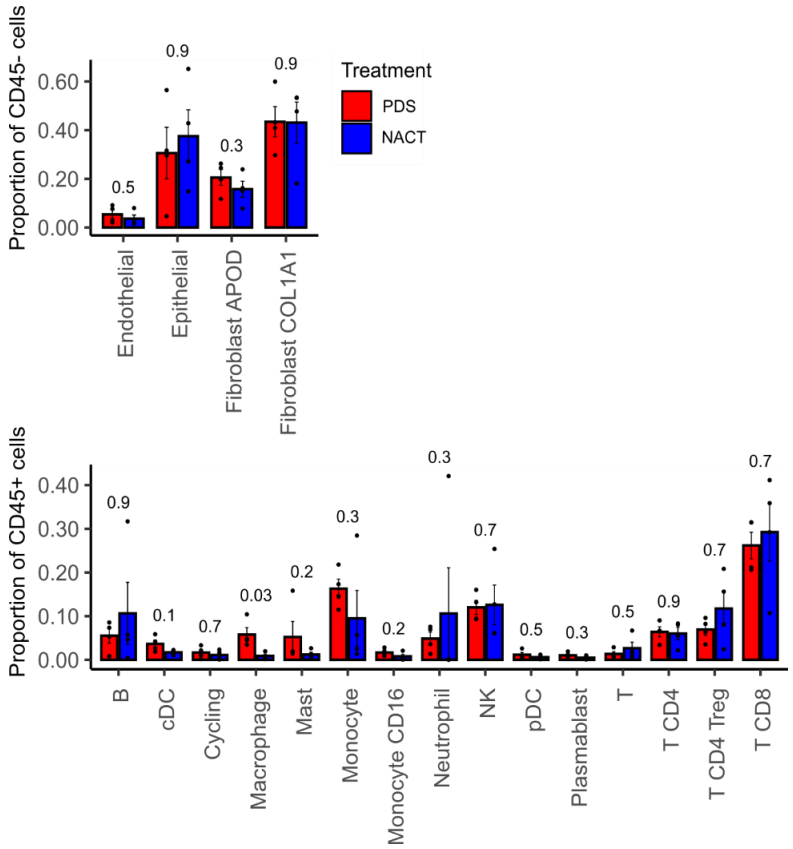


Figure 3.7: The proportion of major cell types in the CD45-ve and CD45+ve populations based on NACT treatment.

The proportion of major lineage cell types within the non-immune and immune cell compartments of OC omental metastatic tissue, stratified by NACT treatment (PDS vs NACT).

The genes expressed by the major cell types were compared between the chemotherapy-naïve group (labelled 'pre') and the chemotherapy-exposed group (labelled 'post'). The modulation of gene expression following chemotherapy exposure is shown in Figure 3.8, indicating the cell populations which were most affected by treatment. By observing the differentially expressed genes (DEGs), it was evident that the epithelial cells, fibroblasts and myeloid populations were the most transcriptionally divergent following chemotherapy. The differential gene expression analysis of pre versus post treatment demonstrated over-expression of the *MGP* gene by epithelial cells following chemotherapy, while *PPP1R14B* was expressed significantly more by the pre-chemotherapy epithelial cells.

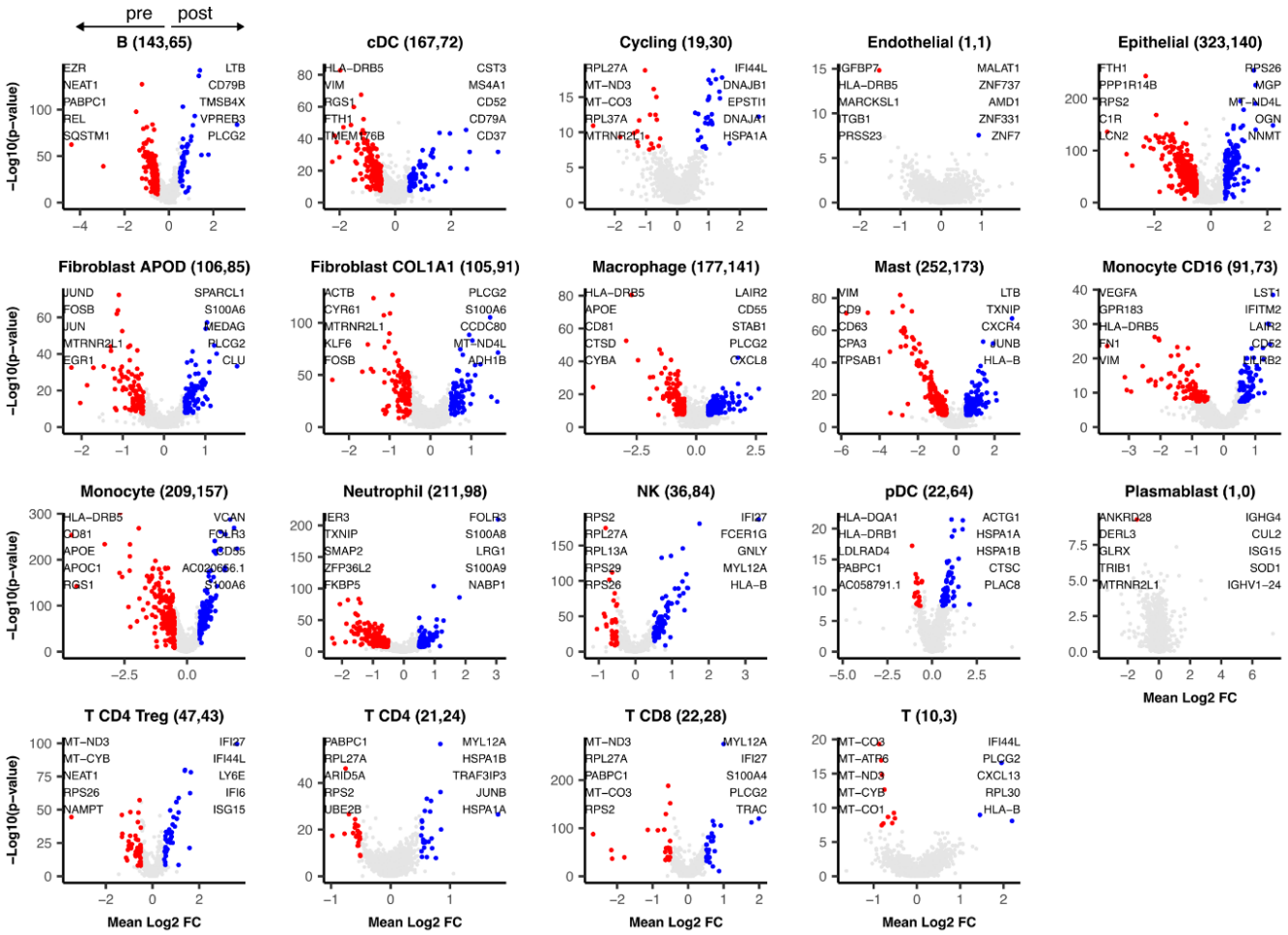


Figure 3.8: Modulation of gene expression within major cell types following chemotherapy exposure.

Summary of genes identified as differentially expressed in comparison of post-chemotherapy (NACT group) to pre-chemotherapy (PDS group) samples. Total DEG counts are noted alongside the cell type label. Coloured points indicate DEGs (Benjamini Hochberg adjusted $p < 0.01$), with those coloured red indicating genes expressed significantly more in pre-chemotherapy tissue and blue points indicating genes over-expressed in post-chemotherapy tissue.

Focusing on the 4 patients who had NACT, CD45+ and CD45- cells were stratified by the chemotherapy response score (CRS; described in the Methods section 2.1.3.1). There were 3 patients with CRS 2 (moderate response) and 1 patient with CRS 3 (complete response). The patient that demonstrated a complete response had elevated epithelial cells and reduced COL1A1 (cancer-associated) fibroblasts compared to the patients with CRS 2 and also to the primary surgery patients, who had not been exposed to chemotherapy (Figure 3.9). The patient with CRS 3 also had increased proportions of monocytes and neutrophils, plus fewer B cells, NK cells and T cells.

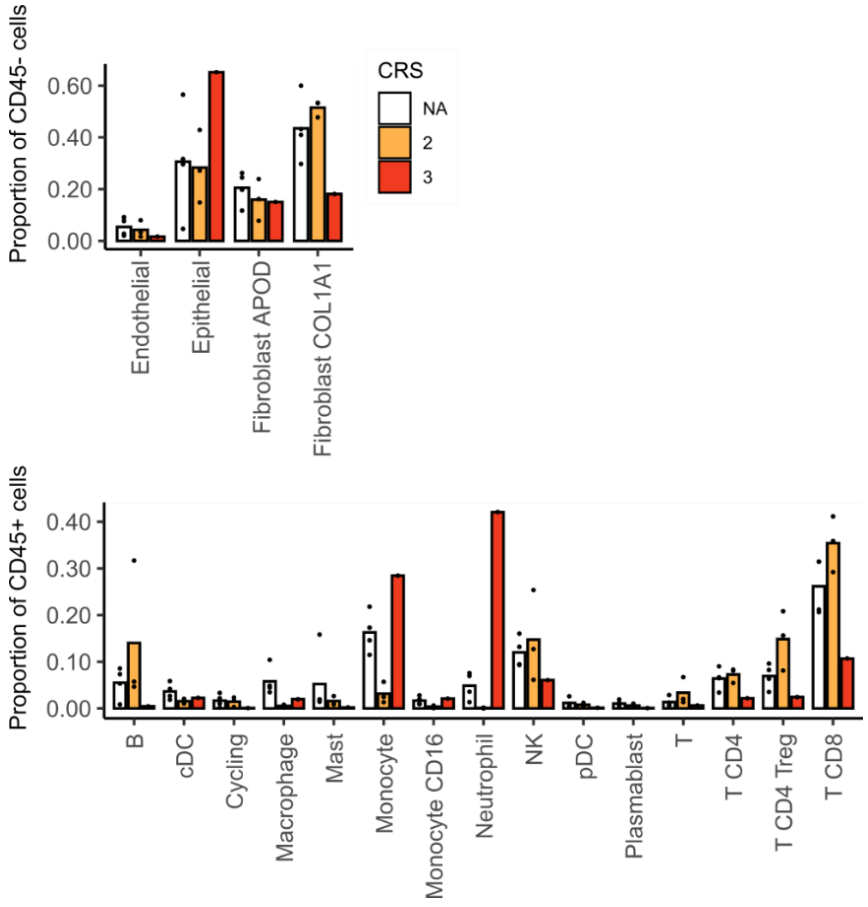


Figure 3.9: The proportion of cell types in the CD45-ve and CD45+ve populations based on chemotherapy response score.

The proportion of major lineage cell types within the non-immune and immune cell compartments of OC omental metastasis tissue stratified by chemotherapy response score (CRS).

The same analysis was undertaken on the 4 patients who had received NACT, but patients were divided into those who did not recur within 18 months following completion of treatment (n=2) and those who did have a recurrence of OC within 18 months (n=2) (Figure 3.10). Of the non-immune cell types, there was no difference in the proportion of epithelial cells between the two groups. Although not significant, those that recurred had a higher proportion of COL1A1 fibroblasts and fewer APOD fibroblasts and endothelial cells. In the immune cell population, patients who recurred had a trend towards higher proportions of CD8+ T cells, Treg cells, NK cells and cycling cells. The recurrence patients also had reduced proportions of B cells, macrophages, monocytes and neutrophils.

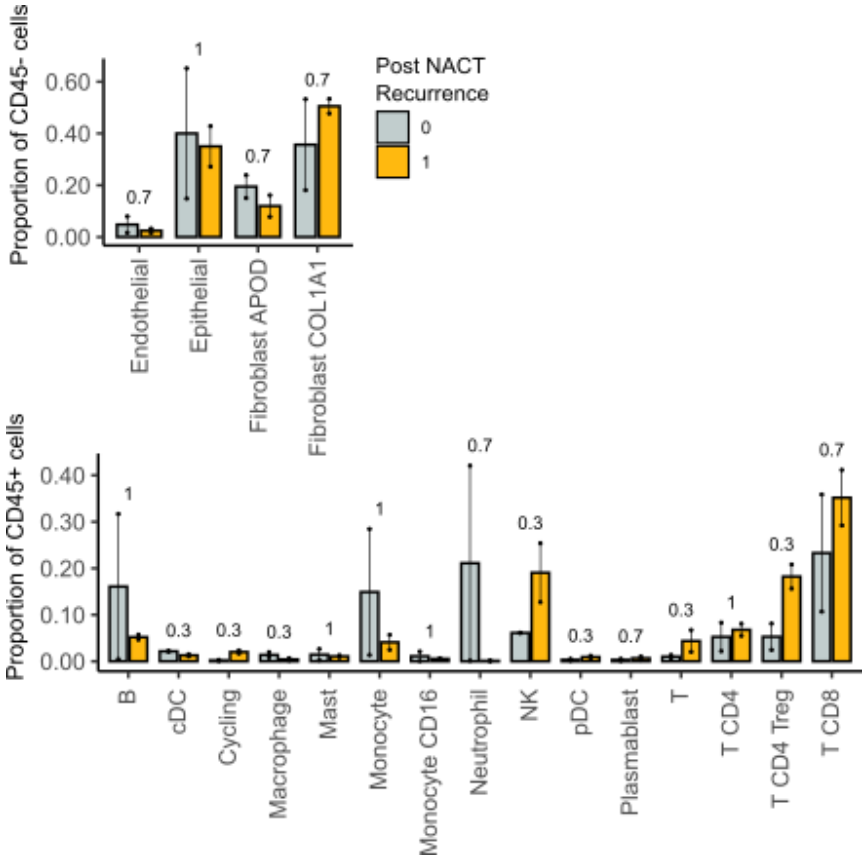


Figure 3.10 The proportion of cell types in the CD45-ve and CD45+ve populations based on disease recurrence within 18 months following chemotherapy treatment.

The proportion of major lineage cell types within the non-immune and immune cell compartments of chemotherapy-treated, metastatic omental tumour tissue, stratified by disease recurrence within 18 months following chemotherapy (0: no recurrence, 1: HGSOvCa recurred following completion of treatment).

3.2.3.4 Interrogation of NK cell ligands within omental tissue

A finer analysis then focused on NK cells and their relationship with the omental tissue. The expression of NK ligands on major cell types was examined initially. Figure 3.11 shows the average expression of key NK activating and inhibitory ligands on the 19 major cell types described previously. The ligands that activate NK cells included MICB/A, ULBP1/2/3, PVR (CD155), Nectin-2 (PVRL2 or CD112). The ligands that inhibit NK cells were HLA-E, CD274 (PDL-1), Nectin-1 (PVRL1 or CD111), PDCD1LG2 (PD-L2), Nectin-3 (PVRL3 or CD113), MUC16 (CA-125) and Nectin-4 (PVRL4). Based on the expression patterns of these ligands, the degree of NK stimulation and the overriding behaviour of the major cells towards NK cells could be postulated. The epithelial cell population had high expression of MUC16 and Nectin-4, which implies an inhibiting function toward NK cells. Endothelial cells showed high levels of Nectin-2 and PVR, which are ligands for both the activating receptor DNAM-1 and the inhibitory receptors TIGIT and CD96. The fibroblast populations seemed to be inhibitory towards NK cells, with elevated expression of inhibitory ligands Nectin-1/2/3 and PD-L2. There were high expression levels of the NKG2D ligands on the immune cell populations, which could be an indicator of the activation status of these cells.

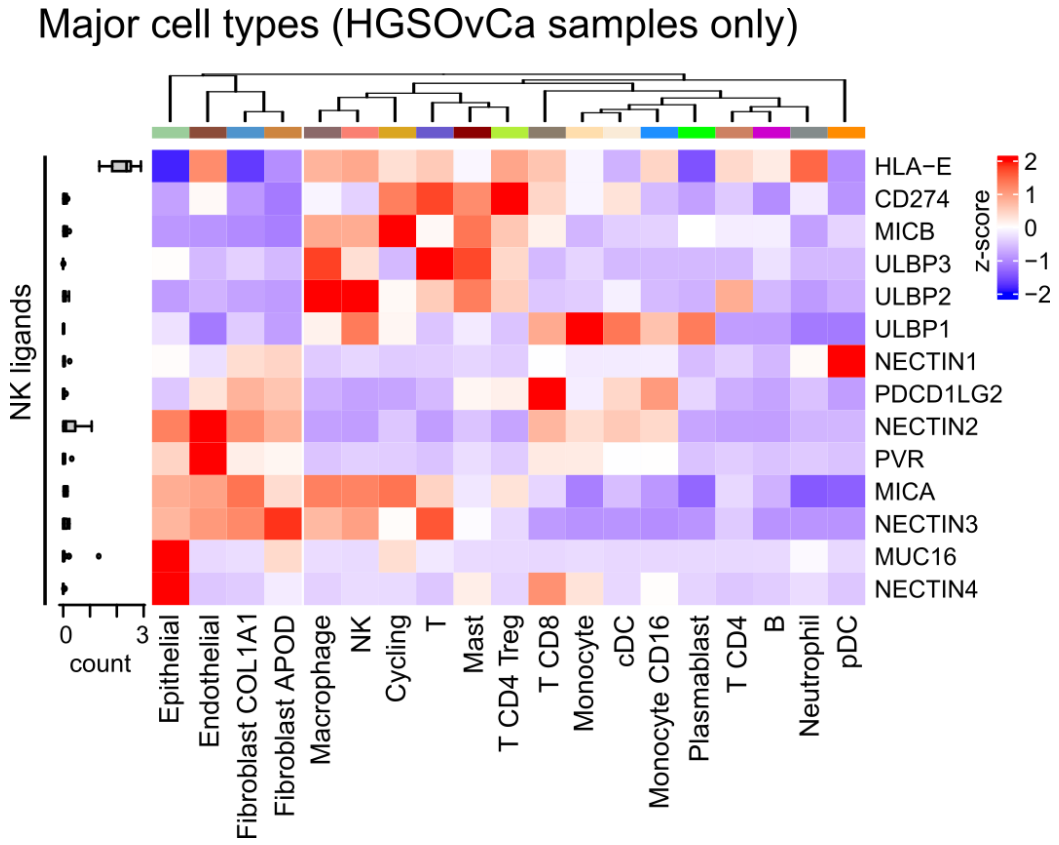


Figure 3.11: The expression of NK cell ligands on major cell types within omental tumour.
Cluster-wise average expression profile (heatmap) and UMI count (boxplots) of selected NK ligands of interest.

The modifications in NK ligand expression following exposure to chemotherapy were then examined in the non-immune cell populations. Figure 3.12 demonstrates the differential expression of the key NK ligands between the chemotherapy-naïve (pre-NACT) and the chemotherapy-exposed (post-NACT) groups. The epithelial cell population in the chemotherapy-naive tissue was typically inhibitory, with greater expression of ligands MUC16, Nectin-2, Nectin-5 and HLA-E. There were no other significant changes in expression across the different cell populations.

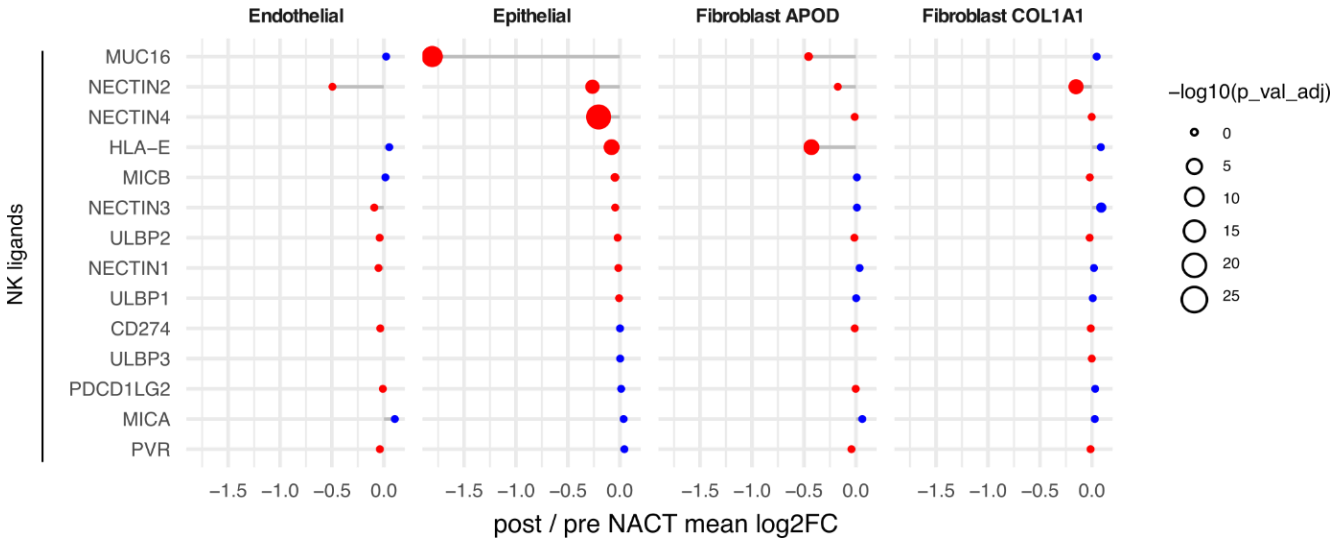


Figure 3.12: Profile of differential expression of NK ligands following chemotherapy exposure. The differential expression of NK ligands on Endothelial, Epithelial and Fibroblast cells in post-chemotherapy (NACT group) vs pre-chemotherapy (PDS group), where red dots represent increased expression pre-chemotherapy and blue represent greater expression post-chemotherapy.

3.2.3.5 Clustering and identification of NK cell subpopulations

Finer analysis of the NK cells identified 5 different subpopulations across the 9 omental samples (Figure 3.13) based on differential expression of key marker genes (Figure 3.14). These allowed functional allocation of cell subtypes (Figure 3.15). A cytotoxic NK subset was seen with high expression of cytotoxicity marker genes *NKG7, FGFBP2, GZMB* and *FCGR3A.* A similar subset but with raised activation markers *CCL4* and *CCL4L2* was identified as an activated NK subset. An exhausted NK subset had low levels of the cytotoxic marker *GZMB,* no CD16, and raised inhibitory markers *KLRC1* and *GZMK*. In addition, there were tissue resident (with increased *CCL4*, *CCL3*, *JUN*, *HSPA1A* and *CD69* genes) and immature (increased *IL7R, TPT1, AREG* and *XCL1/2* genes) NK clusters. The population of NK cells as a whole was comprised of relatively equal proportions of these subsets, except for the immature NK subpopulation which was comparatively smaller than the other subpopulations.

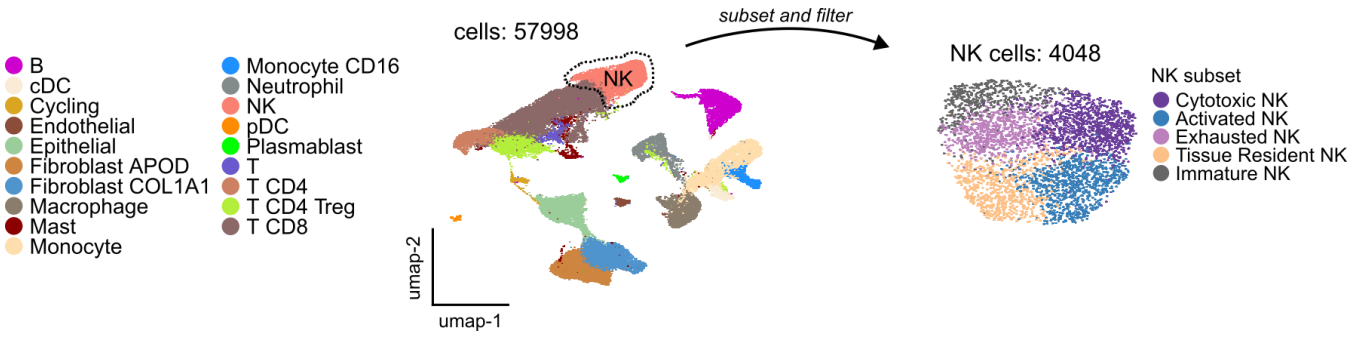


Figure 3.13: Clustering of the major lymphocyte cell populations in all omental samples.
UMAP embedding of isolated NK cell populations overlaid with the NK cell subpopulations identified by unsupervised clustering.

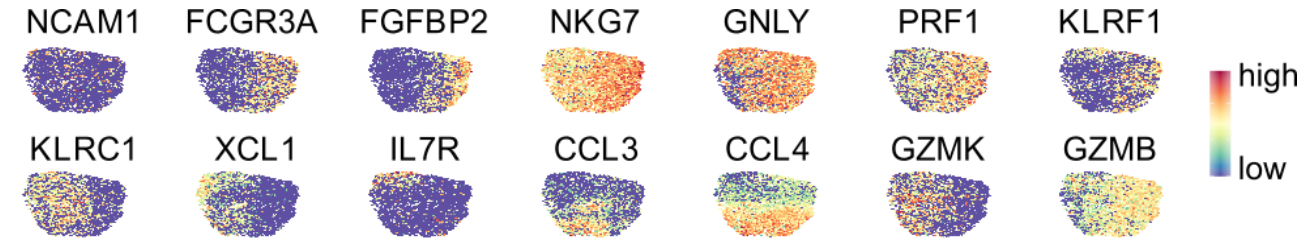


Figure 3.14: Identification of NK subtypes within omental tissue.
UMAP embeddings of NK cells overlaid with the expression of marker genes for NK cell subtypes.

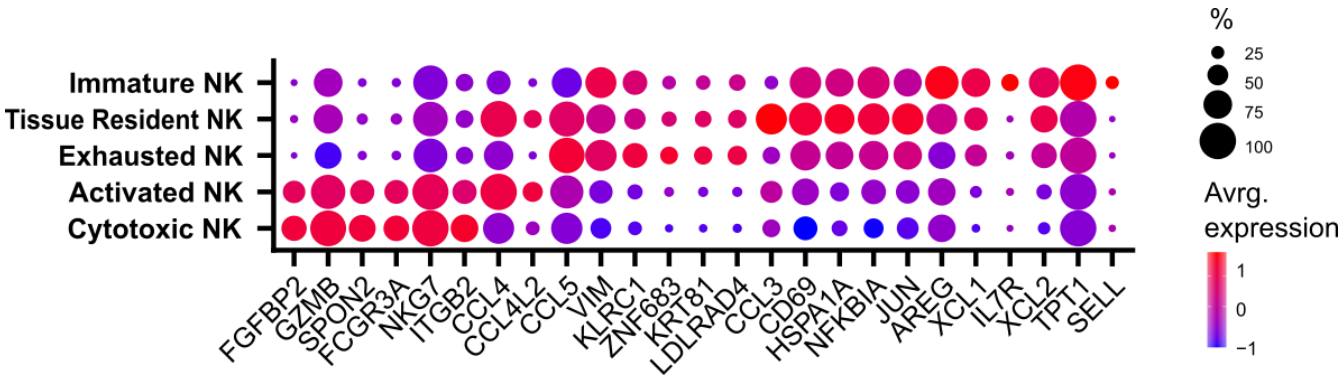


Figure 3.15 Expression of makers genes within the different NK cell clusters.
Dotplot to show the average expression of the top marker genes identified as being overexpressed in NK subpopulations. The size of the dots indicates the proportion of cells within the cluster that are expressing the given gene.

3.2.3.6 Interrogation of the NK cell clusters according to tissue type and OC treatment

The NK cell subtypes were then reviewed separately in the omental tumour (n=8) and normal omental (n=1) samples. NK cell marker genes that are representative for NK function were compared between these two groups (Figure 3.16). The expression of genes for NK cytotoxicity were greater across the clusters in the normal omental sample, with few cells in the tumour samples having high expression of the same genes. Agreeing with this, the normal sample had increased expression of the genes for activating receptors, while gene expression for NK exhaustion and inhibitory receptors were higher in the tumour samples.

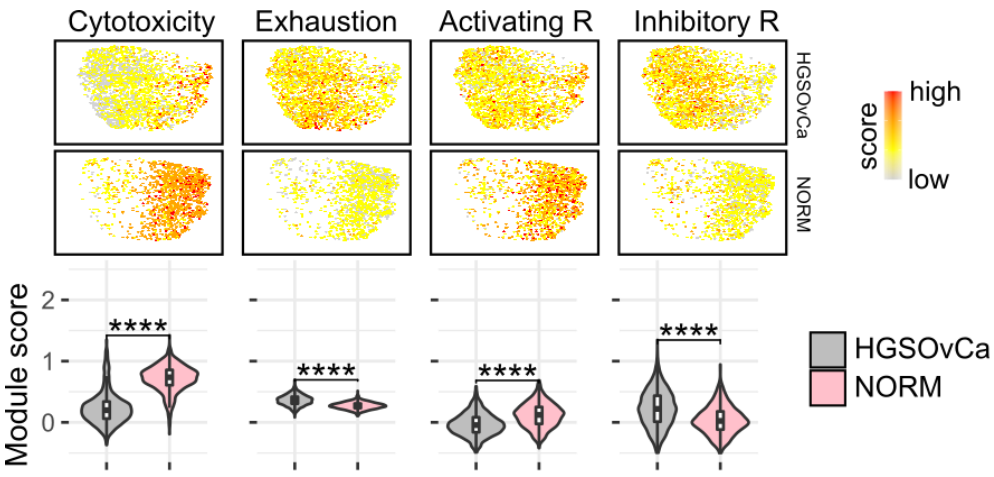


Figure 3.16 Gene expression of NK cell marker genes depicting NK cell function.
UMAP embeddings overlaid with signature module scores for NK cytotoxicity, exhaustion, activating receptors and inhibitory receptors (A). The distributions of module scores stratified by tissue type, comparing omental tumour and normal omentum in HGSOvCa patients (B).

The expression profiles of NK activation and inhibitory receptors were then compared between the tumour and normal omental samples (Figure 3.17). The normal and malignant omentum demonstrated raised expression of both activating and inhibiting receptor genes, with no clear patterns between the two groups. When focusing on the treatment type (PDS compared to NACT), the samples exposed to chemotherapy had raised expression of the genes for NK

activation receptors compared to the chemotherapy-naïve (PDS) group. Increased expression of various genes for NK inhibitory receptors were seen in both of the treatment groups. Next, the expression of the same receptor genes was examined in the NK subsets; the subpopulations all had raised expression of numerous activating receptor genes, apart from the tissue resident cluster where few activating genes were highly expressed. The exhausted and tissue resident NK clusters had a greater number of inhibitory receptor genes that were highly expressed, with minimal overexpression seen in the cytotoxic and activated NK clusters.

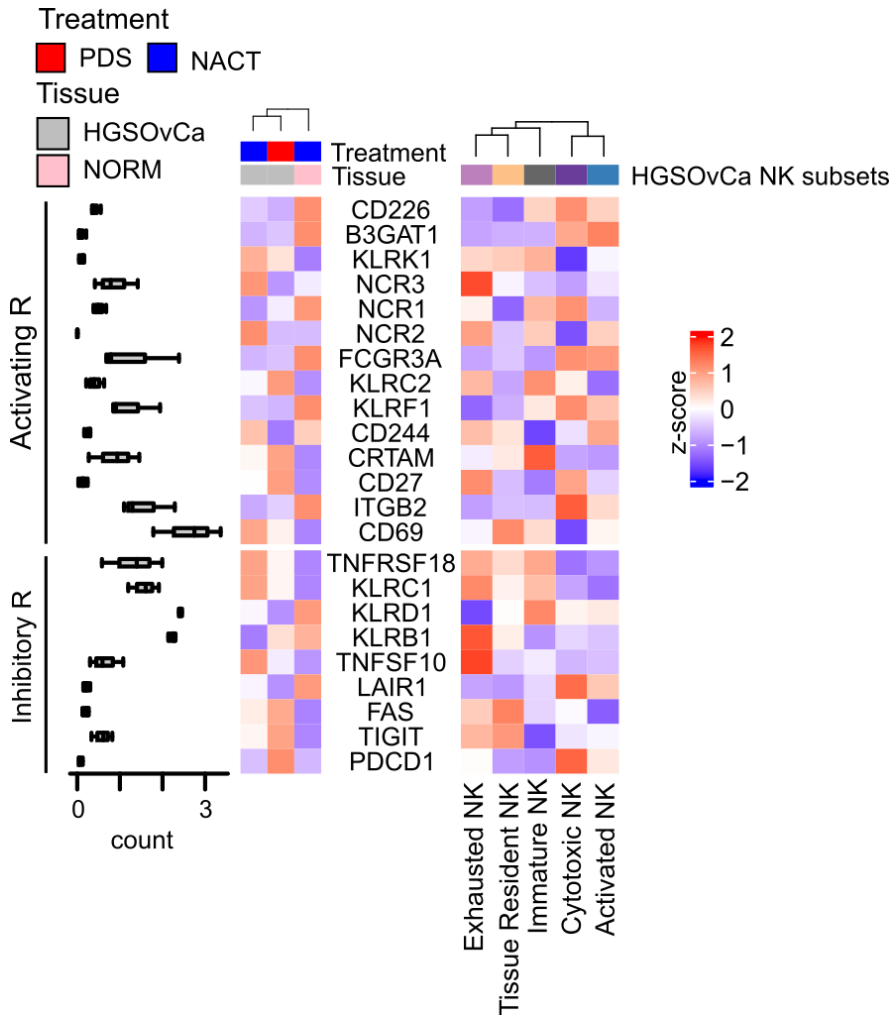


Figure 3.17: Expression profile of receptors for NK activation and inhibition.
Average scaled expression across tissue type / chemotherapy treatment (left heatmap) and average NK cluster-wise expression profile (right heatmap) of NK receptor genes. Boxplots represent total NK raw UMI count for each gene.

The expression profile of the genes for NK cytokines were explored (Figure 3.18), clearly showing increased expression in the omental tumour samples than in the normal omental samples. Within the tumour samples, those that had been exposed to chemotherapy had a greater number of highly expressed cytokine genes than the chemotherapy-naïve omental tumour. In addition, highly expressed cytokine genes differed between the NK cell subsets, with each NK subset having raised expression of different cytokines. The exhausted cluster demonstrated increased expression of the largest number of cytokine genes and also the highest levels of cytokine overexpression. While the tissue resident NK subset also had raised expression of a number of cytokine genes, fewer genes were highly expressed in the activated, cytotoxic and immature NK subsets.

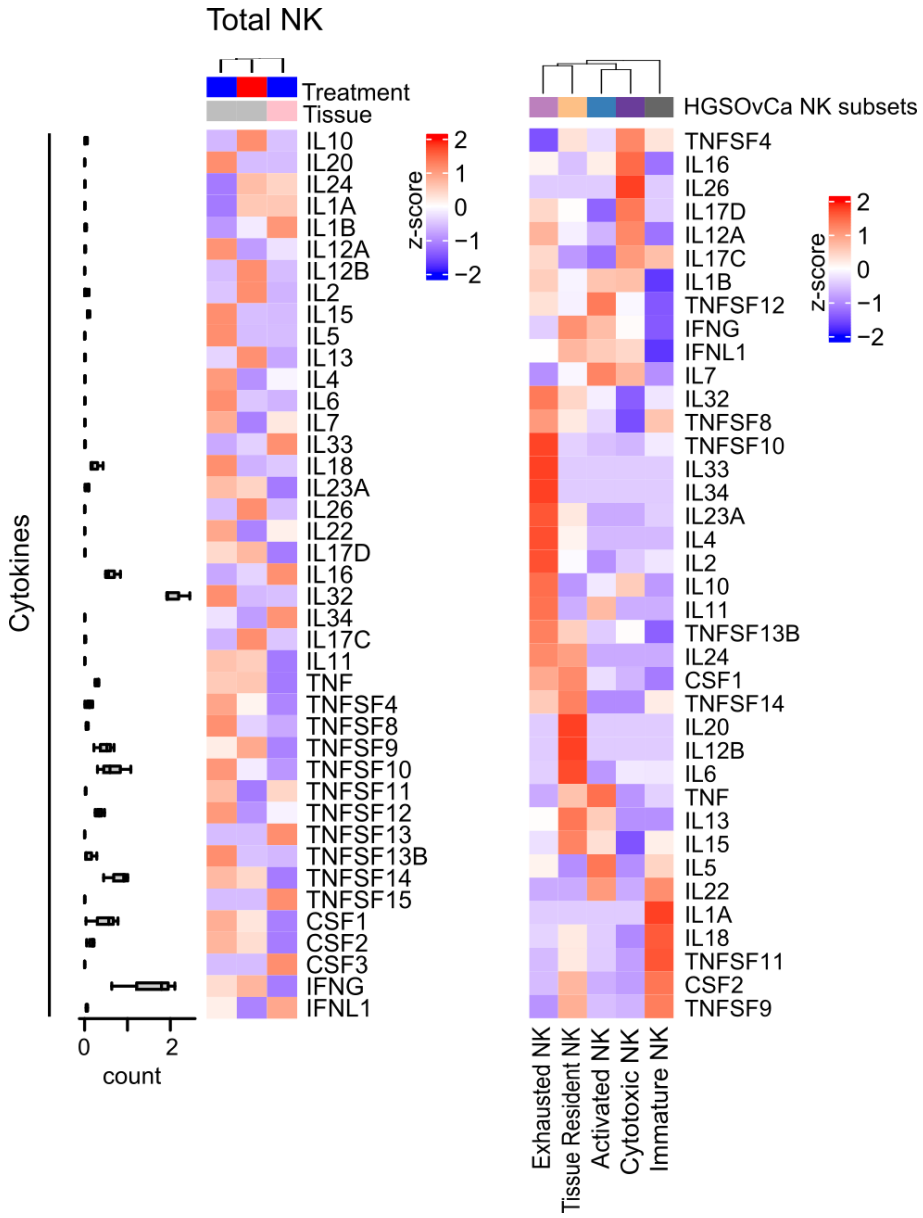


Figure 3.18: Expression profile of genes for NK cytokines.
Average scaled expression across tissue type / chemotherapy treatment (left heatmap) and average NK cluster-wise expression profile (right heatmap) of selected cytokine genes. Boxplots represent total NK raw UMI count for each gene.

The proportion of each of the 5 NK subsets was determined in the samples and compared between tissue type and treatment. Figure 3.19 shows that the normal omental tissue had greater proportions of cytotoxic and activated NK subpopulations than the omental tumour. In comparison, the omentum with HGSOvCa tumour deposits had increased exhausted, immature and tissue resident NK cells. Although not significant, the chemotherapy-exposed tumour had fewer exhausted NK cells alongside higher proportions of activated and cytotoxic NK cells (Figure 3.20).

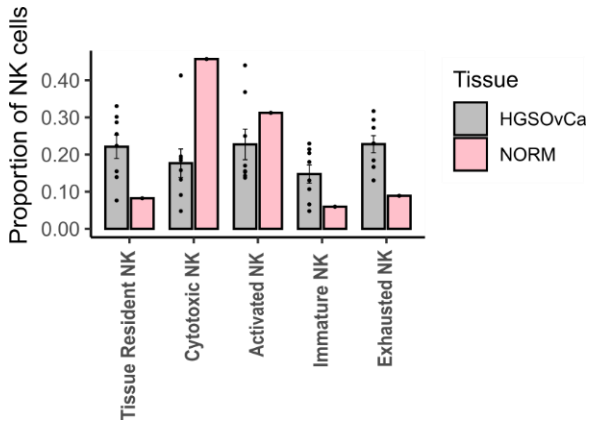


Figure 3.19: The proportion of NK cell clusters based on tissue type.
The proportion of NK cell subtypes in omental tumour and normal omental tissue.

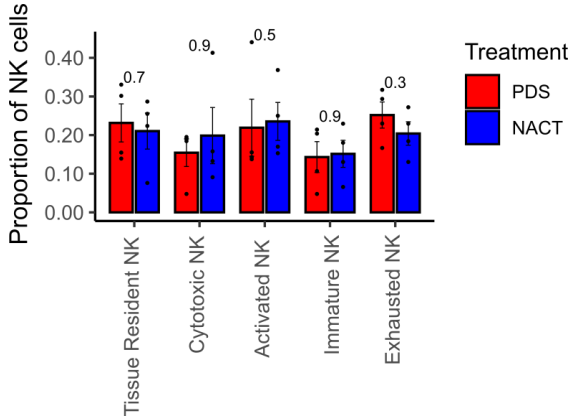


Figure 3.20: The proportion of NK cell clusters based on chemotherapy exposure.
The proportion of NK cell subtypes in the samples prior to (PDS group) and post chemotherapy (NACT group) exposure.

3.2.3.7 Annotation of NK cells with chemotherapy exposure

NK cell clusters were next evaluated according to the cytotoxic effect of chemotherapy towards the omental tumour. By comparing the 3 patients with a moderate chemotherapy response (CRS 2) to the patient with a complete response (CRS 3), there was a greater proportion of activated NK cells and smaller proportion of immature NK cells in patient with CRS 3. Those without a CRS score (PDS group, labelled NA) had an increased proportion of exhausted NK cells compared to the those who had received chemotherapy. This exhausted NK subtype was smallest in the patient with a CRS 3 following neoadjuvant chemotherapy. The proportions of the other NK subsets were similar between the groups.

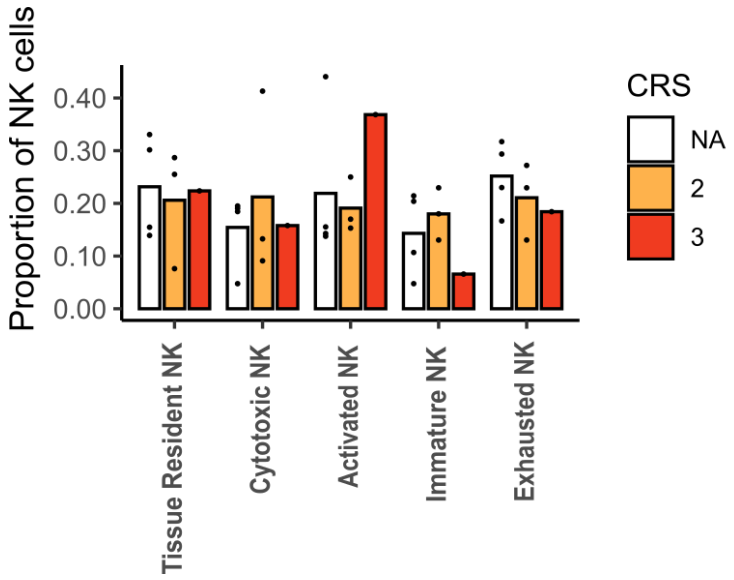


Figure 3.21: The proportion of NK cell clusters by chemotherapy response score.
The proportion of NK cell subtypes stratified according to the tumour response to chemotherapy.

The NK cell clusters varied between those patients with disease recurrence following chemotherapy compared to those who remained disease free (Figure 3.22). Those that recurred had higher proportions of exhausted, immature and tissue resident NK cells, with the disease-free patients having increased cytotoxic and activated NK cells.

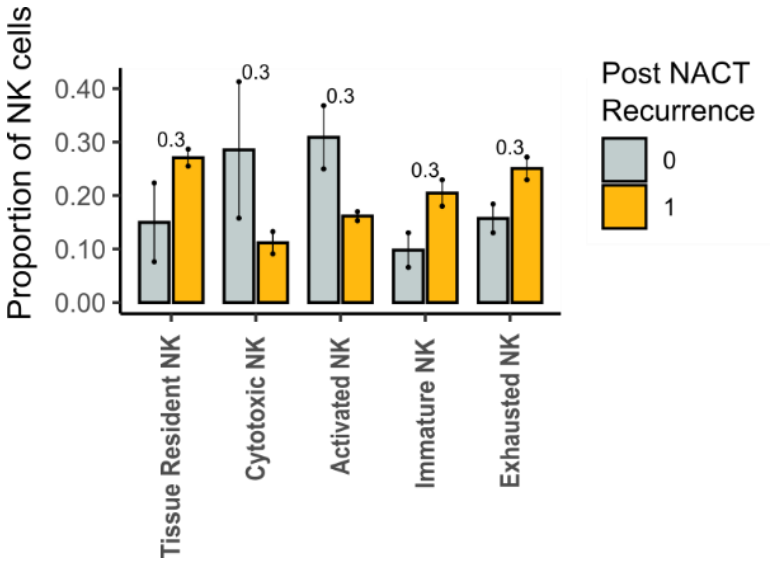


Figure 3.22: The proportion of NK cell clusters by disease recurrence following chemotherapy treatment.
The proportion of NK cell subtypes in those who recurred following chemotherapy (1) compared to those who remained disease free.

Modifications in NK cell gene expression were also seen following chemotherapy exposure. Figure 3.23 shows the genes that were over expressed in the neoadjuvant chemotherapy (post-NACT) and primary surgery (pre-NACT) groups. Following chemotherapy, the most significant changes in NK gene expression were seen in *HLA-B, IFI27, GNLY, FCER1G* and *MYL12A*, all of which were upregulated in response to NACT. In comparison, NK cells in the pre-chemotherapy (PDS) group had increased expression of *MT-CYB, RPS4X* and *RPL27*. Gene set enrichment analysis showed post-chemotherapy enrichments for cytokine production

and an inflammatory response, whilst genes for DNA repair and MYC target genes were enriched prior to treatment. The relative changes in gene expression in the patients who recurred following chemotherapy were seen with over-expression of genes *RGS1*, *BTG1* and *JUN*. Disease recurrence following chemotherapy had gene set enrichments for cytokine production, apoptosis, hypoxia, inflammatory response, epithelial mesenchymal transition and the p53 pathway.

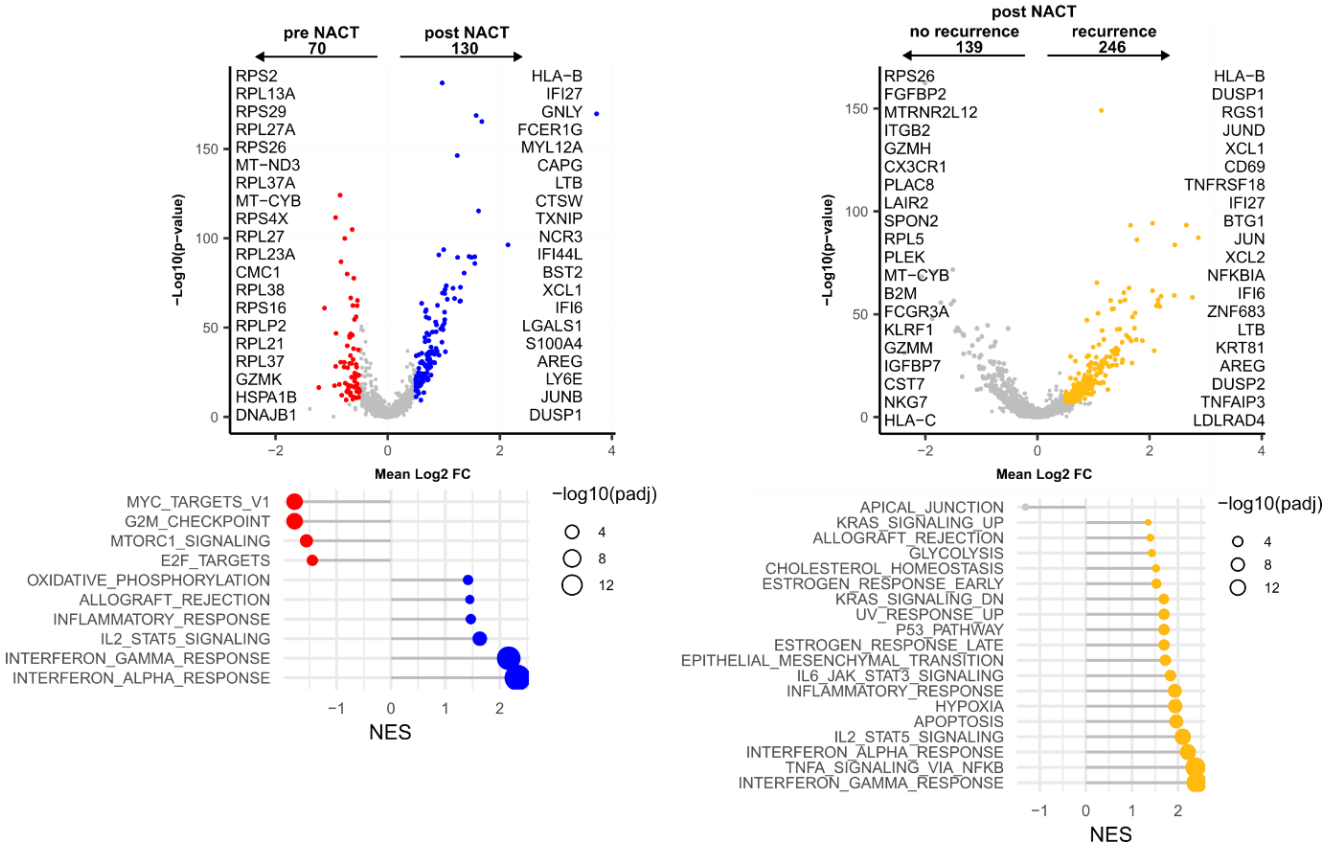


Figure 3.23 Gene expression and functional divergence following chemotherapy treatment and upon disease recurrence.

Summary of genes identified as differentially expressed on NK cells in comparisons of post-chemotherapy (NACT group) vs pre-chemotherapy (PDS group) treatment and no recurrence vs disease recurrence. Coloured points indicate DEGs (Benjamini Hochberg adjusted $p < 0.01$). Significant functional enrichments from GSEA on Hallmark gene sets are displayed below the volcano plots.

3.2.4 Summary of the single cell RNA sequencing analysis in ovarian cancer

A total of 19 transcriptionally distinct major cell types were identified within omental samples from patients with HGSOvCa. While the majority were immune cell populations, a cluster of epithelial cells was detected, which contained a subset of malignant cells. When comparing a normal omental sample with omental tumour samples, greater proportions of epithelial cells and cancer-associated fibroblasts were evident within malignant tissue, with differences in the types of immune populations also seen. Deviations with chemotherapy treatment included changes to the sizes of immune cell populations and variable gene expression profiles. Interestingly, with chemotherapy exposure, the epithelial cell population had upregulation of the *MGP* gene, which is associated with chemoresistance in OC [328].

NK cell ligands expressed by epithelial cells and fibroblasts within omentum were broadly inhibitory towards NK cells. However, modifications with chemotherapy exposure showed elevated activating ligands along with raised checkpoint inhibitors. The finer analysis of the NK cell population identified 5 NK subsets across the omental samples, with differing expression of genes for cytokine production, activation receptors and inhibition receptors in the different subsets. The expression of genes for NK cytokines, cytotoxicity and activating receptors were reduced in omental tumour compared to normal samples, while gene expression for NK exhaustion and inhibitory receptors were increased. As such, tumour tissue had smaller proportions of cytotoxic and activated NK subpopulations alongside larger exhausted, immature and tissue resident NK cell populations. Following chemotherapy, gene expression for NK activation and cytokine production increased, with higher proportions of activated and cytotoxic NK cells in tumour cells. In addition, patients that recurred following chemotherapy had higher proportions of exhausted, immature and tissue resident NK cells, with disease-free patients having increased cytotoxic and activated NK cells.

3.3 Single cell ATAC sequencing of ovarian cancer samples

3.3.1 The sample population

Single cell ATAC sequencing (scATACseq) was undertaken to analyse thousands of individual nuclei within OC tissue biopsies. This analysis of chromatin accessibility detected the open chromatin regions and transcriptionally active genes within each cell. In addition, scATACseq also identified transcription factor binding sites and assisted with evaluating the active genomic pathways. A cohort of 10 samples was obtained from 9 patients with advanced (FIGO stage III/IV) HGSOvCa. Of these, 4 patients had PDS whilst 4 had been treated with platinum-based NACT and then had IDS. Two tissue samples were obtained from a ninth patient, one at the time of diagnosis and then one following NACT at the time of IDS.

The 5 pre-chemotherapy samples (4 from patients undergoing PDS and 1 diagnostic biopsy) were frozen and stored until pathological confirmation of HGSOvCa. The 5 chemotherapy exposed (NACT) samples were obtained from patients who had HGSOvCa confirmed prior to commencing NACT and then underwent IDS. This ensured all processed and sequenced samples had the desired histological diagnosis of HGSOvCa. The tumour biopsies analysed were omental tumour tissues, which corresponded with the scRNAseq samples.

The 9 patients in the cohort were matched for age, ethnicity, disease stage, BRCA status, PCI, CA-125 level and cytoreduction score. Table 3.3 illustrates the characteristics of patients in the cohort, comparing the chemotherapy-naïve (pre-chemotherapy) samples with those following NACT (chemotherapy-exposed samples). Of the 9 patients in the cohort, 4 suffered a recurrence of their disease and subsequently died. Two of these were pre-chemotherapy and two had received NACT. The progression free survival ($p = 0.6962$) and overall survival ($p = 0.8414$) rates between the patient groups were similar.

Table 3.3: Characteristics and baseline variables of patients who provided samples for scATACseq analysis

Variable	Pre-chemotherapy (n=5)	NACT (n=5)	P value
Age (years)			
Mean ± SD	68.6 ± 8.3	64.8 ± 7.7	0.4741
Ethnicity	**n (%)**	**n (%)**	
White	5 (100.0)	4 (80.0)	
Asian	0 (0.0)	1 (20.0)	>0.9999
Disease stage	**n (%)**	**n (%)**	
3	4 80.0)	3 (60.0)	
4	1 (20.0)	2 (40.0)	>0.9999
PCI			
Median (range)	23 (15-30)	16 (12-26)	0.2254
BRCA status	**n (%)**	**n (%)**	
normal	4 (80.0)	5 (100.0)	
mutated	1 (20.0)	0 (0.0)	>0.9999
CA-125 (u/ml)			
Mean ± SD	1251 ± 1303	1380 ± 1270	0.3137
Cytoreduction	**n (%)**	**n (%)**	
R0	3 (60.0)	4 (80.0)	
R2	1 (20.0)	1 (20)	
n/a	1 (20.0)	0 (0.0)	0.8780
Chemotherapy cycles	n/a	**n (%)**	
3		3 (60.0)	
4		2 (40.0)	n/a
Chemotherapy Response Score	n/a	**n (%)**	
2		4 (80.0)	n/a
3		1 (20.0)	
Disease recurrence	**n (%)**	**n (%)**	
Recurred	2 (40.0)	2 (40.0)	
Disease-free	3 (60.0)	3 (60.0)	>0.9999
Survival	**n (%)**	**n (%)**	
Died	2 (40.0)	2 (40.0)	
Alive	3 (60.0)	3 (60.0)	>0.9999

3.3.2 Preparation of specimens

Individual nuclei were extracted from whole tissue samples that had been snap frozen immediately after surgical resection (described in the Methodology section 2.3.2). These individual nuclei were sequenced, with bioinformatic analysis detecting open chromatin regions to measure chromatin accessibility and the transcriptionally active genes within each cell. The number of nuclei sequenced and analysed (Table 3.4) from the OC tumour biopsies ranged from 916 to 7254 for the pre-chemotherapy (chemotherapy naïve) samples and 568 to 2931 for the NACT (chemotherapy exposed) samples.

Table 3.4: The nuclei sequenced in each sample in the scATAC cohort

Sample	Treatment group	Chemotherapy exposure	Nuclei sequenced
1	Pre-chemotherapy PDS	Nil	7254
2	Pre-chemotherapy PDS	Nil	4716
3	Pre-chemotherapy PDS	Nil	1989
4	Pre-chemotherapy PDS	Nil	916
5	Pre-chemotherapy diagnostic biopsy	Nil	3973
6	NACT + IDS	4 cycles	2105
7	NACT + IDS	4 cycles	1443
8	NACT + IDS	4 cycles	2931
9	NACT + IDS	4 cycles	568
10	NACT + IDS	6 cycles	1194

3.3.3 Analysis of single cell ATAC sequencing data

3.3.3.1 Clustering and identification of major cell types

Sequencing analysis generated the data to determine the DNA reads at locations of open chromatin within individual nuclei, as described in Methods section 2.3.2.3. The measurements of chromatin accessibility and recognition of transcriptionally active genes in each cell allowed similar cell types to be clustered together. By combining the data from all 10 samples, 7 different populations of cells were identified. These included the high-level cell types:

lymphocytes, myeloid cells, fibroblasts and epithelial cells. Figure 3.24 demonstrates the clustering of cells from the ten samples with the detection of cell populations.

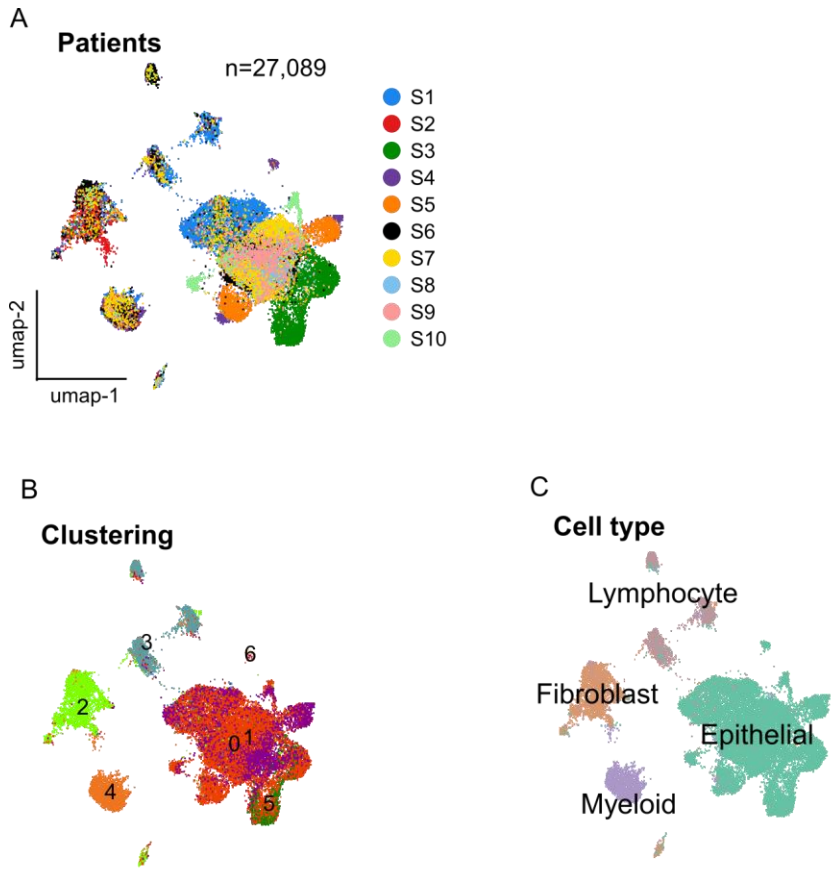


Figure 3.24: Clustering of high-level cell types cells within metastatic omental tumour deposits. UMAP embedding integrates scATACseq data overlaid with patient sample label (A), unsupervised clustering results B) and major lineage cell types (C).

The raised expression of high-level cell marker genes was used to cluster the cells from all samples into different populations and also identify the type of each cell population. Figure 3.25 shows the expression of the key maker genes used to classify the 4 major cell types across all of the cells analysed. The gene activity score of the marker genes for the cells within each of the 4 major cell populations is shown in Figure 3.26. The epithelial tumour cell population

had increased activity of the genes *EPCAM* (epithelial cell adhesion molecule), *MUC16* (mucin16 or CA-125), *WFDC2* (WAP four-disulfide core domain protein 2) and *LAPTM4B* (Lysosome-associated transmembrane protein 4B). The fibroblast population was identified due to raised gene activity of *PDPN* (podoplanin) and *COL1A2* (collagen type I alpha 2 chain). Increased *IKZF1* (IKAROS family zinc finger 1) and *PTPRC* (Protein tyrosine phosphatase, receptor type, C) activity identified the lymphocyte cells, while myeloid cells had raised activity of the genes coding for *CD14* and *TREM1* (Triggering Receptor Expressed On Myeloid Cells 1). Figure 3.27 shows the chromatin accessibility profiles for the key marker genes within the 4 major cell types.

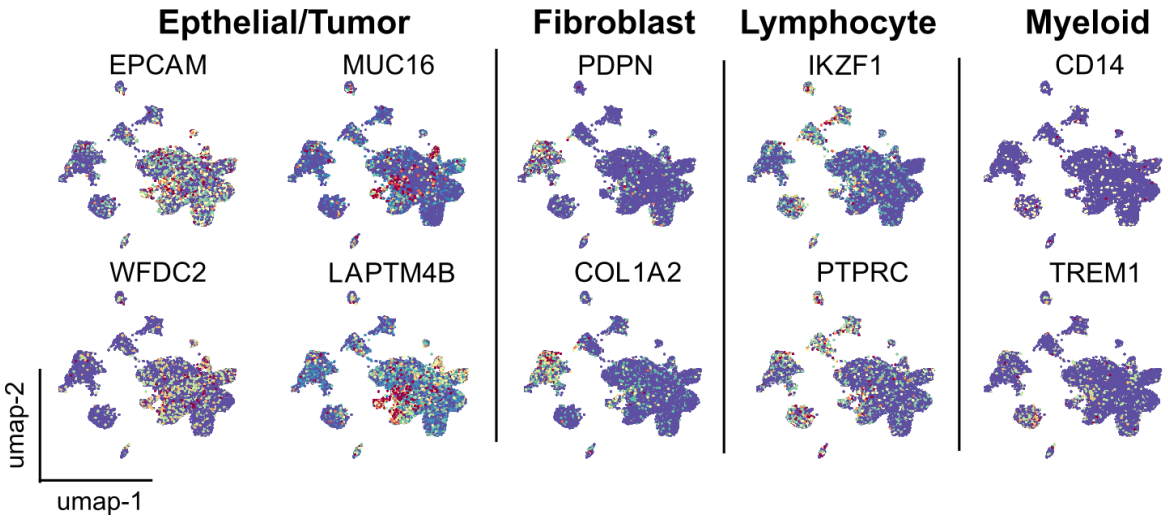


Figure 3.25: Identification of the major high-level cell types within metastatic omental tumour deposits.
UMAP embedding overlaid with gene activity scores for canonical high-level cell marker genes.

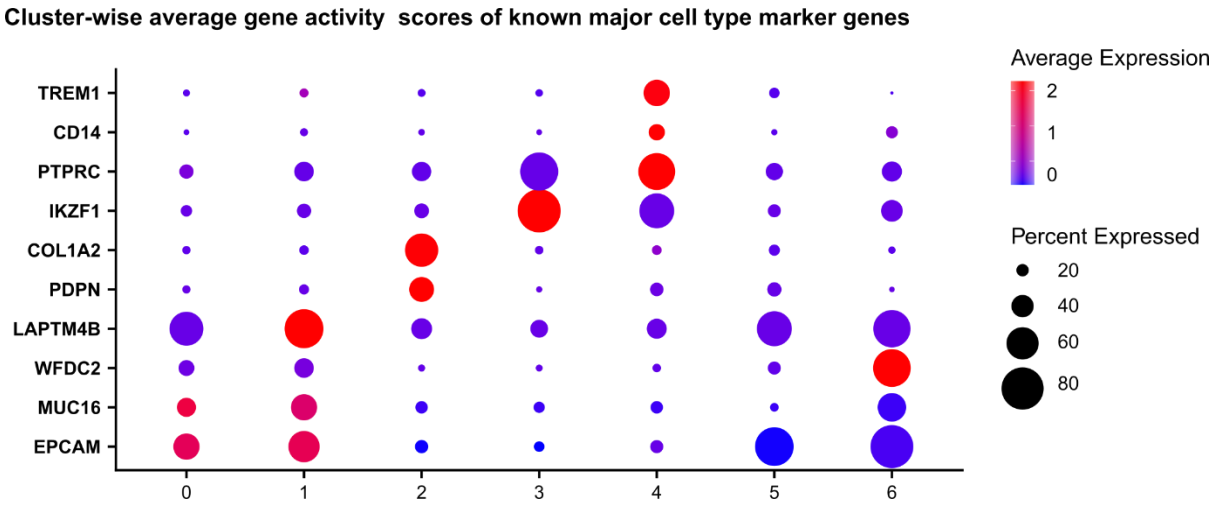


Figure 3.26: Gene activity of major cell type marker genes.
Dotplot showing average gene activity scores of canonical marker genes for major lineage cell types. Dot size indicates the proportion of cells within the cluster that show activity for the given gene. Cluster number 1 is the epithelial tumour cell population, cluster 2 is the fibroblast population, cluster 3 is the lymphocyte population and cluster 4 is the myeloid population.

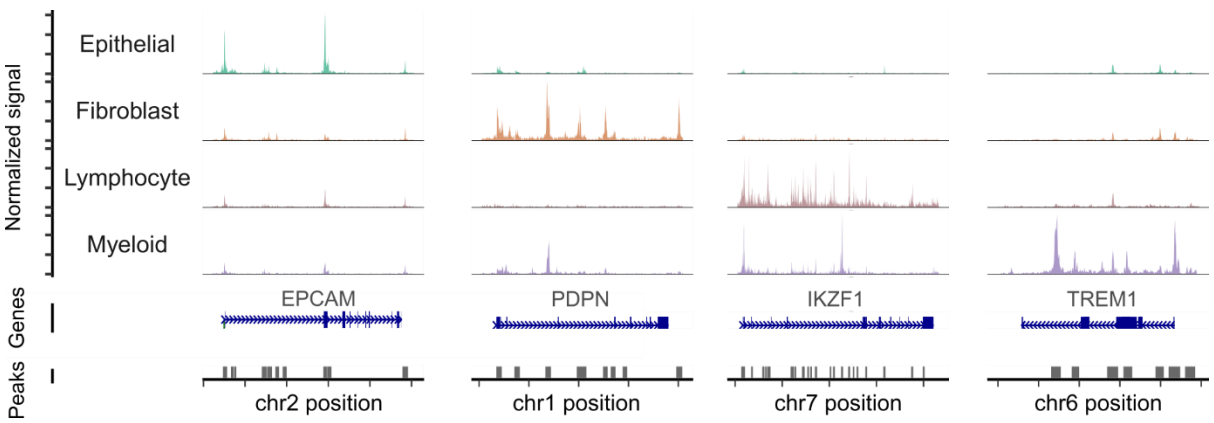


Figure 3.27: Identification of the major high-level cell types marker genes.
Genome coverage plots to demonstrate chromatin accessibility profiles at canonical high-level cell type marker gene loci within the defined major cell types.

The 7 major cell clusters were then analysed in more detail. Figure 3.28 analyses the composition of each major cell cluster according to the patient samples. The cells within the epithelial tumour cluster (cluster 1), originated from all 10 samples, however greater proportions of the cluster were from samples 1, 3, 5 and 7. The fibroblast cluster (cluster 2) was comprised of cells from all samples, except for sample 9, and had larger proportions from samples 1 and 2. While the myeloid cluster (cluster 4) had cells from all samples in roughly equal proportions (apart from having no cells from sample 9), the lymphocyte cluster (cluster 3) was made of cells predominantly from sample 1. Interestingly, sample 9 was only seen in cluster 0 and cluster 1, the epithelial tumour cluster, suggesting this patient sample was predominantly tumour or epithelial tissue. The other patient samples contained cells from the cell clusters 0, 1, 2, 3 and 4, signifying these samples were comprised of a number of different cell types, including epithelial tumour, fibroblasts, myeloid cells and lymphocytes. Clusters 5 and 6 contained cells almost entirely from patient sample 3 and 4, respectively.

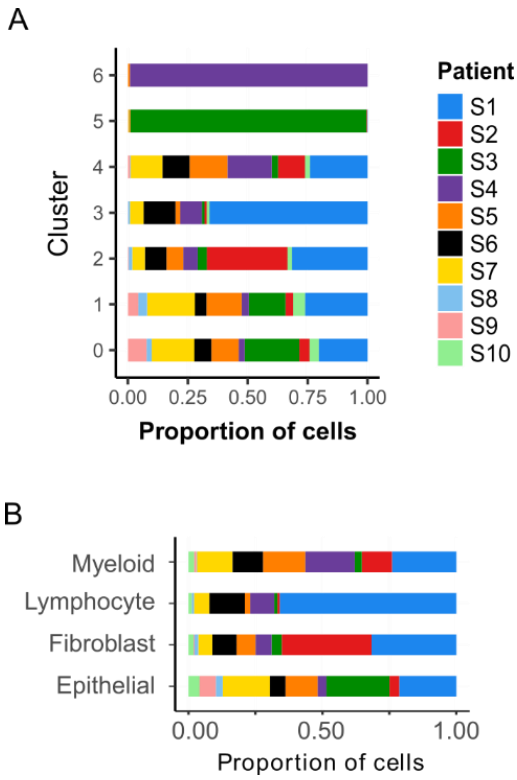


Figure 3.28: Cluster proportions based on patient sample.
The proportion of cells within each of the seven cell clusters (A) and the defined major high-level cell types (B) based on the patient samples.

Further interrogation of the individual patient samples showed that the epithelial tumour cells were the predominant population in all 9 of the 10 patient samples (Figure 3.29). Indeed, half of the samples (samples 3, 7, 8, 9 and 10) were comprised almost entirely of epithelial tumour cells. It may be possible that the epithelial cells were more robust and resistant to damage, while other smaller or more fragile nuclei were lost during the processing of samples for scATACseq.

The proportion of fibroblast cells varied across the patient samples, with the majority of sample 2 shown to be fibroblasts. There were minimal proportions of lymphocyte and myeloid cells in each sample, confirmed in Figure 3.30, where the total number of these cells clusters was

smallest. It is evident from the total cell counts, that there was a far greater number of epithelial tumour cells than the other major cell types across all the samples.

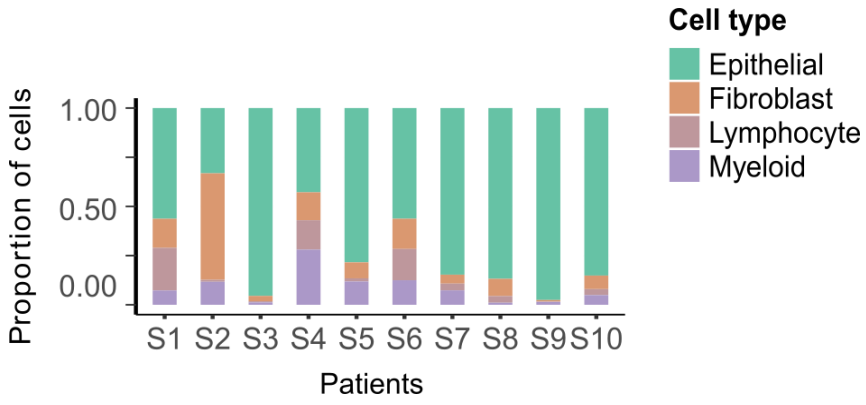


Figure 3.29: Major high-level cell types within patient samples.
A per-sample breakdown of the proportion of the four major lineage cell types cells.

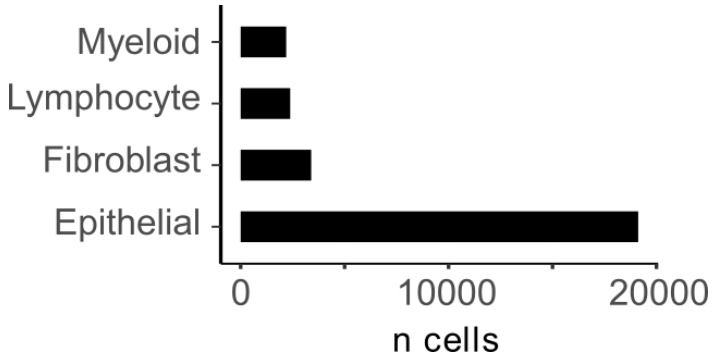


Figure 3.30: Cells within high-level cell clusters.
The total counts of cells within the four main cell populations.

3.3.3.2 Differences in chromatin landscape following chemotherapy exposure

The high-level cell clusters were then stratified by exposure to chemotherapy treatment (Figure 3.31). Each major cell cluster contained cells from pre-chemotherapy samples and samples exposed to NACT. The epithelial tumour population and lymphocyte population were comprised of more pre-chemotherapy cells than NACT cells. The fibroblast and myeloid

populations contained similar amounts of pre-chemotherapy and NACT cells. Figure 3.32 shows that pre-chemotherapy cells contributed to almost 75% of the epithelial tumour population and almost all of the lymphocyte population. There were equal proportions of the pre-chemotherapy and NACT cells in the myeloid and fibroblast populations.

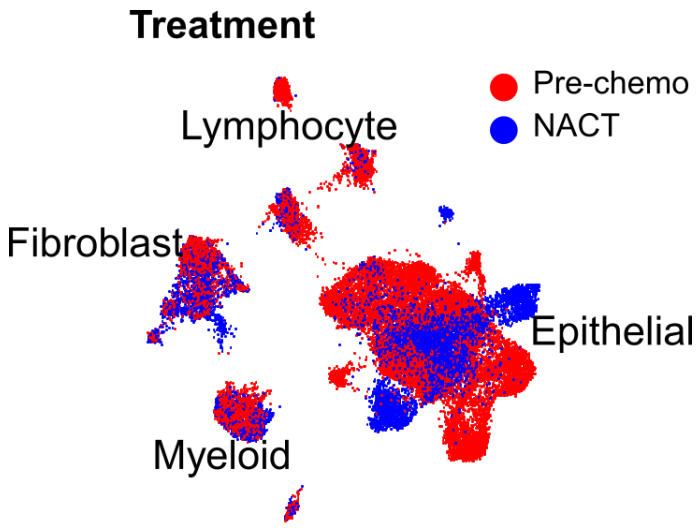


Figure 3.31:UMAP of cells within metastatic omental tumour deposits based on treatment.
UMAP embedding overlaid with cell labelling for chemotherapy naïve cells (pre-chemotherapy) and those exposed to chemotherapy treatment (NACT).

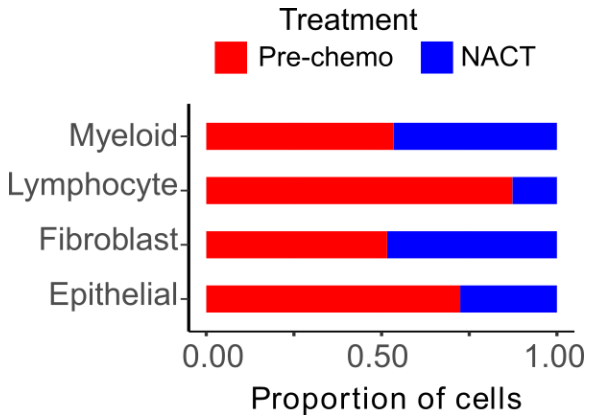


Figure 3.32: Cluster proportions stratified by chemotherapy treatment.
The proportion of treatment-naïve (Pre-chemotherapy) and chemotherapy-exposed (NACT) cells within each of the major high-level cell types.

The key markers that were used to identify individual cells were then reviewed. Figure 3.33 shows the chromatin accessibility of these key markers in each patient sample and in the different major cell clusters. It is evident that the patient samples had varied accessibility of the different chromatin markers. In particular, samples 1, 3, 6, 7, and 10 have clear differences in the major cell markers. The degree of chromatin accessibility for the key markers also differed in each of major cell populations. The key markers were then stratified according to chemotherapy exposure; there were alterations between the chemotherapy naïve (pre-chemotherapy group) and chemotherapy exposed (NACT group) samples, but these were less obvious.

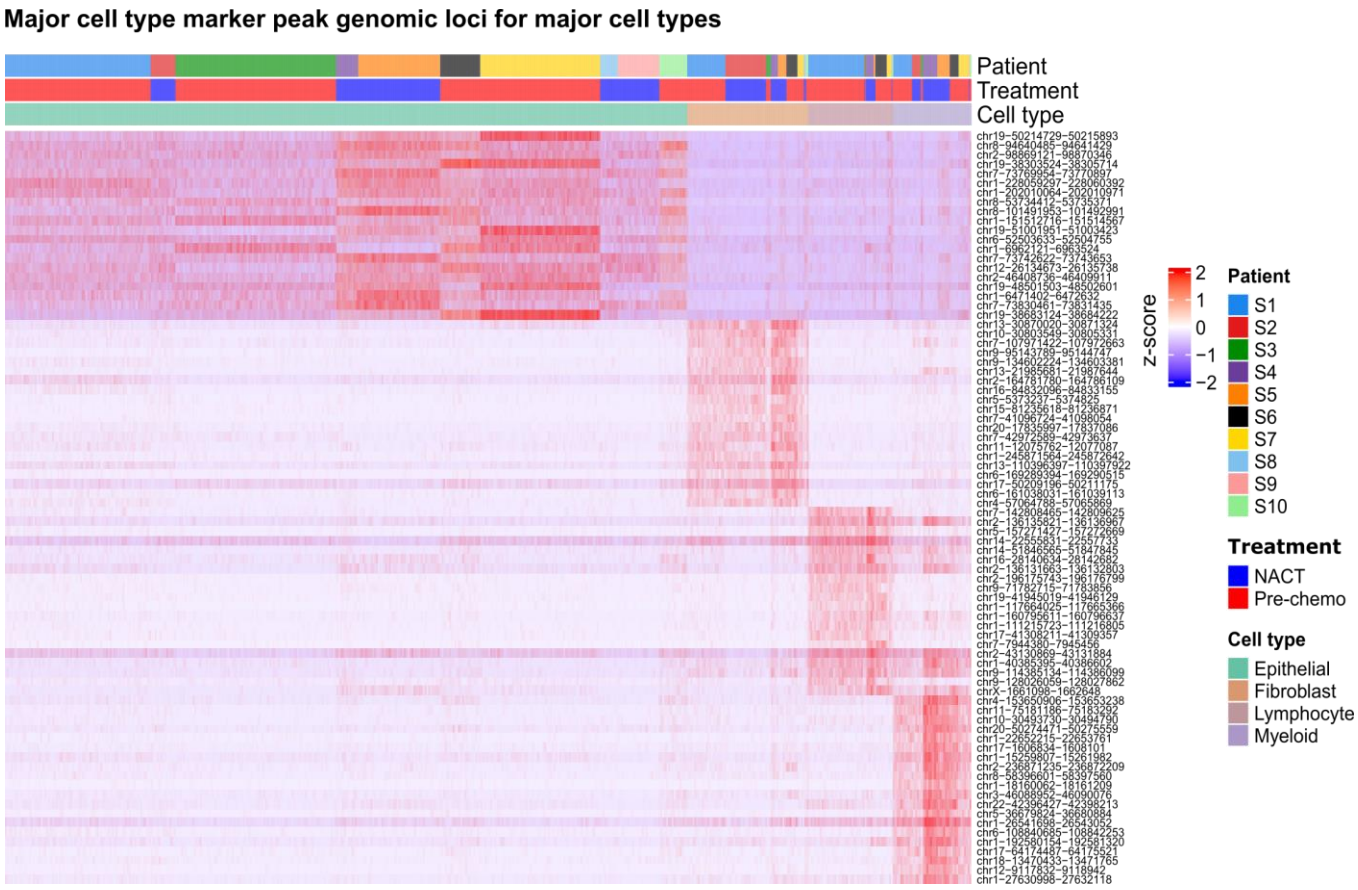


Figure 3.33: Major cell type chromatin accessibility marker peak profile .
Accessibility profile of top marker peaks identified as being differentially accessible in each of the high-level cell types.

The transcription factor motifs that were enhanced in the major cell populations are shown in Figure 3.34. The top markers for these motifs varied across the samples, but there were no clear patterns when comparing the pre-chemotherapy samples with the NACT samples. The epithelial population had increased *MEIS1, MEIS2, PBX2, SMAD2/3/4* and *TP63*, further confirming this as a tumour cell cluster. The fibroblast population had raised *TCF7L2, TCF7* and *FOS*. The enriched transcription factor motifs in the myeloid and lymphocyte populations were similar, with no clear alterations following chemotherapy.

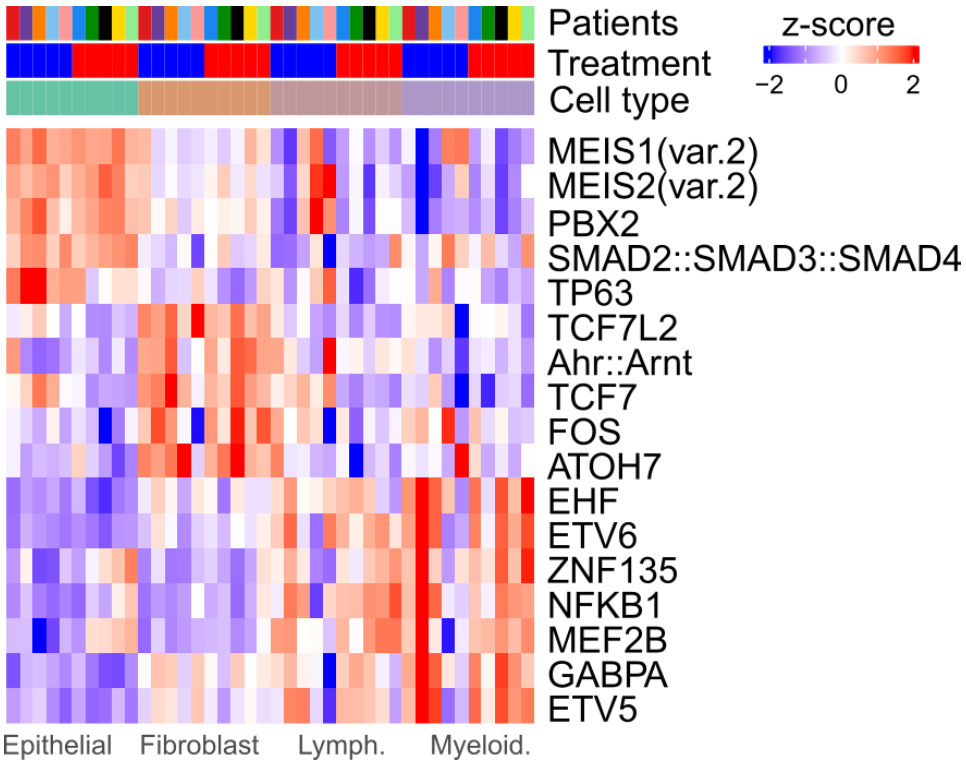


Figure 3.34: Transcription factor motif enrichment profile of marker motifs enriched within major cell type marker peaks.
Profile of sample-wise average enrichment of top transcription factor motifs identified as significantly enriched within major cell type marker peaks.

The modifications in chromatin accessibility following chemotherapy treatment differed between the major cell types (Figure 3.35). There were a high number of differentially accessible peak loci in the epithelial population following chemotherapy, but few in the other cell populations, particularly for the closed chromatin regions. Large deviations in the open and closed chromatin regions for transcription factor motifs were evident in the epithelial population, with the greatest changes seen in *TP63*, *MAFA* and *ZIC2*, which had increased chromatin accessibility after chemotherapy.

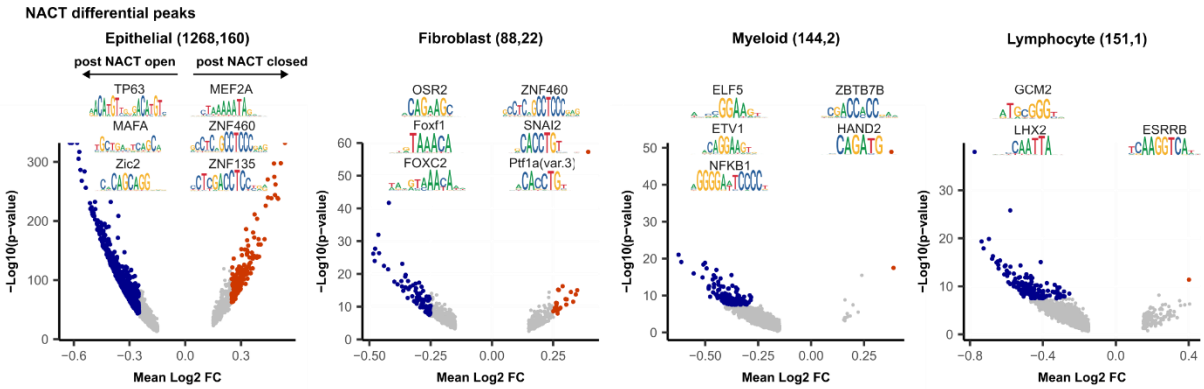


Figure 3.35: Chromatin accessibility in the major cell types following chemotherapy treatment. Differentially open (blue) and closed (red) chromatin regions following NACT (neoadjuvant chemotherapy) in epithelial, fibroblast, myeloid and lymphocyte cell clusters. Coloured points indicate differentially accessible peak loci (BH adjusted $p < 0.01$ and absolute mean log FC > 0.25). Motif logos indicate the top enriched transcription factor motifs within post and pre NACT differential peaks.

Following on from this, the differentially enriched motifs of gene transcription were compared between the pre-chemotherapy and NACT samples (Figure 3.36). While the chemotherapy naïve (pre-chemotherapy) and exposed (NACT) groups in the lymphocyte population were similar, there were clear differences in the epithelial population. There was increased expression of cancer-associated transcription factors in both treatment groups in the epithelial population. The pre-chemotherapy group had raised transcription factors related with tumour

metastasis and progression (such as *MEF2A, ZN460* and *KLF3*), but also transcription factors for tumour dormancy (such as *NR2F1*). In contrast, the NACT group had elevated transcription factors for oncogenes (such as *MAFA* and *ZIC2*) and cancer stem cells (such as *PAX6*). There were no consistent differences in enhanced transcription factor motifs for treatment groups in the myeloid and fibroblast populations.

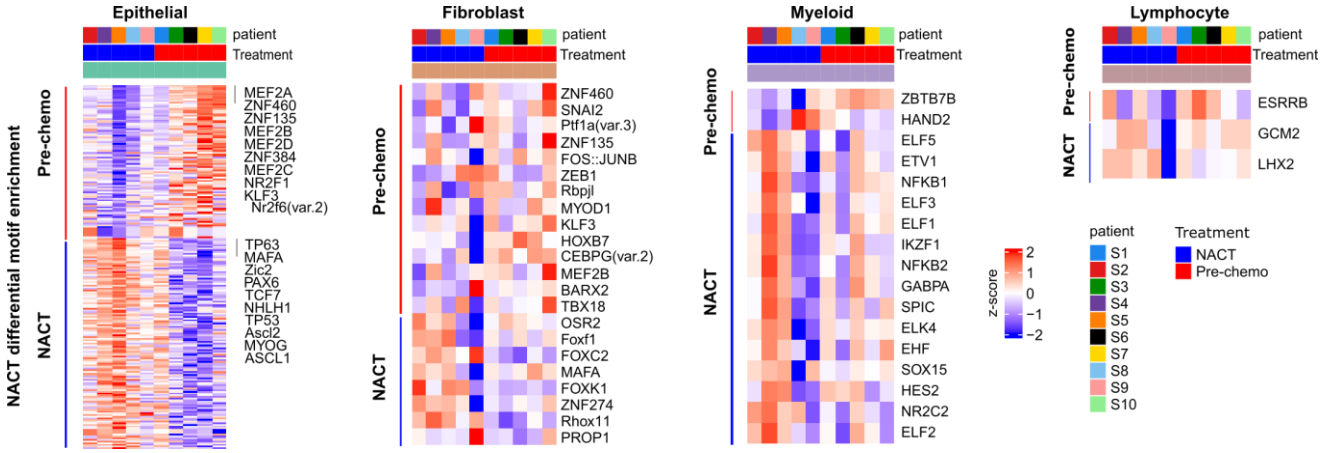


Figure 3.36: Motif enrichment analysis of gene transcription in major cells depending on chemotherapy exposure and patient samples.
Transcription factor motif enrichment profile of motifs identified as differentially enriched between chemotherapy-naive (Pre-chemotherapy) and following chemotherapy exposure (NACT) within each of the major cell types.

3.3.4 Summary of the single cell ATAC sequencing analysis in ovarian cancer

Sequencing analysis of scATAC data identified 7 different high-level cell populations within omental tumour samples obtained from patients with HGSOvCa. These included lymphocytes, fibroblasts, myeloid cells and epithelial cells. An epithelial tumour cell population had increased activity of genes associated with OC, such as *EPCAM* and *MUC16*, and was the predominant cell population in all but one of the samples. Indeed, half of the samples were comprised almost entirely of epithelial tumour cells. In contrast, there were minimal proportions of lymphocyte and myeloid cells in each of the samples. As expected, there was a

reduction in the epithelial tumour population following chemotherapy, while there was also a loss of immune cells.

For the key markers utilised to identify the different cell types, measurements of chromatin accessibility differed greatly between patients. In addition, markers for the transcription factor motifs that were enhanced in the major cell populations varied across samples, showing inter-patient heterogeneity. The modifications in chromatin accessibility and differentially enriched motifs of gene transcription occurred following chemotherapy. While there was increased expression of cancer-associated transcription factors in both chemotherapy-naïve and exposed groups in the epithelial cell population, elevated cancer stem cell transcription was evident post chemotherapy.

3.4 Discussion

A range of techniques such as immunohistochemistry staining, flow cytometry and microarray assays, have endeavoured to categorise the cell populations within HGSOvCa in order to assess their predictive potential and guide the development of new therapies [5, 116, 118-120, 326]. Genomic analysis has failed to discover significant genomic profiles or suitable target genes, despite stratifying samples by treatment outcomes [93]. The Cancer Genome Atlas (TCGA) identified four transcriptionally distinct HGSOvCa cell subtypes through the assessment of RNA expression, promoter methylation and DNA copy number assays [5]. Numerous reviews have utilised bulk RNA sequencing to assess these subtypes, but were unsuccessful in recognising gene expression patterns to classify cell populations and could not detect intra-cellular heterogeneity [5, 116, 119, 329-332]. Recent scRNAseq analyses are of interest although sample sizes were typically small, ascitic fluid samples were utilised instead of solid tumour specimens, the immune cells were not evaluated in depth and chemotherapy-exposed

samples were infrequently included [114, 116-118 122, 333]. In this chapter I was able to overcome some of these challenges and gain new insights into the single cell architecture of HGSOvCa.

Single cell sequencing techniques of omental samples

This chapter utilised two different 10X Genomics sequencing techniques to explore the cellular composition of fresh or snap-frozen tissue samples [305, 308]. Thousands of individual cells (scRNAseq) or nuclei (scATACseq) were examined, mapping reads to the human reference genome [305, 308, 334]. By identifying the cell types within each tissue sample, as well as gene expression (scRNAseq) or the chromatin accessibility (scATACseq) profile, a comprehensive analysis of the cell type contexture within the ovarian TME was undertaken.

scRNAseq analyses allowed assessment of 2271-20494 viable cells per sample although few epithelial or Epcam+ cells were present, likely due to the loss of fragile and stressed tumour cells during tissue digestion. Therefore, cell sorting reconstructed the samples to ensure they contained an adequate proportion of epithelial cells. This enrichment enabled the detection of a subset of epithelial tumour cells with enhanced expression of OC biomarkers, *MUC16* and *WFDC2* [335-336], albeit a relatively smaller population than initially anticipated. As scATACseq samples did not require similar processing, with tissues simply snap frozen immediately after collection, the tumour populations in these biopsies are likely unchanged and representative of the original malignant tissue. Omental tissue was used in both studies as this is typically the first site of metastatic spread in OC [65, 66, 69, 71, 72] and understanding the involvement of the omentum in disease progression is of great clinical importance.

Identification and clustering of high-level cell types

Single cell mRNA sequencing successfully detected cell heterogeneity with 19 distinct major cell types (Figures 3.1 and 3.2), greater than the number reported (2-16) in previous studies [116-123]. This is possibly due to the increased number of cells sequenced within our study and could also have been influenced by the clustering methods used.

Most populations were CD45+ (Figures 3.1 and 3.5) with 5 populations of CD45- non-immune cells, including a small cluster of epithelial tumour cells expressing OC biomarkers, *MUC16* (Mucin16 or CA-125) and *WFDC2* (whey acidic protein four-disulphide core domain protein 2 or HE4) [335, 336]. While others have identified multiple transcriptionally different epithelial cell clusters, these were not apparent in our data and finer grained clustering of the epithelial cells is required to depict them [117, 122, 123]. The proportion of epithelial cells in our samples (approximately 10%) was similar to that in another series [123]. However, there is a large variety in the epithelial cluster proportion reported in other scRNAseq reviews, regardless of the tissue type analysed [116-119]. Typically, epithelial cells are frequently found to be the largest cell population, with some reviews finding that they contribute to over half of all cells, including within similar omental tumour tissues biopsies [119, 120]. The low numbers of epithelial cells within our scRNAseq samples could possibly be associated with the digestion and sample processing of the hypoxic and friable omental tumour tissues collected.

Another non-immune major cell cluster detected by scRNAseq was a fibroblast population, with two distinct types recognised: those with APOD (apolipoprotein D) expression, which were categorised as normal adipose-derived stromal cells, and those expressing COL1A1, the cancer-associated fibroblasts (CAFs) [327]. The APOD fibroblasts transition into CAFs during

tumour development and are associated with cancer invasion, progressive disease and treatment resistance [327, 337].

The composition of the immune cell population varies greatly between scRNAseq studies [118, 123], and was shown to differ between individual patients in our cohort (Figure 3.5). CD8+ T cells were the predominant cell type upon integration of all samples in the scRNAseq cohort. A population of CD4+CD8+ double positive T cells was also seen which have previously been shown to demonstrate tumour reactivity following antigen stimulation [338]. Interestingly, our analysis discovered a relatively large NK cell population, while others have found no or few NK cells [119-121, 123].

In comparison, the single cell chromatin accessibility analysis (scATACseq) detected 7 major cell populations, fewer than the 19 identified in the scRNAseq cohort. The majority of the cells in the scRNAseq samples were immune cells, likely due to the cell sorting and enrichment for CD45+ cells in order to primarily focus on the immune populations. The unsorted samples used in scATACseq revealed a predominant epithelial cluster with a far smaller lymphocyte (or immune cell) cluster (Figure 3.24). This large epithelial cell population identified by scATACseq was comprised of a far greater number of cells than the other major cell types (Figure 3.30). Epithelial cells were present in all 10 analyses but the proportion varied between samples (Figure 3.29). One sample comprised of almost all epithelial cells while another had only 30%, demonstrating tumour cell heterogeneity between patients. Interestingly, of the smaller immune cluster, almost three quarters were derived from a single patient, with other patient samples containing a much lower proportion of immune cells, suggestive of immune cell heterogeneity across samples (Figures 3.28 and 3.29).

These findings vary somewhat from the scRNAseq analysis, despite the patients and samples being similar in both cohorts. As well as the cell sorting and CD45+ cell enrichment in scRNAseq, it is possible that the additional processing and digestion required for scRNAseq may have damaged fragile epithelial cells. A single published OC scATACseq study supports our findings: within two HGSOvCa samples, 6 similar major cell types were identified (compared to our 7) and the main cell population was also an epithelial tumour cell cluster [339]. While they recognised 4 different tumour subpopulations, we confidently detected 1 subpopulation. However, it is possible that there are actually 4 tumour subpopulations within our samples (clusters 0, 1, 5, 6), all with profiles of epithelial markers. Further analysis is required to confirm these clusters as definitive tumour subpopulations, therefore demonstrating a similar level of heterogeneity to the previous study. We discovered a greater number of major cell types in scRNAseq than in scATACseq, with 19 and 7 cell types, respectively. Likewise, Regner et al. described 24 and 14 recognisable sub-clusters of cells in their paired analysis of scRNAseq and scATACseq data, respectively, suggesting that scRNAseq is more sensitive at detecting smaller clusters or populations of cells.

Transcriptional profiling of malignant and normal omental tissues

The inclusion of a normal omental sample in the scRNAseq analysis allowed the comparisons of cell heterogeneity and gene transcription following malignant transformation (Figures 3.4 and 3.5). Despite this single sample, differences were evident in the proportions of the major cell populations (Figure 3.6). The size of the epithelial cell cluster was greater in the omental tumour samples than in the normal omentum. The omentum is an adipose rich organ, with few epithelial cells, so it was expected that this cluster was larger following invasion of an epithelial tumour [339]. In addition, the non-malignant omentum also contained higher levels of normal,

adipose-derived stromal APOD fibroblasts. Likewise, the cancer-associated fibroblasts, with raised COL1A1 expression, were greater within the tumour tissue, as predicted.

The transcriptional landscape following chemotherapy exposure

scRNAseq analysis identified that alterations to the composition of the TME were evident following chemotherapy exposure despite small sample numbers in each treatment group (Figures 3.5 and 3.7). In particular, there were increased proportions of neutrophils, B cells, CD8+ T cells and Treg cells, alongside reduced macrophages and APOD fibroblast populations. The size of the epithelial tumour population was unchanged between the chemotherapy-naïve and chemotherapy-exposed samples. This may indicate inherent chemoresistance within the tumours and a failure to eliminate the malignant epithelial cells, although it is unclear whether clusters sensitive to chemotherapy have been killed, therefore allowing subpopulations of resistant tumour cells to survive and expand.

Interestingly, the patient that demonstrated a complete response to NACT (CRS 3) had a greater proportion of epithelial cells compared to the patients with a reduced chemotherapy response (CRS 2) and the chemotherapy-naïve primary surgery patients (Figure 3.9). With a complete chemotherapy response, all malignant epithelial cells will have been successfully targeted by chemotherapy. It is therefore possible that the epithelial cell population initially identified in the CRS 3 patient were actually mesenchymal stromal cells. As such, additional sequencing analysis is required to further differentiate the epithelial, mesenchymal and stromal cell populations. The patient with CRS 3 also had reduced T cells, B cells and NK cells, with increased proportions of monocytes and neutrophils, suggesting a different response by the TME with successful chemotherapy treatment. As expected, COL1A1

cancer-associated fibroblasts were reduced in the complete responder, whilst recurrence and chemoresistance was associated with increased COL1A1 and fewer APOD fibroblasts.

A recent scRNAseq analysis of 11 paired pre-chemotherapy and post-chemotherapy samples reported outcomes from omental and peritoneal tissues in HGSOvCa [123]. Here, Zhang et al. discovered a similar proportion of epithelial cells in chemotherapy-naïve samples to that in our cohort. Unlike the minimal response seen in our analysis, their epithelial population reduced with treatment, suggesting sensitivity and tumour cell killing. After detecting 12 distinct cancer cell clusters in their analysis, they discovered chemotherapy effectively decreased certain cancer populations, while certain stress-associated populations survived chemotherapy and expanded. The properties and sizes of other stromal and immune populations were analysed based on the stress-associated state of cancer cells, but were not stratified based on chemotherapy exposure. In another study of paired pre and post-chemotherapy tumour biopsies, whole transcriptome analysis has identified T cell expansion, NK cell infiltration and immune activation, but no differences in other cell populations [340].

Despite similar proportions of the epithelial populations in the treatment groups of our scRNAseq analysis, there was significant differential gene expression following chemotherapy in these cells (Figure 3.8). The OC tumour suppressor gene *FTH1* (ferritin heavy chain) was expressed at a higher level in the pre-chemotherapy epithelial cells than following chemotherapy, while *MGP* (matrix gla protein), which is associated with OC progression and treatment resistance, was over-expressed by epithelial cells following chemotherapy [341, 342]. There was also high deviation in gene expression with chemotherapy in the other major cell types, including dendritic cells, fibroblasts and monocytes. In contrast, there was minimal variation in the genes expressed following chemotherapy in the endothelial, plasmablast and T

cell populations. Key alterations in the NK cells included upregulation of *IFI27* (interferon alpha-inducible protein 27), which causes OC invasion, epithelial-mesenchymal transition and chemoresistance, and *GNLY* (granulysin) which stimulates and activates NK cells towards T cells [343, 344]. Chemotherapy modulation also resulted in raised *PLCG2* (phospholipase C gamma 2), which is related to immune activation, in the COL1A1 fibroblast population, and raised *FOL3R* (folate receptor alpha) in neutrophils, which is linked with tumour recurrence and poor survival [345, 346]. The gene *LTB* (lymphotoxin beta), which activates fibroblasts, co-ordinates tumour and stroma interactions and influences OC progression, was upregulated in B cells following chemotherapy [347]. These modifications are associated with immune cell activation and epithelial-mesenchymal transition. It is possible that chemotherapy creates a selection pressure in the TME that ultimately promotes treatment resistance, disease recurrence and progression.

In contrast to scRNAseq, the scATACseq analysis discovered a far greater proportion of epithelial tumour cells and lymphocyte cells prior to chemotherapy than following chemotherapy exposure (Figures 3.31 and 3.32). While this suggests that chemotherapy was successful in eliminating malignant cells, this also seems to have reduced the size of the immune cell populations. Unfortunately, the analysis did not highlight the response of specific types of immune cells to chemotherapy, likely due to the limited number of immune populations detected. While scATACseq has successfully identified detailed immune cell clustering and the differentially accessible genes in other malignancies, there are no other series reported in OC [348, 349]. Chromatin accessibility varied significantly between patients, with obvious differences in major cell markers across samples (Figures 3.33 and 3.34). Alterations following chemotherapy exposure were less clear, although there was greater chromatin accessibility in the epithelial tumour cells (Figure 3.35). Here there were increased open

chromatin regions for *TP63*, the transcription factor for TP53 that influences OC tumorigenesis, and oncogenes *MAFA* and *ZIC2* [350, 351]. Interestingly, the NACT group had elevated transcription factors for cancer stem cells. These undifferentiated stem cells are associated with tumour growth, invasion and metastatic spread. Cancer stem cells in OC have the ability to survive chemotherapy, thereby allowing a small subpopulation of aggressive and treatment-resistant cells to expand, leading to disease recurrence and chemotherapy failure [352-354].

NK cells within the tumour microenvironment

Prior scRNAseq publications have not focussed on NK subsets [119-121, 123]. I assessed the NK cell transcriptome and expression of NK ligands in order to interrogate the relationship between tumour and NK cells and the response to chemotherapy. The data showed that tumour cells and fibroblasts within the omentum are likely to be inhibitory towards NK cells (Figure 3.11). In particular, activating ligands were reduced (MICB and ULBP1/2/3), whilst ligands with inhibitory actions were increased (Nectin and MUC16). In contrast, macrophages and NK cells themselves had increased expression of activatory receptors, with increased MICA/B and ULBP2/3 ligands, and decreased Nectin, MUC16 and PD-L2. A reported scRNAseq analysis of 7 pre-chemotherapy HGSOvCa cases also discovered an immunosuppressive tumour microenvironment and induction of inhibitory immune checkpoints on epithelial cells [117]. However, this increase in the inhibitory ligands occurred in early stage disease and was reduced in advanced disease cases. In addition, genes for the PD-1 ligand and CTLA-4 ligand were low in all stages of HGSOvCa cases, even in advanced disease, which corresponds to our data where the PD-L1 gene had minimal expression. While ligands for T cell inhibition were raised, with corresponding T cell exhaustion, further analysis on additional NK ligands was not reported in this review.

scRNAseq analysis identified 5 different NK subpopulations (Figures 3.13, 3.14 and 3.15), with all showing raised expression of activating receptor genes apart from a tissue resident cluster (Figure 3.16). As expected, the exhausted and tissue resident NK clusters had increased expression of inhibitory receptor genes, while these were reduced in the cytotoxic and activated NK clusters. This NK cell heterogeneity within omental tumour was greater than that identified by scRNAseq in primary ovarian and metastatic peritoneal tumours, where just two main NK clusters were detected [118].

The comparison of NK cells in normal omentum to those within tumour tissue corresponded directly with the examination of NK ligands. Indeed, omental tumour samples had elevated expression for inhibitory NK receptor genes and genes associated with NK cell exhaustion (Figures 3.16 and 3.17), with greater proportions of exhausted, immature and tissue resident NK cells (Figure 3.19). In contrast, the normal omentum had increased gene expression for NK cytotoxicity and NK activating receptors, alongside increased proportions of cytotoxic and activated NK subpopulations than the omental tumour. Supporting the notion that NK cells within solid tumours are dysfunctional, inactive and have reduced cytotoxic function [355-359], this cohort analysis convincingly suggests that NK cells appears inhibited following infiltration into ovarian tumours when compared to those within normal tissue. However, the tumour samples within this cohort had increased gene expression for NK cytokine production compared to normal omentum (Figure 3.18), which differs to previous reports [354, 360].

Of note, chemotherapy treatment functioned to increase expression of activatory receptors on NK cells (Figure 3.17), increase NK cytokine production (Figure 3.18) and increase the proportion of activated and cytotoxic NK subpopulations (Figure 3.20). Furthermore, despite

assessing small sample numbers, there was a greater proportion of activated NK cells and reduced immature NK cells following a complete chemotherapy response (CRS 3), when compared to a moderate response (Figure 3.21). In addition, the proportion of exhausted NK cells was raised in those who did not receive chemotherapy. With NK activity and cytotoxicity seemingly elevated with chemotherapy, especially following a complete response, similar findings occurred in those who remained disease free after chemotherapy compared to those that recurred (Figure 3.22). The gene set enrichment analysis (Figure 3.23) showed an increase in genes associated with cytokine production and an inflammatory response following chemotherapy, along with downregulation of genes related to DNA repair. Disease recurrence following chemotherapy had gene enrichment for cytokine production, apoptosis, hypoxia, inflammatory response and epithelial mesenchymal transition. Chemotherapy therefore appears to reverse the degree of tumour-mediated NK inhibition and to promote NK activation. This profile has also been seen in other tumours [361]. Furthermore, a large whole transcriptome analysis of paired pre and post-chemotherapy OC samples has shown NK cell expansion, cytotoxic NK cell infiltration into tumour and increased cytotoxic gene expression following neoadjuvant chemotherapy [340].

Key findings from single cell sequencing of Ovarian Cancer

The two single cell sequencing techniques have successfully detected heterogeneity within metastatic omental tissue samples. While the scRNAseq analysis portrayed an immunogenic tumour microenvironment, scATACseq data showed tissues were dominated by epithelial cells. The greater sensitivity of scRNAseq detected a greater number of major cell types and cell subpopulations. However, scATACseq identified significant tumour and immune cell heterogeneity. Epithelial tumour cells persisted despite chemotherapy, with treatment increasing the expression of genes associated with immune activation, tumour invasion,

treatment resistance and disease progression. Furthermore, chemotherapy was also shown to increase chromatin accessibility for oncogenes, transcription factors related to OC tumorigenesis and cancer stem cells. The comprehensive NK cell interrogation demonstrated an inhibitory tumour microenvironment, leading to NK cell inactivation within tumour tissue. A total of five transcriptionally distinct tumour infiltrating NK cell subpopulations were present within the omentum. Exhausted, immature and tissue resident subtypes prevailed in malignant samples, with NK cells appearing dysfunctional, inhibited and with reduced cytotoxicity. However, chemotherapy activated NK cells, increased NK cytokine production and elevated cytotoxicity towards tumour cells. These findings highlight the importance of NK cells in these heterogenic, aggressive and chemo-resistant tumours. Further understanding of the NK cell phenotype and functional response within OC is essential, with NK cell manipulation a possible approach for targeted immunotherapy.

Chapter 4:

Analysis of NK cell phenotype in Ovarian Cancer

4.1 Introduction

It is known that Natural Killer (NK) cells are directly activated by specific ligands that are highly expressed on the surface of stressed tumours and also following the downregulation of major histocompatibility complex (MHC) class I molecules by tumour cells [141, 184-188]. NK cells possess several activating and inhibiting receptors, enabling targeted NK-mediated killing of tumour cells following stimulation [183, 173, 175, 177, 186]. However, the NK cells infiltrating into solid tumours from the peripheral blood are inactivated and rendered dysfunctional, with reduced NK cell proliferation and a decreased cytotoxic response [150, 156, 157, 177].

Importantly, the NK cells within ovarian tumour tissue are also thought to be impaired by the immunosuppressive tumour microenvironment [151, 154, 210-216]. Nevertheless, a greater understanding of the nature and role of the tumour infiltrating NK cells in ovarian malignancy is essential. As such, this study aims to extensively evaluate the infiltration and activation of NK cells in ovarian cancer (OC). Specifically, the main objective of this chapter is to interrogate the proportions and type of NK cells within peripheral blood, primary ovarian tumour tissue and metastatic omental tumour deposits; establishing their response and interaction with the tumour microenvironment. To this end, a large prospective cohort of OC and control patients who underwent surgical intervention at a tertiary gynaecological cancer centre was established. The comprehensive examination of patient samples was collated with clinical data to explore the characteristics of NK cells within OC and how current chemotherapy treatments influence the NK cell response.

4.2 Study cohort

The study cohort consisted of 80 patients with OC who were managed in the Pan Birmingham Gynaecological Cancer Centre between 2017 and 2022. Of these, 40 patients underwent primary surgery followed by 6 cycles of platinum-based adjuvant chemotherapy. The majority who underwent primary surgery (n=28, 70.0%) had advanced OC (FIGO stage III/IV) so were scheduled for cytoreductive primary debulking surgery, while 30.0% (n=12) had standard upfront surgery for early OC (FIGO stage I/II). The other 40 OC patients in the cohort received platinum-based neoadjuvant chemotherapy, with the plan to have interval debulking surgery and additional adjuvant chemotherapy for advanced OC.

A further 20 patients who did not have OC, or any other type of malignancy, were recruited as controls. These included 10 patients who had surgery for a benign ovarian mass, with final histology showing either ovarian fibroma or cystadenoma. The remaining 10 patients had histologically normal ovaries and fallopian tubes, with surgery undertaken for benign gynaecological conditions (n=8, 80.0%), such as uterine leiomyomas, or had surgery for ovarian cancer risk reduction (n=2, 20.0%).

4.3 Analysis of NK cells within the study cohort

4.3.1 Patient samples evaluated

Utilising the study cohort of 100 patients described above, paired blood and tissue biopsies were obtained during surgery and processed as described in the Methods sections 2.2.2.1 and 2.2.2.2, respectively. Peripheral blood samples were analysed using flow cytometry for all 100 patients within the cohort, along with the corresponding tissue biopsies, whenever these were available. Within the normal ovary and benign ovary control groups, ovarian tissue

samples were processed for 7 and 6 of the patients, respectively. Ovarian samples were obtained from 31 OC patients in the primary surgery group and 18 OC patients in the neoadjuvant chemotherapy group.

As OC typically metastasises in the first instance to the omentum, with metastatic omental disease associated with a poor prognosis and decreased chemotherapy response, an omentectomy is performed in all OC cases [47, 65, 66, 69, 71, 72]. Therefore, omental tissue biopsies were also analysed, with samples processed for 26 patients in the primary surgery group and 13 patients in the neoadjuvant chemotherapy group. Paired omental biopsies were also available for 5 of the normal ovary patients and 6 of the benign ovary patients. All of the blood and tissue samples that were collected and processed were used in the NK cell analysis. Figure 4.1 describes the samples that were collected for each patient group.

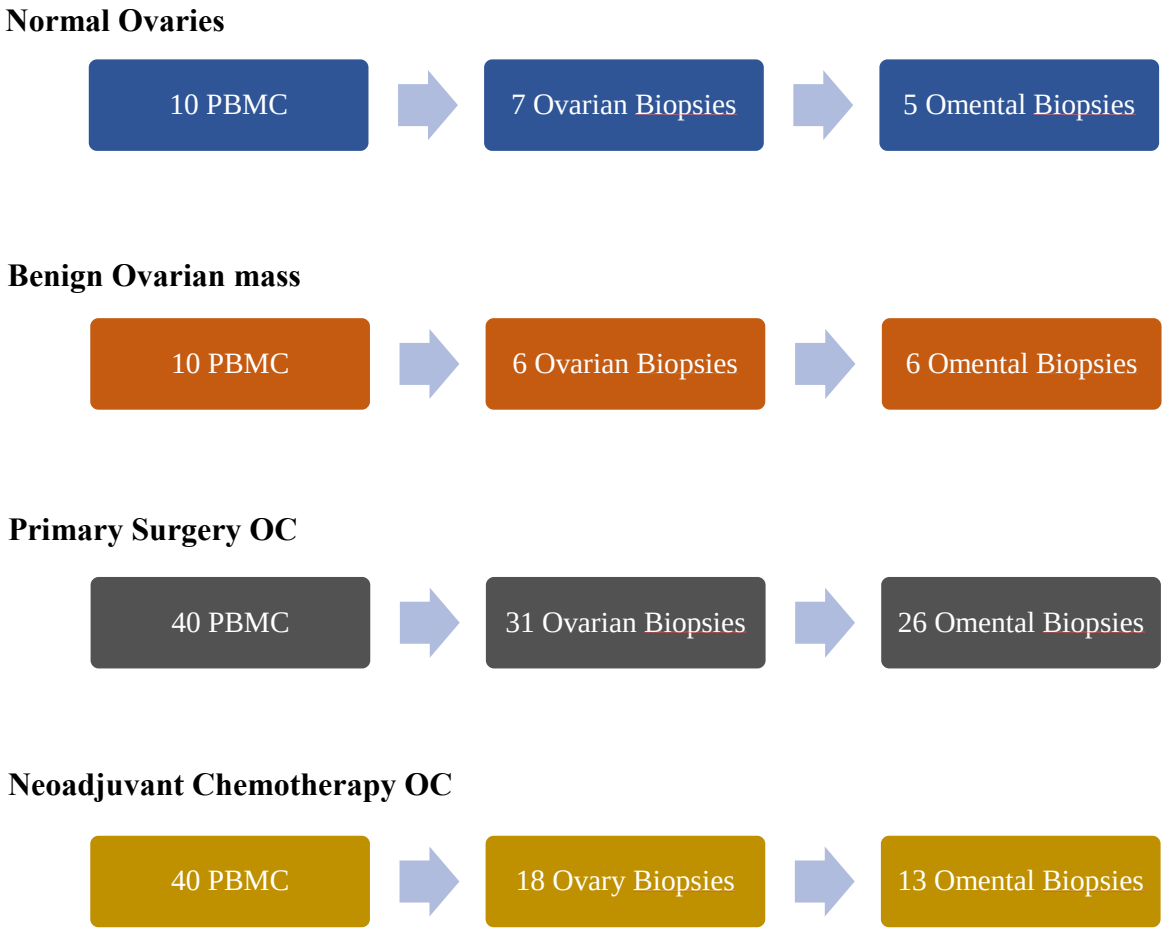


Figure 4.1: Blood and tissue samples collected within the study cohort.
Peripheral blood samples (PBMC) were obtained and analysed for all patients within the cohort. Paired ovarian tissue biopsies were available for 7 (70.0%) and 6 (60.0%) cases in the normal ovary and benign ovary control groups, respectively. Matched omental biopsies were collected from 5 (50.0%) of those with normal ovaries and 6 (60.0%) patients with a benign ovarian mass. A total of 31 (77.5%) ovarian and 26 (65.0%) omental biopsies were collected from the OC patients who underwent primary surgery, with 18 (45.0%) ovarian and 13 (32.5%) omental biopsies obtained from the OC patients in the neoadjuvant chemotherapy group.

4.3.2 Identification of NK cells

The NK cells within blood and tissue biopsies were processed as described in the Methods sections 2.2.2.1 and 2.2.2.2, respectively. Briefly, whole blood was separated to give lymphocyte and monocyte cells, known peripheral blood mononuclear cells (PBMC), and tissue biopsies were sectioned, cultured and filtered to collect tumour infiltrating lymphocyte cells (TILS). The resulting PBMC and TILS were then stained with a bespoke NK antibody panel, detailed in the Methods sections 2.2.3.1. After directing through the Gallios Flow Cytometer, data was analysed with the Kaluza, Flow Cytometry Analysis Software (Beckman Coulter, analysis version 2.1). Figures 4.2 and 4.3 demonstrate the gating strategies implemented to identify the NK cell populations in each PBMC and TILS sample, respectively. Initially samples were gated using FS INT and FS Peak to locate the single cell population. Using these single cells and gating with FS INT and SS INT, the single lymphocyte cells were identified. This lymphocyte population was then used to separate the live cells expressing CD45 from those expressing CD19/CD14, giving the live lymphocyte cells population with B cells, macrophages and dendritic cells all removed. Finally, using the live CD45 positive cells, NK cells were located by CD3 negative and CD56 positive expression.

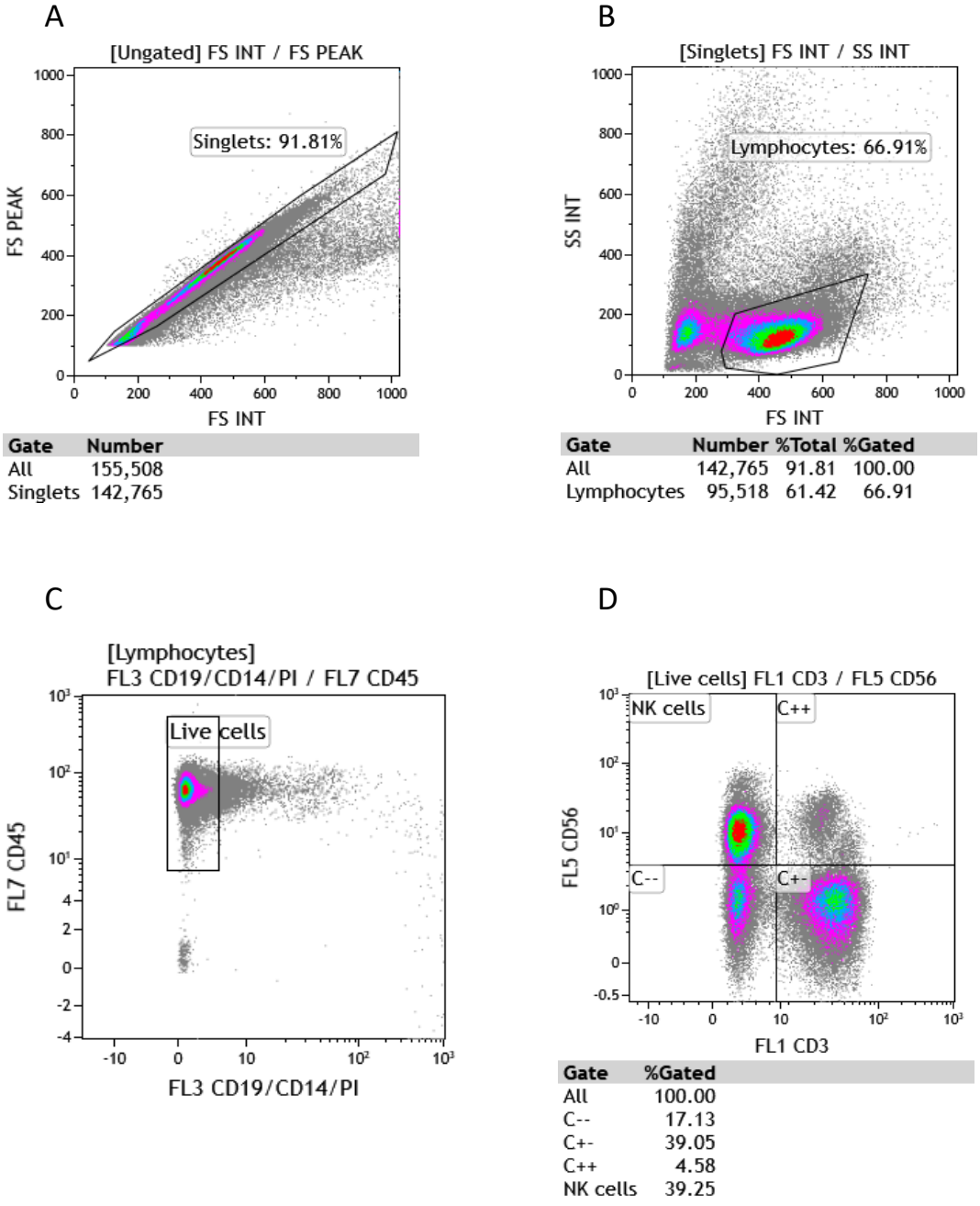


Figure 4.2: The gating strategy implemented to identify the NK cell population within each blood (PBMC) sample following flow cytometry.

Analysis of flow cytometric data allowed the detection of: A) single cells, B) lymphocytes, C) the live cells with CD45 expression, and D) the NK cell population.

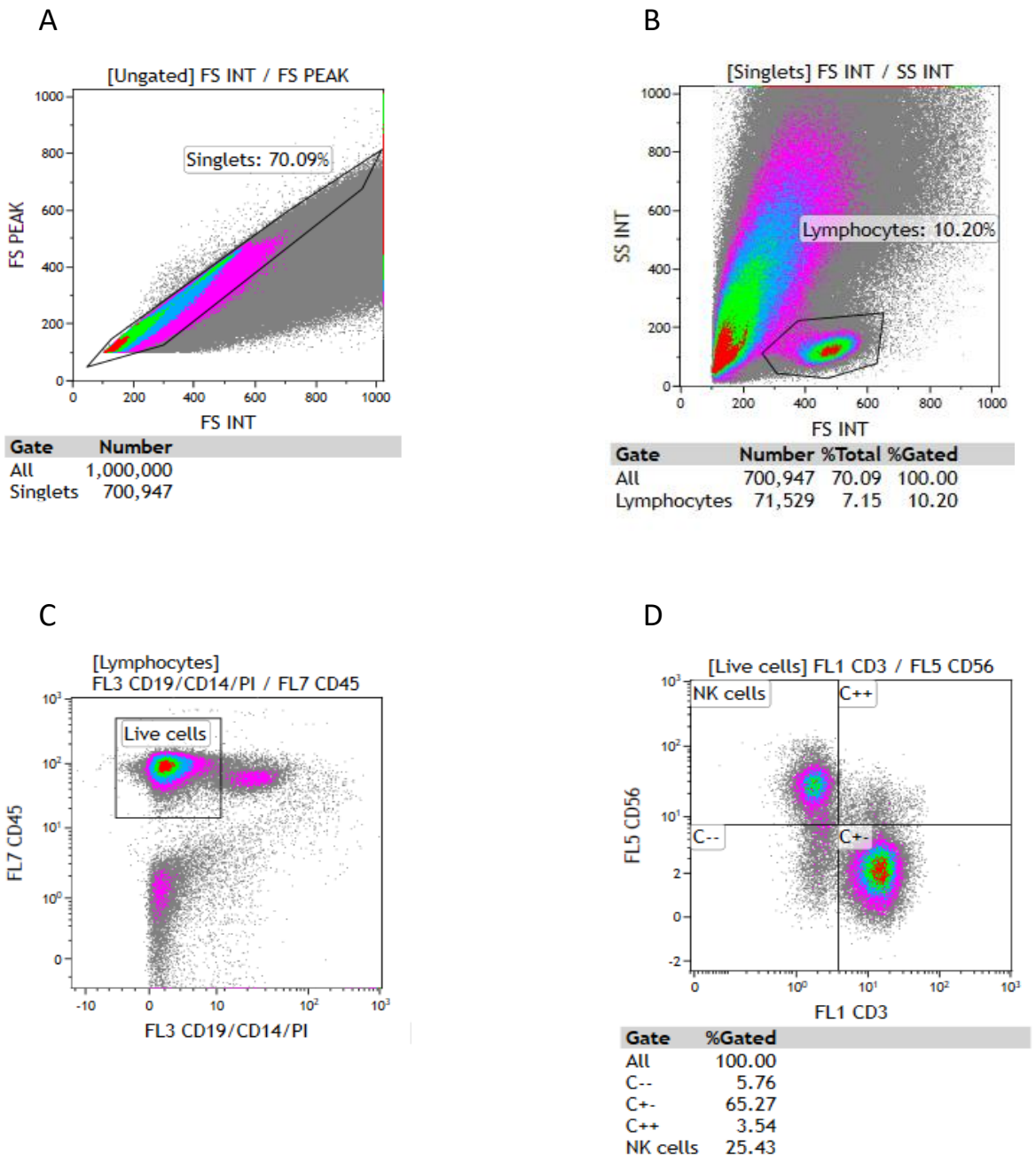


Figure 4.3: The gating strategy implemented to identify the NK cell population within each tissue biopsy (TILS) sample following flow cytometry.

Analysis of flow cytometric data allowed the detection of: A) single cells, B) lymphocytes, C) the live cells with CD45 expression, and D) the NK cell population.

4.3.3 Evaluation of NK cell sub-populations and phenotype

Following the identification of NK cells within each sample, further analysis determined the NK sub-populations, shown in Figure 4.4. Here, gating with CD16 and CD56 expression detected four different types of NK cells: low CD56 expression with either high ($CD56^{dim}CD16^{bright}$) or low ($CD56^{dim}CD16^{dim}$) CD16 expression. Similarly, high CD56 expression accompanied high ($CD56^{bright}CD16^{brigh}$) or low ($CD56^{bright}CD16^{dim}$) CD16 expression.

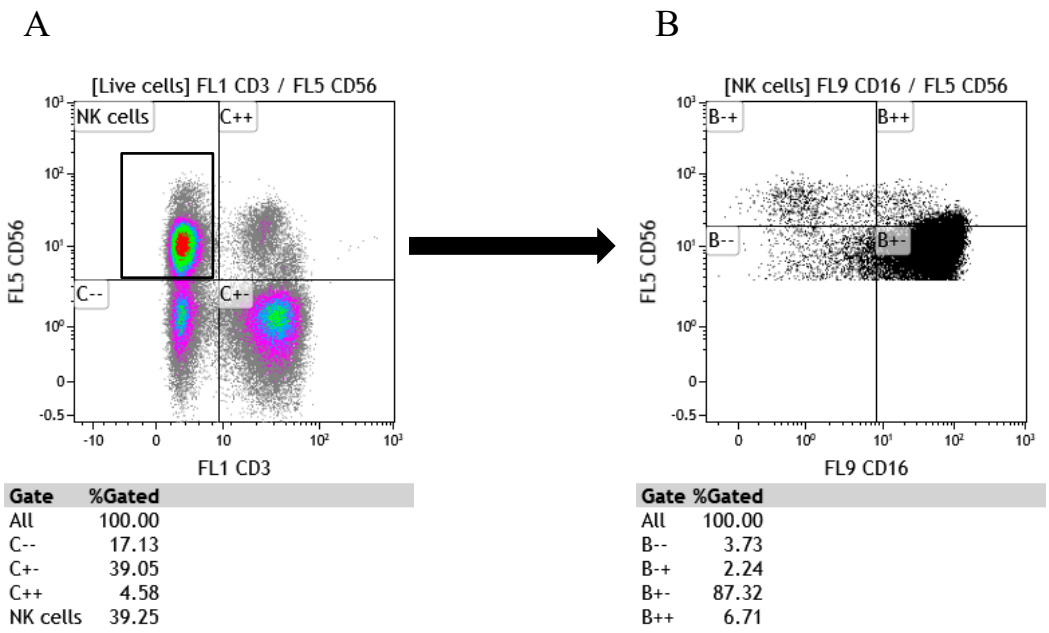


Figure 4.4: The gating strategy used to identify the different NK cell sub-populations.
Flow cytometric analysis separated NK cells (diagram A) into four different subtypes (diagram B). These included NK cells with: 1) low CD16 and low CD56 expression (B--), 2) low CD16 and high CD56 expression (B-+), 3) high CD16 and high CD56 expression (B++), and 4) high CD16 and low CD56 expression (B+-).

Using the flow cytometric data, various NK receptors were interrogated in order to evaluate the phenotype of the NK cells. This included the presence of activatory receptors, such as NKp46, NKG2C, DNAM-1, CD57 and NKG2D, as well as the patterns of inhibitory markers, such as PD-1, CTLA-4, TIGIT and CD94. Their expression measured the degree of activation or inhibition associated with the NK cells in each sample. Figure 4.5 shows the expression of the different cell surface receptors on the NK cells from one sample.

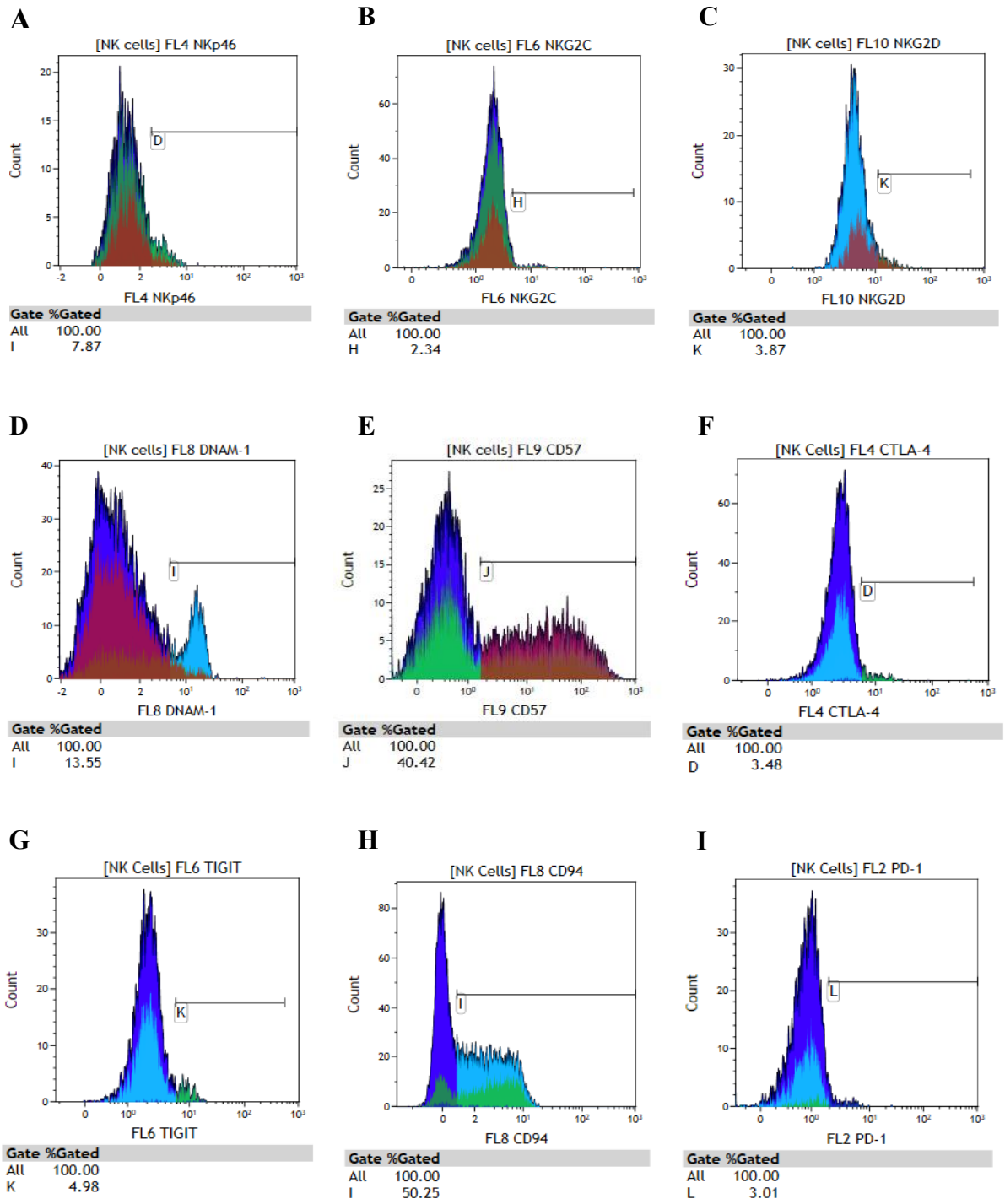


Figure 4.5: Histograms demonstrating the expression of NK cell surface receptors.
Flow cytometric analysis evaluated the expression of activating receptors on the surface of NK cells: A) NKp46, B) NKG2C, C) NKG2D, D) DNAM-1, and E) CD57. The expression of NK inhibiting receptors were also detected, specifically: F) CTLA-4, G) TIGIT, H) CD94, and I) PD-1.

4.4 Analysis of peripheral NK cell phenotype

4.4.1 The proportion of NK cells within the circulating blood

The proportion of NK cells within the CD45 positive, lymphocyte population was calculated from each PBMC sample obtained from every patient in the study cohort. The OC patients had a significantly greater proportion of PBMC NK cells compared to the patients with normal ovaries (p = 0.0226), shown in Figure 4.6. The mean proportion of PBMC NK cells was 23.1% in the OC patients compared to 13.1% in the normal ovary patients.

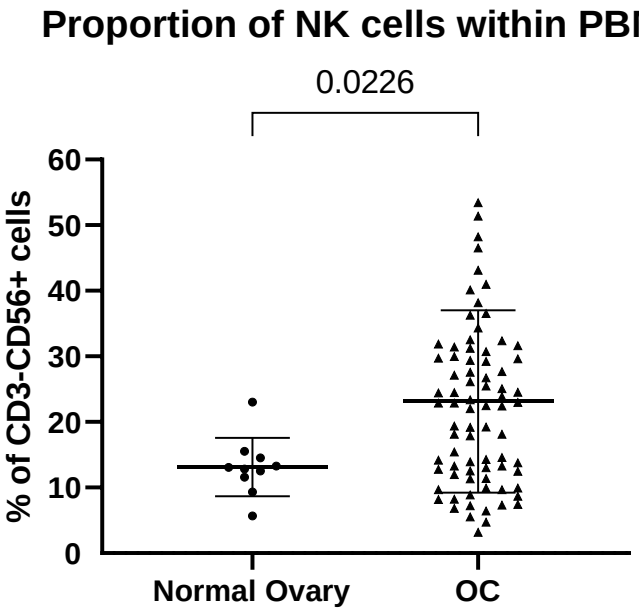


Figure 4.6: The proportion of CD56 positive NK cells within the peripheral blood of patients with OC and with normal ovaries.
The proportion of NK cells in the PBMC samples from OC patients is compared to the PBMC samples from patients with normal ovaries. The OC patients had a significantly greater proportion of peripheral NK cells than those in the normal ovary group (p = 0.0226).

The patient cohort was then divided into the four patient groups to also include those with benign ovarian masses, and the OC patients were separated into those who had undergone primary surgery and those who had received neoadjuvant chemotherapy. Analysis of the four groups showed that those in the primary surgery group had significantly more NK cells than those with normal ovaries ($p = 0.0083$). The neoadjuvant chemotherapy group also had an increased proportion of NK cells compared to those with normal ovaries, although this was not statistically significant ($p = 0.0971$). There were no significant differences in the proportion of PBMC NK cells between the patients with benign ovarian masses and either OC group or the normal ovary group. Figure 4.7 shows the proportion of NK cells within each PBMC across the four patient groups. The mean proportion of PBMC NK cells was highest in the primary surgery group at 24.4%, compared to 21.8% in the neoadjuvant chemotherapy group ($p = 0.4070$), 19.9% in the benign group ($p = 0.3350$) and was significantly greater than mean proportion of 13.1% in the normal ovary group ($p < 0.001$).

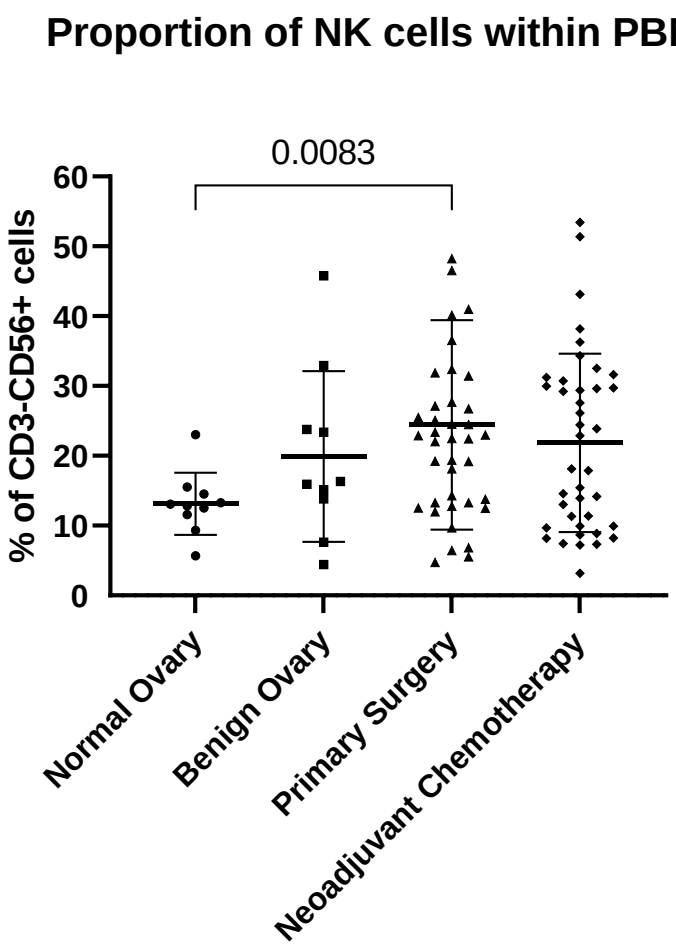


Figure 4.7: The proportion of CD56 positive NK cells within the peripheral blood of all patients in the study cohort.

The proportion of NK cells in each PBMC sample is shown across the four patient groups. The primary surgery group had a significantly greater proportion of peripheral NK cells compared to those in the normal ovary group ($p = 0.0083$; analysed with Analysis of Variance (ANOVA)). There was no significant difference in the proportion of peripheral NK cells between the neoadjuvant chemotherapy group and the normal ovary group.

4.4.2 The type of NK cells within the circulating blood

The CD16 and CD56 expression pattern on the NK cells in each PBMC sample was then determined. The majority of NK cells in the patient cohort had low CD56 and high CD16 expression, termed $CD56^{dim}CD16^{bri}$ NK cells which are the mature cytotoxic NK cells. The mean proportion of NK cells with this phenotype were similar in the normal ovary group (76.5%), benign ovary group (73.1%) and primary surgery OC group (75.0%). However, the

mean proportion of $CD56^{dim}CD16^{bri}$ NK cells was lower when all OC patients were combined (67.7%) and in the neoadjuvant chemotherapy group (60.4%). In contrast, the proportion of NK cells with high CD56 and low CD16 expression, the immature cytokine producing $CD56^{bri}CD16^{neg}$ NK cells, were higher in the combined OC group (6.7%) and in the neoadjuvant chemotherapy group (9.1%) compared to the other groups. The mean proportions of $CD56^{bri}CD16^{neg}$ NK cells were 4.2% in the primary surgery OC group, 6.0% in the benign ovary and 3.1% in the normal ovary groups. The $CD56^{dim}CD16^{neg}$ subset, where both CD56 and CD16 expression was low, was highest following neoadjuvant chemotherapy with a mean proportion of 18.9%. This compared to 6.2%, 5.7% and 13.3% in the primary surgery, benign ovary and normal ovary groups, respectively. There were no clear differences in the NK cells highly expressing both CD56 and CD16 ($CD56^{bri}CD16^{bri}$) across the four patient groups. Table 4.1 shows the mean proportion of each of the four types of NK cells within the different patient groups.

Table 4.1: The mean proportion of PBMC NK subsets in the different patient groups

Ovary status	Mean % CD56dim CD16neg	Mean % CD56bri CD16neg	Mean % CD56dim CD16bri	Mean % CD56bri CD16bri
Normal ovary (n=10)	13.3	3.1	76.5	7.0
Benign ovary (n=10)	5.7	6.0	73.1	16.8
All OC (n=80)	12.6	6.7	67.7	12.1
Primary surgery OC (n=40)	6.2	4.2	75.0	14.5
Neoadjuvant chemotherapy OC (n=40)	18.9	9.1	60.4	9.7

When interrogating the NK subsets in each individual PBMC sample, shown in Figure 4.8, the samples from OC patients were evidently different to the samples from patients with normal ovaries. In addition, the neoadjuvant chemotherapy samples clearly differed to the samples from the other patient groups. Those who had been exposed to chemotherapy had fewer $CD56^{dim}CD16^{bri}$ NK cells but increased $CD56^{bri}CD16^{neg}$ and $CD56^{dim}CD16^{neg}$ subsets.

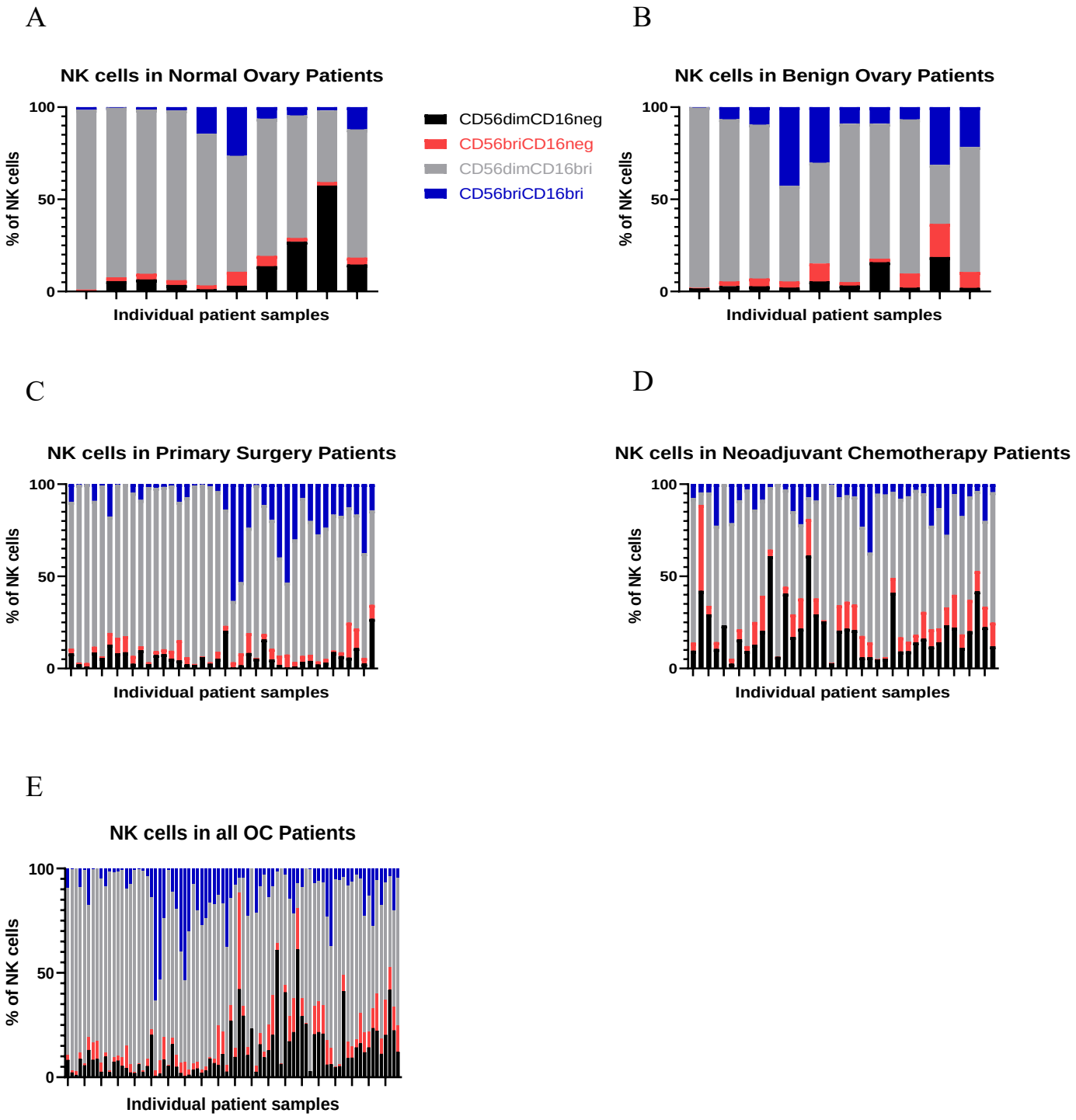


Figure 4.8: The proportion of the NK subsets within each PBMC sample in the study cohort.
The type of NK cells in each PBMC sample is shown in: A) patients with normal ovaries, B) patients with a benign ovarian mass, C) OC patients who underwent primary surgery, D) OC patients who underwent neoadjuvant chemotherapy, and E) all OC patients combined.

Indeed, when directly comparing each NK subset in normal ovary PBMC samples to those from all OC patients, there was a significant increase in $CD56^{bri}CD16^{neg}$ NK cells in the OC patients ($p = 0.0367$), shown in Figure 4.9. Upon interrogation of each NK subset across the four patient groups, there were a greater number of $CD56^{dim}CD16^{neg}$ NK cells in neoadjuvant chemotherapy OC patients compared to those OC patients who underwent primary surgery ($p < 0.0001$). The $CD56^{bri}CD16^{neg}$ subset was also higher in the neoadjuvant chemotherapy group than those in both the primary surgery ($p = 0.0011$) and normal ovary ($p = 0.0055$) groups. In contrast, the proportion of $CD56^{dim}CD16^{bri}$ cells in the neoadjuvant chemotherapy group were significantly less than in the primary surgery ($p = 0.0007$) and normal ovary ($p = 0.0152$) groups. The NK cell subsets in the benign ovary samples did not differ significantly to any of the other patient groups. The amount of $CD56^{bri}CD16^{bri}$ NK cells were also similar in all of the patient groups. Figure 4.10 illustrates the proportion of each of the NK subsets in the four patient groups.

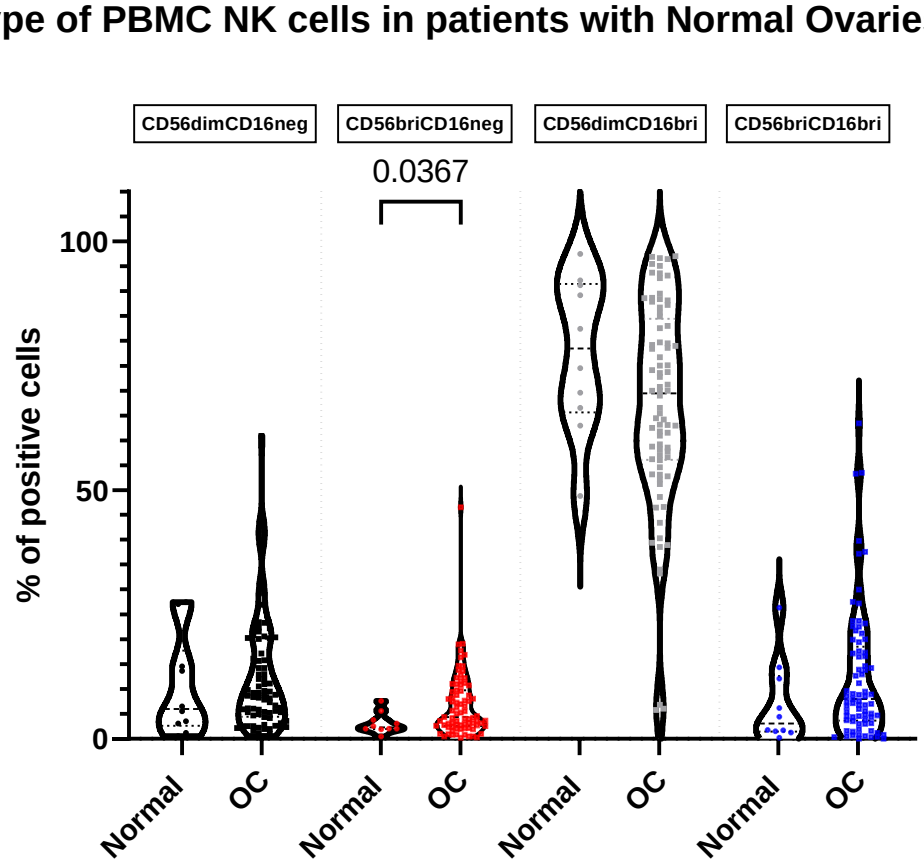


Figure 4.9: Comparison of the proportion of NK cell subsets between patients with normal ovaries and patients with OC.

The $CD56^{bri}CD16^{neg}$ NK cell subset was significantly higher in the OC patients than in the patients with normal ovaries. There was no difference in the other NK subsets between the patients with normal ovaries and patients with OC.

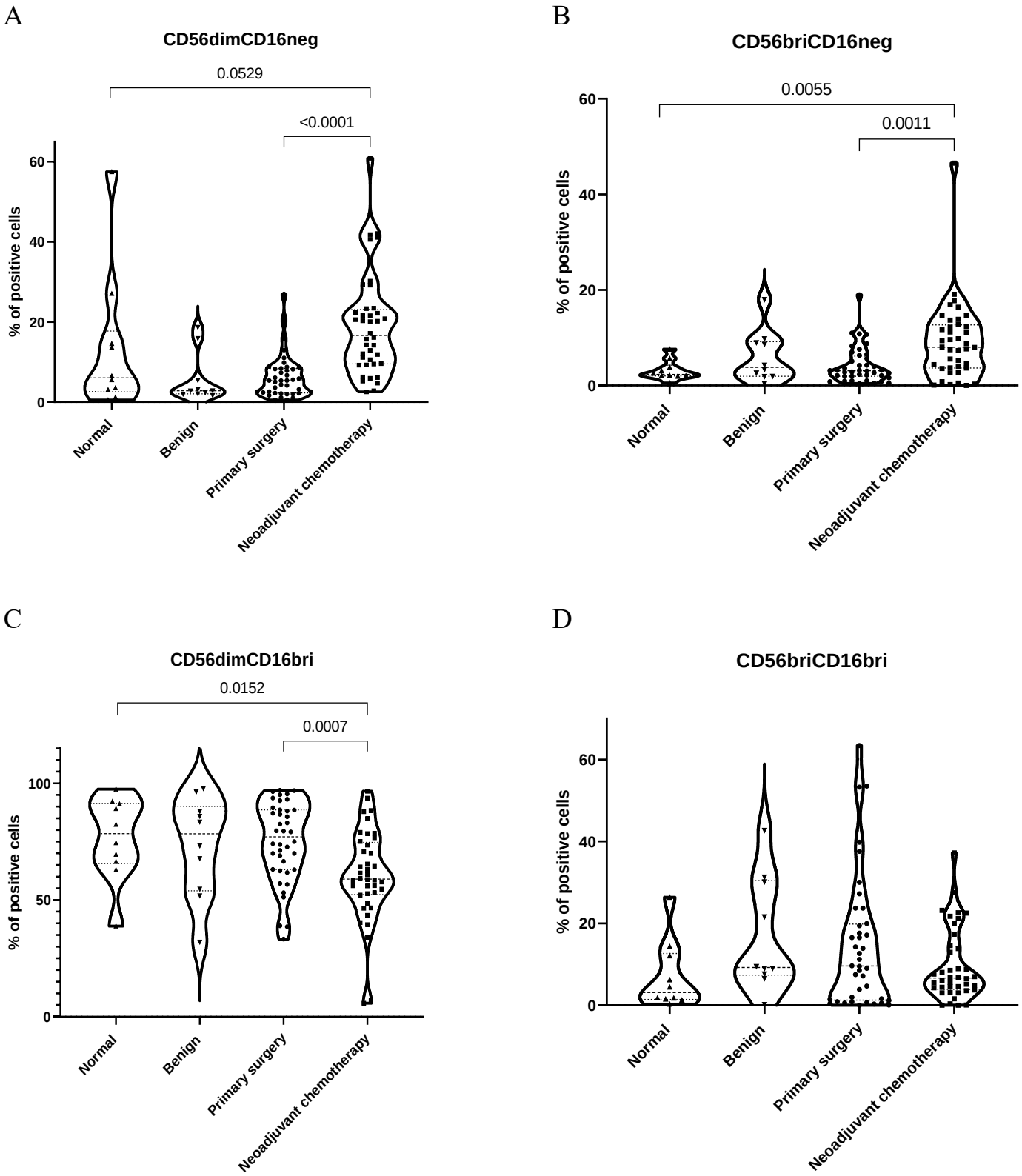


Figure 4.10: The proportion of the NK cell subsets across the different patient groups.
The $CD56^{dim}CD16^{neg}$ (A) and $CD56^{bri}CD16^{neg}$ (B) NK cell subsets occurred more frequently in chemotherapy exposed patients (neoadjuvant chemotherapy group) than in the chemotherapy naïve OC patients (primary surgery group) and in the patents with normal ovaries. The $CD56^{dim}CD16^{bri}$ (C) cells were less common in the neoadjuvant chemotherapy group compared to the primary surgery and normal ovary groups. There were no differences in $CD56^{bri}CD16^{bri}$ (D) NK cells between the patient groups.

4.4.3 The expression of receptors on NK cells within the circulating blood

4.4.3.1 Activation receptors on the peripheral NK cells

The expression of various activation receptors on the whole PBMC NK cells was evaluated by further interrogating the flow cytometric data. The proportion of NK cells with high expression of the activation markers was calculated and any variances observed between the four patient groups. Out of five activation receptors (NKp46, NKG2C, NKG2D, DNAM-1 and CD57), the expression of NKp46 was the only receptor that differed between the patient groups. The proportion of PBMC NK cells with high expression of NKp46 was greater in OC patients (mean proportion of 17.8%) than in patients with normal ovaries (mean proportion of 8.6%), demonstrated in Figure 4.11 ($p = 0.0045$). This increased expression was also seen when the four patient groups were compared, with blood samples from OC patients undergoing primary surgery and neoadjuvant chemotherapy having significantly higher NKp46 levels ($p = 0.0008$ and $p = 0.0481$, respectively) than the blood samples obtained from patients in the normal ovary group. Figure 4.12 summarises the proportion of NK cells expressing the activation receptors across the four groups.

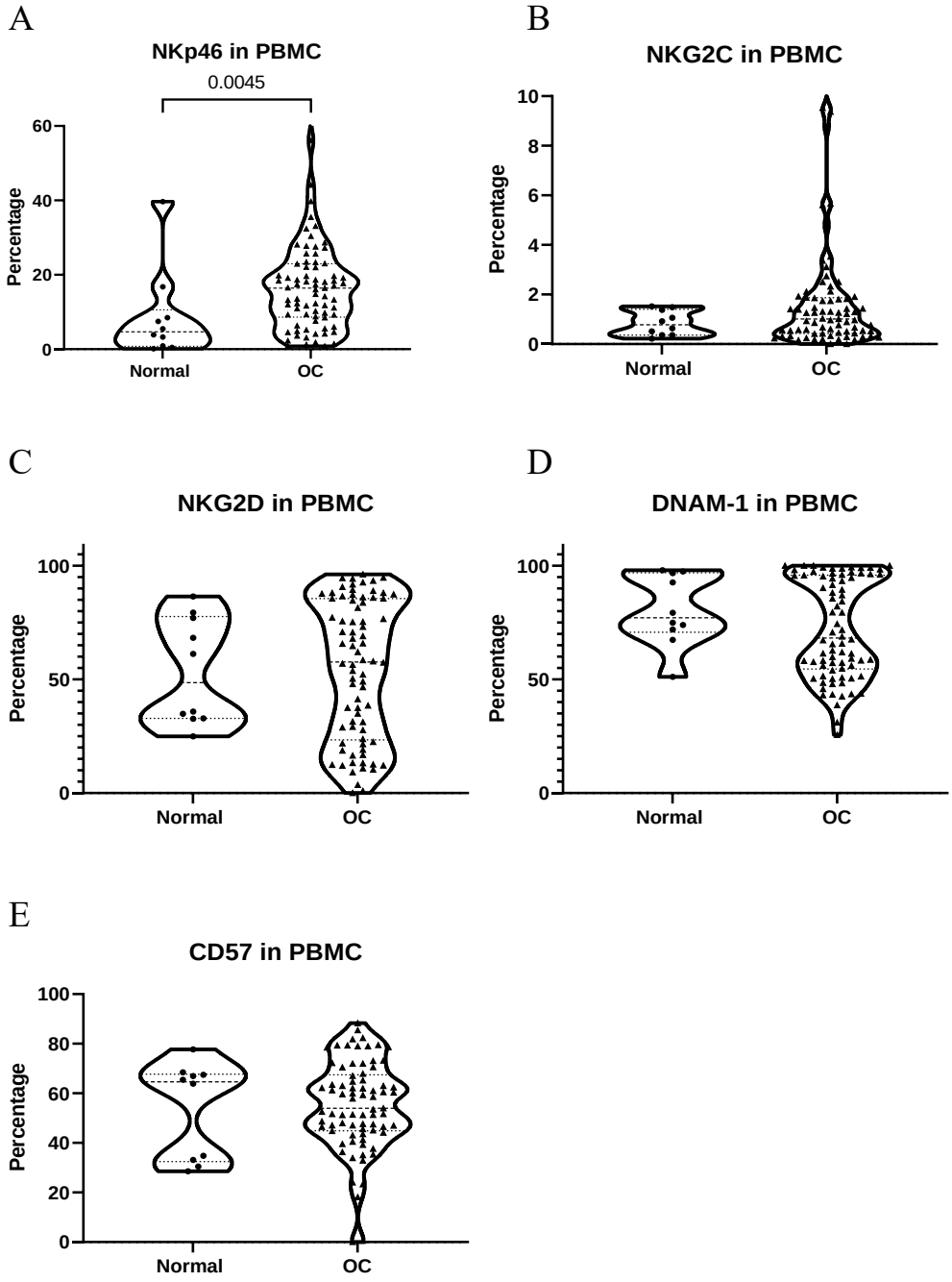


Figure 4.11: PBMC NK cells with high expression of activation receptors in patients with OC and normal ovaries.

The percentages of PBMC NK cells with high expression of activating receptors were compared between the OC patients and control patients with normal ovaries. The PBMC NK cells in OC patients had significantly increased expression of activation receptor (A) NKp46 ($p = 0.0045$). There was no difference between the OC patients and those with normal ovaries in the expression of activation receptors: (B) NKG2C, (C) NKG2D, (D) DNAM-1, and (E) CD57.

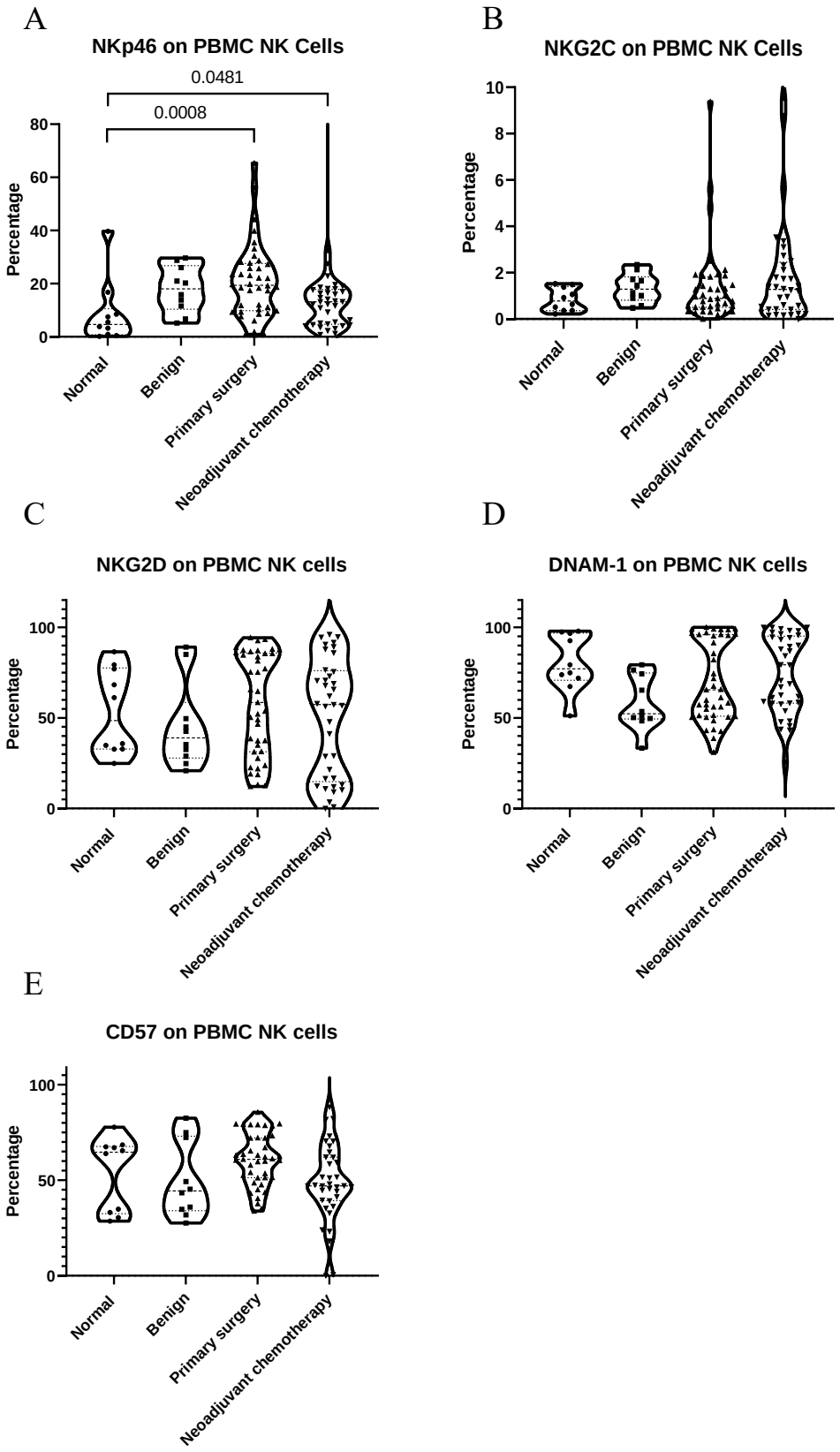


Figure 4.12: PBMC NK cells with high expression of activation receptors in the four patient groups.

PBMC NK cells in primary surgery and neoadjuvant chemotherapy OC patients had increased expression of activation receptor NKp46 (A) compared to patients with normal ovaries ($p = 0.0008$ and $p = 0.0481$, respectively). There was no difference between the patient groups in the expression of activation receptors: (B) NKG2C, (C) NKG2D, (D) DNAM-1, and (E) CD57.

4.4.3.2 Inhibitory receptors on the peripheral NK cells

The expression of the inhibitory receptors on the PBMC NK cells was also calculated. The percentages of NK cells expressing each inhibitory receptor were compared. There was higher expression of both immune checkpoint receptors, PD-1 and CTLA-4, on the peripheral NK cells in OC patients compared to the NK cells in patients with normal ovaries (mean of 7.0% for PD-1 in OC vs 2.1% in the normal ovary group, $p = 0.0607$; mean of 9.8% for CTLA-4 in OC vs 4.1% in the normal ovary group, $p = 0.0403$). There were no differences in the receptors CD94 and TIGIT between the OC and normal ovary groups, seen in Figure 4.13. Upon analysis of the four patient groups (Figure 4.14), it became apparent that the PBMC samples from the neoadjuvant chemotherapy group demonstrated raised immune checkpoint expression. Here, CTLA-4 was found to be significantly higher in the neoadjuvant chemotherapy group than in the normal ovary group ($p = 0.0446$), with PD-1 also significantly raised ($p = 0.0150$).

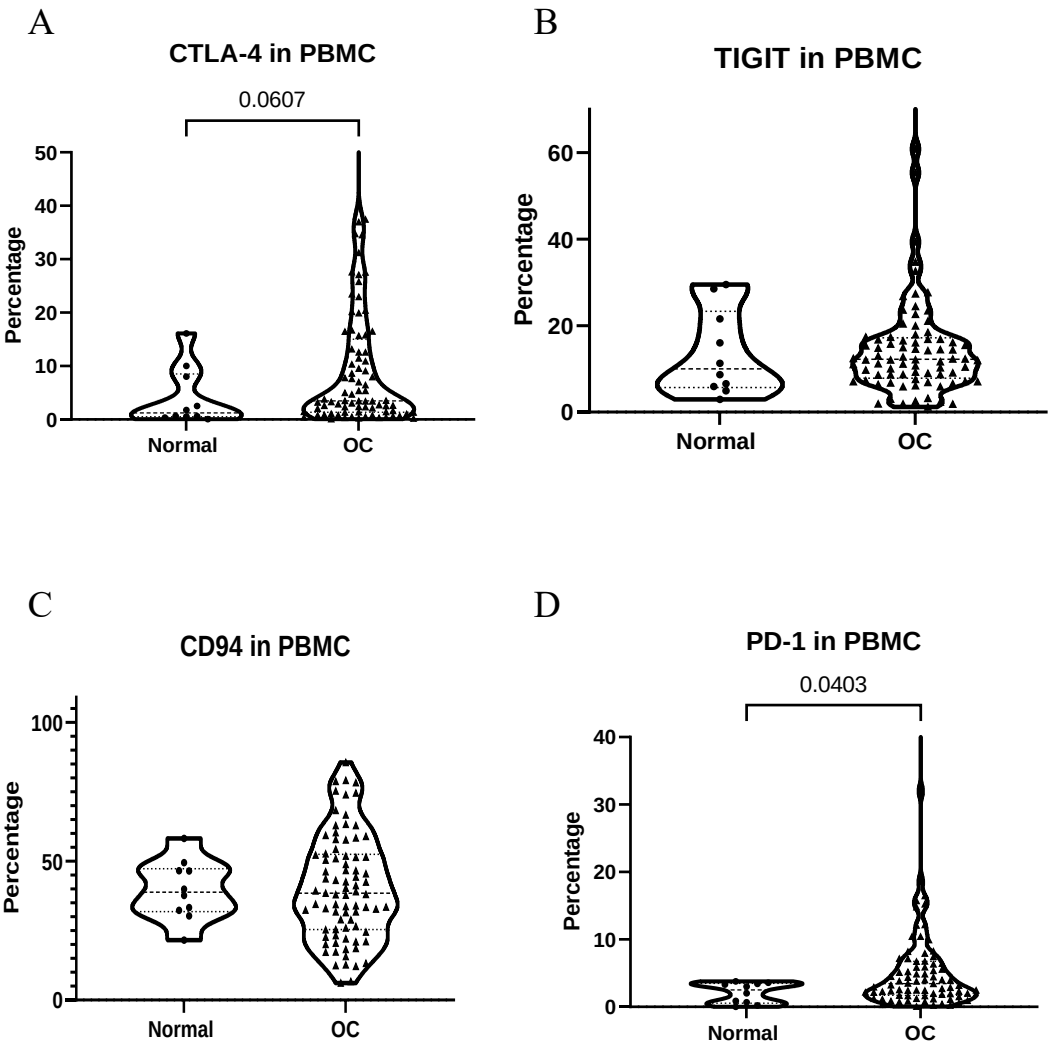


Figure 4.13: PBMC NK cells with high expression of inhibitory receptors in OC patients compared to normal ovary patients.

PBMC NK cells in the OC patients had increased expression of inhibitory immune checkpoints, (A) CTLA-4 ($p = 0.0607$) and (D) PD-1 ($p = 0.0403$), compared to the PBMC NK cells in patients with normal ovaries. There were no differences in the expression of: (B) TIGT and (C) CD94 on the peripheral blood NK cells between patients with OC and normal ovaries.

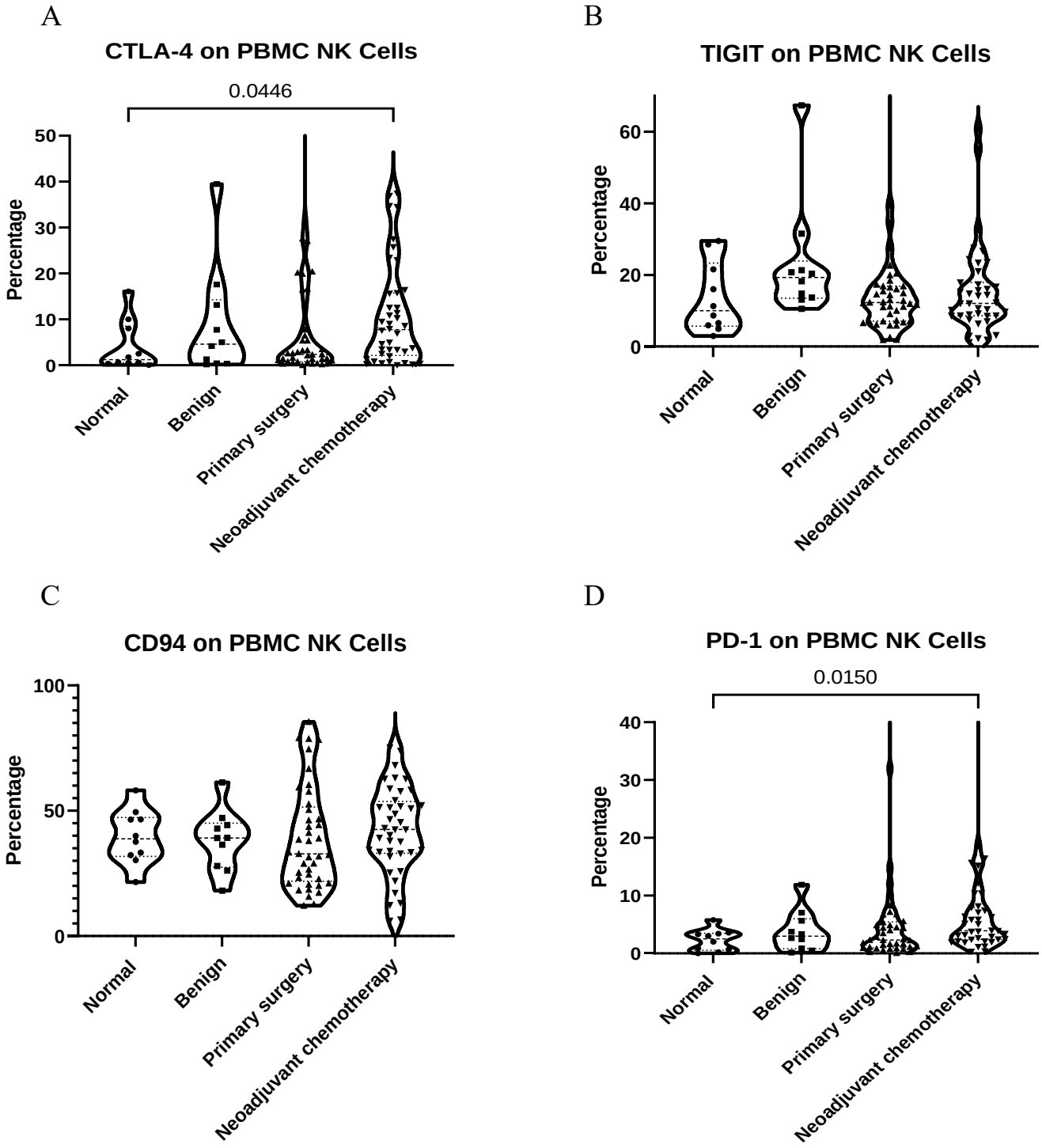


Figure 4.14: PBMC NK cells with high expression of inhibitory receptors in the four patient groups.

PBMC NK cells in the neoadjuvant chemotherapy OC patients had increased expression of inhibitory immune checkpoints, (A) CTLA-4 and (D) PD-1, compared to normal ovary patients ($p = 0.0446$ and $p = 0.0150$, respectively). There were no differences in the expression of these inhibitory checkpoints on peripheral NK cells in the primary surgery and benign ovary groups. There were also no differences between the expression of: (B) TIGT and (C) CD94 on the PBMC NK cells between the patient groups.

4.4.4 Summary of the peripheral NK cell phenotype

The investigation of patient PBMC samples has identified clear variations between the number, subset and activation of the peripheral NK cells. OC patients had a greater proportion of NK cells (significant in the primary surgery group) compared to the patients with normal ovaries, potentially due to NK proliferation and expansion in response to malignancy. The chemotherapy exposed samples had a reduction in the mature cytotoxic NK cells and increase in immature cytokine producing NK cells, showing chemotherapy treatment renders the NK cells less cytotoxic. However, the $CD56^{dim}CD16^{neg}$ NK subset, which is thought to be responsible for natural cytotoxicity specifically against tumours [213], was higher following chemotherapy indicating NK differentiation in response to treatment. In addition, the NK cells in OC patients had increased expression of activation receptor, NKp46, which indicating a more activating phenotype due to the response to malignancy. Whereas the inhibitory immune checkpoints, CTLA-4 and PD-1, were upregulated in OC particularly following chemotherapy, this observation indicates the NK cells in OC are overstimulated and have the potential to become exhausted.

4.5 Assessment of NK cell phenotype following ovarian infiltration

4.5.1 The proportion of NK cells within ovarian tissue

The proportion of NK cells that had infiltrated into ovarian tissue was calculated using the CD45 positive lymphocyte population. All available ovarian biopsy samples were utilised, giving 7 normal, 6 benign, 31 primary surgery OC and 18 neoadjuvant chemotherapy OC samples. There were no obvious differences in the proportion of tissue infiltrating NK cells when comparing all OC cases to normal ovary, highlighted in Figure 4.15. When evaluating the four separate patient groups, there were also no variations between the two OC groups, benign ovary or normal ovary groups, shown in Figure 4.16. The mean proportion of NK

cells that infiltrated ovarian tissue was highest in benign ovary (26.0%) and primary surgery OC (18.5%) samples. While the mean proportion of NK infiltration was 16.6% when all OC samples were classed together, infiltration was reduced in OC tissue following chemotherapy treatment (13.4%). In addition, there were also fewer NK cells found within normal ovarian tissue biopsies (10.9%).

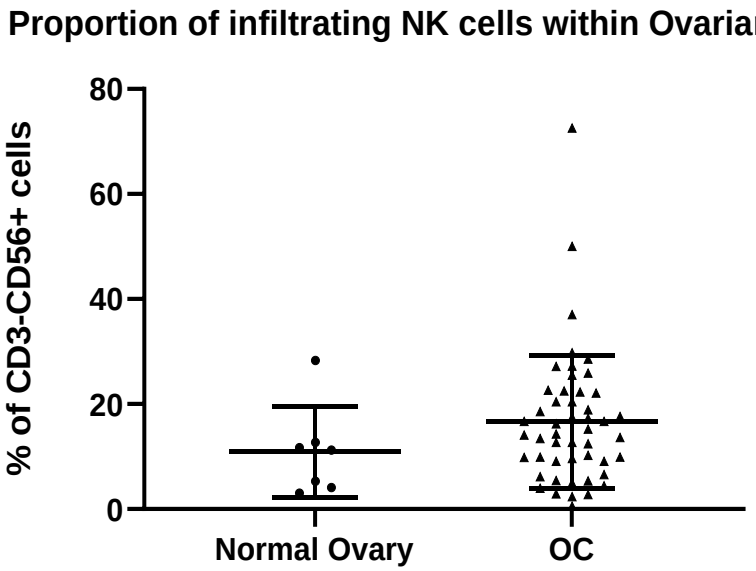


Figure 4.15: The proportion of CD56 positive NK cells infiltrating into ovarian tissue.
The proportion of NK cells in OC tissue biopsies is similar to the proportion of NK cells in biopsies of normal ovarian tissue ($p = 0.1833$). The mean proportion of NK cells in the ovarian tissue from OC patients was 16.6%, compared to 10.9% in the normal ovarian tissue samples.

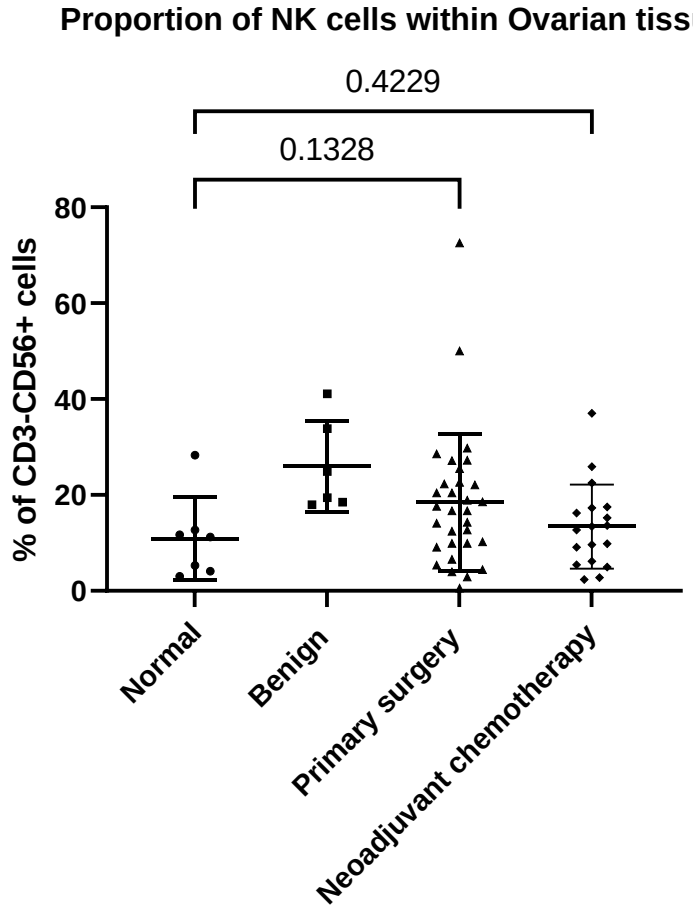


Figure 4.16: The proportion of CD56 positive NK cells infiltrating into ovarian tissue.
The proportion of NK cells in each ovarian tissue biopsy sample is similar across the four patient groups. There was no increased proportion of NK cells within OC samples from patients who had undergone primary surgery (p = 0.1328) or received neoadjuvant chemotherapy (p =0.4229) compared to the proportion of NK cells within the normal ovarian tissue biopsies.

4.5.2 The type of NK cells within the ovarian tissue

The expression patterns of CD16 and CD56 on the NK cells within the ovarian tissue is shown in Table 4.2. While normal ovarian tissue and primary surgery OC tissue have very similar amounts of $CD56^{dim}CD16^{bri}$ NK cells (mean proportions of 49.0% and 45.5%, respectively), decreased amounts of these mature cytotoxic NK cells are seen within the ovarian biopsies from the neoadjuvant chemotherapy group and when all OC samples are combined (mean proportions of 28.3% and 39.1%, respectively). Instead, the mean proportion of $CD56^{dim}CD16^{neg}$ cells within neoadjuvant chemotherapy ovarian tissue was

raised at 51.0%, compared to 22.3% in normal ovarian, 9.0% in benign ovarian, 36.6% in all OC and 30.2% in primary surgery NK cells. While NK cells within normal ovarian tissue were comprised of a higher proportion of $CD56^{bri}CD16^{bri}$ NK cells (mean 15.6%) than benign, primary surgery and neoadjuvant chemotherapy groups (3.1%, 9.4% and 8.4%, respectively), there were no obvious differences in the mean proportion of $CD56^{bri}CD16^{neg}$ NK cells across the four patient groups.

Table 4.2: The mean proportion of NK subsets within ovarian tissue

Ovary status	**Mean % CD56dim CD16neg**	**Mean % CD56bri CD16neg**	**Mean % CD56dim CD16bri**	**Mean % CD56bri CD16bri**
Normal ovary (n=10)	22.3	21.2	49.0	15.6
Benign ovary (n=10)	9.0	12.9	75.0	3.1
All OC (n=80)	36.6	16.7	39.1	9.0
Primary surgery OC (n=40)	30.2	17.9	45.5	9.4
Neoadjuvant chemotherapy OC (n=40)	51.0	14.2	28.3	8.4

The different NK subsets identified within each ovarian tissue biopsy are illustrated in Figure 4.17. Here, ovarian tumour infiltrating NK cells (also in both primary surgery OC and neoadjuvant chemotherapy OC) consist of increased $CD56^{dim}CD16^{neg}$ and decreased C $CD56^{dim}CD16^{bri}$ NK subsets, with the greatest alterations seen in the neoadjuvant chemotherapy group.

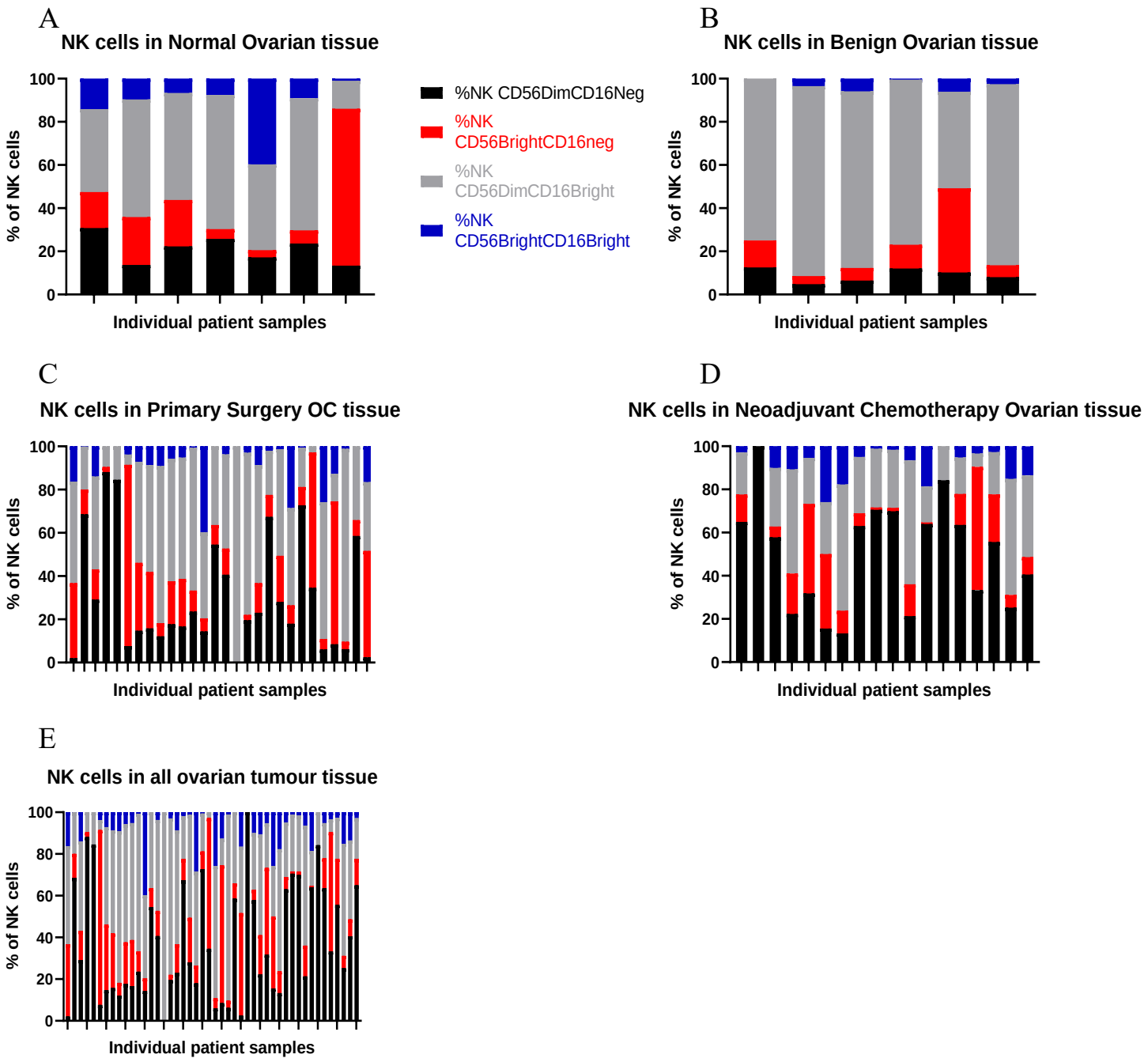


Figure 4.17: The proportion of NK subsets within each ovarian tissue biopsy sample.
The type of NK cells that have infiltrated into: A) normal ovarian tissue, B) benign ovarian tissue, C) primary surgery OC, D) neoadjuvant chemotherapy OC, and E) all OC samples combined. There are increased proportions of $CD56^{dim}CD16^{neg}$ NK subsets within ovarian tissue biopsies obtained from the OC groups. The OC biopsies also have reduced proportions of $CD56^{dim}CD16^{bri}$ NK subsets.

Overall, there were significantly more tissue infiltrating $CD56^{dim}CD16^{neg}$ NK cells in the OC samples than in the normal ovarian biopsies ($p = 0.0210$), Figure 4.18. Further examination revealed that the infiltrating $CD56^{dim}CD16^{neg}$ NK cells were raised solely in the neoadjuvant chemotherapy OC samples, compared to normal ovarian biopsies ($p = 0.0171$), benign ovarian samples ($p < 0.0001$) and primary surgery tumour tissue ($p = 0.0120$). In addition, there were significantly fewer $CD56^{dim}CD16^{bri}$ infiltrating NK cells in the chemotherapy exposed tissue compared to the normal ($p = 0.0205$), benign ($p = 0.0002$) and primary surgery tumour ($p = 0.0154$) tissues. There were no differences in the amount of $CD56^{bri}CD16^{bri}$ or $CD56^{bri}CD16^{neg}$ NK cell infiltration between the four different groups. Figure 4.19 illustrates each of the NK subsets in the four patient groups.

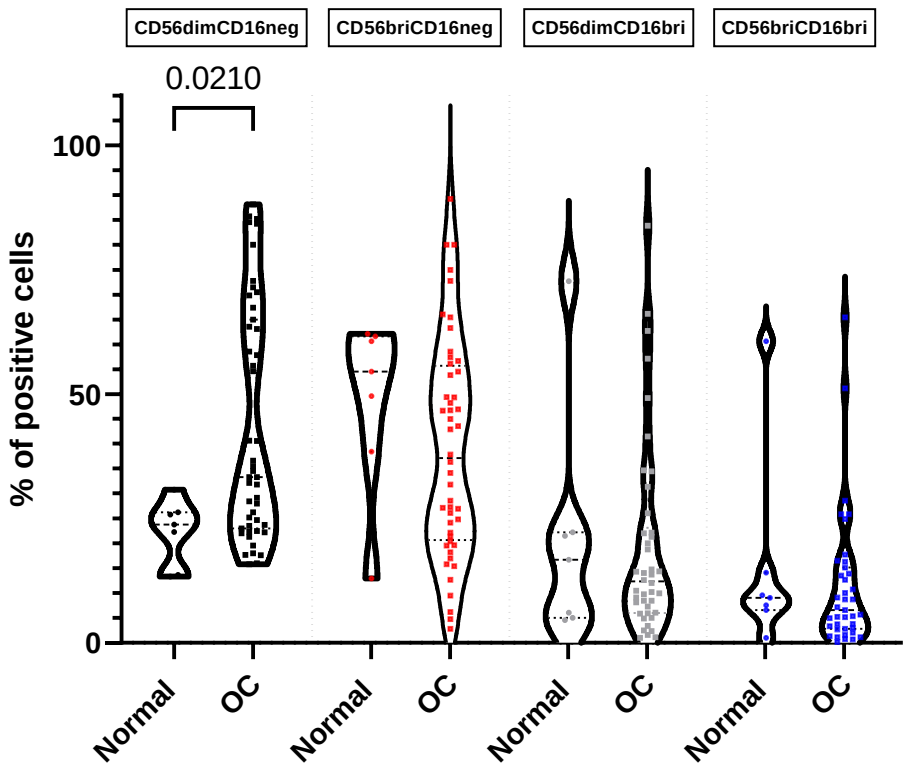


Figure 4.18: The incidence of the ovarian infiltrating NK cell subsets in OC and normal ovarian tissue.

There were significantly more tissue infiltrating $CD56^{dim}CD16^{neg}$ NK cells in the OC samples than in the normal ovarian biopsies ($p = 0.0210$). There were no differences in the other NK subsets within ovarian tissue biopsies between the OC and normal ovary groups.

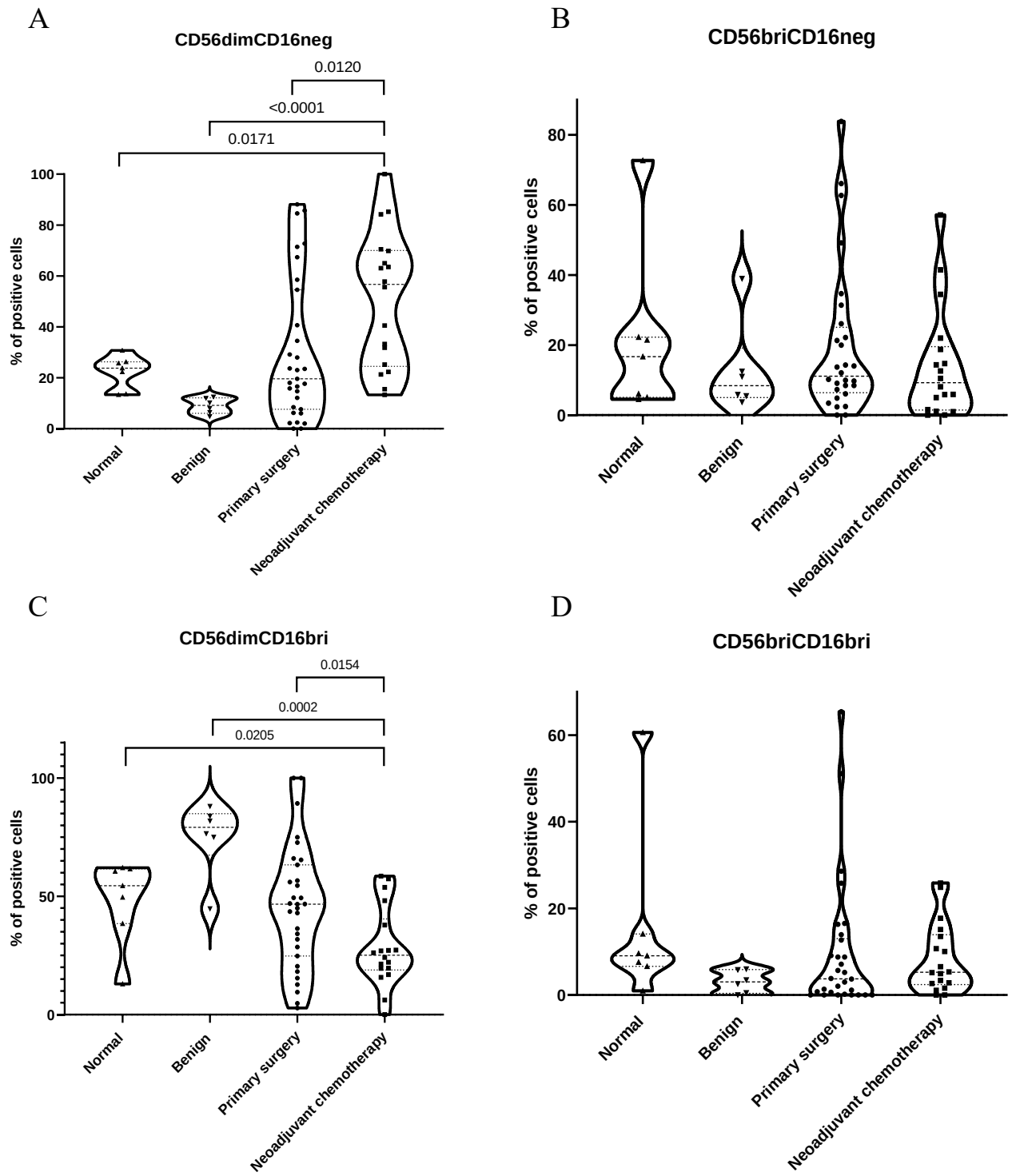


Figure 4.19: The incidence of the ovarian infiltrating NK cell subsets across the different patient groups.

The $CD56^{dim}CD16^{neg}$ (A) subset was significantly greater in the neoadjuvant chemotherapy ovarian tumour tissue compared to primary surgery tumour tissue ($p = 0.0120$), benign ovarian tissue ($p < 0.0001$) and normal ovarian tissue ($p = 0.0171$). The $CD56^{dim}CD16^{bri}$ (C) NK cell subset was significantly reduced in the chemotherapy exposed tumour tissue compared to the primary surgery tumour tissue ($p = 0.0154$), benign ovarian tissue ($p = 0.0002$) and normal ovarian tissue ($p = 0.0205$). There were no differences in the $CD56^{bri}CD16^{neg}$ (B) and $CD56^{bri}CD16^{bri}$ (D) NK subsets between the patient groups.

4.5.3 The expression of receptors on ovarian tissue infiltrating NK cells

4.5.3.1 Activation receptors on the ovarian NK cells

The expression patterns of the activation receptors on the ovarian tissue NK cells were then examined. When comparing NK cells within ovarian tumour tissue to the NK cells in normal ovarian tissue, there was increased expression of NKG2D ($p = 0.0165$), DNAM-1 ($p = 0.0092$) and CD57 ($p = 0.0013$) on the NK cells in the tumour tissue Figure 4.20). When analysing the four patient groups (Figure 4.21), there was clear upregulation of DNAM-1 and CD57 on the NK cells in both primary surgery OC and neoadjuvant chemotherapy OC compared to normal ovarian infiltrating NK cells. The NKG2D receptor however, was only over-expressed on the NK cells within the chemotherapy exposed tissue. There were no differences in NKp46 and NKG2C expression on the ovarian NK cells between the four ovarian tissue groups.

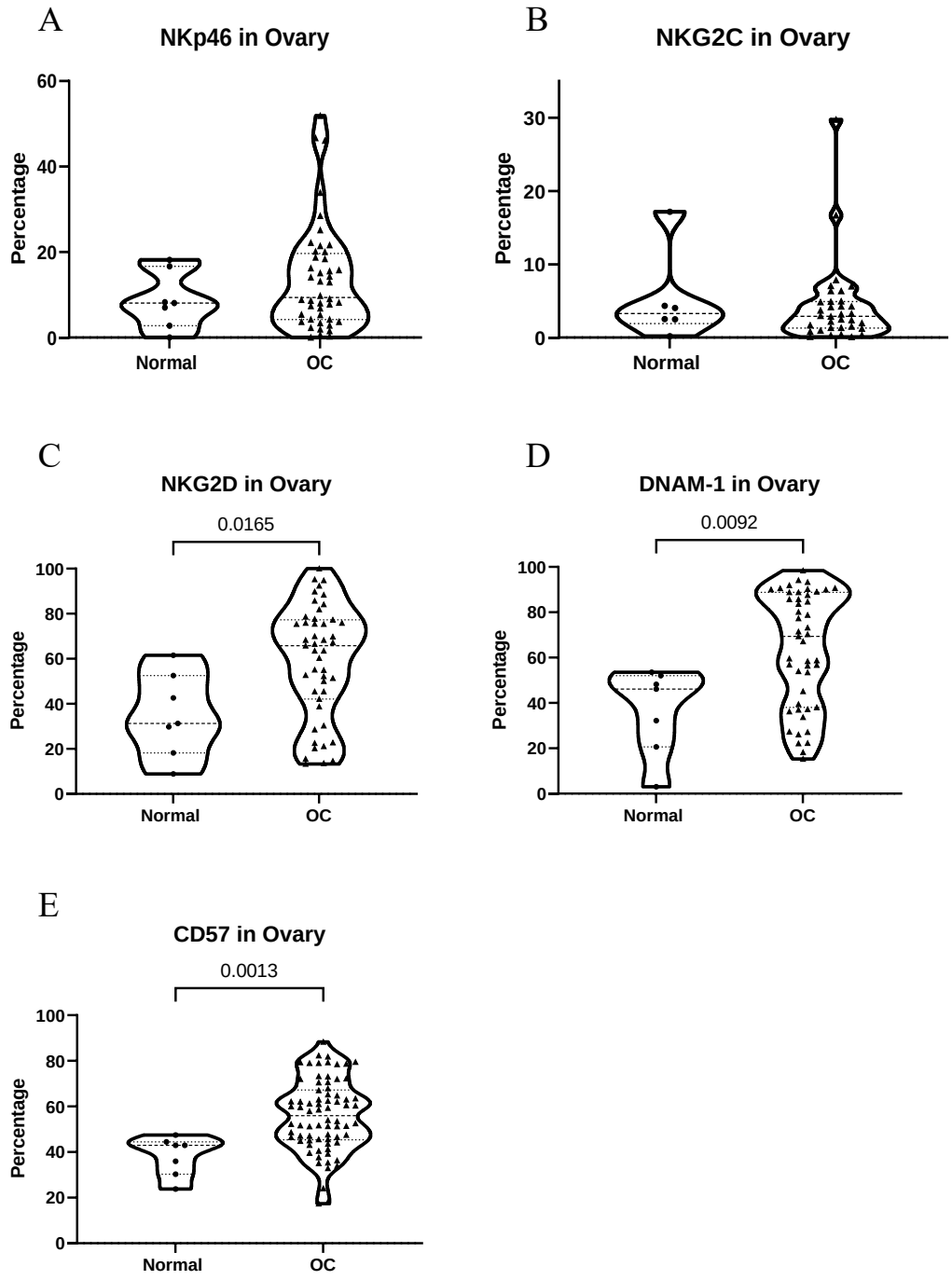


Figure 4.20: Activation receptors in normal ovarian and OC tissue.
Ovarian NK cells within tumour tissue had increased expression of activation receptors: C) NKG2D, D) DNAM-1, and E) CD57 compared to those in normal ovarian tissue ($p = 0.0165$, $p = 0.0092$ and $p = 0.0013$, respectively). There were no differences between the groups in the expression of: A) NKp46 or B) NKG2C.

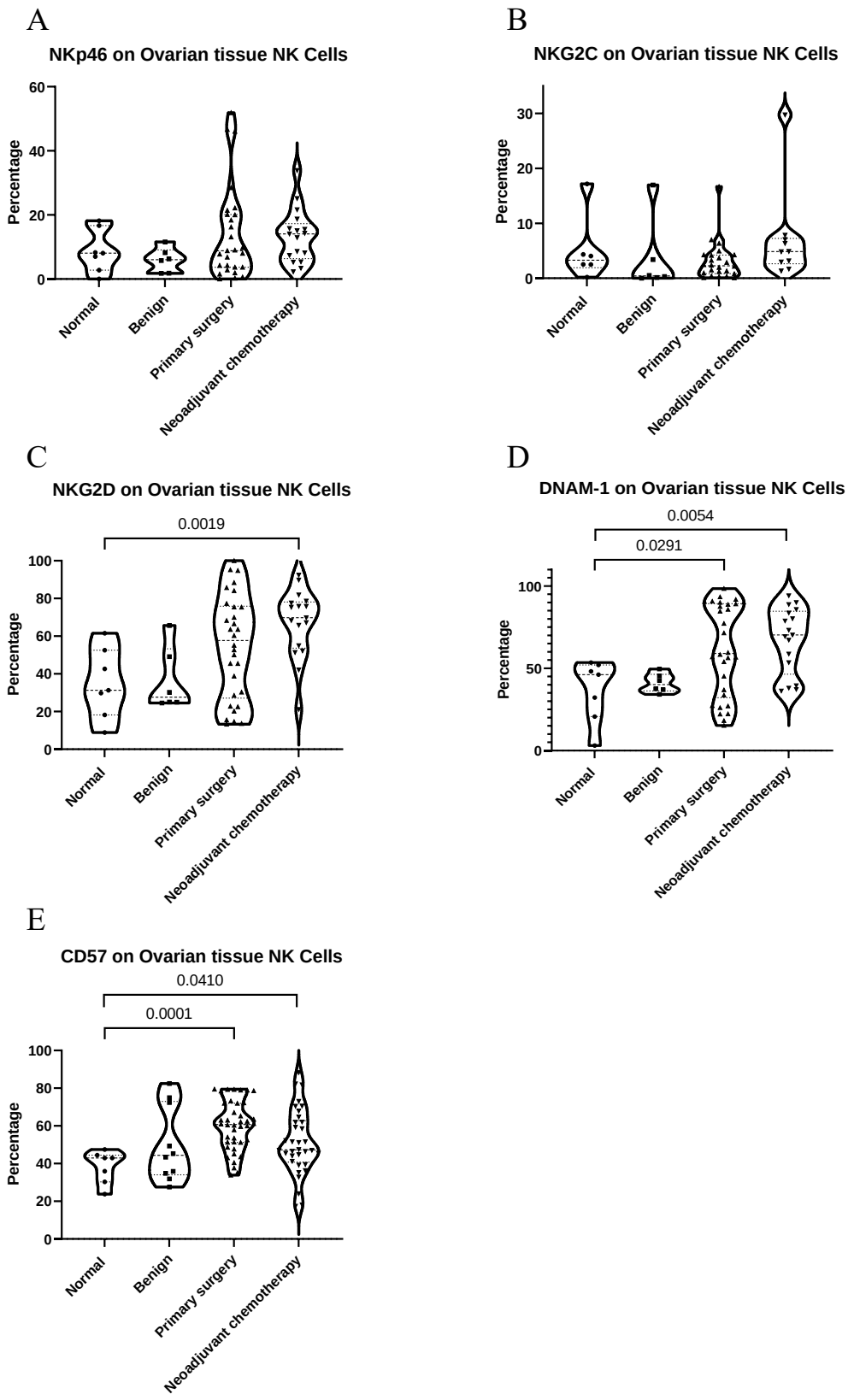


Figure 4.21: Ovarian NK cell activation receptor across four patient groups.
There was increased expression of the activation receptors DNAM-1 (D) and CD57 (E) on NK cells within ovarian tissue in the primary surgery and neoadjuvant chemotherapy OC groups compared to normal ovarian tissue. There was increased expression of NKG2D (C) on the NK cells within the neoadjuvant chemotherapy samples compared to the normal ovarian samples. There were no differences in the expression of NKp46 (A) and NKG2C (B) on the ovarian NK cells between the patient groups.

4.5.3.2. Inhibitory receptors on the ovarian NK cells

The expression of the inhibitory receptors (CTLA-4, TIGIT, CD94 and PD-1) on the ovarian tissue NK cells did not differ between the OC samples and the normal ovary samples, detailed in Figure 4.22. There were also no differences in the expression of inhibitory receptors when comparing the NK cells infiltrating normal ovaries, benign ovaries, treatment naïve primary surgery tumours and chemotherapy exposed tumours (Figure 4.23).

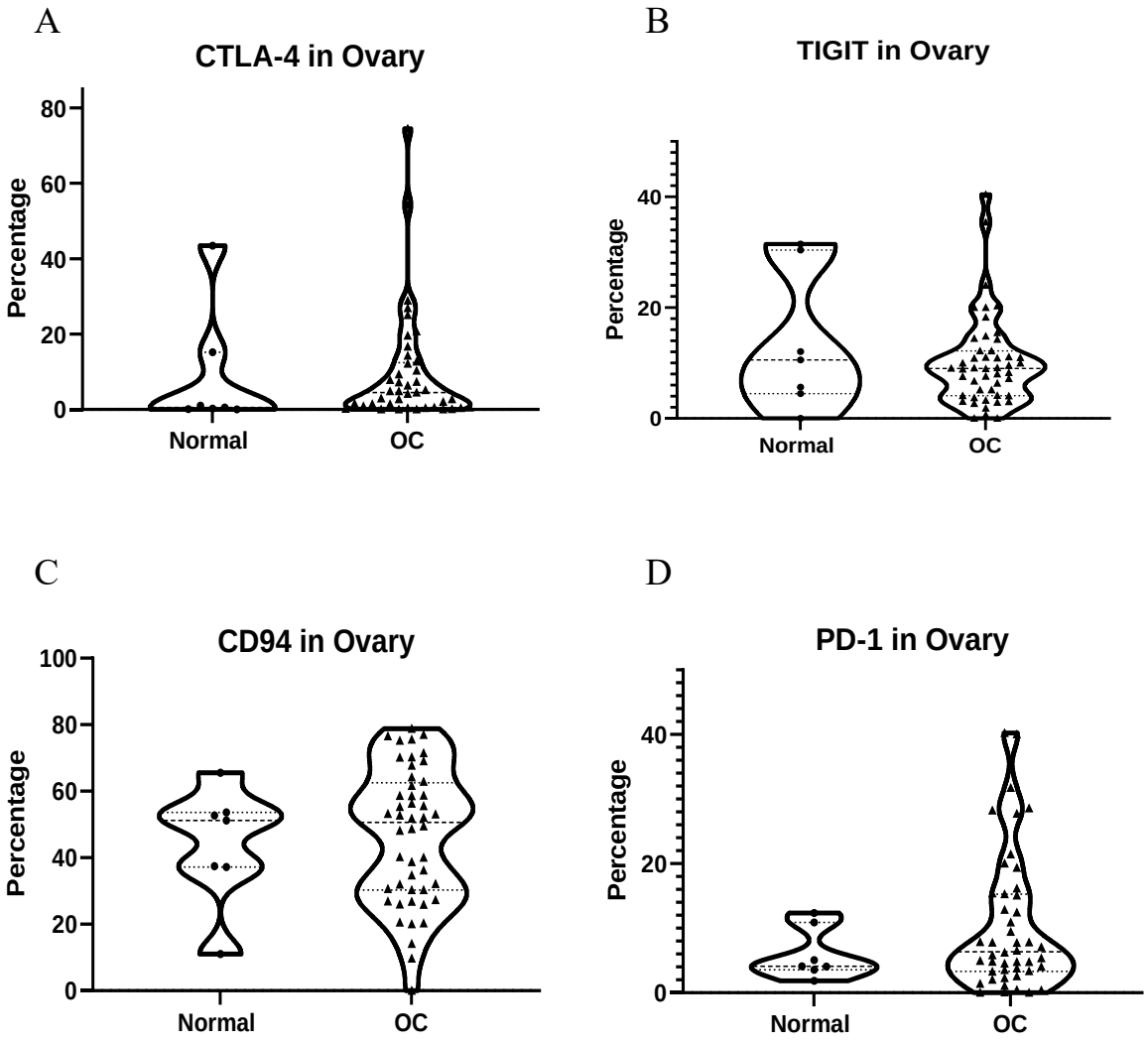


Figure 4.22: Inhibitory receptors on tissue infiltrating NK within OC and normal ovaries.
There were no significant differences in the expression of receptors A) CTLA-4, B) TIGIT, C) CD94, and D) PD-1 on the NK cells within OC and normal ovarian tissue.

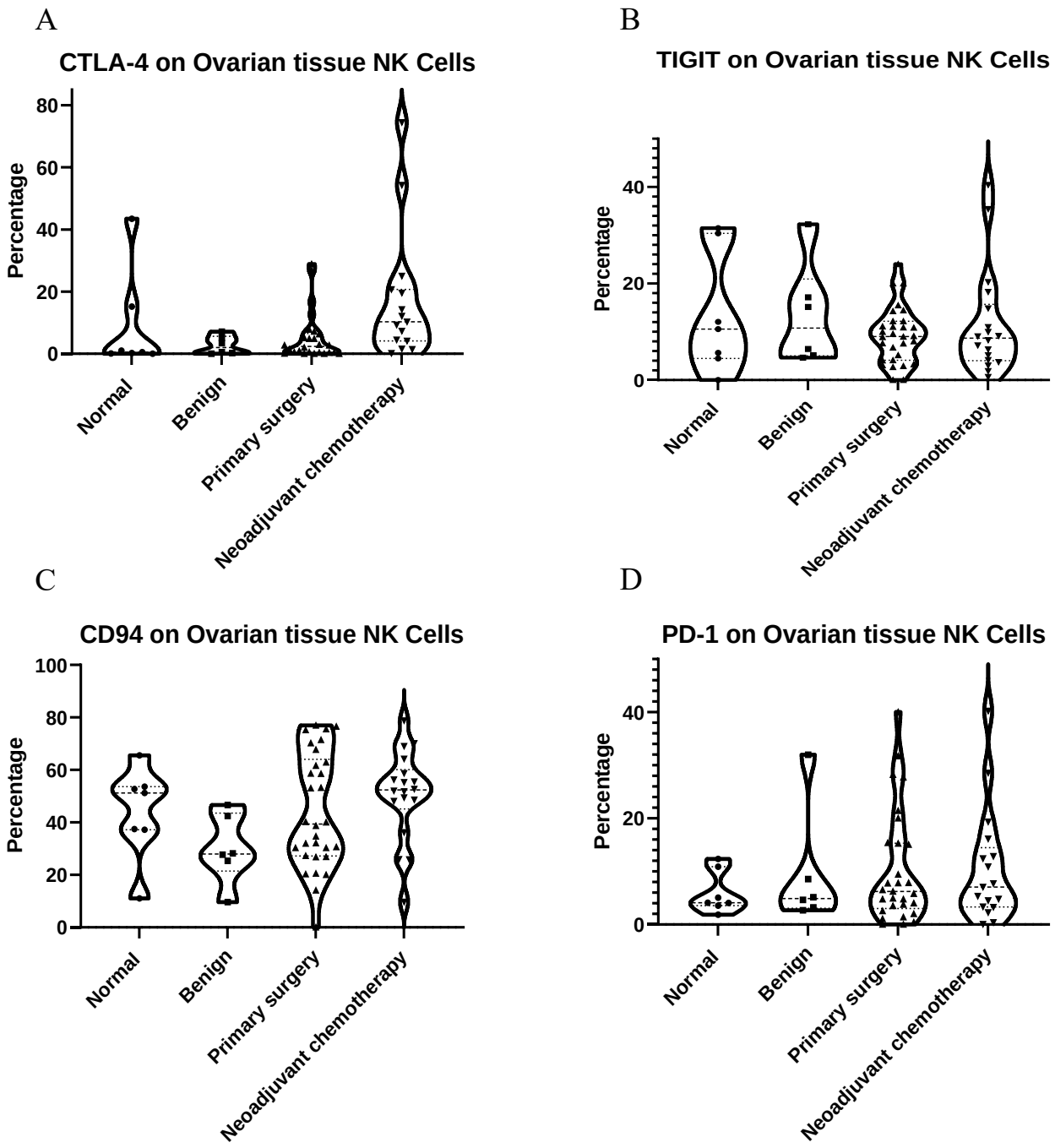


Figure 4.23: Ovarian NK cell inhibitory receptors across four patient groups.
There were no significant differences in the expression of inhibitory receptors A) CTLA-4, B) TIGIT, C) CD94, and D) PD-1 on the ovarian tissue infiltrating NK cells between the patient groups.

4.5.4 Summary of the ovarian infiltrating NK cell phenotype

The number of NK cells were similar in all types of ovarian tissue, suggesting that NK cells retain their ability to penetrate ovarian tissue despite the development of a solid tumour and a malignant microenvironment. However, the type of NK cells differed in the chemotherapy exposed tumour tissue (neoadjuvant chemotherapy group). Here, there were fewer mature cytotoxic $CD56^{dim}CD16^{bri}$ NK cells, yet an increase in the $CD56^{dim}CD16^{neg}$ NK cells that generate tumour specific cytotoxicity, as was seen in the peripheral blood NK analysis. The upregulation of activation receptors NKG2D, DNAM-1 and CD57 on NK cells within OC samples indicated that the NK cells are recognising and responding to the altered ovarian tumour tissue.

4.6 Assessment of NK cell phenotype following omental tissue infiltration

4.6.1 The proportion of NK cells within omental tissue

The proportion of NK cells infiltrating into the omentum was calculated using the same CD45 positive, lymphocyte population. The omental biopsies utilised included: 11 pathologically normal omental samples obtained from patients with normal or benign ovarian masses and 27 omental tumour samples whereby ovarian tumours had metastasised into the omentum. Of these omental tumour samples, there were 14 that had been exposed to chemotherapy (neoadjuvant chemotherapy OC group) and 13 chemotherapy naïve (primary surgery OC group).

The proportion of NK cells infiltrating into the omentum was significantly lower in the omental tumour cases compared to the normal omentum ($p = 0.0105$), shown in Figure 4.24. When the omental tumour cases were divided into the primary surgery and neoadjuvant chemotherapy groups, they both had a reduction in NK cell infiltration compared to normal

omental tissue, but there was no difference between the two tumour groups, highlighted in Figure 4.25. Similarly, the mean proportion of NK cells within the omentum was decreased in the malignant tissue: 19.2% in normal omentum and 11.8% in all omental tumour samples ($p = 0.0260$). The mean proportion in the primary surgery group was also 11.8%, and 11.7% in the neoadjuvant chemotherapy group. This indicates that the NK cells were prevented from or unable to infiltrate the malignant omentum, but their ability to penetrate into omental tumour was not influenced by chemotherapy treatment.

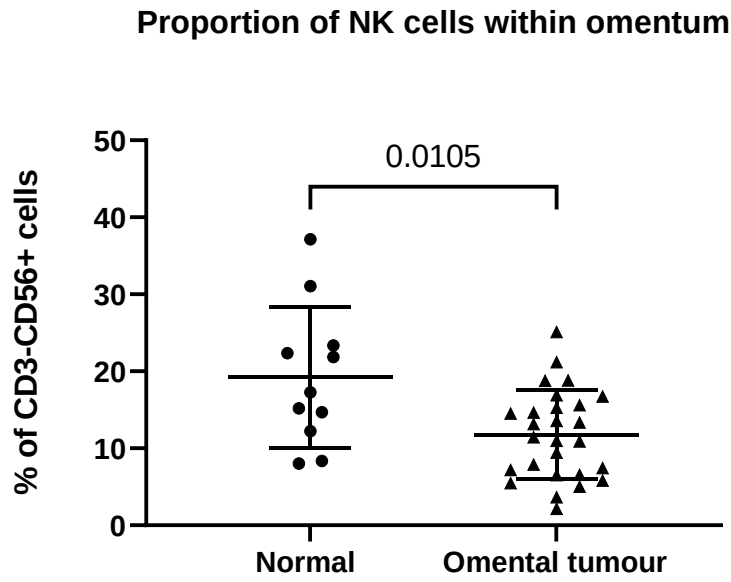


Figure 4.24: Proportion of infiltrating NK cells within omental tissue.
There were significantly fewer NK cells within the omental tumour tissues (biopsies from the primary surgery and neoadjuvant chemotherapy OC groups combined) compared to normal omentum obtained from patients with normal and benign ovaries ($p = 0.0105$).

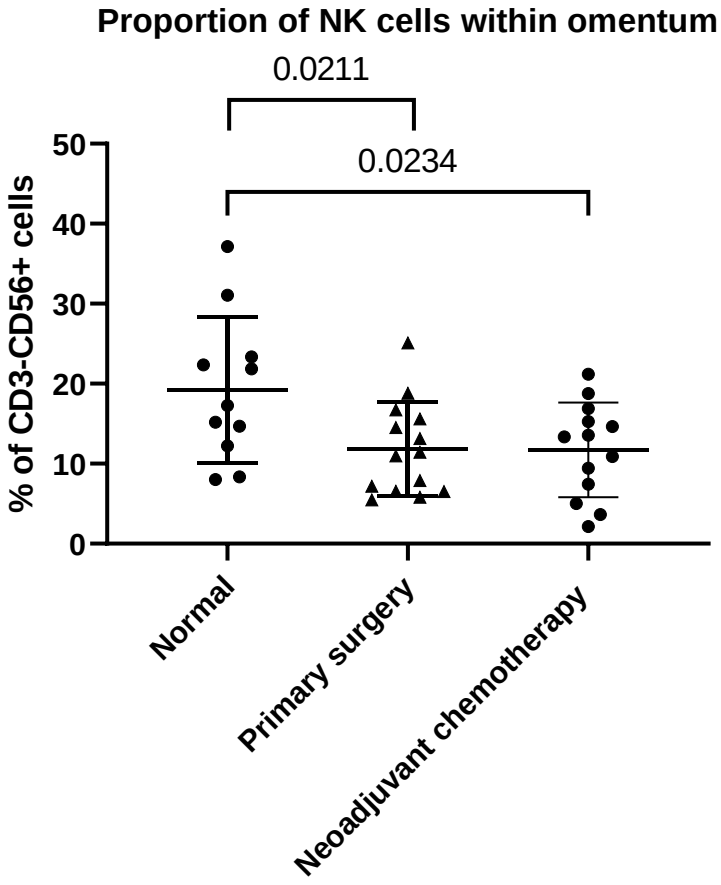


Figure 4.25: Proportion of infiltrating NK cells within normal omentum, chemotherapy naïve omental tumours and chemotherapy exposed omental tumours.
There was no difference in NK cell infiltration between the chemotherapy naïve (primary surgery group) and chemotherapy exposed (neoadjuvant chemotherapy group) omental tumours (p = 0.9810). There were significantly fewer NK cells within both omental tumour groups compared to the proportion in normal omental tissue (p = 0.0211 in primary surgery vs normal omentum; p = 0.0234 in neoadjuvant chemotherapy vs normal omentum).

4.6.2 The type of NK cells within the omental tissue

The CD16 and CD56 expression on the NK cells within the omental tissue was then examined, shown in Table 4.3. The predominant subset in the normal omentum was the mature cytotoxic NK cells with low CD56 and high CD16 expression ($CD56^{dim}CD16^{bri}$), with a mean proportion of 60.5%. This subset of NK cells was reduced in the omental tumour tissue: mean proportion of 34.6% in the primary surgery group (p = 0.0010) and 42.8% in the

neoadjuvant chemotherapy group (p = 0.0930). The $CD56^{dim}CD16^{neg}$ NK cells were increased in the omental tumour compared to the normal tissue: mean proportion of 16.7% in normal omentum vs 34.8% in the primary surgery group (p = 0.0470) and 42.4% in the neoadjuvant chemotherapy group (p = 0.0180). Although the proportion of $CD56^{bri}CD16^{bri}$ NK cells were similar in all the omental samples, the immature cytokine producing $CD56^{bri}CD16^{neg}$ NK cells were reduced in the chemotherapy exposed omental tumour compared to the chemotherapy naïve omental tumour. The mean proportion in the neoadjuvant chemotherapy group was 9.3% compared to 22.7% in the primary surgery group (p = 0.0290). There was no significant difference between the neoadjuvant chemotherapy samples and the normal omentum (9.3% vs 15.7%, p = 0.2840) or the primary surgery samples and the normal omentum (22.7% vs 15.7%, p = 0.3450).

Table 4.3: The mean proportion of NK subsets within omental tissue

Omentum status	**Mean % CD56dim CD16neg**	**Mean % CD56bri CD16neg**	**Mean % CD56dim CD16bri**	**Mean % CD56bri CD16bri**
Normal omentum (n=11)	16.7	15.7	60.5	7.0
All omental tumour (n=27)	38.5	16.2	38.5	6.2
Primary surgery omental tumour (n=13)	34.8	22.7	34.6	7.9
Neoadjuvant chemotherapy omental tumour (n=14)	42.4	9.3	42.8	5.4

The different NK subsets within each individual omental tissue biopsy are detailed in Figure 4.26. The omental tumour infiltrating NK cells (in the primary surgery, neoadjuvant chemotherapy and combined tumour cases) consist of increased $CD56^{dim}CD16^{neg}$ NK cells and decreased $CD56^{dim}CD16^{bri}$ NK subsets.

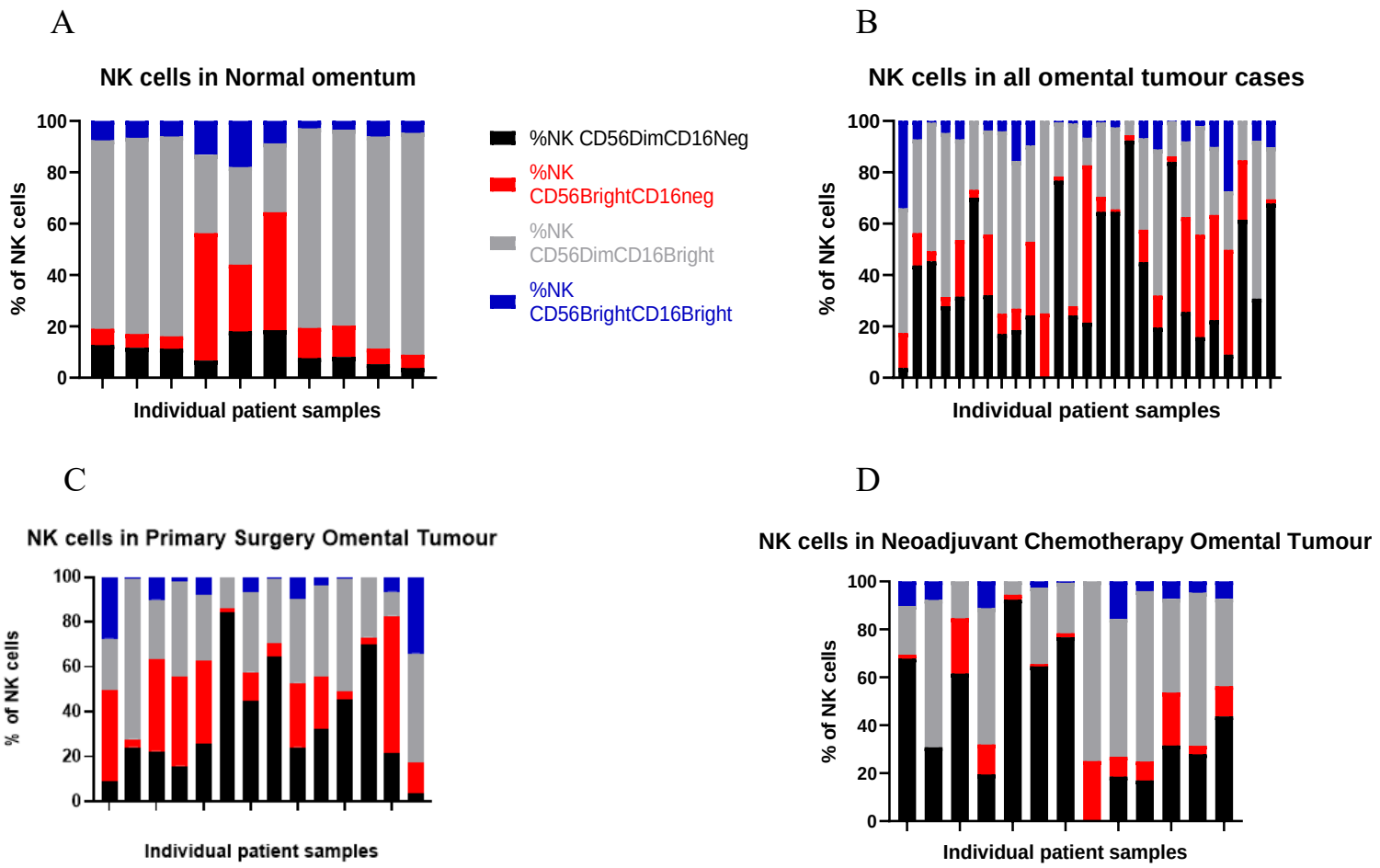


Figure 4.26: The proportion of NK subsets within each omental tissue biopsy sample.
The type of NK cells that have infiltrated into: A) normal omental tissue, B) all omental tumour samples combined, C) primary surgery omental tumour, and D) neoadjuvant chemotherapy omental tumour. Compared to normal omentum, tumour biopsies have increased $CD56^{dim}CD16^{neg}$ and decreased $CD56^{dim}CD16^{bri}$ NK cell subsets.

When the individual omental samples were compared, the $CD56^{dim}CD16^{neg}$ NK subset was significantly larger in all omental tumour cases, compared to normal omental tissue ($p < 0.0001$). In contrast, the $CD56^{dim}CD16^{bri}$ NK population was significantly smaller in the omental tumour ($p = 0.0021$), demonstrated in Figure 4.27. The malignant omental cases were then separated into primary surgery and neoadjuvant chemotherapy groups, and compared to normal omentum (Figure 4.28). Here, the $CD56^{dim}CD16^{neg}$ subset was significantly increased in both the omental tumour groups ($p = 0.0075$ for primary surgery and $p = 0.0051$ for neoadjuvant chemotherapy) compared to normal omentum. The $CD56^{dim}CD16^{bri}$ NK cell subset was significantly reduced in both the tumour groups ($p = 0.0179$ and $p = 0.0474$ for primary surgery and neoadjuvant chemotherapy groups, respectively) compared to normal omentum. The $CD56^{bri}CD16^{neg}$ NK cell subset was decreased in the tumour tissue following chemotherapy compared to the chemotherapy naïve tumour tissue ($p = 0.0222$).

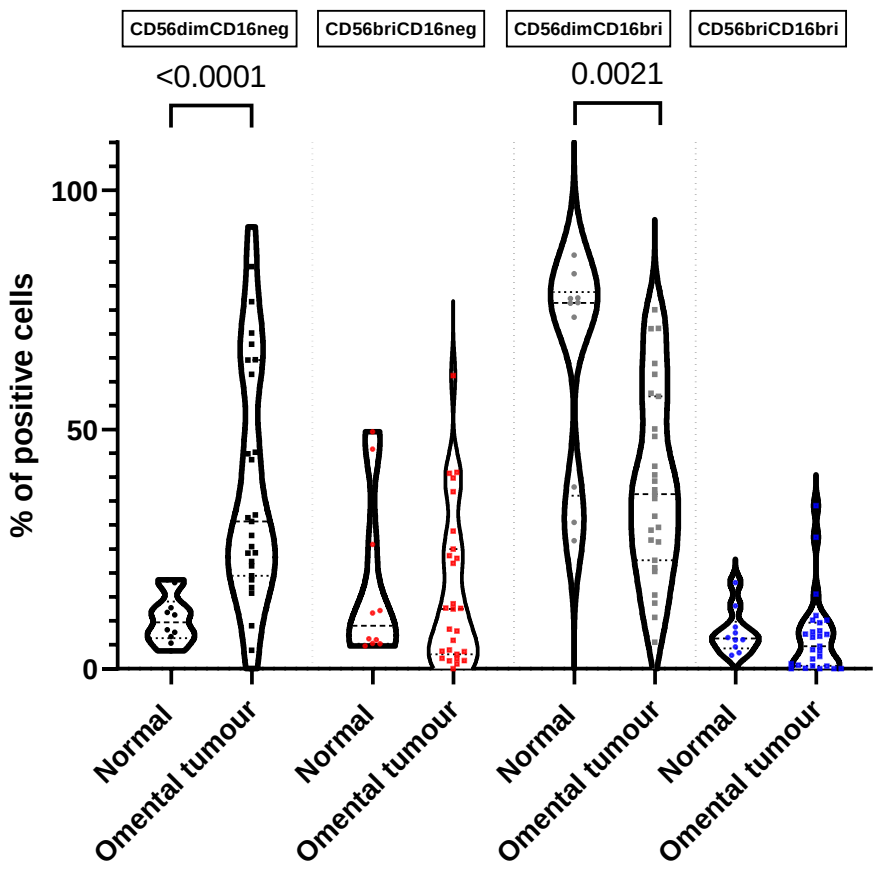


Figure 4.27: The type of infiltrating NK cell subsets in omental tumour and normal omental tissue. There were significantly more tissue infiltrating $CD56^{dim}CD16^{neg}$ NK cells ($p < 0.0001$) and fewer $CD56^{dim}CD16^{bri}$ NK cells ($p = 0.0021$) in the omental tumour samples than in the normal omentum.

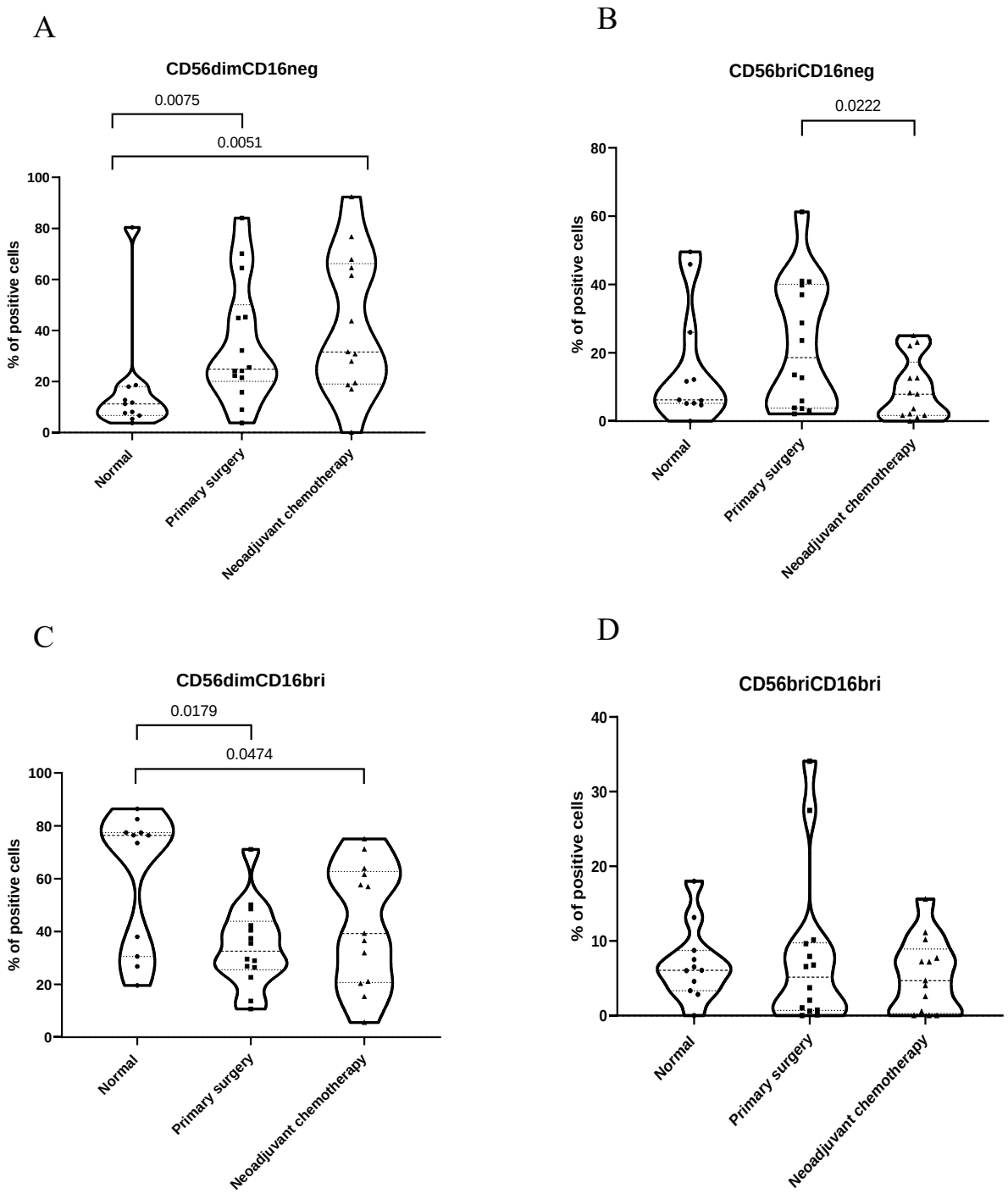


Figure 4.28: The proportion of the omental infiltrating NK cell subsets across the different patient groups.

The $CD56^{dim}CD16^{neg}$ (A) subset was significantly increased in both the primary surgery and neoadjuvant chemotherapy omental tumour tissue, while the $CD56^{dim}CD16^{bri}$ (C) NK cell subset was significantly reduced in both the tumour groups. The $CD56^{bri}CD16^{neg}$ (B) NK cell subset was decreased in the neoadjuvant chemotherapy group compared to the primary surgery group.

4.6.3 The expression of receptors on omental tissue infiltrating NK cells

4.6.3.1 Activation receptors on the omental NK cells

Evaluation of the NK activation receptors on the NK cells infiltrating into the omental tissue found that DNAM-1 was significantly higher in all OC omental tumour cases compared to normal omentum ($p = 0.0095$). There were no differences in the expression of other activation receptors (NKp46, NKG2C, NKG2D and CD57) between normal omentum and omental tumour as shown in Figure 4.29. DNAM-1 expression was significantly higher in the tumours exposed to chemotherapy compared to the normal omentum ($p = 0.0473$), but not in the primary surgery tumours (Figure 4.30). In addition, NKp46 was shown to be reduced on the NK cells in the untreated omental tumour compared to normal omentum ($p = 0.0091$), but this was significantly raised following chemotherapy ($p = 0.0021$). The expression of the other activation receptors was similar between the OC groups and normal tissue.

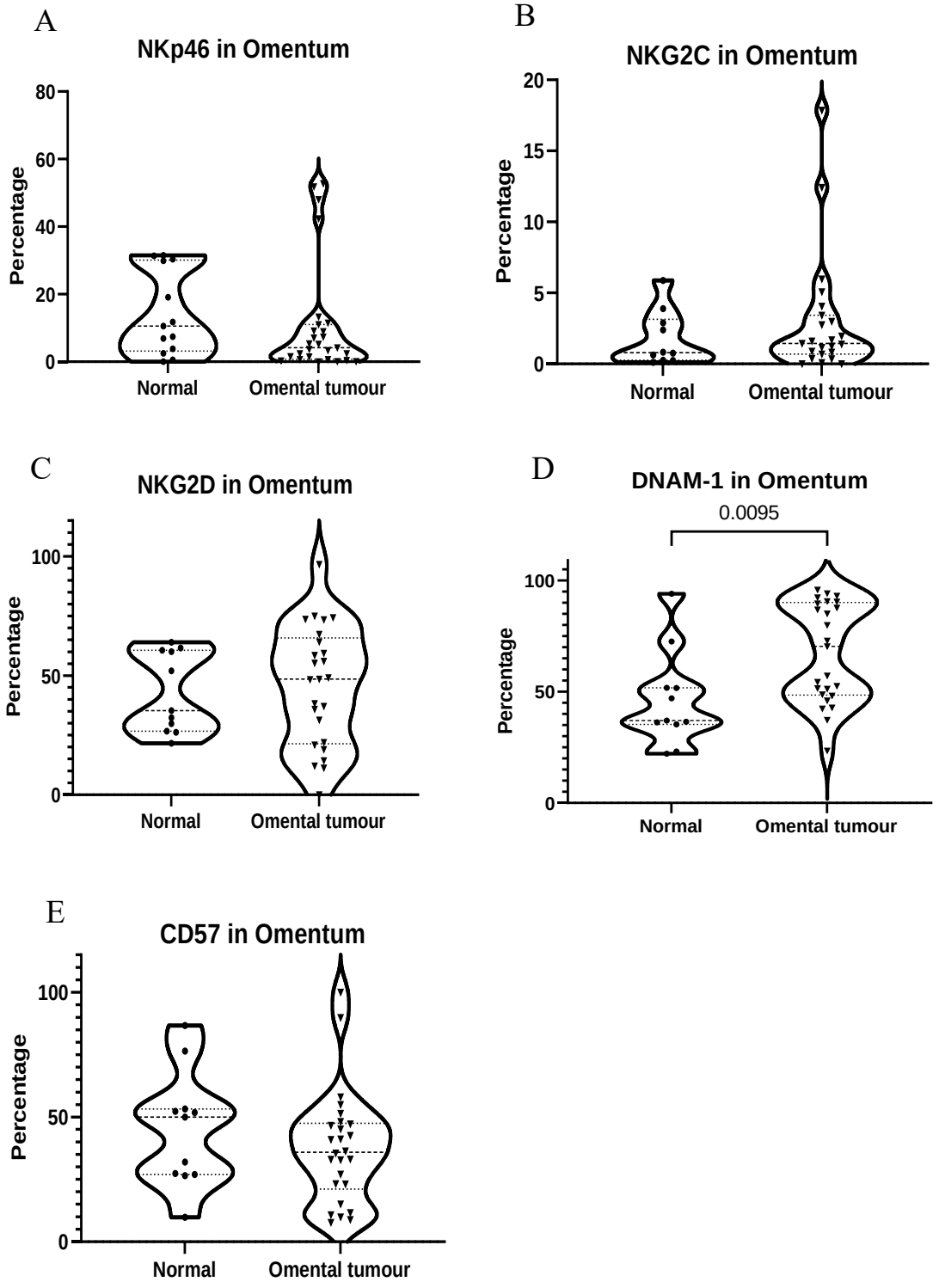


Figure 4.29: NK activation receptors in normal omentum and omental tumour.
Omental NK cells within tumour tissue had increased expression of activation receptor DNAM-1 (D) compared to those in normal omental tissue (p = 0.0095). There were no differences in the expression of: A) NKp46, B) NKG2C, C) NKG2D, or E) CD57.

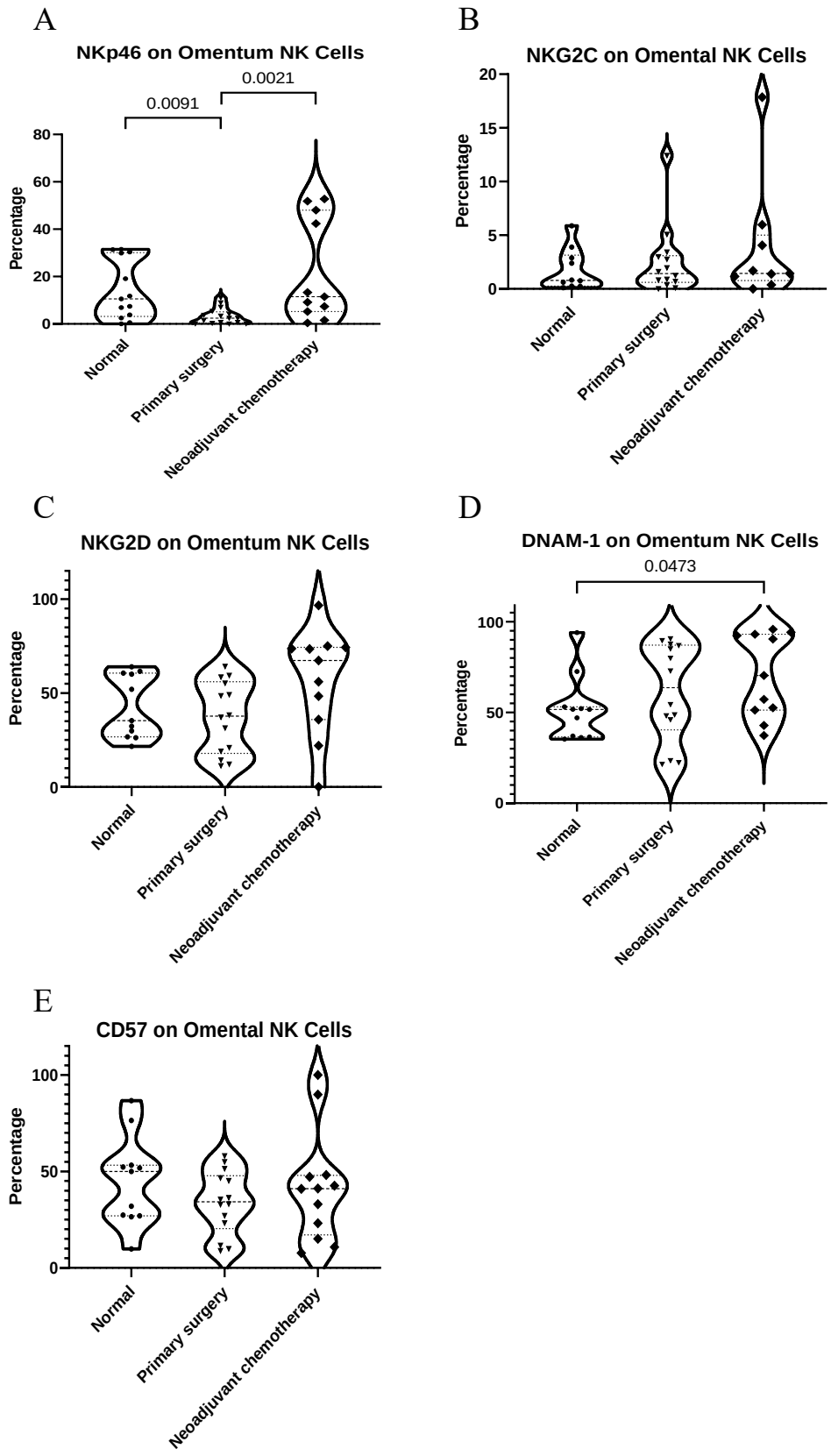


Figure 4.30: Omental NK cell activation receptors across the patient groups.
Receptor NKp46 (A) was reduced on the NK cells within untreated omental tumour compared to normal omentum ($p = 0.0091$), but was then increased following chemotherapy ($p = 0.0021$). The receptor DNAM-1 (D) was also increased on chemotherapy treated omental tumour compared to normal omentum ($p = 0.0473$). There were no differences in the expression of NKG2C (B), NKG2D (C) and CD56 (E) between the different groups.

4.6.3.2 Inhibitory receptors on the omental NK cells

There was no difference in the expression of all four inhibitory receptors (CTLA-4, TIGIT, CD94 and PD-1) on the NK cells within normal omentum and the omental tumour tissues (Figure 4.31). There was also no difference in the expression of these NK receptors between omental biopsies taken from primary surgery and neoadjuvant chemotherapy OC patients (Figure 4.32).

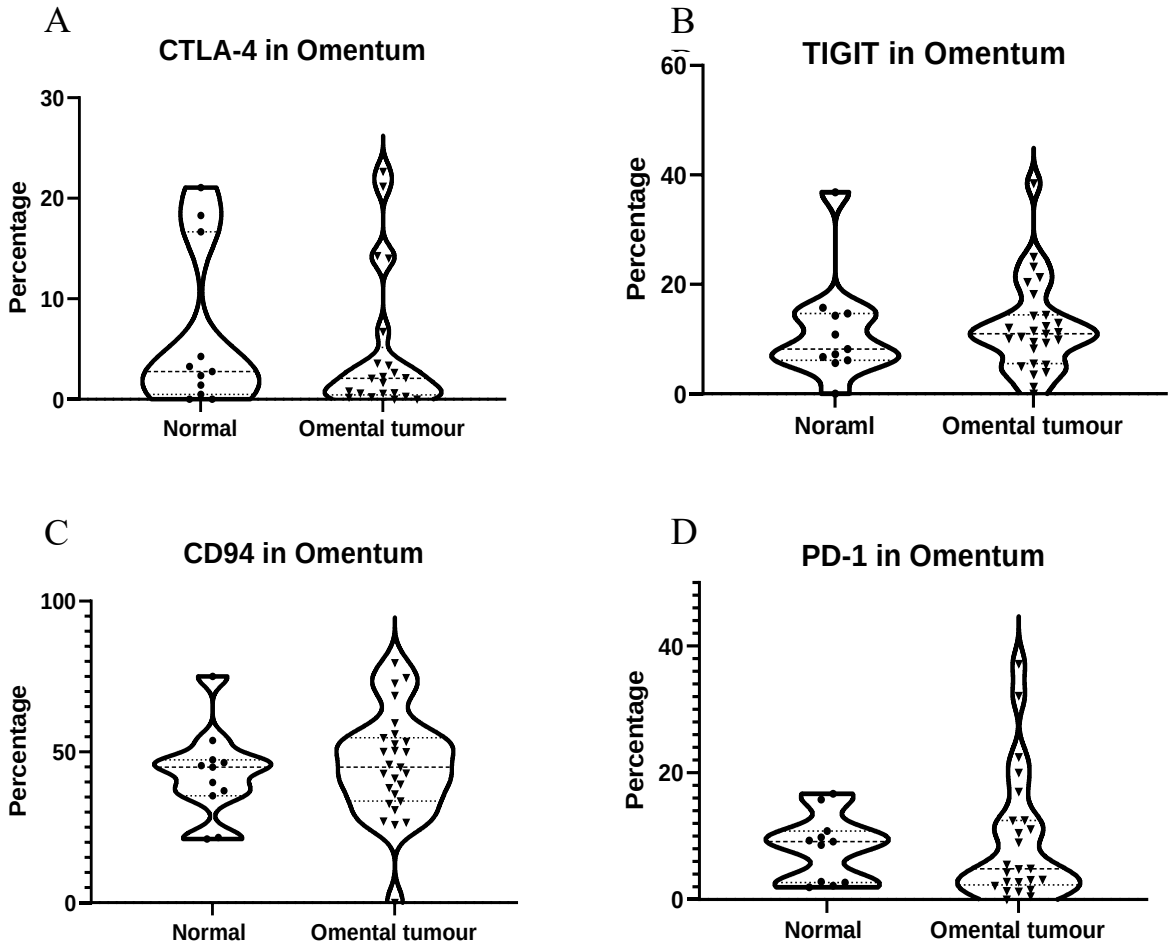


Figure 4.31: NK cell inhibitory receptors in normal omentum and omental tumour.
The omental tumour and normal omentum infiltrating NK cells had similar expression patterns for the inhibitory receptors: A) CTLA-4, B) TIGIT, C) CD94, and D) PD-1.

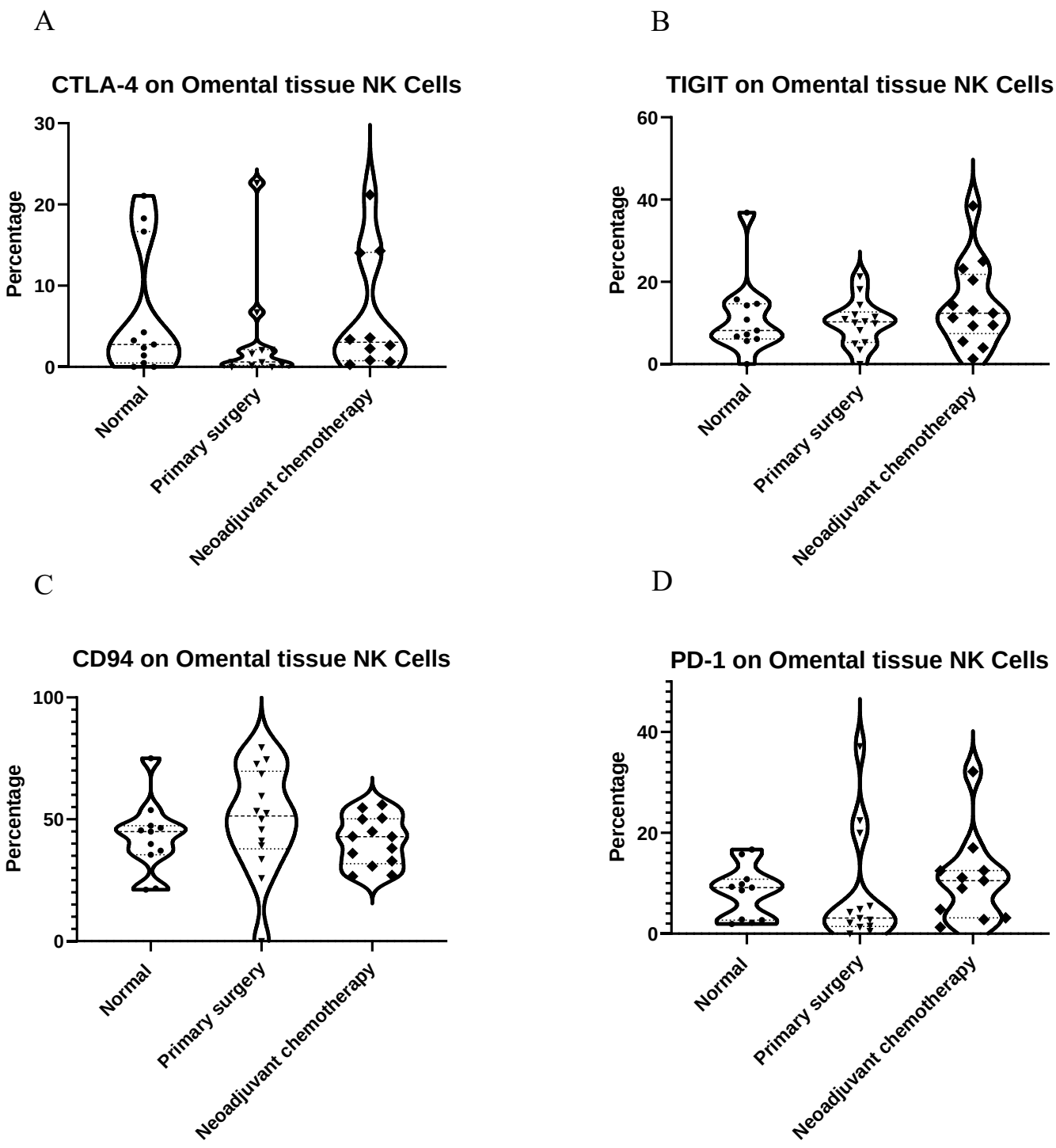


Figure 4.32: Omental NK cell inhibitory receptors across three patient groups.
There were no differences in the expression of inhibitory receptors: A) CTLA-4, B) TIGIT, C) CD94, and D) PD-1 when comparing normal omentum, primary surgery omental tumour and neoadjuvant chemotherapy omental tumour.

4.6.4 Summary of the omental infiltrating NK cell phenotype

The ability of the NK cells to infiltrate into omental tissue was impaired in metastatic omental disease. This was evident with fewer NK cells found within the omental tumours than in the normal omental tissue. However, the amount of NK tumour infiltration was not influenced by chemotherapy treatment. There were increased $CD56^{dim}CD16^{neg}$ NK cells and decreased mature cytotoxic $CD56^{dim}CD16^{bri}$ NK cells within both the chemotherapy naïve and chemotherapy exposed omental tumours, with chemotherapy also reducing the amount of immature cytokine producing $CD56^{bri}CD16^{neg}$ NK cells. The NK cells in untreated omental tumours had lower expression of the activating receptor NKp46 compared to normal tissue, but this was then greatly increased upon chemotherapy exposure. In addition, there was increased expression of the activating receptor DNAM-1 in omental tumours than in the normal omental tissue, which is particularly highly expressed on NK cells following chemotherapy. The expression of inhibitory receptors was not altered when NK cells infiltrated tumour tissue or following chemotherapy treatment.

4.7 The correlation between peripheral, ovarian tissue and omental tissue NK cells

4.7.1 The association between paired PBMC NK cells and ovarian NK cells

4.7.1.1 The proportion and type of NK cells

For every ovarian tissue sample, the data obtained was compared directly to the matched peripheral blood sample that had been taken from the same patient. This included matched PBMC-ovarian samples from the 7 patients with normal ovaries, 6 patients with benign ovaries, 31 who underwent primary surgery for OC and 18 who were given neoadjuvant chemotherapy for OC. The differences between the NK cells from the PBMC and matched ovary was determined for each patient.

In OC patients, there was a reduction in the number of NK cells infiltrating into the tumour tissue than in PBMC (Figure 4.33). Tumour infiltrating NK cells showed a downregulation of CD16 compared to their corresponding PBMC NK cells. Figure 4.34 shows an increase in both the proportion of $CD56^{dim}CD16^{neg}$ NK cells ($p < 0.0001$) and the $CD56^{bri}CD16^{neg}$ NK cells ($p = 0.0009$) in ovarian tumour when compared to PBMC. As expected, there was a reduction in the $CD56^{bri}CD16^{bi}$ ($p = 0.0084$) and $CD56^{dim}CD16^{bri}$ ($p < 0.0001$) NK cell populations in the tumour tissue compared to PBMC. This indicates either the CD16 bright NK cells had been excluded and prevented from infiltrating into tumour tissue or the CD16 had been downregulated by the ovarian tumour microenvironment.

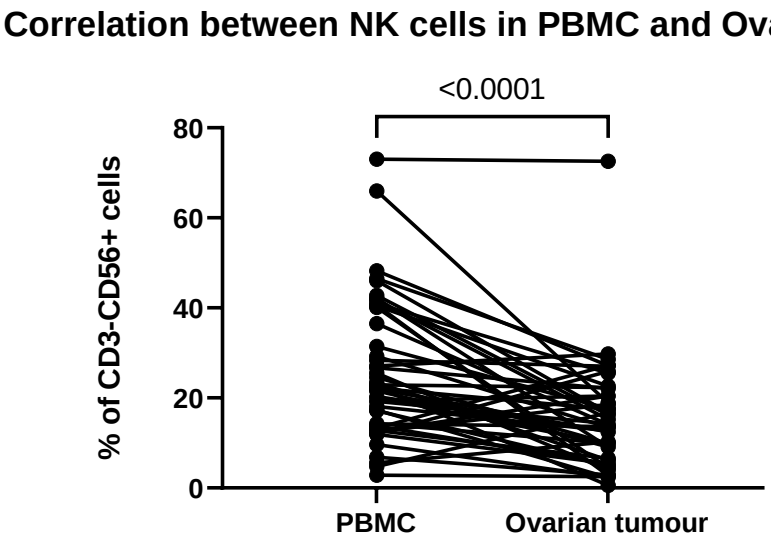


Figure 4.33: Correlation between the proportion of NK cells within the PBMC to matched ovarian tumour.
Fewer NK cells infiltrated into the ovarian tumour tissue than were circulating in the peripheral blood ($p < 0.0001$).

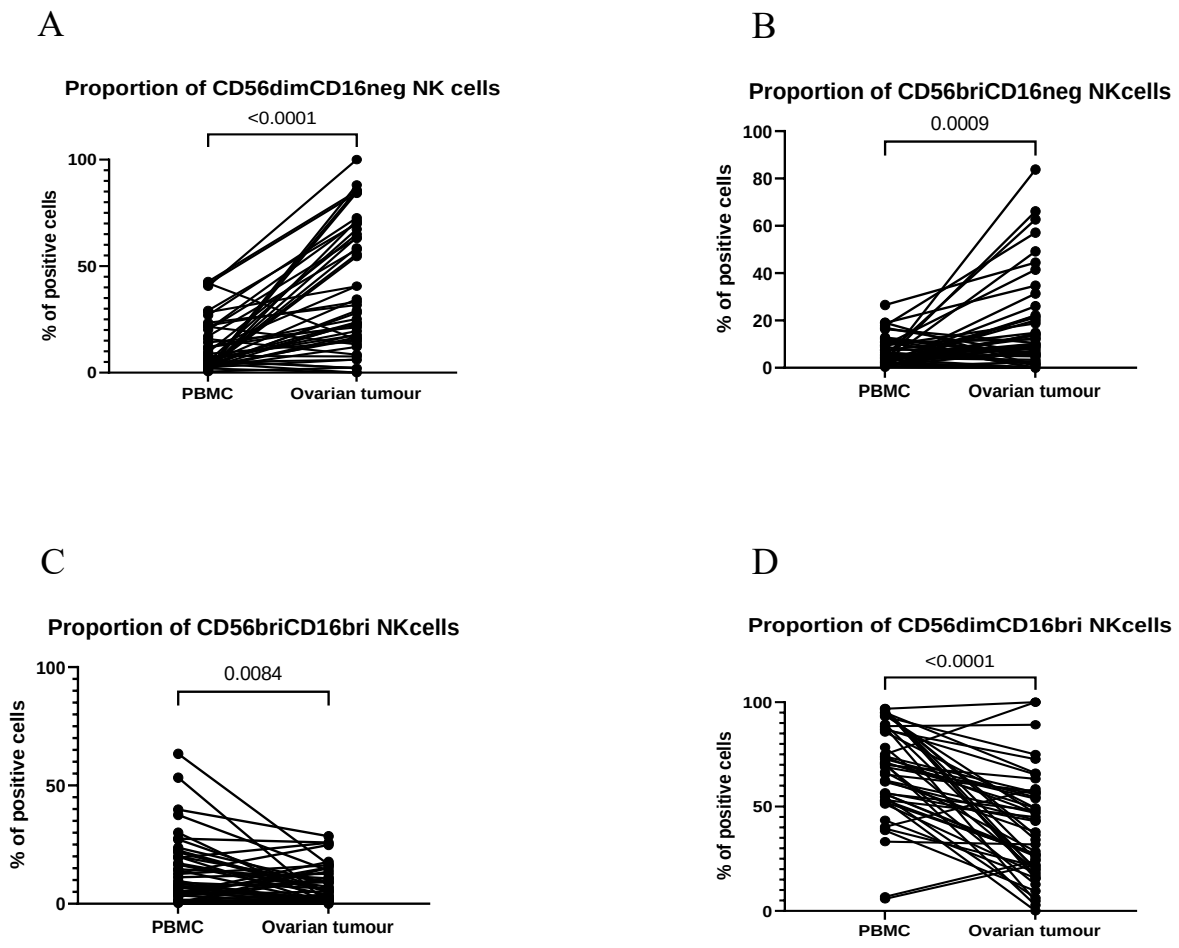
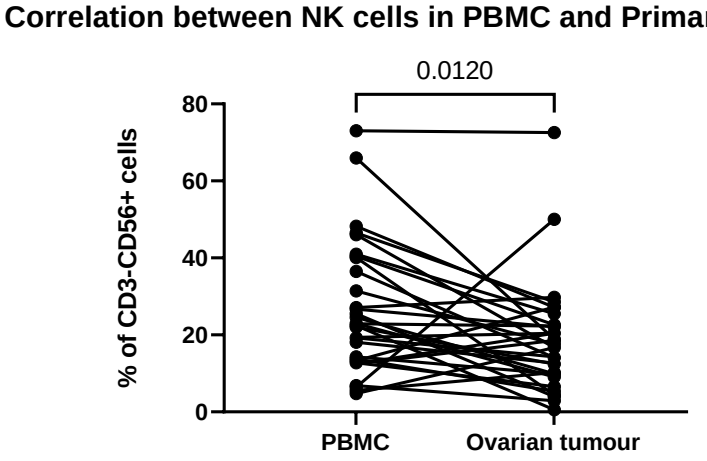


Figure 4.34: Correlation between CD56 and CD16 expression in PBMC NK cells and paired ovarian tumour NK cells.

The ovarian tumour infiltrating NK cells had a greater proportion of $CD56^{dim}CD16^{neg}$ (A) and $CD56^{bri}CD16^{neg}$ NK cells (B), along with a reduced proportion of $CD56^{bri}CD16^{bri}$ (C) and $CD56^{dim}CD16^{bri}$ NK cells (D) compared to their paired peripheral blood samples.

When the tumour samples were separated into primary surgery and neoadjuvant chemotherapy groups, the results were similar. The proportion of tumour infiltrating NK cells were decreased in both groups when compared to their matched PBMC samples ($p = 0.0121$ and $p = 0.0004$, respectively), shown in Figure 4.35. CD16 expression was found to be reduced in the NK cells in the tumour when compared to their corresponding PBMC in both the primary surgery and neoadjuvant chemotherapy groups (Figure 4.36).

A



B

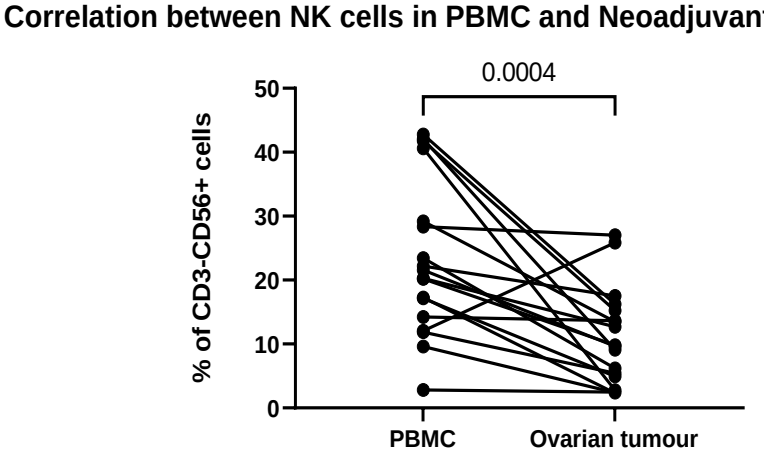
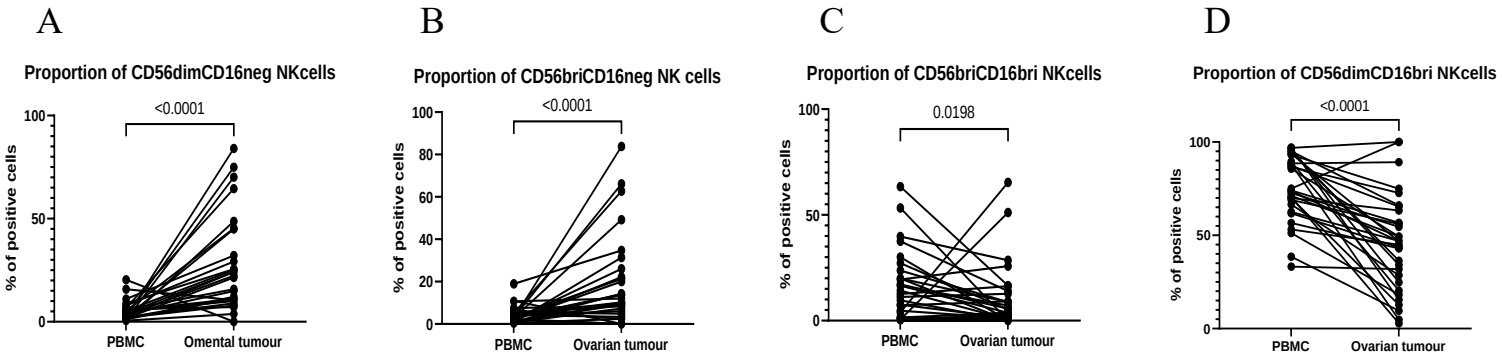


Figure 4.35: Correlation between the proportion of NK cells within the PBMC to matched ovarian tumour in both primary surgery and neoadjuvant chemotherapy OC patients.
There were fewer NK cells within the ovarian tumour tissue than in the peripheral blood in both primary surgery (A) and neoadjuvant chemotherapy (B) OC patients.

PBMC and Ovarian tumour in the primary surgery group



PBMC and Ovarian tumour in the neoadjuvant chemotherapy group

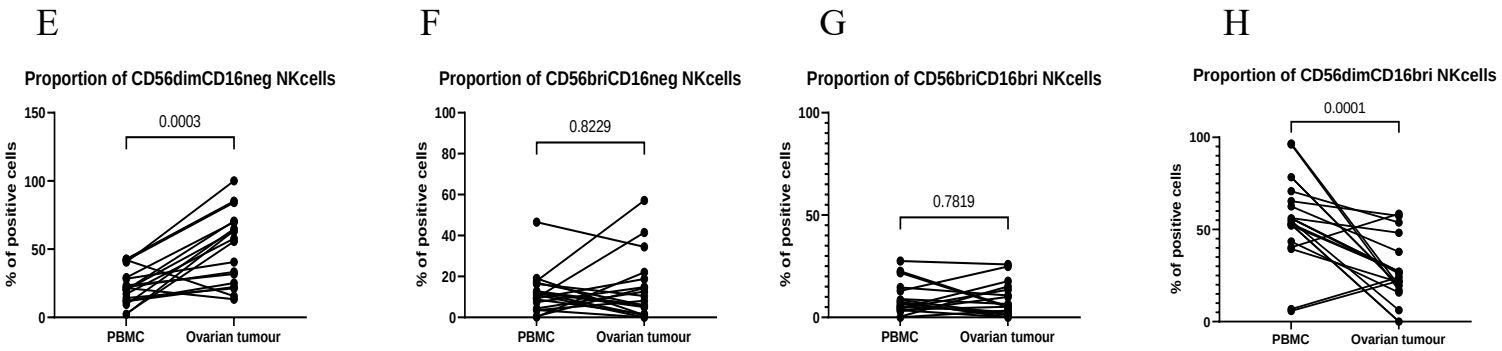


Figure 4.36: Correlation between PBMC and ovarian NK cell CD56 and CD16 expression in both primary surgery and neoadjuvant chemotherapy patients.
In the primary surgery patients, the tumour infiltrating NK cells had a greater proportion of $CD56^{dim}CD16^{neg}$ (A) and $CD56^{bri}CD16^{neg}$ NK cells (B), along with a reduced proportion of $CD56^{bri}CD16^{bri}$ (C) and $CD56^{dim}CD16^{bri}$ NK cells (D). Likewise, the neoadjuvant chemotherapy patients had increased $CD56^{dim}CD16^{neg}$ (E) and decreased $CD56^{dim}CD16^{bri}$ NK cells (H).

In contrast, there was a similar proportion of NK cells in matched PBMC samples and normal ovarian tissue, and paired PBMC and benign ovarian tissue samples (Figure 4.37). When comparing the CD56 and CD16 expression between matched PBMC and normal ovary samples, the ovarian tissue infiltrating NK cells had a greater proportion of $CD56^{dim}CD16^{neg}$ and $CD56^{bri}CD16^{neg}$ NK cells. There was also a reduced proportion of $CD56^{dim}CD16^{bri}$ NK

cells within the normal ovarian tissue, while there was no difference in the $CD56^{bri}CD16^{bri}$ NK cells. Upon evaluation of the benign ovarian tissue biopsies to their paired PBMC samples, there was a reduction in the $CD56^{bri}CD16^{bri}$ NK cells in the ovarian tissue, while there were no differences in the other NK subtypes between the benign ovarian tissue and peripheral blood (Figure 4.38).

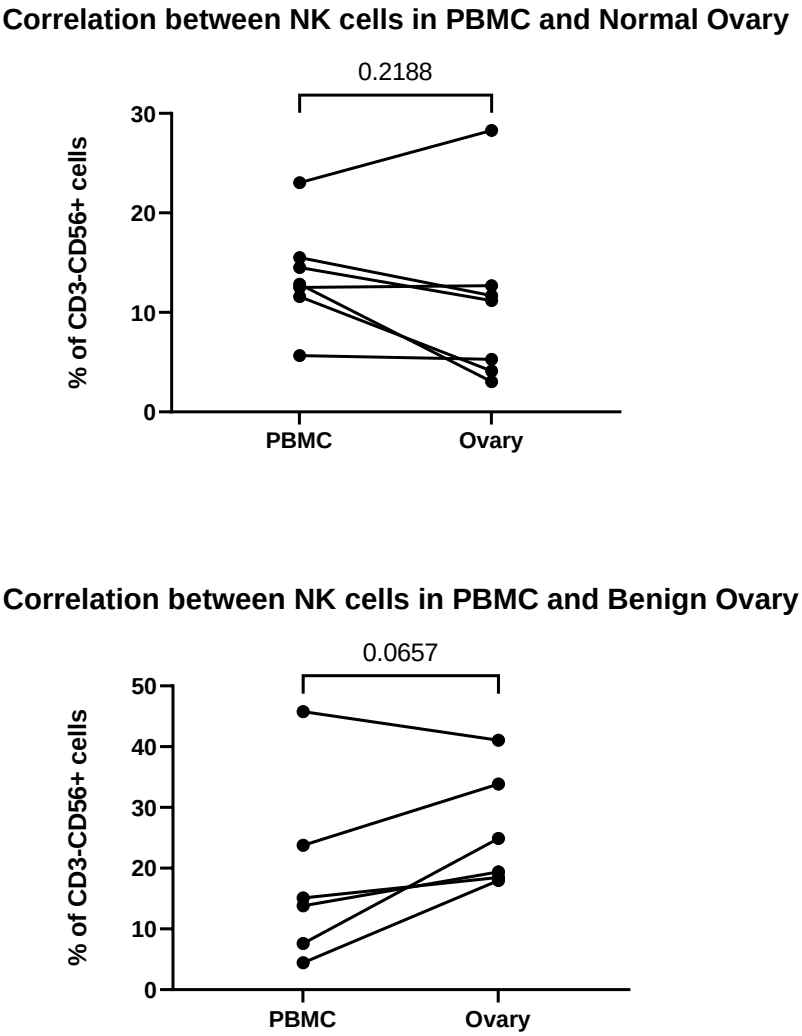
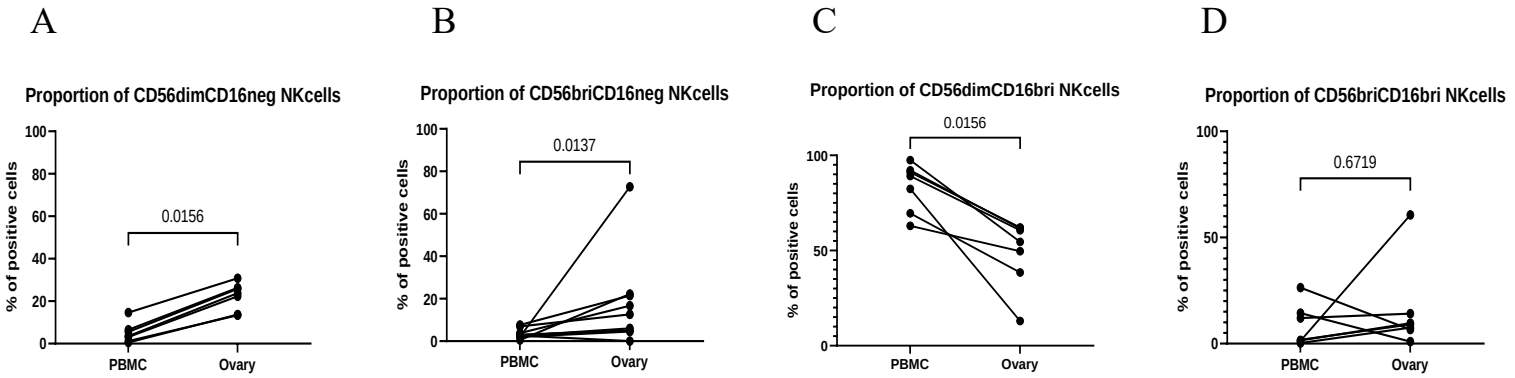


Figure 4.37: Correlation between the proportion of NK cells within PBMC to matched ovarian tissue in patients with normal ovaries and benign ovaries.
There were similar proportions of NK cells in normal ovarian tissue to matched PBMC (A), and in benign ovarian tissue to matched PBMC (B).

PBMC and Normal Ovarian tissue



PBMC and Benign Ovarian tissue

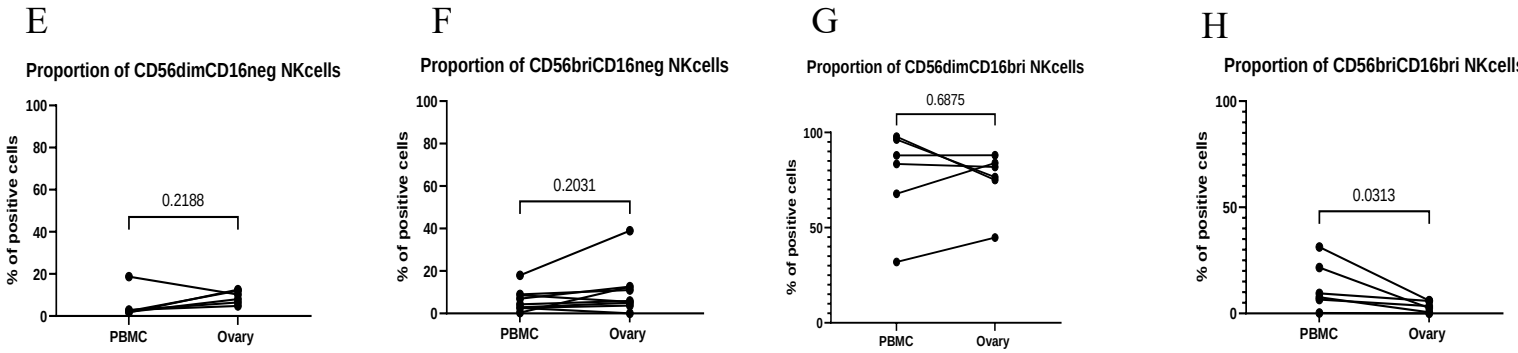


Figure 4.38: Correlation between paired PBMC and ovarian NK cell CD56 and CD16 expression in patients with normal and benign ovaries.

In the normal ovary patients, the tissue infiltrating NK cells had a greater proportion of $CD56^{dim}CD16^{neg}$ (A) and $CD56^{bri}CD16^{neg}$ NK cells (B), along with a reduced proportion of $CD56^{dim}CD16^{bri}$ (C) NK cells. There was no difference in the $CD56^{bri}CD16^{bri}$ NK cells between normal ovarian and paired PBMC NK cells (D). In the benign ovary patients, there was a reduction in $CD56^{bri}CD16^{bri}$ NK cells in the ovarian tissue compared to matched PBMC (H). There were no differences in the $CD56^{dim}CD16^{neg}$ (E), $CD56^{bri}CD16^{neg}$ (F) and $CD56^{dim}CD16^{bri}$ (G) NK cells between the PBMC and benign ovarian tissue samples.

4.7.1.2 Analysis of NK activation receptors

The expression of activation receptors on the ovarian tumour infiltrating NK cells in all OC patients were compared to the NK cells in their matched PBMC cells (Figure 4.39). The expression of activation receptors, NKp46, DNAM-1 and CD57 were found to be significantly reduced on the NK cells in in OC tumour samples when compared to their corresponding PBMC samples ($p = 0.0013$, $p < 0.0001$ and $p < 0.0001$, respectively). However, there was no differences in the expression of activation receptors NKG2C and NKG2D between the PBMC and ovarian tumour NK cells.

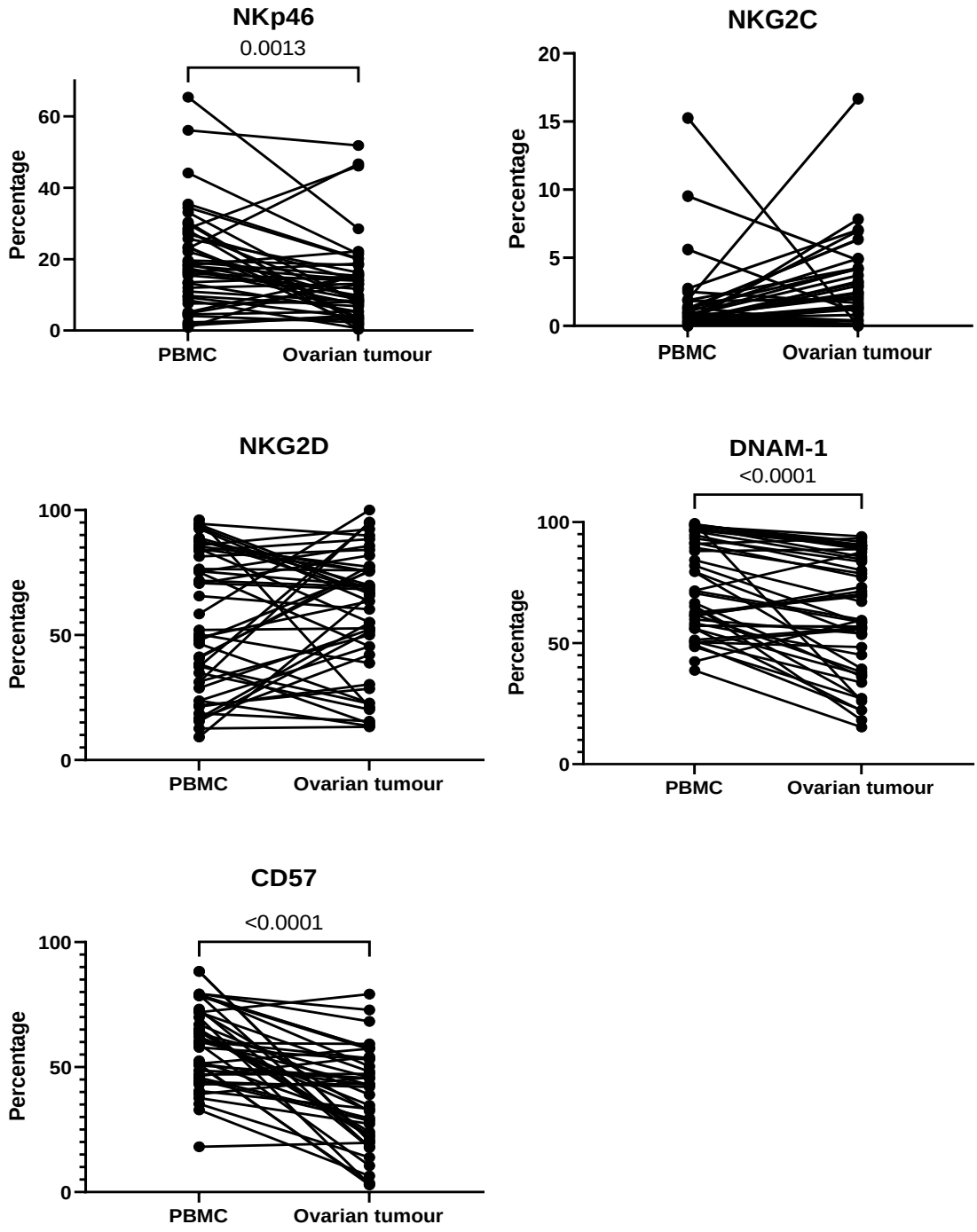


Figure 4.39: Expression of activation receptors on ovarian tumour infiltrating NK cells and matched PBMC NK cells in all OC patients.

There was a reduction in the expression of activation receptors NKp46, DNAM-1 and CD57 on NK cells within ovarian tumour tissue compared to the corresponding NK cells in the peripheral blood. There were no differences in the expression of NKG2C and NKG2D between the ovarian tumour tissue and peripheral blood.

4.7.1.3 Analysis of NK inhibition receptors

The expression of inhibition receptors on the ovarian tumour infiltrating NK cells in all OC patients were compared to the NK cells in their matched peripheral blood samples (Figure 4.40). There was a decrease in the expression of receptor TIGIT on the NK cells within the tumour tissue compared to the corresponding NK cells in the peripheral blood ($p = 0.0016$). In addition, there was an increase in the inhibitory checkpoint PD-1 on the NK cells within ovarian tumour tissue compared to the PBMC ($p = 0.0003$). There was no difference in the expression of inhibitory receptor CD94 and inhibitory checkpoint CTLA-4 between the blood and tumour NK cells.

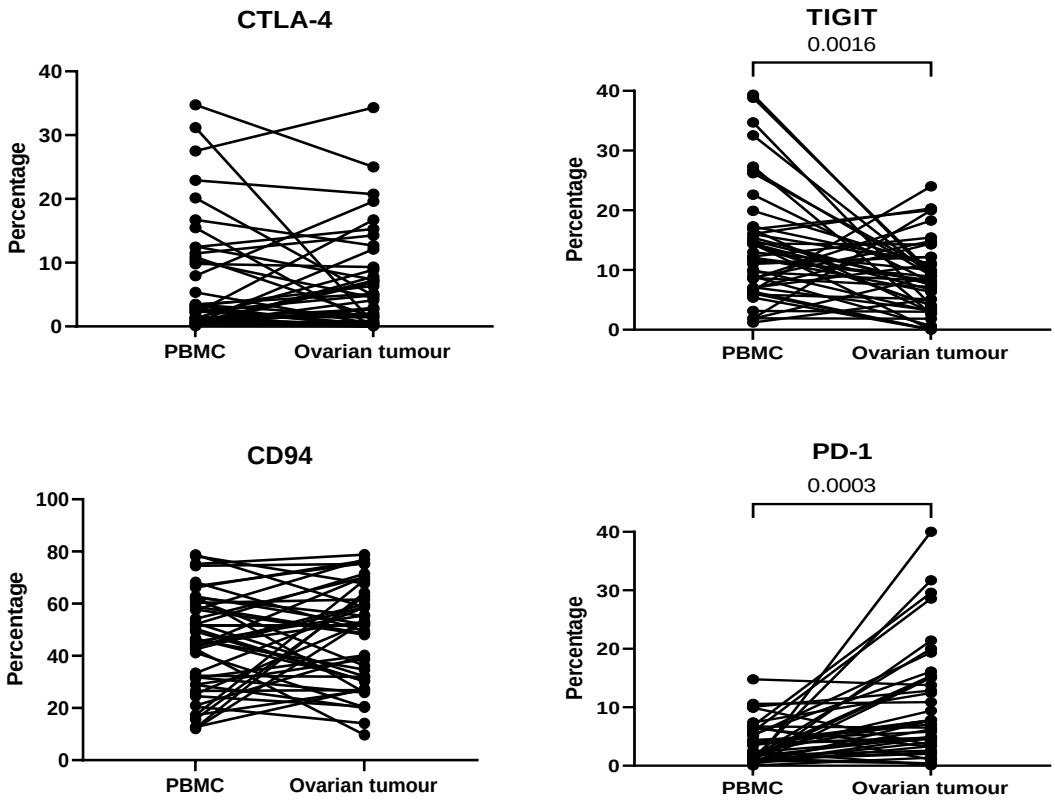


Figure 4.40: Expression of inhibitory receptors on tumour infiltrating NK cells and matched peripheral blood NK cells in all OC patients.
There was a reduction in the expression of inhibition receptor TIGIT and an increase in the inhibitory checkpoint PD-1 on the NK cells within ovarian tumour tissue compared to the corresponding NK cells in the peripheral blood.

4.7.2 The association between matched PBMC NK cells and omental NK cells

4.7.2.1 The proportion and type of NK cells

The data obtained from every omental tissue sample was then compared directly to the matched peripheral blood sample that had been taken from the same patient. This included matched PBMC-omental tissue samples from the 11 patients with histologically normal omentum (from the patients with either normal ovaries or benign ovarian masses), and 27 omental tumour samples from patients with ovarian tumours. Of these tumour samples, 14 had received chemotherapy (neoadjuvant chemotherapy group) and 13 were untreated (primary surgery group). The NK cells from the PBMC and matched omentum were analysed for each patient.

In patients with omental tumours, the proportion of the NK cells infiltrating the omental tissue was significantly lower than the proportion of NK cells within each of the matched blood samples ($p < 0.0001$), shown in Figure 4.41. Evaluation of the CD56 and CD16 expression showed that the omental tumour infiltrating NK cells had downregulation of CD16 compared to their corresponding PBMC NK cells. Figure 4.42 shows an increase in both the populations of $CD56^{dim}CD16^{neg}$ NK cells ($p < 0.0001$) and the $CD56^{bri}CD16^{neg}$ NK cells ($p = 0.0002$) in the omental tumour infiltrating NK cells when compared to the NK cells in the corresponding PBMC samples. In addition, there were reductions in the $CD56^{bri}CD16^{bri}$ ($p = 0.0073$) and $CD56^{dim}CD16^{bri}$ ($p < 0.0001$) NK cell populations within the tumour tissue compared to the PBMC samples.

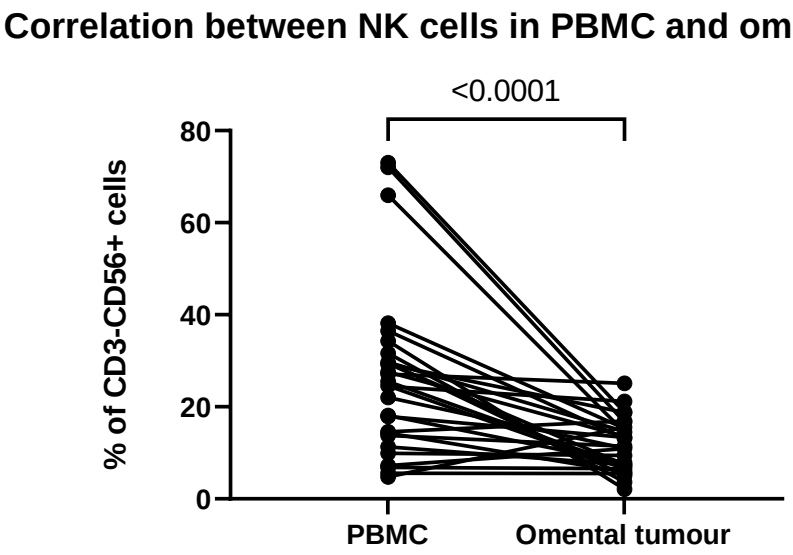


Figure 4.41: Correlation between the proportion of NK cells within the PBMC to matched omental tumour tissue.

There was a reduction in the proportion of NK cells within the omental tumour tissue than in the peripheral blood ($p < 0.0001$).

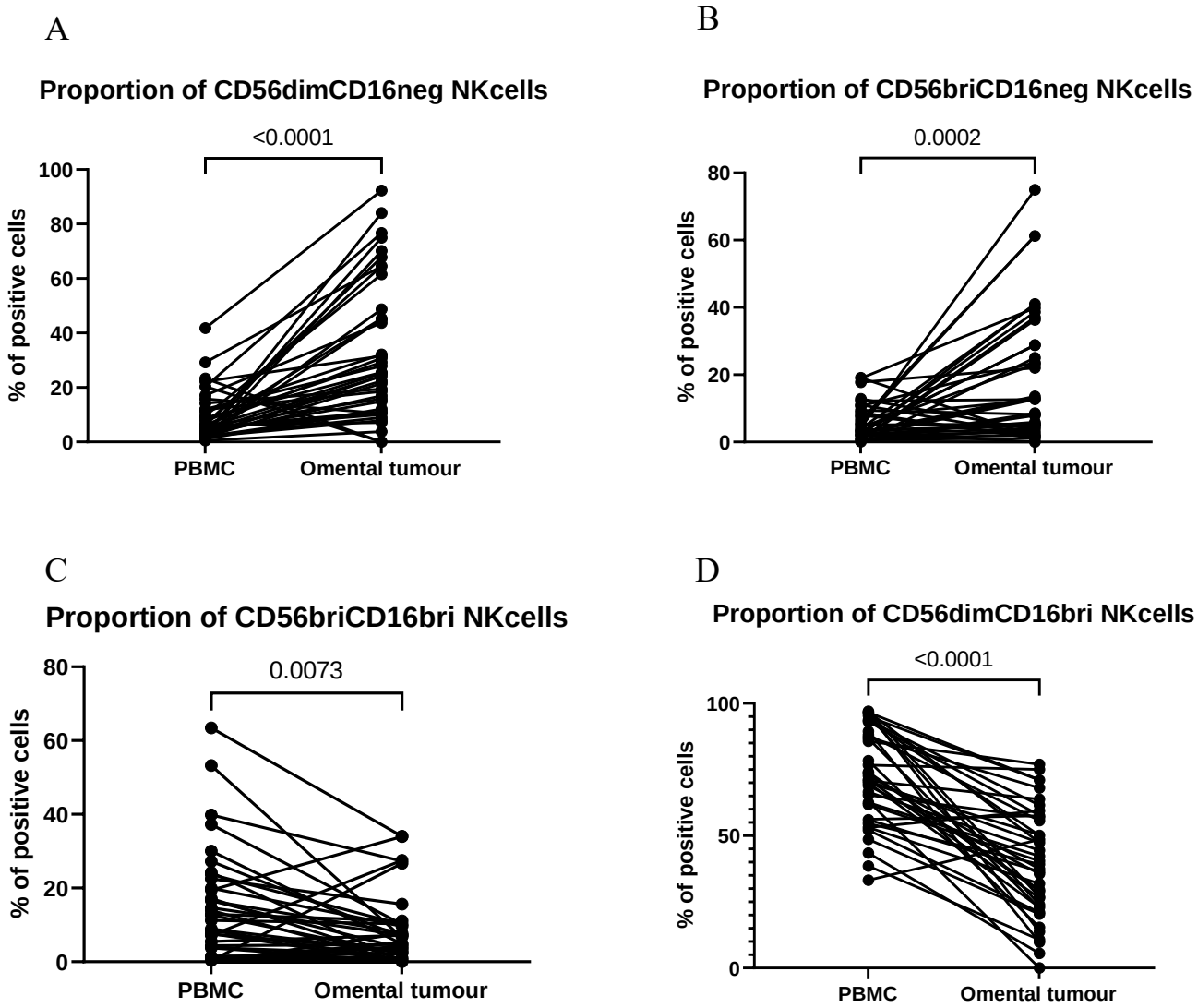


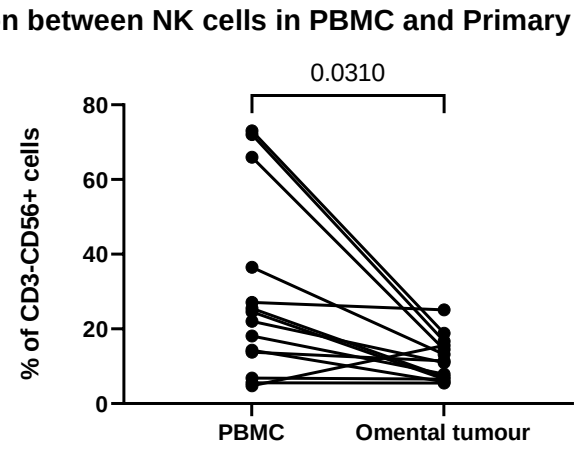
Figure 4.42: Correlation between CD56 and CD16 expression in PBMC NK cells and matched omental tumour NK cells

The tumour infiltrating NK cells had a greater proportion of $CD56^{dim}CD16^{neg}$ (A) and $CD56^{bright}CD16^{neg}$ NK cells (B), along with a reduced proportion of $CD56^{bri}CD16^{bi}$ (C) and $CD56^{dim}CD16^{bi}$ NK cells (D).

When omental tumours were further categorised into primary surgery and neoadjuvant chemotherapy groups, both showed a decrease in the proportion of tumour infiltrating NK cells compared to their matched PBMC ($p = 0.0310$ in primary surgery and $p = 0.0021$ in neoadjuvant chemotherapy patients), shown in Figure 4.43. The expression of CD16 and CD56 on the NK cells within omental tumour and matched PBMC samples were then

reviewed (Figure 4.44), which showed a loss of CD16 expression as the NK cells infiltrated the omental tumour. In the primary surgery group, there was a higher proportion of $CD56^{dim}CD16^{neg}$ and $CD56^{bri}CD16^{neg}$ NK cells, and lower populations of $CD56^{bri}CD16^{bri}$ and $CD56^{dim}CD16^{bri}$ NK cells in omental tumour compared to the PBMC. In the neoadjuvant chemotherapy group, there was an increase in $CD56^{dim}CD16^{neg}$ and reduction in $CD56^{dim}CD16^{bri}$ NK cell populations within the omental tumour tissues compared to the paired PBMC samples. There were no differences in the $CD56^{bri}CD16^{neg}$ and $CD56^{bri}CD16^{bri}$ NK populations.

A



B

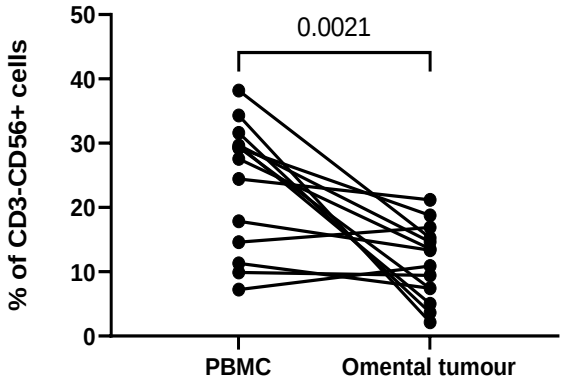
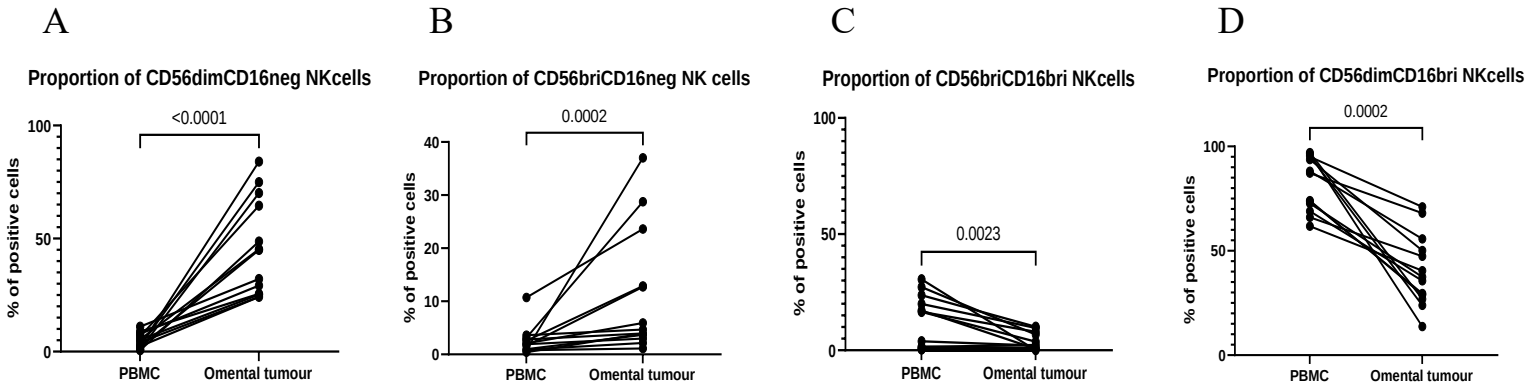


Figure 4.43: Correlation between the proportion of NK cells within the PBMC to matched omental tumour in both primary surgery and neoadjuvant chemotherapy groups.
There was a reduction in the proportion of NK cells within the omental tumour tissue compared to the peripheral blood in both primary surgery (A) and neoadjuvant chemotherapy (B) OC patients.

PBMC and Omental tumour in the primary surgery group



PBMC and Omental tumour in the neoadjuvant chemotherapy group

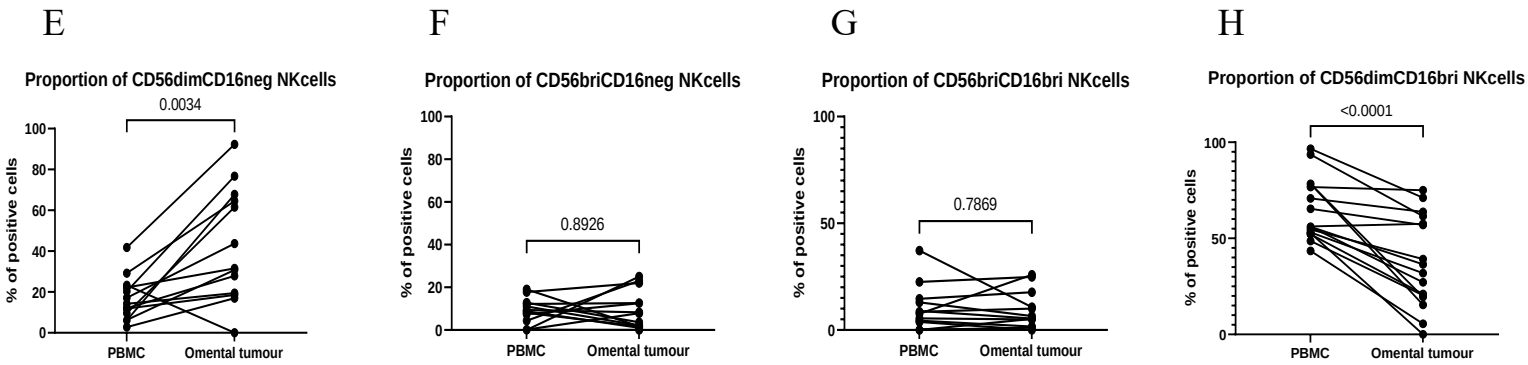


Figure 4.44: Correlation between PBMC and omental NK cell CD56 and CD16 expression in both primary surgery and neoadjuvant chemotherapy OC patients.

In the primary surgery patients, the omental tumour infiltrating NK cells had a greater proportion of $CD56^{dim}CD16^{neg}$ (A) and $CD56^{bri}CD16^{neg}$ NK cells (B) and reduced proportions of both $CD56^{bri}CD16^{bri}$ (C) and $CD56^{dim}CD16^{bri}$ NK cells (D). The neoadjuvant chemotherapy patients had increased $CD56^{dim}CD16^{neg}$ (E) and reduced $CD56^{dim}CD16r^{bri}$ NK cells (H), while there were no differences between $CD56^{bri}CD16^{neg}$ NK cells (F) and $CD56^{bri}CD16^{bri}$ (G).

When normal omental samples were compared to the corresponding PBMC, there were similar proportions of NK cells in the peripheral blood as in the omental tissue (Figure 4.45). However, the omental tissue infiltrating NK cells had a greater proportion of $CD56^{bri}CD16^{neg}$ NK cells and a reduced proportion of $CD56^{dim}CD16^{bri}$ NK cells compared to the matched PBMC samples (Figure 4.46). There was no difference in the proportion of $CD56^{dim}CD16^{neg}$ and $CD56^{bri}CD16^{bri}$ NK cells between PBMC and the normal omental tissue.

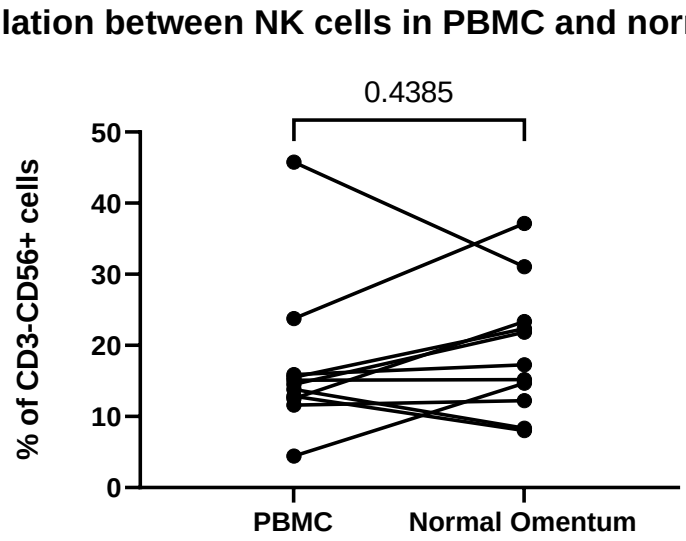


Figure 4.45: Correlation between the proportion of NK cells within the PBMC to matched normal omental tissue in patients with normal or benign ovaries.
There were similar proportions of NK cells in normal omental tissue to the matched PBMC samples.

PBMC and Normal Omentum

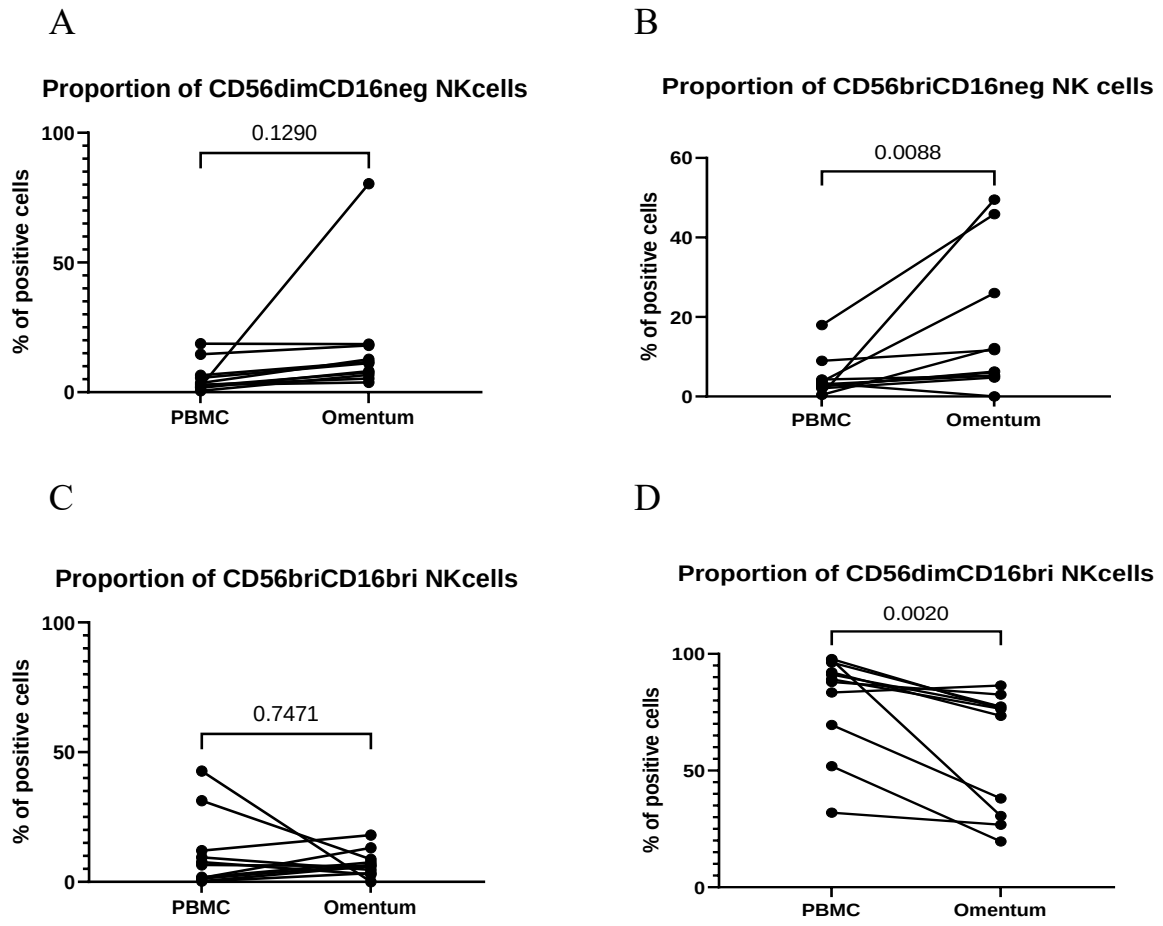


Figure 4.46: Correlation between PBMC and normal omental NK cell CD56 and CD16 expression in patients with normal and benign ovaries.

Evaluation of the PBMC and corresponding normal omental tissue biopsies from patients with normal and benign ovaries found that the omental tissue infiltrating NK cells had a greater proportion of $CD56^{bri}CD16^{neg}$ NK cells (B) and a reduced proportion of $CD56^{dim}CD16^{bri}$ (D) NK cells. There was no difference in the proportion of the $CD56^{dim}CD16^{neg}$ NK cells (A) or $CD56^{bri}CD16^{bri}$ NK cells (C) between PBMC and these normal omental tissues.

4.7.2.2 Analysis of NK activation receptors

The activation receptors on NK cells were compared between omental tumour from all OC patients with the corresponding PBMC NK. There was a reduction in the expression of NKp46 ($p < 0.0001$), DNAM-1 ($p < 0.0001$) and CD57 ($p < 0.0001$) on the NK cells within omental tumour when compared to PBMC (Figure 4.47). There was no difference in the expression of activation receptors NKG2C or NKG2D between them the PBMC and omental tumour samples.

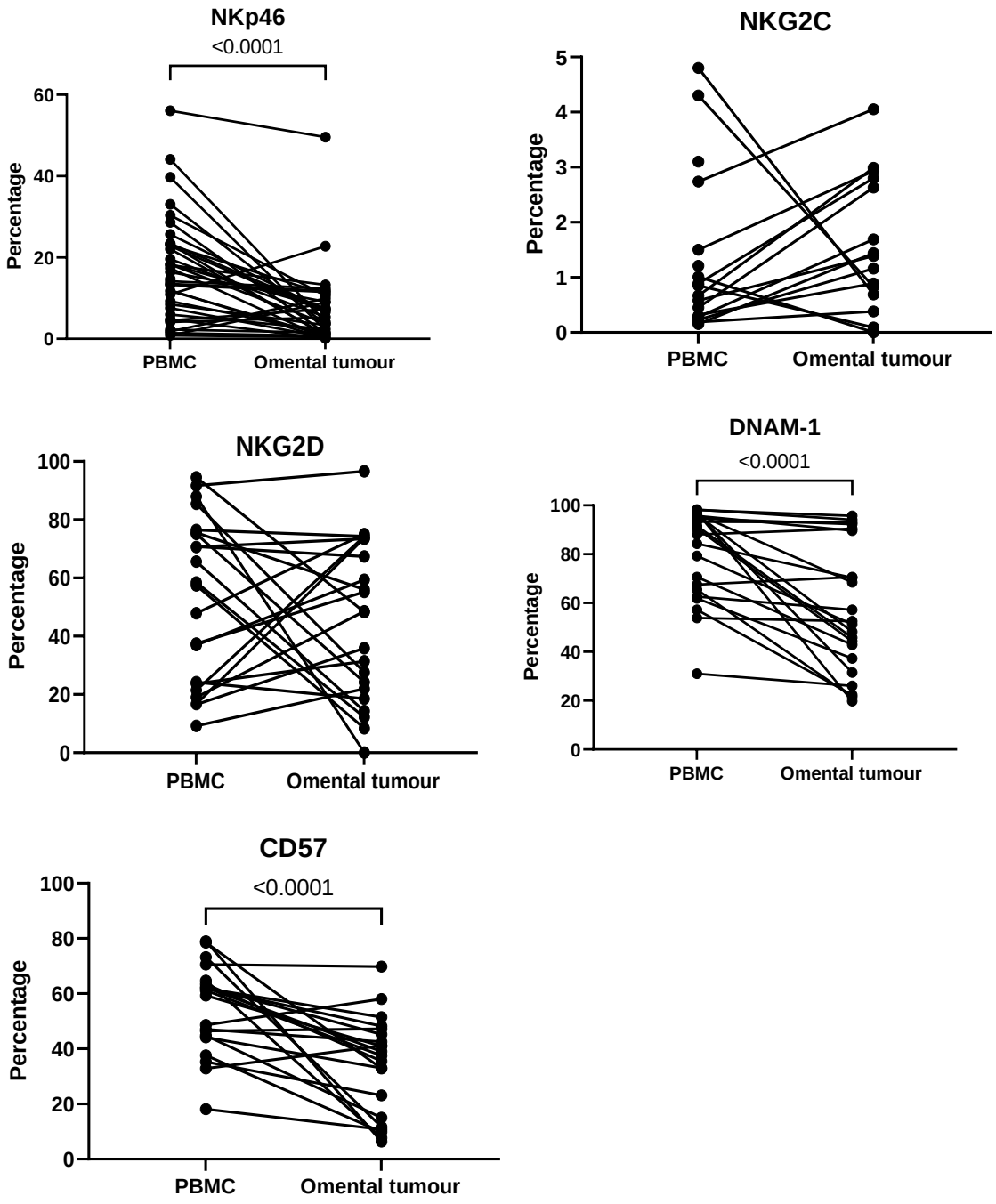


Figure 4.47: Expression of activation receptors on omental tumour infiltrating NK cells and matched PBMC NK cells in all OC patients.

There was a reduction in the expression of activation receptors NKp46, DNAM-1 and CD57 on NK cells within omental tumour tissue compared to the corresponding NK cells in the peripheral blood. There was no difference in the expression of NKG2C and NKG2D between the omental tumour and PBMC samples.

4.7.2.3 Analysis of NK inhibition receptors

Examination of the inhibition receptors of infiltrating NK cells in omental tumour of OC patients and the corresponding PBMC cells (Figure 4.48) revealed an increase in the expression of inhibitory checkpoint PD-1 receptor on the NK cells in omental tumour ($p = 0.0004$). However, there was no difference in the expression of inhibitory receptors CD94, TIGIT or CTLA-4 between the blood and omental tumour NK cells.

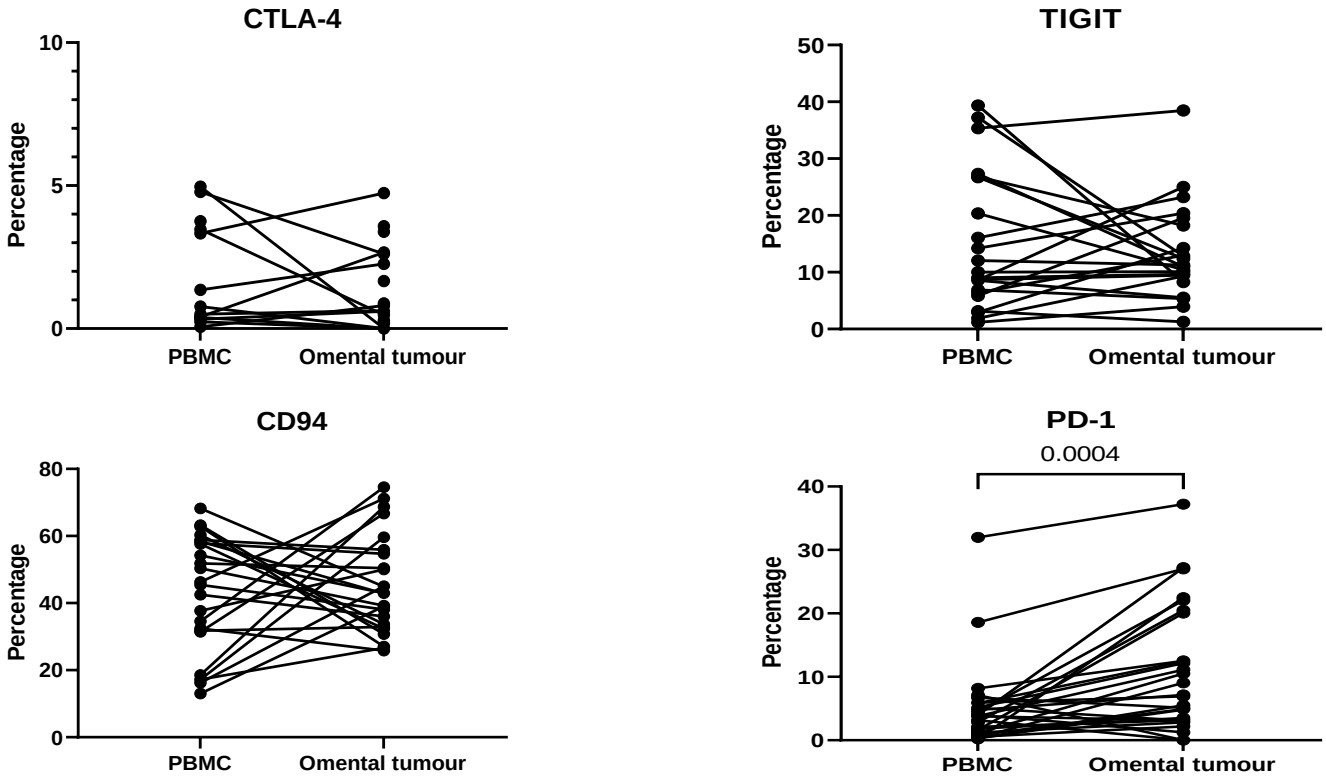


Figure 4.48: Expression of inhibitory receptors on omental tumour infiltrating NK cells and matched PBMC NK cells in all OC patients.
There was an increase in the expression of inhibitory receptor PD-1 on the NK cells within omental tumour tissue compared to the corresponding NK cells in the peripheral blood.

4.7.3 The association between paired ovarian tumour and omental tumour NK cells

4.7.3.1 The proportion and type of NK cells

The proportion and subtypes of NK cells were compared between ovarian tumour tissue and their corresponding omental tumour biopsies from each patient. There were 23 cases where matched ovarian tumour and omental tumour samples were available:13 from the primary surgery OC group and 10 from the neoadjuvant chemotherapy group. Overall, there was no difference in the proportion of the infiltrating NK cells between the omental tumour and the ovarian tumour (Figure 4.49). In addition, there was no difference in the subtypes of NK cells between ovarian and omental tumour tissue (Figure 4.50). Similarly, there was no difference in the distribution and subtypes of NK cells between ovarian and omental tumour in primary surgery and neoadjuvant chemotherapy groups (Figures 4.51 and 4.52).

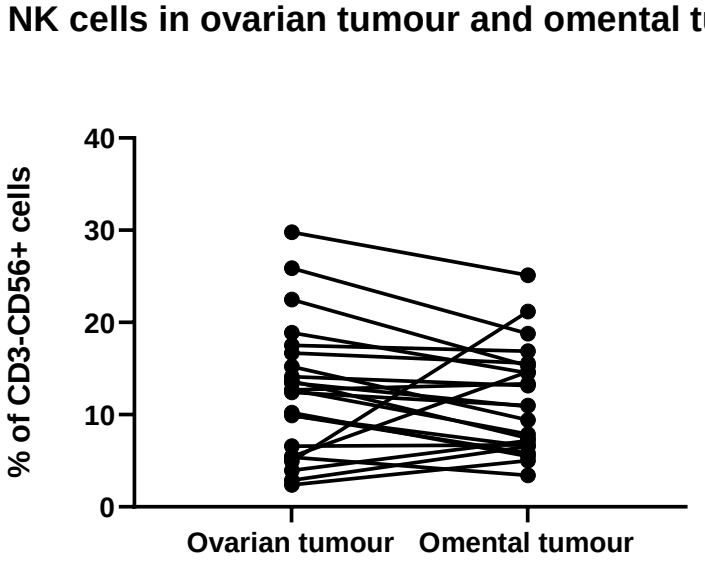


Figure 4.49: Correlation between the proportion of NK cells within ovarian tumour and matched omental tumour samples.

There was no difference in the proportion of NK cells within the ovarian tumour tissue compared to the omental tumour tissue.

Ovarian tumour and Omental tumour

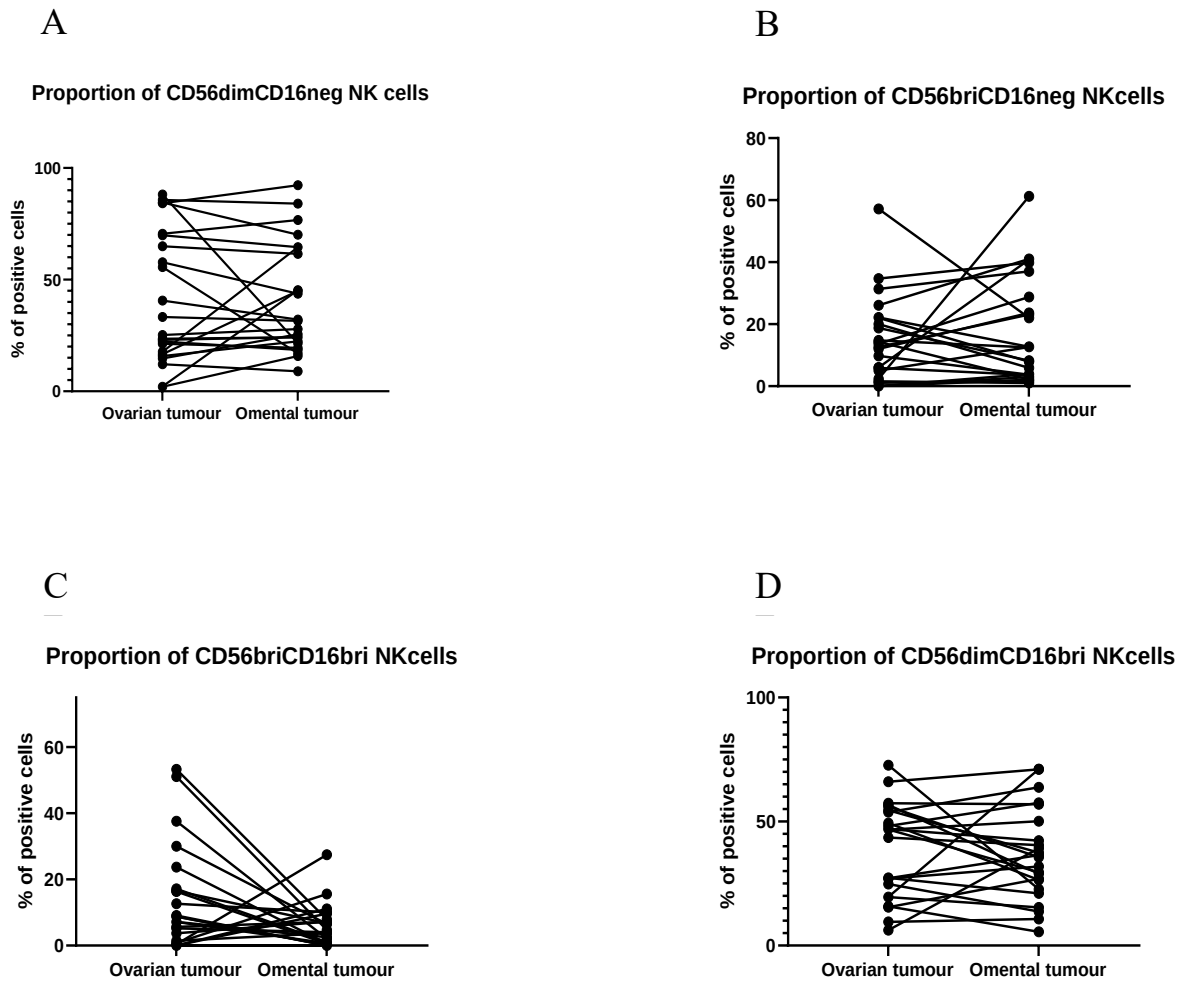
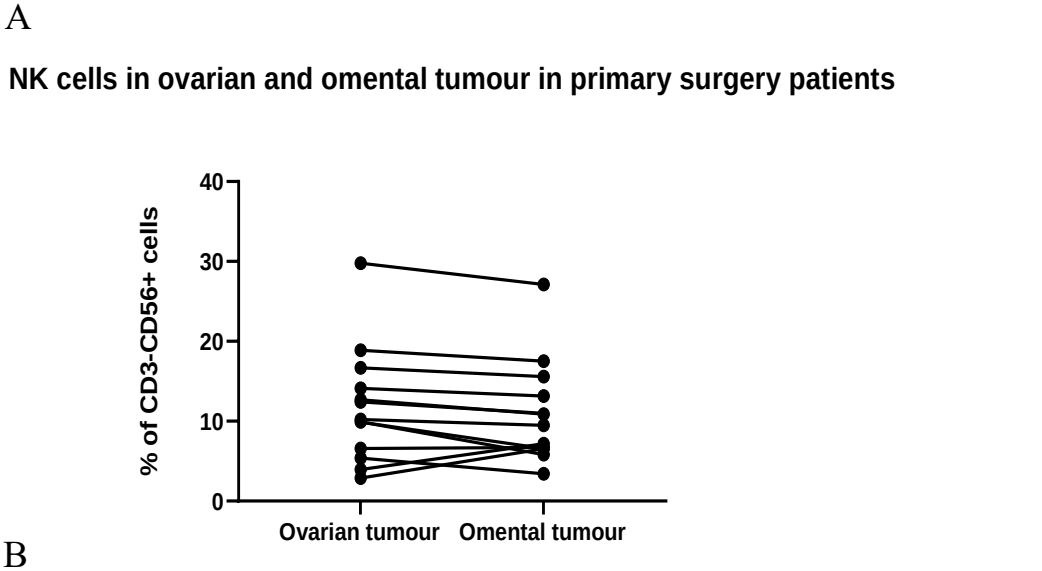


Figure 4.50: Correlation between CD56 and CD16 expression in ovarian tumour NK cells and paired omental tumour NK cells.

Within the ovarian and omental tumour there were similar distribution of infiltrating $CD56^{dim}CD16^{neg}$ (A), $CD56^{bri}CD16^{neg}$ (B), $CD56^{bri}CD16^{bri}$ (C) and $CD56^{dim}CD16^{bri}$ NK cells (D).

A



B

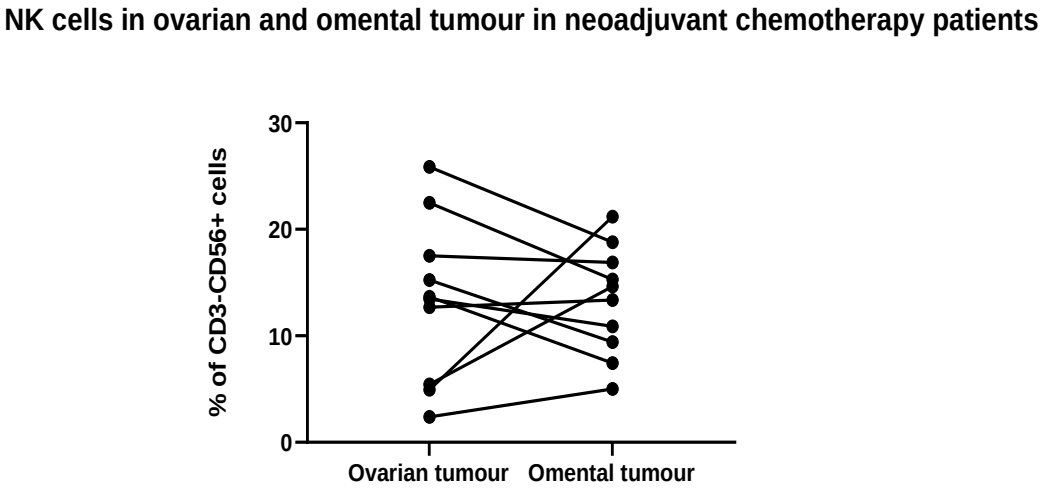
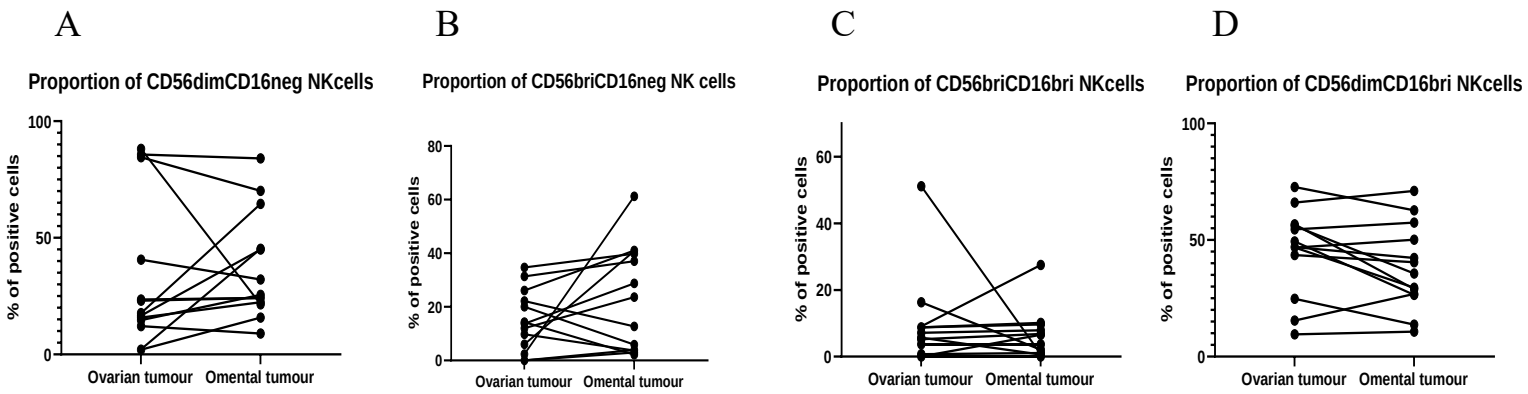


Figure 4.51: Correlation between the proportion of NK cells within ovarian tumour and matched omental tumour in both primary surgery and neoadjuvant chemotherapy OC patients.
There were no differences in the proportion of NK cells within the omental tumour tissue compared to those in the ovarian tumour tissue in both primary surgery (A) and neoadjuvant chemotherapy (B) OC patients.

Ovarian and Omental tumour in the primary surgery group



Ovarian and Omental tumour in the neoadjuvant chemotherapy group

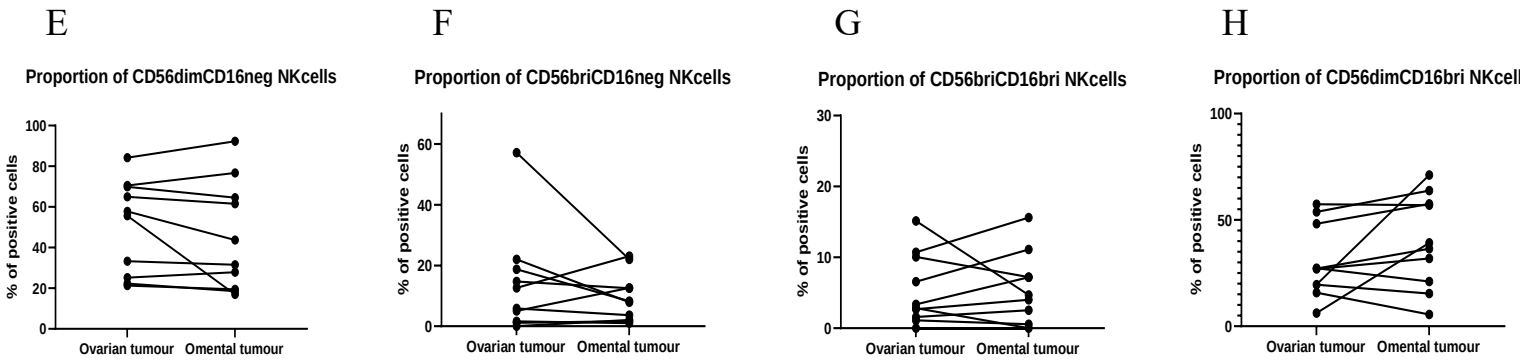


Figure 4.52: Correlation between ovarian tumour and omental tumour NK cell CD56 and CD16 expression in both primary surgery and neoadjuvant chemotherapy OC patients.
There were no differences in the CD56 and CD16 expression patterns on NK cells within ovarian tumour compared to omental tumour in either the primary surgery OC or neoadjuvant chemotherapy OC groups.

4.7.3.2 Analysis of NK activation receptors

The activation receptors on the ovarian tumour infiltrating NK cells were compared to the matched omental tumour infiltrating NK cells. There were no differences between the tissue types except for the expression of NKG2D (Figure 4.53), which was reduced on the NK cells within the omental tumour tissue ($p = 0.0060$).

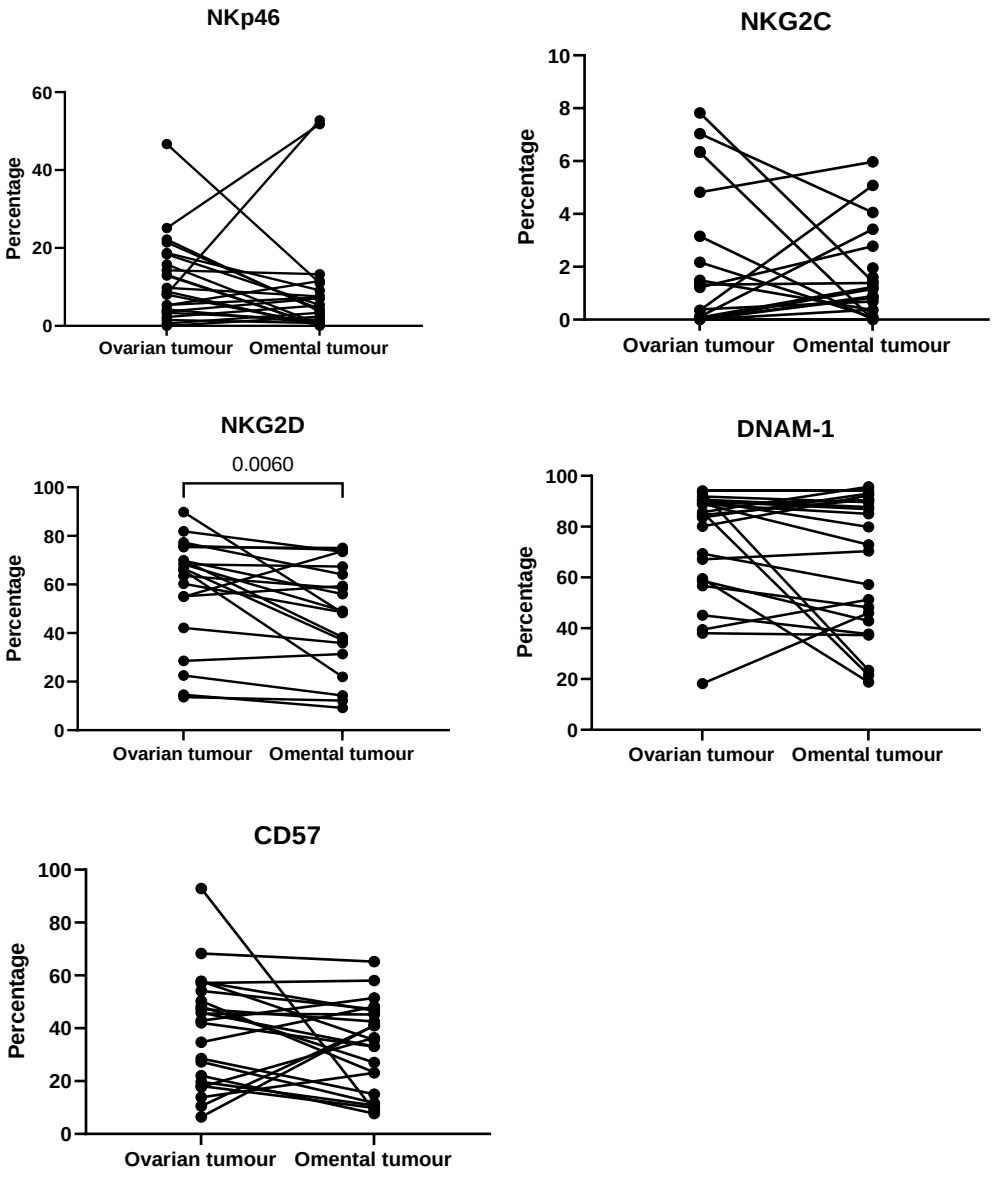


Figure 4.53: Expression of activation receptors on ovarian tumour infiltrating NK cells and matched omental tumour NK cells in all OC patients.
There was a reduction in the expression of activation receptor NKG2D on the NK cells within the omental tumour tissue compared to the ovarian tumour tissue. All other activation receptors were similar between ovarian and omental tumour tissue samples.

4.7.3.3 Analysis of NK inhibition receptors

On evaluation of inhibitory receptors on the matched ovarian and omental tumour infiltrating NK cells in all OC patients, there were no differences in the expression of CTLA-4, TIGIT, CD94 or PD-1 (Figure 4.54).

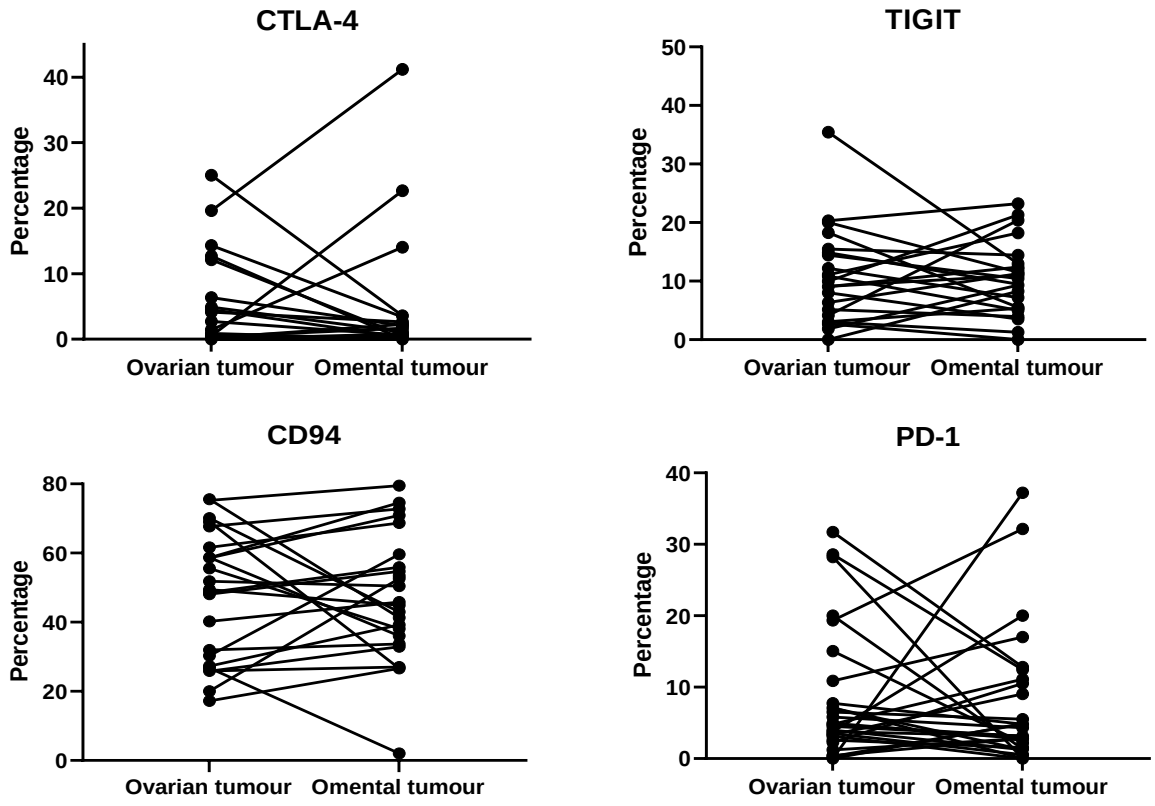


Figure 4.54: Expression of inhibitory receptors on ovarian tumour infiltrating NK cells and matched omental tumour NK cells in all OC patients.
There were no differences in the expression of inhibitory receptors on NK cells in ovarian tumour and omental tumour.

4.7.4 Summary of the correlation between peripheral, ovarian and omental NK cells

While there were no significant differences between the peripheral NK cells and those in normal ovary and omental tissue, there were clear differences between the NK cells in the peripheral blood and those infiltrating into both ovarian and omental tumour tissue. Firstly, the proportion of NK cells able to penetrate into ovarian tumour and omental tumour was reduced compared to those in the circulating blood. The type of NK cells also varied, with downregulation of CD16 expression on the ovarian and omental tumour NK cells in comparison to their corresponding peripheral NK cells. In particular, the $CD56^{dim}CD16^{neg}$ and $CD56^{bri}CD16^{neg}$ NK cells were in higher proportion in tumour tissue compared with PBMC samples. In addition, the ovarian tumour and omental tumour NK cells were in an inhibitory state compared to their matched peripheral NK cells. Both the ovarian and omental tumour NK cells had reduced expression of activation receptors NKp46, DNAM-1 and CD57, along with an increase in the inhibitory checkpoint PD-1; thus, implying a potential suppression of NK cell function by the tumour and the microenvironment.

Interestingly, when the ovarian tumour and omental tumour NK cells were compared directly, there was no difference in the subtypes and distribution of different NK cell populations between these two tumours. Apart from omental tumour NK cells having a reduction in NKG2D expression when compared to ovarian tumour NK cells, there was no other difference in the expression of inhibitory or activation receptors between the two tumour tissue types.

In summary, the distribution, subtype and activation state of tumour infiltrating NK cells differ significantly to the peripheral NK cells, regardless of whether the tumour is a primary ovarian mass or metastatic omental deposit. In addition, chemotherapy did not affect the

distribution patterns and proportions of NK cells within primary or metastatic ovarian tumour, as NK cells within chemotherapy naïve tumours exhibited a similar phenotype to those within chemotherapy exposed tumours.

4.8 Discussion

This large patient cohort not only allowed the direct comparison of ovarian tumours with benign and normal ovarian tissue, it also evaluated primary ovarian malignancies with metastatic omental tumour deposits and peripheral blood. In addition, the differences between chemotherapy naïve OC and tumours exposed to chemotherapy treatment were explored, making this NK cell flow cytometric analysis one of the most substantial studies reported in OC.

The proportion of NK cells and Ovarian cancer

The comprehensive analysis performed describes how the proportion, subtype and activation state of tumour infiltrating NK cells within the ovarian and omental tissues were similar, yet differed significantly to the peripheral NK cells. With NK cells typically accounting for 10-15% of circulating peripheral blood lymphocyte cells [173], the 13% average seen in the peripheral blood samples from our normal ovary control patients mirrored this. In comparison, the peripheral NK cell populations were increased in the OC patients (Figure 4.6), with an average proportion of 23%, demonstrating NK cell proliferation within the circulating blood in response to malignancy. Although peripheral NK cells are known to expand in other cancer types, albeit to a lesser extent, previous conflicting reports suggest similar proportions of peripheral NK cells in healthy donors to OC patients [362, 363].

A reduction in the proportion of NK cells was evident upon infiltration into both the ovarian tumour (average proportion 16%) and omental tumour (11%) from the circulating blood (Figures 4.15, 4.24, 4.33 and 4.41), which is related to disease progression and poor outcomes [110, 175, 362-366]. However, there were similar portions of NK cells within normal and benign ovary to the neoplastic ovarian samples (Figure 4.16), suggesting that NK cells retain their ability to penetrate the solid ovarian tissues upon malignant transformation and can initially withstand the immunosuppressive ovarian tumour microenvironment. In comparison, NK cell infiltration into omental tissue was impaired in metastatic omental disease, with fewer NK cells within omental tumours than in the normal omental tissue (Figure 4.25). As earlier reports suggest, with OC progression, shown with metastatic spread and advancing stage, the proportion of NK cells within both malignant ovary and omental tissue decline [110, 175, 362-366]. This possibly indicates immunosuppressive alterations in the tumour environment or an escape response from the tumour to eliminate or prevent further NK infiltration.

NK cell subtypes in Ovarian cancer

The majority of peripheral NK cells across the patient cohort were of the mature cytotoxic $CD56^{dim}CD16^{bri}$ subtype, yet OC patients had an increase in the immature cytokine producing $CD56^{bri}CD16^{neg}$ NK cells within the circulating blood compared to patients without malignancy (Figures 4.8 and 4.9). This reduction in NK function within OC patients is associated with advancing disease and unfavourable outcomes [110, 175, 362-366]. Confirming the notion that tumour infiltrating NK cells are less cytotoxic than the peripheral NK cells [156, 210, 211], there were fewer mature cytotoxic $CD56^{dim}CD16^{bri}$ NK cells within tumour tissue (average of 39% in ovarian tumour and 38% in omental tumour) compared to the peripheral blood of the cancer patients (average of 67%). The tumour NK cells also had downregulation of CD16 expression, with greater amounts of $CD56^{dim}CD16^{neg}$ cells (Figures

4.17, 4.26, 4.34 and 4.42). These have been shown to be raised in ovarian malignancy and are believed to generate natural tumour specific cytotoxicity [367, 368].

Activating and inhibitory receptors on NK cells in Ovarian cancer

The degree of NK activation was lower in the ovarian tumour tissue and metastatic omental deposits when these tumour NK cells were matched to their corresponding circulating blood samples (Figures 4.39 and 4.47). An increase in the inhibitory checkpoint, PD-1, in both ovarian tumour and omental tumour tissues compared to the paired blood samples (Figures 4.40 and 4.48) also confirmed NK cell dysfunction and inactivation following tumour infiltration [150, 211, 212, 217].

However, peripheral blood and tissue infiltrating NK cells had greater activation in cases of malignancy when compared to the non-cancerous samples, showing cancer recognition and an anti-tumour response. There was increased expression of various NK activation receptors: NKp46 was raised in the PBMC samples of OC patients compared to control patients (Figures 4.11. and 4.12), while NKG2D, DNAM-1 and CD57 were all raised in the ovarian tumour biopsies compared to the normal ovarian samples (Figures 4.20 and 4.21). Although NK cells in omental tumour biopsies demonstrated increased expression of the activation receptor DNAM-1 compared to normal omentum (Figure 4.29), there was also a reduction of NKp46 expression in the untreated omental tumour samples (Figure 4.30). This is consistent with the belief that the immunosuppressive metastatic environment attempts to inactivate NK cells, thereby preventing an NK-mediated attack towards tumour cells in progressive disease [131, 150, 151, 154, 177, 180, 199, 200, 212-216, 225, 226].

The effect of Chemotherapy on NK cells

Although chemotherapy did not influence the amount of NK cell infiltration into ovarian tumour and omental tumour tissue, the NK cell phenotype was modified with treatment. The impeding chemotherapy effect on peripheral and ovarian tumour NK cells, reducing the mature cytotoxic subpopulation and increasing the immature cytokine producing subtype (Figures 4.10 and 4.19), is in contrast to earlier studies where neoadjuvant chemotherapy enhanced the immune response in OC [104, 166, 356, 369]. It is possible that the reduction in mature cytotoxic NK cells following neoadjuvant chemotherapy in our cohort was influenced by granulocyte-colony stimulatory factor (G-CSF), which is utilised in our cancer centre for the treatment of lymphocytopenia after chemotherapy. It is known that G-CSF is associated with NK cell suppression, decreased activity and reduced cytotoxicity [370-372]. Nevertheless, this cohort analysis identified higher levels of the $CD56^{dim}CD16^{neg}$ NK subset, which is responsible for natural cytotoxicity specifically targeted against tumours [368], in both peripheral and ovarian NK cells following chemotherapy (Figures 4.8, 4.10 and 4.19). Chemotherapy did however, render the peripheral NK cells dysfunctional, with upregulation of the inhibitory immune checkpoints, CTLA-4 and PD-1 (Figure 4.14), as previously noted in OC cases [166]. The omental tumour NK cells, on the contrary, demonstrated increased activation with greater NKp46 and DNAM-1 expression (Figure 4.30), as expected following chemotherapy [104, 166, 354, 362].

In summary, this comprehensive analysis of NK phenotype successfully compared primary ovarian tumour and metastatic omental deposits to controls, interrogating the impact of chemotherapy and evaluating differences between peripheral blood and tissue biopsies. The findings reveal the challenges associated with innate immune function within the

immunosuppressive ovarian and omental tumour microenvironment where NK cell infiltration, cytotoxicity and activation are impaired.

Chapter 5:

The correlation of NK cell phenotype with clinical outcomes in Ovarian Cancer

5.1 Introduction

The majority of ovarian cancer (OC) cases develop resistance to current chemotherapy treatments and suffer a recurrence of disease within two years. As such, there is an urgent need to identify novel therapeutic approaches for OC patients [1, 64, 73]. It remains hopeful that Natural Killer (NK) cell immunotherapy can improve outcomes for patients and assist in overcoming the current therapeutic failures. It is known that NK cells have prognostic implications in solid and haematological malignancies, including OC. Here, dysfunctional and inhibited NK cells are associated with tumour progression, metastatic disease and poor survival [100, 152, 175, 192, 223, 225, 230. 231, 285, 364-366]. However, consideration of the specific function, interactions and activation of NK cells within advanced and treatment resistant ovarian tumours is needed to maximise the potential of NK cell immunotherapy in OC [110].

Therefore, this chapter explores the associations between NK cells and clinical outcomes in a large cohort of patients with OC. Utilising the comprehensive flow cytometric evaluation undertaken in chapter 4 of this thesis, the detailed NK cell phenotype analysis on blood and tumour samples from OC patients is correlated to prospectively collected clinical data. This aims to establish how NK infiltration and activation influences outcomes such as disease recurrence, survival, tumour burden and response to current treatments.

5.2 Study cohort

The study cohort described in Chapter 4 was utilised to correlate NK cell phenotype with clinical outcomes. This included 80 patients with OC, 40 who underwent primary surgery followed by 6 cycles of platinum-based adjuvant chemotherapy and 40 who received neoadjuvant chemotherapy followed by interval surgery. In addition, 20 patients without OC

(10 with a benign ovarian mass and 10 with pathologically normal ovaries and fallopian tubes) were also included in the assessment as controls. These four patient groups (primary surgery OC, neoadjuvant chemotherapy OC, benign ovary and normal ovary) were used to examine the relationships between NK cell phenotype and clinical outcomes.

5.3 Explanatory variables of the study cohort

5.3.1 Patient characteristics and histopathological variables (Table 5.1)

5.3.1.1 Patient age at the time of surgical intervention

The ages of women at the time of surgical intervention did not differ statistically between the four different patient groups ($p = 0.4480$). The mean ages were: 60 and 64 years in the primary surgery and neoadjuvant chemotherapy groups, respectively. Those in the benign and normal ovary groups had a mean age of 62 and 57 years, respectively. The median ages were also similar across the categories: 64 years (range 31-84) in the primary surgery group, 64 years (range 45-82) in the neoadjuvant chemotherapy group, 63 years (range 38-79) in the benign ovary group and 56 years (range 39-87) in the normal ovary group.

5.3.1.2 Patient ethnicity

The majority of the OC patients in the cohort were of White ethnicity: 82.5% (n=33) and 80% (n=32) of the primary surgery and neoadjuvant chemotherapy patients, respectively. The non-cancerous patients were also predominantly of White ethnicity, including 60.0% (n=6) of those with benign ovarian masses and 70.0% (n=7) with normal ovaries. The remaining women were of Asian, Black or mixed ethnicities.

5.3.1.3 Disease stage

The disease stage was determined using the 2014 FIGO staging system for OC. Staging data was complete for all cancer patients. All of the neoadjuvant chemotherapy patients had advanced disease: 52.5% (n=21) with stage III and 47.5% (n=19) with stage IV disease. While most of the primary surgery patients also had advanced OC; 52.5% (n=21) and 17.5% (n=7) with stages III and IV, respectively, a small proportion in this group had early stage OC. Here, 27.5% (n=11) had stage I and 2.5% (n=1) stage II OC. However, there was no statistical difference in disease stage between the two OC groups ($p = 0.7429$).

5.3.1.4 Peritoneal Cancer Index

The Peritoneal Cancer Index (PCI) assesses the degree of metastatic peritoneal disease in cases of advanced OC and is also a significant factor in patient survival [77]. The size and number of tumour masses within the abdominal cavity are used to calculate the PCI, where a greater value equates to more extensive disease. The PCI was calculated for all OC patients within the cohort. Although the median PCI in the neoadjuvant chemotherapy group was higher (16; interquartile range of 5-18) than in the primary surgery group (11; interquartile range of 3-15), there was no significant difference in PCI value between the two treatment groups ($p = 0.1485$).

5.3.1.5 Histopathological findings

Histopathological data was available for all of the patients in the cohort. The majority of the ovarian tumours were identified as serous epithelial cancers: 85.0% (n=34) in the primary surgery group and 97.5% (n=39) in the neoadjuvant chemotherapy group. All of the serous tumours in the neoadjuvant chemotherapy group were of the high-grade serous (HGSOvCa)

subtype. In the primary surgery group, 30 out of the 34 (88.2%) were HGSOvCa, while the remaining 4 were low-grade serous tumours.

The neoadjuvant chemotherapy group had just one (2.5%) case of non-serous OC, whereas 6 (15.0%) tumours in the primary surgery group had alternative pathologies, including clear cell (n=3, 7.5%), mucinous (n=2, 5.0%) and endometrioid (n=1, 2.5%) tumours. However, the discrepancies in pathological findings between the two OC treatment groups were not significant (p = 0.4000).

5.3.1.6 Metastatic Omental disease

The omentum plays an important role in OC: it is typically the first site of tumour metastases in progressive disease, histological assessment evaluates the tumour response to chemotherapy and tumour deposits are associated with poor patient outcomes [47, 65, 66, 69, 72]. As such, an omentectomy is routinely performed during OC surgery. Omental biopsies were therefore also collected, where possible, for the patients in this cohort and were examined alongside primary ovarian tissue in the NK phenotype analysis.

All OC cases in the cohort had either an omental biopsy or omentectomy to determine the presence of metastatic tumour deposits within the omental tissue. There were significantly more cases with omental disease in the neoadjuvant chemotherapy group than in the primary surgery group, where 92.5% (n=37) and 55.0% (n=22), respectively, had confirmation of metastatic disease (p = 0.0001). All patients with a benign ovarian mass had an omental biopsy as part of their staging surgery; all were histologically normal.

5.3.1.7 Serum CA-125 level at the time of surgical intervention

The glycoprotein Mucin-16, also known as MUC16 or CA-125, is produced by epithelial ovarian tumours and is expressed on the surface of cancer cells [226, 228]. Here it inhibits NK cells, supresses the cytotoxic activity of NK cells towards tumour tissue and reduces NK cytokine secretion. In addition, CA-125 is associated with OC progression and metastatic disease [223-229]. Serum CA-125 is utilised as a tumour biomarker for OC, where levels are used to monitor disease burden and treatment response. As standard of care for all OC patients, serum CA-125 levels are collected upon diagnosis (pre-treatment), during chemotherapy and also post-treatment for surveillance testing.

As such, the serum CA-125 levels obtained upon diagnosis were evaluated for the patients within the cohort. Women who had surgery for non-ovarian related pathology (normal ovary group) typically had normal serum CA-125 levels (<35 U/ml), as expected. However, CA-125 is not routinely measured in these women and only six (60%) had a pre-operative serum CA-125 level taken. In the women diagnosed with a benign ovarian mass, 90% had serum CA-125 measured and the mean value was 150 U/ml. In comparison, the mean serum CA-125 value was significantly raised in the OC patients, with a mean value of 1049 U/ml (OC vs normal ovary: $p < 0.0001$; OC vs benign ovary: $p = 0.0020$). The mean value was higher in the neoadjuvant chemotherapy group (1146 U/ml) than in the primary surgery group (734 U/ml), but not significantly so ($p = 0.3930$).

The proportion of women with a raised CA-125 level was significantly higher in those with any ovarian mass, be that malignant or non-malignant, than in women with normal ovaries ($p = 0.0001$). Although most women with OC had an elevated serum CA-125 level (95.0% (n=38) in the primary surgery group and 87.5% (n=35) in the neoadjuvant chemotherapy

group), 7 OC patients had a normal serum CA-125 level. In comparison, 3 (30.0%) patients in the normal ovary group had an elevated serum CA-125.

5.3.1.8 Absolute lymphocyte count at the time of surgical intervention

The absolute lymphocyte count is a routine serum haematology test that determines the total number of lymphocyte cells in the peripheral blood. In OC it is believed to be associated with survival, tumour burden and treatment response [373]. It is normally undertaken at diagnosis, during treatment and as part of the baseline pre-operative screening blood tests. In this cohort, pre-operative results were available for 80% of patients in the benign and normal ovary group (n=16), and 77.5% (n=62) of patients with OC. Cases of lymphocytopenia (less than 1x10*9/L) were observed in 3 patients; 2 in the primary surgery group and another in the neoadjuvant chemotherapy group. There were no cases of lymphocytosis (levels above the upper limit of 4.5x10*9/L) in either group. The mean lymphocyte counts were similar across all four groups.

Table 5.1: Patient characteristics and histopathological variables

Variable	Normal ovary (n=10)	Benign ovary (n=10)	Primary surgery (n=40)	Neoadjuvant chemotherapy (n=40)	P value
Age (years)					
Mean ± SD	57.3 ± 13.7	62.1 ± 12.8	60.7 ± 14.6	64.5 ± 11.6	0.4480
Ethnicity	**n (%)**	**n (%)**	**n (%)**	**n (%)**	
White	7 (70.0)	6 (60.0)	33 (82.5)	32 (80.0)	
Asian	1 (10.0)	2 (20.0)	5 (12.5)	6 (15.0)	
Black	1 (10.0)	1 (10.0)	0 (0.0)	1 (2.5)	
Mixed	1 (10.0)	1 (10.0)	2 (5.0)	1 (2.5)	0.2960
Disease stage	n/a	n/a	**n (%)**	**n (%)**	
1			11 (27.5)	0 (0.0)	
2			1 (2.5)	0 (0.0)	
3			21 (52.5)	21 (52.5)	
4			7 (17.5)	19 (47.5)	0.7429
PCI					
Median ± IQR	n/a	n/a	11 (3-15)	16 (5-18)	0.1485
Histopathology	n/a	n/a	**n (%)**	**n (%)**	
Serous			34 (85.0)	39 (97.5)	
Clear cell			3 (7.5)	0 (0.0)	
Mucinous			2 (5.0)	0 (0.0.)	
Endometrioid			1 (2.5)	1 (2.5)	0.4000
Omental disease	n/a	n/a	**n (%)**	**n (%)**	
Metastasis Present			22 (55.0)	37 (92.5)	**0.0001**
CA-125 (u/ml)	**n (%)**	**n (%)**	**n (%)**	**n (%)**	
-Patients with raised level	3 (30.0)	8 (80.0)	38 (95.0)	35 (87.5)	**0.0001**
-No level taken	4 (40.0)	1 (10.0)	0 (0.0)	0 (0.0)	
CA-125 (u/ml)					
Mean ± SD	32.0 ± 20	150 ± 98	734 ± 370	1146 ± 253	0.2649
Absolute lymphocyte count (x10*9/L)					
Mean ± SD	1.71 ±0.45	1.88 ±0.39	1.93 ±0.99	1.67 ±0.72	0.8321

5.3.2 Patient management and treatment variables (Table 5.2)

5.3.2.1 Type of surgical intervention

The surgical procedures performed were analysed for all patients in the cohort. The 10 patients with normal ovaries and fallopian tubes either had surgery for benign gynaecological conditions (80%, n=8) or had risk reduction surgery with the aim of preventing OC (20%, n=2). These patients underwent a total abdominal hysterectomy and bilateral salpingo-oopherectomy (TAH + BSO) or oophorectomy alone (70.0% and 30.0%, respectively). The 10 patients with a benign ovarian mass were managed with a TAH + BSO (60.0%), oophorectomy alone (20.0%) or TAH + BSO and omentectomy (20.0%).

Of the 40 patients who had primary surgery, 12 (30.0%) had FIGO stage I/II disease so had standard upfront surgery consisting of TAH+BSO and omentectomy. The remaining 28 patients (70.0%) were scheduled to have cytoreductive primary debulking surgery (PDS) for advanced disease (FIGO stage III/IV). PDS was successfully performed in 26 patients (65.0%), with 13 having a TAH+BSO and omentectomy, and the remaining 13 cases (32.5%) requiring additional procedures including bowel resection or upper abdominal surgery. All 40 patients in the neoadjuvant chemotherapy group were booked for cytoreductive interval debulking surgery (IDS) for FIGO stage III/IV disease. IDS was performed in 28 (70.0%) of the patients in the neoadjuvant chemotherapy group, with 18 (45.0%) having additional bowel or upper abdominal surgical procedures.

A total of 68 patients in the cohort had advanced (FIGO stage III/IV) OC and were deemed suitable for cytoreductive debulking surgery: 28 in the primary surgery group and 40 in the neoadjuvant chemotherapy group. Of these advanced cases, 31 patients (45.6%) required bowel or upper abdominal surgery. There was no significant difference in the proportion of

patients who required these additional surgical procedures between the primary surgery and neoadjuvant chemotherapy groups: 46.4% (n=13) vs 45.0% (n=18), respectively (p = 0.9073).

Despite all 68 patients with advanced OC being scheduled for cytoreductive surgery, debulking surgery was performed in 54 (79.4%); 26 who underwent PDS and 28 who had IDS. Surgeons were unable to proceed with surgery in the remaining 14 patients (20.6%) due to extensive disease burden which prevented optimal surgical resection. Hence, these patients only had a diagnostic procedure to assess disease distribution, a procedure also known as "open and close". This was more commonly seen in those who had already received neoadjuvant chemotherapy than in the primary surgery patients, with debulking surgery abandoned in 12 (30.0%) and 2 (7.1%) patients with advanced OC, respectively (p = 0.0218). These patients recommenced chemotherapy treatment.

5.3.2.2 Cytoreduction

OC surgery aims to remove all visible disease, known as complete cytoreduction or R0. This is associated with improved overall survival and progression free survival when compared to optimal (R1) or suboptimal (R2) cytoreduction, where residual disease following surgery is less than or greater than 1cm in size, respectively [47, 61-64]. The cytoreduction score has significant prognostic implications for OC and is not applicable to benign disease. It is therefore calculated for all patients having surgical resection of an ovarian tumour.

Complete cytoreduction (R0) was achieved in 33 (82.5%) of the patients who underwent primary surgery. This included all 12 of the OC patients with stage I/II disease who underwent standard primary surgery. Of the 28 patients in the primary surgery group with

advanced (stage III/IV) OC, complete cytoreduction (R0) was achieved in 75.0% (n=21). In comparison, complete cytoreduction was achieved in 65.0% (n=26) of patients in the neoadjuvant chemotherapy group. There was no significant difference in the rate of R0 when comparing the patients with advanced disease in the primary surgery and neoadjuvant chemotherapy groups (p = 0.3797). There was also no difference in complete cytoreduction when including all primary surgery patients (those with early and advanced OC) and comparing to the neoadjuvant chemotherapy group (p = 0.0753). When removing those patients with such extensive disease that cytoreductive debulking surgery had to be abandoned (2 in the primary surgery group and 12 in the neoadjuvant chemotherapy group), R0 was achieved in 80.8% following PDS and 92.9% in the patients who received neoadjuvant chemotherapy and had IDS (p = 0.1864).

Optimal cytoreduction (R1) was achieved in 1 patient (2.5%) in each treatment group, while suboptimal cytoreduction (R2) occurred in 4 (10.0%) and 1 (2.5%) of those in the primary surgery and neoadjuvant chemotherapy groups, respectively. Overall, there was no difference in cytoreduction score between the two groups (p = 0.1274)

5.3.2.3 Chemotherapy treatment and response

All of the OC patients who received neoadjuvant chemotherapy were given two chemotherapeutic agents, carboplatin and paclitaxel. The majority had either three (n=15, 37.5%) or four (n=12, 30.0%) cycles of neoadjuvant chemotherapy before proceeding to surgery. Some patients received five (n=3, 7.5%) or six (n=10, 25.0%) cycles of chemotherapy prior to undergoing ovarian cytoreductive surgery. The timing and decision of surgery was based on individual case discussions in the gynaecological oncology multidisciplinary team (MDT) meeting.

Chemotherapy response score (CRS) is assigned through pathological examination of the omentum that is removed during ovarian debulking surgery in patients who received prior chemotherapy (neoadjuvant chemotherapy group). CRS measures the degree of cell death following chemotherapy and is used as a surrogate marker to determine the response to chemotherapy treatment. CRS is scored in 3 levels: CRS 3 indicates a complete response to chemotherapy; CRS 2 indicates a moderate response; and CRS 1 indicates a poor response. Within our cohort of patients who had neoadjuvant chemotherapy, 20.0% (n=8) had CRS 3, 35.0% (n=14) had CRS 2, and 42.5% (n=17) had CRS 1.

Table 5.2: Patient management and treatment variables

Variable	Normal ovary (n=10)	Benign ovary (n=10)	Primary surgery (n=40)	Neoadjuvant chemotherapy (n=40)	P value
Type of surgery - Inspection + biopsies - Oophorectomy only - TAH + BSO - TAH + BSO, omentectomy - TAH + BSO, omentectomy + additional procedures	**n (%)** 0 (0.0) 3 (30.0) 7 (70.0) 0 (0.0) 0 (0.0)	**n (%)** 0 (0.0) 2 (20.0) 6 (60.0) 2 (20.0) 0 (0.0)	**n (%)** 2 (5.0) 0 (0.0) 0 (0.0) 25 (62.5) 13 (32.5)	**n (%)** 12 (30.0) 0 (0.0) 0 (0.0) 10 (25.0) 18 (45.0)	< **0.0001**
Cytoreduction score R0 R1 R2 n/a	n/a	n/a	**n (%)** 33 (82.5) 1 (2.5) 4 (10.0) 2 (5.0)	**n (%)** 26 (65.0) 1 (2.5) 1 (2.5) 12 (30.0)	0.1274
Number of Neoadjuvant chemotherapy cycles 3 4 5 6	n/a	n/a	n/a	**n (%)** 15 (37.5) 12 (30.0) 3 (7.5) 10 (25.0)	n/a
Chemotherapy Response Score 1 2 3 n/a	n/a	n/a	n/a	**n (%)** 17 (42.5) 14 (35.0) 8 (20.0) 1 (2.5)	n/a

5.4 Patient outcomes

All OC patients at the cancer centre are followed up for 5 years after completion of treatment. At the time of analysis, no patients had been lost to follow-up and there was no difference in the post-operative follow up duration between those who had primary surgery or neoadjuvant chemotherapy. The mean follow-up duration for patients in the primary surgery group was 27 months (range 2-60 months), while patients in the neoadjuvant chemotherapy group had a mean follow-up of 32 months (range 6-60 months).

5.4.1 Disease recurrence and analysis of progression free survival

Information regarding disease recurrence was obtained from patient notes and electronic records. Disease recurrence was defined as pathological or radiological confirmation of disease following the completion of adjuvant chemotherapy. The time to disease recurrence was calculated from the treatment completion date (the date of completing adjuvant chemotherapy) to the date that a recurrence was confirmed. This time period was used to give the progression free survival (PFS). In cases where there was no evidence of disease recurrence at the time of analysis, the PFS was determined using the date the patient was last seen and remained free of disease.

During the follow-up period, 36 (45.0%) OC patients suffered a recurrence of their disease, described in Table 5.3. This accounted for 7 (17.5%) in the primary surgery group and 29 (72.5%) in the neoadjuvant chemotherapy group, with the latter being significantly more likely to recur ($p < 0.001$). Of the 36 patients who developed a disease recurrence, over half (52.8%, n=19) occurred within the first 12 months and almost three quarters (72.2%, n=26) within the first 24 months. Although not significant ($p = 0.3137$), the patients who recurred by 12 months were more likely to have had neoadjuvant chemotherapy (58.6%, n=17) than

primary surgery (28.6%, n=2). This was also seen in patients who recurred by 24 months: 57.1% (n=4) compared to 75.9% (n=22) in primary surgery and neoadjuvant chemotherapy groups, respectively (p = 0.3210).

Disease recurrence was then examined in those patients who had advanced disease (FIGO stage III/IV): the 40 patients in the neoadjuvant chemotherapy group and 28 patients in the primary surgery group. Those in the neoadjuvant chemotherapy group were significantly more likely to suffer a disease recurrence than the patients with advanced OC in the primary surgery group (72.5% (n=29) vs 17.9% (n=5), respectively; p < 0.0001). Again, there was no significant difference in recurrence by 12 months (p = 0.1101) or 24 months (p = 0.1041) between the advanced cases who had primary surgery and neoadjuvant chemotherapy.

Table 5.3: Disease recurrence based on treatment modality

Disease recurrence	**All OC (n=80)**	**All Primary Surgery (n=40)**	**Primary Surgery Advanced OC (n=28)**	**Neoadjuvant Chemotherapy (n=40)**
All recurrences	36/80 (45.0%)	7/40 (17.5%)	5/28 (17.9%)	29/40 (72.5%)
Recurrences occurring within 12 months	19/36 (52.8%)	2/7 (28.6%)	1/5 (20.0%)	17/29 (58.6%)
Recurrences occurring within 24 months	26/36 (72.2%)	4/7 (57.1%)	2/5 (40.0%)	22/29 (75.9%)

The PFS time periods were worse in the neoadjuvant chemotherapy patients. Figure 5.1 shows the Kaplan-Meier plot for PFS in all OC patients, comparing the primary surgery group (early and advanced disease) to the neoadjuvant chemotherapy group ($p < 0.0001$). The average PFS times were lower in the neoadjuvant chemotherapy group, with a median and mean PFS of 13.6 and 17.9 months, respectively. In comparison, the median and mean PFS for all patients in the primary surgery group were 19.1 and 22.1 months, respectively. The poor PFS outcomes in the neoadjuvant chemotherapy patients correlated to this group having more advanced and aggressive disease, for example more cases of FIGO stage III/IV disease, higher PCI values, more cases of omental metastases, a greater number of high-grade serous cases and fewer patients with complete cytoreduction following debulking surgery. Therefore, the PFS was compared between advanced (FIGO stage III/IV) OC patients only, shown in Figure 5.2. The PFS remained decreased in the patients with advanced OC who received neoadjuvant chemotherapy compared to those who had primary surgery for advanced disease ($p = 0.0006$). The median and mean PFS for the patients with advanced OC who underwent primary surgery were 19.1 and 22.2 months, respectively.

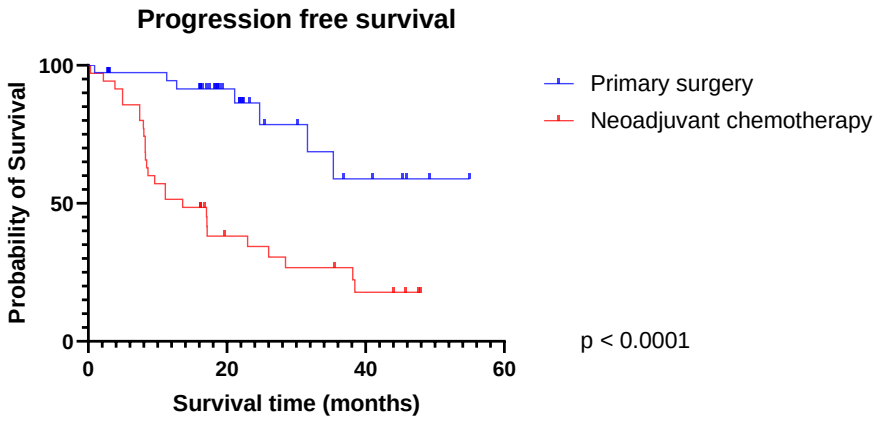


Figure 5.1: Kaplan-Meier plot demonstrating progression free survival in all OC patients in the primary surgery and neoadjuvant chemotherapy treatment groups.
PFS was significantly lower in the neoadjuvant chemotherapy group than in the primary surgery group when analysing patients with all stages of disease ($p < 0.0001$).

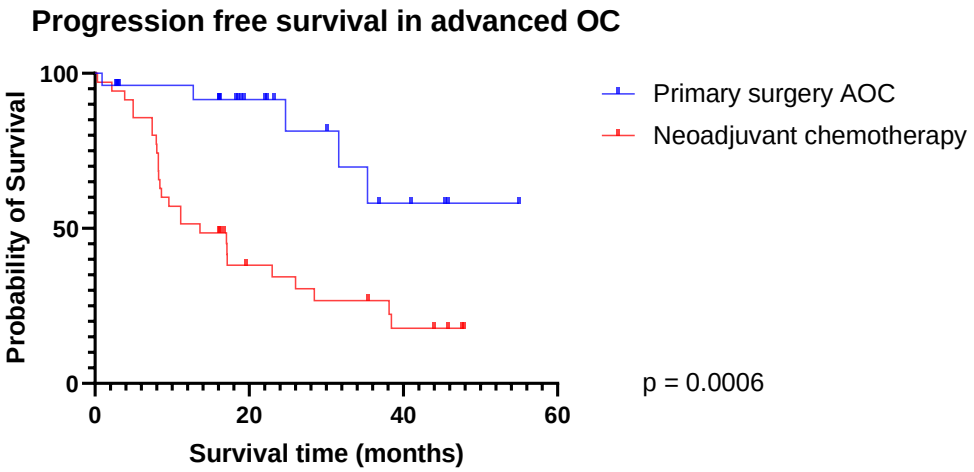


Figure 5.2: Kaplan-Meier plot demonstrating progression free survival in advanced OC (AOC) patients in the primary surgery and neoadjuvant chemotherapy treatment groups.
PFS was significantly lower in the neoadjuvant chemotherapy group than in the primary surgery group when comparing patients with stage III/IV OC (p = 0.0006).

5.4.2 Analysis of disease specific death

Information regarding death and the cause of death was obtained from patient notes, electronic hospital records and death certificates. The survival status for all patients in the cohort were reviewed on the study end date (10.1.2023). The time to disease-specific death (death from OC) was calculated from the date of diagnosis to the recorded date of death. This time period gave the overall survival (OS). When patients remained alive, their OS was established from the diagnosis date to the end date of the study follow-up period.

During the follow-up period, a total of 36 (45.0%) women died from OC, demonstrated in Table 5.4. There were no deaths attributed to other causes. Death rates were higher in the neoadjuvant chemotherapy group, where 28 (70.0%) died. This compared to 8 (20.0%) patients with all stages (early and advanced OC) in the primary surgery group ($p < 0.0001$) and 6 (21.4%) patients in the primary surgery group when including only those with advanced disease ($p = 0.0001$). Of those who died, 33.3% (n=12/36) did so by 12 months,

which gave an overall one-year survival rate of 85.0% (n=68/80). In addition, 58.3% (n=21/36) of those who died did so by 24 months, giving an overall two-year survival rate of 73.8% (n=59/80) within the whole OC cohort. With 26 patients dying within 36 months, the three-year survival rate was 67.5% (n=54/80).

Women who died within 12 months were just as likely to have had primary surgery (all stages) than neoadjuvant chemotherapy: 37.5% (n= 3) in the primary surgery group for all cases vs. 32.1% (n=9) in the neoadjuvant chemotherapy group ($p = 0.7768$). Similarly, there was no significant difference in mortality over 24 months between the primary surgery group (50.0%, n=4) and neoadjuvant chemotherapy group (60.7%, n=17), ($p = 0.5877$). When focusing on patients with advanced OC only, those who died within 12 months and 24 months were just as likely to have undergone primary surgery as those who received neoadjuvant chemotherapy ($p = 0.9549$ and $p = 0.2203$, respectively).

However, the proportion of patients who were still alive and disease-free at the end of the follow-up period was significantly higher in the patients of all stages in the primary surgery group ($p < 0.0001$) compared to those in the neoadjuvant chemotherapy group. When comparing those with advanced OC, the proportion alive and disease-free was again significantly higher in the primary surgery group compared to the neoadjuvant chemotherapy group ($p < 0.0001$). Overall, 40 (50.0%) women with OC in the study cohort were alive and remained disease free after treatment: 77.5% (n=31/40) with all stages of OC in the primary surgery group and 75.0% (n=21/28) with advanced OC in the primary surgery group, compared to 22.5% (n=9/40) from the neoadjuvant chemotherapy group.

Table 5.4: OC related death based on treatment modality

OC related deaths	All OC (n=80)	All Primary Surgery (n=40)	Primary Surgery Advanced OC (n=28)	Neoadjuvant Chemotherapy (n=40)
All OC deaths	36/80 (45.0%)	8/40 (20%)	6/28 (21.4%)	28/40 (70.0%)
Deaths occurring within 12 months	12/36 (33.3%)	3/8 (37.5%)	2/6 (33.3%)	9/28 (32.1%)
Deaths occurring within 24 months	21/36 (58.3%)	4/8 (50.0%)	2/6 (33.3%)	17/28 (60.7%)

The neoadjuvant chemotherapy group had significantly shorter overall survival (OS) rates. Figure 5.3 shows the Kaplan-Meier plot with OS for patients with all stages of OC: the neoadjuvant chemotherapy group had decreased OS compared to patients with early and advanced disease who underwent primary surgery ($p = 0.0171$). Figure 5.4 shows the OS of patients with advanced disease: OS was again worse in the neoadjuvant chemotherapy group compared to the patients with stage III/IV OC who had primary surgery ($p = 0.0418$). The median and mean OS for the neoadjuvant chemotherapy group was 22.6 and 29.7 months, respectively. This compared to 20.6 and 22.4 months in all primary surgery cases, respectively, and 20.7 and 22.4 months in the advanced OC cases in the primary surgery group.

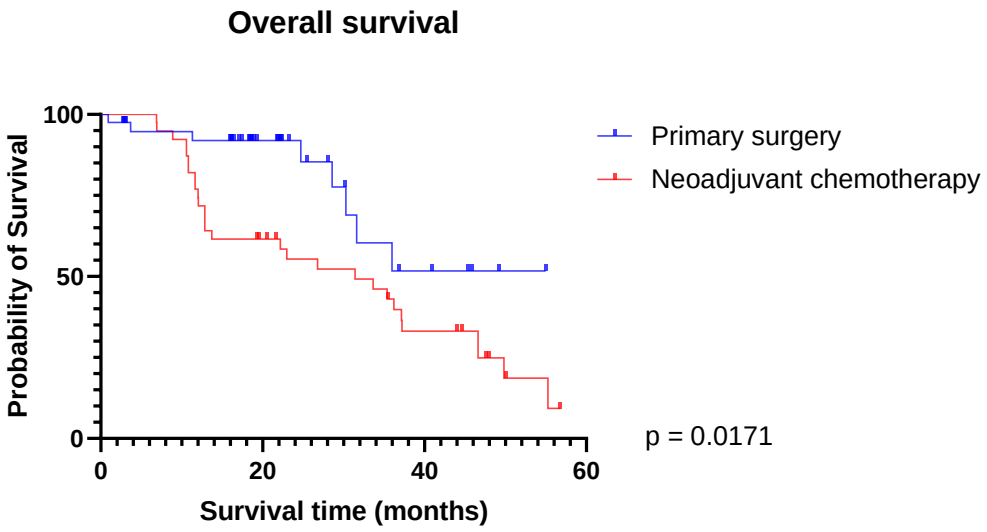


Figure 5.3: Kaplan-Meier plot demonstrating overall survival in all OC patients in the primary surgery and neoadjuvant chemotherapy treatment groups.
OS was reduced in the neoadjuvant chemotherapy group when compared to patients with early and advanced OC who underwent primary surgery (p = 0.0171).

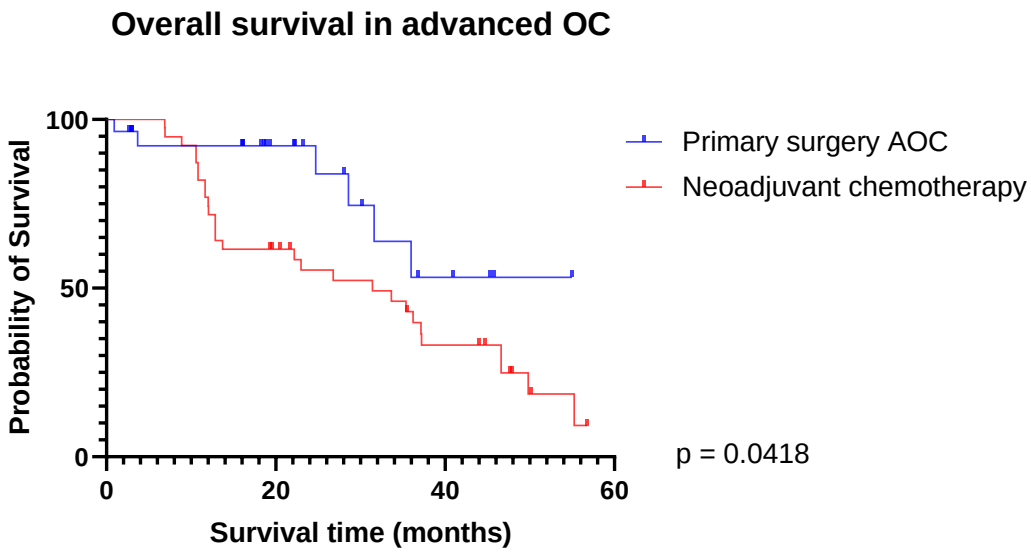


Figure 5.4: Kaplan-Meier plot demonstrating overall survival in advanced OC (AOC) managed with primary surgery and neoadjuvant chemotherapy.
OS was decreased in the neoadjuvant chemotherapy group when compared to the patients who had primary surgery for stage III/IV OC (p = 0.0418).

5.5 The association between NK cell phenotype and clinical outcomes

5.5.1 The correlation between NK cells, patient survival and disease recurrence

5.5.1.1 Recurrence of disease and the proportion of NK cells

Throughout the study collection period, 36 (45.0%) of the 80 OC patients suffered a recurrence of their disease. To determine the association between the amount of NK cells and disease recurrence, patients were divided into two categories based on the proportion of NK cells in the CD45 positive lymphocyte population within their blood and tissue samples: those with an NK cell proportion at or below the median value (group 1) and those with a proportion above the median value (group 2). Analysis of the NK cells within the PBMC samples revealed that 17 (47.2%) of the disease recurrence cases occurred in group 1, and 19 (52.8%) in group 2. There was no difference in the incidence of recurrence between the two groups ($p = 0.6531$), shown in Table 5.5. There was also no significant difference in the incidence of disease recurrence when comparing the proportions of NK cells within ovarian tumour biopsies ($p = 0.4651$). Disease recurrence was also similar between the two groups when analysing NK cells within omental biopsies ($p = 0.3933$).

Table 5.5: OC recurrences based on the proportion of NK cells

Samples	Proportion of NK cells	Recurrence	P value
PBMC (n=36)	1. ≤ median	17 (47.2%)	0.6531
	2. > median	19 (52.8%)	
Ovary (n=18)	1. ≤ median	8 (44.4%)	0.4651
	2. > median	10 (55.6%)	
Omentum (n=13)	1. ≤ median	6 (46.2%)	0.3933
	2. > median	7(53.8%)	

The relationship between PFS and the proportion of NK cells was then examined. Focusing on the proportion of NK cells within PBMC samples, there was no difference in PFS between patients with NK cells at or below the median (group 1) and those with NK cells above the median value (group 2), shown in Figure 5.5 ($p = 0.9138$). The PFS was also similar between groups 1 and 2 when analysing the proportion of NK cells within ovarian biopsies (Figure 5.6, $p = 0.9728$) and within omental biopsies (Figure 5.7, $p = 0.8716$).

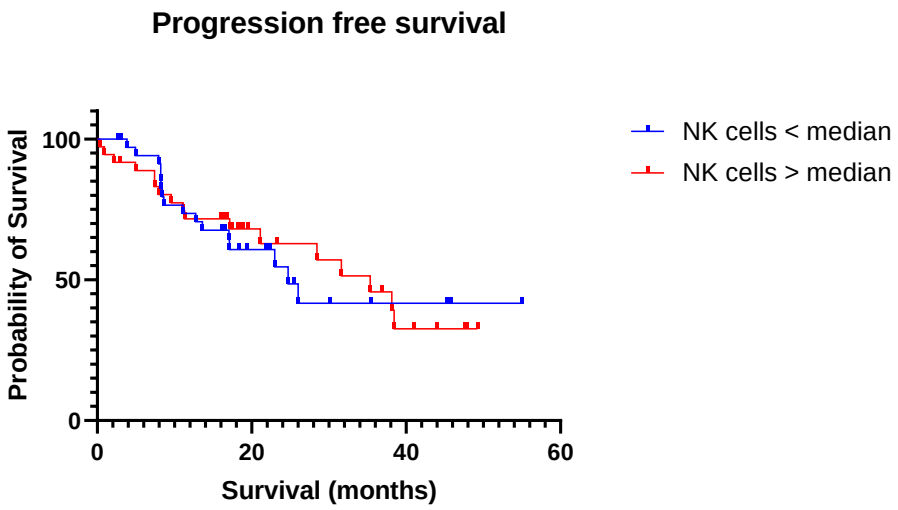


Figure 5.5: The progression free survival of OC patients based on the proportion of NK cells within their peripheral blood.
There was no difference in PFS between patients who had a PBMC NK cell proportion below the median value to those with a PBMC NK cell proportion above the median value ($p = 0.9138$).

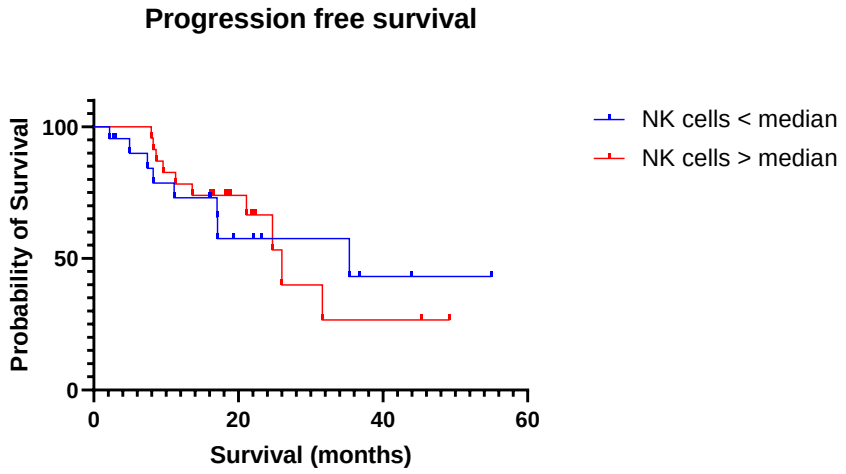


Figure 5.6: The progression free survival of OC patients based on the proportion of NK cells within the ovarian tumour tissue samples.
There was no difference in PFS between patients who had an ovarian NK cell proportion below the median value to those with an NK cell proportion above the median value (p = 0.9728).

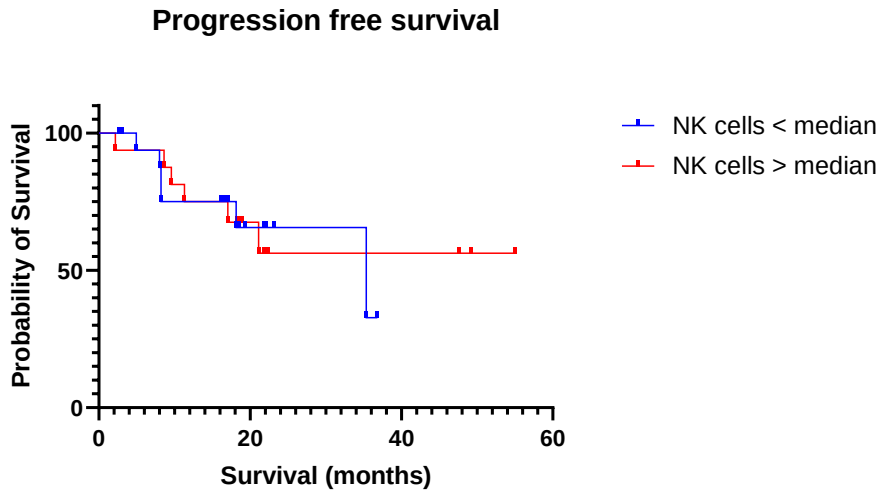


Figure 5.7: The progression free survival of OC patients based on the proportion of NK cells within the omental tumour tissue samples.
There was no difference in PFS between patients who had an omental NK cell proportion below the median value to those with an NK cell proportion above the median value (p = 0.8716).

5.5.1.2 Patient survival and the proportion of NK cells

During the follow-up period, a total of 36 (45.0%) women died from OC. To analyse the association between the number of NK cells and patient death, patients were separated into the same two categories: those with NK cell proportion below and above the median value, (groups 1 and 2, respectively), shown in Table 5.6. Based on PBMC samples, there were equal number of deaths (n=18/36; 50.0%) reported between the groups with no difference in OS (Figure 5.8, p = 0.5929). Analysis of the proportion of NK cells within ovarian biopsies showed no difference in patient death between groups 1 and 2 (p = 0.2964). Disease-specific death was also similar between the two groups of NK cells within omental tissue (p = 0.1349). Figures 5.9 and 5.10 show that OS was also similar between the group 1 and 2 in ovarian and omental tissue, respectively.

Table 5.6: Disease-specific death and the proportion of NK cells

Samples	Proportion of NK cells	Death	P value
PBMC (n=36)	1. ≤ median	18 (50.0%)	1.0
	2. > median	18 (50.0%)	
Ovary (n=20)	1. ≤ median	8 (40.0%)	0.2964
	2. > median	12 (60.0%)	
Omentum (n=12)	1. ≤ median	4 (33.3%)	*0.1349*
	2. > median	8 (66.6%)	

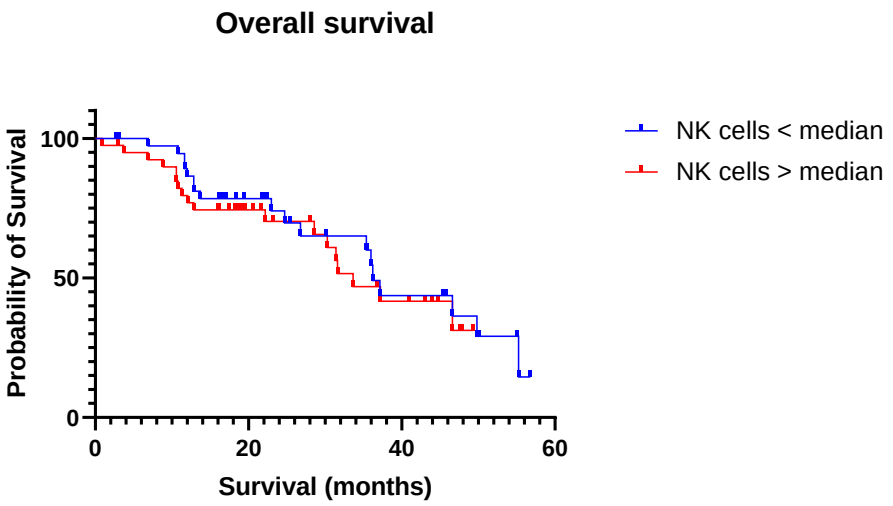


Figure 5.8: The overall survival of OC patients based on the proportion of NK cells within the peripheral blood.

There was no difference in OS between patients who had a PBMC NK cell proportion below the median value to those with an NK cell proportion above the median value (p = 0.5929).

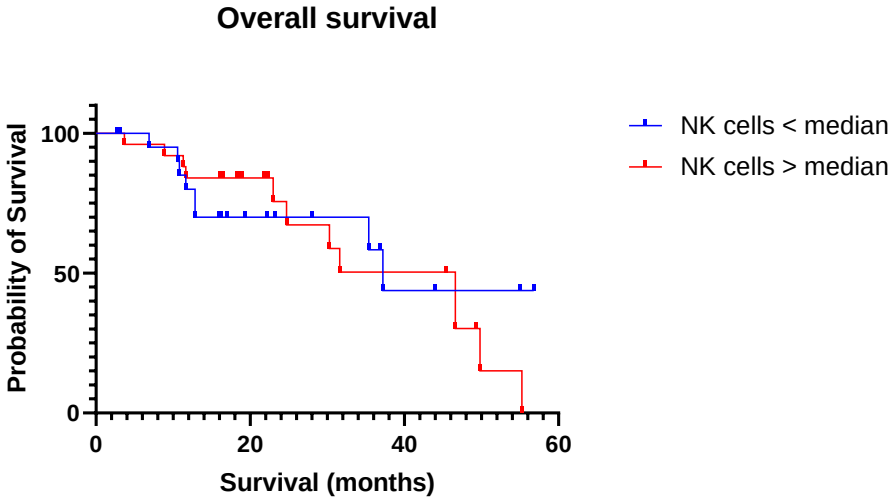


Figure 5.9: The overall survival of OC patients based on the proportion of NK cells within ovarian tumour tissue.

There was no difference in OS between patients who had an ovarian NK cell proportion below the median value to those with an NK cell proportion above the median value (p = 0.7700).

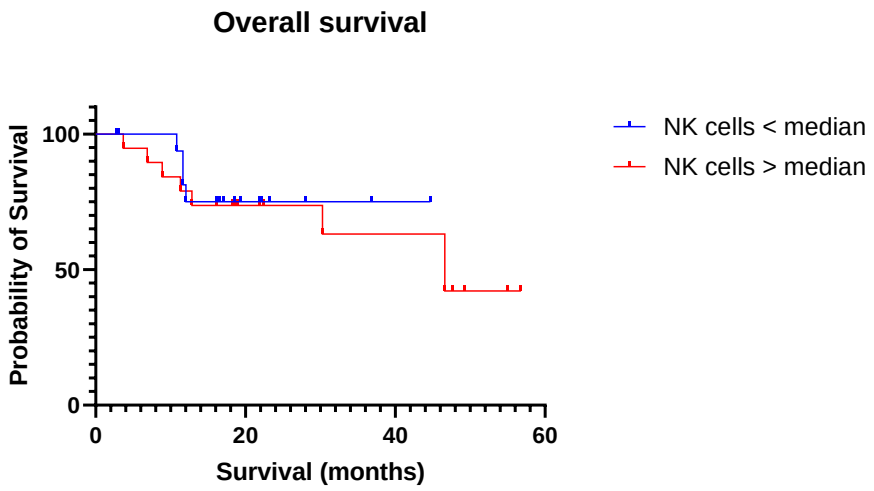


Figure 5.10: The overall survival of OC patients based on the proportion of NK cells within omental tumour tissue.
There was no difference in OS between patients who had an omental NK cell proportion below the median value to those with an NK cell proportion above the median value (p = 0.7334).

5.5.1.3 Disease recurrence based on the NK cell subpopulation

The different NK subpopulations were then correlated to disease recurrence. The samples were separated into two categories based on the proportion of each of the NK subpopulations: those samples with a proportion of each NK subpopulation at or below the median value (group 1) and those with a proportion above the median value (group 2). There were no differences in disease recurrence when groups 1 and 2 for the NK subpopulations within ovarian and omental tissue were compared. However, differences in disease recurrence were evident when the proportions of NK subpopulations in PBMC samples were compared. Table 5.7 shows the recurrences that occurred in groups 1 and 2 for each of the NK subpopulations in PBMC samples. When $CD56^{dim}CD16^{neg}$ NK cells were divided into the two groups, 11 patients in group 1 (27.5%) and 25 in group 2 (62.5%) suffered a recurrence (p = 0.0017). Of the $CD56^{bri}CD16^{neg}$ NK cells within PBMC samples, there were 12 (30.0%) recurrences in group 1 and 24 (60.0%) in group 2 (p = 0.0070). There was also a significant difference in

disease recurrence between group 1 of the PBMC $CD56^{dim}CD16^{bri}$ NK cells and group 2: 23 (57.5%) vs 13 (32.5%) recurrences, respectively (p = 0.0246). There was no difference in disease recurrence between samples with the proportion of $CD56^{bri}CD16^{bri}$ NK cells less than the median when compared to samples with the proportion above the median value (p = 0.01775).

Table 5.7: OC recurrences based on the proportion of PBMC NK cell subpopulations.

PBMC NK Subpopulation	Proportion of NK cells	Recurrence	P value
$CD56^{dim}CD16^{neg}$	1. ≤ median	11/40 (27.5%)	
	2. > median	25/40 (62.5%)	**0.0017**
$CD56^{bri}CD16^{neg}$	1. ≤ median	12/40 (30.0%)	
	2. > median	24/40 (60.0%)	**0.0070**
$CD56^{dim}CD16^{bri}$	1. ≤ median	23/40 (57.5%)	
	2. > median	13/40 (32.5%)	**0.0246**
$CD56^{bri}CD16^{bri}$	3. ≤ median	21/40 (52.5%)	
	4. > median	15/40 (37.5%)	0.1775

The association between PFS and the proportion of the NK cell subpopulations was then examined. The PFS was significantly reduced when OC patients had increased (above the median value; group 2) $CD56^{dim}CD16^{neg}$ NK cells in PBMC samples compared to patients with $CD56^{dim}CD16^{neg}$ NK cells below the median value (group 1), shown in Figure 5.11(A), (p = 0.0091). Similarly, PFS was significantly decreased in patients with a higher proportion (group 2) of PBMC $CD56^{bri}CD16^{neg}$ NK cells (Figure 5.11(B); p = 0.0004). In contrast, the patients with a greater proportion of PBMC $CD56^{dim}CD16^{bri}$ NK cells above the median value (group 2) had improved PFS (Figure 5.11(C); p = 0.0244). There was no difference in

PFS between the patients who had increased and decreased proportions of $CD56^{bri}D16^{bri}$ NK cells in PBMC (Figure 5.11(D)).

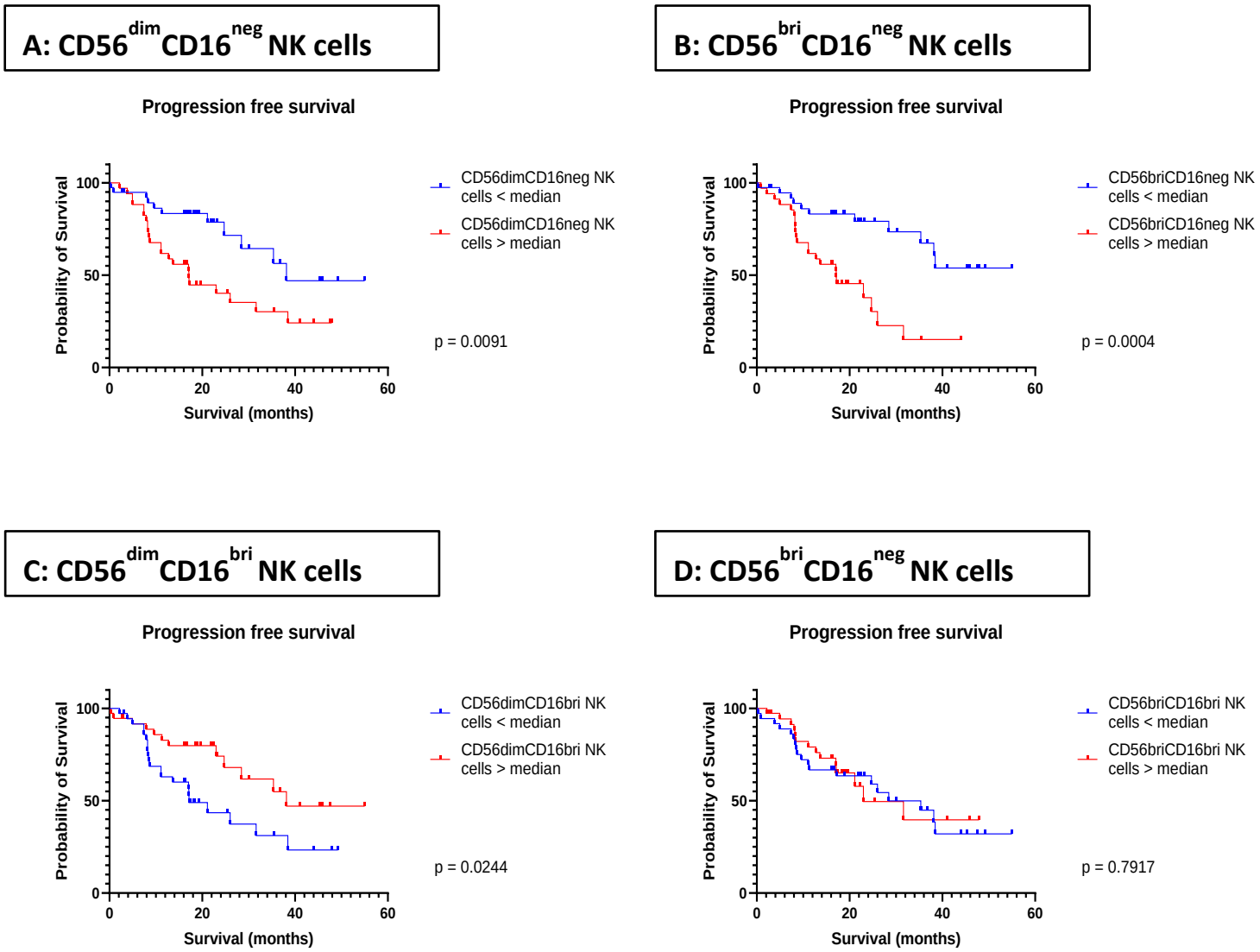


Figure 5.11: The progression free survival of OC patients based on the proportion of NK cell subpopulations within peripheral blood samples.

PFS was reduced in patients who had an increased proportion of $CD56^{dim}CD16^{neg}$ NK cells (A) and increased $CD56^{bri}CD16^{neg}$ NK cells (B) in PBMC samples. Patients who had an increased proportion of $CD56^{dim}CD16^{bri}$ NK cells had improved PFS (C). There was no difference in PFS between patients who had reduced or increased proportions of $CD56^{bri}CD16^{bri}$ NK cells (D) in PBMC samples.

5.5.1.4 Patient survival based on the NK cell subpopulation

The proportions of NK subpopulations were then correlated to disease specific death. Samples were again divided into those with a proportion at or below the median value (group 1) and those with a proportion above the median value (group 2) for each of the different NK subpopulations. Table 5.8 shows the cases of disease specific death that occurred in groups 1 and 2 for each of the NK subpopulations in PBMC samples. When $CD56^{dim}CD16^{neg}$ NK cells were reviewed, 10 patients in group 1 (25.0%) and 26 in group 2 (62.5%) died from OC (p = 0.0003). On examination of the $CD56^{bri}CD16^{neg}$ NK cells, there were 9 (22.5%) deaths in group 1 and 27 (67.5%) in group 2 (p < 0.0001). In contrast, there were a greater number of deaths in group 1 of the $CD56^{dim}CD16^{bri}$ NK cells (n=23, 57.5%) compared to group 2 (n=13, 32.5%, p = 0.0246). There was no difference in disease specific death between the proportions of $CD56^{bri}CD16^{bri}$ NK cells (p = 0.3687).

Table 5.8: OC related death based on the proportion of PBMC NK cell subpopulations.

PBMC NK Subpopulation	Proportion of NK cells	Death	P value
$CD56^{dim}CD16^{neg}$	1. ≤ median	10/40 (25.0%)	
	2 > median	26/40 (65.0%)	**0.0003**
$CD56^{bri}CD16^{neg}$	1. ≤ median	9/40 (22.5%)	
	2. > median	27/40 (67.5%)	**< 0.0001**
$CD56^{dim}CD16^{bri}$	1. ≤ median	23/40 (57.5%)	
	2. > median	13/40 (32.5%)	**0.0246**
$CD56^{bri}CD16^{bri}$	1. ≤ median	20/40 (50.0%)	
	2. > median	16/40 (40.0%)	0.3687

The proportions of the PBMC NK cell subpopulations were then correlated to OS. Patients who had an increased proportion of $CD56^{dim}CD16^{neg}$ NK cells had a significantly lower OS when compared to the patients with reduced levels of $CD56^{dim}CD16^{neg}$ NK cells in PBMC samples ($p = 0.0372$), shown in Figure 5.12(A). Likewise, OS was significantly reduced in patients with a higher proportion of PBMC $CD56^{bri}CD16^{neg}$ NK cells ($p = 0.0002$), shown in Figure 5.12(B). There was no difference in OS when patients with raised $CD56^{dim}CD16^{bri}$ NK cells were compared to those with $CD56^{dim}CD16^{bri}$ NK cells below the median value (Figure 5.12 (C); $p = 0.0803$). There was also no difference in OS between increased and decreased proportions of $CD56^{bri}D16^{bri}$ NK cells (Figure 5.12(D); $p = 8809$).

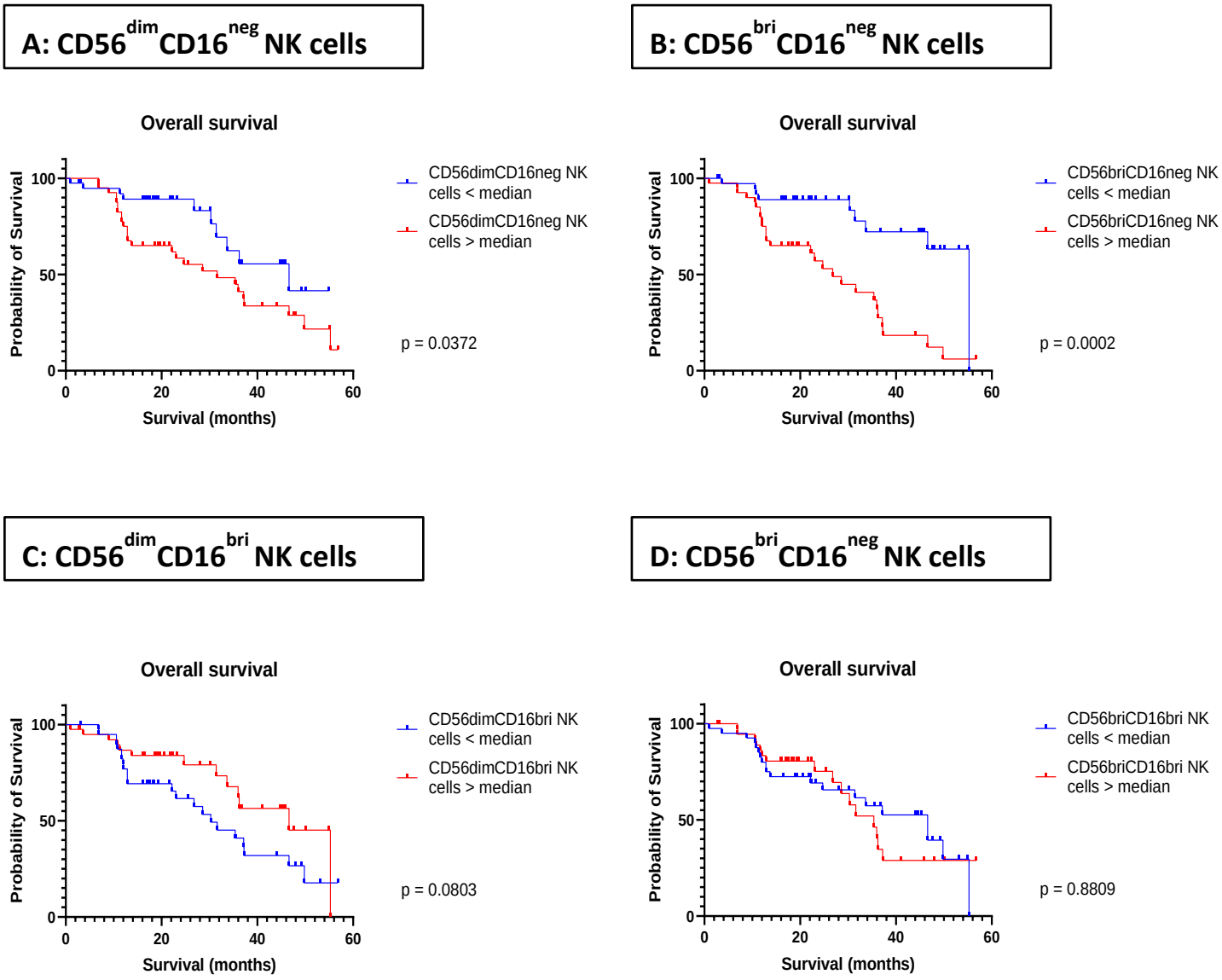


Figure 5.12: The overall survival of OC patients based on the proportion of NK cell subpopulations within peripheral blood samples.

OS was reduced in patients who had an increased proportion of $CD56^{dim}CD16^{neg}$ NK cells (A) and increased $CD56^{bri}CD16^{neg}$ NK cells (B) in PBMC samples. There was no significant difference in OS when proportions of $CD56^{dim}CD16^{bri}$ NK cells (C) and $CD56^{bri}CD16^{bri}$ NK cells (D) in peripheral blood samples were above or below the median.

5.5.1.5 Disease recurrence based on NK cell receptors

Phenotypic analysis of NK cells in both the ovarian and omental tumour revealed a significant reduction in the expression of activation receptors NKp46, DNAM-1 and CD57, along with increased expression of the inhibitory checkpoint PD-1 receptor. Following on from this, these NK cell receptors were interrogated to determine whether their expression patterns on peripheral, ovarian and omental NK cells correlate with disease recurrence. Using flow cytometry, tumour samples were divided into those with low expression of each receptor below the median value, and those with high expression above the median value. The incidence of disease recurrence associated with high and low receptor expression is detailed in Table 5.9. Of the 80 PBMC samples from OC patients, the incidence of disease recurrence was 57.5% in the samples with low NKp46 expression, compared to a recurrence rate of 32.5% when NK cells had high NKp46 expression ($p = 0.0246$). There was no difference in the incidence of disease recurrence between high and low DNAM-1, CD57 or PD-1 expressing NK cells.

Of the 49 ovarian tumour tissue samples available for analysis, there were 18 patients who developed disease recurrences (36.7%) within the study period. The incidence of recurrence was significantly higher in NK cells expressing PD-1 receptors above the median level (n=13/24, 54.2%) when compared to the low expressers (n=5/25, 20.0%, p=0.0066). There was no difference in recurrence rates between high and low expressers for DNAM-1, NKp46 or CD57 receptors in the ovarian tumour infiltrating NK cells.

Of the 39 omental tumour tissue samples available, there were 12 patients who developed disease recurrences (30.8%). The proportion of patients with recurrent disease was significantly greater in patients with NK cells showing NKp46 and CD57 expression above

the median value: 47.4% vs 15.0% for NKp46 (p = 0.0286) and 52.6% vs 10.0% for CD57 (p = 0.0039). The level of DNAM-1 and PD-1 expression did not influence the recurrence rate.

Table 5.9: Proportion of women with disease recurrence based on low and high expression of NK receptors

NK cell receptor	Disease recurrence with NK receptor expression <u>below</u> median	Disease recurrence with NK receptor expression <u>above</u> median	P Value
Peripheral NK cells (n=80)	**n (%)**	**n (%)**	
DNAM-1	16 (40.0)	20 (50.0)	0.3687
NKp46	23 (57.5)	13 (32.5)	**0.0246**
CD57	21 (52.5)	15 (37.5)	0.1755
PD-1	19 (47.5)	17 (42.5)	0.6531
Ovarian NK cells (n=49):	**n (%)**	**n (%)**	
DNAM-1	10 (40.0)	8 (33.3)	0.6284
NKp46	10 (40.0)	8 (33.3)	0.6284
CD57	11 (44.0)	7 (29.2)	0.3913
PD-1	5 (20.0)	13 (54.2%)	**0.0066**
Omental NK cells (n=39):	**n (%)**	**n (%)**	
DNAM-1	7 (35.0)	5 (26.3)	0.5570
NKp46	3 (15.0)	9 (47.4)	**0.0286**
CD57	2 (10.0)	10 (52.6)	**0.0039**
PD-1	5 (25.0)	7 (36.8)	0.4232

The expression of these receptors in NK cells from PBMC samples was then correlated to PFS. Peripheral NK cells with NKp46 expression below the median level was associated with a reduced PFS (p = 0.0386) when compared to those with expression above the median level (Figure 5.13). Similarly, PBMC NK cells with CD57 expression below the median value correlated with decreased PFS (p = 0.0324) when compared to NK cells with expression above the median value (Figure 5.14). The expression of DNAM-1 and PD-1 in PBMC NK cells did not influence PFS (Figures 5.15 and 5.16).

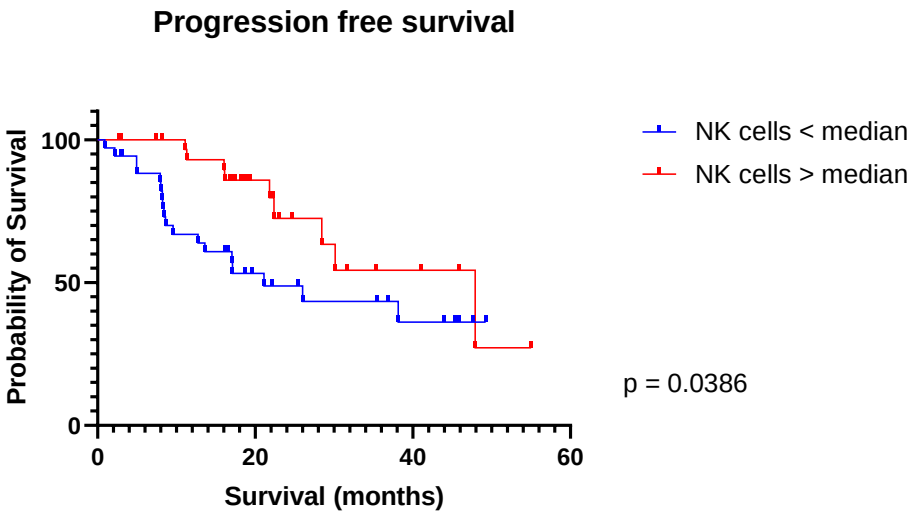


Figure 5.13: The progression free survival of OC patients based on peripheral NK cell expression of activation receptor NKp46.
There was a reduction in PFS when expression of NKp46 was below the median value on PBMC NK cells (p = 0.0386).

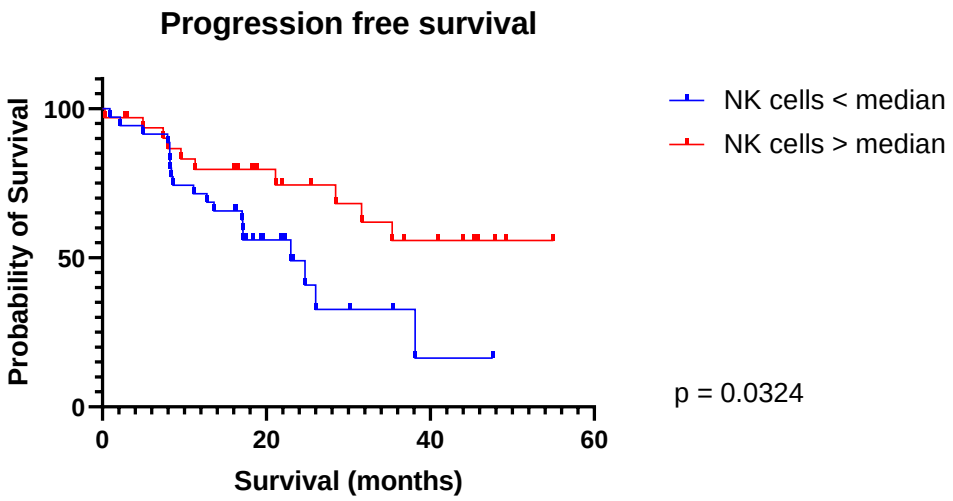


Figure 5.14: The progression free survival of OC patients based on peripheral NK cell expression of activation receptor CD57.

There was a reduction in PFS when expression of CD57 was below the median value on PBMC NK cells (p = 0.0324).

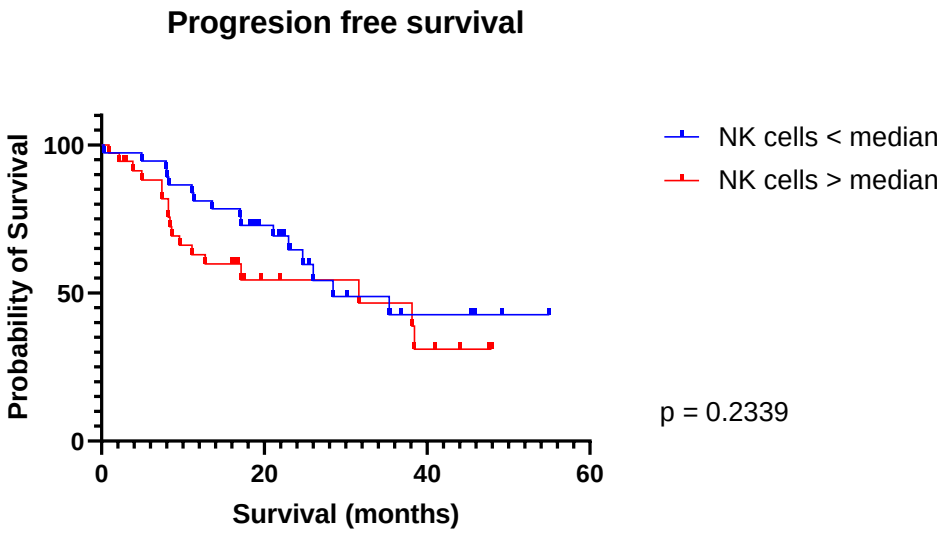


Figure 5.15: The progression free survival of OC patients based on peripheral NK cell expression of activation receptor DNAM-1.

There was no difference in PFS between patients who had PBMC NK expression of DNAM-1 above the median compared to expression below the median value (p = 0.2339).

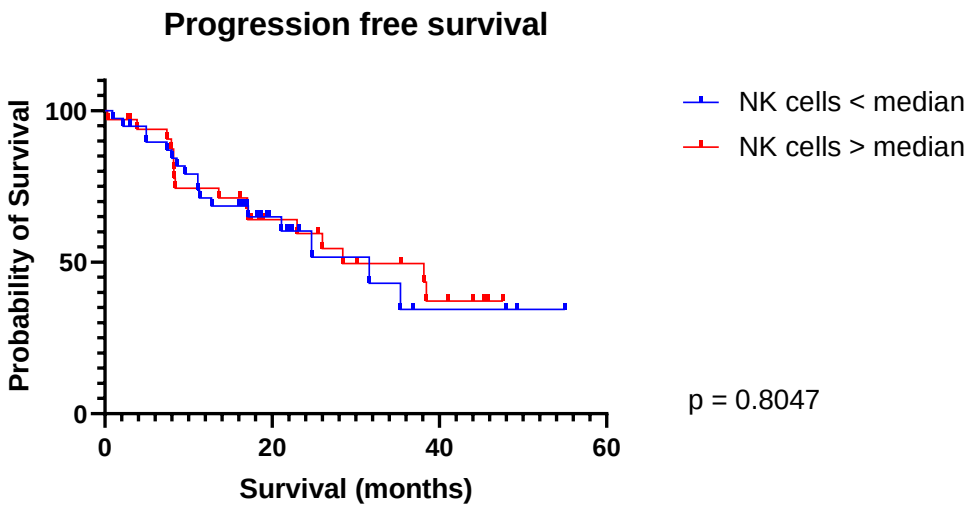


Figure 5.16: The progression free survival of OC patients based on peripheral NK cell expression of inhibiting receptor PD-1.
There was no difference in PFS between patients who had PBMC NK expression of PD-1 above the median compared to expression below the median value (p = 0.8047).

PFS was then correlated to the expression of the receptors in NK cells within ovarian tumour samples. There was no difference in PFS between patients who had expression of NKp46, DNAM-1, CD57 and PD-1 in ovarian NK cells above the median values compared to expression below the median (Figures 5.17, 5.18, 5.19 and 5.20, respectively). Likewise, there was no difference in PFS when receptor expression above the median values was compared to expression below the median in NK cells within omental tumour tissue (Figures 5.21, 5.22, 5.23 and 5.24).

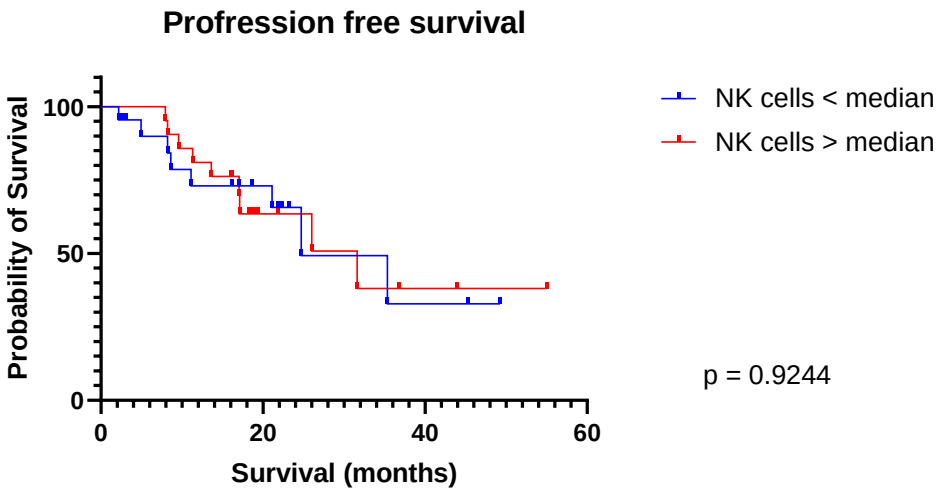


Figure 5.17: The progression free survival of OC patients based on ovarian NK cell expression of activation receptor NKp46.

There was no difference in PFS between patients who had ovarian NK expression of NKp46 above the median compared to expression on ovarian NK cells below the median value (p = 0.9244).

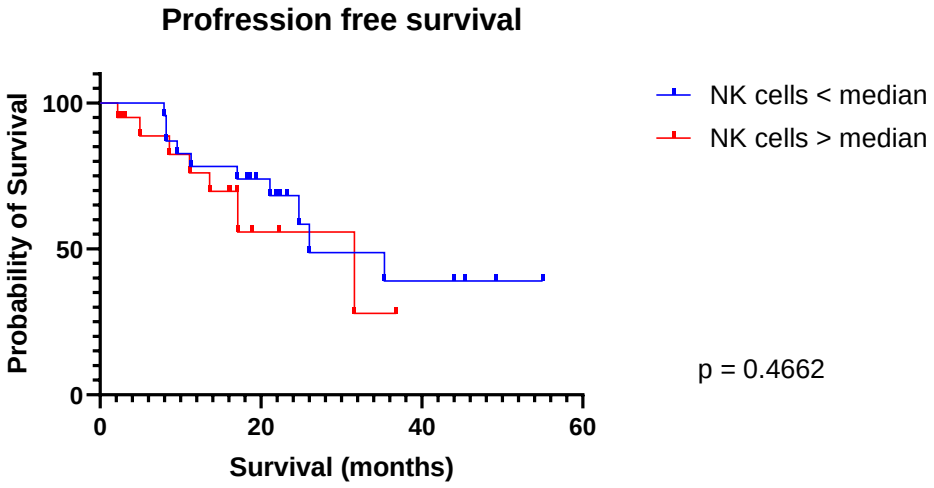


Figure 5.18: The progression free survival of OC patients based on ovarian NK cell expression of activation receptor DNAM-1.

There was no difference in PFS between patients who had ovarian NK expression of DNAM-1 above the median compared to expression on ovarian NK cells below the median value (p = 0.4662).

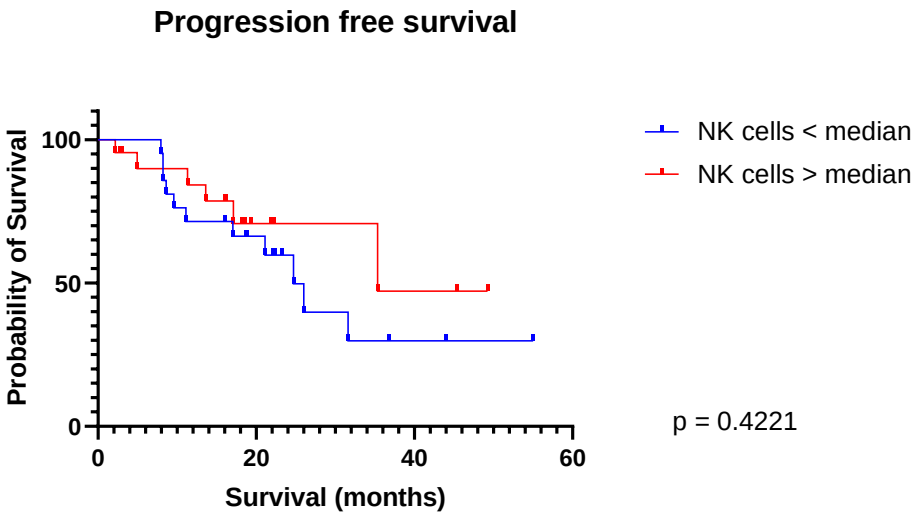


Figure 5.19: The progression free survival of OC patients based on ovarian NK cell expression of activation receptor CD57.

There was no difference in PFS between patients who had ovarian NK expression of CD57 above the median compared to expression on ovarian NK cells below the median value (p = 0.4221).

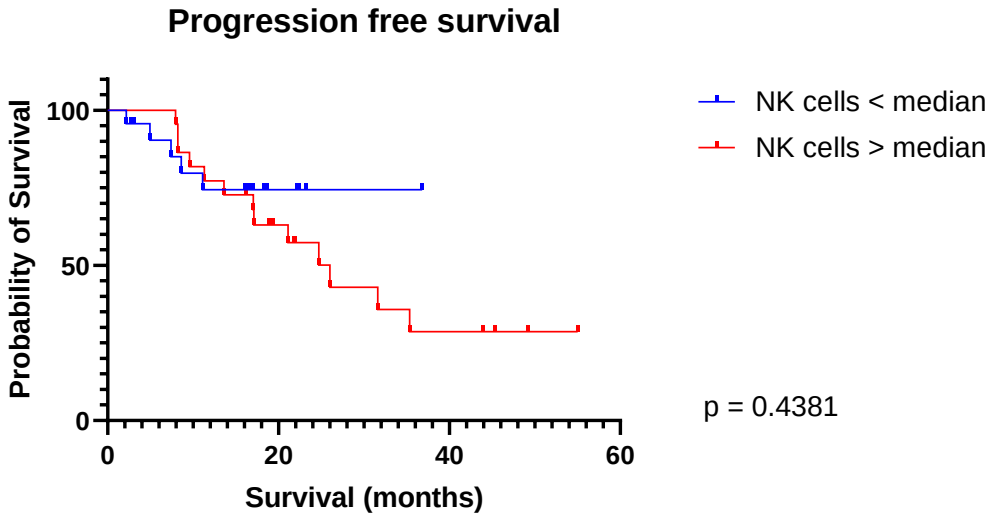


Figure 5.20: The progression free survival of OC patients based on ovarian NK cell expression of inhibiting receptor PD-1.

There was no difference in PFS between patients who had ovarian NK expression of PD-1 above the median compared to expression on ovarian NK cells below the median value (p = 0.4381).

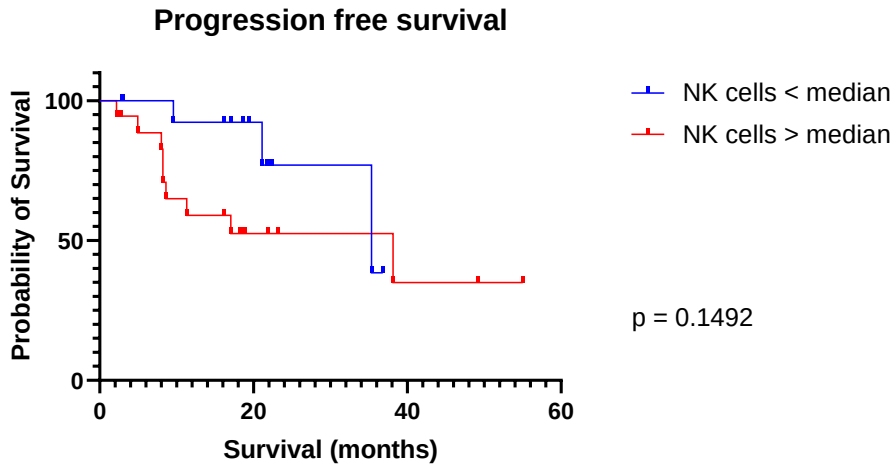


Figure 5.21: The progression free survival of OC patients based on omental NK cell expression of activation receptor NKp46.

There was no difference in PFS between patients who had omental NK expression of NKp46 above the median compared to expression on omental NK cells below the median value (p = 0.1492).

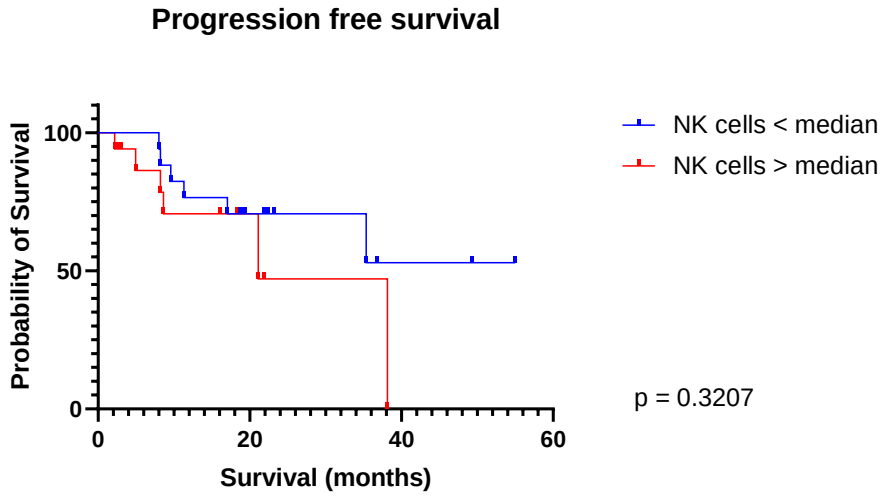


Figure 5.22: The progression free survival of OC patients based on omental NK cell expression of activation receptor DNAM-1.

There was no difference in PFS between patients who had omental NK expression of DNAM-1 above the median compared to expression on omental NK cells below the median value (p = 0.3207).

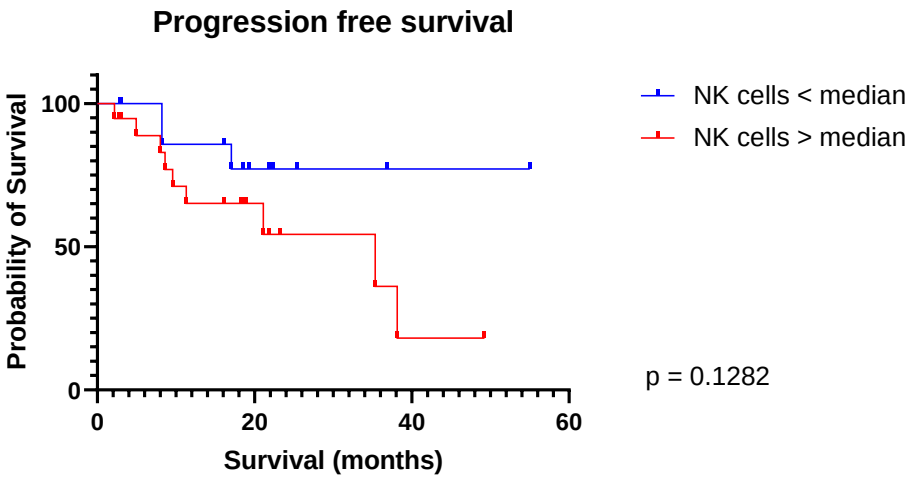


Figure 5.23: The progression free survival of OC patients based on omental NK cell expression of activation receptor CD57.

There was no difference in PFS between patients who had omental NK expression of CD57 above the median compared to expression on omental NK cells below the median value (p = 0.1282).

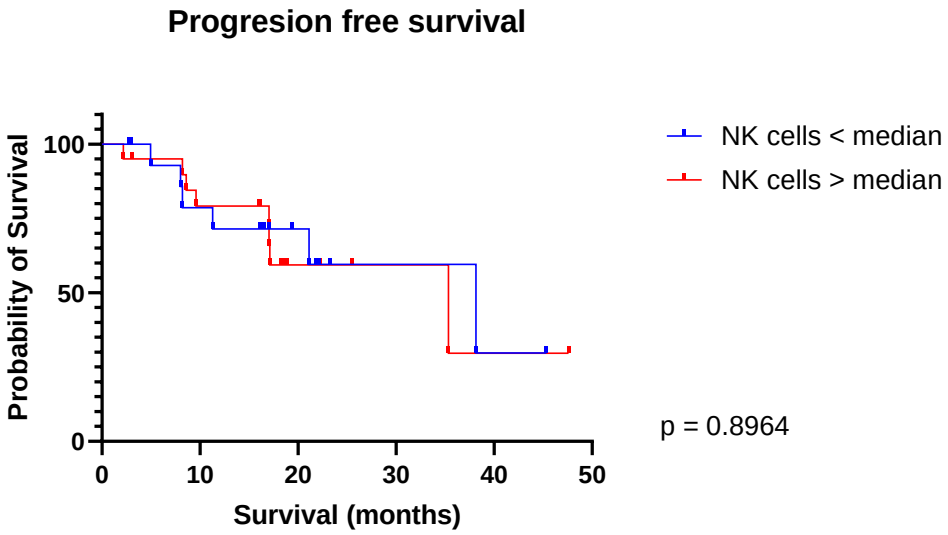


Figure 5.24: The progression free survival of OC patients based on omental NK cell expression of inhibiting receptor PD-1.

There was no difference in PFS between patients who had omental NK expression of PD-1 above the median compared to expression on omental NK cells below the median value (p = 0.8964).

5.5.1.6 Patient survival based on NK cell receptors

The same NK cell receptors were examined to determine whether their expression on peripheral, ovarian and omental NK cells were associated with disease-specific death and overall survival (OS). With samples again separated into those with receptor expression below the median value and expression above the median value, the proportion of patients who died in each group was established, as shown in Table 5.10.

Of the 80 PBMC samples available from patients with OC, disease-specific death was not related to the expression level of NKp46, DNAM-1, CD57 or PD-1 receptors in NK cells. Similarly, NK cells receptor expression was not associated with death from OC in the 49 patients where ovarian tumour tissue samples were available for analysis. However, in 39 patients with omental tumour tissue available for analysis, disease-specific death was significantly higher in those patients with NK cells showing CD57 expression above the median ($p=0.0286$). Death was not associated with the level of NKp46, DNAM-1 or PD-1 expression in the NK cells which infiltrated the omental tumour.

Table 5.10: Mortality from OC with low and high expression of NK receptors

NK cell receptor	Women who died with NK receptor expression <u>below</u> median	Women who died with NK receptor expression <u>above</u> median	P Value
Peripheral NK cells (n=80)	**n (%)**	**n (%)**	
DNAM-1	15 (37.5)	21 (52.5)	0.1775
NKp46	20 (50.0)	16 (40.0)	0.3687
CD57	21 (52.5)	15 (37.5)	0.1755
PD-1	17 (42.5)	19 (47.5)	0.6531
Ovarian NK cell (n=49):	**n (%)**	**n (%)**	
DNAM-1	11 (45.8)	9 (37.5)	0.6435
NKp46	11 (40.0)	9 (33.3)	0.6435
CD57	12 (48.0)	8 (33.3)	0.2964
PD-1	7 (28.0)	13 (54.2%)	0.0625
Omental NK receptor (n=39):	**n (%)**	**n (%)**	
DNAM-1	5 (25.0)	7 (36.8)	0.4232
NKp46	4 (20.0)	8 (42.1)	0.1349
CD57	3 (15.0)	9 (47.4)	**0.0286**
PD-1	5 (25.0)	7 (36.8)	0.4232

The expression of the receptors in NK cells from PBMC samples was then correlated to OS. Peripheral NK cells with DNAM-1 expression above the median value was associated with decreased OS (p = 0.0455) when compared to those with expression below the median level (Figure 5.25). The expression of NKp46, CD57 and PD-1 in PBMC NK cells did not influence OS (Figures 5.26, 5.27 and 5.28).

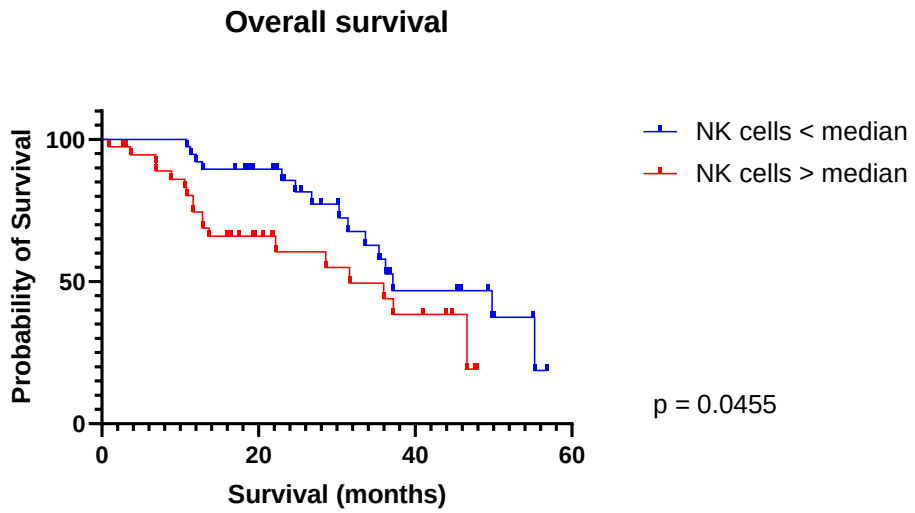


Figure 5.25: The overall survival of OC patients based on peripheral NK cell expression of activation receptor DNAM-1.
There was a reduction in OS when expression of DNAM-1 was above the median value on PBMC NK cells (p = 0.0455).

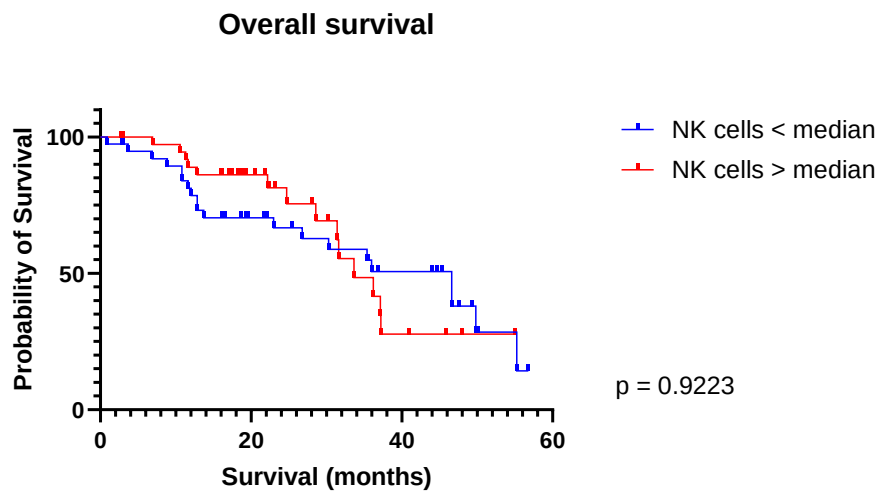


Figure 5.26: The overall survival of OC patients based on peripheral NK cell expression of activation receptor NKp46.

There was no difference in OS between patients who had PBMC NK expression of NKp46 above the median compared to expression below the median value (p = 0.9223).

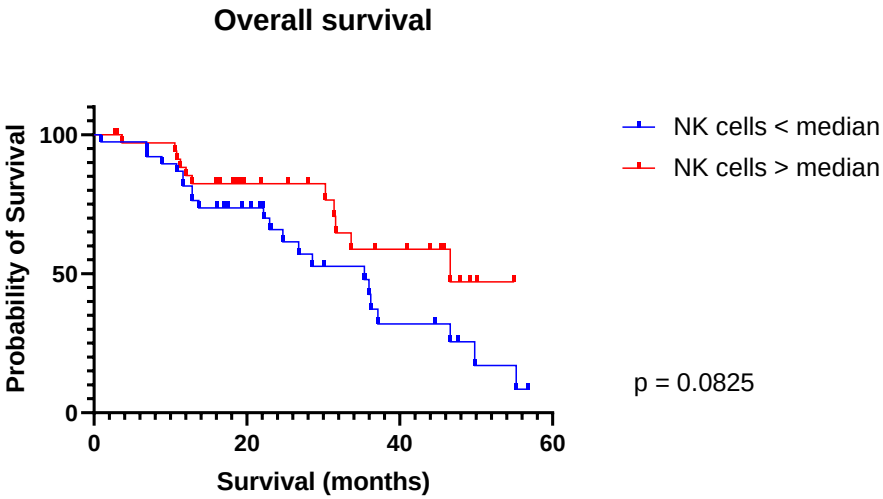


Figure 5.27: The overall survival of OC patients based on peripheral NK cell expression of activation receptor CD57.

There was no difference in OS between patients who had PBMC NK expression of CD57 above the median compared to expression below the median value (p = 0.0825).

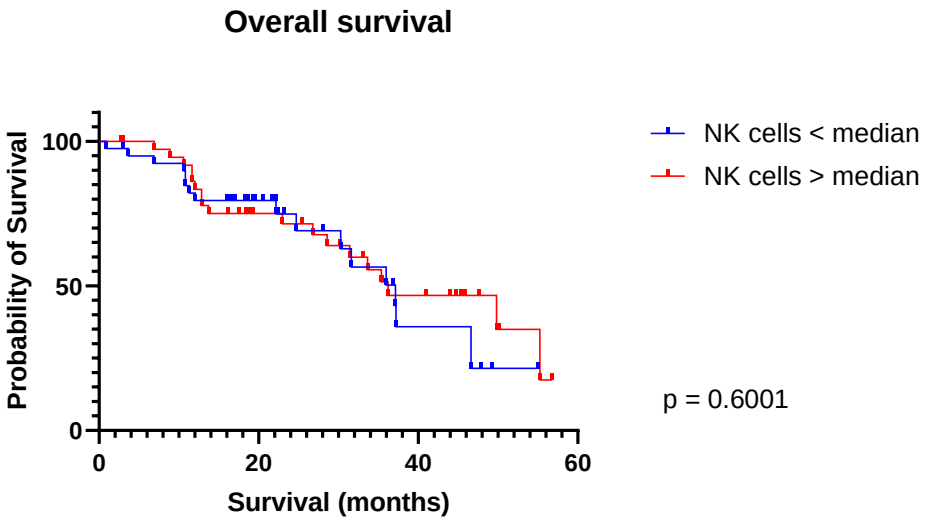


Figure 5.28: The overall survival of OC patients based on peripheral NK cell expression of inhibiting receptor PD-1.
There was no difference in OS between patients who had PBMC NK expression of PD-1 above the median compared to expression below the median value (p = 0.6001).

OS was then correlated to the expression of receptors in NK cells within ovarian tumour samples. Figure 5.29 shows that OS was reduced when DNAM-1 expression on the ovarian NK cells was above the median (p = 0.0315). There was no difference in OS when expression of NKp46, CD57 and PD-1 was above the median on ovarian NK cells compared to expression below the median (Figures 5.30, 5.31 and 5.32). Upon review of OS and the expression of receptors in NK cells within omental tissue, DNAM-1 expression above the median was also associated with a poorer OS (p = 0.0234), shown in Figure 5.33. Again, there was no correlation between OS and the expression of receptors in omental NK cells (Figures 5.34, 5.35 and 5.36).

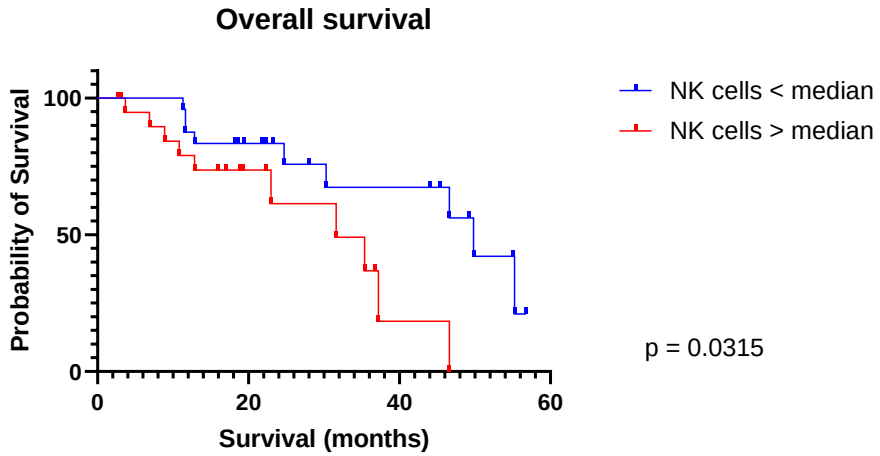


Figure 5.29: The overall survival of OC patients based on ovarian NK cell expression of activation receptor DNAM-1.

There was a reduction in OS when expression of DNAM-1 was above the median value on ovarian NK cells (p = 0.0315).

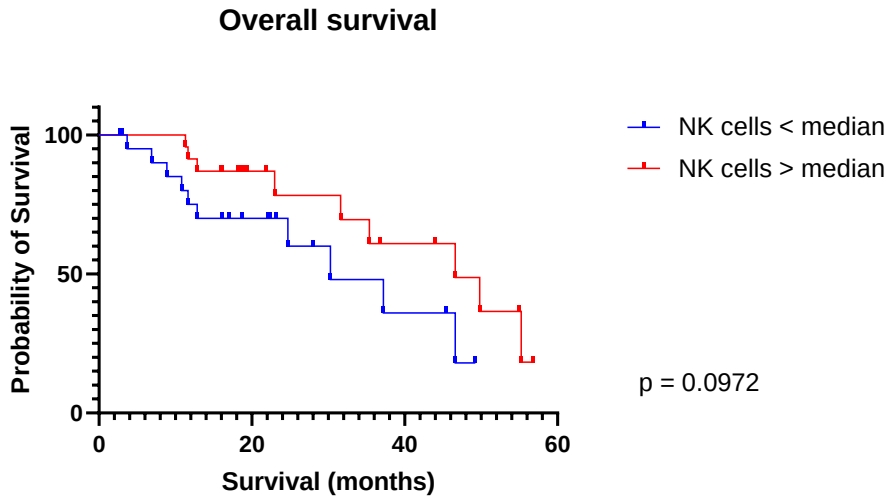


Figure 5.30: The overall survival of OC patients based on ovarian NK cell expression of activation receptor NKp46.

There was no difference in OS between patients who had ovarian NK expression of NKp46 above the median compared to expression below the median value (p = 0.0972).

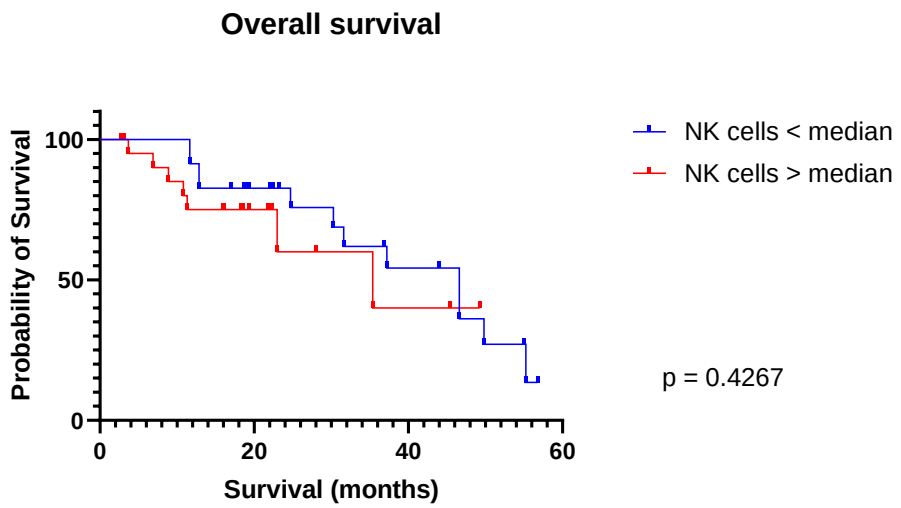


Figure 5.31: The overall survival of OC patients based on ovarian NK cell expression of activation receptor CD57.

There was no difference in OS between patients who had ovarian NK expression of CD57 above the median compared to expression below the median value (p = 0.4267).

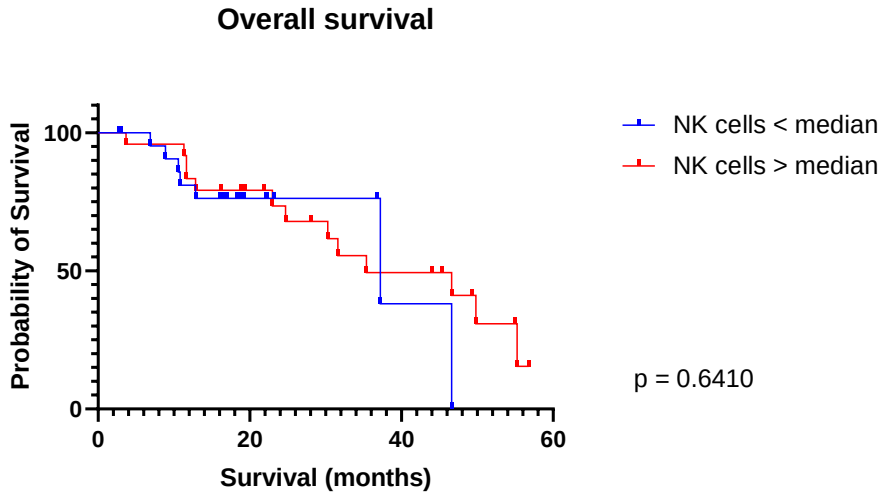


Figure 5.32: The overall survival of OC patients based on ovarian NK cell expression of inhibiting receptor PD-1.

There was no difference in OS between patients who had ovarian NK expression of PD-1 above the median compared to expression below the median value (p = 0.6410).

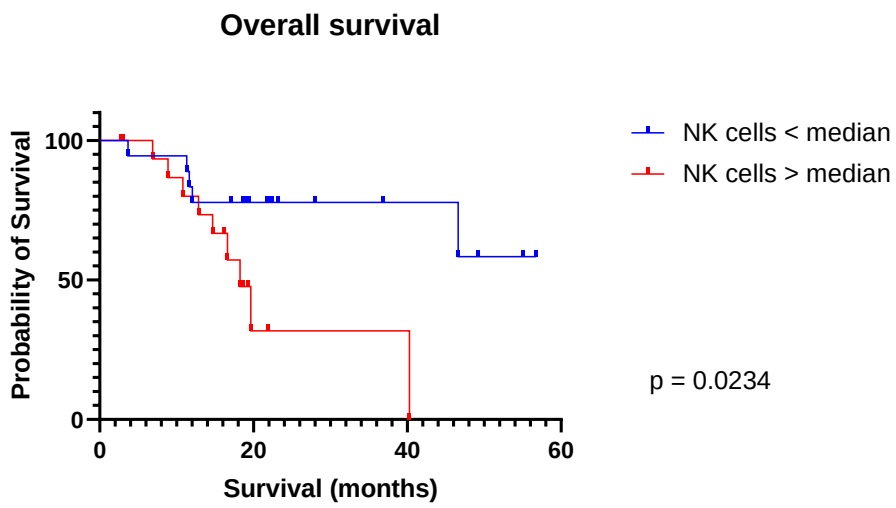


Figure 5.33: The overall survival of OC patients based on omental NK cell expression of activation receptor DNAM-1.

There was a reduction in OS when expression of DNAM-1 was above the median value on omental NK cells (p = 0.0234).

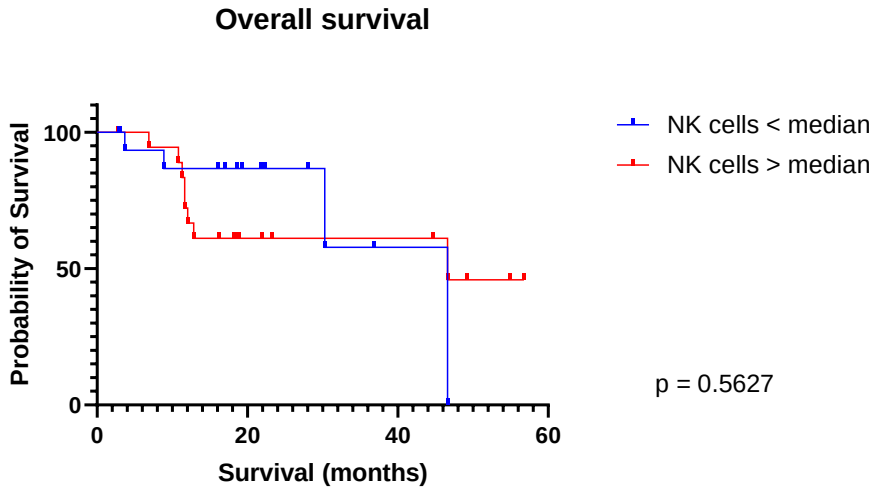


Figure 5.34: The overall survival of OC patients based on omental NK cell expression of activation receptor NKp46.

There was no difference in OS between patients who had omental NK expression of NKp46 above the median compared to expression below the median value (p = 0.5627).

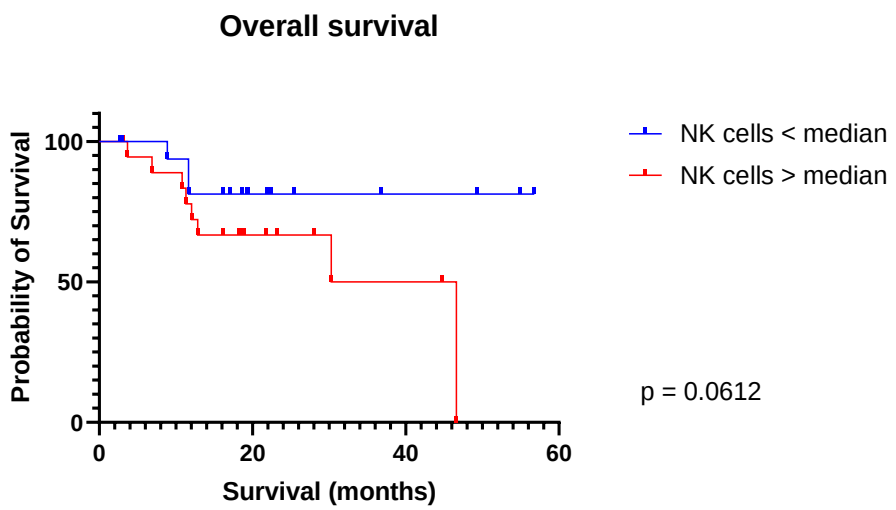


Figure 5.35: The overall survival of OC patients based on omental NK cell expression of activation receptor CD57.

There was no difference in OS between patients who had omental NK expression of CD57 above the median compared to expression below the median value (p = 0.0612).

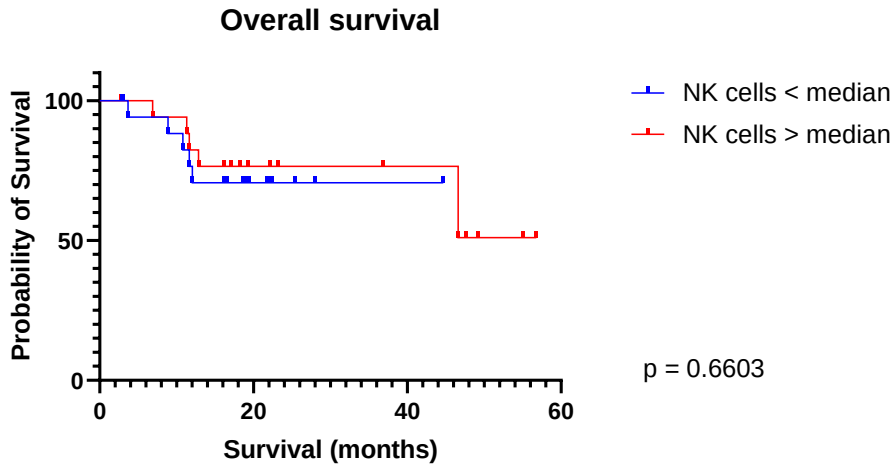


Figure 5.36: The overall survival of OC patients based on omental NK cell expression of inhibiting receptor PD-1.

There was no difference in OS between patients who had omental NK expression of PD-1 above the median compared to expression below the median value (p = 0.6603).

5.5.2 Disease severity and NK cell phenotype

5.5.2.1 NK cells and disease stage

To establish whether the severity of OC corresponds with the NK cell phenotype, the stage of disease was compared to the proportion and type of NK cells. The mean proportions of PBMC NK cells were similar in early stage OC (FIGO stages I and II) and advanced disease (FIGO stages III and IV). However, the proportion of NK cells within ovarian tumours and omental tumours were significantly lower in cases of advanced OC than in early disease ($p = 0.0236$). Figure 5.37 shows the mean proportion of NK cells within peripheral blood, ovarian tumour and omental tumour for each disease stage. Based on CD16 and CD56 expression, there was no difference in the type of PBMC NK cells between the four OC stages (Figure 5.38).

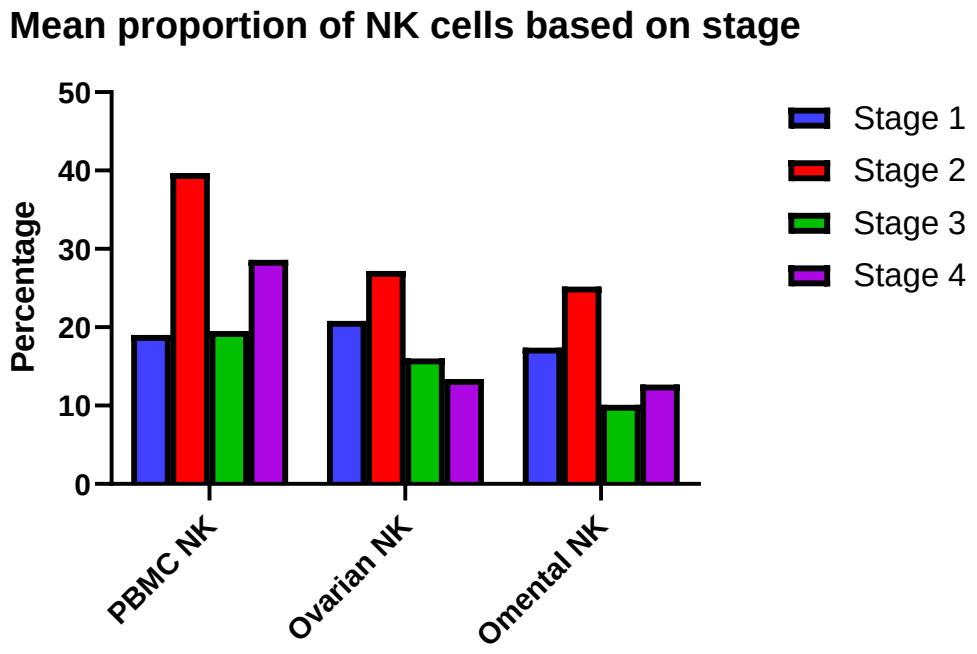


Figure 5.37: The mean proportion of NK cells in peripheral blood, ovarian tumour and omental tumour depending on disease stage.
Patients with advanced OC (stage III or IV) had lower proportions of ovarian tumour and omental tumour NK cells compared to early disease.

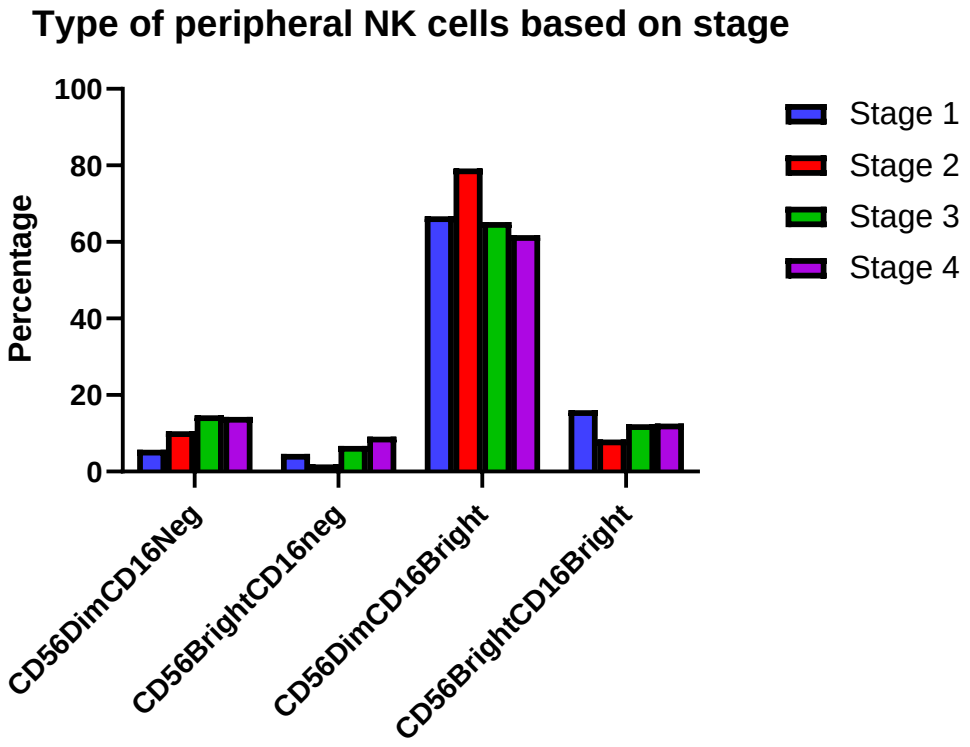


Figure 5.38: The proportion of each NK cell subtype within the peripheral blood depending on disease stage.
There were no differences in the type of PBMC NK cells across the different disease stages.

5.5.2.2 NK cells and tumour burden

To review the severity of disease and NK cell phenotype, the tumour burden, or peritoneal cancer index (PCI), was evaluated. With PCI data available for 67 patients, 27 had a low PCI ≤ 10, while 40 patients had a PCI >10, indicating a higher disease burden. There was no difference in the proportion of NK cells between the low and high PCI groups. This was true for the NK cells in PBMC, ovarian tumour and omental tumour samples. Figure 5.39 shows that disease burden did not influence the proportion of NK cells in peripheral blood and tumour biopsies.

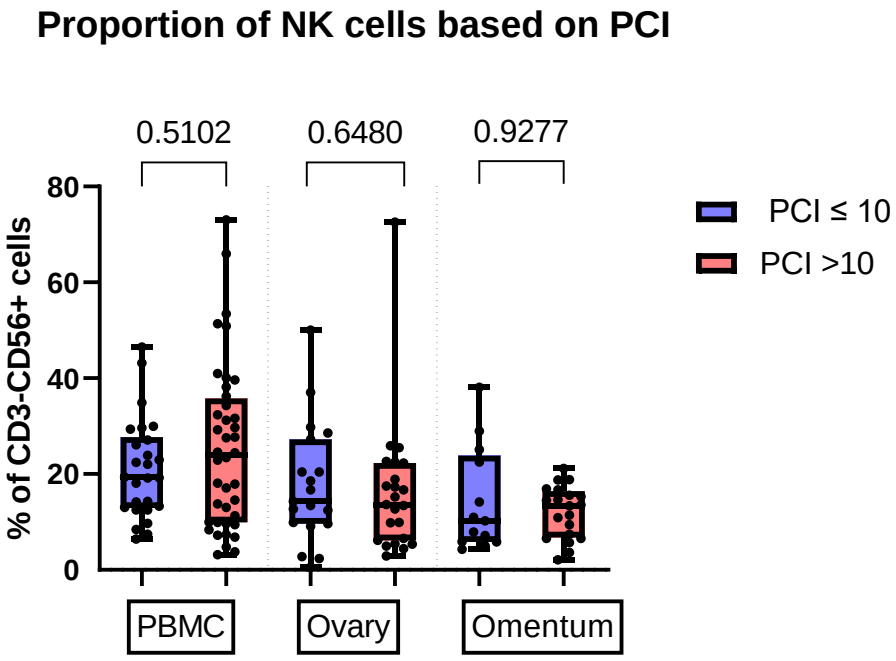


Figure 5.39: The proportion of NK cells within the peripheral blood, ovarian tumour and omental tumour depending on PCI value.
There were no differences in the proportion of NK cells between the low PCI and high PCI groups.

Examination of NK activation receptors and PCI (Figure 5.40) showed that patients with a greater tumour burden (high PCI), had an increased proportion of ovarian and omental tumour NK cells with overexpression of activation receptors NKp46 and NKG2D compared to patients with low PCI. Those patients in the high PCI group also had a greater proportion of PBMC NK cells with increased DNAM-1 expression. In contrast, there were fewer PBMC and ovarian NK cells with high CD57 expression in the high PCI group compared to the low PCI group.

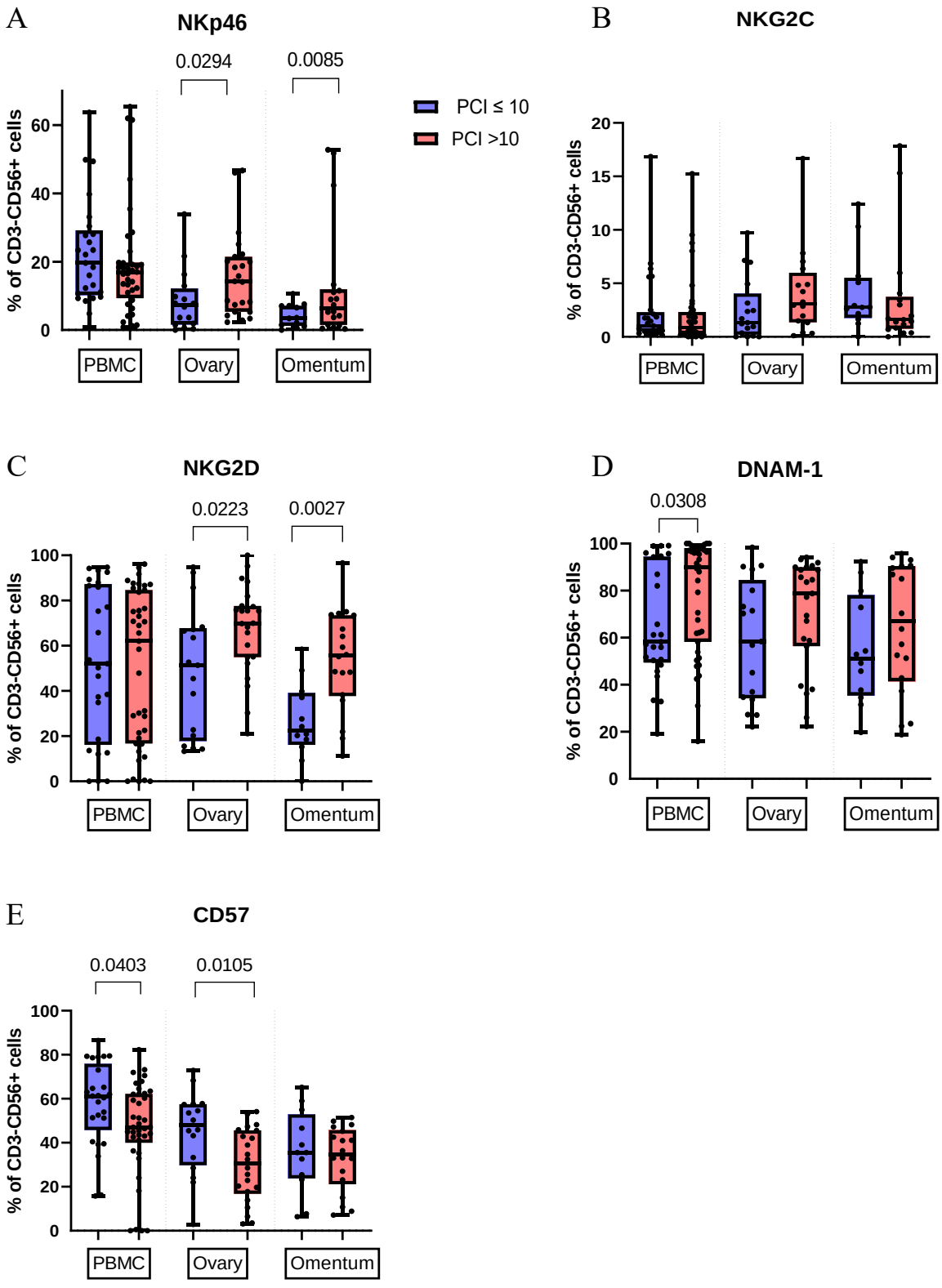


Figure 5.40: The proportion of NK cells with high expression of activation receptors based on PCI. Patients with high PCI had a greater proportion of ovarian and omental tumour NK cells with overexpression of NKp46 (A) and NKG2D (C) compared to patients with low PCI. Those in the high PCI group also had increased PBMC NK cells with upregulation of DNAM-1 (D). There were fewer PBMC and ovarian NK cells with high CD57 expression in the high PCI group (E).

Next, correlation was made between the level of expression of inhibitory receptors and PCI value. There was no difference in the proportion of NK cells with high receptor expression between the low PCI and high PCI groups (Figure 5.41).

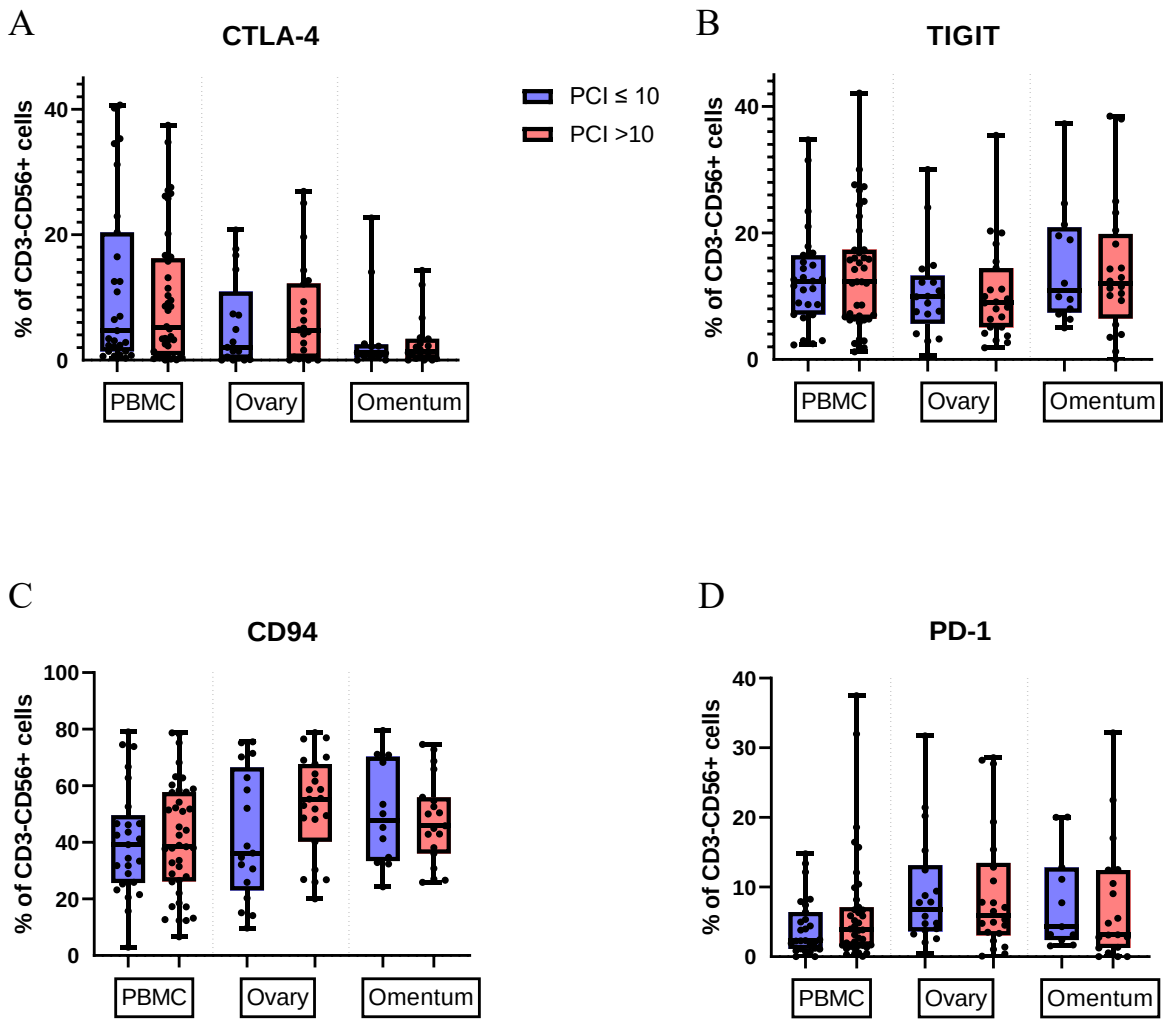


Figure 5.41: The proportion of NK cells with high expression of inhibitory receptors based on PCI value.
There were no differences in the proportion of NK cells with high expression of inhibitory receptors CTLA-4 (A), TIGIT (B), CD94 (C), and PD-1 (D) between the low PCI and high PCI groups.

5.5.3 NK cells and chemotherapy response

The NK cell proportion was then correlated to the chemotherapy response score (CRS) in patients who underwent neoadjuvant chemotherapy. Within this group of patients, there were 20.0% (n=8) who showed an excellent chemotherapy response (CRS 3), 35.0% (n=14) had a partial response to chemotherapy (CRS 2) and 42.5% (n=17) had no response to chemotherapy (CRS 1). Figure 5.42 shows that the proportion of PBMC NK cells were similar despite the differing CRS results. The proportion of ovarian NK cells and omental tumour NK cells were also not altered by the response to chemotherapy. When focusing solely on the samples with CRS 2, there were fewer NK cells in tumour tissues than in the peripheral blood, but there were no other differences between the proportion of NK cells based on the CRS results.

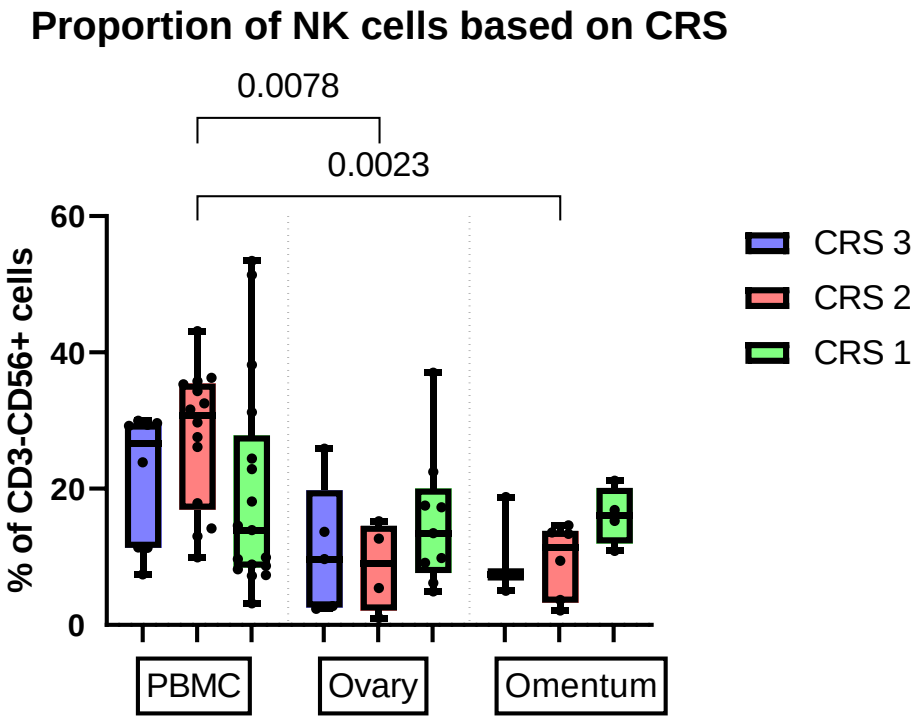


Figure 5.42: The proportion of NK cells in peripheral blood and tumour tissue based on CRS. Ovarian and omental tumour samples with CRS 2 had fewer NK cells than their corresponding PBMC samples (p = 0.0078 and p = 0.0023, respectively).

The amount of NK cells with high expression of the activation and inhibitory receptors (based on the CRS result) were then determined. Focusing on the activation receptors, Figure 5.43 shows the correlation of NKG2C and NKG2D with the chemotherapy response. There are fewer NKG2C positive NK cells in the PBMC and omentum samples from patients who generated a better response to chemotherapy, particularly the patients with complete response (CRS 3) compared to patients with CRS 2 (Figure 5.43 B). There were more NKG2D positive NK cells in the PBMC samples of those patients who generated a better response to chemotherapy, specifically the patients with CRS 3 compared to those with CRS 1 (Figure 5.43 C). When interrogating the inhibitory receptors (Figure 5.44), the amount of NK cells with high expression of CD94 was less frequent in the ovarian samples of patients who responded well to chemotherapy (CRS 3) compared to the ovarian samples of patients who did not respond (CRS 1). There were no other differences in activation or inhibitory receptor expression based on chemotherapy response.

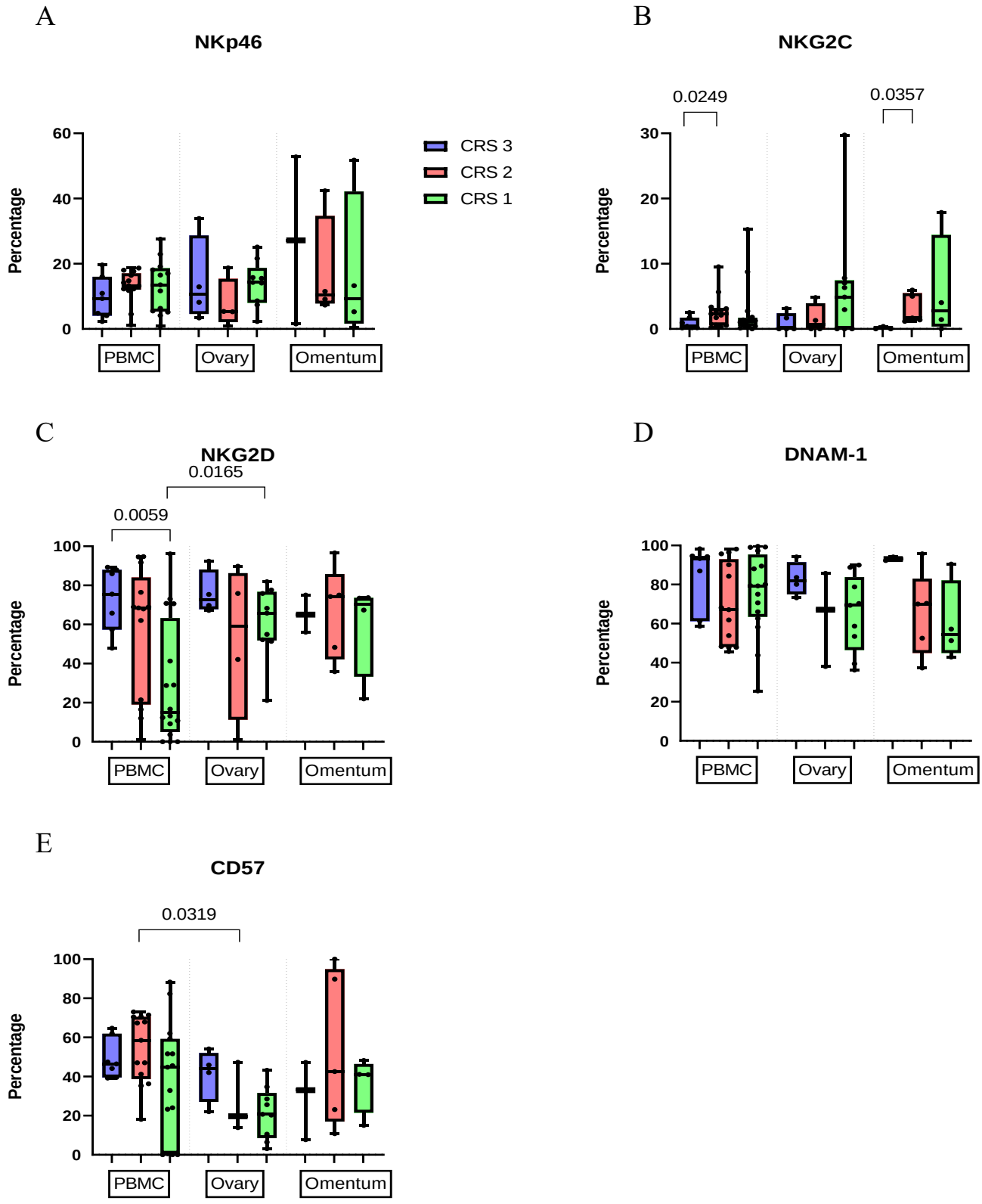


Figure 5.43: The proportion of NK cells with high expression of activation receptors based on CRS. NK cells with upregulation of A) NKp46, B) NKG2C, C) NKG2D, D) DNAM-1, and E) CD57 in the peripheral blood, ovarian tumour and omental tumour depending on CRS.

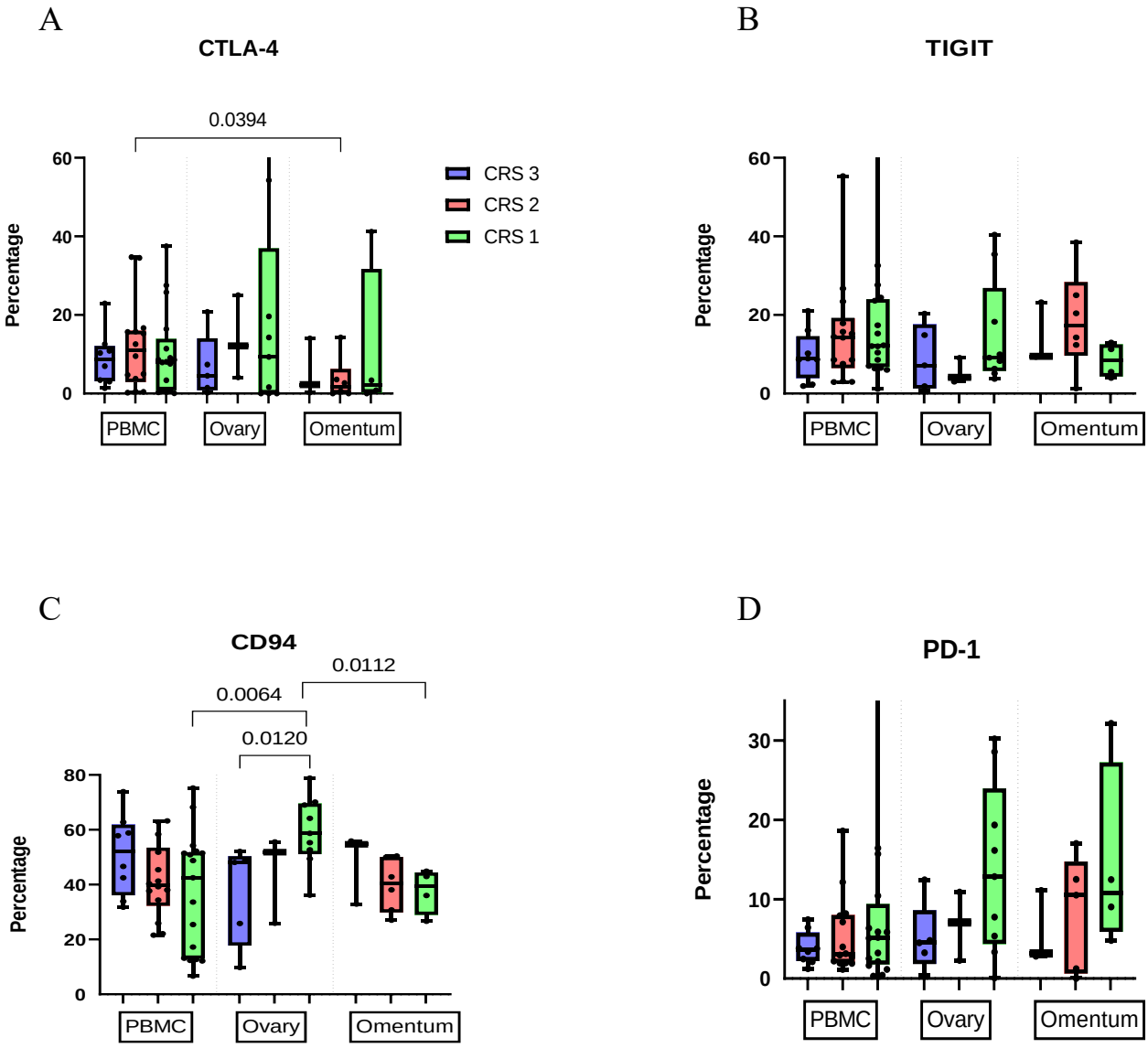


Figure 5.44: The proportion of NK cells with high expression of inhibitory receptors based on CRS. NK cells with upregulation of A) CTLA-4, B) TIGIT, C) CD94 and, D) PD-1 in the peripheral blood, ovarian tumour and omental tumour depending on CRS.

5.5.4 DNAM-1 expression and patient outcomes

Following on from earlier observations that the overall survival of OC patients is significantly reduced when the activation receptor DNAM-1 is over expressed in peripheral blood, ovarian tumour and omental tumour NK cells (section 5.5.1.6), DNAM-1 expression was further interrogated to assess its association with clinical outcomes.

5.5.4.1 DNAM-1 expression and disease stage

The expression of DNAM-1 on NK cells was correlated to disease stage, showing that the proportion of NK cells with high DNAM-1 expression were more likely in advanced disease (stages III and IV) when compared to those in stages I and II disease. Indeed, there is significantly greater DNAM-1 expression on PBMC NK cells in both stage III and IV disease when compared to early staged disease (Figure 5.45). Although DNAM-1 expression was raised in both the ovarian and omental tumour NK cells in stage III and IV disease when compared to those with early stage disease, the difference was only significant in the omentum of patients with stage IV disease.

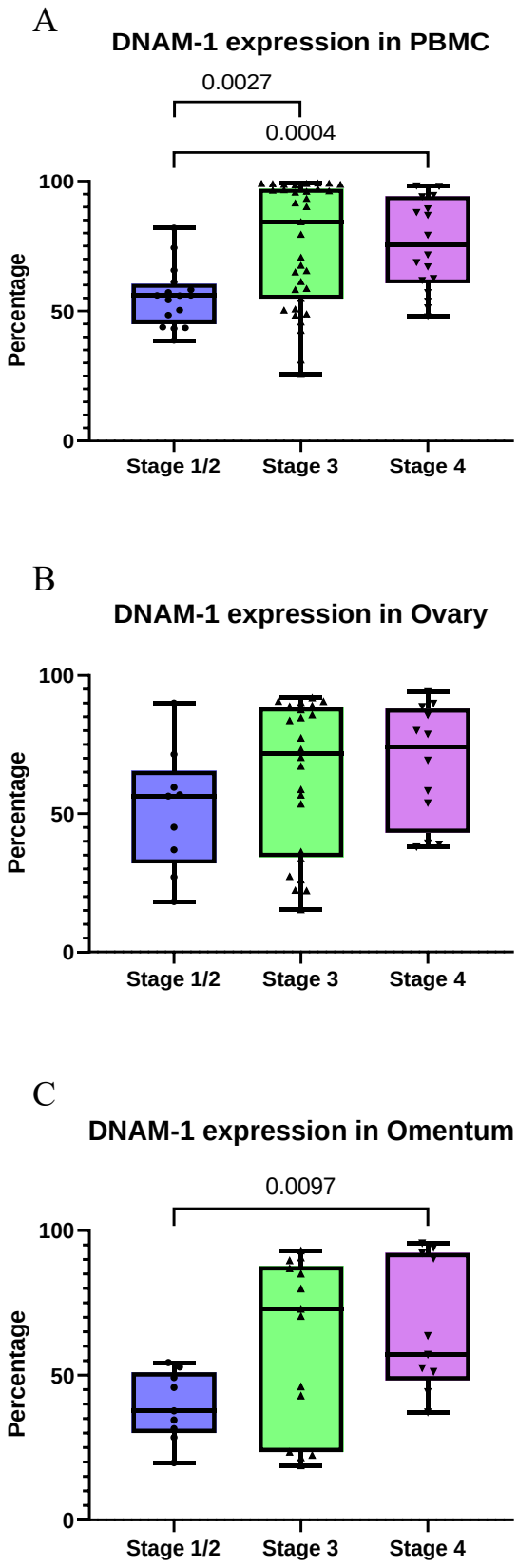
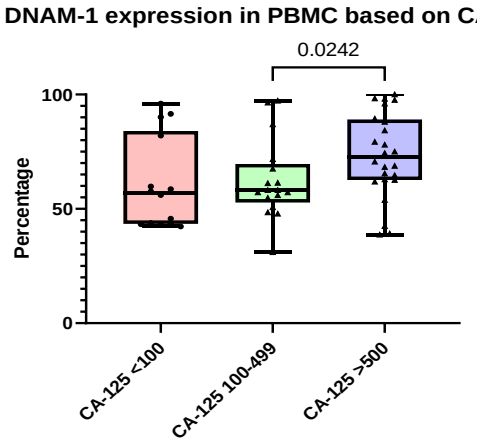


Figure 5.45: NK cells with high expression of DNAM-1 based on disease stage.
NK cells within A) PBMC, B) ovarian tumour, and C) omental tumour have increased DNAM-1 expression in advanced stage III and IV disease.

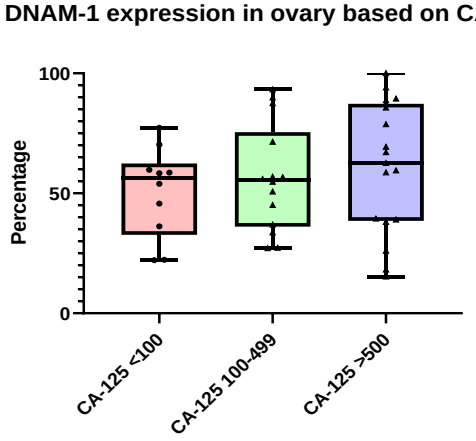
5.5.4.2 DNAM-1 expression and CA-125 level

Further analysis was undertaken to correlate DNAM-1 expression with the level of serum CA-125, the tumour marker which is usually raised in OC. The CA-125 values at the time of surgery within this OC cohort ranged from 17 to 4297 U/ml (mean value of 1049 U/ml) and were categorised into three groups: <100 U/ml, 100 – 499 U/ml and ≥500 U/ml. The expression of DNAM-1 was correlated to the CA-125 level by examining the amount of NK cells over expressing DNAM-1 in the three CA-125 groups. Figure 5.46 shows that there is a higher DNAM-1 expression in PBMC and omental tumour when CA-125 levels were above 500 U/ml.

A



B



C

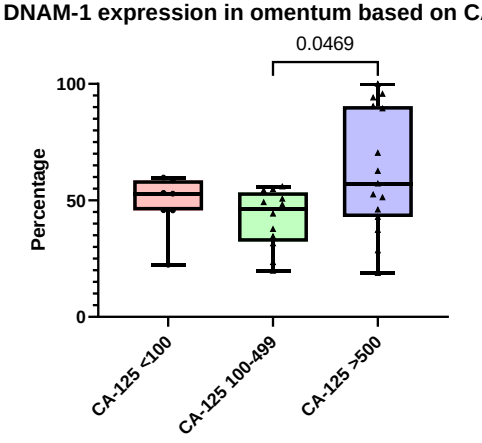


Figure 5.46: NK cells with high expression of DNAM-1 based on CA-125 level.
NK cells within A) PBMC, B) ovarian tumour, and C) omental tumour have increased DNAM-1 expression when CA-125 is greater than 500 U/ml.

5.5.4.3 DNAM-1 expression and omental metastatic disease

The majority of the OC patients within this cohort had histological confirmation of metastatic omental disease at the time of surgical resection (n=59, 73.8%). To evaluate if DNAM-1 expression was associated with omental metastasis, the OC patients were divided into those who had omentum tumours (n=59) and those who had histologically disease free or normal omentum (n=21). The proportion of NK cells exhibiting elevated DNAM-1 expression was then evaluated within these groups. Figure 5.47 shows that the OC patients with omental tumours have a significantly increased proportion of NK cells with DNAM-1 overexpression when compared to normal omentum. This was observed in the NK cells within PBMC, ovarian tumour and omental tumour samples.

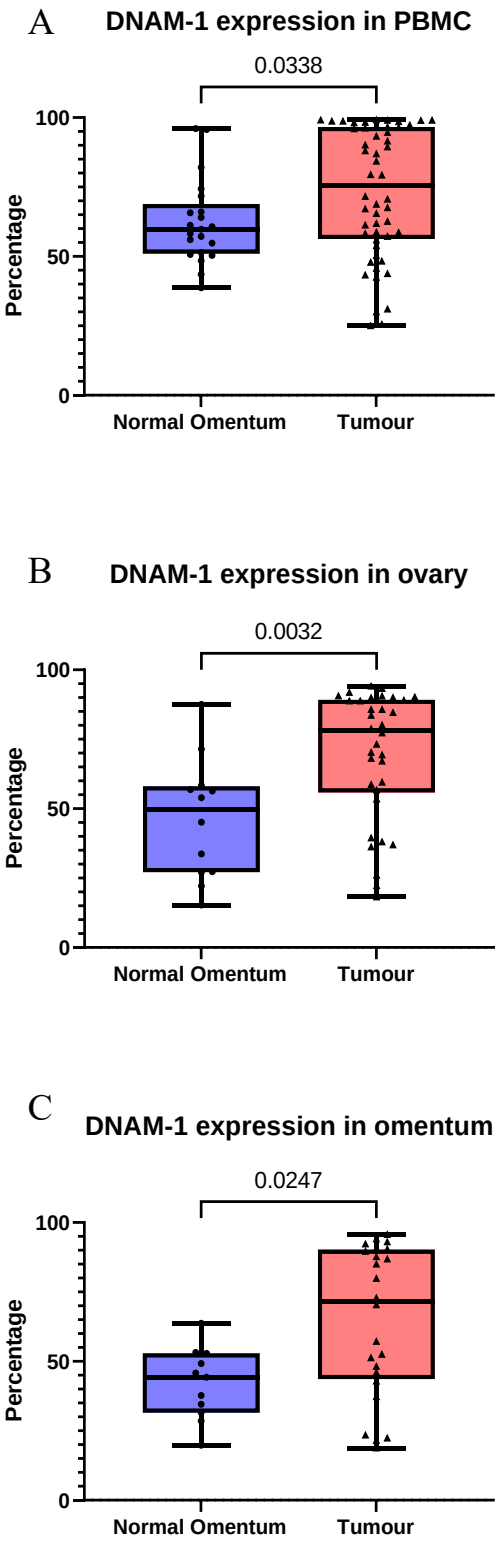


Figure 5.47: NK cells with high expression of DNAM-1 based on the presence of omental tumours in OC patients.

NK cells within A) PBMC, B) ovarian tissue, and C) omental tissue have increased DNAM-1 expression in the patients who have metastatic omental disease compared to those with normal omentum.

5.5.5 Summary of the association between NK cell phenotype and clinical outcomes

There were direct associations between clinical outcomes, NK subtypes and the level of expression of activation/inhibitory receptors. The proportions of peripheral, ovarian and omental NK cells were not associated with disease recurrence, disease-specific death, PFS or OS. However, poor patient outcomes were typically related to an inhibitory PBMC and ovarian tumour NK phenotype. Disease recurrence occurred more frequently when: PBMC NK cells had reduced NKp46, ovarian tumour NK cells had raised PD-1 expression and both PBMC and ovarian NK cells had increased expression of CD94. In addition, PFS was decreased in the patients who had low NKp46 expression in PBMC samples. Mortality was associated with increased CD94 expression in PBMC and ovarian tumour samples, while OS was decreased when NK cells showed an over expression of DNAM-1 in PBMC, ovarian and omental tumour. Supporting the notion that NK inactivation was related to poor clinical outcomes; disease recurrence and death were greater in the patients with increased PBMC proportions of immature cytokine producing $CD56^{bri}CD16^{neg}$ NK cells and a reduction in the mature cytotoxic $CD56^{dim}CD16^{bri}$ NK cells. In accordance to these findings, raised immature $CD56^{bri}CD16^{neg}$ NK cells were associated with decreased PFS and OS, while reduced cytotoxic $CD56^{dim}CD16^{bri}$ NK cells were found in those with poor PFS.

There were fewer NK cells within ovarian and omental tumours in advanced stage OC and in patients with high PCI, when compared to early stage and low PCI cases. Nevertheless, the tumour infiltrating NK cells in high PCI cases were in an activated state as they showed increased expression of DNAM-1, NKp46 and NKG2D. NK cells with raised expression of DNAM-1 in PBMC, ovarian tumour and omental tumour samples were associated with advanced stage disease, elevated serum CA-125 levels and increased omental metastases.

In addition, the patients who responded well to chemotherapy (CRS 3) were also found to have an altered NK phenotype, with reduced PBMC and omental NK expression of NKG2C, increased PBMC expression of NKG2D and decreased ovarian CD94 expression.

5.6 Discussion

This chapter builds on the comprehensive flow cytometric analysis of NK cells described in Chapter 4 of this thesis. A large, prospective cohort of OC and control patients was established, allowing the NK cell phenotype in blood and tissue samples to be interrogated. This chapter correlates these findings to collected clinical data. It examines the relationship between the proportion of NK cells, type of NK cells and the expression of NK receptors to patient outcomes, such as disease recurrence and survival. The associations between NK cells and the disease stage, tumour burden, presence of metastatic omental disease, CA-125 levels and response to chemotherapy are also evaluated.

The cohort of Ovarian cancer patients.

Within our patient cohort, the population who received neoadjuvant chemotherapy had more advanced and aggressive disease; unsurprisingly their surgical interventions were more complex and their PFS and OS outcomes were poor (Figures 5.1 and 5.3). This remained true when comparing only those patients with advanced stage III/IV OC (Figures 5.2 and 5.4). This was unexpected given that previous data has shown that interval debulking surgery is non-inferior to primary surgery, with similar survival and recurrence outcomes reported [64]. The discrepancies and variable characteristics between the two OC treatment groups described here are possibly due to our standard practice of offering upfront chemotherapy in cases of significant disease burden, resulting in poorer clinical outcomes [47, 63, 64].

There were challenges in patient recruitment to the cohort during the study period due to the coronavirus pandemic. As well as reduced opportunities to enlist patients to research studies and collect tissue samples, the tertiary gynaecology cancer centre performed fewer cytoreductive primary debulking operations [374]. This prevented the described OC cohort being unanimously composed of advanced and aggressive high-grade serous cases, our desired and intended study population. Instead, early stage OC, less aggressive tumours and cases with reduced disease burden were included in the primary surgery group. In addition, the management pathways for some OC patients at the cancer centre were slightly altered during this period [374]. Although patients still received optimal treatment, some received additional neoadjuvant chemotherapy treatment (more than the intended three cycles) before interval debulking surgery could be undertaken.

The proportion of NK cells and Ovarian cancer clinical outcomes.

The flow cytometric analysis in Chapter 4 describes how the proportion of peripheral NK cells increases in OC patients, with reduced populations upon infiltration into ovarian and omental tumour tissue. While the amounts of peripheral, ovarian and omental NK cells are believed to be related to patient outcomes [231, 232], in this cohort they were not associated with disease recurrence and patient death (Figures 5.5 – 5.10). This could be due to the inclusion of non-consecutive cases and a lack of available tumour samples from certain patients during the collection period. The recruitment of less aggressive tumours and patients with reduced disease burden may also have influenced findings. With the majority of patients suffering treatment resistance and disease relapse within two years [1, 64, 73], the follow-up of patients in this cohort was comprehensive and allowed the detection of OC recurrence and cases of disease specific death. However, a larger cohort is required, which may demonstrate a correlation between NK cell populations and clinical outcomes.

NK cell receptors and clinical outcomes in Ovarian cancer.

The NK cell analysis in Chapter 4 demonstrates NK cell inactivation in ovarian and omental tumour tissue compared to paired circulating blood samples. However, peripheral and tissue infiltrating NK cells had greater activation in cases of malignancy when compared to the corresponding non-cancerous samples. As tumours progressed, seen with advancing stage, raised PCI and the development of metastatic omental deposits, the NK cells within blood and tumour samples demonstrated further overexpression of activation receptors. Indeed, activation receptors were raised in patients with a high PCI: NKp46 and NKG2D in both ovarian and omental tumour biopsies, and DNAM-1 in PBMC samples (Figure 5.40). Advanced OC (FIGO stage III/IV) was associated elevated DNAM-1 expression in the NK cells within PBMC and omental biopsies (Figure 5.45). Furthermore, patients with metastatic omental disease had NK cells with increased DNAM-1 expression in peripheral blood, ovarian and omental samples (Figure 5.47). This implies possible tumour escape mechanisms or soluble tumour ligand release, which work to chronically upregulate and saturate activation receptors, driving the NK cells to an exhausted phenotype and further preventing an NK immune response [213, 218-220]. One feature to support this possibility is the increased expression of inhibiting receptors PD-1 and CTLA-4 on NK cells in PBMC samples of OC patients compared with control patients (Figure 4.15). In addition, the upregulation of PD-1 was more pronounced in the ovarian and omental tumour tissues compared with the corresponding PBMC samples (Figures 4.42 and 4.50, respectively).

Poor patient outcomes were typically related to an inhibitory PBMC and ovarian tumour NK phenotype: disease recurrence occurred more frequently with low PBMC NKp46 and raised ovarian PD-1 (Table 5.9). Furthermore, PFS was reduced with low expression of NKp46 (Figure 5.11) and CD57 (Figure 5.12) on peripheral NK cells. Previous findings coincide with

this, as improved clinical outcomes and prolonged survival occurs when peripheral NK cells are activated and there is upregulation of NK activation receptors [192, 175, 223, 225, 231, 285]. Perhaps due to chronic ligand exposure in advancing disease, and the subsequent altered receptor expression [212], disease recurrence was seen with high omental NKp46 and CD57 expression (Table 5.9), while disease specific death was associated with raised CD57 on omental NK cells (Table 5.10). In addition, OS was decreased with the overexpression of DNAM-1 on PBMC, ovarian and omental tumour NK cells (Figures 5.25, 5.29 and 5.33, respectively).

The chemotherapeutic effect on NK cells and clinical outcomes

Almost half of patients who received neoadjuvant chemotherapy within the cohort had no response (CRS 1) to the treatment, while only 20% showed an excellent response (CRS 3), which is similar to other previously reported OC cohorts [233]. Despite the response to chemotherapy having no influence on the proportions of NK cells within blood and tissue samples (Figure 5.42), the NK cell phenotype was altered. The NK cells in patients who responded well to chemotherapy (with a CRS 3) were found to be in an activated state. Here there was increased expression of NKG2D on peripheral blood NK cells (Figure 5.43) and decreased ovarian CD94 expression (Figure 5.44). This supports the anticipated chemotherapeutic response of downregulation of inhibiting receptors and overexpression of activation receptors [366]. However, it is important to note that patients may have received granulocyte-colony stimulatory factor (G-CSF), which is given to treat lymphocytopenia during chemotherapy treatment. This is known to effect NK activity and may therefore have influenced the findings [368-370].

In summary, this chapter further evaluates the NK cell phenotype in OC by correlating the flow cytometric analysis to clinical data. The interrogation of NK cell proportions, subtypes and receptor expression examined any associations with patient outcomes. By collating extensive clinical information, the importance and influence of NK cells in OC was explored. Possible tumour evasion mechanisms were considered with the identification of significant targets, such as DNAM-1, which are directly related to patient outcomes and warrant further investigation. Additional analysis will evaluate the significance of continuous variables and other clinical factors, such as the type of OC treatment received and chemotherapy exposure. This will be conducted with a multivariate analysis and a Cox proportional hazards regression analysis, and will also evaluate how the type and proportion of NK cell populations influence patient survival and recurrence.

Chapter 6:

Functionality study of NK cells and Interaction with Primary Ovarian Cancer cells

6.1 Introduction

Natural Killer (NK) cells interact with their target cells through various ligands, either recognise “self”, causing NK cell inhibition, or detect abnormal and damaged cells, stimulating an NK cell attack [173, 177, 182, 184-186, 187, 188]. In cases of malignancy, the overriding NK cell action is dependent on the balance between the activating and inhibiting NK receptor and tumour ligand interactions [182, 197, 198]. Tumours have the ability to downregulate, overexpress or secrete specific molecules to avoid NK recognition and alter NK signalling pathways, thus preventing an NK-mediated immune response [141, 150, 154, 177, 186, 190-195, 187, 213]. If NK cells are successfully activated towards malignant cells, their functional response aims to destroy the tumour cells via several mechanisms [173, 177, 186, 187, 201-208].

The cytotoxic nature of NK cells and their ability to produce cytokines is impeded upon infiltration into cancer tissue. Tumours often utilise various escape mechanisms to evade immunity and create an immunosuppressive microenvironment that inactivates the NK cells, rendering them dysfunctional [150, 151, 153, 156, 177, 180, 187, 212-216, 221-226, 228, 210, 211]. Directly related to patient prognosis, NK cell activation is associated with improved outcomes and survival, while disease progression, metastases and poor outcomes are linked with NK inhibition and reduced NK function [110, 175, 192, 223, 225, 285, 231, 364-366].

The overarching aim of this chapter is to explore the functional aspect and behaviour of NK cells. In vitro experiments using NK cells obtained from ovarian cancer (OC) patients will focus specifically on the NK response to their ovarian tumours. By stimulating and challenging the NK cells to mount an attack, their ability to produce cytokines and directly

kill tumour cells will be interrogated. This chapter will build on the NK cell analysis and clinical correlation described in chapters 4 and 5. Having previously established the phenotype and activation of the NK cells in OC patients, here we focus on how the tumour microenvironment influences the NK cell function, evaluating possible causes of NK dysfunction and tumour evasion. Using tissue biopsies and peripheral blood NK cells from the established patient cohort, the interactions and relationships between NK cells and tumour cells will be reviewed. Finally, the manipulation of NK activating signalling pathways, and the resulting cytotoxic capabilities, will further explore credible targets for NK immunotherapies.

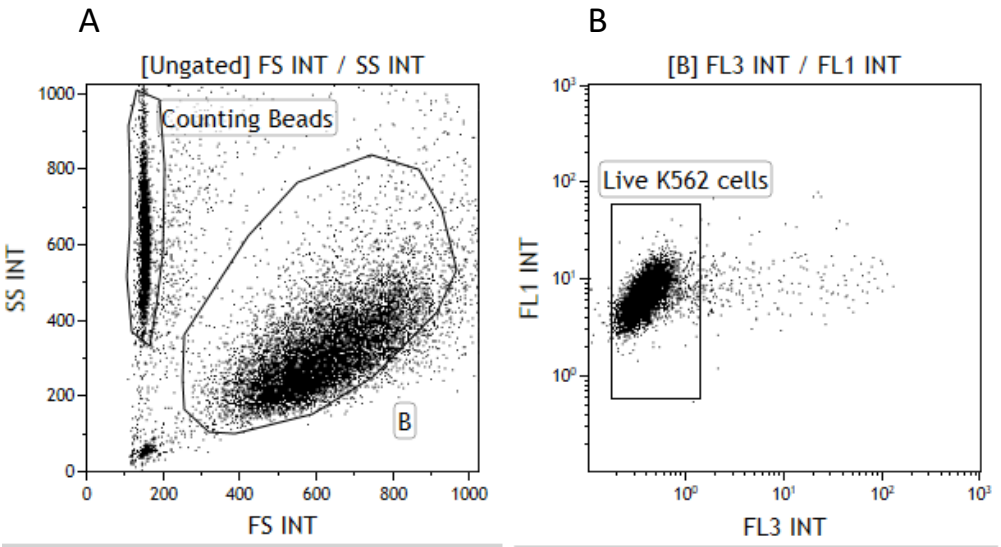
6.2 Function of the peripheral NK cells

6.2.1 NK cell cytotoxicity

6.2.1.1 Defining NK cell killing

To ascertain the killing ability of the peripheral NK cells, the cytotoxicity assay described in the Methods section 2.2.4 was undertaken. The assay utilised the immortalised K-562 cell line, which originated from a patient with chronic myelogenous leukaemia and lacks HLA expression, therefore directly stimulating NK cells and initiating a cytotoxic response [304]. The K-562 cells were labelled with CFSE (carboxyfluorescein succinimidyl ester), a fluorescent staining dye, and either cultured alone or in combination with NK cells obtained from peripheral blood samples. Flow cytometric analysis was undertaken to measure the absolute cell counts. Figure 6.1 shows an example of the gating strategy used to identify the counting beads in each sample by gating on FS INT and SS INT, while the live K-562 cell population was measured by gating with CFSE and PI. The ratio of viable K-562 cells to the number of counting beads was established, with the control sample (K-562 cells only) compared to the combined K-562 and NK cell sample to calculate the percentage of K-562

killing achieved by the NK cells. An example of the remaining live K-562 cells from the NK cell co-culture is shown in Figure 6.2, and is compared to the K-562 cells from the isolated control culture.

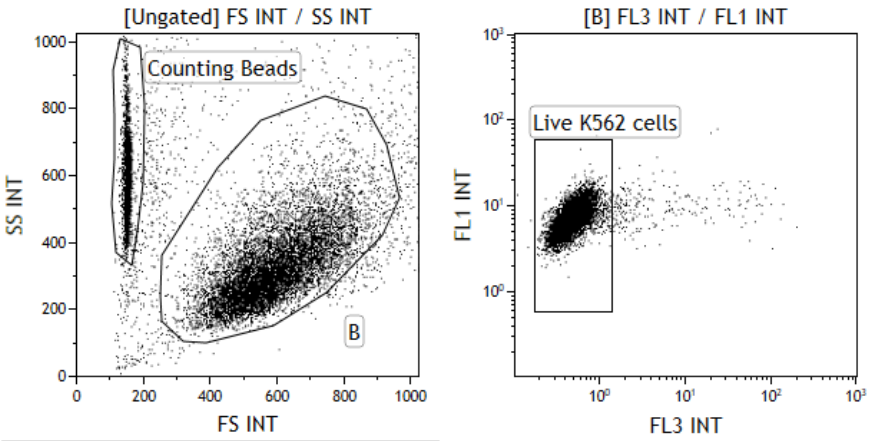


Gate	Number
All	17,606
B	10,715
Counting Beads	4,624

Gate	Number
All	10,715
Live K562 cells	10,470

Figure 6.1: The gating strategy implemented to identify live K-562 cells
Analysis of flow cytometric data allowed the detection of: A) counting beads, and B) live K-562 cells, which were used to calculate NK cell cytotoxicity

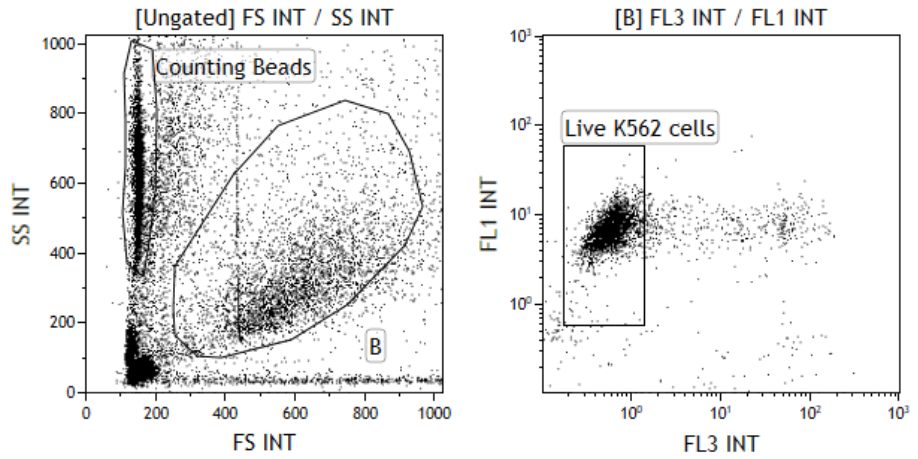
A. Control sample



Gate	Number
All	14,159
B	9,421
Counting Beads	3,204

Gate	Number
All	9,421
Live K562 cells	9,173

B. Co-culture of K-562 and NK cells



Gate	Number
All	31,396
B	4,354
Counting Beads	4,813

Gate	Number
All	4,354
Live K562 cells	2,902

Figure 6.2: Identification of live K-562 cells following NK cell co-culture.
The NK cell cytotoxicity was calculated by comparing A) isolated live K-562 cells to B) viable K-562 cells following co-culture with NK cells.

6.2.1.2 The NK cell cytotoxicity study cohort

The cohort for the cytotoxicity assay consisted of samples from 10 healthy donor controls and 20 patients with advanced (stage II/IV), high-grade serous OC (HGSOvCa) previously described in the NK phenotype analysis. Of the OC patients, 10 were chemotherapy naïve and blood samples were collected at the time of primary surgery. The remaining 10 patients had received either three or four cycles of platinum-based neoadjuvant chemotherapy, with blood samples taken at the time of their interval debulking surgery. The patients in the two HGSOvCa groups had very comparable baseline characteristics, shown in Table 6.1, and there were also no differences in surgical outcomes, disease recurrence and survival. In addition, progression free survival (Figure 6.3) and overall survival (Figure 6.4) were similar between the primary surgery and neoadjuvant chemotherapy patients.

Table 6.1: Cytotoxicity assay patient characteristics and outcomes

Variable	Primary surgery (n=10)	Neoadjuvant chemotherapy (n=10)	P value
Age (years) Mean ± SD	63.4 ± 6.7	69.7 ± 7.5	0.2048
Ethnicity	**n (%)**	**n (%)**	
White	9 (90.0)	8 (80.0)	
Asian	1 (10.0)	1 (10.0)	
Black	0 (0.0)	1 (10.0)	>0.9999
Disease stage	**n (%)**	**n (%)**	
3	7 (70.0)	6 (60.0)	
4	3 (40.0)	4 (40.0)	0.6392
CRS	n/a	**n (%)**	
1		2 (20.0%)	
2		7 (70.0%)	
3		1 (10.0)	n/a
Cytoreduction	**n (%)**	**n (%)**	
R0	8 (80.0)	7 (70.0)	
R1	0 (0.0)	1 (10.0)	
R2	2 (20.0)	2 (20.0)	>0.9999
Omental disease	**n (%)**	**n (%)**	
Present	8 (80.0)	7 (70.0)	
Absent	2 (20.0)	3 (30.0)	0.5312
Recurrence	**n (%)**	**n (%)**	
Disease free	6 (60.0)	5 (50.0)	
Recurred	4 (40.0)	5 (50.0)	0.6531
Survival	**n (%)**	**n (%)**	
Died	3 (30.0)	4 (40.0)	
Alive	7 (70.0)	6 (60.0)	0.6392

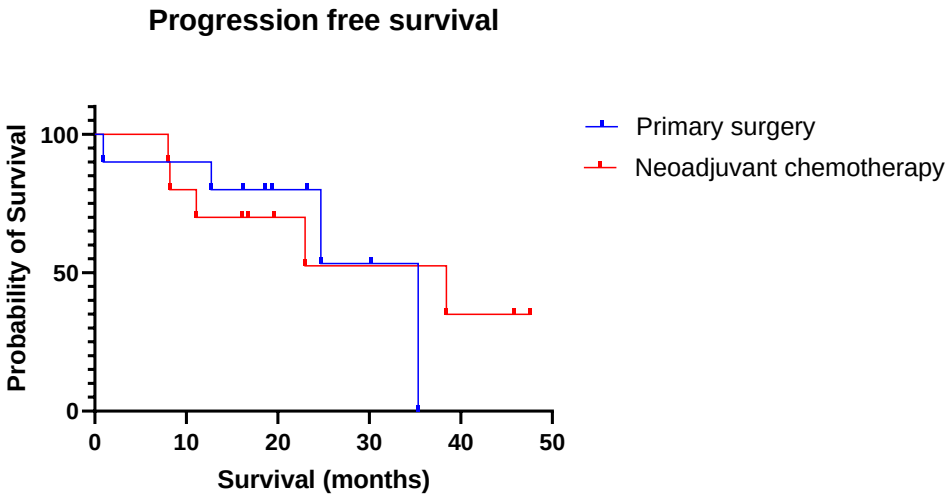


Figure 6.3: Kaplan-Meier plot demonstrating progression free survival in the primary surgery and neoadjuvant chemotherapy patients utilised in the cytotoxicity assay.
There was no significant difference in PFS between the two OC groups.

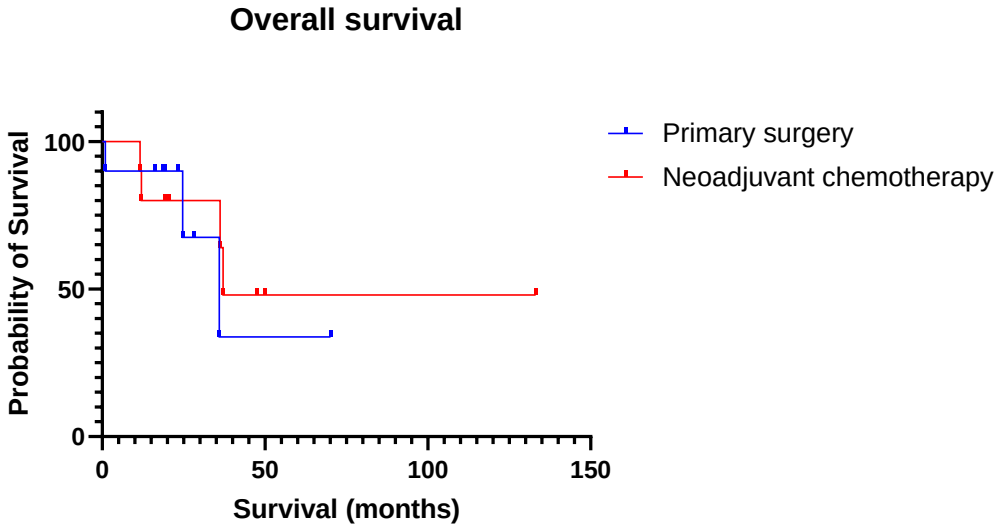
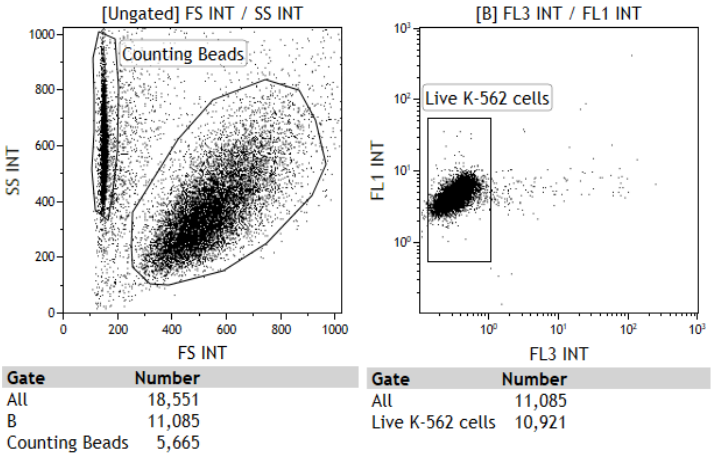


Figure 6.4: Kaplan-Meier plot demonstrating overall survival in the primary surgery and neoadjuvant chemotherapy patients utilised in the cytotoxicity assay.
There was no significant difference in OS between the two OC groups.

6.2.1.3 Peripheral NK cell cytotoxicity analysis

Upon detection of the live K-562 target cells following co-culture with the NK cells, the percentage of cell killing achieved by each patients NK cell sample could be determined. Figure 6.5 demonstrates the remaining viable K-562 cells following co-culture with NK cells from healthy donor samples and from patients with OC.

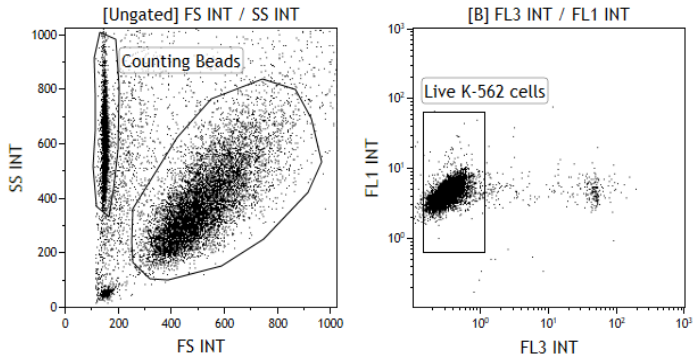
A. K-562 cells + NK cells from healthy donor



Gate	Number
All	18,551
B	11,085
Counting Beads	5,665

Gate	Number
All	11,085
Live K-562 cells	10,921

B. K-562 cells + NK cells from OC patient



Gate	Number
All	16,311
B	9,557
Counting Beads	4,684

Gate	Number
All	9,557
Live K-562 cells	9,201

Figure 6.5: Killing of K-562 cells by NK cells from healthy donor sample and OC sample
The ability of NK cells to kill K-562 cells is shown using A) healthy donor NK cells, and B) NK cells from a patient with OC.

Overall, the mean percentage of NK cytotoxicity in the 10 healthy donor samples was 12.6%, significantly lower than in the OC patients 31.2% in the OC patients, ($p < 0.001$), demonstrated in Table 6.2. The mean cytotoxicity of the chemotherapy naïve (primary surgery) group was 27.5%, while the chemotherapy exposed (neoadjuvant chemotherapy) group had a mean cytotoxicity of 34.9%, both significantly higher than the healthy donor samples ($p = 0.004$ and $p < 0.001$, respectively). There was no significant difference in the mean cytotoxicity values between the two OC groups ($p = 0.2830$).

Table 6.2: Mean cytotoxicity of peripheral NK cells in healthy donors and OC patients

Sample group	Mean NK cytotoxicity (%)
Healthy Donor (n=10)	12.6
All OC patients (n=20)	31.2
Primary surgery OC patients (n=10)	27.5
Neoadjuvant chemotherapy OC patients (n=10)	34.9

The peripheral NK cell cytotoxicity was found to be significantly raised in the OC patients when compared to the normal healthy donor NK samples ($p < 0.0001$), shown in Figure 6.6. Similarly, NK cytotoxicity was significantly raised in the chemotherapy naïve and chemotherapy exposed groups when compared to healthy controls (chemotherapy naive vs control, $p = 0.0002$; chemotherapy exposed vs control, $p = 0.0013$), seen in Figure 6.7. However, there was no difference in NK cytotoxicity between the two OC groups.

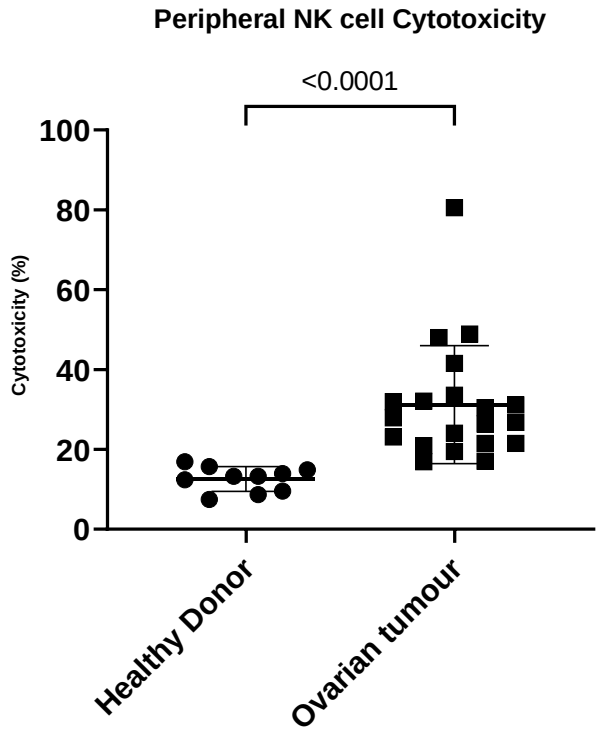


Figure 6.6: Cytotoxicity of peripheral NK cells obtained from healthy donors and patients with OC. The cytotoxicity of peripheral NK cells in OC patients was significantly greater than the peripheral NK cells from healthy donor samples ($p < 0.0001$).

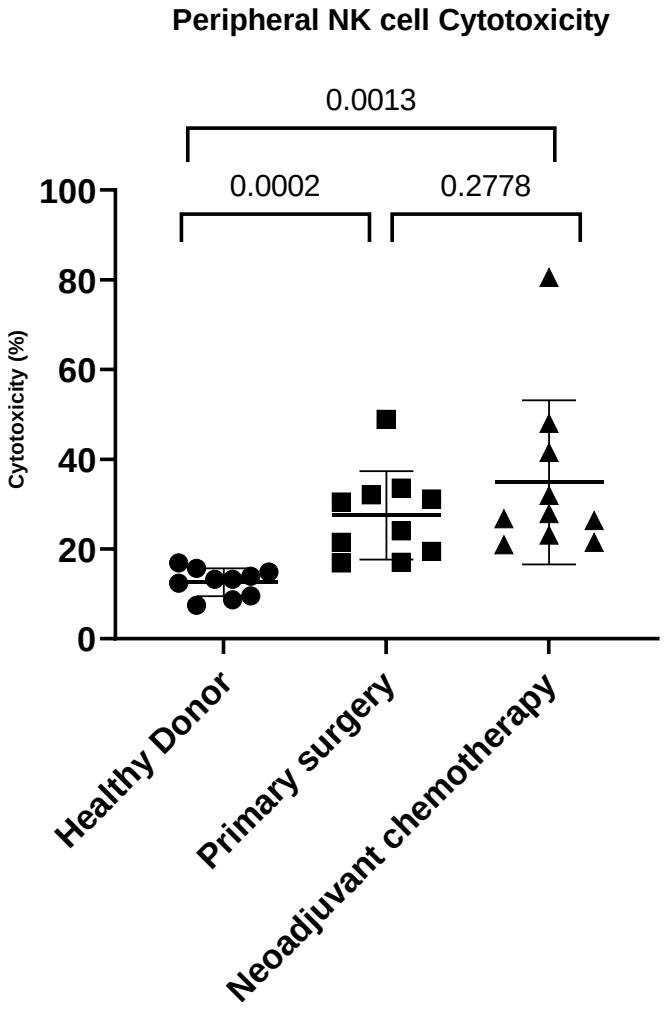


Figure 6.7: Cytotoxicity of peripheral NK cells obtained from healthy donors, primary surgery OC patients and neoadjuvant chemotherapy OC patients.

The cytotoxicity of peripheral NK cells from both primary surgery OC and neoadjuvant chemotherapy OC patients was significantly raised compared to the cytotoxicity of the healthy donor blood samples ($p = 0.002$ and $p = 0.0013$, respectively). There was no difference in NK cytotoxicity between the PBMC samples from primary surgery patients and neoadjuvant chemotherapy patients ($p = 0.2778$).

6.2.1.4 Correlations between NK cell cytotoxicity and clinical findings

The NK cytotoxicity data was then correlated with clinical findings and patient outcomes. Focusing initially on OC progression and metastatic disease, there were 5 patients in the OC groups without histological evidence of omental metastasis. Their average peripheral NK cell cytotoxicity was 22.6%. In comparison, those with omental metastasis has an increased NK cytotoxicity level of 34.0% but the difference was not significant (p=0.0806), shown in Figure 6.8.

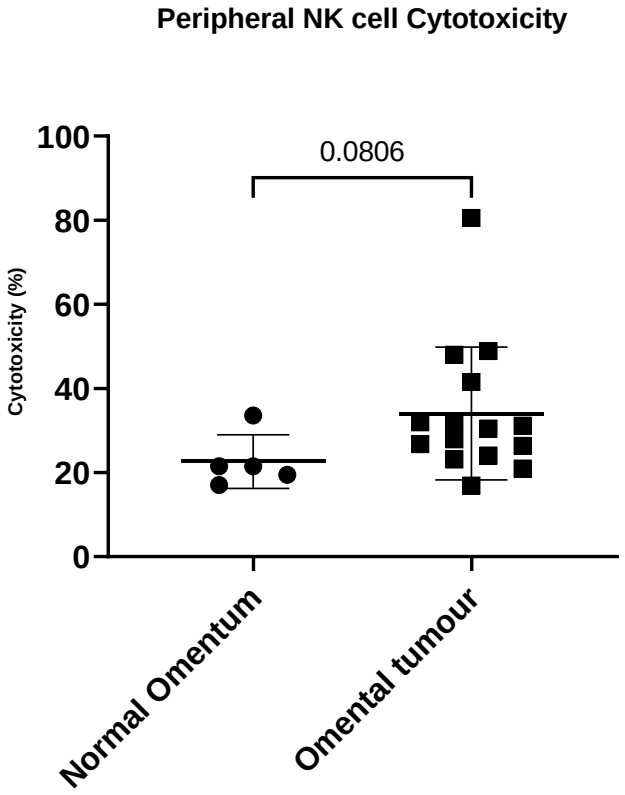


Figure 6.8: Cytotoxicity of peripheral NK cells in OC patients based on the presence of metastatic omental disease.
The ability of peripheral NK killing was raised in the OC patients with omental tumours compared to the OC patients with normal omentum, but not significantly so (p = 0.0806).

Of the 20 OC patients, a total of 9 patients suffered a disease recurrence and 7 died. There were no differences in peripheral blood NK cytotoxicity between those who recurred and those who remained disease free (p = 0.5516), shown in Figure 6.9. In addition, there was no difference in the PBMC NK cytotoxicity levels in the patients who died compared to those who were alive (p = 0.4378), seen in Figure 6.10.

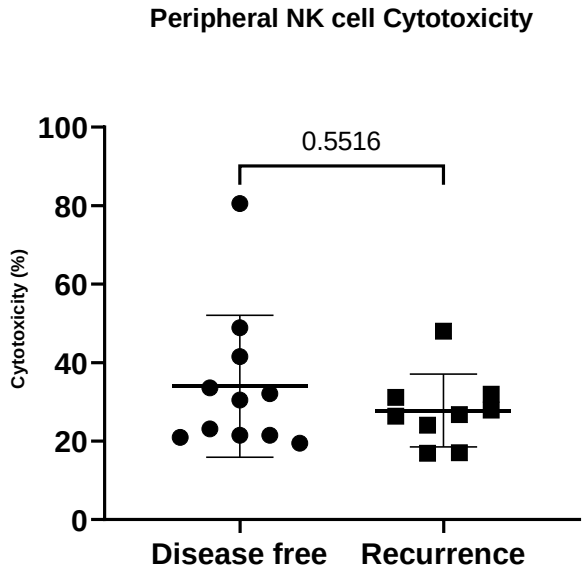


Figure 6.9: Cytotoxicity of peripheral NK cells in OC patients who recurred compared to those who remained disease free.
There was no difference in PBMC NK cytotoxicity between those who recurred and those who did not (p = 0.5516).

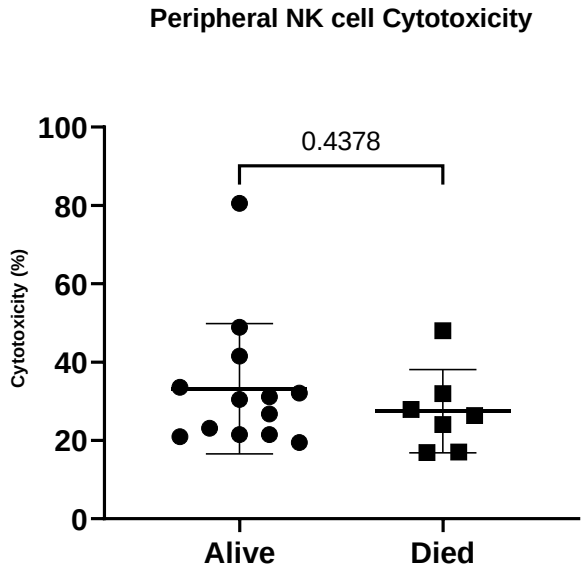


Figure 6.10: Cytotoxicity of peripheral NK cells in OC patients who died compared to those who were alive.
There was no difference in cytotoxicity between those who died and those who were alive (p = 0.4378).

The OC patients were then divided into two groups: those with an NK cytotoxicity level below the median value and those above the median cytotoxicity value. The progression free survival (Figure 6.11) and overall survival (Figure 6.12) were both alike when comparing those with raised NK cell killing to those with lower NK killing (p = 0.0716 for PFS; p = 0.7968 for OS).

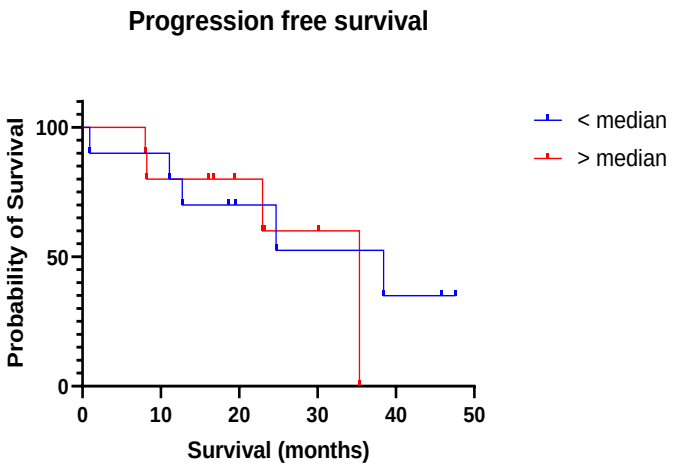


Figure 6.11: Kaplan-Meier plot demonstrating progression free survival in OC patients with NK cytotoxicity below and above the median value.

There was no significant difference in PFS between those OC patients with peripheral blood NK cytotoxicity below the median value and those with cytotoxicity above the median value (p = 0.0716).

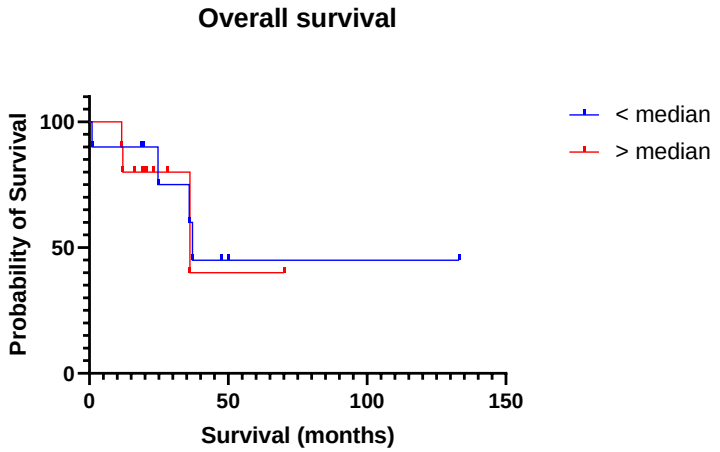


Figure 6.12: Kaplan-Meier plot demonstrating overall survival in OC patients with NK cytotoxicity below and above the median value.

There was no significant difference in OS between those OC patients with peripheral blood NK cytotoxicity below the median value and those with cytotoxicity above the median value (p = 0.7968).

6.2.1.5 Correlations between NK cell cytotoxicity and NK phenotype

To facilitate further analysis, NK cytotoxicity was correlated to findings from the NK phenotype analysis. The proportion of NK cells in peripheral blood samples (described in Chapter 4, section 4.4.1) was evaluated in the two NK cytotoxicity groups, those above and below the median cytotoxicity value (high and low cytotoxicity, respectively). There was no significant difference in the amount of NK cells between the two groups (Figure 6.13). The type of NK cells (evaluated in Chapter 4, section 4.4.2) was also similar in the two groups, with no differences in CD56 and CD16 expression between the samples with high and low NK cytotoxicity (Figure 6.14).

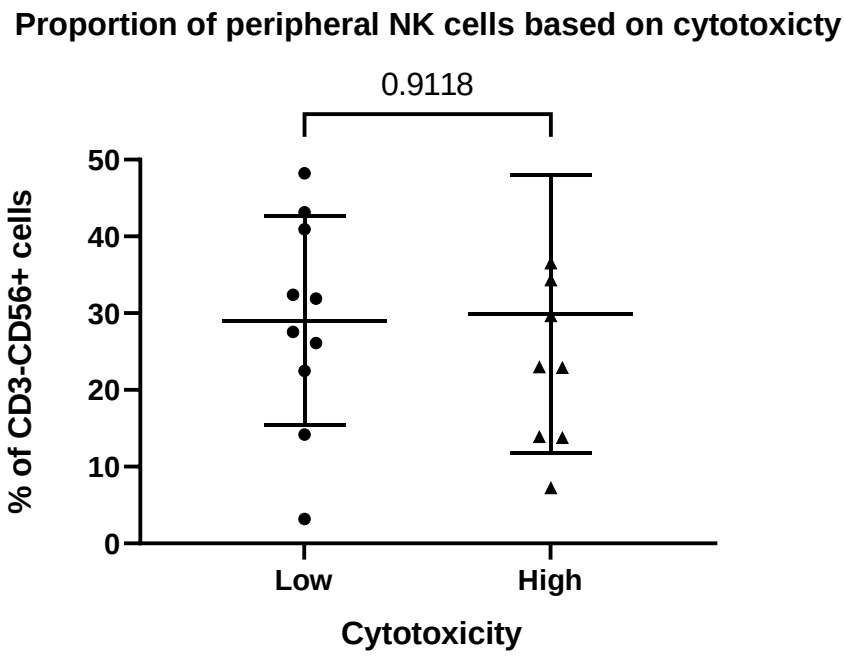


Figure 6.13: Proportion of peripheral NK cells in OC patients based on degree of NK cytotoxicity. There was no difference in the proportion of NK cells in OC patients with NK cytotoxicity below the median (low cytotoxicity) and above the median value (high cytotoxicity).

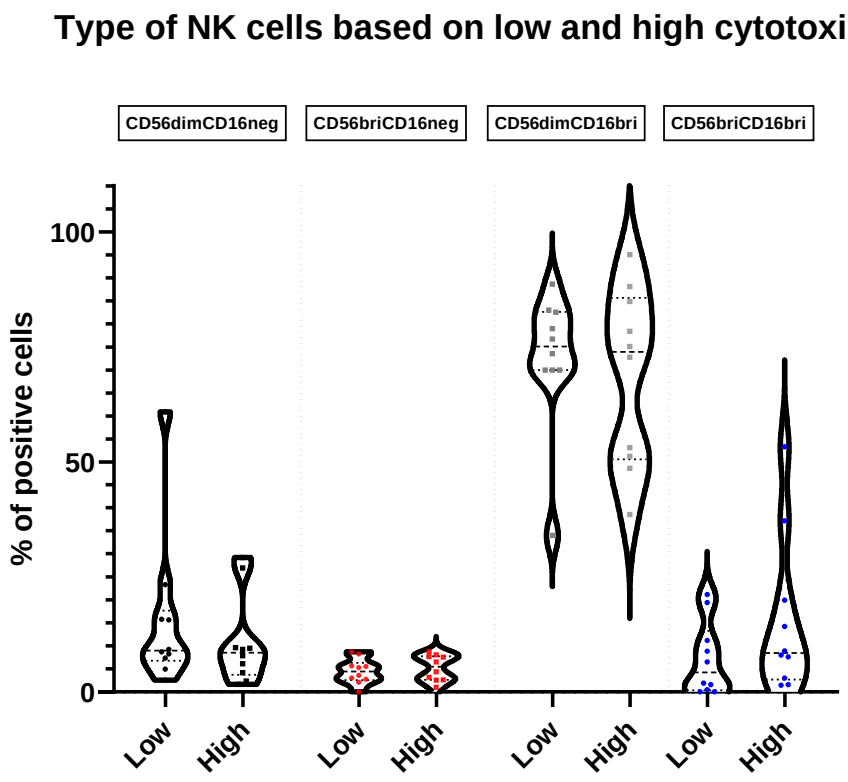


Figure 6.14: Type of peripheral NK cells in OC patients based on degree of NK cytotoxicity. There was no difference in the CD16 and CD56 expression in the peripheral NK cells in OC patients when the samples with low NK cytotoxicity were compared to those with high NK cytotoxicity.

The same NK cytotoxicity groups were then correlated to NK cell receptor expression (shown in Chapter 4, section 4.4.3). NK cells with higher levels of cytotoxicity showed a significant increase in the expression of NKp46 ($p = 0.0443$) and a reduction in NKG2C ($p = 0.0142$) when compared to those NK cells with lower cytotoxicity levels. There was no difference in the expression of the other activation receptors (DNAM-1, NKG2D and CD57), shown in Figure 6.15. The NK cells with higher cytotoxicity levels had decreased expression of checkpoint inhibitors PD-1 and CTLA-4 when compared to the NK cells with lower cytotoxicity, but this was not significant ($p = 0.1655$ and $p= 0.8358$, respectively). There was no difference in the expression of the other inhibitory receptors (TIGIT and CD94), demonstrated in Figure 6.16.

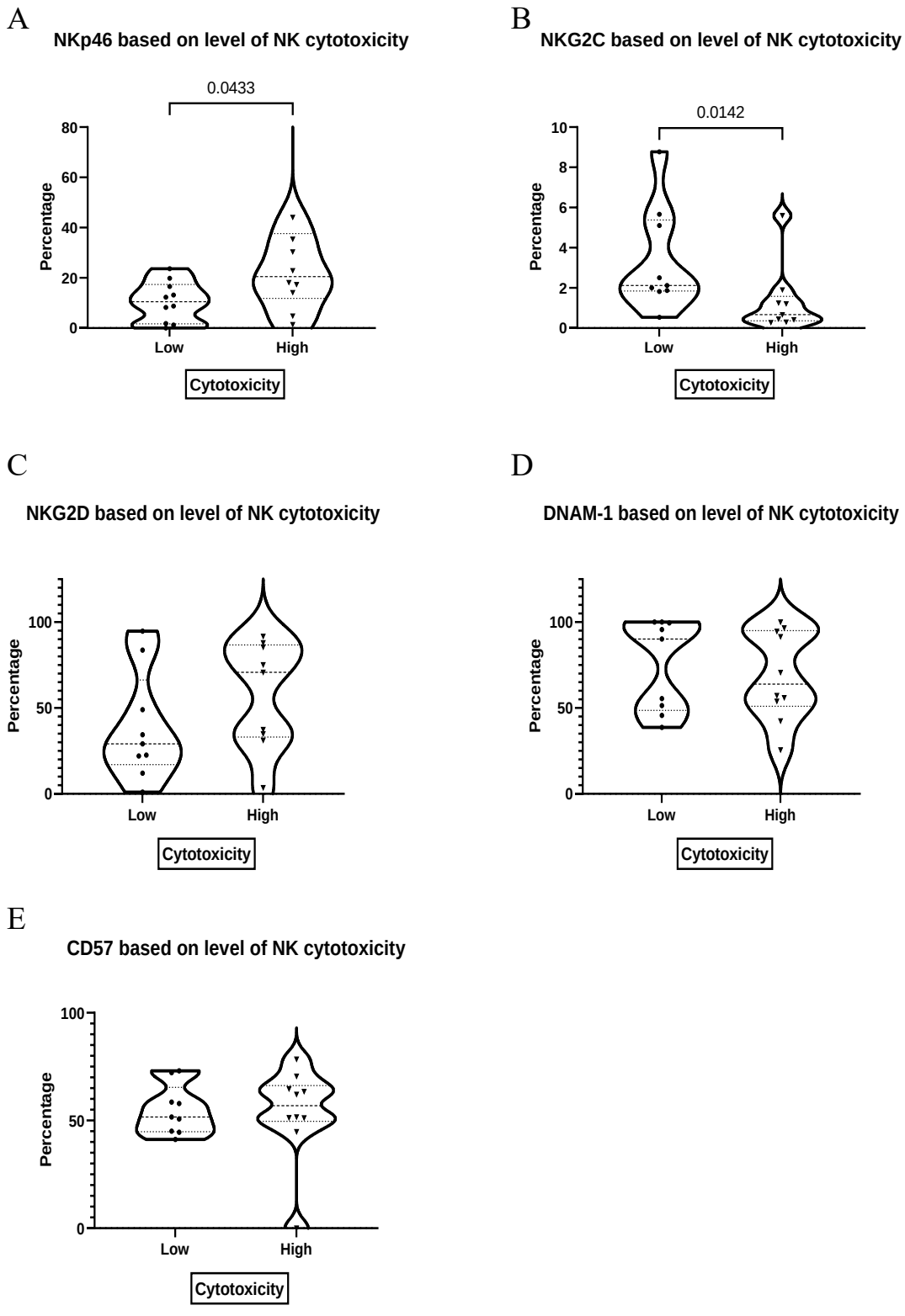


Figure 6.15: Expression of activation receptors on NK cells with low and high levels of cytotoxicity. There was raised expression of Nkp46 (A) and reduced NKG2C (B) on peripheral NK cells with higher cytotoxicity levels (above the median value). There was no difference in the expression of NKG2D (C), DNAM-1 (D), and CD57 (E).

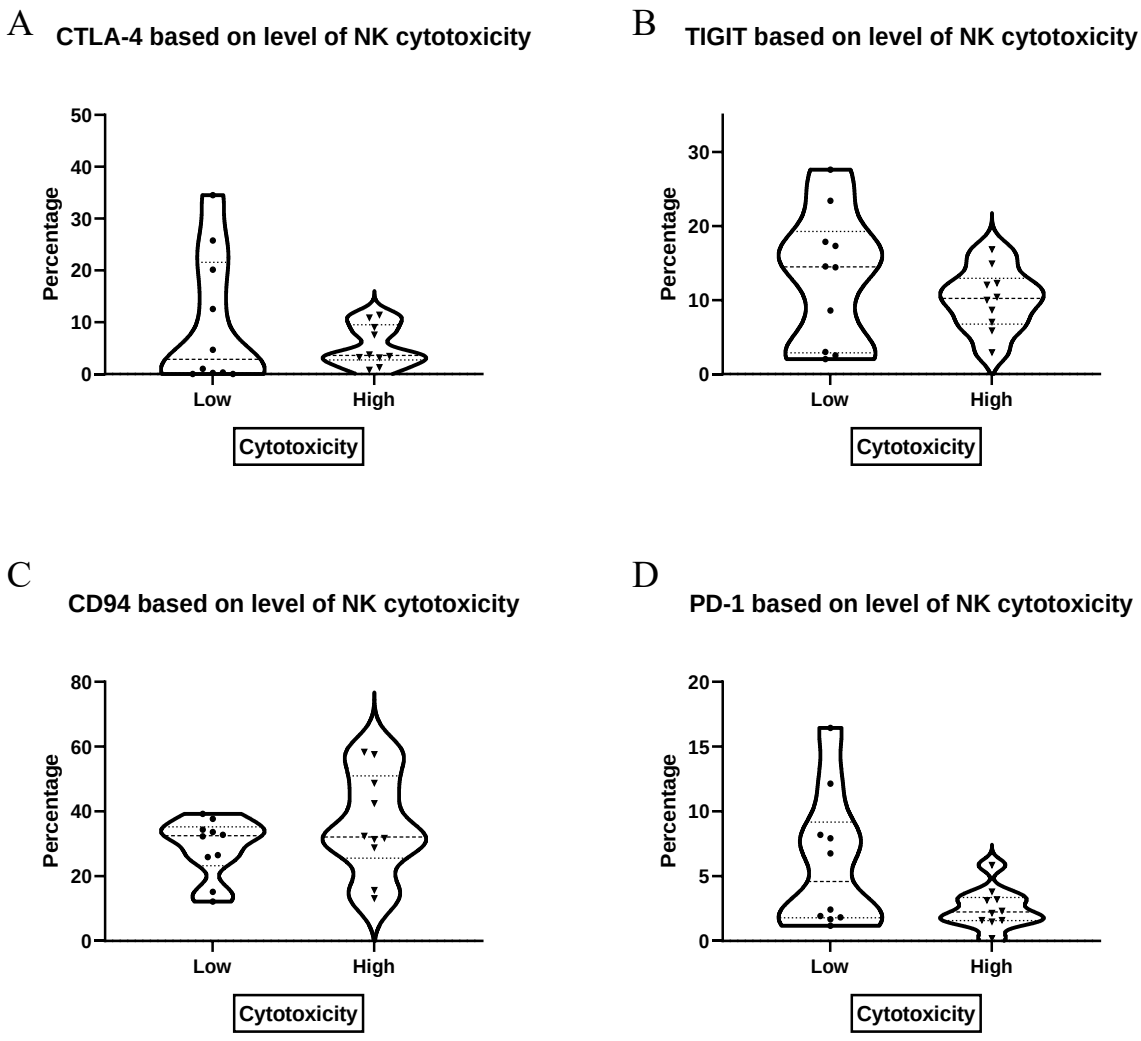


Figure 6.16: Expression of inhibitory receptors on NK cells with low and high levels of cytotoxicity. There were no differences in the expression of CTLA-4 (A), TIGIT (B), CD94 (C), and PD-1 (D) between the peripheral NK cells with high and low cytotoxicity.

6.2.2 NK cell cytokine production

6.2.2.1 Detecting NK cell cytokines

The functional capability of peripheral NK cells in producing cytokines was evaluated utilising the protocol described in the Methods section 2.2.5. Peripheral blood (PBMC) samples were cultured in isolation and in combination with the K-562 cells. This allowed comparison of an unstimulated NK cell population from the isolated PBMC culture and an NK cell population that had been stimulated with the K-562 cell line. A selection of intracellular and cell surface antibodies was then used to detect cytokines produced by the NK cells: tumour necrosis factor (TNF)-alpha, granulocyte-macrophage colony stimulating factor (GM-CSF), interleukin (IL)-10, transforming growth factor (TGF)-beta, interferon (IFN)-gamma and IL-2. The Gallios flow cytometer and Kaluza software (Beckman Coulter, analysis version 2.1) were used to identify the live NK cell population within each sample (Figure 6.17). The single cell population was detected using the FS INT and FS Peak, which was then used to find the single lymphocyte cells (using FS INT and SS INT gating). Utilising these lymphocyte cells, the live cells were retained, while cells with CD19 and CD14 expression (B cells, macrophages and dendritic cells), were removed from the analysis. The live cells were then divided depending on their CD56 and CD3 expression; the NK cell population was located by negative CD3 and positive CD56 expression.

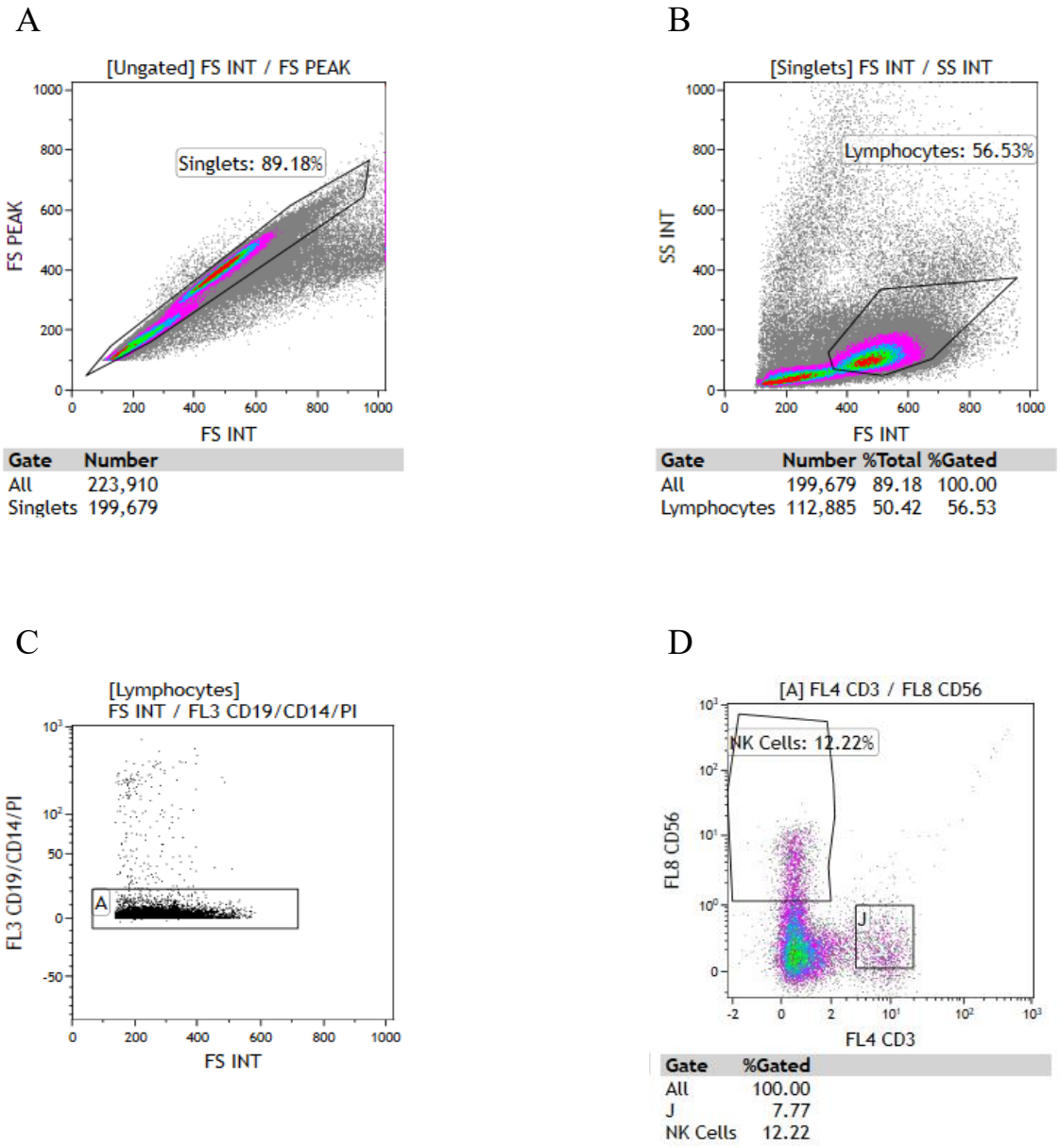


Figure 6.17: The gating strategy implemented to identify the NK cell population within peripheral blood samples following flow cytometry.

Analysis of flow cytometric data allowed the detection of: A) single cells, B) lymphocytes, C) live cells with cells expressing CD14 and CD19 removed, and D) the NK cell population.

The percentage of NK cells in the unstimulated population was then compared to the percentage of NK cells in the stimulated population (those that had been co-cultured with K562 cells) for every sample. Figure 6.18 demonstrates the unstimulated NK cell population and stimulated NK cell population, from the same PBMC sample. These NK cell populations from each sample were then analysed to determine the proportion with increased cytokine expression (Figure 6.19). This was undertaken in the unstimulated NK cells and the NK cells stimulated with K562 for each blood sample.

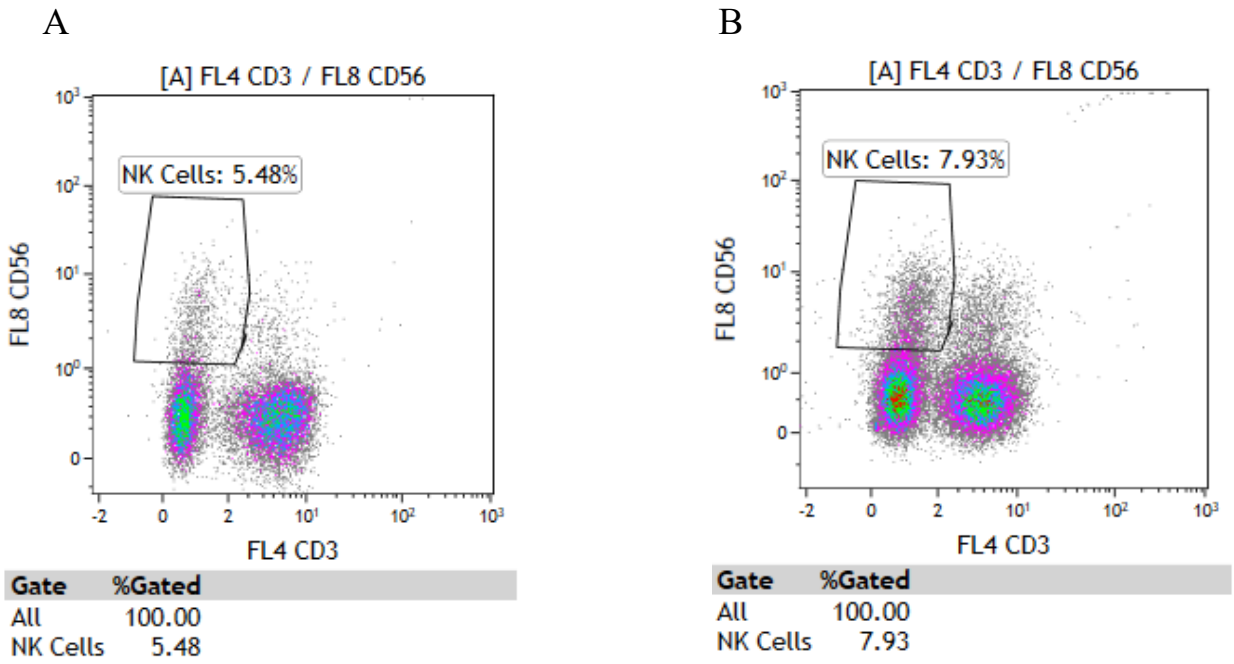


Figure 6.18: The NK cell population from A) an unstimulated PBMC sample, and B) a stimulated PBMC sample co-cultured with K-562 cells.

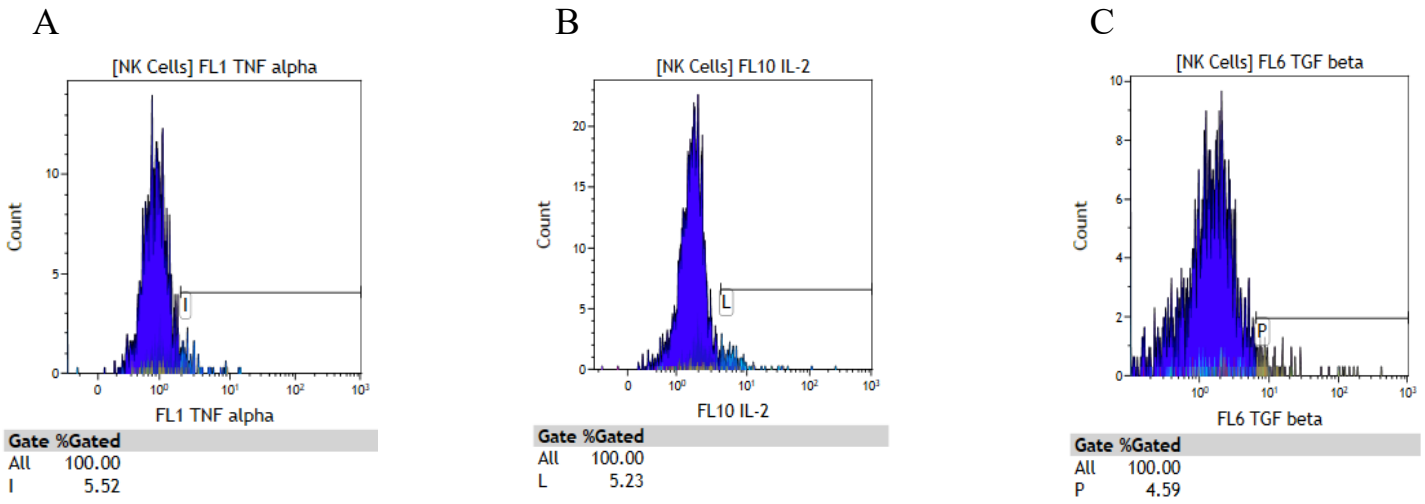


Figure 6.19: Histograms demonstrating NK cell cytokine production.
The expression of A) TNF-alpha, B) IL-2, and C) TGF-beta by peripheral NK cells.

6.2.2.2 The NK cytokine study cohort

Further study was undertaken to evaluate cytokine production by the peripheral NK cells. The samples utilised included 10 controls and 20 advanced (stage III/IV), HGSOvCa patients from the NK phenotype cohort. Again, 10 of the OC patients were chemotherapy naïve (primary surgery group) and 10 had received neoadjuvant chemotherapy, with both groups n having comparable baseline characteristics, shown in Table 6.3. Patients in the neoadjuvant chemotherapy group were significantly more likely to recur and die when compared to the chemotherapy naïve group (80% vs 30%, p = 0.0246), despite patients from both groups having similar demographic variables and presentation.

Table 6.3: Cytokine assay patient characteristics and outcomes

Variable	Primary surgery (n=10)	Neoadjuvant chemotherapy (n=10)	P value
Age (years) Mean ± SD	63.3 ± 14.5	62.9 ± 8.6	0.9847
Ethnicity	**n (%)**	**n (%)**	
White	8 (80.0)	7 (70.0)	
Asian	1 (10.0)	2 (20.0)	
Black	1 (10.0)	1 (10.0)	0.8187
Disease stage	**n (%)**	**n (%)**	
3	9 (90.0)	6 (60.0)	
4	1 (10.0)	4 (40.0)	0.1214
CRS	n/a	**n (%)**	
1		3 (30.0%)	
2		4 (40.0%)	
3		3 (30.0)	n/a
Cytoreduction	**n (%)**	**n (%)**	
R0	8 (80.0)	6 (60.0)	
R1	1 (10.0)	1 (10.0)	
R2	1 (10.0)	3 (30.0)	0.5258
Omental disease	**n (%)**	**n (%)**	
Present	8 (80.0)	9 (90.0)	
Absent	2 (20.0)	1 (10.0)	0.5312
Recurrence	**n (%)**	**n (%)**	
Disease-free	7 (70.0)	2 (20.0)	
Recurred	3 (30.0)	8 (80.0)	**0.0246**
Survival	**n (%)**	**n (%)**	
Died	3 (30.0)	8 (80.0)	
Alive	7 (70.0)	2 (20.0)	**0.0246**

6.2.2.3 Analysis of NK cell cytokine production

Following the culture of each PBMC sample, both in isolation (unstimulated) and in combination with K-562 cells (stimulated), the proportions of NK cells that produce cytokines were determined. The proportion of each NK cell population in the stimulated and unstimulated samples obtained from healthy donors were compared to the stimulated and unstimulated samples in the OC groups. Figure 6.20 demonstrates the proportion of NK cells within each of these groups: there was an increase in the percentage of NK cells in the

stimulated samples from the healthy donors when compared to the corresponding unstimulated samples (p = 0.0355). This determines that the healthy donor NK cells have the ability to proliferate and expand upon interaction with cells that have lost HLA expression. In contrast, there were no significant differences between the stimulated and unstimulated NK populations in either of the OC groups, regardless if the patients were previously exposed to chemotherapy. These results suggest that peripheral NK cells in OC patients have either lost their ability to expand when tumour cell HLA expression is reduced. This can be explored further and validated through the co-culture of NK cells with ovarian cancer cell lines that have confirmed HLA expression as well as with ovarian cancer cell lines that have lost MHC class I expression and should therefore stimulate the NK cells.

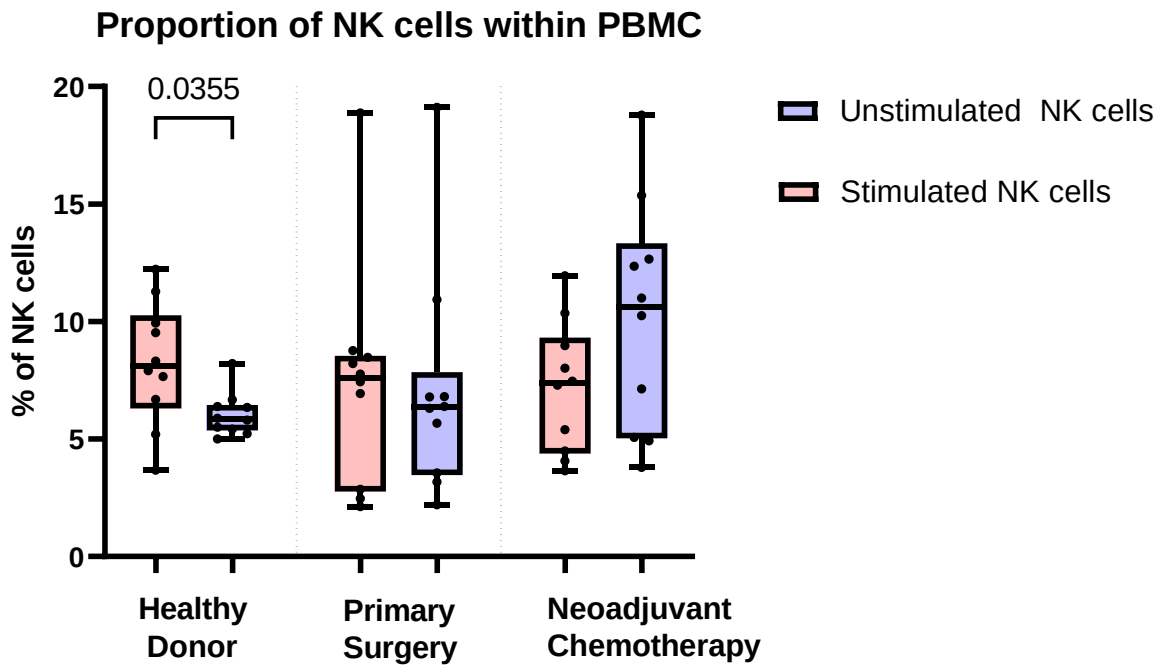


Figure 6.20: Proportion of NK cells within unstimulated and stimulated PBMC samples.
There was an increase in the proportion of NK cells within the stimulated samples from healthy donors compared to the unstimulated healthy donor samples. There were no significant differences in the proportions of NK cells between stimulated and unstimulated samples from patients undergoing primary surgery and neoadjuvant chemotherapy.

Once the NK cell populations had been identified, the percentage of the cytokines produced by the NK cells in each sample could be determined. Table 6.4 displays the mean percentage of each cytokine produced by the NK cells in stimulated and unstimulated samples from healthy donors, primary surgery patients and neoadjuvant chemotherapy patients. The healthy donor samples demonstrated increased production of all cytokines (except for IL-10) upon stimulation when compared to unstimulated NK cells. Similarly, stimulated NK cells in OC patients also produced greater amounts of cytokines when compared to unstimulated NK cells. Comparatively, NK cells from heathy donors, both stimulated and unstimulated, had an increased mean production of all cytokines when compared to OC patients. There was no difference in cytokine production between the two OC groups.

Table 6.4: Mean percentage of cytokines produced by stimulated and unstimulated NK cells within PBMC samples.

Cytokine	Healthy Donor (n=10) Mean production (%)		Primary Surgery (n=10) Mean production (%)		Neoadjuvant Chemotherapy (n=10) Mean production (%)	
	Unstimulated	***Stimulated***	***Unstimulated***	***Stimulated***	***Unstimulated***	***Stimulated***
TNF-α	3.5	5.1	2.2	3.1	1.1	2.4
GM-CSF	2.1	4.2	1.6	2.5	0.9	2.8
IL-2	2.3	4.1	1.8	2.5	1.4	2.2
IFN-ɣ	3.0	3.4	2.3	2.6	1.3	1.7
IL-10	2.9	2.1	0.9	1.4	1.0	1.1
TGF-β	2.5	3.7	2.3	2.4	2.0	2.2

Figure 6.21 shows the proportion of cytokines produced by unstimulated NK cells in healthy donors (HD) and OC patients (primary surgery and neoadjuvant chemotherapy groups). The same analysis was then performed for the stimulated NK cells, shown in Figure 6.22. For the unstimulated NK cells, there were significantly less cytokines (TNF-α, GM-CSF, IL-10 and IFN-γ) produced by the NK cells in the neoadjuvant chemotherapy group when compared to the healthy donor NK cells. In the primary surgery group, there was reduced IL-10 production by the unstimulated NK cells compared to the healthy donor samples. In the K562 stimulated NK cells, the neoadjuvant chemotherapy group produced significantly decreased amounts of TNF-α, IFN-γ and IL-2 compared to the healthy donor group, while the primary surgery group also produced less IL-2 than the healthy donor group.

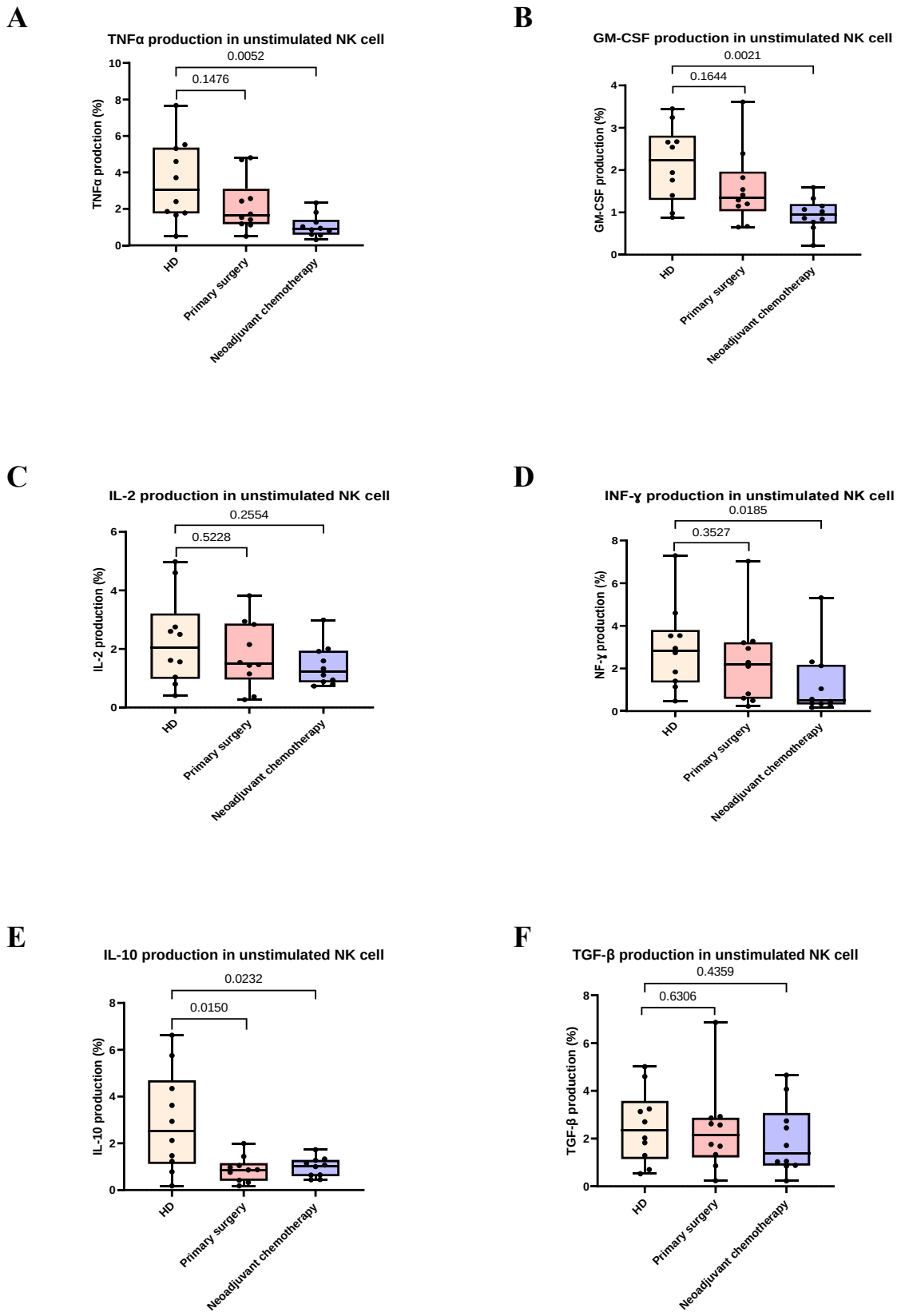


Figure 6.21: Cytokine production from unstimulated peripheral NK cells.
Production of A) TNF-alpha, B) GM-CSF, D) IFN-gamma, and E) IL-10 was significantly reduced in the neoadjuvant chemotherapy group compared to the healthy donor group. The primary surgery group had significantly decreased production of E) IL-10 compared to the healthy donor group. There was no difference in the production of C) IL-2 and F) TGF-beta between the groups.

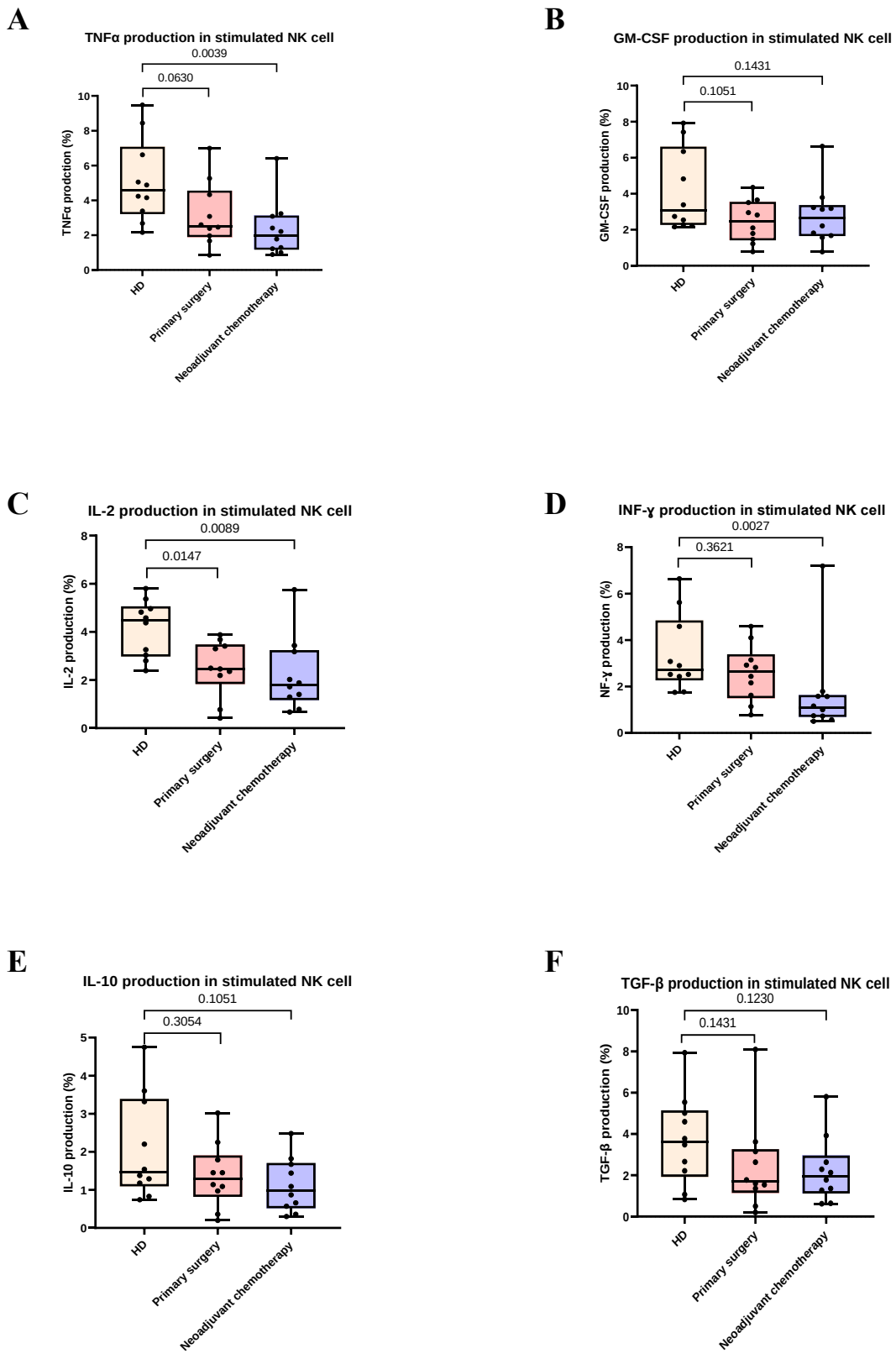


Figure 6.22: Cytokine production from stimulated peripheral NK cells

Production of A) TNF-alpha, C) IL-2, and D) IFN-gamma was significantly lower in the neoadjuvant chemotherapy group compared to the healthy donor group. The primary surgery group produced significantly less C) IL-2 than the healthy donor group. There was no difference in the production of B) GM-CSF, E) IL-10, and F) TGF-beta between the groups.

Next, the increased percentage of cytokine production following NK stimulation was calculated by comparing the unstimulated and stimulated NK cells. Figure 6.23 shows that there is an increase in TNF-alpha, GM-CSF, IL-2 and IFN-γ production following NK stimulation in each of the healthy donor, primary surgery OC and neoadjuvant chemotherapy patients. Although the increase in TNF-alpha, GM-CSF and IL-2 levels following stimulation appeared to be greater in healthy donors than the two OC groups, the difference was not significant. The production of Il-10 decreased in the healthy donor group upon stimulation, while there was no significant change in IL-10 production following stimulation in the primary surgery and neoadjuvant chemotherapy OC patients. The production of TGF-beta was similar before and after NK stimulation between the groups. Figure 6.24 shows the same evaluation, observing the increase in cytokine production following NK stimulation, but compares healthy donor samples to the OC groups combined. The findings were similar, however the increase in IL-2 production following NK stimulation in the healthy donor samples was significantly higher than in the combined OC samples ($p = 0.0357$).

The healthy donor NK cells produced greater amounts of every cytokine compared to the NK cells from the OC patients. The decreased ability of OC NK cells to produce cytokines was seen prior to NK stimulation (representing baseline NK activation) as well as following exposure to HLA-deficient cells. The sustained lack of cytokine production from the peripheral OC NK cells, despite direct stimulation, represented a dysfunctional NK response in cases of ovarian malignancy. While the significant cytokine reductions occurred more frequently when comparing healthy donor NK cells to those exposed to chemotherapy, there were no significant differences in cytokine production between the primary surgery and neoadjuvant chemotherapy groups. This demonstrated that chemotherapy treatment did not impact upon the ability of OC NK cells to produce cytokines, regardless of any NK

stimulation. By deducting the baseline cytokine production (cytokines produced by unstimulated NK cells) from the amount produced by stimulated NK cells, the NK response to K-562 stimulation and the ability to increase cytokine production could be determined. There was no significant difference between the groups, except the increase in IL-2 production following stimulation by the non-cancerous samples compared to the OC samples combined. This implies the NK response and the potential to produce cytokines with NK stimulation, in general, does not differ between healthy donor and OC patients.

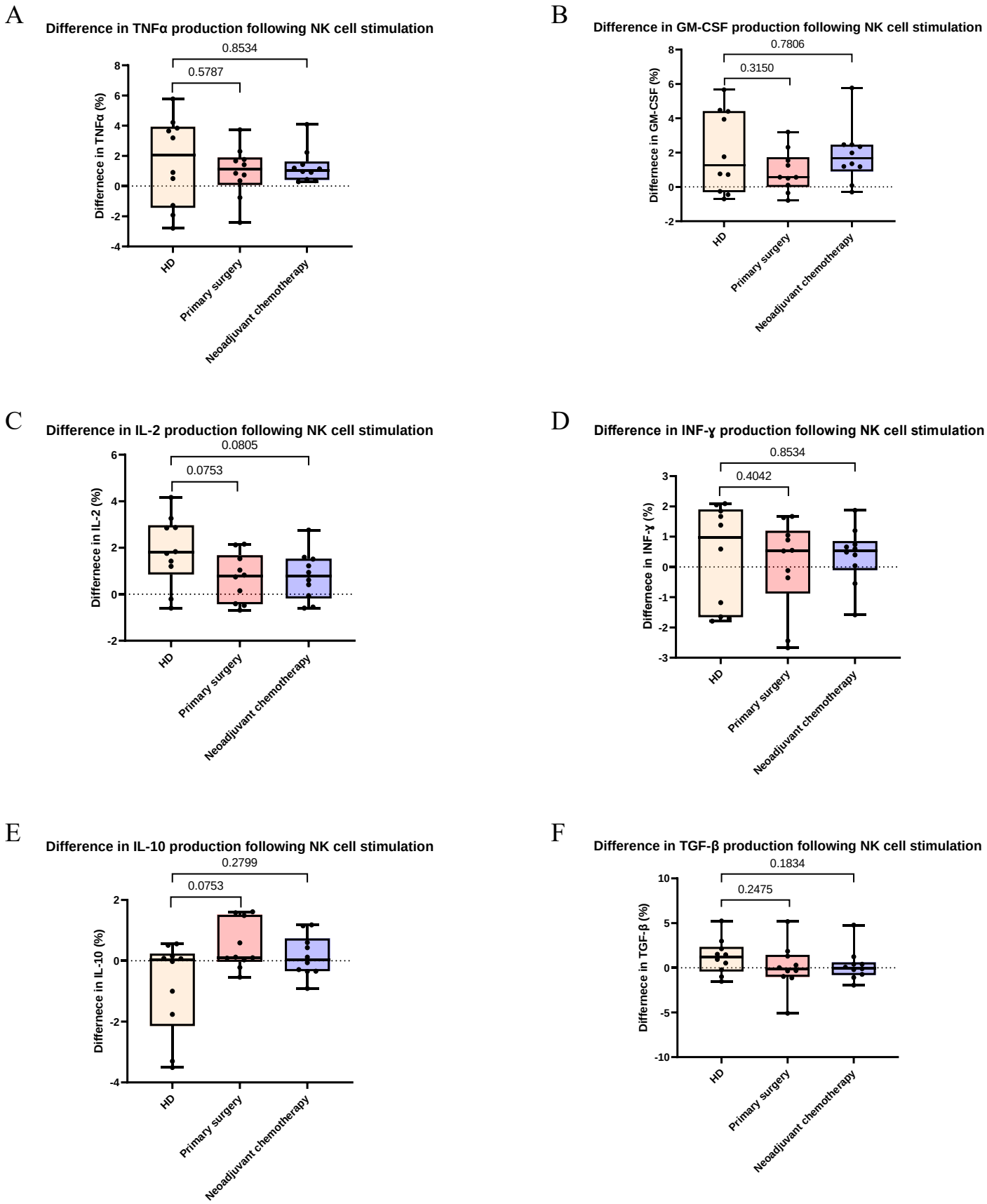


Figure 6.23: The difference in cytokine production between unstimulated and stimulated NK cells in healthy donor, primary surgery and neoadjuvant chemotherapy samples.

The difference in the production of A) TNF-alpha, B) GM-CSF, C) IL-2, D) IFN-gamma, E) IL-10, and F) TGF-beta in healthy donor (HD), primary surgery and neoadjuvant chemotherapy groups following NK cell stimulation. The NK response to stimulation was similar between the groups.

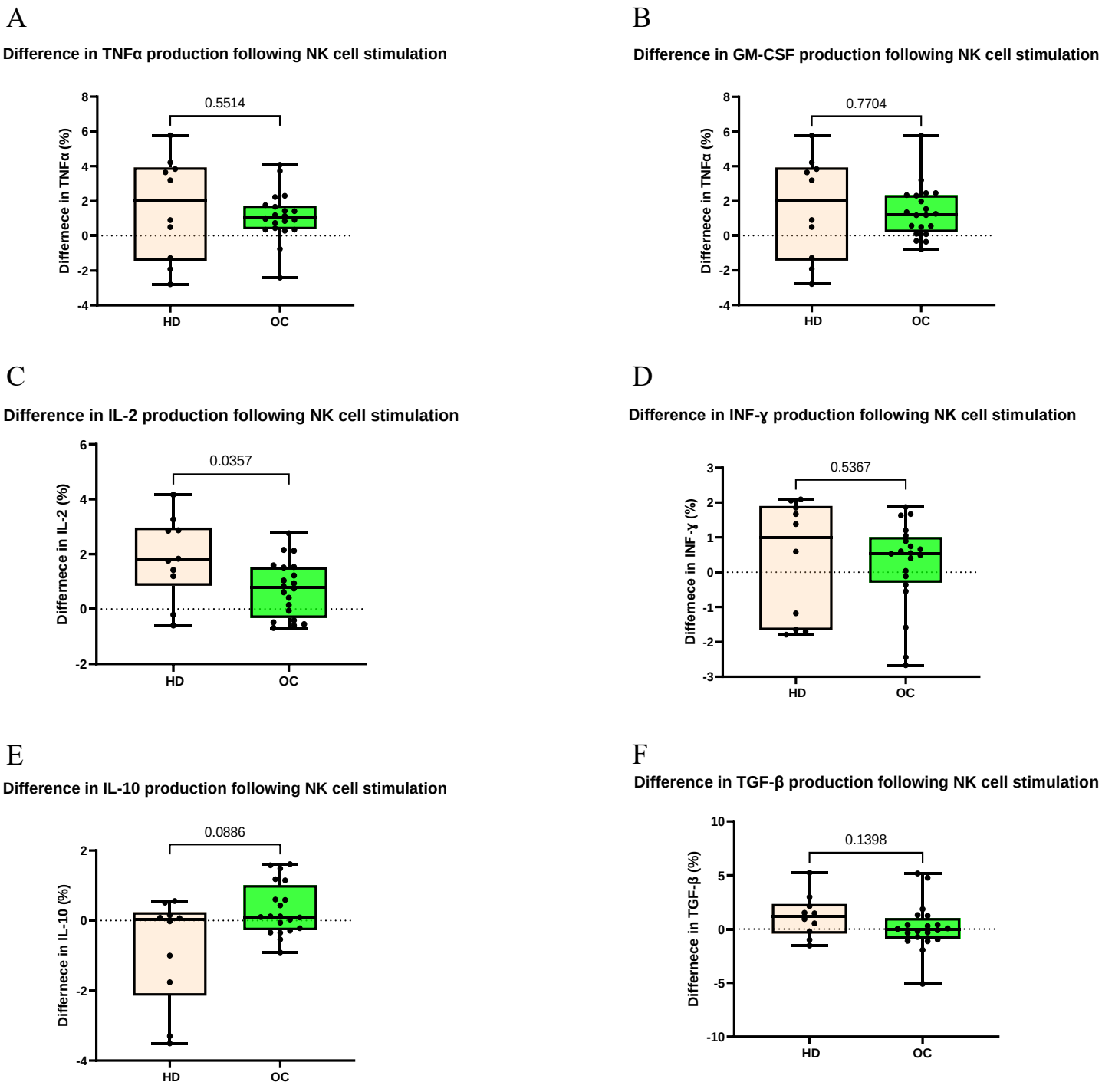


Figure 6.24: The difference in cytokine production between unstimulated and stimulated NK cells in healthy donor and combined OC samples.

The difference in the production of A) TNF-alpha, B) GM-CSF, C) IL-2, D) IFN-gamma, E) IL-10, and F) TGF-beta in healthy donor (HD) and OC groups following NK cell stimulation. The NK response to stimulation and the resulting alterations in cytokine production were similar between the healthy donor and OC groups, apart from greater IL-2 production by the HD samples.

6.2.2.4 Correlations between NK cytokine production and clinical outcomes

Further analyses were undertaken to evaluate the association of NK stimulation and cytokine production with clinical findings and patient outcomes. First of all, the effects of NK stimulation and differences in NK cytokine production were compared between patients who had metastatic omental disease and those with normal omentum. There were 3 OC patients without histological evidence of omental metastasis; the average proportion of peripheral NK cells in these patients was 6.0% prior to stimulation, increasing to 8.2% following NK stimulation ($p = 0.0310$). In contrast, the average proportion of peripheral NK cells in the 17 patients with omental metastasis decreased significantly from 9.1% to 7.1% following stimulation ($p = 0.0120$). While the PBMC NK cells from patients without omental metastasis underwent proliferation upon stimulation as expected, the NK cells from cases with omental metastasis were unable to expand with stimulation. Figure 6.25 demonstrates the PBMC NK cell expansion in response to stimulation in patients with normal omentum, although not significant ($p = 0.1000$). There was no change in the proportion of NK cells with stimulation in the patients with omental tumours.

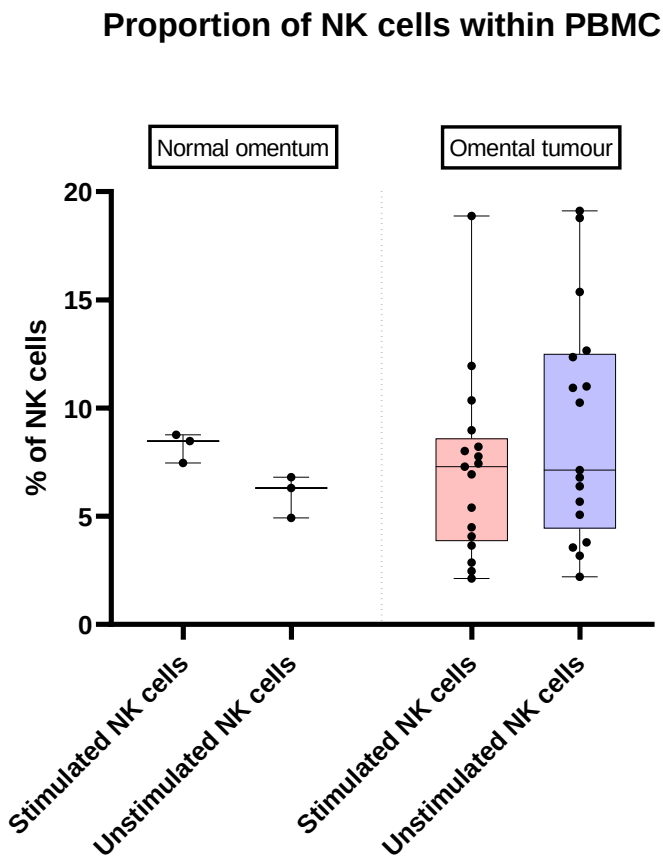


Figure 6.25: Proportion of peripheral NK cells in OC patients based on presence of omental disease.
There was an increase in the proportion of PBMC NK cells following stimulation in the samples from OC patients with normal omentum, although not significantly so ($p = 0.1000$). There was no difference in the amount of NK cells following stimulation in the PBMC samples from OC patients with omental tumours.

Of the 20 OC patients evaluated, a total of 11 suffered a disease recurrence while 9 remained free of disease. There were no differences in the proportion of peripheral NK cells, either before or after stimulation, between the patients who had a recurrence and those who did not (Figure 6.26). This suggests both groups of patients have a similar NK response upon interaction with cells deficient in HLA. In addition, the production of cytokines from stimulated NK cells was similar between those who recurred and those who were disease free (Figure 6.27). The same 11 patients who suffered disease recurrence subsequently died from

the disease shortly after. Thus, there was also no difference in NK cell expansion and cytokine production following stimulation between those patients who were alive and those who died from OC.

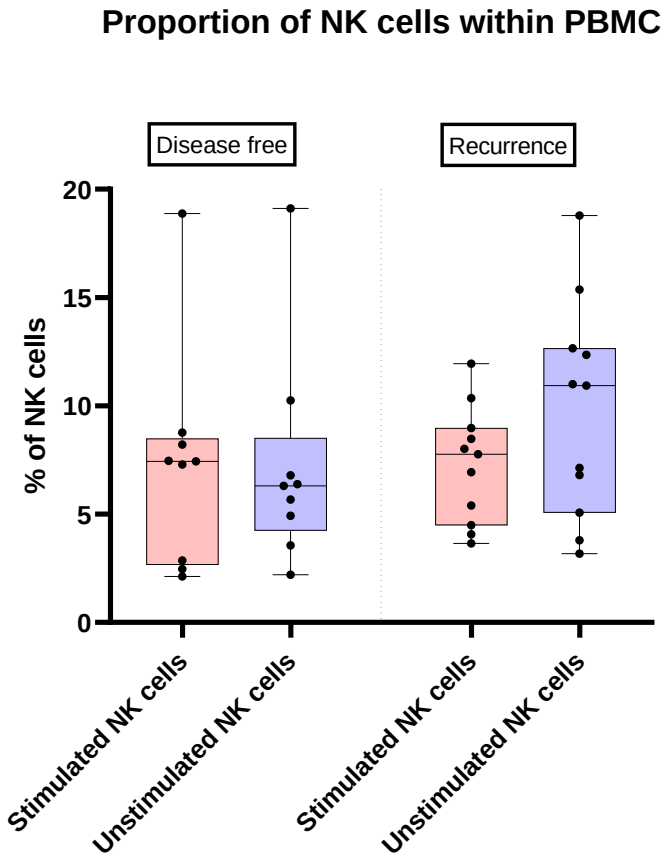


Figure 6.26: The proportion of NK cells with and without stimulation in OC patients who suffered a recurrence of disease compared to those who remained disease free.
There were no differences in the proportion of NK cells following stimulation.

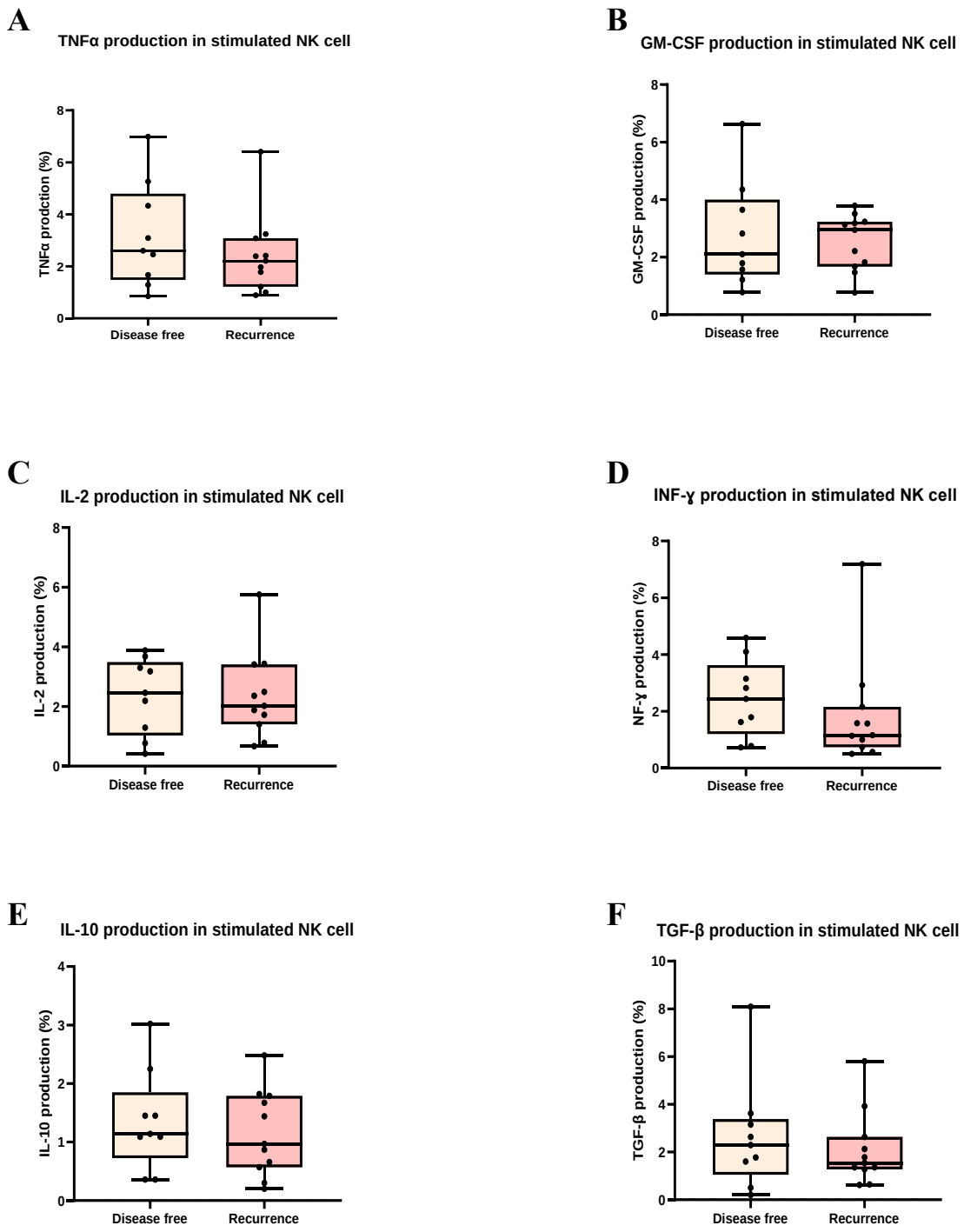


Figure 6.27: Cytokine production in stimulated NK cells based on disease recurrence.
There were no differences in the production of cytokines in patients who remained free of disease compared to those who suffered a recurrence of disease.

To facilitate further analysis on clinical outcomes, the 20 OC patients were then divided into two groups based on the level of cytokine production from the stimulated NK cells: those with cytokines production below the median value (low cytokine production) and above the median (high cytokine production). Progression free survival (PFS) and overall survival (OS) were then measured within these 2 groups of patients as shown in Figure 6.28 and Figure 6.29. There were no differences in PFS and OS with regards to the level of cytokine production.

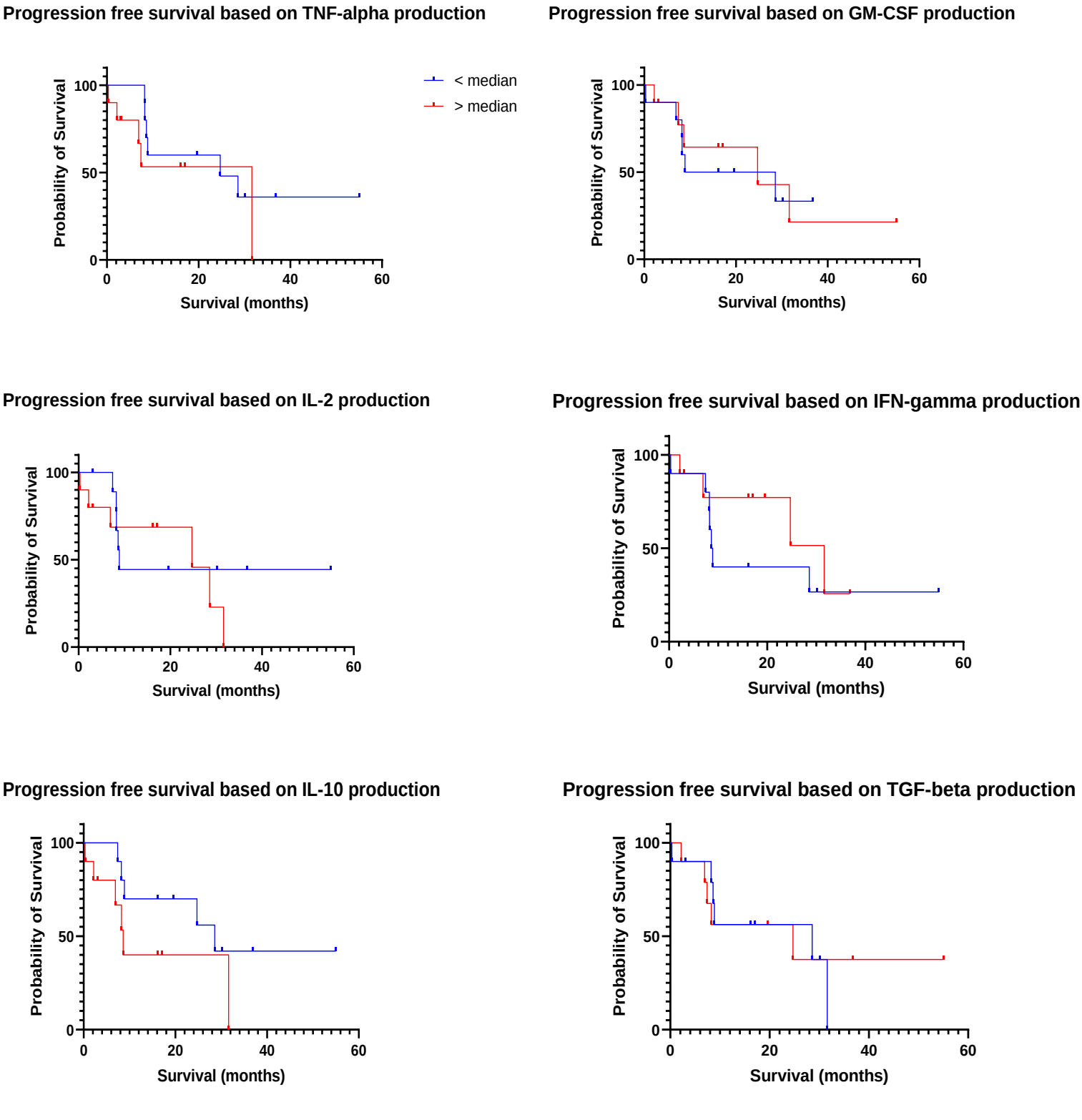


Figure 6.28: Kaplan-Meier plots demonstrating progression free survival in OC patients based on the level of cytokines produced by NK cells.

There were no differences in PFS with low or high NK cell cytokine production.

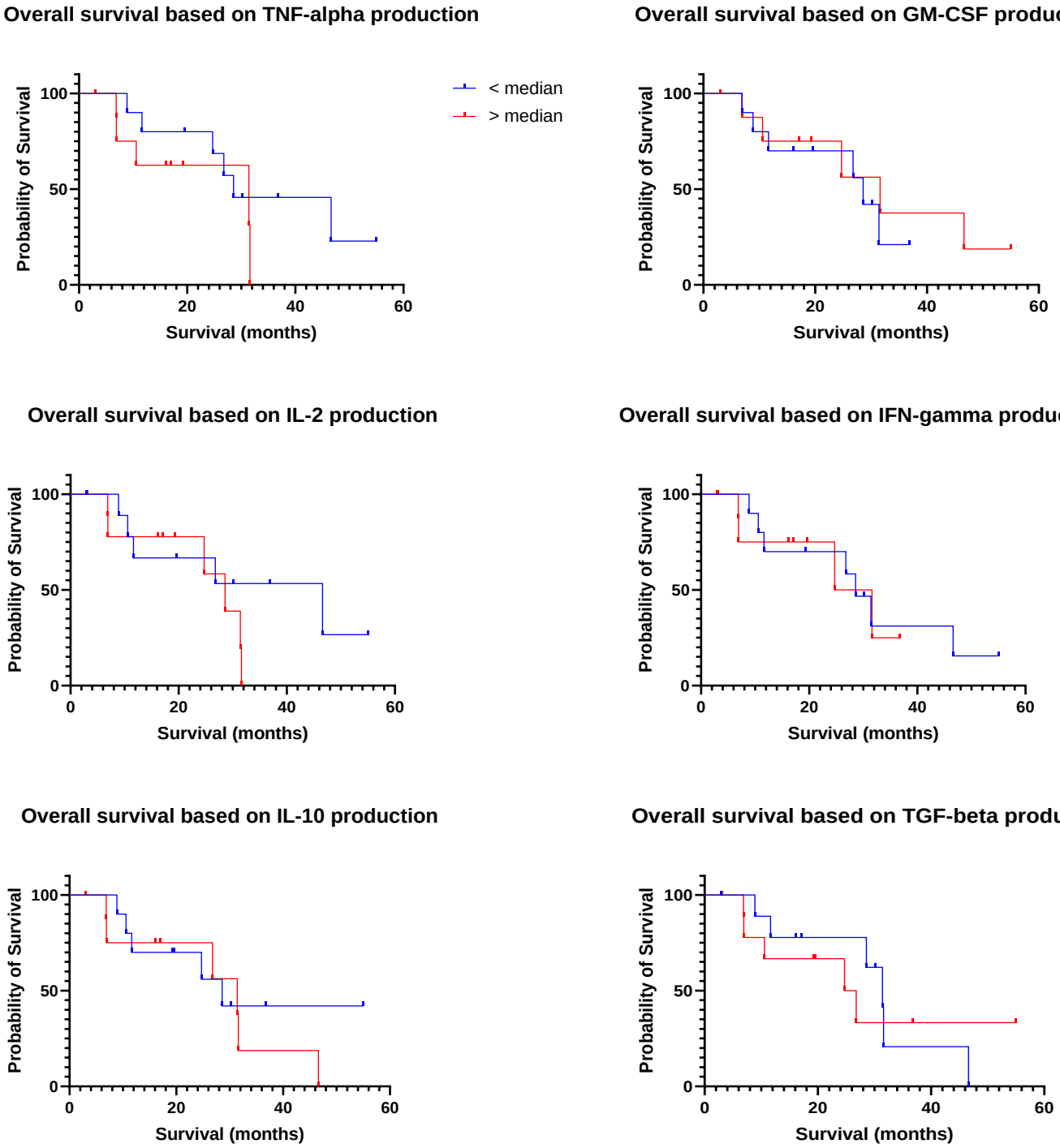


Figure 6.29: Kaplan-Meier plots demonstrating overall survival in OC patients based on amount of cytokine production.

There were no differences in OS with low or high NK cell cytokine production.

6.2.2.5 Correlations between NK cell cytokine production and NK phenotype

The cytokines produced by the stimulated peripheral NK cells from the OC patients were then correlated to the flow cytometry NK phenotype data. The degree of cytokine production was again characterised as being low (below the median value) or high (above the median value), and was compared to the NK subpopulations in the PBMC samples. For each of the six cytokines investigated in this study, the proportion of each NK subpopulation (based on CD56 and CD16 expression) was determined in both of the low and high cytokine groups. The samples with high levels of TNF-alpha, IL-2, IFN-gamma and IL-10 had significantly more $D56^{bri}CD16^{bri}$ NK cells than the samples with low levels of cytokines. There was no difference in this NK subtype based on GM-CSF and TGF-beta production levels. The other NK subtypes were similar between the low and high cytokine groups, shown in Figure 6.30.

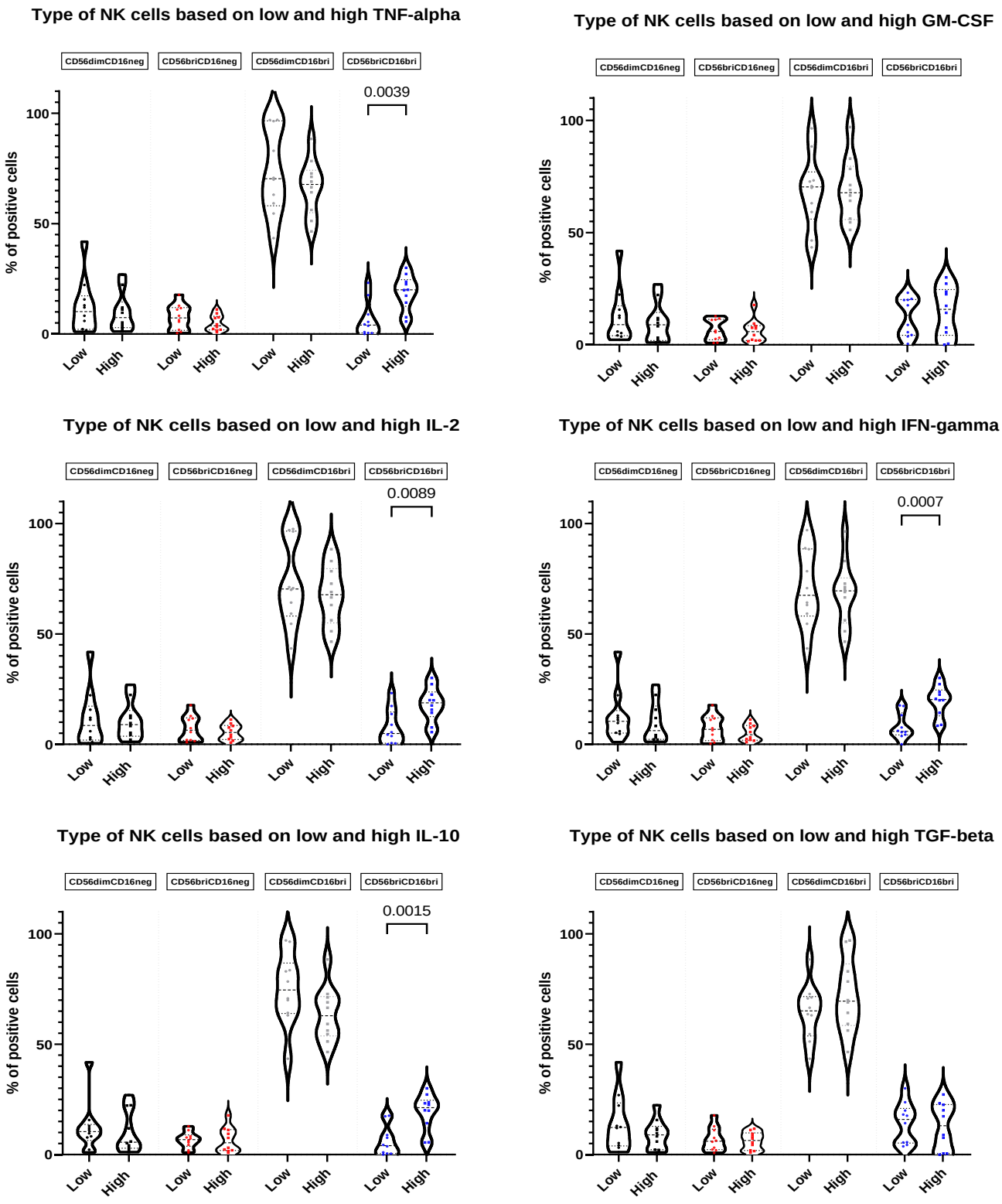


Figure 6.30: Comparison of the proportion of NK cell subpopulations between patients with high and low cytokine production.

There were significantly more $CD56^{bri}CD16^{bri}$ NK cells with high production of TNF-alpha, IL-2, IFN-gamma and IL-10 compared to the cohort with low cytokine production.

The cytokines produced (again categorised as low or high levels of production) by the stimulated peripheral NK cells from OC patients were correlated to the expression of the receptors on the NK cells. Figure 6.31 shows that there were significantly higher levels of NKG2D expression and CD57 expression in the NK cells with high TNF-alpha production compared to NK cells with low TNF-alpha production. There were no associations between the expression of activation receptors NKp46, DNAM-1 and NKG2C and the degree of cytokine production. Focusing on the inhibitory receptors (Figure 6.32), the immune checkpoints CTLA-4 and PD-1 were significantly increased in the NK cells with reduced GM-CSF. PD-1 expression was also upregulated in the NK cells with low IFN-gamma production. There were no alterations in CD94 expression between the cytokine groups, but the expression of TIGIT was greater in NK cells that had high production levels of TNF-alpha, IL-2 and IL-10. These correlations suggest that when the peripheral NK cells in OC patients are activated, along with the upregulation of activation receptors, production of TNF-alpha increases. Supporting this notion, greater NK cell checkpoint inhibition was related to poorer cytokine secretion. In contrast, the upregulation of TIGIT was associated with high cytokine production. TIGIT is also known as an activating receptor for NK cells during the early stage of NK activation. Thus, these findings could represent an escape mechanism whereby the tumour cells attempt to inhibit a stimulated NK cell by causing upregulation of the inhibitory receptor.

.

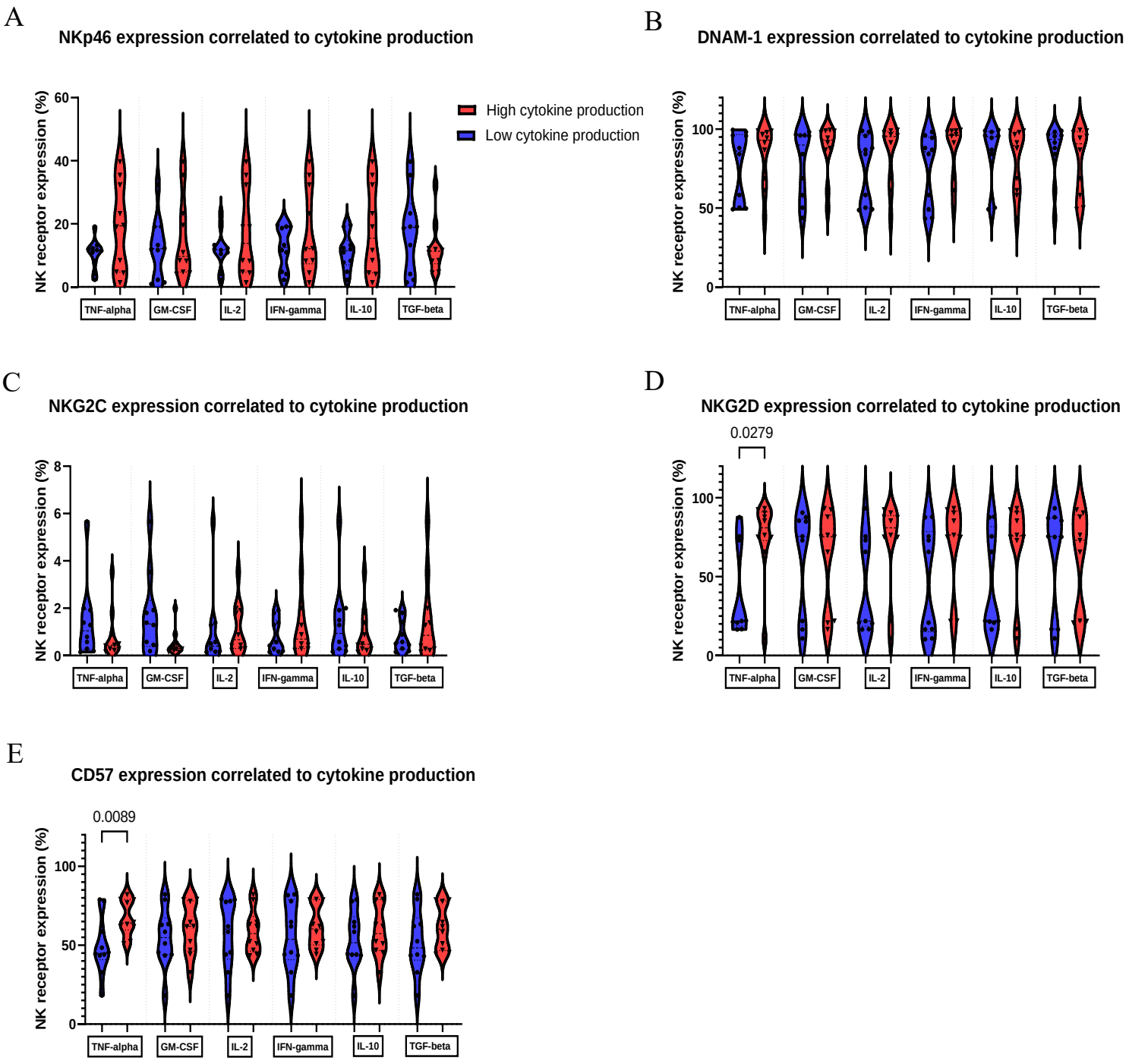


Figure 6.31: The correlation between the expression of NK activation receptors and degree of cytokine production.

There was significantly higher NKG2D (D) and CD57 (E) expression in the cohort with high TNF-alpha production compared to the cohort with low TNF-alpha production. There were no differences in NKp46 (A), DNAM-1 (B), or NKG2C (C) expression based on low or high cytokine production.

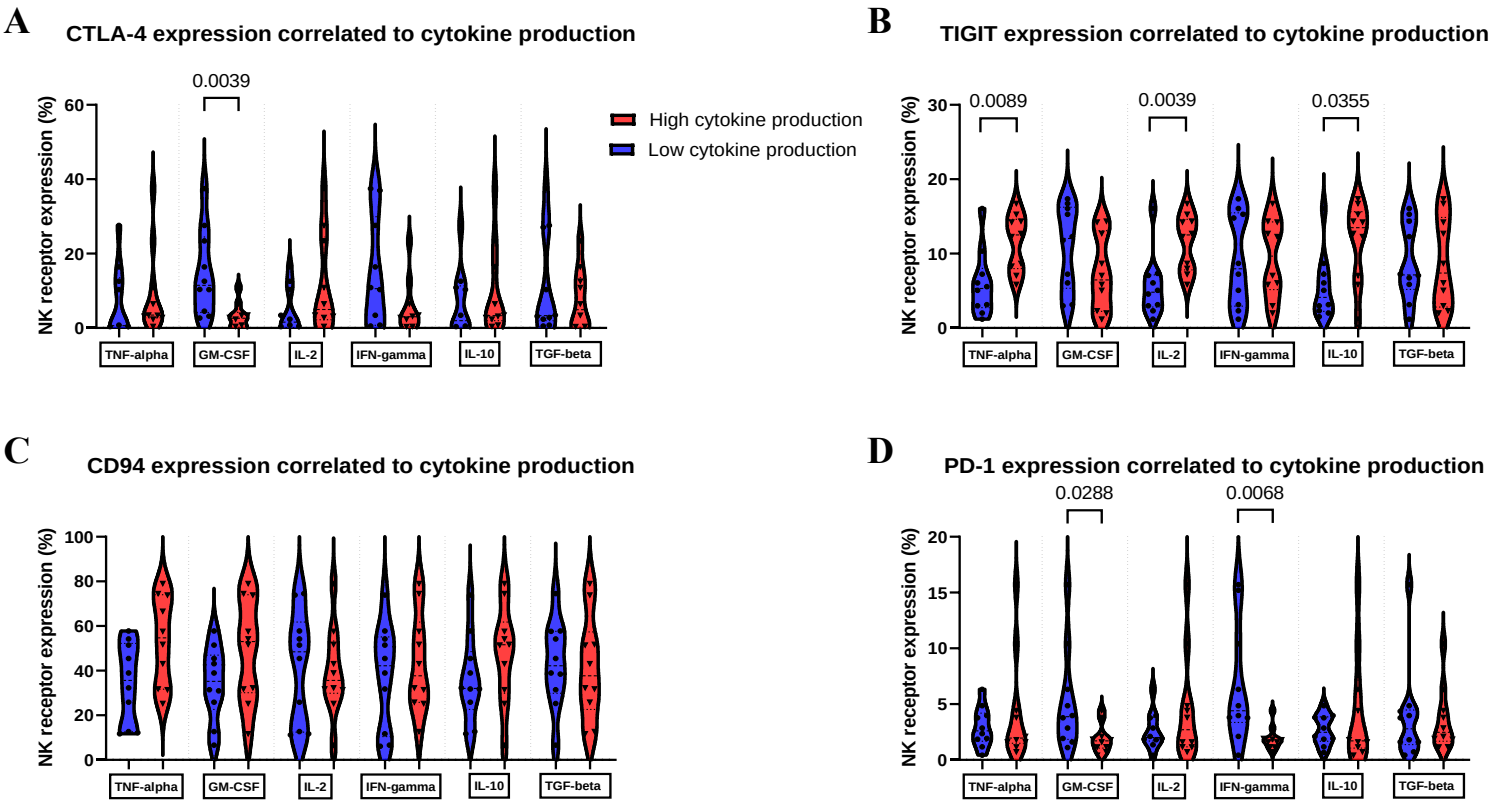


Figure 6.32: The correlation between the expression of NK inhibitory receptors and degree of cytokine production.
There was significantly increased immune checkpoint inhibitors CTLA-4 (A) and PD-1 (D) expression in the cohort with low GM-CSF. PD-1 was also raised in the cohort with low IFN-gamma. The expression of TIGIT (B) was greater in the cohorts with high production of TNF-alpha, IL-2 and IL-10.

6.2.3 Summary of peripheral NK cell function

The function of the peripheral NK cells in OC patients was explored by interrogating NK cell cytotoxicity and cytokine production. Utilising the HLA-deficient cell line, K-562, NK cells were stimulated to emulate their response in the ovarian tumour environment where malignant cells lack HLA. The killing ability achieved by the NK cells was evaluated using an OC patient cohort and comparing to healthy donor non-cancerous cases that shared similar

demographic characteristics. Here, the OC NK cells demonstrated increased cytotoxicity compared to controls, regardless of chemotherapy exposure, which did not enhance or hinder the NK response in the OC patients. However, there was no clear association between cytotoxicity and the presence of omental metastasis, PFS and OS. In addition, the proportions of peripheral cells and NK subtypes were not influenced by the degree of cytotoxicity. The expression of NK receptors was also not associated to NK cell killing, except for decreased NKG2C and raised NKp46 in the NK cells with higher levels of cytotoxicity. This increase in NKp46 with greater NK cytotoxicity correlates with the previous finding of a greater PFS with higher NKp46 expression.

The functional capability of peripheral NK cells to produce cytokines was also examined in a cohort of OC patients and healthy donor controls. While the OC NK cells demonstrated a reduced ability to proliferate and expand upon exposure to cells lacking HLA, their cytokine production improved following direct stimulation. However, the OC NK cells (both unstimulated and stimulated) secreted fewer cytokines than the NK cells in the corresponding healthy donor samples. The NK response to stimulation and the ability to increase cytokine production was similar between healthy donor and cancer samples, except for an increase in IL-2 production by the healthy donor samples compared to the OC samples. This implies there is a lack of cytokine production from peripheral OC NK cells, yet the response to stimulation is comparable with healthy controls.

Again, chemotherapy treatment did not influence NK cell function and cytokine production when compared to chemotherapy naïve NK cells from OC patients. In addition, PFS and OS were not affected by the ability of NK cells to produce cytokines. However, there were changes in the phenotype of the NK cells based on the cytokines produced. There was a

greater proportion of $CD56^{bri}CD16^{bri}$ NK cells and increased expression of activation receptors (NKG2D, CD57) in patients with higher cytokine levels. Similarly, in those with low cytokine levels, there was a greater proportion of NK cells expressing checkpoint inhibition receptors CTLA-4 and PD-1.

In summary, the peripheral NK cells in OC patients are highly cytotoxic, which corresponds with the NK phenotype study (chapter 4) that demonstrated activated NK cells. However, their killing ability does not correlate with clinical outcomes, likely due to the cohort size. The dysfunctional NK cells in OC patients lack the ability to expand following stimulation and have poor cytokine secretion, which is related to the higher expression of checkpoint inhibitor receptors, but again has no relation to clinical outcomes.

6.3 Interaction between ovarian tumour tissue and NK cells

6.3.1 Identification of NK cell ligands on tumour tissue

This analysis explored the ligands expressed on ovarian tumour tissue to gain an understanding of the interactions between malignant ovarian cells and the tumour infiltrating NK cells, as well as evaluating the immune evasion mechanisms utilised by the tumours. The specific ligands which induce activation of NK cells were interrogated: MICA, MICB and ULBP1/2/3/4 which bind to NK activation receptor NKG2D; along with PVR and PVRL2 which bind to activating receptor DNAM-1. NK cell inhibiting ligands were also included in this study: PDL-1 which binds to the immune checkpoint inhibitor PD-1; HLA-E which binds to inhibiting receptors CD94 and NKG2A; HLA-A and HLA-C which are involved in "self" recognition by NK cells; and HLA-DR which is a ligand for inhibiting receptor LAG3 [375].

Real-time quantitative PCR (qPCR) was undertaken to determine the transcription patterns of the NK ligands, as described in the Methods section 2.2.6. Snap frozen, solid tissue biopsies were obtained from both ovarian tumours and benign ovaries, with copy numbers of NK ligand target genes compared to the transcription of reference genes 18S and B2M (β2-microglobulin). This housekeeping control genes normalised any discrepancies in qPCR findings, specifically disparities in cDNA quantity and copy number variation between samples [376-379]. The ratios obtained gave standardised transcription levels for each target gene in both the benign and tumour biopsies.

6.3.2 The study cohort for NK ligand analysis

To explore the NK ligands on ovarian tissue samples, a total of 30 solid tissue biopsy samples from the original study cohort were processed. This included 16 ovarian tumour biopsies from patients with stage III or IV HGSOvCa. There were a further 14 samples from patients with a benign ovarian mass, including ovarian fibroma, cystadenoma and simple cyst. The characteristics of the patients within the HGSOvCa and benign cohorts are shown in Table 6.5. These included 11 OC patients who had not received any previous chemotherapy, with their tissue biopsies collected at the time of primary debulking surgery, and 5 women who had received either three or four cycles of neoadjuvant chemotherapy (NACT), with biopsies obtained at interval debulking surgery. Complete surgical cytoreduction was achieved in 81.3% (n=13/16) of the OC patients, with 60.0% (n=3/5) of those who had neoadjuvant chemotherapy treatment demonstrating a complete chemotherapy response. Within the cohort of OC patients, 56.3% (n=9/16) developed disease recurrence and 50.0% subsequently died at the time of analysis (average follow-up of 26 months).

Table 6.5: Characteristics and outcomes of the patients included in the NK ligand analysis

Variable	Ovarian tumour (n=16)	Benign ovarian mass (n=14)
Age (years) Mean ± SD	64.1 ± 10.9	58.3 ± 14.3
Ethnicity	**n (%)**	**n (%)**
White	14 (87.5)	9 (64.3)
Asian	2 (12.5)	4 (28.6)
Black	0 (0.0)	1 (7.1)
Disease stage	**n (%)**	n/a
3	11 (68.8)	
4	5 (31.3)	
Chemotherapy	**n (%)**	n/a
Nil	11 (68.8)	
NACT	5 (31.3)	
CRS (n=5)	**n (%)**	n/a
2	2 (40.0)	
3	3 (60.0)	
Cytoreduction	**n (%)**	n/a
R0	13 (81.3)	
R1	2 (12.5)	
R2	1 (6.3)	
Recurrence	**n (%)**	n/a
Disease-free	7 (43.8)	
Recurred	9 (56.3)	
Survival	**n (%)**	n/a
Died	8 (50.0)	
Alive	8 (50.0)	

6.3.3 Transcription analysis of NK cell ligands on ovarian tumour tissue

The standardised transcription levels (formulated by comparing copy numbers for each target gene per 25ng of cDNA to 18S copy numbers) were obtained using qPCR. These values from HGSOvCa biopsies were compared to those from benign ovarian biopsies. The transcription levels of housekeeping gene and internal control 18S is shown in Figure 6.33, with no differences evident between the benign and malignant biopsies.

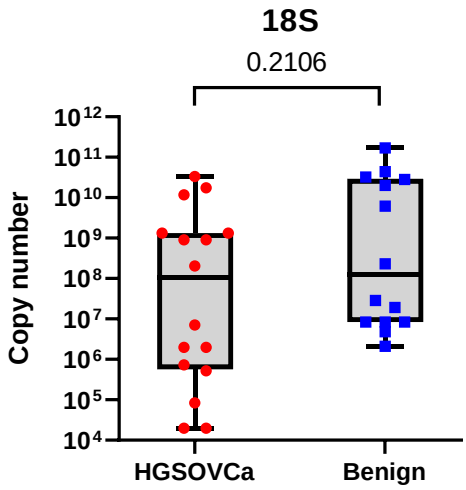


Figure 6.33: Quantitative PCR data demonstrating the transcription level of 18S within HGSOvCa and benign ovarian tissue biopsies.
There was no difference in 18S between the two groups.

The transcription level ratios for the NK ligand target genes are illustrated below. Initially focusing on the ligands for NK activation receptors, shown in in Figure 6.34, the expression levels of MICB, PVR and ULBP1 were significantly raised in the HGSOvCa tissues compared to the benign ovarian tissues ($p = 0.0279$, $p = 0.0007$ and $p = 0.0005$, respectively). There were no significant differences between the expression of MICA, PVRL2, ULBP2, ULBP3 and ULBP4 in HGSOvCa tissues and the benign ovarian tissues biopsies. Figure 6.35 shows the ratios for the inhibitory NK ligands. There was no difference in the expression levels of HLA-A, HLA-C, HLA-E, HLA-DR and PDL-1 between HGSOvCa and benign ovaries.

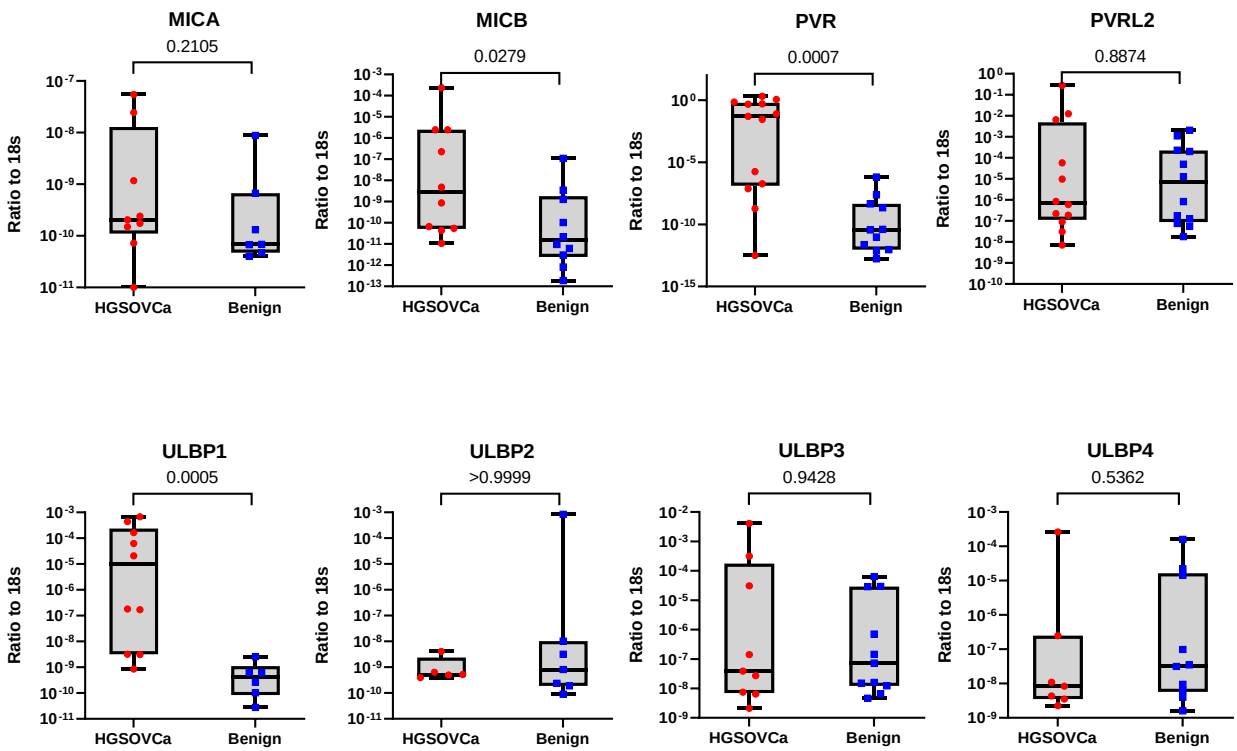


Figure 6.34: Quantitative PCR data demonstrating the relative transcription of NK cell activating ligands on HGSOvCa tissue and benign ovarian tissue.

There was significantly increased MICB, PVR and ULBP1 on HGSOvCa tissue compared to benign ovarian tissue.

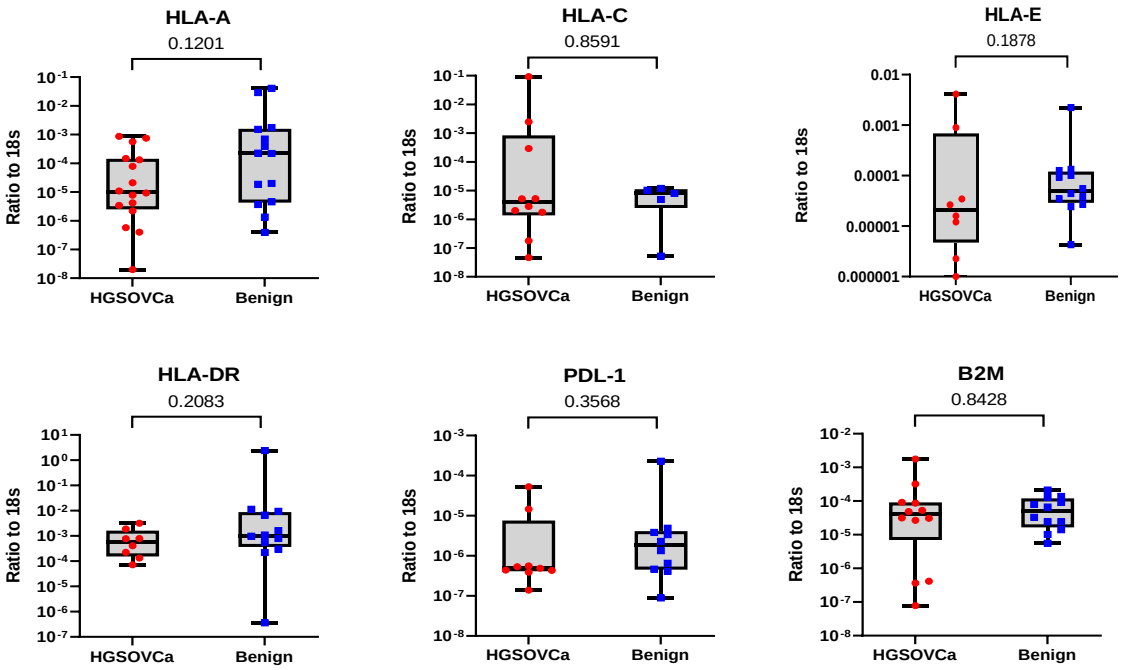


Figure 6.35: Quantitative PCR data demonstrating the relative transcription of NK cell inhibition ligands on HGSOvCa tissue and benign ovarian tissue.
There were no significant differences in the inhibitory ligands between tumour tissue and benign ovarian tissue.

6.3.4 Correlations between tumour ligands and patient outcomes

The transcription level ratios from the HGSOvCa samples were compared with clinical characteristics and outcomes. The expression of NK ligands on ovarian tumour biopsies were first compared between chemotherapy naïve (n=11) and chemotherapy exposed (n=5) patients to determine if chemotherapy treatment influences their expression. There was no observed difference in the level of expression between the two groups except for the two inhibitory ligands, PDL-1 and HLA-DR (Figure 6.36). The expression of both PDL-1 ($p = 0.0286$) and HLA-DR ($p = 0.0022$) was significantly reduced in chemotherapy exposed tumour biopsies when compared to chemotherapy naïve tissue.

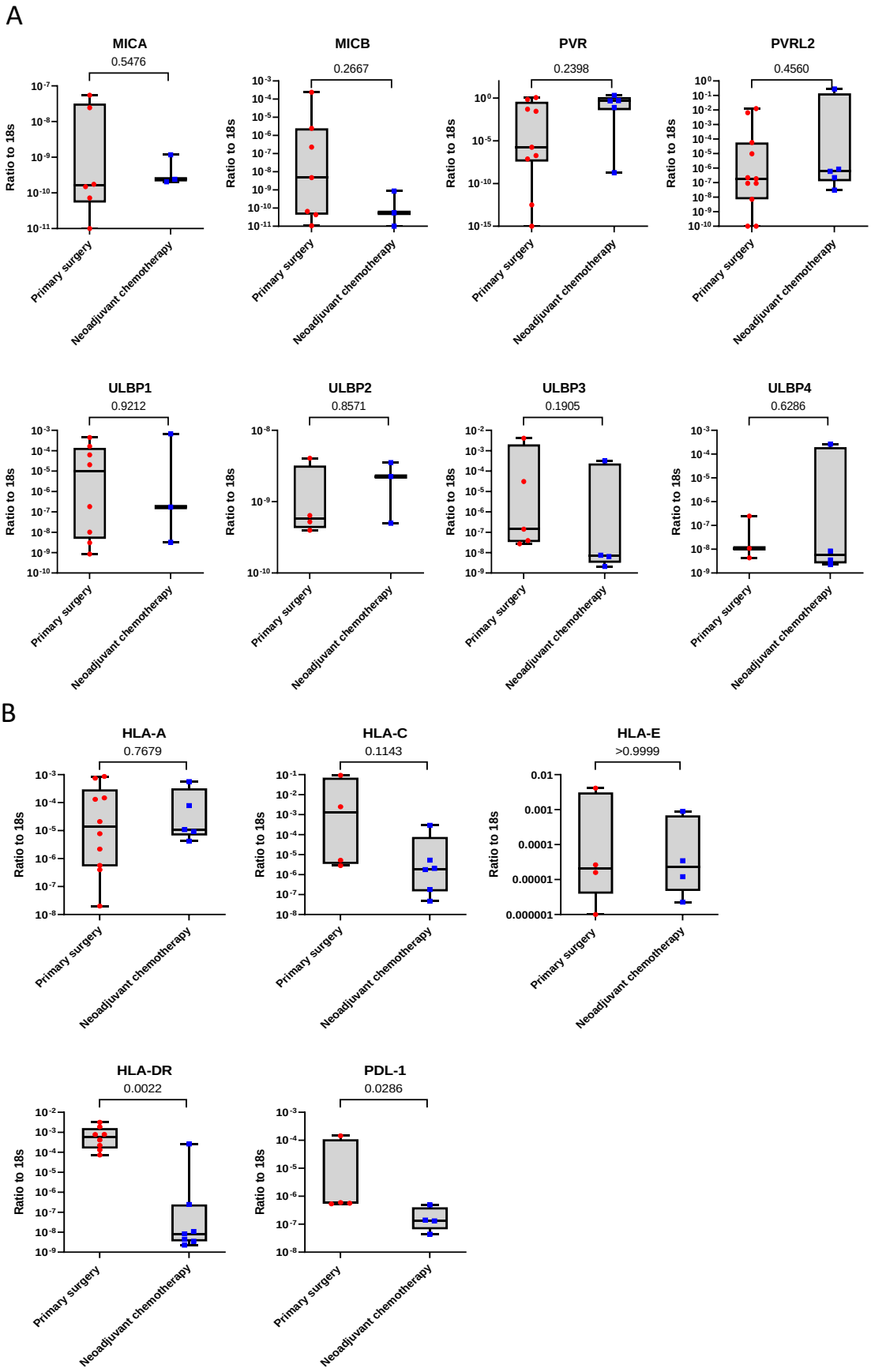


Figure 6.36: Transcription of NK ligands on HGSOvCa tissue based on chemotherapy exposure. There were no significant differences in the ligands for NK cell activation upon tumour tissue that had been exposed to chemotherapy compared to chemotherapy naïve tumour tissue (A). There was a significant reduction in the inhibitory ligands PDL-1 and HLA-DR on tumour tissue following chemotherapy treatment (B).

The transcription level ratios were then compared between the 9 patients who suffered a recurrence of disease and the 7 who remained disease free. Figure 6.37 shows that the expression of NK activating ligands, MICB and ULBP3 were significantly lower ($p = 0.0043$ and $p = 0.0419$) in the tissue biopsies from the disease recurrence group when compared to those who did not recur. Similarly, the inhibitory ligands PDL-1 and HLA-DR were reduced ($p = 0.0190$ and $p = 0.0022$) in patients with recurrent disease. Survival outcomes were then evaluated for these ligands that were associated with disease recurrence (Figure 6.38): MICB, ULBP3, HLA-DR and PDL-1 were all significantly lower in the patients who died compared to the women who were alive at the end of the study follow-up period, which had an average follow-up duration of 26 months ($p = 0.0108$ for MICB, $p= 0.0260$ for ULBP3, $p = 0.0159$ for HLA-DR and $p = 0.0079$ for PDL-1). Patients were then divided into two groups depending on their ligand transcription levels, with ratios below and above the median value classed as low and high expression, respectively. Figures 6.39 and 6.40 show that there were no differences in progression free survival and overall survival between those with low and high expression levels.

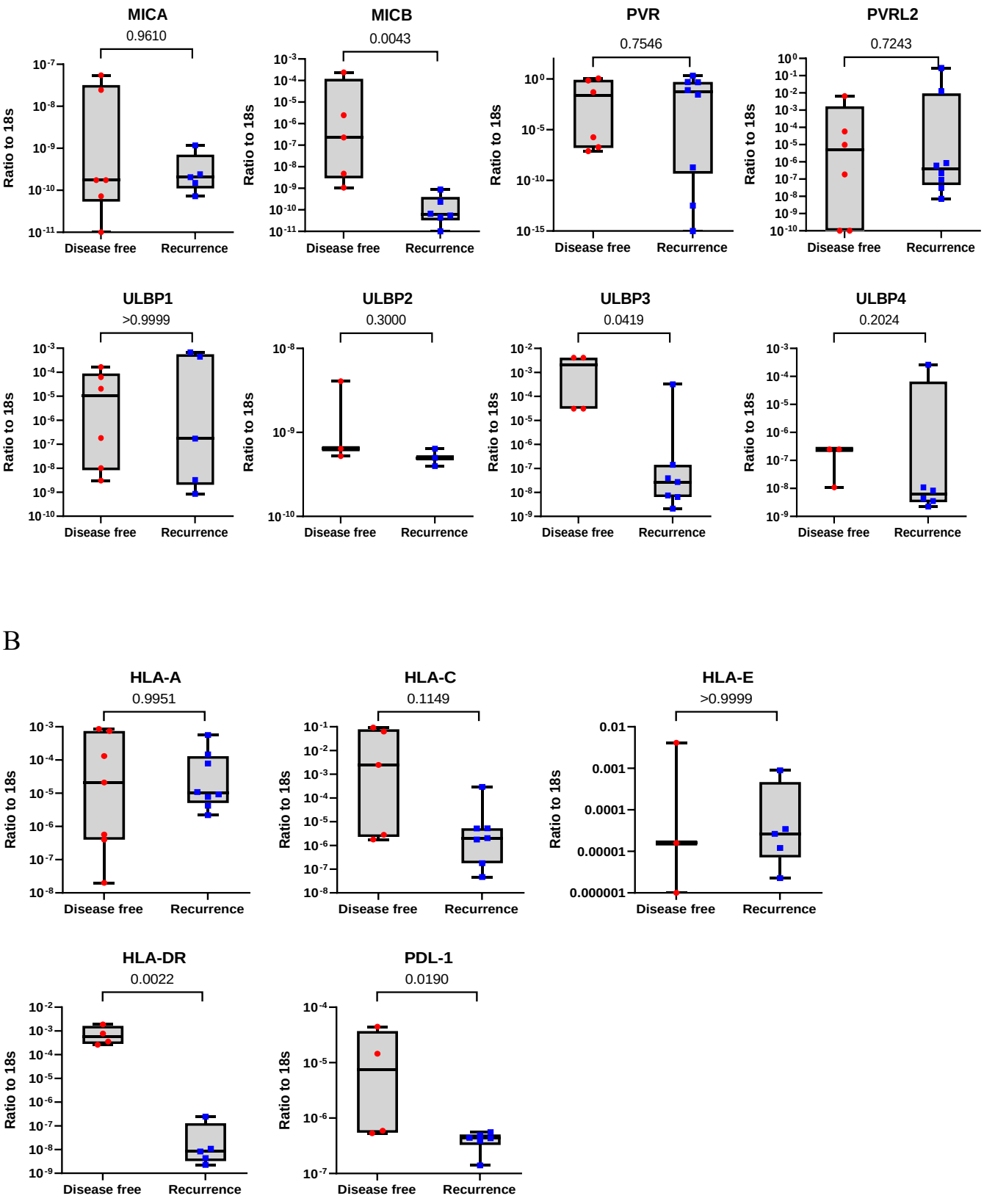


Figure 6.37: Disease recurrence and the transcription of NK ligands on HGSOvCa tissue.
The activation NK ligands MICB and ULBP3 (A) and the inhibitory ligands HLA-DR and PDL-1 (B) were decreased in patients who suffered a recurrence of disease compared to those who remained disease free.

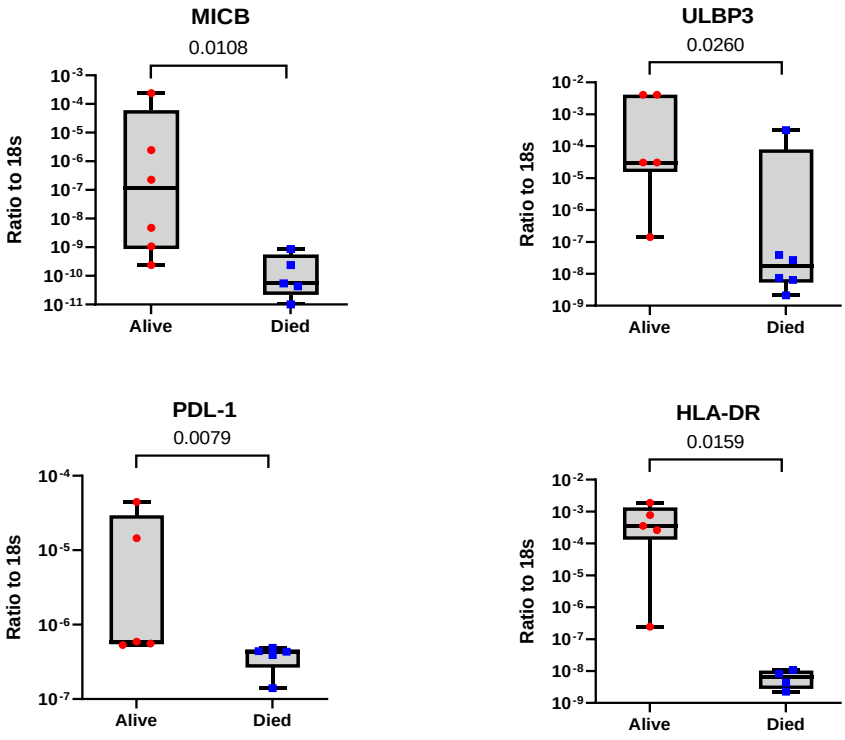


Figure 6.38: Survival and the transcription of NK ligands on HGSOvCa tissue.
The activation NK ligands (MICB and ULBP3) and the inhibitory ligands (HLA-DR and PDL-1) were significantly decreased in the patients who died from OC compared to those who were alive.

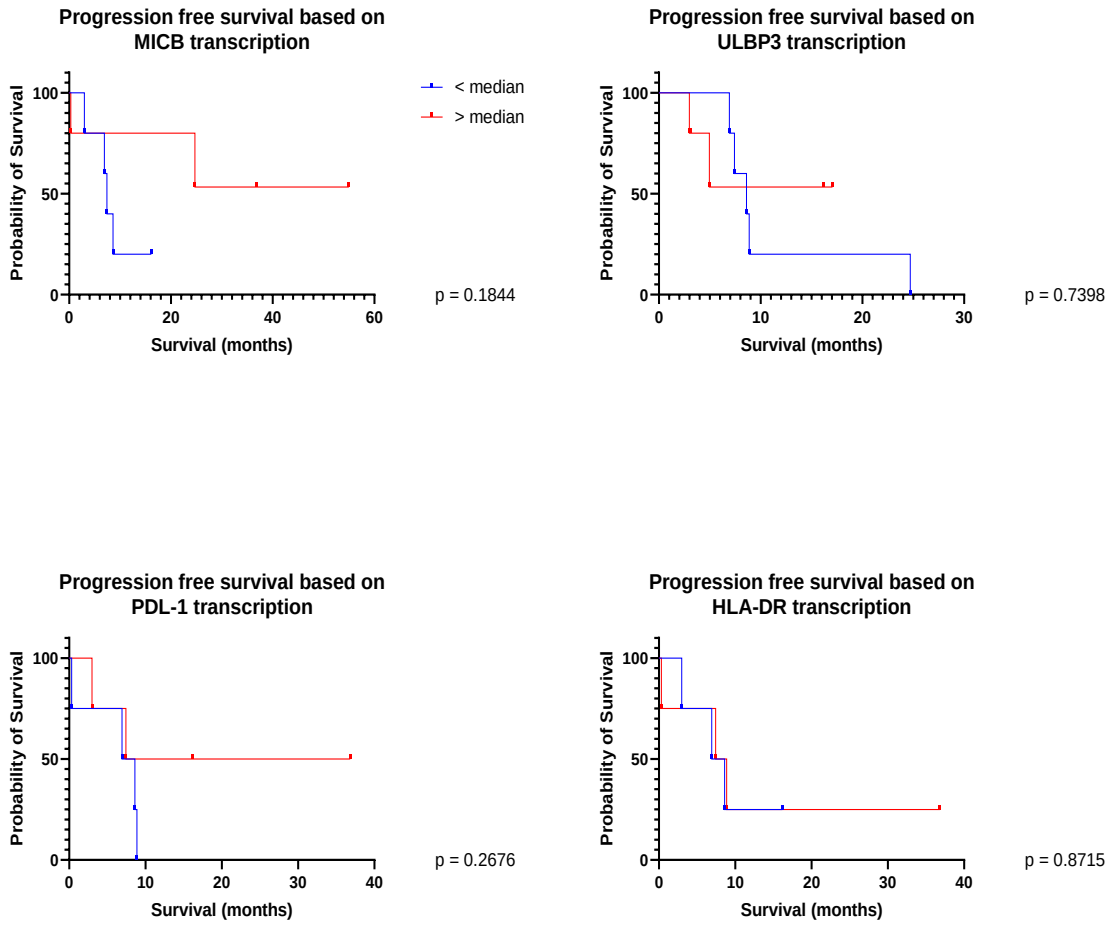


Figure 6.39: Kaplan-Meier plot showing progression free survival based on transcription levels for NK ligands on tumour tissue.

There were no differences in PFS with low or high transcription levels of MICB, ULBP3, PDL-1 and HLA-DR.

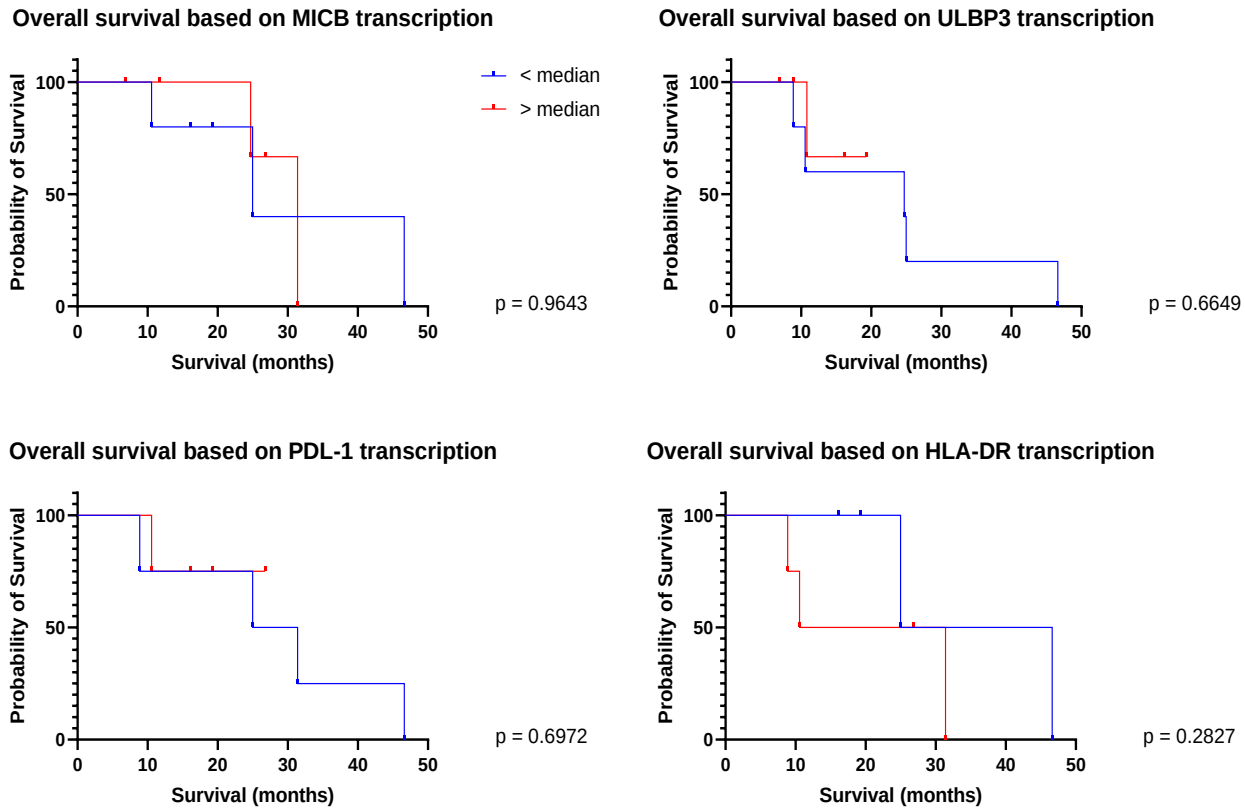


Figure 6.40: Kaplan-Meier plot showing overall survival based on transcription levels for NK ligands on tumour tissue.
There were no differences in OS with low or high transcription levels of MICB, ULBP3, PDL-1 and HLA-DR.

6.3.5 Correlation between NK ligands and NK phenotype data

The transcription levels for the NK ligands on tumour tissue were compared to the NK cell phenotype data. The NK ligands were categorised as having low or high transcription levels (below and above the median value) and correlated to the type of tumour infiltrating NK cells (determined by their CD56 and CD16 expression). Based on the amount of NK ligands expressed by the tumour, there were no differences in the types of NK cells within the ovarian tumour microenvironment, shown in Figure 6.41. The expression of various receptors by the tumour infiltrating NK cells were then correlated to their corresponding ligands on the

tumour tissue. The activating NK receptor-ligand interactions analysed included the DNAM-1 receptor with tumour ligands PVR and PVRL2, the NKG2D receptor with ligands MICA, MICB, ULBP1 and ULBP3 (Figure 6.42). There was no difference in DNAM-1 expression on NK cells between those tumours that had low and high levels of PVR. Similarly, there was no difference in NK expression of DNAM-1 on the NK cells between the tumours with low and high PVRL2 levels. There was a significant increase in the expression of NKG2D on the NK cells found in tumours with low levels of MICB expression compared to those with high expression ($p = 0.0159$). However, there were no differences in NKG2D expression on the NK cells within tumours that had low and high levels of the other NKG2D ligands, MICA, ULBP1 and ULBP3. Figure 6.43 illustrates the inhibiting NK receptor-ligand interactions. There were no differences in the NK expression of CD94 between tumours with low and high levels of HLA-E. The NK expression of PD-1 was also similar in tumours with low and high PDL-1.

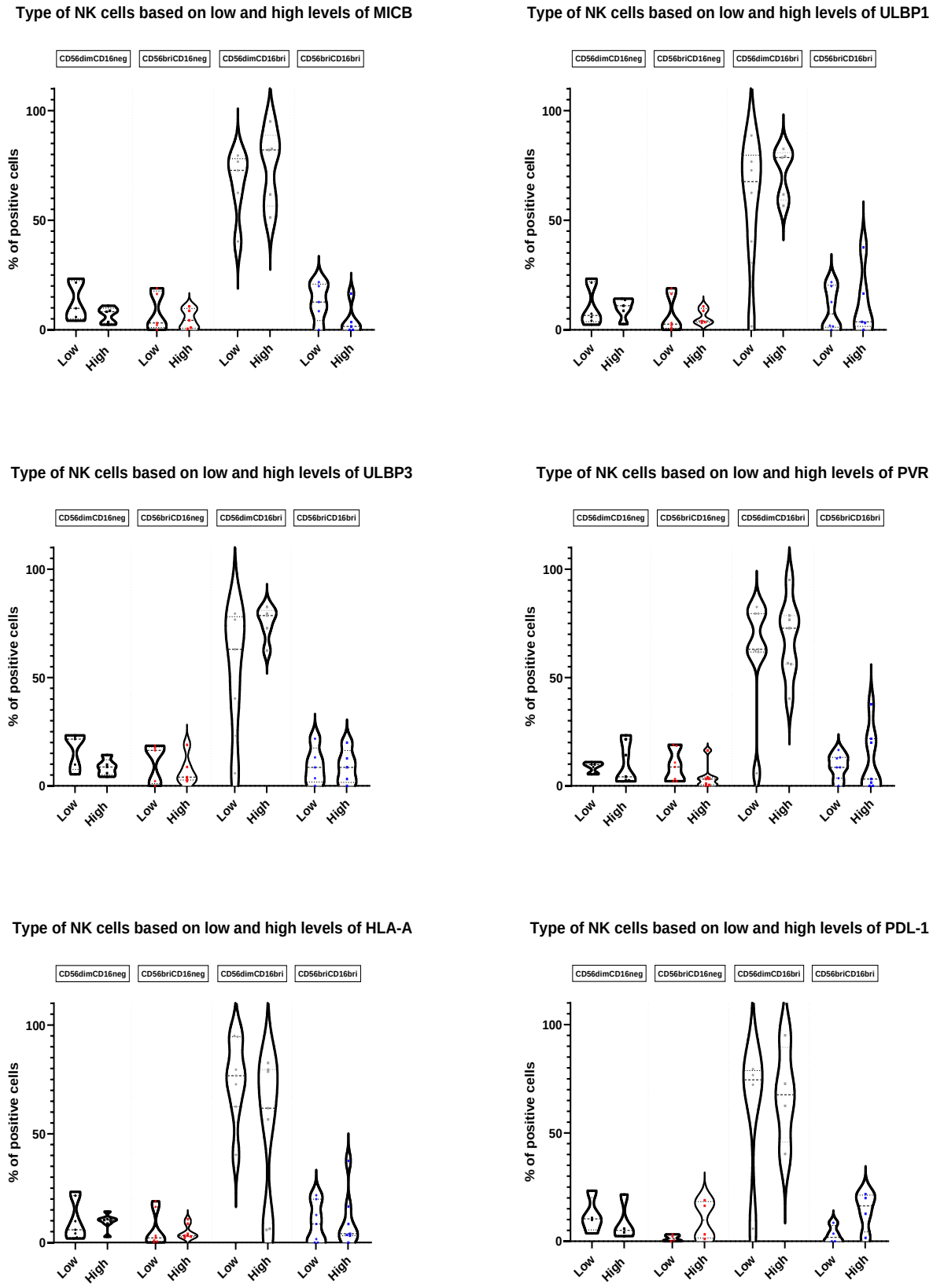


Figure 6.41: Comparison of the type of tumour infiltrating NK cells between tumours with high and low transcription levels for the NK ligands

There were no differences in the type of NK cells based on low and high levels of MICB, ULBP1, ULBP3, PVR, HLA-A and PDL-1.

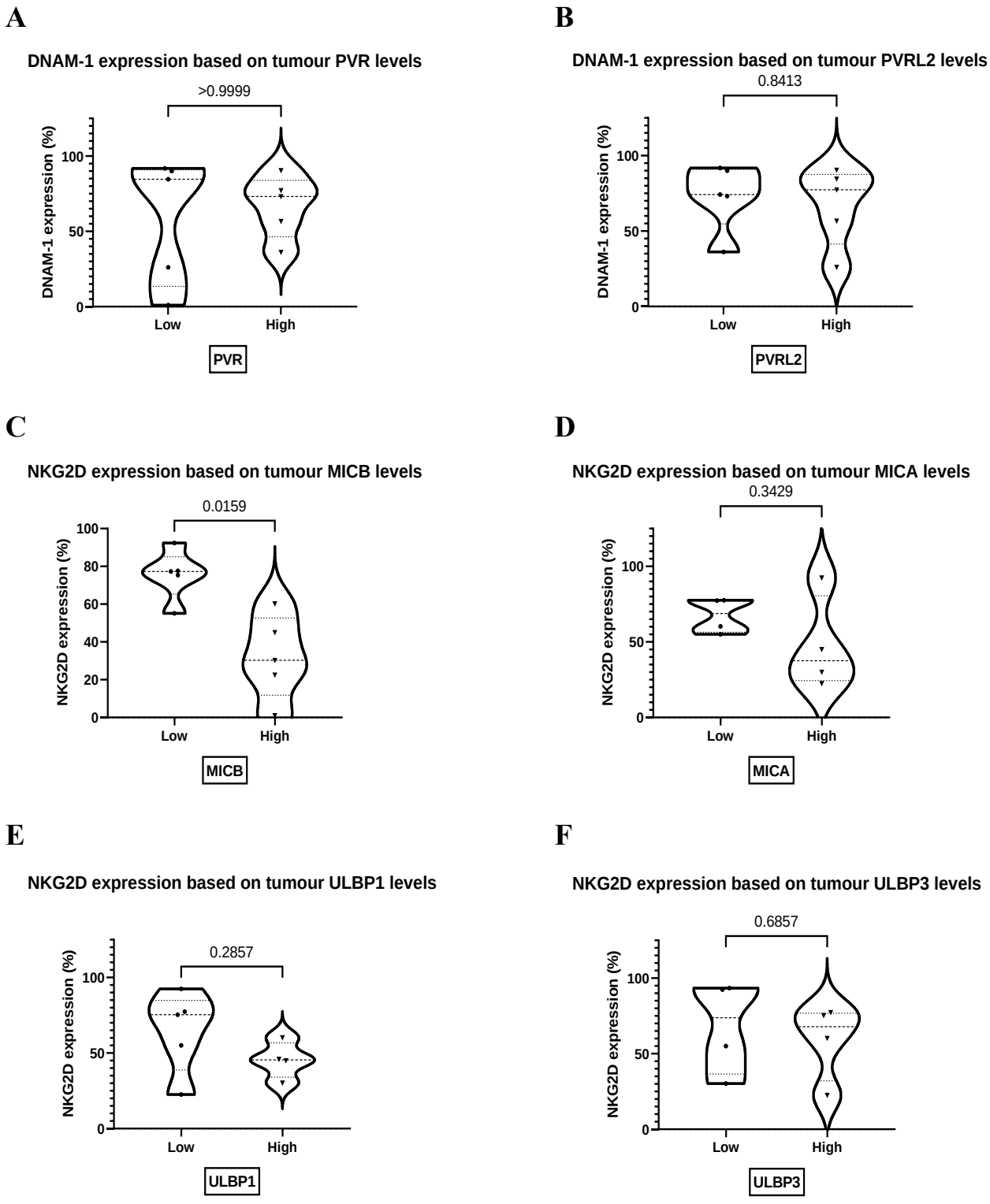


Figure 6.42: Expression of activating receptors on NK cells within tumour tissue based on the levels of corresponding NK ligands.

There were no differences in the NK cell expression of DNAM-1 within tumour that had low and high levels of ligands PVR (A) and PVRL2 (B). NKG2D was significantly upregulated on NK cells within tumours that had low MICB levels compared to tumours that had high MICB (C). There were no differences in NKG2D expression in tumours with low and high levels of the other corresponding NKG2D ligands: MICA (D), ULBP1 (E) and ULBP3 (F).

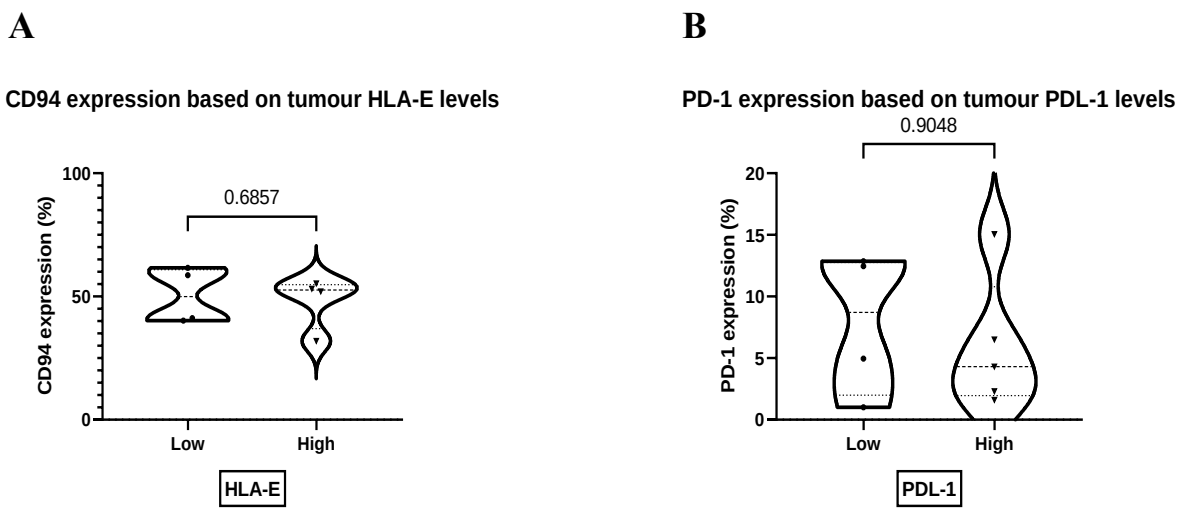


Figure 6.43: Expression of inhibiting receptors on NK cells within tumour tissue based on the levels of corresponding NK ligands.
There were no differences in the NK cell expression of CD94 (A) or PD-1 (B) within tumour tissue that had low and high levels of the corresponding ligands HLA-E and PDL-1.

6.3.6 Summary of NK cell ligand expression upon ovarian tumours

This section interrogates the NK ligands within ovarian tissue, using qPCR to determine the transcription patterns and identify variations in ligand expression between the malignant and benign ovarian biopsies. The ligands MICB, MICA, PVR and ULBP1, which stimulate NK cells through interaction with activation receptors DNAM-1 and NKG2D, were raised on the malignant samples when compared to the benign tissues. Next, the expression of NK ligands and their response to chemotherapy was reviewed by comparing the chemotherapy exposed and chemotherapy naïve OC biopsies. Although there were no alterations in activation ligands, chemotherapy did reduce the inhibitory ligands PDL-1 and HLA-DR. In addition, there was a reduction in both activating ligands (MICB and ULBP3) and inhibiting (HLA-DR and PDL-1) ligands on tumours associated with disease recurrence and patient death. Overall, this shows that the ovarian tumour microenvironment directly stimulates NK cells, with further activation

following chemotherapy and the expression of NK ligands associated with poor clinical outcomes.

6.4 The expression of NK ligands on epithelial cells within ovarian biopsies

6.4.1 Detecting NK ligands expressed by epithelial cells within ovarian biopsies

Following the qPCR transcription level analysis for the NK ligands in whole tumour biopsies, the surface expression of the same ligands on the epithelial cells within OC samples was determined using flow cytometric analysis. By identifying the epithelial cell population within each ovarian tumour biopsy, the normal epithelial cells could be separated from the epithelial tumour cells in every individual sample. This allowed the expression of NK ligands in the normal epithelial cells to be compared to the expression of ligands in the malignant epithelial cells from the same biopsy.

Ovarian tumour samples, obtained from 9 patients with advanced stage HGSOvCa from the cohort described in Chapter 4, were processed according to Methods section 2.2.7 and stained with antibodies for the epithelial cell marker (Epcam) and NK ligands (HLA-A/B/C, MHC class II, PDL-1, MICA, MICB, ULBP1, ULBP2/5/6, ULBP3 and ULBP4). Figure 6.44 demonstrates the gating strategy used to detect the single, live epithelial cells within the ovarian tumour samples before the proportion of Epcam positive epithelial cells was identified. The ovarian tumour cells are generally believed to express high levels of Epcam and have low HLA class I expression levels. Within each HGSOvCa biopsy sample, these tumour cells were separated from likely coinciding normal epithelial cells by the degree of Epcam and HLA-I expression, as shown in Figure 6.45. Although not completely indicative of normal epithelium, HLA class I molecules typically remain upregulated on non-malignant

epithelial cells and Epcam expression was considered to be lower on normal epithelium than that seen on the tumour cells. As such the altered expression of HLA class I and Epcam was used to isolate possible normal epithelial cells from tumour cells. The expression (median florescence intensity, MFI) of the NK ligands within each of the tumour and normal cell populations, obtained from the same biopsy sample, was then be assessed.

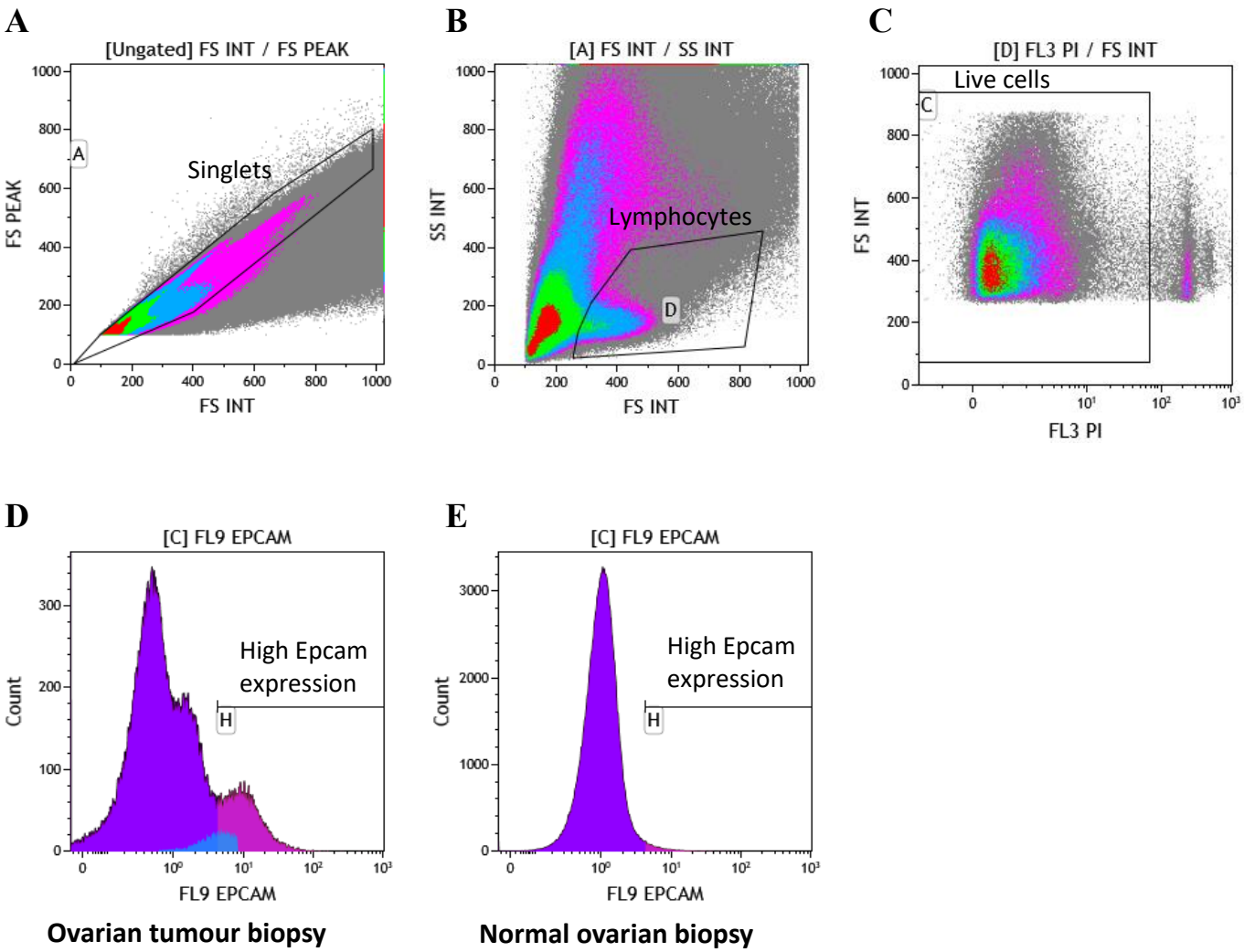


Figure 6.44: The gating strategy to detect Epcam positive epithelial cells within tumour biopsies. Flow cytometric analysis of ovarian tumour biopsies identified: A) singlets, B) lymphocyte cells, and C) live cells. The single, live lymphocyte cells within OC tumour biopsies with upregulation of Epcam could then be detected (D). There was a greater proportion of cells highly expressing Epcam within an OC biopsy, compared to a normal ovarian biopsy (E).

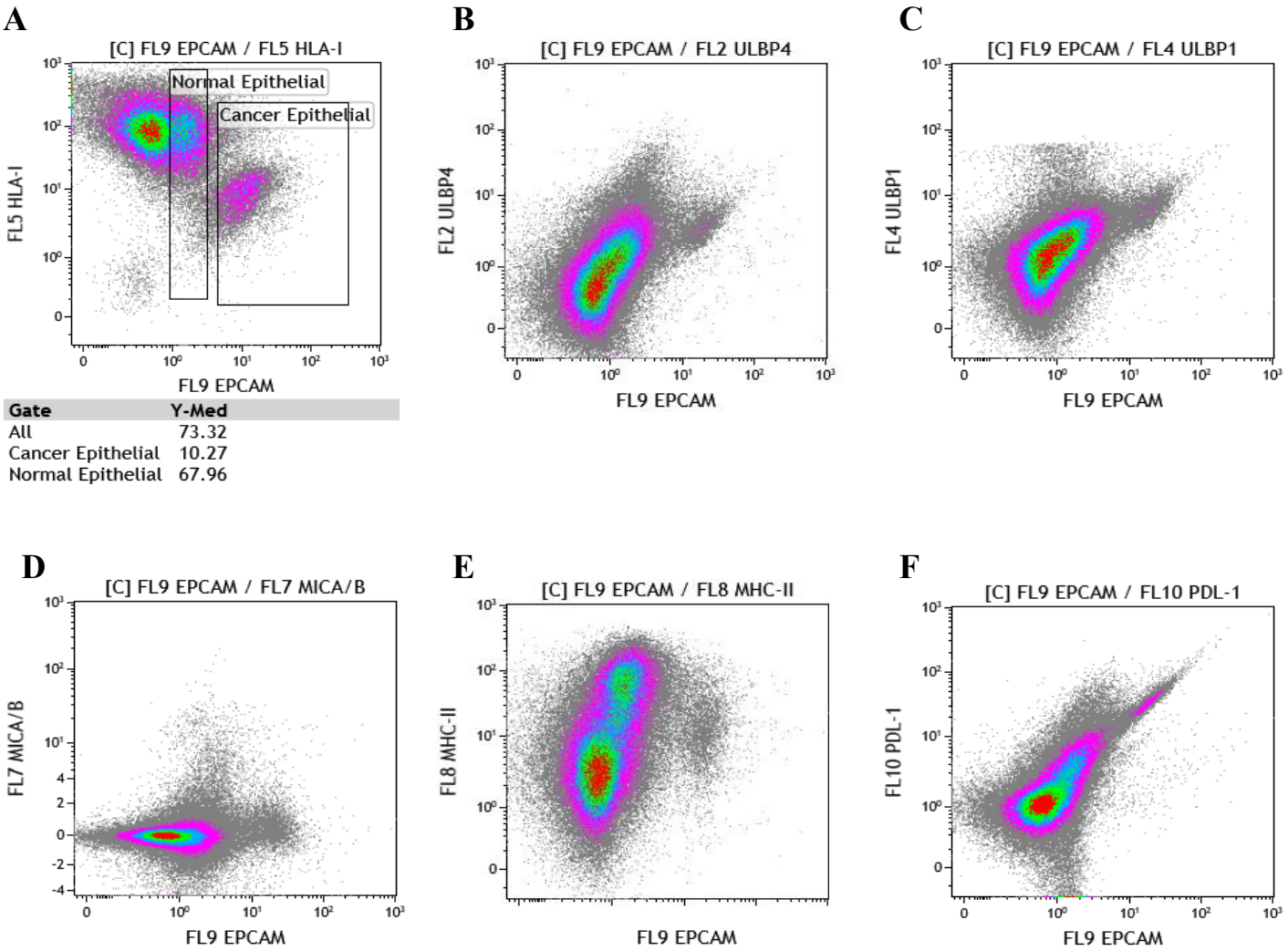


Figure 6.45: Identification of epithelial cell population and their expression of NK ligands.
Within each OC tissue biopsy, the epithelial tumour cells had high Epcam and low HLA-I expression compared to the normal epithelial cells (A). The expression of NK ligands could then be assessed, including: ULBP4 (B), ULBP1 (C), MICA/B (D), MHC class II (E), and PDL-1 (F).

6.4.2 Comparison of NK ligands between normal and malignant epithelial cells

Once the cancer cell population and normal epithelial cell population had been identified within each HGSOvCa biopsy, the expression of NK ligands could be determined. For each of the 9 biopsy samples used in this assay, the median florescence intensity (MFI) value for every ligand was compared between the cancer and normal cell populations. Figure 6.46 shows that there were significantly lower levels of HLA class I on the cancer cells than on the normal cells ($p = 0.0008$). There was upregulation of both PDL-1 and ULBP1 in the tumour cells compared to the normal population ($p = 0.0040$ for both ligands). There were no differences in the expression of MHC class II, MICA/B and ULBP2/3/4/5/6, between the normal and cancer cells.

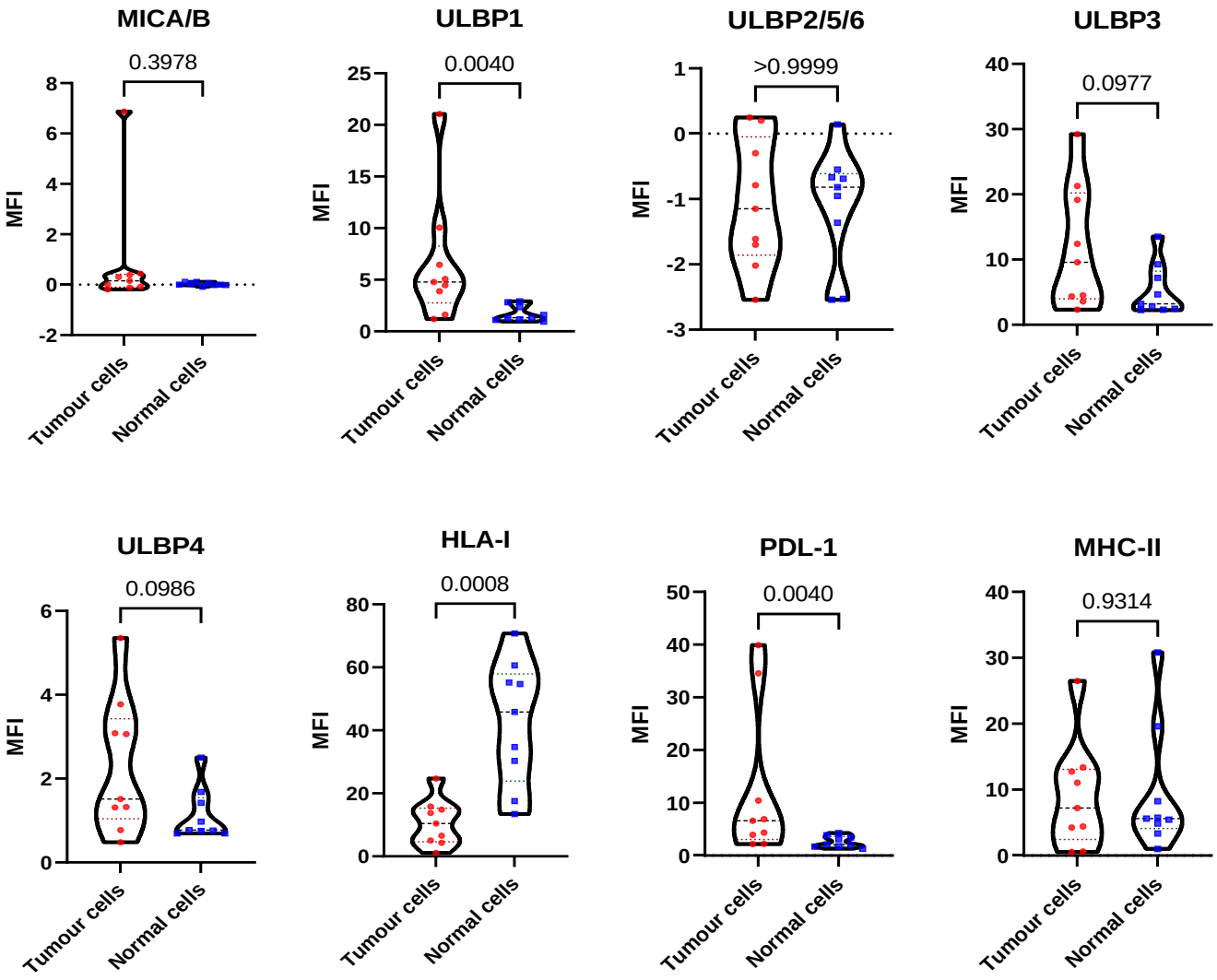


Figure 6.46: The expression of NK ligands upon normal epithelial cells and malignant cells within ovarian tumour biopsies.
Compared to normal epithelial cells, there was significantly less HLA-I on the epithelial tumour cells. There was upregulation of PDL-1 and ULBP1 on tumour epithelial cells compared to normal epithelial cells from the same OC biopsy.

6.4.3 Summary of NK ligand expression in normal and malignant epithelial cells

Within a single ovarian tumour biopsy, it is possible to detect the Epcam positive cancer cell population as well as any coinciding normal epithelial cells that are also present. This allows a detailed analysis of the surface expression levels of NK ligands on primary ovarian cancer cells. As expected, the expression of NK cell ligands on the surface of ovarian cells change

with malignant transformation. The MHC class I molecules (HLA-A/B/C), which bind to inhibitory receptors on NK cells, were reduced on the cancer cells compared to the normal epithelial cells. Decreased HLA-A was also apparent from the qPCR analysis, where HGSOvCa tissue had lower transcription levels than the benign ovarian tissue. The expression of the immune checkpoint ligand, PDL-1 was raised in the ovarian tumour cell population, where it acts to inhibit NK cells. The activating NKG2D ligands (ULBP1, ULBP3, and UBP4) were all overexpressed on the tumour cell populations compared to the normal epithelial cells. The upregulation of the NKG2D ligand, ULBP1 was consistent with the qPCR analysis where the transcription of ULBP1 was greater on the tumour tissue compared to benign ovarian tissue.

6.5 The recognition of primary ovarian tumour cells by NK cells

6.5.1 NK cell cytotoxicity following co-culture with ovarian tumour cells

6.5.1.1 Detecting NK cell killing of tumour cells

To establish the NK response and degree of cytotoxicity towards ovarian tumour cells, NK cells isolated from peripheral blood were co-cultured with processed primary ovarian tumour cells in a 1:1 ratio, as described in the Methods section 2.2.8. The cultured samples were stained with antibodies for Epcam (the epithelial cell marker that is overexpressed in epithelial ovarian tumours [377, 378]), HLA-I (the MHC class I molecule that is present on healthy cells but downregulated on tumour cells) and CD56 (the NK cell identifying marker). The population of the Epcam positive cancer cells was detected using Gallios flow cytometry and Kaluza analysis software, shown in Figure 6.47. The FS INT and FS Peak gates identified the single cells within the samples, which gave rise to the single lymphocyte cells and subsequently the live single lymphocyte cells using PI staining. High CD56 expression identified the NK cells within the co-cultured samples, which were removed to leave the

Epcam positive tumour cells (high Epcam expression with low HLA-I expression). Those remaining cells with raised HLA-I expression were classed as healthy non-cancerous epithelial cells, and were not used for the analysis. The absolute count of the Epcam positive cancer cell population following co-culture with NK cells was compared to the same primary cancer cells cultured without NK cells. This established whether the NK cells were able to recognise and destroy the primary cancer cells. To determine the efficacy of the peripheral NK cells obtained from OC patients towards their own tumour tissue, NK cells from autologous PBMC samples were compared to unrelated healthy donor PBMC samples.

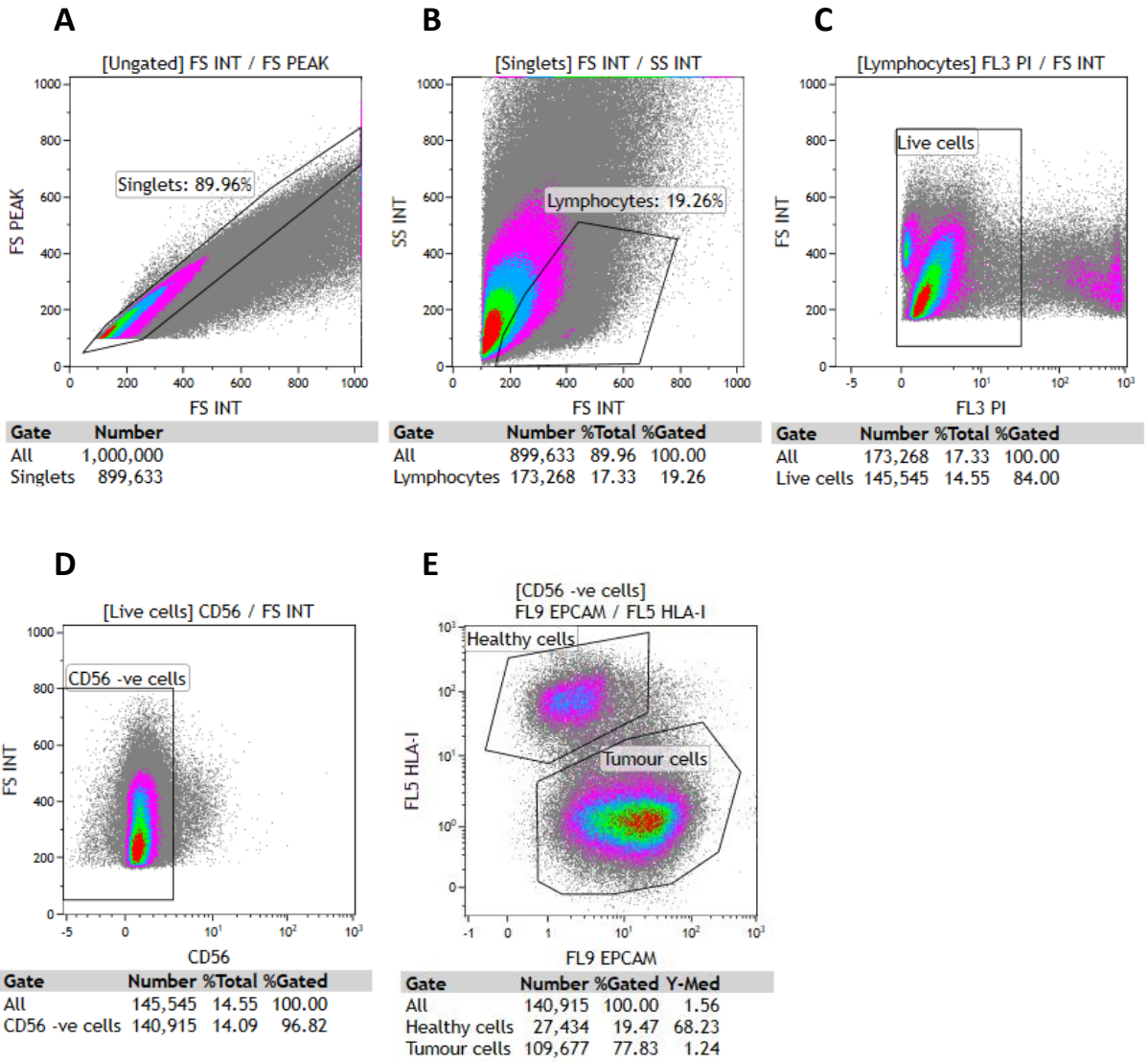


Figure 6.47: The gating strategy implemented to identify the live ovarian tumour cells following co-culture with NK cells.

Analysis of flow cytometric data allowed the detection of: A) single cells, B) lymphocytes, C) live cells, D) live cells with the NK cell (high CD56 expression) population removed, and E) the tumour cell population (high Epcam and low HLA-I expression).

6.5.1.2 The co-culture study population

The patient cohort used for the NK-ovarian cell co-culture is described in Figure 6.48. The study population included ovarian tumour samples from 20 patients with advanced, stage III or IV HGSOvCa from the original NK phenotype cohort, where biopsies were taken from the ovarian mass at the time of surgical resection. All 20 of these cancer samples were cultured alone and also in combination with healthy donor peripheral NK cells. In addition, 5 of these tumour samples were also co-cultured with autologous NK cells, with PBMC samples obtained at the time of surgery. To thoroughly interrogate the killing ability of NK cells towards tumour tissue, these 20 HGSOvCa samples were compared to 10 of the normal ovary samples. All 10 normal samples were processed and cultured with healthy donor peripheral NK cells, with two of these also cultured with autologous NK cells. As a further control, 2 benign ovarian masses were cultured with both healthy donor peripheral NK cells and autologous NK cells. The characteristics of the study cohort are shown in Table 6.6. Of the 20 HGSOvCa patients, 9 (45.0%) had received neoadjuvant chemotherapy, while the other 11 (55.0%) had primary surgery without prior chemotherapy. Complete surgical resection (R0) was achieved in 70% (n=14), with 60.0% (n=12) suffering a recurrence of their disease and 55.0% (n=11) of the patients died.

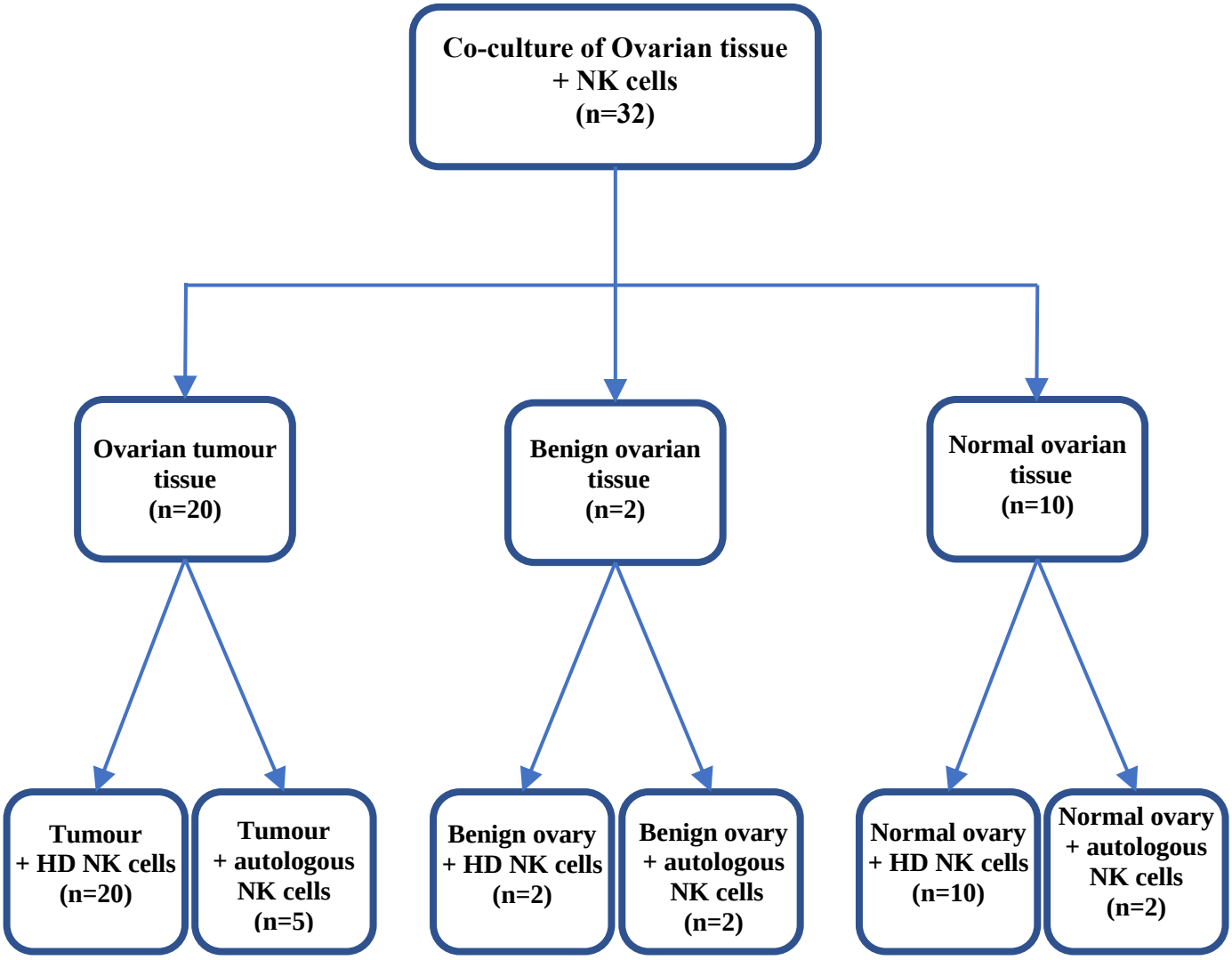


Figure 6.48: The cohort of samples used in the NK cell – ovarian tissue co-culture assay
Of the total cohort of 32 patients, 20 had OC while there were 12 controls (2 with a benign ovarian mass and 10 with normal ovaries). A combination of NK cells from healthy donor (HD) peripheral blood samples and autologous blood samples were used.

Table 6.6: Characteristics and outcomes of the patients included in the Ovarian-NK cell co-culture analysis

Variable	Ovarian tumour (n=20)	Benign ovarian mass (n=2)	Normal ovary (n=10)
Age (years) Mean ± SD	62.2 ± 10.1	70.5 ± 4.9	57.9 ± 15.6
Ethnicity	**n (%)**	**n (%)**	**n (%)**
White	18 (90.0)	2 (100.0)	5 (50.0)
Asian	2 (10.0)	0 (0.0)	4 (40.0)
Black	0 (0.0)	0 (0.0)	1 (10.0)
Disease stage	**n (%)**	n/a	n/a
3	11 (55.0)		
4	9 (45.0)		
Chemotherapy	**n (%)**	n/a	n/a
Nil	11 (55.0)		
NACT	9 (45.0)		
CRS (n=9)	**n (%)**	n/a	n/a
1	1 (11.1)		
2	3 (33.3)		
3	5 (55.6)		
Cytoreduction	**n (%)**	n/a	n/a
R0	14 (70.0)		
R1	4 (20.0)		
R2	2 (10.0)		
Recurrence	**n (%)**	n/a	n/a
Disease-free	8 (40.0)		
Recurred	12 (60.0)		
Survival	**n (%)**	n/a	n/a
Died	11 (55.0)		
Alive	9 (45.0)		

6.5.1.3 Ovarian - NK cell co-culture analysis

Upon detection of the Epcam positive tumour cell populations, cultured alone and with the addition of peripheral NK cells, the killing ability of the NK cells could be calculated for each tumour biopsy. Figure 6.49 shows an example of healthy donor NK killing of both a tumour sample and a normal ovarian sample. The capacity of autologous NK cells to kill tumour cells is shown in Figure 6.50. The average cytotoxicity of healthy donor NK cells when combined for the 20 HGSOvCa samples was 57.1% (range of 18.8% to 95.1%). The autologous NK cells had an average cytotoxicity of 39.3% against the tumour cells (range of

17.7% to 81.3%). While the average NK cytotoxicity rates in the benign ovarian co-cultures were similar to the HGSOvCa samples, the average NK cytotoxicity was lower when co-cultured with normal ovarian tissue (Table 6.7). Although the healthy donor NK cells were more cytotoxic than the autologous NK cells towards the primary tumour cells, seen in each of the different ovarian tissue types, this was not significant.

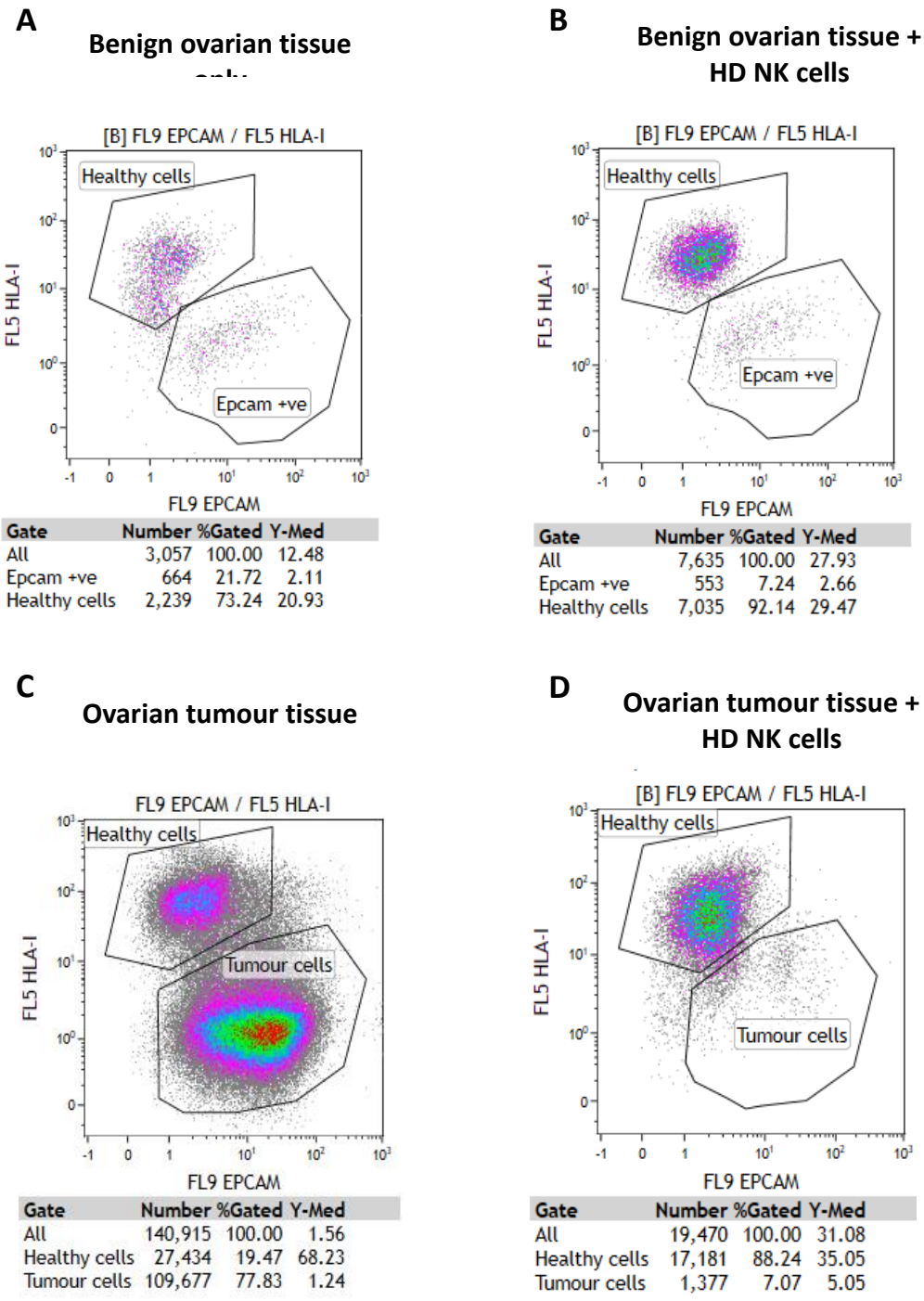


Figure 6.49: Healthy donor NK cell killing after co-culture with ovarian tissue.
NK cell cytotoxicity was determined by comparing the population of live Epcam positive tumour cells in C) isolated ovarian tumour tissue to D) ovarian tumour cells co-cultured with healthy donor (HD) NK cells. NK cell killing was also observed in non-malignant ovaries by comparing the Epcam positive populations in A) benign ovarian tissue to B) co-cultured benign ovarian tissue and healthy donor (HD) NK cells.

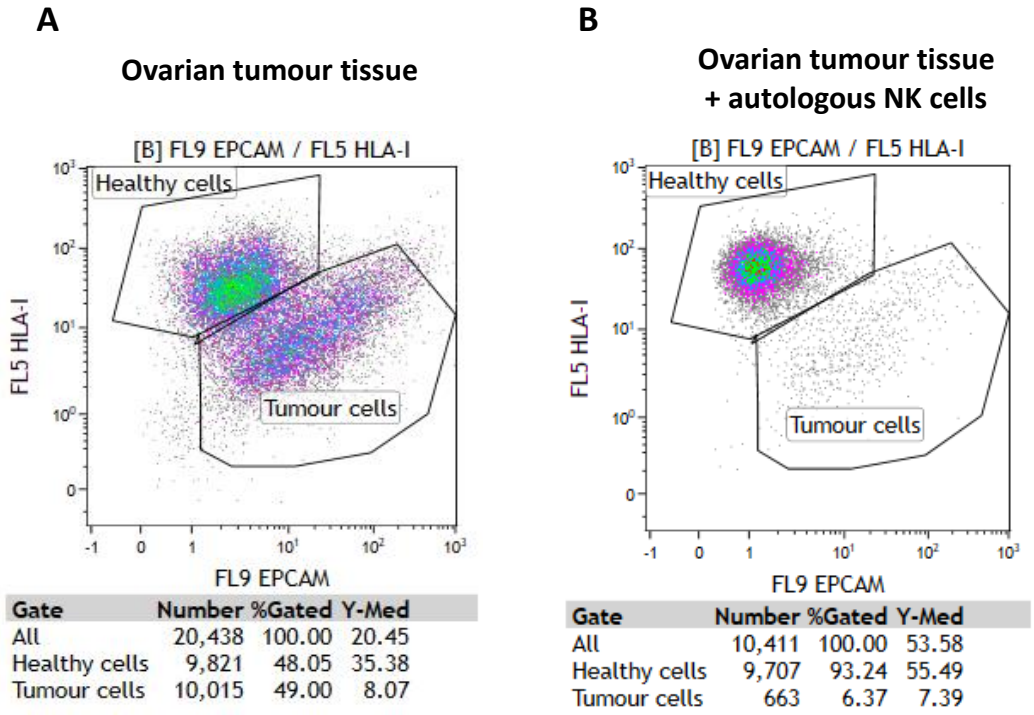


Figure 6.50: Autologous NK cell killing after co-culture with ovarian tissue.
The killing ability of autologous NK cells was determined by comparing A) the population of live Epcam positive tumour cells cultured in isolation to B) the tumour cell population cultured with autologous NK cells.

Table 6.7: Cytotoxicity of healthy donor (HD) NK cells and autologous NK cells when cultured with ovarian tumour, benign ovary and normal ovary

Co-culture	Cytotoxicity average (%)	Cytotoxicity range (%)	P Value
Ovarian tumour			
+ *HD NK cells*	57.1	18.8 - 95.1	
+ *autologous NK cells*	39.3	17.7 - 81.3	0.1690
Benign ovary			
+ *HD NK cells*	67.9	66.7 – 69.2	
+ *autologous NK cells*	31.6	12.5 – 50.7	0.3333
Normal ovary			
+ *HD NK cells*	25.6	7.8 – 37.1	
+ *autologous NK cells*	20.7	16.7 – 24.7	0.6061

Figure 6.51 shows that the healthy donor NK cells were more cytotoxic towards ovarian tumour cells than the normal ovarian cells (p = 0.0019). Healthy donor NK cytotoxicity was also greater in the benign ovary co-cultures than with the normal ovary samples (p = 0.0303). There was no difference in healthy donor NK cell killing between tumour and benign ovary co-cultures.

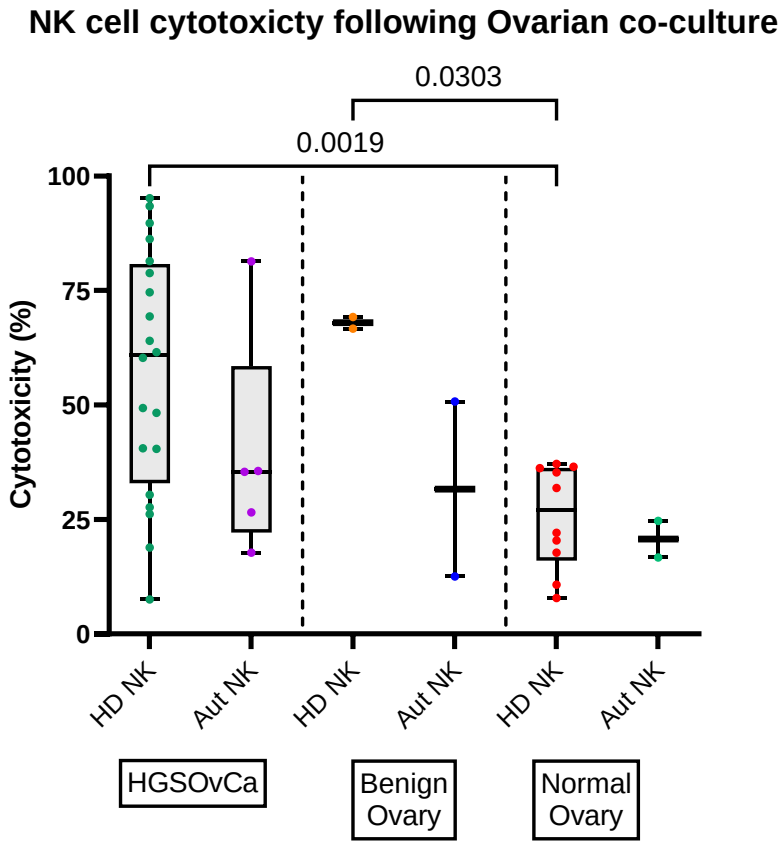


Figure 6.51: NK cell killing after co-culture with ovarian tissue.
The killing ability of healthy donor (HD) NK cells and autologous (Aut) NK cells in ovarian tumour, benign ovary and normal ovary samples. Healthy donor NK cells were more cytotoxic in tumour and benign ovary samples than in normal ovary samples.

6.5.1.4 Correlation between NK cell killing and clinical outcomes

The sensitivity of NK cell killing following culture with ovarian tumour tissue was examined in those patients who received neoadjuvant chemotherapy and those who were chemotherapy naïve. Figure 6.52 demonstrates there was no variation in sensitivity to cytotoxicity following chemotherapy treatment, in cultures with both HD NK cells ($p = 0.8820$) and autologous NK cells ($p = 0.8000$). However, when cytotoxicity was correlated to recurrence data, healthy donor NK cytotoxicity was greater against the tumours derived from patients with recurrent disease when compared to those who remained disease free after treatment ($p = 0.0096$), shown in Figure 6.53. Furthermore, there was amplified tumour cell killing by the healthy donor NK cells in the cohort of patients that died (Figure 6.54), compared to those who were still alive at the end of the follow-up period ($p = 0.0381$). There were no differences in autologous NK cell cytotoxicity between those who recurred and remained disease free, or those who were alive and died.

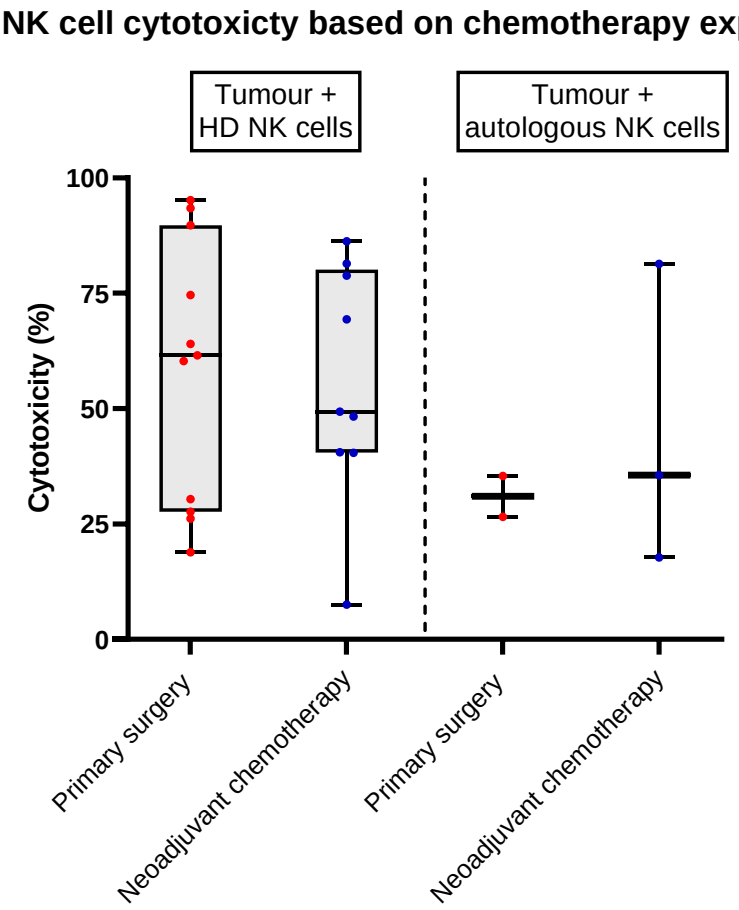


Figure 6.52: NK cell killing after co-culture with ovarian tumour treated with and without chemotherapy.

The killing ability of healthy donor (HD) NK cells and autologous NK cells in ovarian tumour was similar prior to any chemotherapy (primary surgery group) and following chemotherapy exposure (neoadjuvant chemotherapy group).

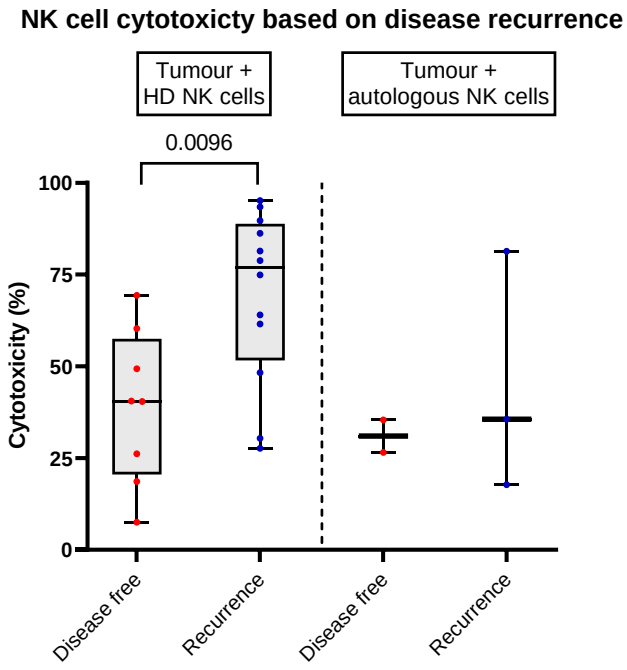


Figure 6.53: NK cell killing of ovarian tumour in those who recurred and those who remained free of disease.
Healthy donor NK cells had increased cytotoxicity when cultured with tumours that recurred compared to those tumours that did not recur.

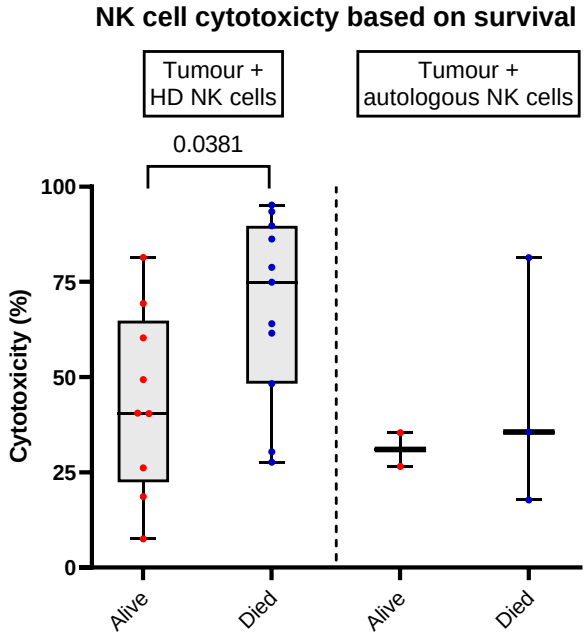


Figure 6.54: NK cell killing of ovarian tumour in those who died and those alive.
Healthy donor NK cells had increased cytotoxicity when cultured with tumours from patients who died compared to those from patients who were alive at the end of the follow-up period.

The tumour tissue associated with raised NK cell cytotoxicity was from the patients with poorer progression free and overall survival. For the 20 ovarian tumours cultured with healthy donor NK cells, those with the higher levels of NK cytotoxicity (above the median value) were compared to those with reduced levels (cytotoxicity below the median value). Both progression free survival (Figure 6.53) and overall survival (Figure 6.54) were significantly decreased in the population with high NK cytotoxicity and tumour cell killing ($p = 0.0009$ and $p = 0.0002$, respectively).

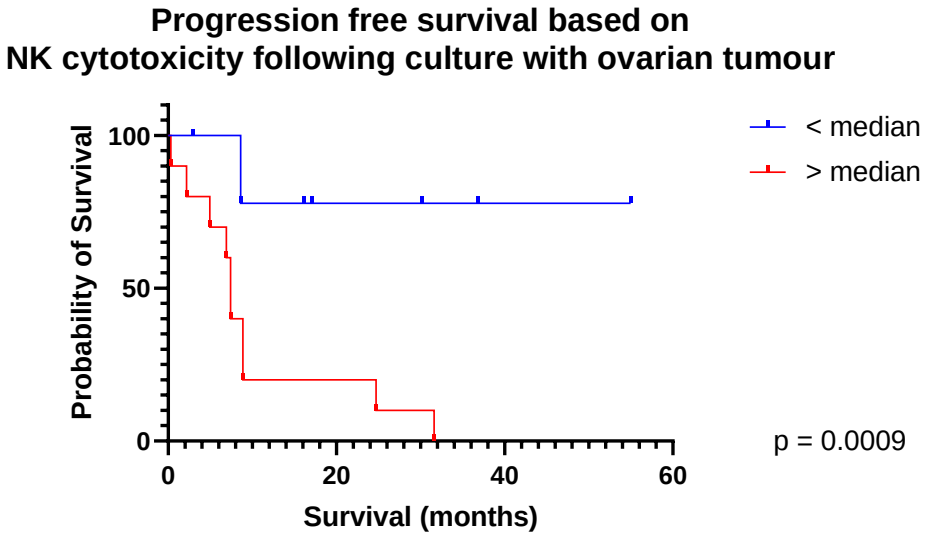


Figure 6.55: Kaplan-Meier plot showing progression free survival in those with low and high levels of NK cell cytotoxicity following culture with ovarian tumour tissue.
Increased tumour killing by healthy donor NK cells (above the median value) was associated with poorer progression free survival.

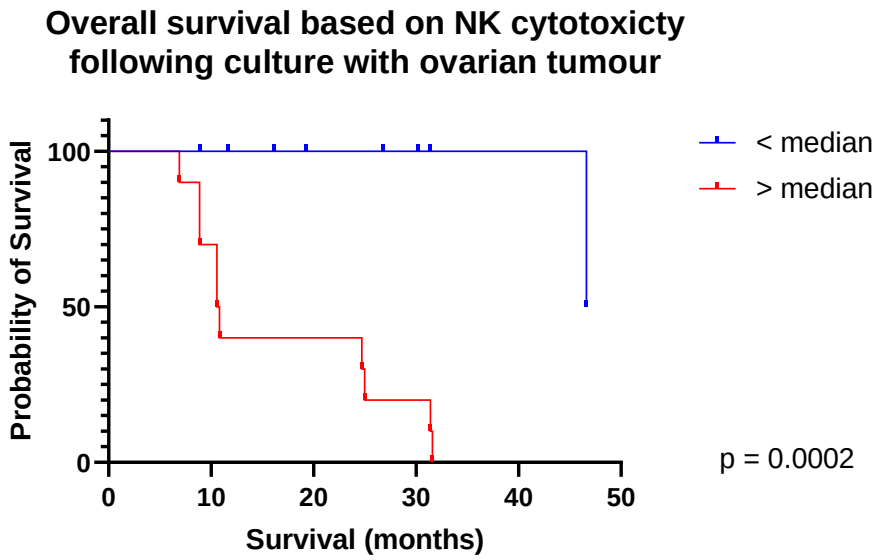


Figure 6.56: Kaplan-Meier plot showing overall survival in those with low and high levels of NK cell cytotoxicity following culture with ovarian tumour tissue.
Increased tumour killing by healthy donor NK cells (above the median value) was associated with reduced overall survival.

6.5.2 The contribution of NK activating receptors to NK cell cytotoxicity

6.5.2.1 Receptor inhibition and NK cell killing

To explore which activating signalling pathways stimulate NK cells to exert their cytotoxic effects on ovarian tumour tissue, selected inhibitors were used to suppress NK cells. NK cells isolated from the peripheral blood of healthy donors were cultured with primary ovarian tumour cells, as described in the previous co-culture assay (Methods section 2.2.8.1). The NK-ovarian co-cultures were then treated with NK receptor inhibiting antibodies and NK cell cytotoxicity compared to untreated control cultures (Methods section 2.2.8.3). The NK activation receptors that were impeded were DNAM-1, NKG2D, NKp46 and NKp30, with each inhibited separately by their respective antibody. Following the co-culture +/- antibody treatment, samples were again stained for Epcam, HLA-I and CD56. The absolute count of the Epcam positive tumour cells was calculated as previously defined in Figure 6.45 using Gallios flow cytometry and Kaluza analysis. The proportion of tumour cells that were still

alive following NK cell co-culture were measured to determine the cytotoxic effects of the NK cells towards OC cells after selective receptor inhibition.

6.5.2.2 The co-culture population for receptor inhibition

A total of 15 of the primary ovarian tumour samples from the co-culture analysis were used. All were from patients with stage III or IV HGSOvCa, with 6 (40.0%) previously exposed to chemotherapy and 9 (60.0%) from the chemotherapy naïve group. At the end of the study period, 8 were still alive and disease free, 7 (46.7%) had suffered a recurrence and 6 (40.0%) had died from the disease.

6.5.2.3 Analysis of NK activation receptor inhibition

The mean cytotoxicity of healthy donor NK cells towards ovarian tumour tissue was 62.4%. This was reduced to 10.9% when DNAM-1 receptors were inhibited ($p = 0.008$) and 44.0% with NKG2D receptor inhibition ($p = 0.257$). There were no changes in the NK cell cytotoxicity when the NKp46 and NKp30 receptors were inhibited, with mean cytotoxicity levels of 75.2% and 69.0%, respectively. There were no significant differences in NK cell cytotoxicity between control and experimental arms where NKG2D, NKp46 and NKp30 receptors were inhibited with their respective antibody. However, there was a significant reduction in NK cytotoxicity when the DNAM-1 receptor was inhibited ($p = 0.0012$), shown in figure 6.57. Representative examples of the flow cytometric analysis are shown in Figure 6.58, where the DNAM-1 inhibiting antibody prevented NK cell killing.

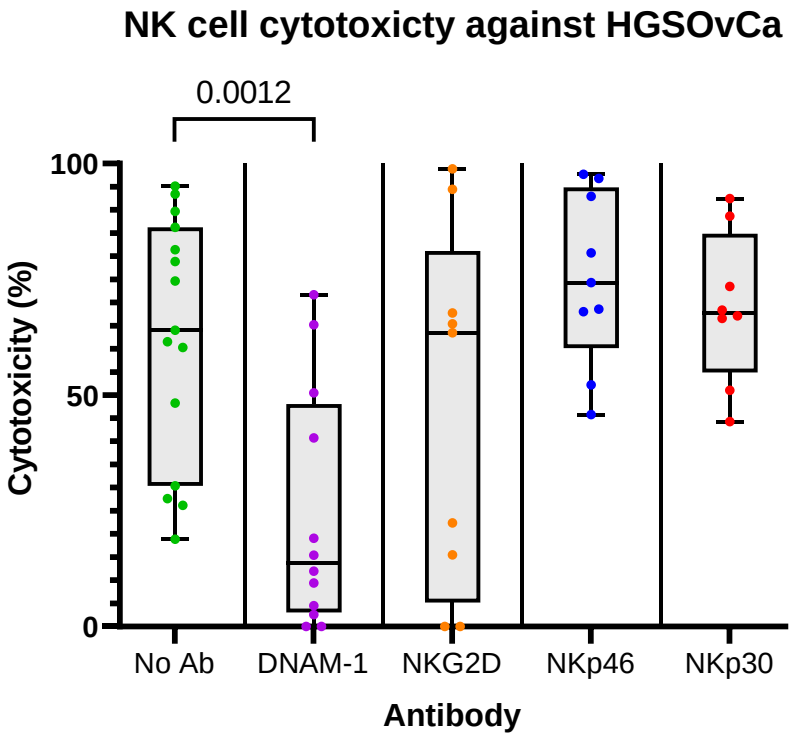
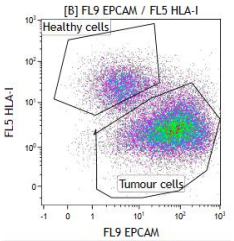


Figure 6.57: NK cell killing of ovarian tumour cells with the inhibition of NK activating receptors. NK cell cytotoxicity was reduced when the DNAM-1 receptor was inhibited on the NK cells, while there were no differences in cytotoxicity when NK receptors NKG2D, NKp46 and NKp30 were inhibited.

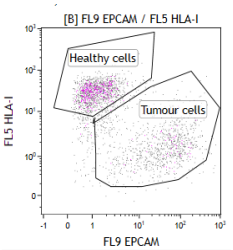
A

Ovarian tumour tissue



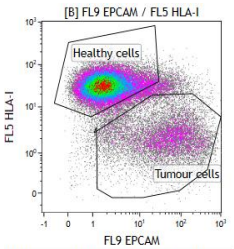
Gate	Number	%Gated	Y-Med
All	27,305	100.00	3.11
Healthy cells	4,942	18.10	27.68
Tumour cells	20,537	75.21	2.36

Ovarian tumour tissue + NK cells



Gate	Number	%Gated	Y-Med
All	2,538	100.00	14.37
Healthy cells	1,342	52.88	30.39
Tumour cells	996	39.24	1.68

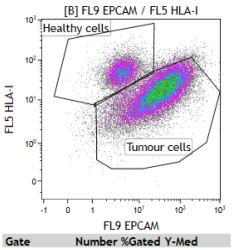
Ovarian tumour tissue + NK cells + DNAM-1 antibody



Gate	Number	%Gated	Y-Med
All	60,491	100.00	26.19
Healthy cells	43,574	72.03	31.26
Tumour cells	12,167	20.11	2.18

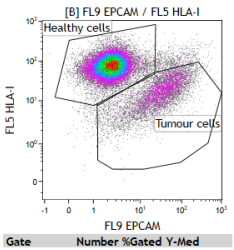
B

Ovarian tumour tissue



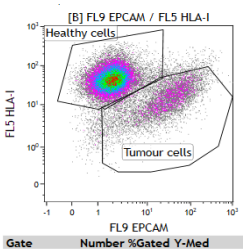
Gate	Number	%Gated	Y-Med
All	35,358	100.00	19.49
Healthy cells	6,483	18.34	48.36
Tumour cells	27,841	78.74	15.04

Ovarian tumour tissue + NK cells



Gate	Number	%Gated	Y-Med
All	39,477	100.00	64.64
Healthy cells	31,446	79.66	72.23
Tumour cells	7,070	17.91	14.75

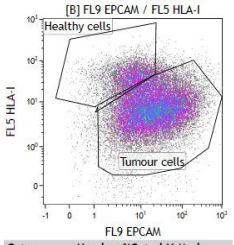
Ovarian tumour tissue + NK cells + NKp30 antibody



Gate	Number	%Gated	Y-Med
All	35,646	100.00	37.59
Healthy cells	27,419	76.92	43.12
Tumour cells	7,397	20.75	12.66

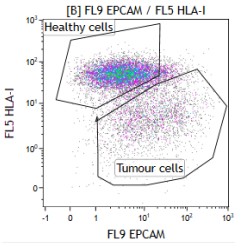
C

Ovarian tumour tissue



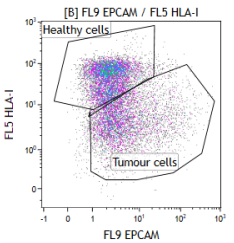
Gate	Number	%Gated	Y-Med
All	32,197	100.00	7.96
Healthy cells	4,921	15.28	42.91
Tumour cells	25,845	80.27	6.27

Ovarian tumour tissue + NK cells



Gate	Number	%Gated	Y-Med
All	10,295	100.00	39.53
Healthy cells	6,612	64.23	49.84
Tumour cells	2,663	25.87	4.77

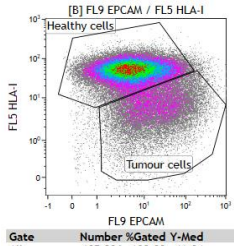
Ovarian tumour tissue + NK cells + NKp46 antibody



Gate	Number	%Gated	Y-Med
All	11,435	100.00	17.30
Healthy cells	5,968	52.19	51.91
Tumour cells	5,049	44.15	3.97

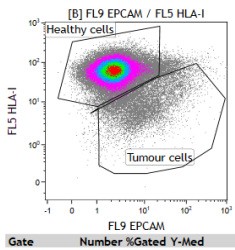
D

Ovarian tumour tissue



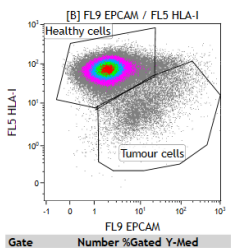
Gate	Number	%Gated	Y-Med
All	105,336	100.00	41.04
Healthy cells	78,428	74.46	49.76
Tumour cells	25,182	23.91	5.77

Ovarian tumour tissue + NK cells



Gate	Number	%Gated	Y-Med
All	127,434	100.00	57.67
Healthy cells	115,077	90.30	60.15
Tumour cells	9,562	7.50	8.79

Ovarian tumour tissue + NK cells + NKG2D antibody



Gate	Number	%Gated	Y-Med
All	122,309	100.00	67.12
Healthy cells	112,809	92.23	69.01
Tumour cells	7,769	6.35	9.64

Figure 6.58: Flow cytometric analysis of NK cell killing following NK receptor inhibition. NK cell cytotoxicity with inhibition of A) DNAM-1, B) NKp30, C) NKp46, and D) NKG2D.

6.5.3 Summary of the NK cell response to ovarian tumour tissue

Ovarian cancer primary cultures were incubated with autologous NK cells and NK cells derived from health donors to evaluate their ability to respond to and kill ovarian cancer cells. It was evident that healthy donor NK cells had a higher cytotoxicity level towards tumour tissue than the autologous NK cells. The small sample size of ovarian co-cultures with autologous NK cells prevented a thorough assessment of their cytotoxic abilities towards the primary ovarian tissue, however it is important to note that autologous NK cells were indeed cytotoxic with K-562 cells as their target as shown earlier in this chapter.

When co-cultured with chemotherapy exposed primary OC cultures, the cytotoxic effects of NK cells were not altered, with no changes to the live tumour cell populations when compared to the chemotherapy naïve OC co-cultures. However, when healthy donor NK cells were co-cultured with primary OC cells from patients with poor PFS and OS, there was an increase in tumour cell death when compared to the co-cultures of tumours from patients who were remained disease-free. This implies an increase in NK cell cytotoxicity towards cancer cells from those with poor clinical outcomes. This is related to the observation that upregulated activating receptor (DNAM-1) expression is related to worse OS; the tumour cells from these patients likely have greater expression of ligands, increasing their sensitivity to NK killing.

When NK cells derived from healthy donors were manipulated by selectively inhibiting the NK activating receptors, DNAM-1 receptor inhibition led to an increase in cytotoxicity against cancer cells, while inhibition of other activation receptors had no impact on the level of cytotoxicity activities.

6.6 Discussion

The extensive interrogation of NK cell phenotype and clinical correlation in a large OC cohort was described in the previous chapters. Following on from these, this chapter has focused on the NK functionality and the interaction with the tumour microenvironment. The relationship between NK cells and ovarian tumour cells has been explored, highlighting possible causes of NK dysfunction and tumour evasion. The chapter has evaluated the fundamental NK activation pathways necessary to produce a successful NK-cell mediated attack towards ovarian tumours, highlighting possible targets for potential NK immunotherapies.

Ovarian tumour microenvironment

The interactions between ovarian tumours and NK cells were explored using qPCR to quantify the transcription levels of the key NK ligands expressed by the tumour tissues. The comparison to benign ovarian controls gave an insight into the relationship between the malignant tissues and the tumour infiltrating NK cells, as well as an understanding of alterations and adaptations made by the tumours. Highly expressed NK activation receptors are known to bind to their corresponding ligands that are upregulated by tumour cells, including the receptor DNAM-1 and its ligand PVR, triggering an NK-mediated attack [182, 184-186]. The NKG2D ligands, specifically major histocompatibility complex (MHC) class I-related chain A (MICA) and B (MICB), are produced by stressed tumour cells, also activating NK cells upon interaction with the receptor NKG2D [187, 188]. The chronic expression of these activating ligands is an escape mechanism that tumours use to desensitise the NK activation receptors, prevent NK activation signalling and reduce cytotoxicity [150, 192, 200, 225, 226]. This cohort analysis confirmed these notions, where HGSOvCa samples had significantly raised levels of NK activating ligands MICB, MICA, PVR and ULBP1,

another NKG2D ligand, compared to the controls (Figure 6.34). In addition, the comparison of NK ligands expressed on the surface of malignant epithelial cells to normal epithelial cells from within the same tumour biopsies also confirmed that ovarian tumours have elevated activating ligands. Here there was increased expression of the NKG2D ligands ULBP1, ULBP3, and UBP4 on the tumour epithelial cells (Figure 6.46).

OC cells attempt to avoid immune recognition by deliberately downregulating the classical MHC class I molecules, such as the class I human leucocyte antigens (HLA-A, HLA-B and HLA-C). While typically allowing self recognition of normal healthy cells and preventing an NK attack, their loss upon tumour tissue eliminates their inhibiting function and NK activation towards the tumour ensues [154 173, 177, 182, 186, 189-192]. Indeed, our series of advanced HGSOvCa cases demonstrated a reduction of HLA-A transcription (Figures 6.35). Upon comparison of NK ligand expression between epithelial tumour cells and normal epithelial cells from the same OC biopsy (Figure 6.46), the tumour cells had a reduction of the MHC class I molecules, supporting our qPCR analysis. Tumours are also known to upregulate the atypical MHC class I molecules, such as HLA-E, which binds to the NK inhibitory receptor NKG2A and inactivates NK cells [193-196]. However, our cohort did not show a reduction in these ligands compared to controls or compared to their coinciding normal cells. Although not evident from the qPCR transcription evaluation, the inhibitory immune checkpoint ligand, PDL-1, was overexpressed on the ovarian tumour cells compared to the normal cell populations within tumour tissue (Figure 6.46). The infiltrating lymphocytes within ovarian tumours can cause upregulation of PDL-1 on tumour cells, increasing NK cell inhibition [150, 200, 225, 226, 379].

Overall, these findings portray a tumour microenvironment that serves to directly stimulate NK cells. The tumour behaviour following chemotherapy was then reviewed by comparing the tumours exposed to neoadjuvant therapies to untreated cancer biopsies. Although there were no alterations in activation ligands, chemotherapy downregulated the inhibitory ligands PDL-1, HLA-C and HLA-DR (Figure 6.36). This suggests the ovarian tumour response to chemotherapy is to further activate the NK cells. Indeed, chemotherapies have been shown to sensitise other tumours to immune cells by modulating their ligands, including a reduction of inhibitory molecules, thus improving NK cell activation and attack [361].

The NK ligands differed in the tumours obtained from patients with poor clinical outcomes. Specifically, a reduction of both activating (MICB and ULBP3) and inhibiting (HLA-DR and PDL-1) ligands were associated with disease recurrence and death (Figures 6.37 and 6.38). This supports previous studies that have shown increased levels of the MICB, ULBP3 and PDL-1 ligands are linked to improved survival and favourable outcomes in OC and other malignancies [380-384].

The functionality of NK cells in OC patients

The function of peripheral NK cells in OC patients was determined by the degree of tumour cell killing and cytokine production. OC NK cells from peripheral blood were highly cytotoxic, demonstrating increased elimination of the HLA-deficient cell line compared to NK cells from healthy non-cancerous controls (Figure 6.6). This supports the phenotype analysis where PBMC NK cells in OC patients had an increase in NKp46 expression which has been demonstrated to be related to higher NK cytotoxicity and is associated with lower rates of recurrence. However, with inferior expansion and proliferation following similar stimulation, the peripheral NK cells from OC patients had reduced cytokine production

compared to the controls (Figures 6.20, 6.21 and 6.22). This suggests that the NK cells in the peripheral blood of OC patients have a highly activated phenotype, but are unable to mount an effective response following direct stimulation [156, 210]. This could be due to these NK cells being overstimulated, leading to an exhausted phenotype, which has been corroborated with high expression of checkpoint receptors, including PD-1 and CTLA4.

The NK cell function in the presence of low HLA, shown with high cytotoxicity levels and poor cytokine secretion, was not influenced by chemotherapy treatment and had no association with clinical outcomes (Figures 6.7, 6.9 - 6.12, 6.21, 6.22, 6.27 - 6.29). The main chemotherapeutic agent used in OC, carboplatin, has been shown to have minimal effects on NK cell populations and does not interfere with their cytotoxic effects. However, the addition of the drug paclitaxel to treatment regimes, which all but one of our cohort received, does alter NK cell function and prevent tumour killing [385]. However, these effects from paclitaxel were not apparent in our study population.

The NK killing ability was also unrelated to phenotypical features, yet enhanced cytokine secretion was seen in the $CD56^{bri}CD16^{bri}$ NK cells (Figure 6.30). The immature $CD56^{bri}$ NK subpopulations are known to be the predominant cytokine producing NK cells with the aim of regulating and improving the tumour immune response [154, 173, 175, 177-180]. As expected, NK activation, seen with upregulation of activation receptors CD57 and NKG2D, was related to increased cytokine production (Figure 6.31), while NK cell checkpoint inhibition through PD-1 and CTLA-4 was linked with impaired NK function and poor cytokine secretion (Figure 6.32) [386].

The sensitivity of primary OC tumour cells to NK killing

The abilities of both healthy donor allogeneic and autologous NK cells to respond to and directly kill primary ovarian tumour tissue were evaluated in the co-culture assay. In line with the literature [199, 218], healthy donor NK cells had higher cytotoxicity levels towards the same cultured tumour tissue than the autologous NK cells (Table 6.7 and Figure 6.51). Nevertheless, the autologous NK cells were still able to kill the primary tumour cells, even without pre-activation with IL-2. In addition, while the NK cells demonstrated greater cytotoxicity towards tumour cells, they were, importantly, still cytotoxic towards the normal ovarian tissue (Figure 6.51). This raises the question of why tumour cells have not been eliminated by NK cells in patients with OC. Firstly, the infiltration of NK cells into the malignant tissue is poor, particularly within metastatic tumour deposits such as the omentum. Secondly, the hostile microenvironment of ovarian tumours acts to quickly inactivate and impair the function of the infiltrated NK cells. However, the demonstrated sensitivity of primary ovarian tumours to NK cells implies that NK therapy has the potential to effectively treat OC, even with autologous NK cells, which provide a safer therapeutic option.

Furthermore, the tumours associated with poor clinical outcomes generated an increased killing response from the healthy donor NK cells (Figures 6.53 – 6.56), suggesting further alterations within the TME occurred with advancing disease that stimulated a greater NK response. The previous NK analysis (chapter 5) demonstrated that increased NK activating receptors, like DNAM-1, are related with advanced disease and higher tumour burden. It is reasonable to hypothesize that elevated DNAM-1 expression on NK cells is associated with increased DNAM-1 ligands on the OC tissue, which renders the tumour cells sensitive to NK killing. This increased NK killing response is related with poorer patient outcomes.

Through the manipulation of NK activation signalling pathways following tumour recognition, the activation receptors NKG2D, NKp46 and NKp30 were found to have limited significance for NK cells to successfully target tumour cells. Nevertheless, the DNAM-1 receptor was shown to be critical for effective NK cell killing of ovarian tumour tissue (Figure 6.57). Others have also recognised the importance of interactions between the tumour PVR ligand and the DNAM-1 receptor for NK cell degranulation and cytotoxicity in ovarian tumours [199]. In the transcription assay (Figure 6.34), the PVR ligand was shown to be upregulated in tumour biopsies compared with normal ovarian tissue. As DNAM-1 expression was downregulated on the tumour infiltrating NK cells compared to the peripheral blood NK cells (chapter 4, Figures 4.39 and 4.4.7), NK cells that overexpress DNAM-1 have therapeutic potential in OC, assuming they can be protected in the tumour microenvironment.

In conclusion, the large NK cell populations present in OC were highly cytotoxic when stimulated by cell lines, yet showed minimal expansion capabilities and poor cytokine secretion. While the interrogation of the ovarian tumour ligands revealed a TME that should support NK activation, tumour evasion mechanisms in advancing disease seemingly prevented the OC NK cells from mounting an effective response. Interestingly, both allogenic and autologous NK cells have shown strong cytotoxicity to primary OC tumour cells without activation. Finally, the interaction between PVR and DNAM-1 was highlighted as an essential signalling pathway, warranting further exploration and manipulation for possible targeted NK cell therapy.

Chapter 7:

General Discussion and Future Work

7.1 Tumour Heterogeneity and Transcriptional Profiling of Ovarian Cancer

Utilising metastatic omental tumour samples, single cell sequencing interrogated the heterogeneity and transcriptional profiles of advanced high-grade serous OC. This chapter (Chapter 3) aimed to perform a comprehensive analysis of the cell type contexture within the ovarian TME and evaluate the characteristics and relationship of the tumour and immune cell populations. Another key objective of this sequencing study was to examine any alterations to the TME following chemotherapy exposure and the molecular adaptations associated with treatment resistance.

Two different single cell sequencing techniques were successfully optimised and detected multiple immune, tumour and stromal cell populations within the omental tissue. Indeed, significant tumour and immune cell heterogeneity was detected across the patient samples using both sequencing techniques. Substantial modifications occurred following chemotherapy, with scRNAseq analysis showing elevated expression of genes associated with immune activation, tumour invasion, treatment resistance and disease progression. In addition, scATACseq revealed that chemotherapy increased chromatin accessibility for oncogenes, transcription factors related to OC tumorigenesis and cancer stem cells.

The detailed analysis of the NK cell population provided insight into the characteristics of this important immune subtype, and how interactions with the TME influence the NK cell response to ovarian malignancy. The scRNAseq analysis was able to identify and classify 5 transcriptionally distinct tumour-infiltrating NK cell subpopulations. Notably, the inhibitory features of the TME correlated to dysfunctional features of the NK cells, with inhibition and reduced cytotoxicity towards tumour cells. The reactivation and stimulation of NK cells

following chemotherapy was also evident, confirming the significance of this population for disease control and treatment response.

While our scRNA sequencing study is the first to undertake such a comprehensive immunogenomic analysis of OC and describe the complex modifications with chemotherapy, it also complements the earlier studies reported [114, 116-123, 333, 340]. With just a single published OC scATACseq study [339], where just two HGSOvCa samples were utilised, our in-depth analysis of the major cell subpopulations, transcription factor activity and chromatin accessibility following chemotherapy, provided additional insight into the chromatin landscape in OC.

The single cell solutions utilised for the scRNAseq analysis were cell sorted and enriched for CD45 positive immune cells. This ensured that adequate numbers of small cell clusters could be detected for the immunogenomic analysis and allowed me to focus on the immune environment for OC. There were small numbers of Epcam positive epithelial cells within our samples, likely due to the processing of fragile and hypoxic tumour tissue or due to low mRNA levels of Epcam within these cells. However, cell sorting and the reconstruction of samples also allowed the maximum possible number of epithelial cells to be sequenced.

An advantage of scATACseq is the ability to utilise stored frozen tissue biopsies. This enables histological diagnosis to be confirmed prior to undertaking sequencing, allowing samples to be selected for desired outcomes and characteristics. This also gives the option of including matched samples from the same patient, where tissue can be collected at the time of diagnosis, and again following chemotherapy when IDS is performed. These paired chemotherapy-naïve and chemotherapy-exposed samples from the same patient can provide a direct insight of

treatment modifications within individual patients. Indeed, within our scATACseq cohort there was one pair of these matched biopsies collected and sequenced. Future work includes obtaining additional paired samples and performing a detailed patient specific analysis of these corresponding pre and post chemotherapy samples. In addition, using frozen tissues gives the possibility of matching the stored scATACseq samples to selected scRNAseq samples following successful sequencing of the fresh tissues. Within our cohort, adjacent biopsies obtained from the same tissue site were used in both scRNAseq and scATACseq for three patients. Further data analysis is required to investigate these samples, comparing the two sequencing methods using the same patients and tissue samples. This will provide additional insight into the link between gene expression and chromatin accessibility.

Additional work required to enhance this single cell study of OC is a more comprehensive cancer stem cell analysis, following the detection of this population following chemotherapy. Further interrogation of the scATACseq dataset will also aid the discovery of the different lymphocyte subpopulations. A deeper review of the tumour cell cluster identified in both sequencing techniques is also required. By categorising the subpopulations of tumour cells, those that are inherently chemo-resistant can be recognised and examined in more detail. Here, possible targets could be detected for immunotherapeutic strategies to try and overcome the current treatment failures.

7.2 NK cell Phenotype, Functionality and Clinical Relevance in Ovarian Cancer

Building on the findings from previous NK cell studies, which are summarised in Figure 7.1, my subsequent chapters explored the characteristics, behaviour and clinical significance of NK cells in OC. The primary aim of Chapter 4 was to interrogate the proportions, types and features of NK cells within peripheral blood, primary ovarian tumour tissue and metastatic omental tumour deposits obtained from patients with OC. By evaluating the degree of activation, the NK cell response to the ovarian TME could be explored along with the impact of chemotherapy on NK cell phenotype. To this end, a large prospective cohort of OC and control patients was established. Utilising this cohort, a direct comparison of ovarian tumours with benign and normal ovarian tissue was made, while also evaluating chemotherapy naïve and exposed tumours.

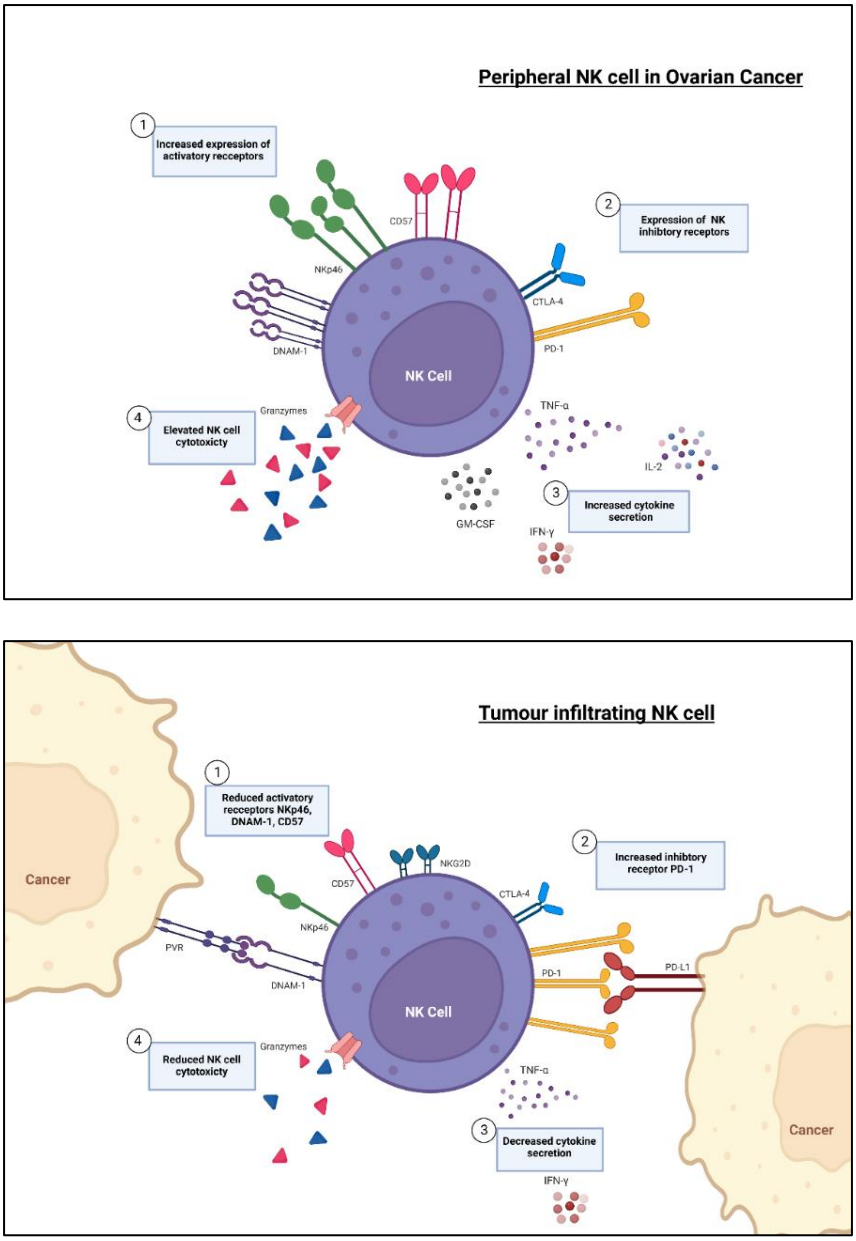


Figure 7.1: Comparison of tumour-infiltrating NK cells and peripheral NK cells in OC

The peripheral NK cells in OC patients have increased expression of activating receptors, such as DNAM-1 and NKp46, and have elevated cytotoxicity levels. In comparison, the tumour-infiltrating NK cells are impaired by the suppressive ovarian tumour microenvironment. They develop an inhibitory phenotype with reduced activation receptors, particularly DNAM-1, NKp46 and CD57, and increased expression of the checkpoint inhibitor, PD-1 [150, 200, 211, 212, 217, 225, 226]. Tumour NK cells have reduced proliferation, produce fewer cytokines and decreased cytotoxicity levels [156, 210, 211].

7.2.1 NK cell Phenotype

The complex flow cytometric analysis undertaken in Chapter 4 detected clear differences in the NK cells within samples from OC patients. There was an increased proportion of peripheral NK cells in cases of OC compared to non-cancerous control patients, suggesting stimulation and proliferation in malignancy. While NK cells retained their ability to penetrate the solid ovarian tissues upon malignant transformation, NK cell infiltration into metastatic omental tumour was impaired compared to normal omental tissue. However, following infiltration into tumour tissues, the NK cells had less cytotoxic capacity (with fewer mature cytotoxic $CD56^{dim}CD16^{bri}$ NK cells) and expressed a less activated phenotype (with decreased expression of activation receptors and increased inhibitory checkpoint PD-1) compared to the peripheral blood NK cells. Nevertheless, when compared to controls, NK cells in the blood and tissue of OC patients had increased expression of various NK activation receptors, showing the potential for cancer recognition and an anti-tumour response.

The analysis also showed that NK cell phenotype was modified following chemotherapy; peripheral NK cells were rendered less functional, with upregulation of the inhibitory immune checkpoints (CTLA-4 and PD-1), while there was increased activation of the omental tumour NK cells. There was also a reduction in the mature cytotoxic NK subpopulation in blood and ovarian samples following chemotherapy, which contradicts previous findings of an increased immune response [104, 166, 361, 369].

It is important to note that patients who receive chemotherapy are more likely to develop lymphocytopenia. While lymphocyte counts often normalise spontaneously prior to surgery, patients may require treatment with granulocyte-colony stimulatory factor (G-CSF) for persistent lymphocytopenia in order to reduce intra-operative and post-operative sepsis.

However, G-CSF can cause NK cell suppression, reduced NK activity and decreased cytotoxicity [370-373]. Therefore, it is possible that the reduction in mature cytotoxic NK cells following chemotherapy in our cohort was influenced by G-CSF administration. Unfortunately, the use of G-CSF in the cohort was unknown at the time of analysis and it was not possible to stratify NK cell subtypes accordingly. However, this data can now be acquired and future work will determine the impact of G-CSF on the NK populations in this cohort.

In addition, patients typically undergo interval debulking surgery four to six weeks after their last cycle of NACT, allowing the immune system and NK populations to recover from chemotherapy prior to surgery. As our samples were all collected at the time of surgery, the immediate impact of NACT on the NK cells could not be entirely appreciated. Future studies should aim to assess NK cells at the time of diagnosis (prior to any treatment) and when NACT is completed, comparing to the samples obtained at the time of surgery. This would allow the direct influence of chemotherapy on NK cells to be assessed, as well as the alterations as they recover in the period between NACT and surgery. Further collection points, post-operatively and with adjuvant chemotherapy, will allow NK cells to be reviewed after treatment is completed and also as disease is progressing and recurring. Additional correlations, such as the relation between CA-125 and NK phenotype, can be made as patients respond to treatment or develop chemoresistance.

7.2.2 NK cell Phenotype and Clinical Relevance

Following on from this assessment of the NK cell phenotype, Chapter 5 examined the relationship between NK cells and clinical outcomes in the same cohort of patients with OC. Thus, the overarching aim was to determine how NK cell infiltration and activation influences disease recurrence, patient survival, tumour burden and response to current treatments. It was

evident that as tumours progressed, seen with advancing stage, raised PCI and the development of metastatic omental deposits, the expression of activation receptors increased on NK cells within blood and tumour samples. This implies possible tumour escape mechanisms or the release of soluble tumour ligands acting to chronically upregulate and saturate activation receptors, leading to exhausted NK cells and a diminished NK response [213, 218-220]. In support of this notion, checkpoint inhibitors (PD-1 and CTLA-4) were raised in OC blood samples compared to controls, with PD-1 also raised in ovarian and omental tumour tissues.

Poor patient outcomes, specifically disease recurrence and reduced PFS, were typically related to an inhibitory NK phenotype (reduced activation receptors and raised checkpoint inhibitors) in blood and ovarian tumour samples. In contrast, disease recurrence and disease specific death were associated with omental NK activation, perhaps caused by chronic ligand exposure in advancing disease and a subsequent increase in activation receptors [212]. A noteworthy discovery was the significant reduction in OS when activating receptor DNAM-1 was increased on PBMC, ovarian and omental tumour NK cells. The biological basis for this association is not clear and requires additional study. Further associations were evident between NK cells and chemotherapy treatment: NK cells were in an activated state in patients who responded well to chemotherapy (CRS 3), however it is unclear whether G-CSF also influenced these findings.

7.2.3 NK cell Functionality

The assays described in Chapter 6 explored the interactions between NK cells and primary ovarian tumour. This supplemented existing knowledge of the tumour-NK cell relationship, highlighted in Figure 7.2. Not only did my assessment aim to establish the functionality and cytotoxic abilities of NK cells, it also focused on the ways in which the TME influences and

responds to the NK cells. Finally, I attempted to manipulate NK activating signalling pathways to identify credible targets for NK immunotherapies.

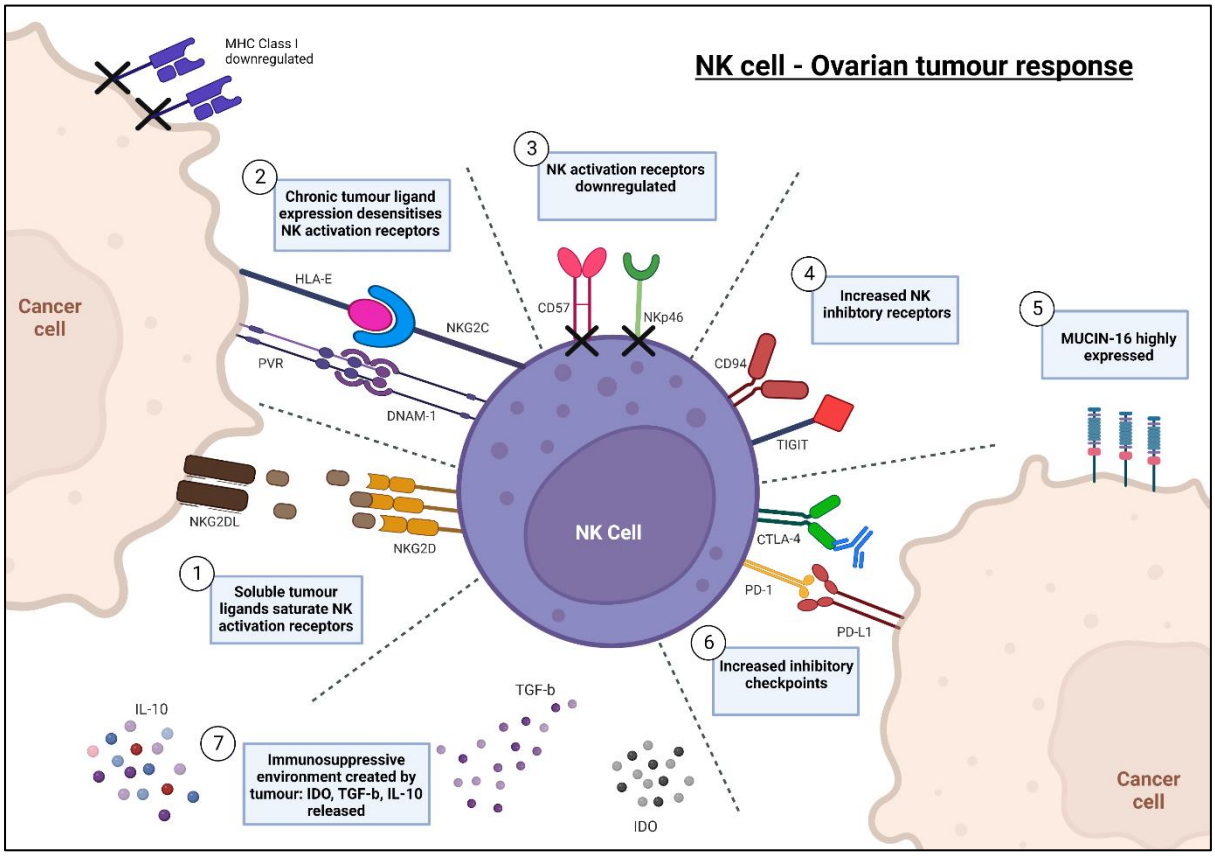


Figure 7.2: The mechanisms utilised by ovarian cancer cells to inactivate NK cells and reduce NK cell-mediated cytotoxicity.

Tumour cells respond to cytotoxic NK cells by: 1) secreting soluble ligands to saturate and deactivate NK activation receptors, 2) chronically expressing ligands to desensitise NK activation receptors, 3) downregulating NK activation receptors, 4) increasing NK inhibitory receptors, 5) expressing Mucin-16 (CA-125) which protects them from an NK cell attack, 6) increasing immune checkpoint ligands to inhibit NK cells, and 7) secreting cytokines and immunosuppressive factors into the TME [131,132, 150, 151, 154, 177, 180, 192, 199, 200, 211-217, 223-229].

Interrogation of the key NK ligands expressed by tumour cells portrayed a TME that serves to directly stimulate NK cells; tumour cells had elevated levels of numerous NK activating ligands alongside a reduction of MHC class I molecules. Downregulation of MHC class I on tumours is thought to reflect selection of cells that can evade T cell immune recognition, but this also serves to increase their susceptibility to NK cell recognition [154, 173, 177 182, 186, 189-192]. A number of NK inhibitory ligands are also downregulated following chemotherapy [361].

The functionality of NK cells towards ovarian tumours was determined by the degree of tumour cell killing and cytokine production. In the presence of an HLA-deficient cell line, peripheral blood NK cells from OC patients were highly cytotoxic yet had poor cytokine secretion and minimal expansion capabilities, suggesting that NK cells are unable to mount a comprehensive functional response following stimulation. This may be due to overstimulation resulting in NK exhaustion, which is supported by the corresponding high expression of checkpoint inhibitors.

Co-culture assays evaluated the sensitivity of primary ovarian tumours to NK killing and here it was notable that both healthy donor and autologous NK cells were able to kill the primary tumour cells without pre-activation with IL-2. This therefore suggests that NK therapy has the potential to effectively treat OC, even with autologous NK cells, which is a safer therapeutic option. Interestingly, tumours associated with poor clinical outcomes generated an increased killing response from the healthy donor NK cells, implying alterations within the TME in advancing disease stimulated a greater NK response. Manipulation of NK activation signalling pathways identified the DNAM-1 receptor as being essential for effective NK cell killing of the primary ovarian tumour tissue.

7.2.4 DNAM-1 in Ovarian Cancer

Throughout the NK cell analysis, the importance of the NK activating receptor DNAM-1 became clear with several significant findings. Primarily, DNAM-1 was shown to be highly expressed on ovarian and omental tumour compared to normal tissues, with expression greater still in the peripheral blood of OC patients. DNAM-1 was increased in cases with advanced stage, high tumour burden, omental metastasis and elevated CA-125, showing the consistent association with worsening disease state. Indeed, DNAM-1 expression was significantly elevated in peripheral blood, ovarian and omental tumour in patients with reduced OS. Upon examination of the tumour tissue, the corresponding activating ligand, PVR was increased in HGSOvCa tissue compared to normal ovary. Furthermore, NK cytotoxicity towards primary ovarian tumour was reduced when DNAM-1 was inhibited, highlighting the significance of the receptor in NK killing.

Others have also recognised the importance of the DNAM-1 receptor in the cytotoxic NK response towards ovarian tumours [199, 387, 388]. Carleston et al. have demonstrated that the interaction between DNAM-1 and PVR is critical for NK activation and tumour killing in OC [199]. Here, they also report a reduction in NK degranulation and cytotoxicity upon DNAM-1 inhibition, but using peritoneal effusion samples and from a small number of OC patients. In addition, while ascitic fluid NK cells had reduced DNAM-1 expression, Maas et al. show the NK cell response towards OC cells is increased when inhibitory receptor TIGIT is blocked, principally when PVR/DNAM-1 signalling occurs concurrently [387].

These findings, along with ours, therefore highlight the significant therapeutic potential of DNAM-1 as a target in OC management. With ovarian NK cells having lower DNAM-1 expression than the NK cells in the blood of OC patients, elevating the DNAM-1 expression

within tumour tissue is likely to potentiate the NK response, provided these NK cells can be protected in the TME. Direct stimulation of DNAM-1, through manipulation of the tumour ligands and activating pathways, is also likely to enhance an NK-mediated attack. Examination of tumour ligands in the single cell sequencing analysis revealed that the DNAM-1 ligands PVR and Nectin-2 were not strongly over-expressed by tumour cells, suggesting that downregulation may potentially act to evade NK activation or possibly that additional unknown DNAM-1 ligands are present in OC. Indeed, further understanding of the interactions between tumour tissue ligands and the DNAM-1 receptor is crucial for effective manipulation of DNAM-1 signalling pathways with immunotherapy. There is a rationale to simultaneously target multiple activating and inhibitory receptors, synergistically stimulating DNAM-1 and other activating receptors, while also blocking the critical inhibitory signalling pathways. Further approaches for DNAM-1 based therapy in OC could explore the use of engineered NK cells. Indeed, in other malignancies, in vitro studies have reported greater cytotoxicity following the adoptive transfer of NK cells that have been engineered to stimulate and manipulate cell signalling through the DNAM-1 receptor [389, 390].

7.3 Limitations and Future Directions

Although the NK cell analysis and functional experiments described in Chapters 4, 5 and 6 have demonstrated important findings and have identified a potential target for immunotherapy, a major limitation of the research was being restricted to performing each assay just once per patient sample. The sample collection relied on patients agreeing to additional blood tests and tumour biopsies being obtained for research, with clinical specimens rightly prioritised for diagnostic and treatment purposes in the first instance. Following the processing and manipulation of samples for multiple assays, the tissue lymphocyte populations were exhausted after just one experimental run. As such, it was not possible to undertake

additional assays, but ideally each would have been performed three times per patient sample. Therefore, the number of patients in the cohort was increased to compensate for this insufficiency. However, it is recognised that biological variation between patients could influence findings. Nevertheless, the large patient cohort, with blood and multiple tissue samples for every patient, is the most substantial and comprehensive reported in the literature.

The analysis of this cohort can be further explored with statistical review of continuous variables and multivariant analysis. Additional understanding of the relationship between NK cells and tumour cells will be acquired through tissue microarrays and multiplex immunostaining of primary ovarian and metastatic omental tissue. Here, the anatomical distribution of NK cells within the ovarian and omental tumours can be determined and will be compared to the NK cells in normal ovarian tissue. As well as locating the NK cells within the tissue, the expression of key NK cell receptors, such as DNAM-1, TIGIT, NKG2D and NKp46, will be reviewed. The presence of NK cell ligands, such as PVR and HLA class I molecules, will also be detected and located within the tumour and normal tissues, observing their association with the tissue-infiltrating NK cells. Finally, chemotherapy-naïve tumour will be compared to chemotherapy resistant samples (CRS 1 following NACT) to evaluate the differences in NK cell distribution and the expression of NK cell ligands with treatment.

7.4 Conclusion

In summary, this thesis has examined the heterogeneity in ovarian cancer using single cell sequencing, identifying transcriptionally distinct tumour and immune cell populations. The detailed characterisation of the OC landscape has detected alterations to the cell type contexture and molecular modifications following chemotherapy treatment. Indeed, it has recognised the genes and transcription factors associated with immune activation, tumorigenesis and treatment

resistance. A comprehensive immunogenomic analysis of the NK cell population has described the characteristics of differing NK cell subtypes, showing how inhibitory features of the tumour microenvironment influence the NK cell response to malignancy. Additional exploration determined how the dysfunctional NK cells, which were inhibited and with decreased cytotoxicity, were reactivated with chemotherapy.

Utilising a large prospective cohort of OC patient samples, the thesis has also explored the phenotype and function of NK cells in peripheral blood, primary ovarian tumour and metastatic omental tumour. Flow cytometric analysis has shown the expansion and activation of peripheral NK cells in OC patients, alongside NK inhibition upon tumour infiltration. Alterations with chemotherapy treatment highlighted further inhibition and reduced cytotoxicity of blood and ovarian tumour NK cells. Furthermore, the nature and role of the tumour-infiltrating NK cells in progressive disease was evaluated, showing adaptations to NK receptors and possible methods of tumour evasion. By examining the relationship of NK cells to clinical data, specific inhibitory NK features were shown to be significantly associated with poor patient outcomes. The importance of NK cells in metastatic disease was evident with reduced NK infiltration into omental tumours, an activated omental NK response to chemotherapy and clear correlations with survival. Finally, primary ovarian tumours were shown to be sensitive to NK killing, but dependent on the activation receptor, DNAM-1. The importance of DNAM-1 has been demonstrated throughout this thesis, identifying it as a likely biomarker that can be used as a target for NK-mediated immunotherapy.

Chapter 8:

References

References

1. Cancer Research UK; Ovarian Cancer Statistics [Internet]. Available at: http://www.cancerresearchuk.org/health-professional/cancer-statistics/statistics-by-cancer-type/ovarian-cancer
2. Smittenaar CR, Petersen KA, Stewart K, Moitt N. Cancer incidence and mortality projections in the UK until 2035. Br J Cancer. 2016 Oct 25;115(9):1147-1155.
3. Delon C, Brown KF, Payne NWS, Kotrotsios Y, Vernon S, Shelton J. Differences in cancer incidence by broad ethnic group in England, 2013-2017. Br J Cancer. 2022 Jun;126(12):1765-1773.
4. Manchanda R, Abdelraheim A, Johnson M, Rosenthal AN, Benjamin E, Brunell C, et al. Outcome of risk-reducing salpingo-oophorectomy in BRCA carriers and women of unknown mutation status. BJOG 2011; 118(7): 814-24.
5. Cancer Genome Atlas Research Network. Integrated genomic analyses of ovarian carcinoma. Nature 2011; 474(7353): 609–615.
6. Lynch HT, Snyder C, Casey MJ. Hereditary ovarian and breast cancer: What have we learned? Ann. Oncol. 2013; 24 (Suppl. S8): viii83–viii95.
7. Hunn J, Rodriguez GC. Ovarian cancer: etiology, risk factors, and epidemiology. Clin Obstet Gynecol. 2012 Mar;55(1):3-23.
8. Crum CP, Drapkin R, Kindelberger D, Medeiros F, Miron A, Lee Y. Lessons from BRCA: the tubal fimbria emerges as an origin for pelvic serous cancer. Clin Med Res. 2007 Mar;5(1):35-44.
9. Labidi-Galy SI, Papp E, Hallberg D, Niknafs N, Adleff V, Noe M, et al. High grade serous ovarian carcinomas originate in the fallopian tube. Nat Commun. 2017 Oct 23;8(1):1093.
10. Reade CJ, McVey RM, Tone AA, Finlayson SJ, McAlpine JN, Fung-Kee-Fung M, et al. The fallopian tube as the origin of high grade serous ovarian cancer: review of a paradigm shift. J Obstet Gynaecol Can. 2014 Feb;36(2):133-140.
11. BMJ Best Practice; Ovarian Cancer [Internet]. Available at: https://bestpractice.bmj.com/topics/en-gb/260
12. Raulet DH, Guerra N. Oncogenic stress sensed by the immune system: role of natural killer cell receptors. Nat Rev Immunol. 2009; 9(8): 568-80
13. Saint John's Cancer Institute; Ovarian cancer signs, symptoms and diagnoses [Internet]. Available at: https://www.saintjohnscancer.org/gynecology/conditions-we-treat/ovarian-cancer/
14. Rose PG, Piver MS, Tsukada Y, Lau TS. Metastatic patterns in histologic variants of ovarian cancer. An autopsy study. Cancer. 1989 Oct 1;64(7):1508-13.
15. Risch HA, Weiss NS, Lyon JL, Daling JR, Liff JM. Events of reproductive life and the incidence of epithelial ovarian cancer. Am J Epidemiol. 1983 Feb;117(2):128-39.
16. Schildkraut JM, Bastos E, Berchuck A. Relationship between lifetime ovulatory cycles and overexpression of mutant p53 in epithelial ovarian cancer. J Natl Cancer Inst. 1997;89:932–93.
17. Joly DJ, Lilienfeld AM, Diamond EL, Bross ID. An epidemiologic study of the relationship of reproductive experience to cancer of the ovary. Am J Epidemiol. 1974 Mar;99(3):190-209.
18. Hakim AA, Barry CP, Barnes HJ, Anderson KE, Petitte J, Whitaker R, et al. Ovarian adenocarcinomas in the laying hen and women share similar alterations in p53, ras, and HER-2/neu. Cancer Prev Res (Phila). 2009 Feb;2(2):114-21.
19. Purdie DM, Bain CJ, Siskind V, Webb PM, Green AC. Ovulation and risk of epithelial ovarian cancer. Int J Cancer. 2003 Mar 20;104(2):228-32.
20. Wu ML, Whittemore AS, Paffenbarger RS Jr, Sarles DL, Kampert JB, Grosser S, et al. Personal and environmental characteristics related to epithelial ovarian cancer. I. Reproductive and menstrual events and oral contraceptive use. Am J Epidemiol. 1988 Dec;128(6):1216-27.

21. Králíčková M, Vetvicka V. Endometriosis and ovarian cancer. World J Clin Oncol. 2014 Dec 10;5(5):800-5.
22. Shan W, Liu J. Inflammation: a hidden path to breaking the spell of ovarian cancer. Cell Cycle. 2009 Oct 1;8(19):3107-11.
23. Risch HA. Hormonal etiology of epithelial ovarian cancer, with a hypothesis concerning the role of androgens and progesterone. J Natl Cancer Inst. 1998 Dec 2;90(23):1774-86.
24. Cramer DW, Welch WR. Determinants of ovarian cancer risk. II. Inferences regarding pathogenesis. J Natl Cancer Inst. 1983 Oct;71(4):717-21.
25. Huncharek M, Geschwind JF, Kupelnick B. Perineal application of cosmetic talc and risk of invasive epithelial ovarian cancer: a meta-analysis of 11,933 subjects from sixteen observational studies. Anticancer Res. 2003;23:1955–1960.
26. Tworoger SS, Fairfield KM, Colditz GA, Rosner BA, Hankinson SE. Association of oral contraceptive use, other contraceptive methods, and infertility with ovarian cancer risk. Am J Epidemiol. 2007 Oct 15;166(8):894-901.
27. Olsen CM, Green AC, Whiteman DC, Sadeghi S, Kolahdooz F, Webb PM. Obesity and the risk of epithelial ovarian cancer: a systematic review and meta-analysis. Eur J Cancer. 2007 Mar;43(4):690-709.
28. Jordan SJ, Whiteman DC, Purdie DM, Green AC, Webb PM. Does smoking increase risk of ovarian cancer? A systematic review. Gynecol Oncol. 2006 Dec;103(3):1122-9.
29. Lawrence MS, Stojanov P, Polak P, Kryukov GV, Cibulskis K, Sivachenko A, et al. Mutational heterogeneity in cancer and the search for new cancer-associated genes. Nature. 2013 Jul 11;499(7457):214-218.
30. Martin SD, Brown SD, Wick DA, Nielsen JS, Kroeger DR, Twumasi-Boateng K, et al. Low Mutation Burden in Ovarian Cancer May Limit the Utility of Neoantigen-Targeted Vaccines. PLoS One. 2016 May 18;11(5):e0155189.
31. Wick DA, Webb JR, Nielsen JS, Martin SD, Kroeger DR, Milne K, et al. . Surveillance of the tumor mutanome by T cells during progression from primary to recurrent ovarian cancer. Clin. Cancer Res. 2014;20:1125–1134.
32. Sabatier R, Garnier S, Guille A, Carbuccia N, Pakradouni J, Adelaide J, et al. Whole-genome/exome analysis of circulating tumor DNA and comparison to tumor genomics from patients with heavily pre-treated ovarian cancer: subset analysis of the PERMED-01 trial. Front Oncol. 2022 Jul 29;12:946257.
33. Kmet LM, Cook LS, Magliocco AM. A review of p53 expression and mutation in human benign, low malignant potential, and invasive epithelial ovarian tumors. Cancer. 2003 Jan 15;97(2):389-404.
34. Schuijer M, Berns EM. TP53 and ovarian cancer. Hum Mutat. 2003 Mar;21(3):285-91.
35. Chen X, Li X, Wang X, Zhu Q, Wu X, Wang X. MUC16 impacts tumor proliferation and migration through cytoplasmic translocation of P120-catenin in epithelial ovarian cancer cells: An original research. BMC Cancer 2019; 19(1): 171.
36. Jacobs I, Lancaster J . The molecular genetics of sporadic and familial epithelial ovarian cancer. Int J Gynecol Cancer 1996;6:337–355.
37. Ross JS, Yang F, Kallakury BVS, Sheehan CE, Ambros RA, Muraca PJ. HER-2/neu oncogene amplification by fluorescence in situ hybridization in epithelial tumors of the ovary. American Journal of Clinical Pathology. 1999;111(3):311–316.
38. Cheng JQ, Godwin AK, Bellacosa A, Taguchi T, Franke TF, Hamilton TC, et al. AKT2, a putative oncogene encoding a member of a subfamily of protein-serine/threonine kinases, is amplified in human ovarian carcinomas. Proc Natl Acad Sci U S A. 1992 Oct 1;89(19):9267-71.

39. Atallah GA, Kampan NC, Chew KT, Mohd Mokhtar N, Md Zin RR, Shafiee MNB, et al. Predicting Prognosis and Platinum Resistance in Ovarian Cancer: Role of Immunohistochemistry Biomarkers. Int J Mol Sci. 2023 Jan 19;24(3):1973.
40. Singer G, Stöhr R, Cope L, Dehari R, Hartmann A, Cao DF, et al. Patterns of p53 mutations separate ovarian serous borderline tumors and low- and high-grade carcinomas and provide support for a new model of ovarian carcinogenesis: a mutational analysis with immunohistochemical correlation. Am J Surg Pathol. 2005 Feb;29(2):218-24.
41. Shih IeM, Kurman RJ. Ovarian tumorigenesis: a proposed model based on morphological and molecular genetic analysis. Am J Pathol. 2004 May;164(5):1511-8.
42. Karst AM, Drapkin R. Ovarian cancer pathogenesis: a model in evolution. J Oncol. 2010;2010:932371.
43. Lancaster JM, Powell CB, Chen LM, Richardson DL; SGO Clinical Practice Committee. Society of Gynecologic Oncology statement on risk assessment for inherited gynecologic cancer predispositions. Gynecol Oncol. 2015 Jan;136(1):3-7.
44. Alsop K, Fereday S, Meldrum C, deFazio A, Emmanuel C, George J, et al. BRCA mutation frequency and patterns of treatment response in BRCA mutation-positive women with ovarian cancer: a report from the Australian Ovarian Cancer Study Group. J Clin Oncol. 2012 Jul 20;30(21):2654-63.
45. Ledermann JA, Drew Y, Kristeleit RS. Homologous recombination deficiency and ovarian cancer. Eur J Cancer. 2016;60:49-58.
46. Baci D, Bosi A, Gallazzi M, Rizzi M, Noonan DM, Poggi A, et al. The Ovarian Cancer Tumor Immune Microenvironment (TIME) as Target for Therapy: A Focus on Innate Immunity Cells as Therapeutic Effectors. Int J Mol Sci. 2020; 21(9) :3125
47. BGCS Guidelines Ovarian Cancer: Recommendations for Practice [Internet]. [cited 2017]. Available at: https://www.bgcs.org.uk/wp-content/uploads/2019/05/BGCS-Guidelines-Ovarian-Guidelines-2017.pdf.
48. Whittemore AS, Gong G, Itnyre J. Prevalence and contribution of BRCA1 mutations in breast cancer and ovarian cancer: result from three U.S. population-based case-control studies of ovarian cancer. Am J Hum Genet. 1997;60:496–504.
49. Ford D, Easton DF, Stratton M, Narod S, Goldgar D, Devilee P, et al. Genetic heterogeneity and penetrance analysis of the BRCA1 and BRCA2 genes in breast cancer families. The Breast Cancer Linkage Consortium. Am J Hum Genet. 1998 Mar;62(3):676-89.
50. Bonadona V, Bonaïti B, Olschwang S, Grandjouan S, Huiart L, Longy M, et al.; French Cancer Genetics Network. Cancer risks associated with germline mutations in MLH1, MSH2, and MSH6 genes in Lynch syndrome. JAMA. 2011 Jun 8;305(22):2304-10.
51. Peltomäki P. Update on Lynch syndrome genomics. Fam Cancer. 2016 Jul;15(3):385-93.
52. Taylor N, Mutch DG. Gynecologic manifestations of hereditary nonpolyposis colorectal cancer. From inherited to sporadic disease. Oncology (Huntington). 2006;20:85–94.
53. Lu KH, Broaddus RR. Gynecologic cancers in Lynch syndrome/HNPCC. Fam Cancer. 2005;4:249–254.
54. NICE Clinical Guideline; CG122; Ovarian cancer: recognition and initial management [Internet]. Available at: https://www.nice.org.uk/guidance/cg122/chapter/Key-priorities-for-implementation
55. FIGO; Staging for OVFTP malignancies [Internet]. Available at https://www.figo.org/news/staging-ovftp-malignancies
56. Society of Gynecologic Oncology; FIGO OVARIAN CANCER STAGING GUIDELINES (JANUARY 2014) [Internet]. Available at:New FIGO ovarian cancer staging guidelines (sgo.org) https://www.sgo.org/resources/new-figo-ovarian-cancer-staging-

guidelines/#:~:text=New%20FIGO%20ovarian%20cancer%20staging%20guidelines.%20January%202014.,concluded%20in%20Italy%20at%20the%20end%20of%202012.
57. Berek JS, Kehoe ST, Kumar L, Friedlander M. Cancer of the ovary, fallopian tube, and peritoneum. Int J Gynaecol Obstet. 2018 Oct;143 Suppl 2:59-78
58. NICE Clinical Guidance; IPG470; Ultra-radical (extensive) surgery for advanced ovarian cancer [Internet]. Available at https://www.nice.org.uk/guidance/ipg470
59. NICE Clinical Guidance; TA55; Guidance on the use of paclitaxel in the treatment of ovarian cancer [Internet]. Available at: https://www.nice.org.uk/guidance/ta55
60. National Cancer Guidance Steering Group. Improving outcomes in gynaecological cancers - the manual. London: NHS Executive, Department of Health, 1999.
61. du Bois A, Reuss A, Pujade-Lauraine E, Harter P, Ray-Coquard I, Pfisterer J. Role of surgical outcome as prognostic factor in advanced epithelial ovarian cancer: a combined exploratory analysis of 3 prospectively randomized phase 3 multicenter trials: by the Arbeitsgemeinschaft Gynaekologische Onkologie Studiengruppe Ovarialkarzinom (AGO-OVAR) and the Groupe d'Investigateurs Nationaux Pour les Etudes des Cancers de l'Ovaire (GINECO). Cancer 2009; 115(6): 1234-44.
62. van der Burg ME, van Lent M, Buyse M, Kobierska A, Colombo N, Favalli G, et al. The effect of debulking surgery after induction chemotherapy on the prognosis in advanced epithelial ovarian cancer. Gynecological Cancer Cooperative Group of the European Organization for Research and Treatment of Cancer. N Engl J Med 1995; 332(10): 629-34.
63. Vergote I, Trope CG, Amant F, Kristensen GB, Ehlen T, Johnson N, et al. Neoadjuvant chemotherapy or primary surgery in stage IIIC or IV ovarian cancer. N Engl J Med 2010; 363(10): 943-53.
64. Kehoe S, Hook J, Nankivell M, Jayson GC, Kitchener H, Lopes T, et al. Primary chemotherapy versus primary surgery for newly diagnosed advanced ovarian cancer (CHORUS): an open-label, randomised, controlled, non-inferiority trial. Lancet 2015; 386(9990): 249-57.
65. Vedantu; Omentum: Anatomy, functions and structure [Internet]. Available at: https://www.vedantu.com/biology/omentum
66. Iwagoi Y, Motohara T, Hwang S, Fujimoto K, Ikeda T, Katabuchi H. Omental metastasis as a predictive risk factor for unfavorable prognosis in patients with stage III-IV epithelial ovarian cancer. Int J Clin Oncol. 2021 May;26(5):995-1004.
67. Meza-Perez S, Randall TD. Immunological Functions of the Omentum. Trends Immunol. 2017 Jul;38(7):526-536.
68. Koppe MJ, Nagtegaal ID, de Wilt JH, Ceelen WP. Recent insights into the pathophysiology of omental metastases. J Surg Oncol. 2014 Nov;110(6):670-5..
69. Arie AB, McNally L, Kapp DS, Teng NN. The omentum and omentectomy in epithelial ovarian cancer: a reappraisal: part II--The role of omentectomy in the staging and treatment of apparent early stage epithelial ovarian cancer. Gynecol Oncol. 2013 Dec;131(3):784-90.
70. Motohara T, Masuda K, Morotti M, Zheng Y, El-Sahhar S, Chong KY, et al. An evolving story of the metastatic voyage of ovarian cancer cells: cellular and molecular orchestration of the adipose-rich metastatic microenvironment. Oncogene. 2019 Apr;38(16):2885-2898.
71. Böhm S, Faruqi A, Said I, Lockley M, Brockbank E, Jeyarajah A, et al. Chemotherapy Response Score: Development and Validation of a System to Quantify Histopathologic Response to Neoadjuvant Chemotherapy in Tubo-Ovarian High-Grade Serous Carcinoma. J Clin Oncol. 2015 Aug 1;33(22):2457-63.
72. Bergman F. Carcinoma of the ovary. A clinicopathological study of 86 autopsied cases with special reference to mode of spread. Acta Obstet Gynecol Scand. 1966;45(2):211–231.

73. McGuire WP, Hoskins WJ, Brady MF, Kucera PR, Partridge EE, Look KY, et al. Cyclophosphamide and cisplatin compared with paclitaxel and cisplatin in patients with stage III and stage IV ovarian cancer. N Engl J Med 1996; 334(1): 1-6.
74. Atallah D, Moubarak M, Dagher B, et al. 396 Predictive factors of survival and recurrence in patients with epithelial ovarian cancer after complete cytoreductive surgery: series of 185 patients. International Journal of Gynecologic Cancer 2020;30:A164-A165
75. Reles A, Wen WH, Schmider A, Gee C, Runnebaum IB, Kilian U, et al. Correlation of p53 mutations with resistance to platinum-based chemotherapy and shortened survival in ovarian cancer. Clin Cancer Res. 2001 Oct;7(10):2984-97.
76. NICE Clinical Guidance; TA389; Topotecan, pegylated liposomal doxorubicin hydrochloride, paclitaxel, trabectedin and gemcitabine for treating recurrent ovarian cancer [Internet]. Available at: https://www.nice.org.uk/guidance/ta389
77. Tentes AA, Tripsiannis G, Markakidis SK, Karanikiotis CN, Tzegas G, Georgiadis G, et al. Peritoneal cancer index: a prognostic indicator of survival in advanced ovarian cancer. Eur J Surg Oncol. 2003 Feb;29(1):69-73.
78. Jammal MP, Martins Filho A, Bandeira GH, Murta BMT, Murta EFC, Nomelini RS. Laboratory predictors of survival in ovarian cancer. Rev Assoc Med Bras (1992). 2020 Feb 27;66(1):61-66
79. Nagle CM, Bain CJ, Webb PM. Cigarette smoking and survival after ovarian cancer diagnosis. Cancer Epidemiol Biomarkers Prev. 2006 Dec;15(12):2557-60.
80. Yang L, Klint A, Lambe M, Bellocco R, Riman T, Bergfeldt K, et al. Predictors of ovarian cancer survival: a population-based prospective study in Sweden. Int J Cancer. 2008 Aug 1;123(3):672-9.
81. Pavelka JC, Brown RS, Karlan BY, Cass I, Leuchter RS, Lagasse LD, et al. Effect of obesity on survival in epithelial ovarian cancer. Cancer. 2006 Oct 1;107(7):1520-4.
82. Cress RD, Chen YS, Morris CR, Petersen M, Leiserowitz GS. Characteristics of long-term survivors of epithelial ovarian cancer. Obstet.Gynecol., 126 (2015): 491-497.
83. Hamilton CA, Miller A, Casablanca Y, Horowitz NS, Rungruang B, Krivak TC, at al. Clinicopathologic characteristics associated with long-term survival in advanced epithelial ovarian cancer: an NRG Oncology/Gynecologic Oncology Group ancillary data study. Gynecol Oncol. 2018 Feb;148(2):275-280.
84. Peres LC, Sinha S, Townsend MK, Fridley BL, Karlan BY, Lutgendorf SK, et al. Predictors of survival trajectories among women with epithelial ovarian cancer. Gynecol Oncol. 2020 Feb;156(2):459-466.
85. Candido-dos-Reis FJ, Song H, Goode EL, Cunningham JM, Fridley BL, Larson MC, et al. for EMBRACE; kConFab Investigators; Australian Ovarian Cancer Study Group. Germline mutation in BRCA1 or BRCA2 and ten-year survival for women diagnosed with epithelial ovarian cancer. Clin Cancer Res. 2015 Feb 1;21(3):652-7.
86. Yang SYC, Lheureux S, Karakasis K, Burnier JV, Bruce JP, Clouthier DL, et al. Landscape of genomic alterations in high-grade serous ovarian cancer from exceptional long- and short-term survivors. Genome Med. 2018 Oct 31;10(1):81.
87. Berchuck A, Iversen ES, Lancaster JM, Pittman J, Luo J, Lee P, et al. Patterns of gene expression that characterize long-term survival in advanced stage serous ovarian cancers. Clin Cancer Res. 2005 May 15;11(10):3686-96.
88. Peres LC, Schildkraut JM. Racial/ethnic disparities in ovarian cancer research. Adv Cancer Res. 2020;146:1-21.
89. Hennessy BT, Coleman R, Markman M. Ovarian cancer. Lancet 2009; 374:1371–1382.
90. Yang Y, Yang Y, Yang J, Zhao X, Wei X. Tumor Microenvironment in Ovarian Cancer: Function and Therapeutic Strategy. Front. Cell Dev. Biol. 2020;8: 758.

91. van Zyl B, Tang D, Bowden NA. Biomarkers of platinum resistance in ovarian cancer: what can we use to improve treatment. Endocr Relat Cancer. 2018 May;25(5):R303-R318.
92. Wei SH, Balch C, Paik HH, Kim YS, Baldwin RL, Liyanarachchi S, et al. Prognostic DNA methylation biomarkers in ovarian cancer. Clin Cancer Res. 2006; 12:2788–2794.
93. Patch AM, Christie EL, Etemadmoghadam D, Garsed DW, George J, Fereday S, et al. Whole-genome characterization of chemoresistant ovarian cancer. Nature. 2015;521:489–494.
94. Hartwich Y, Soteras MG, Lin ZP, Holmberg J, Sumi N, Craveiro V, et al. p53 protein aggregation promotes platinum resistance in ovarian cancer. Oncogene. 2015;34: 3605–3616.
95. Barakat BM, Wang QE, Han C, Milum K, Yin DT, Zhao Q, et al. Overexpression of DDB2 enhances the sensitivity of human ovarian cancer cells to cisplatin by augmenting cellular apoptosis. Int J Cancer. 2010;127:977–988.
96. Steg AD, Bevis KS, Katre AA, Ziebarth A, Dobbin ZC, Alvarez RD, et al. Stem cell pathways contribute to clinical chemoresistance in ovarian cancer. Clin Cancer Res. 2012 Feb 1;18(3):869-81.
97. Roberts CM, Cardenas C, Tedja R. The Role of Intra-Tumoral Heterogeneity and Its Clinical Relevance in Epithelial Ovarian Cancer Recurrence and Metastasis. Cancers (Basel). 2019 Jul 30;11(8):1083.
98. Brabletz T, Kalluri R, Nieto MA, Weinberg RA. EMT in cancer. Nat Rev Cancer. 2018 Feb;18(2):128-134.
99. Marchini S, Fruscio R, Clivio L, Beltrame L, Porcu L, Fuso Nerini I, et al. Resistance to platinum-based chemotherapy is associated with epithelial to mesenchymal transition in epithelial ovarian cancer. Eur J Cancer. 2013 Jan;49(2):520-30.
100. Marusyk A, Polyak K. Tumor heterogeneity: causes and consequences. Biochim Biophys Acta. 2010 Jan;1805(1):105-17.
101. Heppner GH. Tumor heterogeneity. Cancer Res. 1984;44:2259–2265
102. Fidler IJ, Hart IR. Biological diversity in metastatic neoplasms: origins and implications. Science. 1982;217:998–1003.
103. Tellez-Gabriel M, Ory B, Lamoureux F, Heymann MF, Heymann D. Tumour Heterogeneity: The Key Advantages of Single-Cell Analysis. Int J Mol Sci. 2016 Dec 20;17(12):2142.
104. Jiménez-Sánchez A, Cybulska P, Mager KL, Koplev S, Cast O, Couturier DL, et al. Unraveling tumor-immune heterogeneity in advanced ovarian cancer uncovers immunogenic effect of chemotherapy. Nat Genet. 2020 Jun;52(6):582-593.
105. Fox EJ, Loeb LA. Cancer: One cell at a time. Nature. 2014 Aug 14;512(7513):143-4.
106. Swanton C. Intratumor heterogeneity: evolution through space and time. Cancer Res. 2012 Oct 1;72(19):4875-82.
107. Dagogo-Jack I, Shaw AT. Tumour heterogeneity and resistance to cancer therapies. Nat Rev Clin Oncol. 2018 Feb;15(2):81-94.
108. Anderson NM, Simon MC. The tumor microenvironment. Curr Biol. 2020 Aug 17;30(16):R921-R925.
109. Binnewies M, Roberts EW, Kersten K, Chan V, Fearon DF, Merad M, et al. Understanding the tumor immune microenvironment (TIME) for effective therapy. Nat Med. 2018 May;24(5):541-550.
110. Nersesian S, Glazebrook H, Toulany J, Grantham SR, Boudreau JE. Naturally Killing the Silent Killer: NK Cell-Based Immunotherapy for Ovarian Cancer. Front Immunol. 2019 Aug 9;10:1782.
111. Cui Y, Guo G. Immunomodulatory Function of the Tumor Suppressor p53 in Host Immune Response and the Tumor Microenvironment. Int J Mol Sci. 2016 Nov 19;17(11):1942.

112. Zhang J, Veeramachaneni N. Targeting interleukin-1β and inflammation in lung cancer. Biomark Res. 2022 Jan 27;10(1):5.
113. Yang Y, Yang Y, Yang J, Zhao X, Wei X. Tumor Microenvironment in Ovarian Cancer: Function and Therapeutic Strategy. Front Cell Dev Biol. 2020 Aug 11;8:758.
114. Olalekan S, Xie B, Back R, Eckart H, Basu A. Characterizing the tumor microenvironment of metastatic ovarian cancer by single-cell transcriptomics. Cell Rep. 2021 May 25;35(8):109165.
115. Jiménez-Sánchez A, Cybulska P, Mager KL, Koplev S, Cast O, Couturier DL, et al. Unraveling tumor-immune heterogeneity in advanced ovarian cancer uncovers immunogenic effect of chemotherapy. Nat Genet. 2020 Jun;52(6):582-59.
116. Winterhoff BJ, Maile M, Mitra AK, Sebe A, Bazzaro M, Geller MA, et al. Single cell sequencing reveals heterogeneity within ovarian cancer epithelium and cancer associated stromal cells. Gynecol Oncol. 2017 Mar;144(3):598-606.
117. Xu J, Fang Y, Chen K, Li S, Tang S, Ren Y, et al. Single-Cell RNA Sequencing Reveals the Tissue Architecture in Human High-Grade Serous Ovarian Cancer. Clin Cancer Res. 2022 Aug 15;28(16):3590-3602.
118. Deng Y, Tan Y, Zhou D, Bai Y, Cao T, Zhong C, et al. Single-Cell RNA-Sequencing Atlas Reveals the Tumor Microenvironment of Metastatic High-Grade Serous Ovarian Carcinoma. Front Immunol. 2022 Jul 22;13:923194.
119. Olalekan S, Xie B, Back R, Eckart H, Basu A. Characterizing the tumor microenvironment of metastatic ovarian cancer by single-cell transcriptomics. Cell Rep. 2021 May 25;35(8):109165.
120. Shih AJ, Menzin A, Whyte J, Lovecchio J, Liew A, Khalili H, et al. Identification of grade and origin specific cell populations in serous epithelial ovarian cancer by single cell RNA-seq. PLoS One. 2018 Nov 1;13(11):e0206785.
121. Hornburg M, Desbois M, Lu S, Guan Y, Lo AA, Kaufman S, et al. Single-cell dissection of cellular components and interactions shaping the tumor immune phenotypes in ovarian cancer. Cancer Cell. 2021 Jul 12;39(7):928-944.e6.
122. Izar B, Tirosh I, Stover EH, Wakiro I, Cuoco MS, Alter I, et al. A single-cell landscape of high-grade serous ovarian cancer. Nat Med. 2020 Aug;26(8):1271-1279.
123. Zhang K, Erkan EP, Jamalzadeh S, Dai J, Andersson N, Kaipio K, et al. Longitudinal single-cell RNA-seq analysis reveals stress-promoted chemoresistance in metastatic ovarian cancer. Sci Adv. 2022 Feb 25;8(8):eabm1831.
124. Vivier E, Malissen B. Innate and adaptive immunity: specificities and signaling hierarchies revisited. Nat Immunol. 2005 Jan;6(1):17-21.
125. Marshall JS, Warrington R, Watson W, Kim HL. An introduction to immunology and immunopathology. Allergy Asthma Clin Immunol. 2018 Sep 12;14(Suppl 2):49.
126. Dunn GP, Old LJ, Schreiber RD. The three Es of cancer immunoediting. Annu Rev Immunol. 2004;22:329-60
127. Mittal D, Gubin MM, Schreiber RD, Smyth MJ. New insights into cancer immunoediting and its three component phases--elimination, equilibrium and escape. Curr Opin Immunol. 2014 Apr;27:16-25.
128. Schreiber RD, Old LJ, Smyth MJ. Cancer immunoediting: integrating immunity's roles in cancer suppression and promotion. Science. 2011;331:1565–1570.
129. Dunn GP, Old LJ, Schreiber RD. The immunobiology of cancer immunosurveillance and immunoediting. Immunity: 2004;21:137–148.
130. Wang HF, Wang SS, Huang MC, Liang XH, Tang YJ, Tang YL. Targeting Immune-Mediated Dormancy: A Promising Treatment of Cancer. Front Oncol. 2019 Jun 26;9:498.

131. Curiel TJ, Coukos G, Zou L, Alvarez X, Cheng P, Mottram P, et al. Specific recruitment of regulatory T cells in ovarian carcinoma fosters immune privilege and predicts reduced survival. Nat. Med 2004; 10(9): 942-9.
132. Pepper MS. Transforming growth factor-beta: vasculogenesis, angiogenesis, and vessel wall integrity. Cytokine Growth Factor Rev. 1997; 8(1): 21-43.
133. Curiel TJ, Cheng P, Mottram P, Alvarez X, Moons L, Evdemon-Hogan M, et al. Dendritic cell subsets differentially regulate angiogenesis in human ovarian cancer. Cancer Res. 2004; 64(16): 5535-8.
134. Kryczek, S. Wei, G. Zhu, L. Myers, P. Mottram, P. Cheng, et al.Relationship between B7-H4, regulatory T cells, and patient outcome in human ovarian carcinoma. Cancer Res 2007; 67(18): 8900–05.
135. Rodriguez GC, Haisley C, Hurteau J, Moser TL, Whitaker R, Bast RC, et al. Regulation of invasion of epithelial ovarian cancer by transforming growth factor-beta. Gynecol. Oncol 2001; 80(2): 245-53.
136. Norgaard P, Hougaard S, Poulsen HS, Spang-Thomsen M. Transforming growth factor beta and cancer. Cancer Treat Rev. 1995; 21(4): 367-403.
137. Okamoto, T. Nikaido, K. Ochiai, S. Takakura, M. Saito, Y. Aoki, et al. Indoleamine 2,3-dioxygenase serves as a marker of poor prognosis in gene expression profiles of serous ovarian cancer cells Clin. Cancer Res 2005; 11 (16): 6030–39.
138. Grohmann FU, Hwang KW, Orabona C, Vacca C, Bianchi R, et al. Modulation of tryptophan catabolism by regulatory T cells. Nat Immunol. 2003; 4(12): 1206-12.
139. De Smedt T, Van Mechelen M, De Becker G, Urbain J, Leo O, Moser M. Effect of interleukin-10 on dendritic cell maturation and function. Eur J Immunol. 1997;27:1229-35.
140. Chae CS, Teran-Cabanillas E, Cubillos-Ruiz JR. Dendritic cell rehab: new strategies to unleash therapeutic immunity in ovarian cancer. Cancer Immunol Immunother. 2017;66:969–77.
141. Morvan, M., Lanier, L. NK cells and cancer: you can teach innate cells new tricks. Nat Rev Cancer 16, 7–19 (2016).
142. Rask K, Zhu Y, Wang W, Hedin L, Sundfeldt K. Ovarian epithelial cancer: a role for PGE2-synthesis and signalling in malignant transformation and progression. Mol Cancer. 2006 Nov 16;5:62.
143. Rodriguez GM, Galpin KJC, McCloskey CW, Vanderhyden BC. The Tumor Microenvironment of Epithelial Ovarian Cancer and Its Influence on Response to Immunotherapy. Cancers (Basel). 2018; 10(8): 242.
144. Maas RJ, Hoogstad-van Evert JS, Van der Meer JM, Mekers V, Rezaeifard S, Korman AJ, et al. TIGIT blockade enhances functionality of peritoneal NK cells with altered expression of DNAM-1/TIGIT/CD96 checkpoint molecules in ovarian cancer. Oncoimmunology. 2020; 9(1): 1843247 9.
145. Hwang WT, Adams SF, Tahirovic E, Hagemann IS, Coukos G. Prognostic significance of tumor-infiltrating T cells in ovarian cancer: a meta-analysis. Gynecol Oncol. 2012; 124(2):192-8.
146. Ma D, Gu MJ. Immune effect of tumor-infiltrating lymphocytes and its relation to the survival rate of patients with ovarian malignancies. J Tongji Med Univ. 1991; 11(4): 235-9.
147. Zhang L, Conejo-Garcia JR, Katsaros D, Gimotty PA, Massobrio M, Regnani G, et al. Intratumoral T cells, recurrence, and survival in epithelial ovarian cancer; N Engl J Med 2003; 348(3): 203-13.
148. Sato E, Olson SH, Ahn J, Bundy B, Nishikawa H, Qian F, et al. Intraepithelial CD8+ tumor-infiltrating lymphocytes and a high CD8+/regulatory T cell ratio are associated with favorable prognosis in ovarian cancer. Proc Natl Acad Sci U S A. 2005; 102(51): 18538-43.

149. Donskov F, Bennedsgaard KM, Von Der Maase H, Marcussen N, Fisker R, Jensen JJ, et al. Intratumoural and peripheral blood lymphocyte subsets in patients with metastatic renal cell carcinoma undergoing interleukin-2 based immunotherapy: association to objective response and survival. Br J Cancer. 2002; 87(2): 194–201.
150. Pesce S, Greppi M, Tabellini G, Rampinelli F, Parolini S, Olive D, et al. Identification of a subset of human natural killer cells expressing high levels of programmed death 1: A phenotypic and functional characterization. J Allergy Clin Immunol. 2017; 139(1): 335-346.
151. Yigit R, Massuger LF, Figdor CG, Torensma R. Ovarian cancer creates a suppressive microenvironment to escape immune elimination. Gynecol Oncol. 2010; 117(2): 366-72.
152. Webb JR, Milne K, Watson P, deLeeuw RJ, Nelson BH. Tumor-infiltrating lymphocytes expressing the tissue resident memory marker CD103 are associated with increased survival in high-grade serous ovarian cancer. Clin Cancer Res. 2014; 20: 434- 44.
153. Nelson BH. New insights into tumor immunity revealed by the unique genetic and genomic aspects of ovarian cancer. Curr Opin Immunol. 2015; 33:93-100.
154. Cai DL, Jin LP. Immune Cell Population in Ovarian Tumor Microenvironment. J Cancer. 2017; 8: 2915–23.
155. Alexandrov LB, Nik-Zainal S, Wedge DC, Aparicio SA, Behjati S, Biankin AV, et al. Signatures of mutational processes in human cancer. Nature. 2013; 500: 415–21.
156. Miescher S, Whiteside TL, Carrel S, von Fliedner V. Functional properties of tumor-infiltrating and blood lymphocytes in patients with solid tumors: effects of tumor cells and their supernatants on proliferative responses of lymphocytes. J Immunol. 1986; 136: 1899–907.
157. Zsiros E, Tanyi J, Balint K, Kandalaft LE. Immunotherapy for ovarian cancer: recent advances and perspectives. Curr Opin Oncol. 2014; 26: 492-55.
158. Hamanishi J, Mandai M, Ikeda T, Minami M, Kawaguchi A, Murayama T, et al. Safety and antitumor activity of anti-PD-1 antibody, nivolumab, in patients with platinum-resistant ovarian cancer. J Clin Oncol. 2015; 33: 4015-22.
159. Fialová A, Partlová S, Sojka L, Hromádková H, Brtnický T, Fučíková J, et al. Dynamics of T-cell infiltration during the course of ovarian cancer: the gradual shift from a Th17 effector cell response to a predominant infiltration by regulatory T-cells. Int J Cancer. 2013 Mar 1;132(5):1070-9.
160. Strickland KC, Howitt BE, Shukla SA, Rodig, Ritterhouse LL, Liu JF et al. Association and prognostic significance of BRCA1/2-mutation status with neoantigen load, number of tumor-infiltrating lymphocytes and expression of PD-1/PD-L1 in high grade serous ovarian cancer. Oncotarget. 2016;7:13587–13598.
161. Clarke B, Tinker AV, Lee CH, Subramanian S, van de Rijn M, Turbin D, et al. Intraepithelial T cells and prognosis in ovarian carcinoma: Novel associations with stage, tumor type, and BRCA1 loss. Mod. Pathol. 2009;22:393–402.
162. Shah CA, Allison KH, Garcia RL, Gray HJ, Goff BA, Swisher EM. Intratumoral T cells, tumor-associated macrophages, and regulatory T cells: Association with p53 mutations, circulating tumor DNA and survival in women with ovarian cancer. Gynecol. Oncol. 2008;109:215–219.
163. Klemm F, Joyce JA. Microenvironmental regulation of therapeutic response in cancer. Trends Cell Biol. 2015 Apr;25(4):198-213.
164. Leung F, Dimitromanolakis A, Kobayashi H, Diamandis EP, Kulasingam V. Folate-receptor 1 (FOLR1) protein is elevated in the serum of ovarian cancer patients. Clin Biochem. 2013 Oct;46(15):1462–8.

165. de Biasi AR, Villena-Vargas J, Adusumilli PS. Cisplatin-induced antitumor immunomodulation: a review of preclinical and clinical evidence. Clin Cancer Res. 2014 Nov 1;20(21):5384-91.
166. Böhm S, Montfort A, Pearce OM, Topping J, Chakravarty P, Everitt GL, et al.. Neoadjuvant Chemotherapy Modulates the Immune Microenvironment in Metastases of Tubo-Ovarian High-Grade Serous Carcinoma. Clin Cancer Res. 2016 Jun 15;22(12):3025-36.
167. Hirata E, Sahai E. Tumor Microenvironment and Differential Responses to Therapy. Cold Spring Harb Perspect Med. 2017 Jul 5;7(7):a026781.
168. Croft W, Evans RPT, Pearce H, Elshafie M, Griffiths EA, Moss P. The single cell transcriptional landscape of esophageal adenocarcinoma and its modulation by neoadjuvant chemotherapy. Mol Cancer. 2022 Oct 17;21(1):200.
169. Kroemer G, Galluzzi L, Kepp O, Zitvogel L. Immunogenic cell death in cancer therapy. Annu Rev Immunol. 2013;31:51-72.
170. Krysko DV, Garg AD, Kaczmarek A, Krysko O, Agostinis P, Vandenabeele P. Immunogenic cell death and DAMPs in cancer therapy. Nat Rev Cancer. 2012 Dec;12(12):860-75.
171. Bracci L, Schiavoni G, Sistigu A, Belardelli F. Immune-based mechanisms of cytotoxic chemotherapy: implications for the design of novel and rationale-based combined treatments against cancer. Cell Death Differ. 2014 Jan;21(1):15-25.
172. Lee M-CW, Lopez-Diaz FJ, Khan SY, Tariq MA, Dayn Y, Vaske CJ, et al. Single-cell analyses of transcriptional heterogeneity during drug tolerance transition in cancer cells by RNA sequencing. Proc Natl Acad Sci U S A [Internet]. 2014 Nov;111(44):E4726—35.
173. Robertson MJ, Ritz J. Biology and clinical relevance of human natural killer cells. Blood. 1990 Dec 15;76(12):2421-38.
174. Scoville SD, Freud AG, Caligiuri MA. Modeling Human Natural Killer Cell Development in the Era of Innate Lymphoid Cells. Front Immunol. 2017 Mar 27;8:360
175. Perera Molligoda Arachchige AS. Human NK cells: From development to effector functions. Innate Immun. 2021 Apr;27(3):212-229.
176. Kannan GS, Aquino-Lopez A, Lee DA. Natural killer cells in malignant hematology: A primer for the non-immunologist. Blood Rev. 2017 Mar;31(2):1-10.
177. Vivier E, Raulet DH, Moretta A, Caligiuri MA, Zitvogel L, Lanier LL, et al. Innate or adaptive immunity? The example of natural killer cells. Science 2011; 331: 44-49.
178. Lanier LL, Le AM, Civin CI, Loken MR, Phillips JH. The relationship of CD16 (Leu-11) and Leu-19 (NKH-1) antigen expression on human peripheral blood NK cells and cytotoxic T lymphocytes. J Immunol. 1986; 136(12): 4480-6.
179. Pegram HJ, Andrews DM, Smyth MJ, Darcy PK, Kershaw MH; Activating and inhibitory receptors of natural killer cells. Immunol Cell Biol. 2011; 89: 216-224.
180. Duska LR, Kohn EC. The new classifications of ovarian, fallopian tube, and primary peritoneal cancer and their clinical implications. Ann. Oncol. 2017; 28: viii8–viii12.
181. Lanier LL, Corliss B, Phillips JH. Arousal and inhibition of human NK cells. Immunol Rev 1997; 155: 145-54.
182. Long E. Regulation of immune responses through inhibitory receptors. Annual Review of Immunology. 1999; 17: 875–904.
183. Pegram HJ, Andrews DM, Smyth MJ, Darcy PK, Kershaw MH. Activating and inhibitory receptors of natural killer cells. Immunol Cell Biol. 2011 Feb;89(2):216-24.
184. Soriani A, Zingoni A, Cerboni C, Iannitto ML, Ricciardi MR, Di Gialleonardo V, et al. ATM-ATR-dependent up-regulation of DNAM-1 and NKG2D ligands on multiple myeloma cells by therapeutic agents results in enhanced NK-cell susceptibility and is associated with a senescent phenotype. Blood. 2009 Apr 9;113(15):3503-11.

185. Raulet, DH, Guerra N. Oncogenic stress sensed by the immune system: role of natural killer cell receptors. Nature Reviews Immunology. 2009; 9(8):568–580.
186. Gonzalez-Gugel E, Saxena M, Bhardwaj N. Modulation of innate immunity in the tumor microenvironment. Cancer Immunol Immunother 2016; 65: 1261-1268.
187. Bauer S, Groh V, Wu J, Steinle A, Phillips JH, Lanier LL, et al. T. Activation of NK cells and T cells by NKG2D, a receptor for stress-inducible MICA. Science. 1999; 285(5428): 727-9.
188. Liu G, Lu S, Wang X, Page ST, Higano CS, Plymate SR, et al. Perturbation of NK cell peripheral homeostasis accelerates prostate carcinoma metastasis. J Clin Invest. 2013; 123(10): 4410-22.
189. James FR, Jiminez-Linan M, Alsop J, Mack M, Song H, Brenton JD, et al. Association between tumour infiltrating lymphocytes, histotype and clinical outcome in epithelial ovarian cancer. BMC Cancer. 2017; 17(1): 657.
190. Hoogstad-van Evert JS, Maas RJ, van der Meer J, Cany J, van der Steen S, Jansen JH, et al. Peritoneal NK cells are responsive to IL-15 and percentages are correlated with outcome in advanced ovarian cancer patients. Oncotarget. 2018; 9(78): 34810-20.
191. Hoogstad-van Evert J, Bekkers R, Ottevanger N, Schaap N, Hobo W, Jansen JH, et al. Intraperitoneal infusion of ex vivo-cultured allogeneic NK cells in recurrent ovarian carcinoma patients (a phase I study). Medicine 2019; 98(5): e14290.
192. Shehata M, Mukherjee A, Deen S, Al-Attar A, Durrant LG, et al. Human leukocyte antigen class I expression is an independent prognostic factor in advanced ovarian cancer resistant to first-line platinum chemotherapy. Br J Cancer. 2009; 101(8): 1321-8.
193. Andersson E, Poschke I, Villabona L, Carlson JW, Lundqvist A, Kiessling R, et al. Non-classical HLA-class I expression in serous ovarian carcinoma: Correlation with the HLA-genotype, tumor infiltrating immune cells and prognosis. Oncoimmunology. 2015 Jul 25;5(1):e1052213.
194. Tomasec P, Braud VM, Rickards C, Powell MB, McSharry BP, Gadola S, et al. Surface expression of HLA-E, an inhibitor of natural killer cells, enhanced by human cytomegalovirus gpUL40. Science. 2000; 287:1031.
195. Lee N, Llano M, Carretero M, Ishitani A, Navarro F, Lopez-Botet M, et al. HLA-E is a major ligand for the natural killer inhibitory receptor CD94/NKG2A. Proc Natl Acad Sci U S A 1998; 95:5199-204.
196. Marchesi M, Andersson E, Villabona L, Seliger B, Lundqvist A, Kiessling R, et al. HLA-dependent tumour development: a role for tumour associate macrophages? J Transl Med 2013; 11:247.
197. Vivier E, Tomasello E, Baratin M, Walzer T, Ugolini S. Functions of natural killer cells. Nat Immunol. 2008; 9: 503–10.
198. Chávez-Galán L, Arenas-Del Angel MC, Zenteno E, Chávez R, Lascurain R. Cell death mechanisms induced by cytotoxic lymphocytes. Cell Mol Immunol. 2009; 6(1): 15-25.
199. Carlsten M, Björkström NK, Norell H, Bryceson Y, van Hall T, Baumann BC, et al. DNAX accessory molecule-1 mediated recognition of freshly isolated ovarian carcinoma by resting natural killer cells. Cancer Res. 2007; 67: 1317-1325.
200. Koshiyama M, Matsumura N, Konishi I. Subtypes of Ovarian Cancer and Ovarian Cancer Screening. Diagnostics (Basel) 2017; 7(1): 12.
201. Gwalani LA, Orange JS. Single degranulations in natural killer cells can mediate target cell killing. J Immunol 2018; 200: 3231–3243.
202. Hsu HT, Mace EM, Carisey AF, Viswanath DI, Christakou AE, Wiklund M, et al. NK cells converge lytic granules to promote cytotoxicity and prevent bystander killing. J Cell Biol. 2016 Dec 19;215(6):875-889.

203. Chávez-Galán L, Arenas-Del Angel MC, Zenteno E, Chávez R, Lascurain R. Cell death mechanisms induced by cytotoxic lymphocytes. Cell Mol Immunol. 2009 Feb;6(1):15-25.
204. Martínez-Lostao L, Anel A, Pardo J. How Do Cytotoxic Lymphocytes Kill Cancer Cells? Clin Cancer Res. 2015 Nov 15;21(22):5047-56.
205. Screpanti V, Wallin RP, Grandien A, Ljunggren HG; Impact of FASL-induced apoptosis in the elimination of tumor cells by NK cells; Mol Immunol; 2005: 42:495-9.
206. Yoon S, Kim T, Choi I. Understanding of molecular mechanisms in natural killer cell therapy. Exp Mol Med 2015; 47: e141.
207. Mitra R, Singh S, Khar A. Antitumour immune responses. Expert Rev Mol Med. 2003 Jan 13;5(3):1-19.
208. Lo Nigro C, Macagno M, Sangiolo D, Bertolaccini L, Aglietta M, Merlano MC. NK-mediated antibody-dependent cell-mediated cytotoxicity in solid tumors: biological evidence and clinical perspectives. Ann Transl Med. 2019 Mar;7(5):105.
209. Stevenson GT. Three major uncertainties in the antibody therapy of cancer. Haematologica 2014;99:1538-46.
210. Moy PM, Holmes EC, Golub SH. Depression of natural killer cytotoxic activity in lymphocytes infiltrating human pulmonary tumors. Cancer Res. 1985; 45: 57–60.
211. Zhou Y, Xu Y, Chen L, Xu B, Wu C, Jiang J. B7-H6 expression correlates with cancer progression and patient's survival in human ovarian cancer. Int J Clin Exp Pathol. 2015; 8: 9428–33.
212. Carlsten M, Norell H, Bryceson YT, Poschke I, Schedvins K, Ljunggren HG, et al. Primary human tumor cells expressing CD155 impair tumor targeting by down-regulating DNAM-1 on NK cells. J Immunol. 2009; 183: 4921-4930.
213. Lukesova S, Vroblova V, Tosner J, Kopecky J, Sedlakova I, Čermáková E, et al. Comparative study of various subpopulations of cytotoxic cells in blood and ascites from patients with ovarian carcinoma. Contemp Oncol (Pozn). 2015; 19: 290-299.
214. Vyas M, Reinartz S, Hoffmann N, Reiners KS, Lieber S, Jansen JM, et al. Soluble NKG2D ligands in the ovarian cancer microenvironment are associated with an adverse clinical outcome and decreased memory effector T cells independent of NKG2D downregulation. Oncoimmunology. 2017; 6: e1339854.
215. Berek JS, Bast RC, Jr, Lichtenstein A, Hacker NF, Spina CA, Lagasse LD, et al. Lymphocyte cytotoxicity in the peritoneal cavity and blood of patients with ovarian cancer. Obstet Gynecol. 1984; 64:708–14.
216. Lai P, Rabinowich H, Crowley-Nowick PA, Bell MC, Mantovani G, Whiteside TL. Alterations in expression and function of signal-transducing proteins in tumor-associated T and natural killer cells in patients with ovarian carcinoma. Clin Cancer Res. 1996; 2:161–73.
217. Bellora F, Castriconi R, Dondero A, Pessino A, Nencioni A, Liggieri G, et al. TLR activation of tumor-associated macrophages from ovarian cancer patients triggers cytolytic activity of NK cells. Eur J Immunol. 2014; 44: 1814–22.
218. Miller JS, Soignier Y, Panoskaltsis-Mortari A, McNearney SA, Yun GH, Fautsch SK, et al. Successful adoptive transfer and in vivo expansion of human haploidentical NK cells in patients with cancer. Blood. 2005; 105: 3051–7.
219. McGilvray RW, Eagle RA, Rolland P, Jafferji I, Trowsdale J, Durrant LG. ULBP2 and RAET1E NKG2D ligands are independent predictors of poor prognosis in ovarian cancer patients. Int. J. Cancer; 2010;127: 1412-20.
220. Nersesian S, Glazebrook H, Toulany J, Grantham SR, Boudreau JE. Naturally Killing the Silent Killer: NK Cell-Based Immunotherapy for Ovarian Cancer. Front Immunol. 2019; 10: 1782.

221. Krockenberger M, Dombrowski Y, Weidler C, Ossadnik M, Hönig A, Häusler S, et al. Macrophage migration inhibitory factor contributes to the immune escape of ovarian cancer by down-regulating NKG2D. J Immunol. 2008 Jun 1;180(11):7338-48.
222. Pesce S, Tabellini G, Cantoni C, Patrizi O, Coltrini D, Rampinelli F, et al. B7-H6-mediated downregulation of NKp30 in NK cells contributes to ovarian carcinoma immune escape. Oncoimmunology. 2015 Jan 22;4(4):e1001224.
223. Childs RW, Carlsten M. Therapeutic approaches to enhance natural killer cell cytotoxicity against cancer: The force awakens. Nat. Rev. Drug Discov. 2015; 14: 487–498.
224. Trotta R, Dal Col J, Yu J, Ciarlariello D, Thomas B, Zhang X, et al. TGF-beta utilizes SMAD3 to inhibit CD16-mediated IFN-gamma production and antibody-dependent cellular cytotoxicity in human NK cells. J Immunol. 2008; 181: 3784–92.
225. Cooper MA, Fehniger TA, Caligiuri MA. The biology of human natural killer-cell subsets. Trends Immunol. 2001 Nov; 22(11): 633-40.
226. Patankar MS, Jing Y, Morrison JC, Belisle JA, Lattanzio FA, Deng Y, et al. Potent suppression of natural killer cell response mediated by the ovarian tumor marker CA125. Gynecol Oncol. 2005; 99(3): 704-13.
227. Recchia F, Di Orio F, Candeloro G, Guerriero G, Piazze J, Rea S. Maintenance immunotherapy in recurrent ovarian cancer: long term follow-up of a phase II study. Gynecol Oncol. 2010; 116(2): 202-7.
228. Gubbels JA, Felder M, Horibata S, Belisle JA, Kapur A, Holden H, et al. MUC16 provides immune protection by inhibiting synapse formation between NK and ovarian tumor cells. Mol Cancer. 2010; 9:11.
229. Robinson TO, Schluns KS. The potential and promise of IL-15 in immuno-oncogenic therapies. Immunol Lett. 2017; 190: 159–68.
230. Dong HP, Elstrand MB, Holth A, Silins I, Berner A, Trope CG, et al. NK- and B-cell infiltration correlates with worse outcome in metastatic ovarian carcinoma. Am J Clin Pathol. 2006 Mar;125(3):451-8.
231. Henriksen JR, Nederby L, Donskov F, Waldstrøm M, Adimi P, Jakobsen A, et al. Blood natural killer cells during treatment in recurrent ovarian cancer. Acta Oncol. 2020; 59(11): 1365-1373.
232. Henriksen JR, Donskov F, Waldstrøm M, Jakobsen A, Hjortkjaer M, Petersen CB, et al. Favorable prognostic impact of Natural Killer cells and T cells in high-grade serous ovarian carcinoma. Acta Oncol. 2020 Jun;59(6):652-659.
233. Hu G, Wang S. Prognostic role of tumor-infiltrating CD57-positive lymphocytes in solid tumors: a meta-analysis. Oncotarget. 2018; 9(8): 8111–8119.
234. Chalmers ZR, Connelly CF, Fabrizio D, Gay L, Ali SM, Ennis R, et al. Analysis of 100,000 human cancer genomes reveals the landscape of tumor mutational burden. Genome Med. 2017; 9(1): 34.
235. Yarchoan M, Hopkins A, Jaffee EM. Tumor mutational burden and response rate to PD-1 inhibition. N Engl J Med 2017; 377(25): 2500–1.
236. Hu-Lieskovan S, Bhaumik S, Dhodapkar K, Grivel J-CJB, Gupta S, Hanks BA, et al. SITC cancer immunotherapy resource document: a compass in the land of biomarker discovery. J Immunother Cancer. 2020; 8(2): e000705.
237. Samstein RM, Lee C-H, Shoushtari AN, Hellmann MD, Shen R, Janjigian YY, et al. Tumor mutational load predicts survival after immunotherapy across multiple cancer types. Nat Genet 2019; 51(2): 202–6
238. Alberts DS, Marth C, Alvarez RD, Johnson G, Bidzinski M, Kardatzke DR, et al. Bradford WZ, Loutit J, Kirn DH, Clouser MC, Markman M; GRACES Clinical Trial Consortium.

Randomized phase 3 trial of interferon gamma-1b plus standard carboplatin/paclitaxel versus carboplatin/paclitaxel alone for first-line treatment of advanced ovarian and primary peritoneal carcinomas: results from a prospectively designed analysis of progression-free survival. Gynecol Oncol. 2008 May;109(2):174-81.

239. Vlad AM, Budiu RA, Lenzner DE, Wang Y, Thaller JA, Colonello K, et al. A phase II trial of intraperitoneal interleukin-2 in patients with platinum-resistant or platinum-refractory ovarian cancer. Cancer Immunol Immunother. 2010 Feb;59(2):293-301.
240. NICE Clinical Guideline; ESUOM21; Ovarian cancer (advanced): bevacizumab 7.5 mg/kg in combination with paclitaxel and carboplatin for first-line treatment [Internet]. Available at: https://www.nice.org.uk/advice/esuom21/chapter/Key-points-from-the-evidence.
241. NICE Clinical Guideline; TA284; Bevacizumab in combination with paclitaxel and carboplatin for first-line treatment of advanced ovarian cancer [Internet]. Available at: https://www.nice.org.uk/guidance/ta284.
242. NICE Clinical Guideline; TA693; Olaparib plus bevacizumab for maintenance treatment of advanced ovarian, fallopian tube or primary peritoneal cancer [Internet]. Available at: https://www.nice.org.uk/guidance/ta693.
243. NICE Clinical Guideline; TA598; Olaparib for maintenance treatment of BRCA mutation-positive advanced ovarian, fallopian tube or peritoneal cancer after response to first-line platinum-based chemotherapy [Internet]. Available at: https://www.nice.org.uk/guidance/ta598.
244. NICE Clinical Guideline; TA784; Niraparib for maintenance treatment of relapsed, platinum-sensitive ovarian, fallopian tube and peritoneal cancer [Internet]. Available at: https://www.nice.org.uk/guidance/ta784.
245. NICE Clinical Guideline; TA620; Olaparib for maintenance treatment of relapsed platinum-sensitive ovarian, fallopian tube or peritoneal cancer [Internet]. Available at: https://www.nice.org.uk/guidance/ta620.
246. NICE Clinical Guideline; TA673; Niraparib for maintenance treatment of advanced ovarian, fallopian tube and peritoneal cancer after response to first-line platinum-based chemotherapy [Internet]. Available at: https://www.nice.org.uk/guidance/ta673.
247. NICE Clinical Guideline; TA784; Niraparib for maintenance treatment of relapsed, platinum-sensitive ovarian, fallopian tube and peritoneal cancer [Internet]. Available at: https://www.nice.org.uk/guidance/ta784.
248. Tutt A, Robson M, Garber JE, Domchek SM, Audeh MW, Weitzel JN, et al. Oral poly(ADP-ribose) polymerase inhibitor olaparib in patients with BRCA1 or BRCA2 mutations and advanced breast cancer: a proof-of-concept trial. Lancet. 2010 Jul 24;376(9737):235-44.
249. HealioLeanrn; Colorectal cancer overview [Internet]. Available at: https://www.healio.com/hematology-oncology/learn-immuno-oncology/clinical-indications/colorectal-cancer
250. Iqbal S, Rattu MA, Neal S; Role of PARP Inhibitors in BRCA-Related Malignancies. US Pharmacist; 2018;43(9):HS10-HS17
251. Perren TJ, Swart AM, Pfisterer J, Ledermann JA, Pujade-Lauraine E, Kristensen G, et al. A phase 3 trial of bevacizumab in ovarian cancer. N Engl J Med. 2011; 365(26): 2484-96.
252. Burger RA, Brady MF, Bookman MA, Fleming GF, Monk BJ, Huang H, et al. Incorporation of bevacizumab in the primary treatment of ovarian cancer. N Engl J Med. 2011; 365(26): 2473-83.
253. du Bois A, Floquet A, Kim JW, Rau J, del Campo JM, Friedlander M, et al. Incorporation of pazopanib in maintenance therapy of ovarian cancer. J Clin Oncol. 2014; 32(30): 3374-82.

254. du Bois A, Kristensen G, Ray-Coquard I, Reuss A, Pignata S, Colombo N, et al. Standard firstline chemotherapy with or without nintedanib for advanced ovarian cancer (AGO-OVAR 12): a randomised, double-blind, placebo-controlled phase 3 trial. Lancet Oncol. 2016; 17(1): 78-89.
255. Mirza MR, Monk BJ, Herrstedt J, Oza AM, Mahner S, Redondo A, et al. ENGOT-OV16/NOVA Investigators. Niraparib Maintenance Therapy in Platinum-Sensitive, Recurrent Ovarian Cancer. N Engl J Med. 2016 Dec 1;375(22):2154-2164.
256. Postow MA, Callahan MK, Wolchok JD. Immune Checkpoint Blockade in Cancer Therapy. J Clin Oncol. 2015 Jun 10;33(17):1974-82.
257. Clinical Trial: NCT01611558; Phase II study of ipilimumab monotherapy in recurrent platinum-sensitive ovarian cancer [Internet]. Available at https://clinicaltrials.gov/ct2/show/results/NCT01611558.
258. Disis ML, Taylor MH, Kelly K, Beck JT, Gordon M, Moore KM, et al. Efficacy and Safety of Avelumab for Patients With Recurrent or Refractory Ovarian Cancer: Phase 1b Results From the JAVELIN Solid Tumor Trial. JAMA Oncol. 2019 Mar 1;5(3):393-401.
259. Drew Y, de Jonge M, Hong SH, Park YH, Wolfer A, Brown J, et al. An open-label, phase II basket study of olaparib and durvalumab (MEDIOLA): results in germline BRCA -mutated (gBRCA m) platinum-sensitive relapsed (PSR) ovarian cancer (OC). Gynecol Oncol. 2018; 149: 246–247.
260. Konstantinopoulos PA, Waggoner S, Vidal GA, Mita M, Moroney JW, Holloway R, et al. Single-Arm Phases 1 and 2 Trial of Niraparib in Combination With Pembrolizumab in Patients With Recurrent Platinum-Resistant Ovarian Carcinoma. JAMA Oncol 2019; 5(8): 1141-1149.
261. Brewer M, Angioli R, Scambia G, Lorusso D, Terranova C, Panici PB, et al. Front-line chemo-immunotherapy with carboplatin-paclitaxel using oregovomab indirect immunization in advanced ovarian cancer: A randomized phase II study. Gynecol Oncol 2020; 156(3): 523-529.
262. Pujade-Lauraine E, Fujiwara K, Dychter SS, Devgan G, Monk BJ. Avelumab (anti-PD-L1) in platinum-resistant/refractory ovarian cancer: JAVELIN ovarian 200 phase III study design. Future Oncol. 2018; 14(21): 2103–2113.
263. Liu J, Li H, Cao S, Zhang X, Yu J, Qi J, et al. Maintenance therapy with autologous cytokine-induced killer cells in patients with advanced epithelial ovarian cancer after first-line treatment. J Immunother. 2014; 37(2): 115–122.
264. Matulonis UA, Moore KN, Martin LP. Initial safety and activity findings from a phase IB escalation study of mirvetuximab soravtansine, a folate receptor alpha (FRα-targeting antibody-drug conjugate (ADC), with pembrolizumab in platinum-resistant epithelial ovarian cancer (EOC) patients. Gynecol Oncol 2018; 149: 38.
265. Liu JF, Herold C, Gray KP, Penson RT, Horowitz N, Konstantinopoulos PA, et al. Assessment of Combined Nivolumab and Bevacizumab in Relapsed Ovarian Cancer: A Phase 2 Clinical Trial. JAMA Oncol 2019; 5(12): 1731-1738.
266. Disis ML, Patel MR, Pant S, Hamilton EP, Lockhart AC, Kelly K, et al. Avelumab (MSB0010718C; anti-PD-L1) in patients with recurrent/refractory ovarian cancer from the JAVELIN Solid Tumor phase Ib trial: safety and clinical activity. JCO 2016; 34(15_suppl): 5533.
267. Eddie SL, Quartuccio SM, Ó hAinmhir E, Moyle-Heyrman G, Lantvit DD, Wei JJ, et al. Tumorigenesis and peritoneal colonization from fallopian tube epithelium. Oncotarget. 2015; 6(24): 20500-12.
268. Chekmasova AA, Rao TD, Nikhamin Y, Park KJ, Levine DA, Spriggs DR et al. Successful eradication of established peritoneal ovarian tumors in SCID-Beige mice following adoptive transfer of T cells genetically targeted to the MUC16 antigen. Clin Cancer Res. 2010; 16(14): 3594–3606.

269. Carpenito C, Milone MC, Hassan R, Simonet JC, Lakhal M, Suhoski MM, et al. Control of large, established tumor xenografts with genetically retargeted human T cells containing CD28 and CD137 domains. Proc Natl Acad Sci USA. 2009; 106: 3360–3365.
270. Aoki Y, Takakuwa K, Kodama S, Tanaka K, Takahashi M, Tokunaga A, et al. Use of adoptive transfer of tumor-infiltrating lymphocytes alone or in combination with cisplatin-containing chemotherapy in patients with epithelial ovarian cancer. Cancer Res. 1991; 51(7): 1934–1939.
271. Tanyi JL, Haas AR, Beatty GL, Stashwick C, O'Hara M, Morgan M, et al. Anti-mesothelin chimeric antigen receptor T cells in patients with epithelial ovarian cancer. J Clin Oncol 2016; 34(15_suppl): 5511.
272. Palaia I, Tomao F, Sassu CM, Musacchio L, Benedetti Panici P. Immunotherapy For Ovarian Cancer: Recent Advances And Combination Therapeutic Approaches. Onco Targets. Ther. 2020; 13: 6109-29.
273. Clinical Trial: NCT04679064; Trial on NIraparib-TSR-042 (Dostarlimab) vs Physician's Choice CHEmotherapy in Recurrent, Ovarian, Fallopian Tube or Primary Peritoneal Cancer Patients Not Candidate for Platinum Retreatment (NItCHE-MITO33) [Internet]; Available at https://www.clinicaltrials.gov/ct2/show/NCT04679064.
274. Musacchio L, Salutari V, Pignata S, Braicu E, Cibula D, Colombo N, et al. Randomized phase III trial on niraparib-TSR-042 (dostarlimab) versus physician's choice chemotherapy in recurrent ovarian, fallopian tube, or primary peritoneal cancer patients not candidate for platinum retreatment: NItCHE trial (MITO 33). Int J Gynecol Cancer 2021; 31(10): 1369-1373.
275. Clinical Trial: NCT05092360; Clinical Phase 3 Study of Nemvaleukin Alfa in Combination With Pembrolizumab in Patients With Platinum-Resistant Epithelial Ovarian Cancer (ARTISTRY-7) [Internet]; Available at https://www.clinicaltrials.gov/ct2/show/NCT05092360.
276. Clinical Trial: NCT03737643; Durvalumab Treatment in Combination With Chemotherapy and Bevacizumab, Followed by Maintenance Durvalumab, Bevacizumab and Olaparib Treatment in Advanced Ovarian Cancer Patients (DUO-O) [Internet]; Available at https://clinicaltrials.gov/ct2/show/NCT03737643.
277. Clinical Trial: NCT03642132; Avelumab and Talazoparib in Untreated Advanced Ovarian Cancer (JAVELIN OVARIAN PARP 100) [Internet]; Available at https://clinicaltrials.gov/ct2/show/NCT03642132.
278. Clinical Trial: NCT03430700; A trial of pembrolizumab for ovarian cancer (PROMPT) [Internet]; Available at http://www.ctc.ucl.ac.uk/TrialDetails.aspx?Trial=167&TherA=3.
279. Hodi FS, Mihm MC, Soiffer RJ, Haluska FG, Butler M, Seiden MV, et al. Biologic activity of cytotoxic T lymphocyte-associated antigen 4 antibody blockade in previously vaccinated metastatic melanoma and ovarian carcinoma patients. Proc Natl Acad Sci U S A 2003; 100(8): 4712–17.
280. Clinical Trial: NCT04861181; NIRAPK : Study of the Relationship(s) Between Clinical, Biological and Pharmacokinetic Metrics and Toxicities When Niraparib is Used as Maintenance Treatment for Ovarian Cancer Patients [Internet]. Available at https://clinicaltrials.gov/ct2/show/NCT04861181.
281. Clinical Trial: NCT04644068; A trial of AZD5305 for certain types of solid cancers that are getting worse (PETRA) [Internet]; Available at https://www.cancerresearchuk.org/about-cancer/find-a-clinical-trial/a-trial-of-azd5305-for-certain-types-of-solid-cancers-that-are-getting-worse-petra.
282. Elyashiv O, Ledermann J, Parmar G, Farrelly L, Counsell N, Feeney A, et al. ICON 9-an international phase III randomized study to evaluate the efficacy of maintenance therapy with olaparib and cediranib or olaparib alone in patients with relapsed platinum-sensitive ovarian

cancer following a response to platinum-based chemotherapy. Int J Gynecol Cancer 2021; 31(1): 134-138.
283. Clinical Trial: NCT01706120; Study of Clinical and Biological Prognostic Factors in Patients With Ovarian Cancer Receiving Carboplatin +Paclitaxel With Bevacizumab (MITO16/MANGO-2) [Internet]; Available at https://clinicaltrials.gov/ct2/show/NCT01706120.
284. Clinical Trial: NCT05057013; HMBD-001 in Advanced HER3 Positive Solid Tumours [Internet]. Available at: https://www.clinicaltrials.gov/ct2/show/NCT05057013
285. Geller MA, Cooley S, Judson PL, Ghebre R, Carson LF, Argenta PA, et al. A phase II study of allogeneic natural killer cell therapy to treat patients with recurrent ovarian and breast cancer. Cytotherapy. 2011; 13: 98–107.
286. Clinical Trial: NCT05057013; Clinical Study on Anti-tumor Effect Induced by Activated Primary Natural Killer（NK）Cells [Internet]. Available at https://clinicaltrials.gov/ct2/show/NCT03634501.
287. Recchia F, Saggio G, Cesta A, Candeloro G, Nuzzo A, Lombardo M, Carta G, Rea S. Interleukin-2 and 13-cis retinoic acid as maintenance therapy in advanced ovarian cancer. Int J Oncol. 2005 Oct;27(4):1039-46. PMID: 16142321.
288. Felices M, Chu S, Kodal B, Bendzick L, Ryan C, Lenvik AJ, et al. IL-15 super-agonist (ALT-803) enhances natural killer (NK) cell function against ovarian cancer. Gynecol Oncol. 2017; 145(3): 453-61.
289. Liu J, Li H, Cao S, Zhang X, Yu J, Qi J, et al. Maintenance therapy with autologous cytokine-induced killer cells in patients with advanced epithelial ovarian cancer after first-line treatment. J Immunother. 2014; 37: 115–22.
290. Geller MA, Knorr DA, Hermanson DA, Pribyl L, Bendzick L, McCullar V, et al. Intraperitoneal delivery of human natural killer cells for treatment of ovarian cancer in a mouse xenograft model. Cytotherapy. 2013; 15(10): 1297-306.
291. Clinical Trial: NCT03213964; Intraperitoneal Delivery of Adaptive Natural Killer (NK) Cells (FATE-NK100) With Intraperitoneal Int [Internet]. Available at https://clinicaltrials.gov/ct2/show/NCT03213964.
292. Clinical Trial: NCT03539406; Intraperitoneal Infusion of ex Vivo-cultured Allogeneic NK Cells in Recurrent Ovarian Carcinoma Patients [Internet]. Available at https://clinicaltrials.gov/ct2/show/NCT03539406.
293. Oyer JL, Gitto SB, Altomare DA, Copik AJ. PD-L1 blockade enhances anti-tumor efficacy of NK cells. Oncoimmunology. 2018; 7: e1509819.
294. Zhang Q, Bi J, Zheng X, Chen Y, Wang H, Wu W, et al. Blockade of the checkpoint receptor TIGIT prevents NK cell exhaustion and elicits potent anti-tumor immunity. Nat Immunol. 2018; 19: 723–32.
295. Kamiya T, Seow SV, Wong D, Robinson M, Campana D. Blocking expression of inhibitory receptor NKG2A overcomes tumor resistance to NK cells. J Clin Invest. 2019; 130: 2094.
296. Fossati M, Buzzonetti A, Monego G, Catzola V, Scambia G, Fattorossi A, et al. Immunological changes in the ascites of cancer patients after intraperitoneal administration of the bispecific antibody catumaxomab (anti-EpCAMxanti-CD3). Gynecol Oncol. 2015; 138: 343–51.
297. Moore KN, Vergote I, Oaknin A, Colombo N, Banerjee S, Oza A, et al. FORWARD I: a Phase III study of mirvetuximab soravtansine versus chemotherapy in platinum-resistant ovarian cancer. Future Oncol. 2018; 14: 1669–78.

298. Li Y, Hermanson DL, Moriarity BS, Kaufman DS. Human iPSC-Derived Natural Killer Cells Engineered with Chimeric Antigen Receptors Enhance Anti-tumor Activity. Cell Stem Cell. 2018; 23(2): 181-92.
299. Clinical Trial: NCT03415100; Pilot Study of NKG2D-Ligand Targeted CAR-NK Cells in Patients With Metastatic Solid Tumours [Internet]. Available at https://clinicaltrials.gov/ct2/show/NCT03415100.
300. Clinical Trial: NCT03692637; Study of Anti-Mesothelin Car NK Cells in Epithelial Ovarian Cancer [Internet]. Available at https://clinicaltrials.gov/ct2/show/NCT03692637.
301. Fan CA, Reader J, Roque DM. Review of Immune Therapies Targeting Ovarian Cancer. Curr Treat Options Oncol. 2018; 19(12): 74.
302. Gilly FN, Cotte E, Brigand C, Monneuse O, Beaujard AC, Freyer G, Glehen O. Quantitative prognostic indices in peritoneal carcinomatosis. Eur J Surg Oncol. 2006 Aug;32(6):597-601.
303. ATCC: Human Cells; CCL-243, K-562 cell line [Internet]. Available at: https://www.atcc.org/products/ccl-243.
304. Klein E, Ben-Bassat H, Neumann H, Ralph P, Zeuthen J, Polliack A, et al. Properties of the K562 cell line, derived from a patient with chronic myeloid leukemia. Int J Cancer. 1976 Oct 15;18(4):421-31.
305. 10X Genomics: Chromium Next GEM Single Cell 3' Reagent Kits v3.1, User Guide [Internet]. Available at: https://cdn.10xgenomics.com/image/upload/v1668017706/support-documents/CG000315_ChromiumNextGEMSingleCell3-_GeneExpression_v3.1_DualIndex__RevE.pdf
306. Zheng GXY, Terry JM, Belgrader P, Ryvkin P, Bent ZW, Wilson R, et al. Massively parallel digital transcriptional profiling of single cells. Nat Commun [Internet]. 2017;8(1):14049. Available from: https://doi.org/10.1038/ncomms14049
307. 10X Genomics: What is Cell Ranger? - Software -Single Cell Gene Expression -Official 10x Genomics Support [Internet]. Available at https://support.10xgenomics.com/single-cell-gene-expression/software/pipelines/latest/what-is-cell-ranger#:~:text=What%20is%20Cell%20Ranger%3F%20Cell%20Ranger%20is%20a,Single%20Cell%20Gene%20Expression%20Solution%20and%20related%20products%3A
308. 10X Genomics: Chromium Next GEM Single Cell ATAC Reagent Kits v1.1, User Guide [Internet]. Available at: chrome-extension://efaidnbmnnnibpcajpcglclefindmkaj/https://cdn.10xgenomics.com/image/upload/v1666737555/support-documents/CG000209_Chromium_NextGEM_SingleCell_ATAC_ReagentKits_v1.1_UserGuide_RevG.pdf
309. Chang PY, Liao YP, Wang HC, Chen YC, Huang RL, Wang YC, et al. An epigenetic signature of adhesion molecules predicts poor prognosis of ovarian cancer patients. Oncotarget. 2017 Jun 16;8(32):53432-53449.
310. Ng SS, De Labastida Rivera F, Yan J, Corvino D, Das I, Zhang P, et al. The NK cell granule protein NKG7 regulates cytotoxic granule exocytosis and inflammation. Nat Immunol. 2020 Oct;21(10):1205-1218.
311. Malarkannan S. NKG7 makes a better killer. Nat Immunol. 2020;21:1139–1140
312. Gene Cards: CD3G Gene [Internet]. Available at: https://www.genecards.org/cgi-bin/carddisp.pl?gene=CD3G
313. National Library of Medicine; Genetic testing registry; CD8A [Internet]. Available at: https://www.ncbi.nlm.nih.gov/gtr/genes/925/
314. Hori S, Nomura T, Sakaguchi S. Control of regulatory T cell development by the transcription factor Foxp3. Science. 2003 Feb 14;299(5609):1057-61.

315. Sprenkeler EGG, Zandstra J, van Kleef ND, Goetschalckx I, Verstegen B, Aarts CEM, et al. S100A8/A9 Is a Marker for the Release of Neutrophil Extracellular Traps and Induces Neutrophil Activation. Cells. 2022 Jan 11;11(2):236.
316. Torsteinsdóttir I, Håkansson L, Hällgren R, Gudbjörnsson B, Arvidson NG, Venge P, Serum lysozyme: a potential marker of monocyte/macrophage activity in rheumatoid arthritis. Rheumatology. 1999;38(12):1249–1254.
317. Wu Z, Zhang Z, Lei Z, Lei P. CD14: Biology and role in the pathogenesis of disease. Cytokine Growth Factor Rev. 2019 Aug;48:24-31.
318. ScienceDirect; CD163: an overview [Internet]. Available at: https://www.sciencedirect.com/topics/neuroscience/cd163
319. Gene Cards: MS4A1 Gene [Internet]. Available at: genecards.org/cgi-bin/carddisp.pl?gene=MS4A1#:~:text=MS4A1%20(Membrane%20Spanning%204-Domains,Cells%20and%20Lineage-specific%20Markers.
320. Cancer Genetics Web; KRT18 [Internet]. Available at: https://www.cancer-genetics.org/KRT18.htm
321. Privratsky JR, Newman PJ. PECAM-1: regulator of endothelial junctional integrity. Cell Tissue Res. 2014 Mar;355(3):607–19.
322. Bozoky B, Savchenko A, Guven H, Ponten F, Klein G, Szekely L. Decreased decorin expression in the tumor microenvironment. Cancer Med. 2014 Jun;3(3):485-91.
323. Muhl L, Genové G, Leptidis S, Liu J, He L, Mocci G, et al. Single-cell analysis uncovers fibroblast heterogeneity and criteria for fibroblast and mural cell identification and discrimination. Nat Commun. 2020 Aug 7;11(1):3953.
324. National Library of Medicine; Centre for Biotechnology information; COL1A1 [Internet]. Available at: https://www.ncbi.nlm.nih.gov/gene/1277
325. National Library of Medicine; Centre for Biotechnology information; MFAP5 [Internet]. Available at: https://www.ncbi.nlm.nih.gov/gene/8076
326. Uxa S, Castillo-Binder P, Kohler R, Stangner K, Müller GA, Engeland K. Ki-67 gene expression. Cell Death Differ [Internet]. 2021;28(12):3357–70. Available from: https://doi.org/10.1038/s41418-021-00823-x
327. Zhu K, Cai L, Cui C, de Los Toyos JR, Anastassiou D. Single-cell analysis reveals the pan-cancer invasiveness-associated transition of adipose-derived stromal cells into COL11A1-expressing cancer-associated fibroblasts. PLoS Comput Biol. 2021 Jul 20;17(7):e1009228.
328. Sterzyńska K, Klejewski A, Wojtowicz K, Świerczewska M, Andrzejewska M, Rusek D, Sobkowski M, et al. The Role of Matrix Gla Protein (MGP) Expression in Paclitaxel and Topotecan Resistant Ovarian Cancer Cell Lines. Int J Mol Sci. 2018 Sep 25;19(10):2901.
329. Ahmed N, Escalona R, Leung D, Chan E, Kannourakis G. Tumour microenvironment and metabolic plasticity in cancer and cancer stem cells: Perspectives on metabolic and immune regulatory signatures in chemoresistant ovarian cancer stem cells. Semin Cancer Biol. 2018 Dec;53:265-281.
330. Verhaak RGW, Tamayo P, Yang J-Y, Hubbard D, Zhang H, Creighton CJ, et al. Prognostically relevant gene signatures of high-grade serous ovarian carcinoma. J Clin Invest. 2012;123(1).
331. Talukdar S, Chang Z, Winterhoff B, Starr TK. Single-Cell RNA Sequencing of Ovarian Cancer: Promises and Challenges. Adv Exp Med Biol. 2021;1330:113–23.
332. Konecny GE, Wang C, Hamidi H, Winterhoff B, Kalli KR, Dering J, et al. Prognostic and therapeutic relevance of molecular subtypes in high-grade serous ovarian cancer. J Natl Cancer Inst. 2014 Oct;106(10).

333. Shih AJ, Menzin A, Whyte J, Lovecchio J, Liew A, Khalili H, et al. Identification of grade and origin specific cell populations in serous epithelial ovarian cancer by single cell RNA-seq. PLoS One. 2018 Nov 1;13(11):e0206785.
334. National Human Genome Research Institute; Human genome reference sequence, updated May 2, 2023 [Internet]. Available at: https://www.genome.gov/genetics-glossary/Human-Genome-Reference-Sequence#:~:text=This%20set%20of%20data%2C%20as%20intended%2C%20was%20a,base%20research%20studies%20or%20compare%20other%20human%20genomes.
335. Zhai Y, Lu Q, Lou T, Cao G, Wang S, Zhang Z. MUC16 affects the biological functions of ovarian cancer cells and induces an antitumor immune response by activating dendritic cells. Ann Transl Med. 2020 Nov;8(22):1494
336. Moore, R., Hill, E., Horan, T. et al. HE4 (WFDC2) gene overexpression promotes ovarian tumor growth. Sci Rep. 2014; 4, 3574
337. Xing F, Saidou J, Watabe K. Cancer associated fibroblasts (CAFs) in tumor microenvironment. Front Biosci (Landmark Ed). 2010 Jan 1;15(1):166-79.
338. Schad SE, Chow A, Mangarin L, Pan H, Zhang J, Ceglia N, et al. Tumor-induced double positive T cells display distinct lineage commitment mechanisms and functions. J Exp Med. 2022 Jun 6;219(6):e20212169.
339. Regner MJ, Wisniewska K, Garcia-Recio S, Thennavan A, Mendez-Giraldez R, Malladi VS, et al. A multi-omic single-cell landscape of human gynecologic malignancies. Mol Cell. 2021 Dec 2;81(23):4924-4941.e10.
340. Jiménez-Sánchez A, Cybulska P, Mager KL, Koplev S, Cast O, Couturier DL, et al. Unraveling tumor-immune heterogeneity in advanced ovarian cancer uncovers immunogenic effect of chemotherapy. Nat Genet. 2020 Jun;52(6):582-593.
341. Lobello N, Biamonte F, Pisanu ME, Faniello MC, Jakopin Ž, Chiarella E, et al. Ferritin heavy chain is a negative regulator of ovarian cancer stem cell expansion and epithelial to mesenchymal transition. Oncotarget. 2016 Sep 20;7(38):62019-62033.
342. Sterzyńska K, Klejewski A, Wojtowicz K, Świerczewska M, Andrzejewska M, Rusek D, et al. The Role of Matrix Gla Protein (MGP) Expression in Paclitaxel and Topotecan Resistant Ovarian Cancer Cell Lines. Int J Mol Sci. 2018 Sep 25;19(10):2901.
343. Li S, Xie Y, Zhang W, Gao J, Wang M, Zheng G, et al. Interferon alpha-inducible protein 27 promotes epithelial-mesenchymal transition and induces ovarian tumorigenicity and stemness. J Surg Res. 2015 Jan;193(1):255-64.
344. Tewary P, Yang D, de la Rosa G, Li Y, Finn MW, Krensky AM, et al. Granulysin activates antigen-presenting cells through TLR4 and acts as an immune alarmin. Blood. 2010 Nov 4;116(18):3465-74.
345. Qi F, Qin WX, Zang YS. Molecular mechanism of triple-negative breast cancer-associated BRCA1 and the identification of signaling pathways. Oncol Lett. 2019 Mar;17(3):2905-2914
346. Kurosaki A, Hasegawa K, Kato T, Abe K, Hanaoka T, Miyara A, et al. Serum folate receptor alpha as a biomarker for ovarian cancer: Implications for diagnosis, prognosis and predicting its local tumor expression. Int J Cancer. 2016 Apr 15;138(8):1994-2002
347. Lau TS, Chung TK, Cheung TH, Chan LK, Cheung LW, Yim SF, et al. Cancer cell-derived lymphotoxin mediates reciprocal tumour-stromal interactions in human ovarian cancer by inducing CXCL11 in fibroblasts. J Pathol. 2014 Jan;232(1):43-56.
348. Zhang Y, Chen H, Mo H, Hu X, Gao R, Zhao Y, et al. Single-cell analyses reveal key immune cell subsets associated with response to PD-L1 blockade in triple-negative breast cancer. Cancer Cell. 2021 Dec 13;39(12):1578-1593.e8.

349. Poos AM, Mallm JP, Tirier SM, Casiraghi N, Susak H, Giesen N, et al. A Comprehensive Analysis of Single-Cell Chromatin Accessibility and Gene Expression Identifies Intra-Tumor Heterogeneity and Molecular Treatment Responses in Relapsed/Refractory Multiple Myeloma. Blood 2019; 134 (Supplement_1): 575.
350. Poli Neto OB, Candido Dos Reis FJ, Zambelli Ramalho LN, Nogueira AA, de Andrade JM. p63 expression in epithelial ovarian tumors. Int J Gynecol Cancer. 2006 Jan-Feb;16(1):152-5.
351. Deng Y, Lu L, Zhang H. The role and regulation of Maf proteins in cancer. Biomark Res 2023; 11: 17
352. Pieterse Z, Amaya-Padilla MA, Singomat T, Binju M, Madjid BD, Yu Y, Kaur P. Ovarian cancer stem cells and their role in drug resistance. Int J Biochem Cell Biol. 2019;106:117–126.
353. Roy L, Cowden Dahl KD. Can Stemness and Chemoresistance Be Therapeutically Targeted via Signaling Pathways in Ovarian Cancer? Cancers (Basel). 2018 Jul 24;10(8):241.
354. Kenda Suster N, Virant-Klun I. Presence and role of stem cells in ovarian cancer. World J Stem Cells. 2019 Jul 26;11(7):383-397.
355. Ardolino M, Azimi CS, Iannello A, Trevino TN, Horan L, Zhang L, et al. Cytokine therapy reverses NK cell anergy in MHC-deficient tumors. J Clin Invest. 2014 Nov;124(11):4781-94
356. Raulet DH, Marcus A, Coscoy L. Dysregulated cellular functions and cell stress pathways provide critical cues for activating and targeting natural killer cells to transformed and infected cells. Immunol Rev. 2017 Nov;280(1):93-101.
357. Rocca YS, Roberti MP, Arriaga JM, Amat M, Bruno L, Pampena MB, et al. Altered phenotype in peripheral blood and tumor-associated NK cells from colorectal cancer patients. Innate Immun. 2013 Feb;19(1):76-85.
358. A. Stojanovic, N. Fiegler, M. Brunner-Weinzierl, A. Cerwenka. CTLA-4 is expressed by activated mouse NK cells and inhibits NK Cell IFN-gamma production in response to mature dendritic cells. J. Immunol. 2014;192:4184-419.
359. Ni J, Wang X, Stojanovic A, Zhang Q, Wincher M, Bühler L, et al. Single-Cell RNA Sequencing of Tumor-Infiltrating NK Cells Reveals that Inhibition of Transcription Factor HIF-1α Unleashes NK Cell Activity. Immunity. 2020 Jun 16;52(6):1075-1087.e8.
360. Parodi M, Raggi F, Cangelosi D, Manzini C, Balsamo M, Blengio F, et al. Hypoxia Modifies the Transcriptome of Human NK Cells, Modulates Their Immunoregulatory Profile, and Influences NK Cell Subset Migration. Front Immunol. 2018 Oct 16;9:2358.
361. Zingoni A, Fionda C, Borrelli C, Cippitelli M, Santoni A, Soriani A. Natural Killer Cell Response to Chemotherapy-Stressed Cancer Cells: Role in Tumor Immunosurveillance. Front Immunol. 2017 Sep 25;8:1194.
362. Ye S, Chen W, Zheng Y, Wu Y, Xiang L, Li T, Ping B, Zhang X, Yang H. Peripheral lymphocyte populations in ovarian cancer patients and correlations with clinicopathological features. J Ovarian Res. 2022 Apr 11;15(1):43.
363. Chen YY, Feng Y, Mao QS, Ma P, Liu JZ, Lu W, et al. Diagnostic and prognostic value of the peripheral natural killer cell levels in gastric cancer. Exp Ther Med. 2020 Oct;20(4):3816-3822.
364. Imai K, Matsuyama S, Miyake S, Suga K, Nakachi K. Natural cytotoxic activity of peripheral-blood lymphocytes and cancer incidence: an 11-year follow-up study of a general population. Lancet. 2000 Nov 25;356(9244):1795-9.
365. Pross HF, Lotzová E. Role of natural killer cells in cancer. Nat Immun. 1993 Jul-Oct;12(4-5):279-92.
366. Holdenrieder S, Stieber P, Peterfi A, Nagel D, Steinle A, Salih HR. Soluble MICB in malignant diseases: analysis of diagnostic significance and correlation with soluble MICA. Cancer Immunol Immunother. 2006 Dec;55(12):1584-9.

367. Möller M, Kammerer R, Von Kleist S . A distinct distribution of natural killer cell subgroups in human tissues and blood. Int J Cancer 1998; 78: 533–538
368. Penack O, Gentilini C, Fischer L, Asemissen AM, Scheibenbogen C, Thiel E, et al. CD56dimCD16neg cells are responsible for natural cytotoxicity against tumor targets. Leukemia. 2005 May;19(5):835-40.
369. Klapdor R, Wang S, Hacker U, Büning H, Morgan M, Dörk T, et al. Improved Killing of Ovarian Cancer Stem Cells by Combining a Novel Chimeric Antigen Receptor-Based Immunotherapy and Chemotherapy. Hum Gene Ther. 2017 Oct;28(10):886-896.
370. Miller JS, Prosper F, McCullar V. Natural killer (NK) cells are functionally abnormal and NK cell progenitors are diminished in granulocyte colony-stimulating factor-mobilized peripheral blood progenitor cell collections. Blood. 1997 Oct 15;90(8):3098-105.
371. Cao X, Zhao X, Peng T, hou Y, Li R, Fan Z, Zhao M, chang Y, chen H, li C, Huang X. P1422: IN VIVO G-CSF TREATMENT ACTIVATES THE GR-SOCS1 AXIS TO SUPPRESS IFN-Γ SECRETION BY NATURAL KILLER CELLS. Hemasphere. 2022 Jun 23;6(Suppl):1306-1307.
372. Schlahsa L, Jaimes Y, Blasczyk R, Figueiredo C. Granulocyte-colony-stimulatory factor: a strong inhibitor of natural killer cell function. Transfusion. 2011 Feb;51(2):293-305.
373. Milne K, Alexander C, Webb JR, Sun W, Dillon K, Kalloger SE, et al. Absolute lymphocyte count is associated with survival in ovarian cancer independent of tumor-infiltrating lymphocytes. J Transl Med. 2012 Feb 27;10:33.
374. Leung E, Pervaiz Z, Lowe-Zinola J, Cree S, Kwong A, Marriott N, et al. Maintaining surgical care delivery during the COVID-19 pandemic: A comparative cohort study at a tertiary gynecological cancer centre. Gynecol Oncol. 2021 Mar;160(3):649-654.
375. Jiang YZ, Couriel D, Mavroudis DA, Lewalle P, Malkovska V, Hensel NF, et al. Interaction of natural killer cells with MHC class II: reversal of HLA-DR1-mediated protection of K562 transfectant from natural killer cell-mediated cytolysis by brefeldin-A. Immunology. 1996 Mar;87(3):481-6.
376. Bas A, Forsberg G, Hammarström S, Hammarström ML. Utility of the housekeeping genes 18S rRNA, beta-actin and glyceraldehyde-3-phosphate-dehydrogenase for normalization in real-time quantitative reverse transcriptase-polymerase chain reaction analysis of gene expression in human T lymphocytes. Scand J Immunol. 2004 Jun;59(6):566-73.
377. Woopen H, Pietzner K, Richter R, Fotopoulou C, Joens T, Braicu EI, et al. Overexpression of the epithelial cell adhesion molecule is associated with a more favorable prognosis and response to platinum-based chemotherapy in ovarian cancer. J Gynecol Oncol. 2014 Jul;25(3):221-8.
378. McCurley AT, Callard GV. Characterization of housekeeping genes in zebrafish: male-female differences and effects of tissue type, developmental stage and chemical treatment. BMC Molecular Biol. 2008; 9: 102
379. Matsuzaki Y, Umemoto T, Tanaka Y, Okano T, Yamato M. β2-Microglobulin is an appropriate reference gene for RT-PCR-based gene expression analysis of hematopoietic stem cells. Regen Ther. 2015 Jun 23;1:91-97.
380. Abiko K, Matsumura N, Hamanishi J, Horikawa N, Murakami R, Yamaguchi K, et al. IFN-γ from lymphocytes induces PD-L1 expression and promotes progression of ovarian cancer. Br J Cancer. 2015 Apr 28;112(9):1501-9.
381. Høgdall E, Høgdall C, Vo T, Zhou W, Huang L, Marton M, Keefe SM, et al. Impact of PD-L1 and T-cell inflamed gene expression profile on survival in advanced ovarian cancer. Int J Gynecol Cancer. 2020 Jul;30(7):1034-104.
382. Zhao Y, Chen N, Yu Y, Zhou L, Niu C, Liu Y, et al. Prognostic value of MICA/B in cancers: a systematic review and meta-analysis. Oncotarget. 2017 Oct 3;8(56):96384-96395.

383. Conejo-Garcia JR, Benencia F, Courreges MC, Gimotty PA, Khang E, Buckanovich RJ, et al. Ovarian carcinoma expresses the NKG2D ligand Letal and promotes the survival and expansion of CD28− antitumor T cells. Cancer Res. 2004;64:2175–2182.
384. Cho H, Chung JY, Kim S, Braunschweig T, Kang TH, Kim J, et al. MICA/B and ULBP1 NKG2D ligands are independent predictors of good prognosis in cervical cancer. BMC Cancer. 2014 Dec 15;14:957.
385. Markasz L, Stuber G, Vanherberghen B, Flaberg E, Olah E, Carbone E, et al. Effect of frequently used chemotherapeutic drugs on the cytotoxic activity of human natural killer cells. Mol Cancer Ther. 2007 Feb;6(2):644-54.
386. Pesce S, Greppi M, Grossi F, Del Zotto G, Moretta L, Sivori S, et al. PD/1-PD-Ls Checkpoint: Insight on the Potential Role of NK Cells. Front Immunol. 2019 Jun 4;10:1242.
387. Maas RJ, Hoogstad-van Evert JS, Van der Meer JM, Mekers V, Rezaeifard S, Korman AJ, et al. TIGIT blockade enhances functionality of peritoneal NK cells with altered expression of DNAM-1/TIGIT/CD96 checkpoint molecules in ovarian cancer. Oncoimmunology. 2020 Nov 8;9(1):1843247.
388. Labani-Motlagh A, Israelsson P, Ottander U, Lundin E, Nagaev I, Nagaeva O, et al. Differential expression of ligands for NKG2D and DNAM-1 receptors by epithelial ovarian cancer-derived exosomes and its influence on NK cell cytotoxicity. Tumour Biol. 2016 Apr;37(4):5455-66.
389. Focaccetti C, Benvenuto M, Pighi C, Vitelli A, Napolitano F, Cotugno N, et al. DNAM-1-chimeric receptor-engineered NK cells, combined with Nutlin-3a, more effectively fight neuroblastoma cells in vitro: a proof-of-concept study. Front Immunol. 2022 Jul 28;13:886319.
390. Huang Y, Zeng J, Liu T, Xu Q, Song X, Zeng J. DNAM1 and 2B4 Costimulatory Domains Enhance the Cytotoxicity of Anti-GPC3 Chimeric Antigen Receptor-Modified Natural Killer Cells Against Hepatocellular Cancer Cells in vitro. Cancer Manag. Res. 2020;12:3247–3255.